SYMPOSIA OF THE
INTERNATIONAL SOCIETY FOR CELL BIOLOGY
VOLUME 4

The Use of Radioautography in Investigating Protein Synthesis

Edited by

C. P. LEBLOND

Department of Anatomy, McGill University
Montreal, Canada

and

KATHERINE BREHME WARREN

National Institutes of Health, Cell Biology Study Section,
Division of Research Grants, Bethesda, Maryland

1965

ACADEMIC PRESS
New York and London

ACADEMIC PRESS INC.
111 Fifth Avenue, New York, New York 10003

United Kingdom Edition published by
ACADEMIC PRESS INC. (LONDON) LTD.
Berkeley Square House, London W.1

LIBRARY OF CONGRESS CATALOG CARD NUMBER: 62-13095

PRINTED IN THE UNITED STATES OF AMERICA

LIST OF CONTRIBUTORS

Numbers in parentheses indicate the pages on which the authors' contributions begin.

T. C. APPLETON, *Medical Research Council, Biophysics Research Unit, Department of Biophysics, King's College, London, England* (9)

L. BACHMANN, *Laboratory of Electron Microscopy, Department of Engineering Physics and Materials Science, Cornell University, Ithaca, New York and The Institute for Physical Chemistry, University of Innsbruck, Innsbruck, Austria* (23)

LEONARD F. BÉLANGER, *Department of Histology and Embryology, University of Ottawa, Ottawa, Canada* (1)

EARL P. BENDITT, *Department of Pathology, University of Washington, Seattle, Washington* (65)

RUTH W. CAFFREY, *Department of Biological Structure, University of Washington, Seattle, Washington* (143)

J. CARNEIRO, *Laboratory for Cell Physiology, Faculdade de Medicina, São Paulo University, São Paulo, Brazil* (247)

KARIN CITOLER, *Institut für Medizinische Isotopenforschung der Universität Köln, Köln, Germany* (107)

P. CITOLER, *Institut für Medizinische Isotopenforschung der Universität Köln, Köln, Germany* (107)

B. DROZ, *Département de Biologie, Commissariat à l'Energie Atomique, Saclay, France* (159)

N. B. EVERETT, *Department of Biological Structure, University of Washington, Seattle, Washington* (143)

LESTER GOLDSTEIN, *Department of Biology, University of Pennsylvania, Philadelphia, Pennsylvania* (79)

PHILIPPE GRANBOULAN, *Institut de Recherches sur le Cancer, Villejuif (Seine), France* (43)

R. C. GREULICH, *Department of Anatomy, School of Medicine, and Division of Oral Biology, School of Dentistry, University of California, Center for the Health Sciences, Los Angeles, California* (199)

K. HEMPEL, *Institut für Medizinische Isotopenforschung der Universität Köln, Köln, Germany and Klinik für Hals-, Nasen-, und Ohrenheilkunde der Medizinischen Akademie Düsseldorf, Düsseldorf, Germany* (107, 177)

E. KOBURG, *Klinik für Hals-, Nasen-, und Ohrenheilkunde der Medizinischen Akademie Düsseldorf, Düsseldorf, Germany, and Institut für medizinische Isotopenforschung der Universität Köln, Köln, Germany* (177)

C. P. LEBLOND, *Department of Anatomy, McGill University, Montreal, Canada* (321)

GEORGE M. MARTIN, *Department of Pathology, University of Washington, Seattle, Washington* (65)

W. MAURER, *Institut für Medizinische Isotopenforschung der Universität Köln, Köln, Germany* (107)

N. J. NADLER, *Department of Anatomy, McGill University, Montreal, Canada* (303)

S. R. PELC, *Medical Research Council, Biophysics Research Unit, Department of Biophysics, King's College, London, England* (9)

HOWARD PLATTER, *Department of Pathology, University of Washington, Seattle, Washington* (65)

D. M. PRESCOTT, *Department of Anatomy, University of Colorado Medical Center, Denver, Colorado* (95)

JEAN-PAUL REVEL, *Department of Anatomy, Harvard Medical School, Boston, Massachusetts* (293)

W. O. RIEKE, *Department of Biological Structure, University of Washington, Seattle, Washington* (143)

RUSSELL ROSS, *Departments of Pathology and Oral Biology, School of Medicine and Dentistry, University of Washington, Seattle, Washington* (273)

M. M. SALPETER, *Laboratory of Electron Microscopy, Department of Engineering Physics and Materials Science, Cornell University, Ithaca, New York, and The Institute for Physical Chemistry, University of Innsbruck, Innsbruck, Austria* (23)

BRIGITTE SCHULTZE, *Institut für Medizinische Isotopenforschung der Universität Köln, Köln, Germany* (107)

M. ROY SCHWARZ, *Department of Biological Structure, University of Washington, Seattle, Washington* (143)

H. C. SLAVKIN, *Department of Anatomy, School of Medicine, and Division of Oral Biology, School of Dentistry, University of California, Center for the Health Sciences, Los Angeles, California* (199)

G. E. STONE, *Department of Anatomy, University of Colorado Medical Center, Denver, Colorado* (95)

EDGAR A. TONNA, *Medical Research Center, Brookhaven National Laboratory, Upton, Long Island, New York* (215)

HUBERTA E. VAN HEYNINGEN, *Department of Anatomy, McGill University, Montreal, Canada* (261)

M. E. WELTON, *Medical Research Council, Biophysics Research Unit, Department of Biophysics, King's College, London, England* (9)

PREFACE

It is a sign of the times that of the thirty-one participants at the three-day symposium on protein metabolism reported in this volume only two described themselves as biochemists, while the others were cytologists, histologists, or pathologists. The common denominator of the participants was their interest in the tracing of labeled proteins with the help of photographic emulsion, that is, by the technique called radioautography or autoradiography. This technique enables us to locate proteins at the site of their synthesis and also to follow their subsequent migration through the cell, thus providing a novel insight into secretion and other processes. Indeed the continuous synthesis of proteins in all cells throughout the body suggests that protein turnover is a basic feature of life. It is hoped that the reader of these proceedings may share some of the excitement that was felt during the entire symposium.

The symposium received generous support not only from its original sponsor, the International Society for Cell Biology (through Dr. J. F. Danielli), but also from the International Union of Biological Sciences (through Dr. M. Chèvremont), and particularly from the Medical Research Council of Canada (through Dr. J. Auer). We should like to thank Mrs. R. Neutra for editing the discussions. A small exhibit of early histology books was provided by the Osler Library of McGill University and was symbolically placed underneath a diagram depicting the latest advances in the biochemical knowledge of protein synthesis.

November, 1965 C. P. LEBLOND

OPENING ADDRESS

LEONARD F. BÉLANGER

Department of Histology and Embryology, University of Ottawa, Ottawa, Canada

Reminiscing is a function of old age, but it may help salvage a few choice items of life. I refer presently to things like dreams of youth, memories of a few days ending in the golden sunset of success, thoughts of former associates and colleagues, the warm glow of friendship, the stimulus of admiration . . . .

I have been asked to open the memory file at the item Radioautography, to all of us a magic word, to some a definite turn in their lives, to the world, a new toy and joy.

To many here, this McGill meeting has meant coming home. To me, this flight into the past will span almost 20 years, to the days when not far from this room, I was initiated into the mysteries of the unstable atom.

It was on a bright and crisp Saturday of February 1946 that the picture now on the screen was first visualized (Figs. 1 and 2). This image in which, for the first time [2], the radioautographic record of ^{32}P was integrated with that of a biological radiating source, was to Charles Leblond, an old hand at this sort of thing, simply another step forward. To me, however, the impact of this first personal experience with atomic energy has been a source of constant wonderment. I remember that going back to the biblical background of my youth, I thought then of the message written in letters of fire, in the great hall of the wicked old Assyrian king. Here was another message written this time in the photographic emulsion, by the fire which had been from the beginning.

Contrary to the writing on the wall, this fire was not recording a message of doom but one of life. For the whole world to see, the section of tissue had written in the emulsion a story in black dots. It was spelling out secrets of synthesis, movement, life-span. A few years later, Charles Leblond was to speak in terms of "Dynamic Histology" to deal with the rapidly accumulating data, some of them unbelievable to the eyes and ears of the rigid classical anatomists.

The McGill integrated radioautographs were produced by coating the histological sections with melted photographic emulsion scraped from lantern slide plates [2]. Some of the background fog present in the early

radioautographs, I remember now, was the result of the early radioautographer having to share the dark room with a phototechnician, a chain-smoking giant who insisted that his cigarettes were producing "only a little bit of light". . . .

Before our days, there had been, of course, a half century of contact radioautography in which the names of Becquerel, London, Lacassagne, Hamilton, and Leblond have been landmarks [5].

Other procedures for the production of *integrated radioautographs* were soon to appear, reminding one that a thing not done at a given time and place soon will be done elsewhere and that scientific thought is a moving train into which one must jump at the right moment. These techniques were the ingenious stripping film method of Pelc [15], the easy mounting method of Evans [9], the practical dipping process of Joftes and Warren [12], and many variants. Looking back at the titles of this literature with a nonprofessional eye, one could easily think of it as joyfully concerned with an altogether different type of activity!

The first 5 years of the integration era were mostly and almost forcibly devoted to bone and tooth work, on account of the labeling substances available: $^{32}PO_4$, $^{45}CaCl_2$, $^{35}SO_4$. There were also at that time new problems for humanity, supplying automatically the tools with which to investigate them. Plutonium, strontium, cesium took their place in the radioautography literature. The names of Arnold and Jee [1], Copp, Axelrod, and Hamilton [8], Comar, Lotz, and Boyd [6] became known in radioautography.

At McGill and elsewhere, history was made in thyroid physiology through ^{131}I radioautography. In evidence were the names of Leblond and Gross [13], Gorbman and Evans [11].

In Chicago, Bloom, Curtis, and McLean [4] had started to use radiocarbon in the form of $^{14}CO_2$. Leblond, Stevens, and Bogoroch [14] were soon to utilize ^{32}P as a label for deoxyribonucleic acid (DNA). In England, Pelc and Howard [16] applied the same isotope to studies of chromosome metabolism.

At this time, the first meeting of radioautographers was called. It was a combination course and symposium for the benefit of U.S. Atomic Energy Commission workers and grantees. This meeting was organized by the Oak Ridge Institute of Nuclear Studies with George Boyd as principal catalyst. Into the inferno of the Atomic City came some of the "veterans" and also the first students. In the picture (Fig. 3), we can recognize Pelc, Arnold, Boyd, Lotz, Leblond, Rita Bogoroch, and others . . . .

The Oak Ridge meeting consisted mainly of papers on theory and technique. As a follow-up, the first textbook on the subject was published by George Boyd 4 years later under the title "Autoradiography in Biology

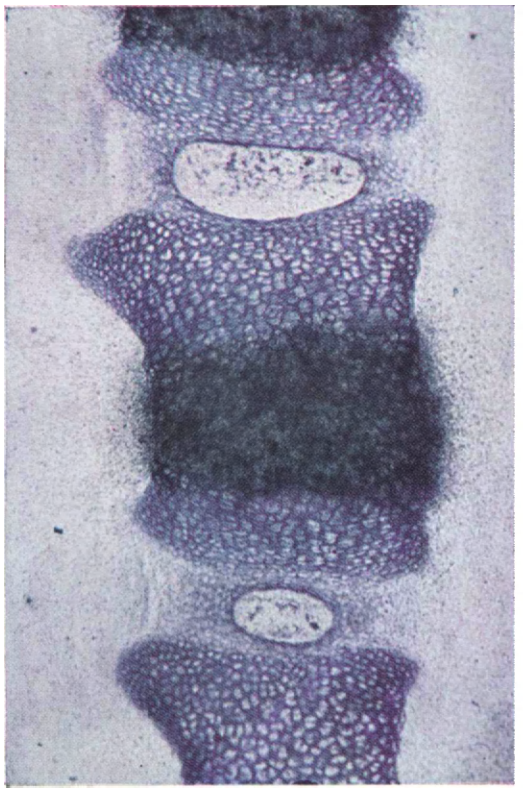

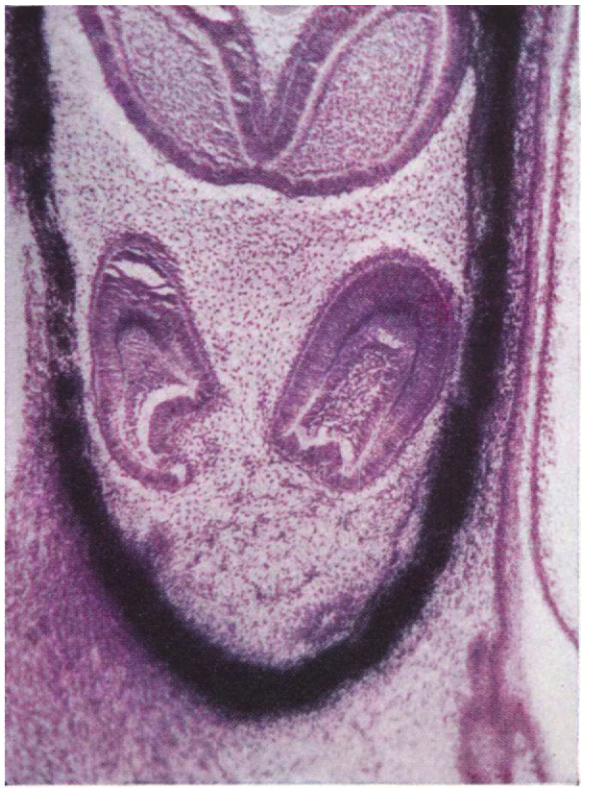

FIG. 1 (left). Methylene blue stained radioautograph of tail vertebra from newborn mouse injected with ^{32}P-phosphate ($\times$ 50). Three (blue stained) cartilaginous vertebrae are separated by whitish, unstained intervertebral discs. The central vertebra is overlaid by a heavy radioautographic reaction in its middle portion where bone coated cartilage spicules take up labeled phosphate.

FIG. 2. (right). *H* and *E* stained radioautographs of the lower jaw region of a newborn mouse injected with ^{32}P-phosphate ($\times$ 50). The ∪-shaped black band is due to heavy radioautographic reaction over the mandible, as there is heavy uptake of labeled phosphate by the trabecular bone of the mandible. The center of the picture shows two (right and left) anterior molar tooth buds within which a thin black crescent may be seen. This is due to uptake of labeled phosphate by dentin [both radioautographs from (5)].

and Medicine" [5]. Radioautographs, autoradiographs, histoautoradiographs, autoradiograms, autographs, whatever they were called and pretty and exciting as they were, did not allow, in general, more than a histological definition. Single cell records were achieved mainly with fortunate isolation or dispersion and one of the conclusions of the Oak Ridge session was that there was little hope for radioautographic records of intracellular constituents.

FIG. 3. The Faculty, First Course in Radioautography, Oak Ridge, 1951 (from the left): Pelc, Bélanger, Arnold, Boyd, Lotz, Leblond, Fitzgerald, Rita Bogoroch.

However, one "student" on that course was to contribute a new tool to radioautography which changed this situation altogether. Here, sitting with the faculty (Fig. 3), is Patrick J. Fitzgerald, the man who was to give us tritium [10].

In 1958, Dr. Fitzgerald was to call another meeting, the Rye Conference [7]. Thirty-eight guests were present at that gathering. Some of the participants talked on bone and techniques, but the general trend was biochemical this time: nucleic acids, proteins, mucopolysaccharides. Carbon-14 and Sulfur-35 had produced superb data in the hands of such people as Pelc, Lajtha and Oliver, Adrienne Ficq [7], but these investigators as well as Cronkite *et al.*, Fitzgerald and Vinijchaikul, Leblond *et al.*, Painter and Drew, Plaut, Woods, and Taylor [7] brought out a magnificent series of tritium records which definitely established radioautography as a choice method for cell physiology investigations. I would like to quote Dr. Fitzgerald in his opening remarks: "A true synthesis of function varying with cytologic change and vice versa, is not impossible nor out of place in this dynamic morphologic world of ours and autoradiography is uniquely fitted for such studies" [7].

The impact of tritium and especially of ^{3}H-thymidine on radioautography has been well illustrated by the following curves presented by W. Maurer at the recent Congress of Histo- and Cytochemistry at Frankfurt (Fig. 4).

Another very important technical advance was introduced at the Rye meeting: commercially available, heavily loaded nuclear emulsions. Bélanger, Cronkite *et al.*, Dziewiatkowski and Woodard, Ficq, Levi, and

Nielsen, Joftes, Leblond *et al.*, Swann *et al.* [7] reported data obtained with these fine-grained, precision emulsions which from then on were here to stay.

Six more years have rolled by in the world of the unstable atom or should we say in the unstable world of the atom and here we are, back where it all started, in old McGill. McGill University which took part in the launching of the atomic age, having been for a time the home of Lord Rutherford, is now host to this meeting in which the role of radioautography in the study of protein synthesis will be discussed.

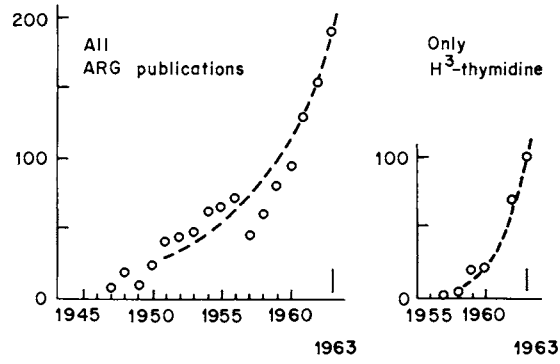

FIG. 4. The growth of radioautography from 1946 to 1963 (W. Maurer).

How nice to be able to meet here, in the realm of my old friend and master Charles Leblond, such distinguished colleagues as Pat Fitzgerald and Steve Pelc, both still painting the sky of radioautography with sunshine. It is also a rare privilege to welcome here such distinguished biochemists, cytologists, and histochemists as Drs. Allfrey, Chèvremont, Danielli, Goldstein, Koburg, and Prescott.

It is highly significant to have with us also the tritium radioautographers, Drs. Carneiro, Droz, Everett, Greulich, Nadler, Brigitte Schultze, Tonna. With beautiful preparations and oh! what patience! they have contributed to establish radioautography as a quantitative method of analysis.

Privately, I have been wondering as to what may happen to the descendants of these disciples of quantitation after several generations of grain counting, especially if grain counters happen to intermarry . . .

Last but not least, I greet the new crew of electron microscope radioautographers, Granboulan, Revel, Ross, Huberta Van Heyningen, and Miriam Salpeter. Their presence will give to the McGill meeting a special orientation. If Oak Ridge (1951) has been the histological phase of radioautography, if the Rye meeting (1958) has marked the beginning of the

cellular era, the present session will probably be remembered as the time when radioautography invaded the realm of electron microscopy.

A few years ago, an important commercial firm took a dim view of some of our efforts:

> "Others find this breadth of choice too narrow. Only with liquid emulsion, these brave souls plead, can they get the radiosensitive layer exactly where they want it and as thick or as thin as they want it. But we, who have worked with liquid emulsion for 75 years, know what delicate, perishable, and variable stuff it is and that its handling is no whit less important than its composition and compounding."

It was nice to see in 1964 this more enthusiastic salute to results obtained by Dr. Salpeter:

> "A work of art! . . .
> "May the marriage of radioautography and electron micrography prosper."

Let us not forget, however, that if a marriage occurred, it took place some 18 years ago. Now the prosperous mature couple, the partners in integrated radioautography, the tissue section and the emulsion, have moved into a new home, the palatial quarters of electron microscopy.

This is one more era of radioautography, but the preceding ones are far from revolved and exhausted. Much will still be done at the light microscope level. In the words of William Blake [3]:

> "I see the Past, Present and Future existing all at once, Before me."

ACKNOWLEDGMENTS

I wish to thank Professor W. Maurer, Director of the Institut für Med. Isotopenforschung, Köln, for the use of Fig. 2.

REFERENCES

1. Arnold, J. S., and Jee, W. S. S., *Am. J. Anat.* **101**, 367 (1957).
2. Bélanger, L. F., and Leblond, C. P., *Endocrinology* **39**, 8 (1946).
3. Blake, William, "Jerusalem," f. 15.6 (1757–1827).
4. Bloom, W., Curtis, H. J., and McLean, F. C., *Science* **105**, 45 (1947).
5. Boyd, G. A., "Autoradiography in Biology and Medicine." Academic Press, New York, 1955.
6. Comar, C. L., Lotz, W. E., and Boyd, G. A., *Am. J. Anat.* **90**, 113 (1952).
7. Conference on Autoradiography, P. J. Fitzgerald, Chairman, *Lab. Invest.* **8**, 59 (1959).
8. Copp, D. H., Axelrod, D., and Hamilton, J. G., *Am. J. Roentgenol. Radium Therapy Nucl. Med.* **58**, 10 (1947).

9. Evans, T. C., *Proc. Soc. Exptl. Biol. Med.* **64**, 313 (1947).
10. Fitzgerald, P. J., Eidinoff, M. L., Knoll, J. E., and Simmel, E. B., *Science* **114**, 494 (1951).
11. Gorbman, A., and Evans, H. M., *Endocrinology* **32**, 113 (1943).
12. Joftes, D. L., and Warren, S., *J. Biol. Phot. Assoc.* **23**, 145 (1955).
13. Leblond, C. P., and Gross, J., *Endocrinology* **43**, 306 (1948).
14. Leblond, C. P., Stevens, C. E., and Bogoroch, R., *Science* **108**, 531 (1948).
15. Pelc, S. R., *Nature* **160**, 749 (1947).
16. Pelc, S. R., and Howard, A., *Brit. Med. Bull.* **8**, 132 (1952).

STATE OF LIGHT AUTORADIOGRAPHY

S. R. PELC, T. C. APPLETON, AND M. E. WELTON

Medical Research Council Biophysics Research Unit,
Department of Biophysics, King's College,
London, England

INTRODUCTION

Although radioactivity was discovered by means of autoradiography, this method of detecting and measuring emitted ionizing particles was not used to a great extent in biology because the naturally occurring unstable elements are relatively rare and of high atomic weight. As soon as artificially produced isotopes of interest to the biologist became available, autoradiography was taken up and three techniques giving improved resolving power were published within 1 year. A theory of the process was produced, the predictions of which proved to be valid guides for evaluating autoradiographs.

For most applications the specimens are fixed, embedded, washed, etc., before applying the photographic emulsion. Labeled compounds soluble in the agents used are removed, and therefore the distribution of labeled precursors in cells was not explored and no work on synthesis of soluble proteins, fat, etc., could be undertaken. Various techniques allowing the retention of soluble labeled compounds were designed and it can be hoped that this field of investigation will now be extended.

RESOLVING POWER

The resolving power has been defined as the distance from a source of radiation at which the grain count declines to one half [7] or as the smallest diameter (d) of two labeled discs separated by a distance d which still gives two distinct images [17]. In high-resolution autoradiography, single grains, rather than continuous densities, are observed and therefore resolving power has to be regarded as a statistical concept.

The factors affecting resolving power are: the geometrical arrangement of the sources of radiation and the photographic film, the size of the photographic grains, and the energy of the ionizing particles emitted by the isotope.

Computations have shown that the resolving power is approximately equal to one half of the sum of the thickness of the specimen plus the

thickness of the photographic emulsion, if these are approximately equal and if scatter and absorption of particles can be neglected. The calculations also show that any gap between the specimen and the emulsion seriously affects the resolving power if such a gap is bigger than 0.1 μ.

The original target for the ionizing particles is silver bromide grains, usually 0.2–0.3 μ in diameter. Exposed grains are reduced to metallic silver by the developer. It is not known whether the developed silver grain is in exactly the same position as the original crystal or whether it is displaced. The total uncertainty in localization due to grain size is therefore of the order of twice the diameter of the original crystal, say 0.4 to 0.6 μ.

As long as the range of the β-particles emitted by an isotope such as ^{32}P or ^{131}I is large compared with the thickness of film and specimen, their energy does not affect the resolving power. For lower energies the improvement is considerable, especially when tritium with a maximum energy of 18 KeV is used.

TECHNIQUES

Originally only the apposition technique was available. The disadvantages of this technique are poor resolving power and difficulty in realigning the specimen and the image. Techniques utilizing differences in grain concentration allowing permanent contact between the specimen and the emulsion were designed by Bélanger and Leblond [4] (coating technique), Endicott and Yagoda [9] (floating technique), Pelc [20] (stripping film technique), Bélanger [3] (inverted autographs), and Joftes [16] (dipping technique). Track autoradiography was pioneered and developed by Boyd and Levi [5] and Ficq [10]. At the present time most workers use either the stripping film technique or the dipping technique. The relative advantages of these techniques are set out in the following paragraphs.

SENSITIVITY

The thickness of the photographic emulsion cannot be adequately controlled when the dipping technique is used and therefore no generally applicable data are available. For Kodak AR.10 stripping film the figures are set out in Table I. Since the β-particles emitted by ^{3}H do not penetrate beyond the first layer of silver bromide crystals, the thickness of the emulsion will not be of great importance when this isotope is used. Baserga and Nemeroff [2], in comparing the two techniques with ^{3}H-labeled tissues, found stripping film to be 15 per cent more sensitive for exposures in air and 36 per cent for exposure in CO_2.

TABLE I. *Sensitivity of AR.10 Stripping Film*

Isotope	Maximum energy (MeV)	Grains per β-particle[a]	μμc/100 grains/ day[b]
^{32}P	1.7	0.78 ± 0.1	0.080
^{131}I	0.25–0.82	1.8 ± 0.2	0.034
^{59}Fe	0.26–0.46	1.6 ± 0.3	0.039
^{14}C	0.15	1.8	0.034
^{3}H	0.018	0.85	0.074

[a] Average number of developed grains per incident β-particle.

[b] The amount of radioactive material (in μμc = 10^{-12} c) in a volume showing 100 grains after 1 day exposure. Valid only if the specimen is sufficiently thin to neglect absorption within the specimen. For exposure times comparable with the half-life of the isotope, radioactive decay has to be taken into account. For ^{3}H the values can be used for a specimen of up to 0.1 μ thickness; for thicker specimens it can be assumed that 100 grains per day represents a concentration of approximately 27.5 μμc in a layer of organic matter 6.75 mg/cm^2 thick.

LATENT IMAGE FADING

Lord [18] investigated latent image fading (see Table II) of Ilford K5 and Gevaert 7.15 emulsion, with and without the use of a drying agent, by exposing ^{3}H autoradiographs prepared by the dipping technique for various periods of time (Ilford K5 and Gevaert 7.15), and by

TABLE II. *Latent Image Fading with Dipping Technique Calculated as Percentage Loss of the Value Expected Without Fading*[a]

	With silica gel		Without silica gel	
Emulsion	2 weeks	5 weeks	2 weeks	5 weeks
Ilford K5	5	29	19	52
Gevaert 7.15A	7	46	1	29
Gevaert 7.15B	23	44	15	36

[a] Calculated from Figs. 4, 8, and 9 of Lord [18].

removing the labeled cells after 1 week exposure and then storing the exposed emulsion for up to 5 weeks (Gevaert 7.15A). It is difficult to interpret the data since Ilford K5 shows less fading when a drying agent is used, whereas Gevaert 7.15 shows more. It can be concluded that with the dipping technique a loss due to latent image fading of 5–20 per cent after 2 weeks exposure and 29–50 per cent after 5 weeks exposure has to be taken into account and that therefore exposure times of more than 10–15 weeks no longer yield appreciably heavier autoradiographs.

Latent image fading in Kodak AR.10 stripping film was investigated by exposing stripping film, mounted emulsion side outward, to standard ^{14}C-labeled methacrylate discs of varying specific activities in such a

way that equal densities would be expected if no fading occurred. For example, a source emitting 2.6×10^4 β per cm^2 per minute was exposed for 3 days and another source emitting 2.6×10^3 β/cm^2/minute was exposed for 30 days. The difference in the densities is a measure of fading. Figure 1 shows that there is no appreciable fading of the latent image with Kodak AR.10 stripping film under our experimental conditions.

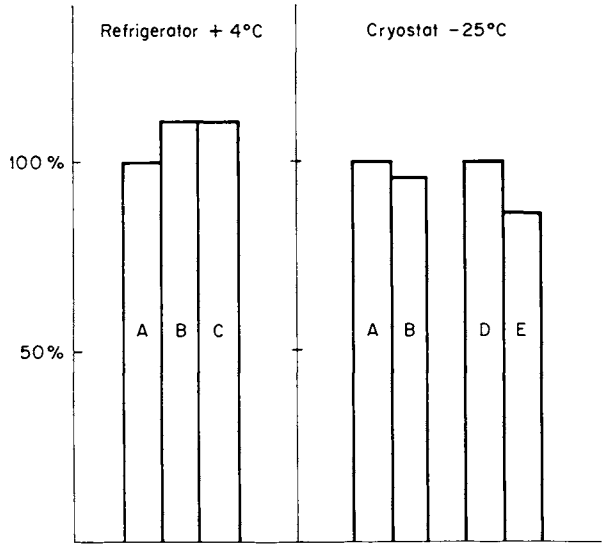

FIG. 1. Latent image fading. A, Taken as 100 per cent exposure for 3 days to 100 × source, developed immediately. B, Exposure as for A, but film stored for 27 days before developing. C, Exposure for 30 days to 10 × source, developed immediately. A, B, and C all developed together, and their optical densities measured on a microdensitometer. D, Taken as 100 per cent; exposure for 1 day to 100 × source, developed immediately. E, Exposure for 100 days to 1 × source, developed immediately. D and E developed together and grain counted.

Specification of standard ^{14}C-methacrylate sources. 1 ×: Specific activity 0.1 μc/gm of polymer Code CFP1; 10 ×: specific activity 1.0 μc/gm of polymer Code CFP2; 100 ×: specific activity 10.3 μc/gm of polymer Code CFP3.

Supplied by the Radiochemical Centre.

The reason for the marked difference in fading between AR.10 stripping film and the emulsions used by Lord is not clear. It may be due to the difference in treatment: floating out on water at 21°C in the stripping film technique versus diluting and melting the emulsion at 45–50°C in the dipping technique. Ray and Stevens [24] found fading of the latent image in Kodak AR.10 stripping film that had not previously been removed from its original base, but none in stripping film transferred to a microscope slide in the usual way and exposed to ^{131}I in an atmos-

phere of nitrogen or carbon dioxide. The difference between their experiments and ours was in the isotope, duration of the exposures, and the densities.

PREPARATION OF AUTORADIOGRAPHS

More equipment is needed for the coating technique than for the stripping film technique. Although presenting no difficulties to persons with reasonable dexterity, stripping film was found more difficult to handle by some workers. Once the photographic emulsion has been diluted and warmed up, up to 60 slides per hour can be coated by the dipping technique, whereas 40–50 slides per hour can be prepared by the stripping technique.

RESOLVING POWER

Since the resolving power depends critically on the thickness of the emulsion, no direct comparison of the two techniques can be made. In the original investigations the first definite autoradiographs of labeled nuclei [14, 23] with ^{32}P and of single chromosomes [22] with ^{35}S, as well as the correct place of binding of ^{131}I in the colloid of the thyroid [7] were made by the stripping film technique.

CONCLUSION

Using ^{3}H as a tracer with short exposure times, the choice of technique can be regarded as a matter of taste. For quantitative work using isotopes other than ^{3}H and for experiments involving long exposure times, the stripping film technique is preferable.

WATER-SOLUBLE AUTORADIOGRAPHY

The requirements that a technique of water-soluble autoradiography has to fulfill are: (1) retention of all labeled materials, (2) no movement by diffusion of the labeled material before or during exposure, (3) resolving power, sensitivity, ease of preparing autoradiographs, and other features should be similar to that of the standard techniques.

It cannot be assumed that all labeled material is retained in a technique which involves washing of cells to remove labeled medium. Experiments [21] have shown that molecules the size of thymidine can diffuse in cells with a velocity of the order of 2 μ per second and therefore washing of cells to remove labeled precursor adhering to the surface can probably not be done without incurring a serious risk of removing water-soluble precursor from the cells. Smearing and squashing techniques when labeled medium might still adhere to the cells are not to be recom-

mended. Similarly, redistribution of soluble labeled material may take place in the interval between killing an animal and the setting up of autoradiographs as well as by diffusion during the exposure. Until more quantitative data are available, techniques of water-soluble autoradiography should be designed in such a way that the danger of diffusion of soluble material is at a minimum.

Various techniques of water-soluble autoradiography have been designed. After freezing and drying, labeled sections were used in an apposition technique [13, 15, 26]. To avoid the disadvantage of separating the section and the autoradiographs, various ways of attaching freeze-dried and embedded sections to the emulsion were tried [6, 8, 11, 12, 25, 30, 31]. Frozen sections cut on a freezing microtome [19, 32] or in a cryostat [11, 15, 27–29] were used, but the problem of attaching a frozen section securely to the emulsion without thawing had remained unsolved.

Recently a simple technique which seems to solve the outstanding problems has been designed [1]. Small pieces of labeled material are placed on an aluminum strip and plunged into isopentane cooled with liquid nitrogen, then slowly warmed up to the temperature of solid CO_2 and kept at that temperature.

Pieces of Kodak AR.10 stripping film floated out on distilled water at 21–23°C and No. 1 cover slips (2 by 7/8 inches) subbed with glycerine–albumin are coated in such a way that the emulsion faces outward. After drying, the coated cover slips are cooled to —5°C before use.

Frozen blocks are slowly brought to the temperature of a Pearse cryostat (—25 to —30°C) and the blocks are mounted and sections cut with normal room lighting. When the sectioning is satisfactory the full light is switched off and a darklight (Wratten No. 1) is placed in such a way that a section can clearly be seen on the knife in reflected light. A cover slip coated with stripping film, hitherto kept in a light-tight box, is touched against the section; in this way the section adheres to the emulsion. These preparations are then kept at a temperature of —25 to —35°C for photographic exposure.

Before photographic processing the preparations are fixed in 5 per cent acetic acid alcohol for 1 minute or methanol for 10 minutes. After thorough washing, photographic processing is carried out in the usual way. Since the sections are not covered by film, staining is even easier than for autoradiographs of embedded sections; afterward the preparations are mounted with Euparal on a normal microscope slide.

The technique was found easy to manipulate. The sections adhere securely to the emulsion and neither shifting nor chemical artifacts have been observed. Since the labeled material is kept well below freezing from the moment of plunging into isopentane at a temperature of

—155°C, loss of water-soluble material can be excluded. No evidence of redistribution by more than a few microns due to diffusion in the solid has been found with ^{3}H-thymidine or $^{22}NaCl$. Some rigorous experiments to determine the accuracy of localization are planned.

The loss of photographic sensitivity at low temperatures was measured by exposing AR.10 stripping film mounted as for water-soluble autoradiography to the radiation of ^{14}C-labeled standard sources. It can be seen from Fig. 2 that at the temperature of solid CO_2 the loss is approximately 30 per cent as compared with exposure at 4°C.

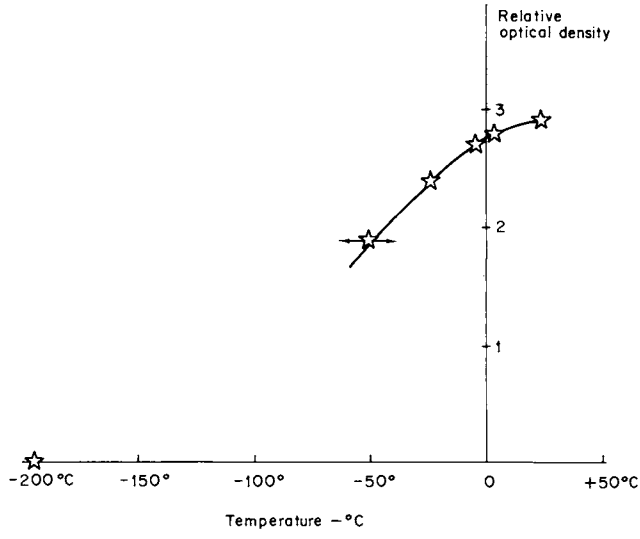

FIG. 2. Variation of film sensitivity with exposure temperature.

The distribution of ^{3}H-thymidine 2 minutes after intravenous and intraperitoneal injection is shown in Figs. 3 and 4. It can be seen that after intravenous injection thymidine is found in equal concentration in smooth muscle and epithelium, whereas after intraperitoneal injection thymidine diffuses across the smooth muscle into the epithelium with a velocity of the order of 2 μ per second. Grain counts show a higher concentration of ^{3}H-thymidine in the muscle for a considerable proportion of the time of availability of this precursor. Therefore grain counts of labeled deoxyribonucleic acid (DNA) are subject to corrections which will have to be based on quantitative counts of the distribution of ^{3}H-thymidine at various times after injection. Our observations also show that ^{3}H-thymidine is available to all cells and nuclei and therefore cannot in itself be regarded as stimulating incorporation into DNA.

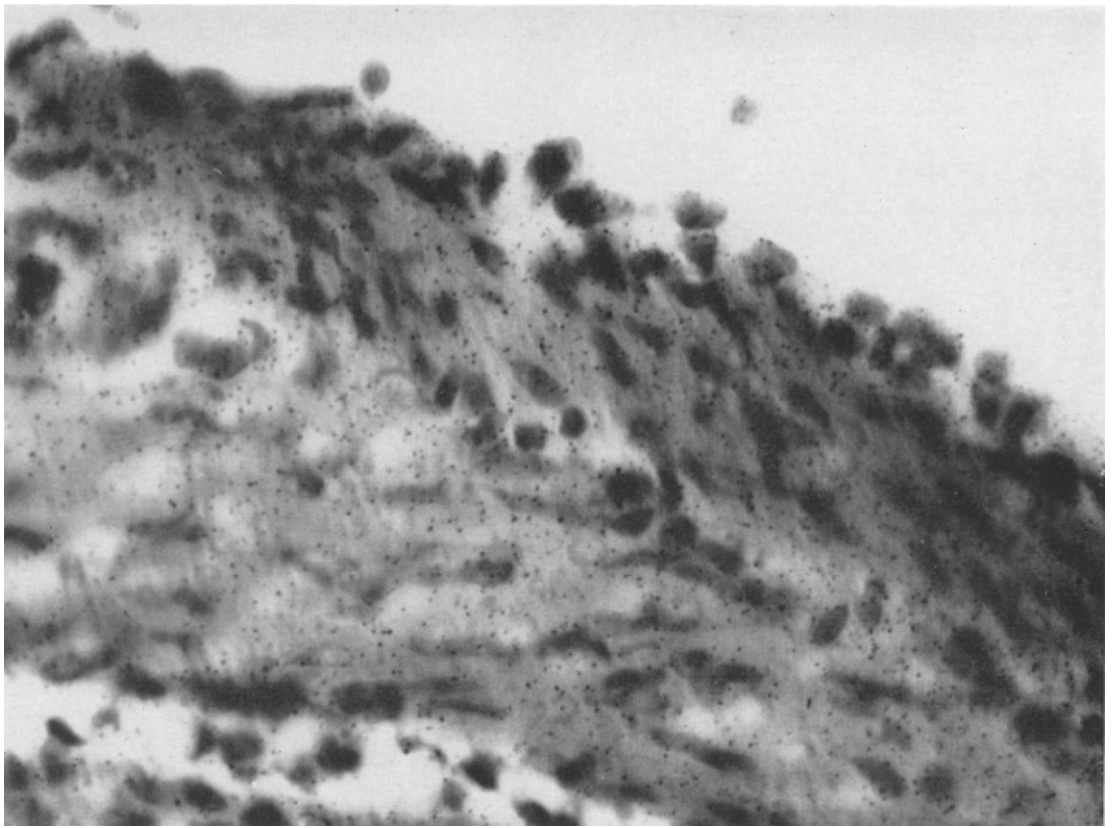

FIG. 3. ^{3}H-Thymidine in smooth muscle of the colon 2 minutes after intravenous injection. The labeling is uniform throughout the muscle. Hematoxylin and eosin stain. Magnification: × 700.

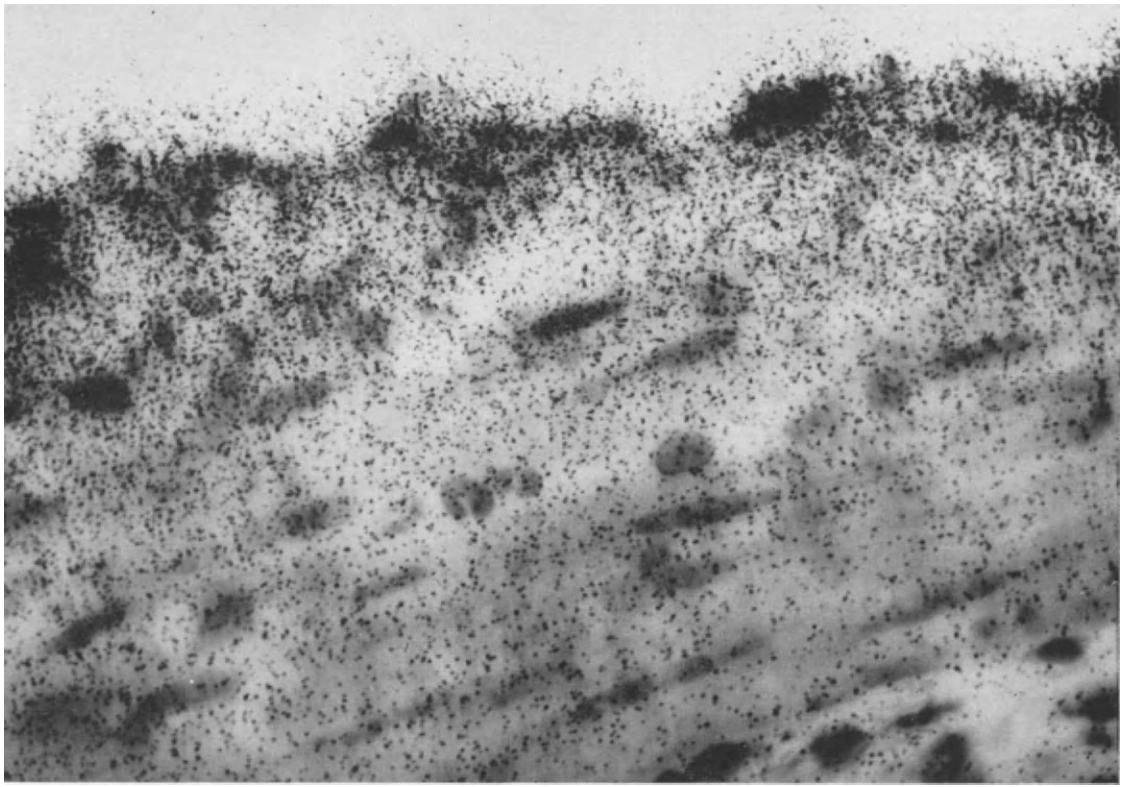

FIG. 4. ^{3}H-Thymidine in smooth muscle 2 minutes after intraperitoneal injection. The thymidine can be seen diffusing in from the peritoneal fluid bathing the outside of the gut; the diffusion seems to be uniform through nuclei or muscle fibers. Hematoxylin and eosin stain. Magnification: × 700.

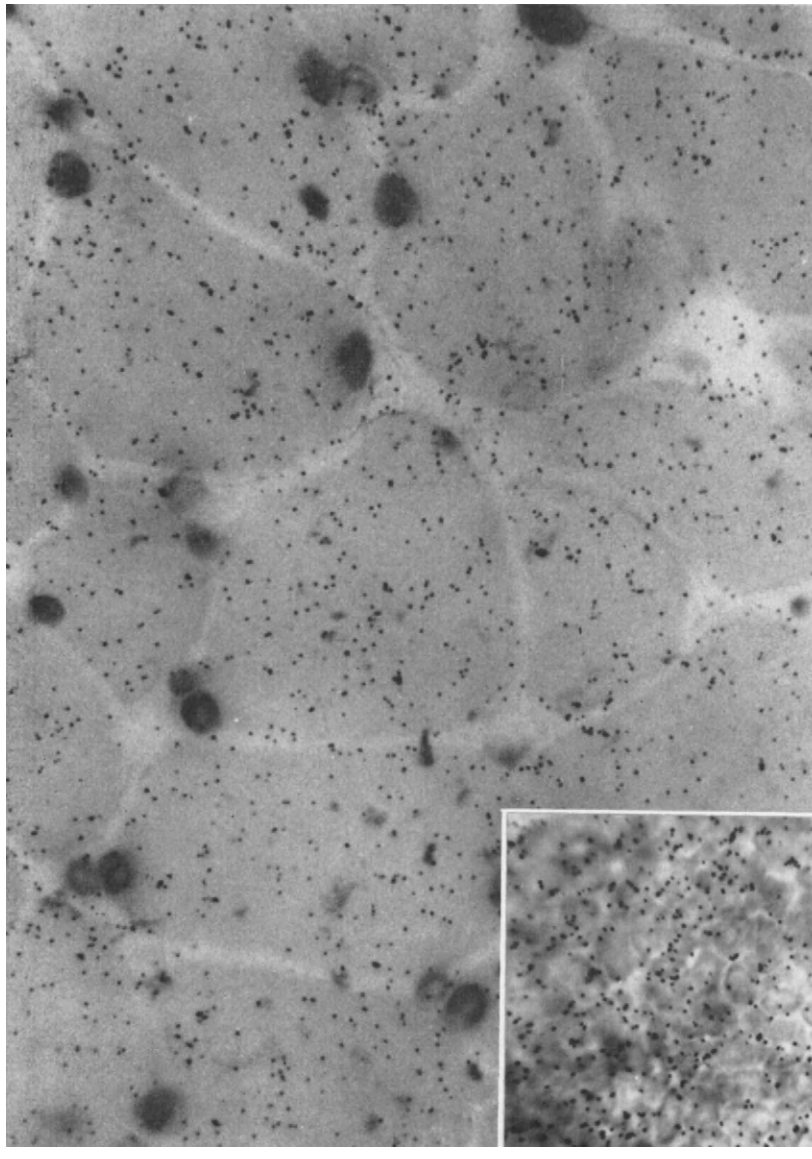

FIG. 5. Transverse section through skeletal muscle of a mouse injected with 50 μc $^{22}NaCl$ as isotonic saline, and killed 1 hour later. The insert shows a section of a blood clot taken from the same animal. The magnification of both photographs is the same: × 950.

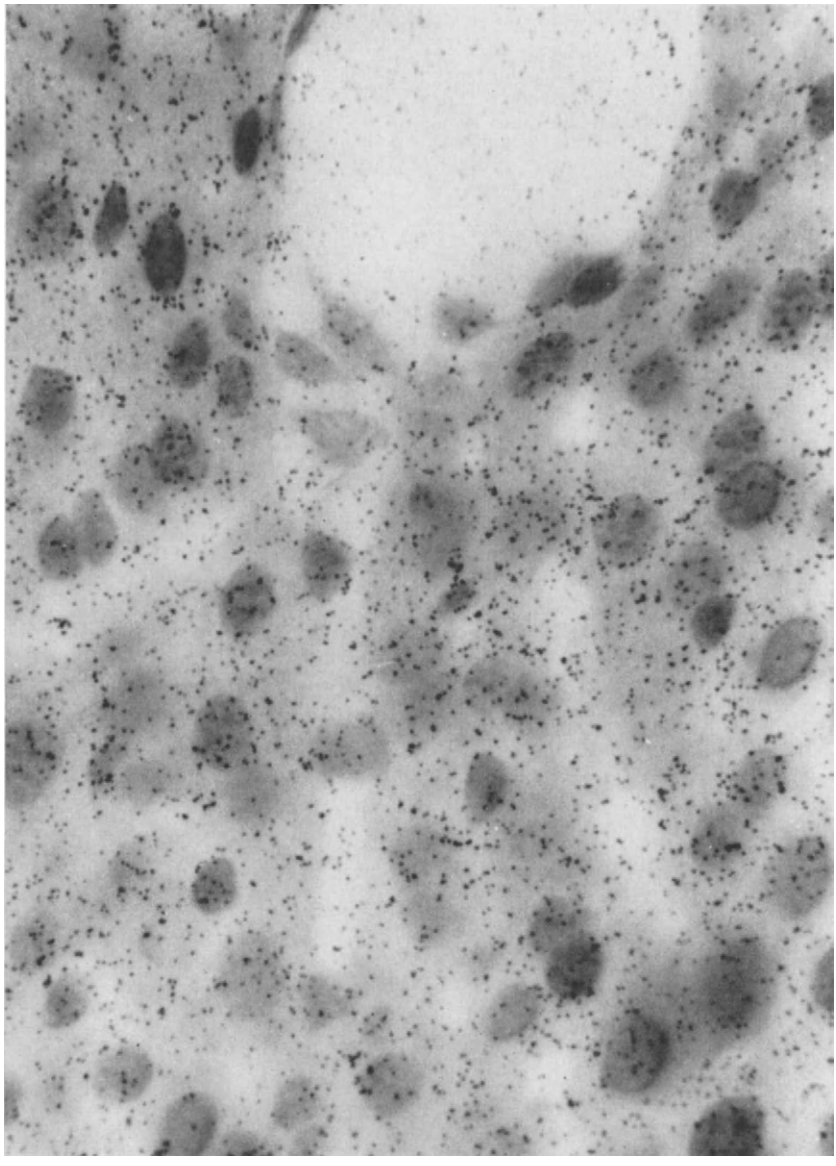

FIG. 6. Section of liver from a mouse killed 1 hour after injection of $^{22}NaCl$. A section through a blood vessel is seen at the top of the print. The level of $^{22}NaCl$ in tissue is approximately equal to that in blood—the grains over the blood vessel are slightly out of focus. Hematoxylin stain. Magnification: × 950.

Experiments on the distribution of $^{22}NaCl$ in animals (Figs. 5 and 6) gave the surprising result that the concentration of ^{22}Na in blood is only approximately twice that in the cells of muscle or liver instead of the expected factor of approximately six. Further work on the distribution of ^{22}Na is in progress.

SUMMARY

The evolution of current techniques of light microscope autoradiography is discussed together with factors that affect their sensitivity, resolving power, and suitability to varying conditions. New evidence on the effect of temperature on sensitivity and latent image fading of stripping film emulsions is presented. The development of techniques of autoradiography suitable for use with soluble compounds is reviewed and a new method is described which fulfills the basic requirements. Results obtained using this technique are illustrated and reveal the need for more extensive work in this field.

REFERENCES

1. Appleton, T. C., *J. Roy. Microscop. Soc.* **83**, 277 (1964).
2. Baserga, R., and Nemeroff, K., *Stain Technol.* **37**, 21 (1962).
3. Bélanger, L. F., *Anat. Record* **107**, 149 (1950).
4. Bélanger, L. F., and Leblond, C. P., *J. Endocrinol.* **39**, 8 (1946).
5. Boyd, G. A., and Levi, H., *Science* **111**, 68 (1950).
6. Branton, D., and Jacobson, L., *Stain Technol.* **37**, 239 (1962).
7. Doniach, I., and Pelc, S. R., *Brit. J. Radiol.* **23**, 184 (1950).
8. Edwards, L. C., and Udupa, K. N. *J. Biophys. Biochem. Cytol.* **3**, 757 (1957).
9. Endicott, K. M., and Yagoda, H., *Proc. Soc. Exp. Biol. Med.* **64**, 170 (1947).
10. Ficq, A., *Compt. Rend.* **233**, 1684 (1951).
11. Fitzgerald, P. J., *J. Histochem. Cytochem.* **9**, 598 (1961).
12. Gallimore, J. C., Bauer, E. C., and Boyd, G., *Stain Technol.* **29**, 95 (1954).
13. Holt, M. W., Cowing, R. F., and Warren, S., *Science* **110**, 328 (1949).
14. Howard, A., and Pelc, S. R., *Exptl. Cell Res.* **2**, 178 (1951).
15. Huang, T., *Intern. J. Appl. Radiation Isotopes* **8**, 234 (1960).
16. Joftes, D. L., *Lab. Invest.* **8**, 131 (1959).
17. Lamerton, L. F., and Harriss, E. B., *J. Phot. Sci.* **2**, 135 (1954).
18. Lord, B. I., *J. Phot. Sci.* **11**, 342 (1963).
19. Oster, H., Kundt, H., and Taugner, R., *Arch. Exptl. Pathol. Pharmakol.* **224**, 476 (1955).
20. Pelc, S. R., *Nature* **160**, 749 (1947).
21. Pelc, S. R., and Appleton, T. C., *Nature* **205**, 1287 (1965).
22. Pelc, S. R., and Howard, A., *Exptl. Cell Res.* **10**, 549 (1956).
23. Pelc, S. R., and Spear, F. G., *Brit. J. Radiol.* **23**, 287 (1950).
24. Ray, R. C., and Stevens, G. W. W., *Brit. J. Radiol.* **26**, 362 (1953).
25. Smitherman, T. C., Debons, A. F., Dittman, J. A., and Stevens, V., *Nature* **198**, 499 (1963).
26. Stirling, C., and Chichester, C. O., *Stain Technol.* **31**, 277 (1956).
27. Stumpf, W. E., and Roth, L. J., *Stain Technol.* **39**, 219 (1964).

28. Taugner, R., and Wagenmann, V. *Arch. Exptl. Pathol. Pharmakol.* **234**, 336 (1958).
29. Taugner, R., Hole, H., Grigoleit, G., and Wagenmann, V. *Arch. Exptl. Pathol. Pharmakol.* **234**, 330 (1958).
30. Williams, A. I., *Nucleonics* 8, 10 (1951).
31. Winteringham, F. P. W., Harrison, A., and Hammond, J. H., *Nature* **165**, 149 (1950).
32. Witten, V. H., and Holstrom, V. *Lab. Invest.* **2**, 368 (1953).

Discussion

Dr. Fitzgerald: With regard to locating diffusible substances by your technique, Dr. Pelc, how sure can you be that the ^{22}Na is not diffusing out of cells or vessels, particularly if freezing in liquid nitrogen destroys membranes? This is what worried me when we found ^{3}H-histamine all over stomach muscles and mucosa. I would also worry about preferential adsorption as an artifact, like the notorious supposed nuclear localization of alkaline phosphatase. I am afraid it would take many types of controls to satisfy these questions.

Dr. Pelc: These possibilities are under investigation.

Dr. Salpeter: You mentioned today that grains smaller than 0.1 μ (1000 Å) may no longer be sensitive to radiation from tritium. I recall that at a meeting of the Royal Microscopical Society in 1963 you gave the value of 0.01 μ (100 Å) (*J. Roy. Microscop. Soc.* 1963, **81**, 131). My own experience with the Kodak NTE emulsion (silver halide crystal size about 500 Å), which is still quite sensitive to tritium, would indicate that your earlier value may be closer to being the true one.

Dr. Pelc: The theoretical value of 0.01 μ was based on the assumption that an absorbed energy of 3 eV was needed to release one electron into the silver-bromide crystal lattice, as in the case of the photoelectric effect of visible light. It is now known, however, that in air one ion pair is formed when approximately 32 eV of ionizing radiation has been absorbed. I have not been able to find any values for silver-bromide, but it is likely that the higher value will apply, hence the new estimate of 0.1 μ. These are averages and it is quite likely that emulsions with smaller grains could be used; the sensitivity might be considerably lower.

Dr. Leblond: The comparison between stripping film technique and liquid emulsion technique (referred to as coating or dipping technique) should be made using the AR-10 stripping film and the Kodak NTB2 emulsion, respectively, since they are the two most widely utilized in actual practice.

With regard to *sensitivity*, Dr. Beatrix Kopriwa counted grains per unit area over ^{3}H-labeled liver sections coated with NTB2 or NTB liquid emulsion, or covered with AR-10 stripping film; the relative numbers of grains were found to be about 1, 0.4, and 0.5, respectively. Hence, the NTB2 emulsion was about twice as sensitive as the AR-10 stripping film. On the other hand, the NTB emulsion had a lesser "sensitivity" than the stripping film emulsion, in confirmation of the results of Baserga and Nemeroff, quoted by Dr. Pelc.

Besides being highly sensitive, the NTB2 emulsion has the advantage of having larger grains, more easily countable than those of the stripping film emulsion.

As for speed, up to 200 slides per hour can be coated with liquid emulsion as against 40 to 50 by the stripping technique.

Finally, under the conditions indicated in an article (*J. Histochem. Cytochem.* 1962, **10**, 269), it is possible to obtain an even layer of emulsion (about 2 μ thick) with the NTB2 emulsion.

DR. KOPRIWA: *Fading* of the latent image does not occur under certain conditions. Thus, we have investigated the increase of reaction intensity with exposure time using Kodak NTB2 emulsion. We used unstained ^3H-containing liver sections developed every 40 days over a 360-day period. The results showed a proportional increase in the number of silver grains up to the end of the 1-year period, provided the drying agent in the exposure box was changed every month. From these results (demonstrated in Figs. 15 and 16 of an article in *J. Histochem. Cytochem.* 1962, **10**, 280), it was concluded that no fading took place.

There are indications, however, that the mode of fixation, the nature of the organ, and prestaining, influence fading, whatever the radioautographic technique used.

DR. PELC: Dr. Lord (Lord, B. I., *J. Phot. Sci.* 1963, **11**, 342) found for the dipping technique, using Ilford K5 and 5 weeks exposure, fading of 28% with a drying agent and of 52% without. Using Gevaert 7.15, the effect of the drying agent was reversed, fading amounting to 34% without and to 45% with silica gel. Since Kopriwa and Leblond found no fading with a drying agent, we have to conclude that something else affects the performance of photographic emulsions and more research seems indicated into fading when the dipping technique is used. As reported in my paper, fading is no problem with stripping film.

DR. CARNEIRO: In my experience, humidity is a much more important factor in latent image fading than is the presence of air during exposure. Exposing AR-10 stripping film under dry atmosphere, we found about the same number of grains as we found under dry CO_2, with ^3H-label exposed for 1 month at 4°C. So we have continued exposing our radioautographs under dry air atmosphere at 4°C.

DR. GREULICH: The Southern California climate is sufficiently dry so that artificial humidity control is not required. Radioautographs exposed with Drierite (one charge only, no changes) at 4°C are without appreciable image fading for over 8 months.

The problem of background was investigated in my laboratory. The use of a safe light has been discontinued, with significant decrease in background (NTB2 liquid emulsion, normal routine; backgrounds 6–8 grains/1000 μ^2).

DR. CARNEIRO: Regarding the safe light arrangement, we use a foot switch, turning on the safe light only when needed. Most of the time we work in total darkness.

DR. PRESCOTT: Fluorescent lights give an afterglow for at least 30 minutes and can contribute to general background fogging. Hence, they should not be used in darkrooms.

DR. GREULICH: I discontinued use of NTB3 emulsion about 3 years ago, since results obtained were variable, and artifacts (such as linear deposition of grains along tissue interfaces) were present too frequently. NTB2 is far more reliable. What is the experience of others in the audience?

DR. EVERETT: Our experience in recent months is the same as that of Dr. Greulich. Many batches of NTB3 emulsion, when received, have high background regardless of how they were shipped. Eastman Kodak informs us that our laboratory is the only one having trouble with the emulsion.

DR. PRESCOTT: All users of radioautographic emulsions should be encouraged to be severe in their demand for the highest quality in emulsion; especially the receipt of high background emulsion should not be tolerated and should be regularly followed by complaint and rejection of the material.

ASSESSMENT OF TECHNICAL STEPS IN ELECTRON MICROSCOPE AUTORADIOGRAPHY[1]

M. M. SALPETER AND L. BACHMANN

Laboratory of Electron Microscopy, Department of Engineering Physics and Materials Science, Cornell University, Ithaca, New York, and The Institute for Physical Chemistry, University of Innsbruck, Innsbruck, Austria

INTRODUCTION

It is very difficult at this stage of rapid development in electron microscope autoradiographic techniques to give a full assessment of such procedures. We would therefore like to limit this paper first to a description of the primary aims in specimen preparation and then to a discussion of only some of the proposed procedures for obtaining them.

AIMS

Resolution

One of the primary aims of electron microscope autoradiography is resolution or accuracy in locating the source of radiation within a specimen. One endeavors to control simultaneously the two independent factors that tend to limit this resolution, the photographic process, and the source detector geometry.

Photographic Process

When an electron hits a silver halide crystal, a latent image may form anywhere within that crystal. During development, a silver grain grows, retaining some contact with the latent image. Very little is known as yet about the growth of such developed silver grains around small silver halide crystals. For the present, therefore, we will assume a random growth. Figure 1 shows such a hypothetical situation. The midpoint of a developed grain can be, at a maximum, one half the diameter of the developed grain away from the latent image, which can, again at a maximum, be the whole diameter of the silver halide crystal away from

[1] This investigation was supported by United States Public Health Service Research Grant GM10422 from The Division of General Medical Sciences; and a Career Development Award NB-K3-3788, to M. M. Salpeter from The Division of Neurological Diseases and Blindness.

the place where the crystal was hit by the electron. Thus the largest error inherent in the photographic process is

$$X_{\max} = a + \tfrac{1}{2} b$$

(where a is the diameter of the undeveloped silver halide crystal and b is the diameter of the smallest circumscribed circle around the developed

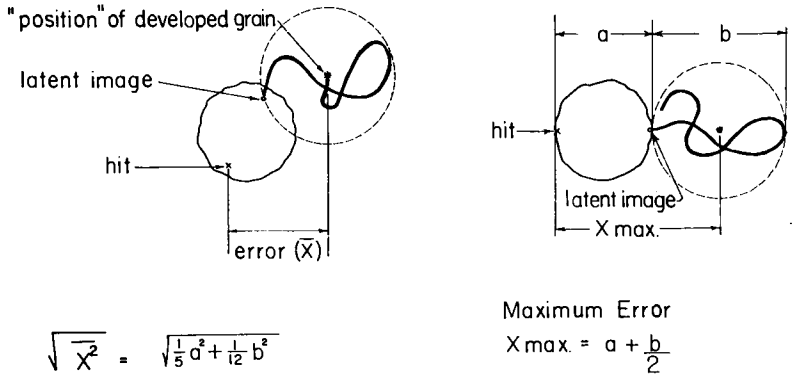

$$\sqrt{\overline{X^2}} = \sqrt{\tfrac{1}{5}a^2 + \tfrac{1}{12}b^2}$$

FIG. 1. Error due to photographic process; a is diameter of silver halide crystal; b is diameter of silver grain.

silver grain). On the average, of course, this error is much less and can be calculated to be more like

$$\overline{X} = \sqrt{\frac{a^2}{5} + \frac{b^2}{12}}$$

We see that very little can be gained by making the developed grain much smaller than the silver halide crystal. Furthermore, there is some indication that the developed grain may not grow in a completely random fashion but may cling more closely to the silver halide crystal, thereby decreasing the importance of the developed grain size still further. The over-all conclusion one can draw, therefore, is that in order to decrease the error due to the photographic process one requires small silver halide crystals and small developed grains, the undeveloped silver halide crystal size being the more important of the two. Table I contains information on photographic resolving power for the Kodak NTE and Ilford L4 emulsions with different developing procedures.

Source-Detector Geometry

The second factor, the source-detector geometry, can be discussed briefly in relation to Fig. 2. Here we have a point source (x) at a distance

TABLE I. *Photographic Resolving Power and Sensitivity for Various Emulsion-Developer Combinations*[a]

Emulsion	Developer	*a*	*b*	X_{max}	$\overline{X}$	Sensitivity[b]
Ilford L4	Microdol X	1000–1600	2000–4000	2500	900	1/12
	p-Phenylenediamine	1000–1600	400–700	1500	600	1/12
Kodak NTE (centrifuged)	Dektol	300–550	800–1500	1000	400	1/12
	Dektol preceded by gold latensification	300–550	800–1500	1000	400	1/4
	Elon-ascorbic acid preceded by gold latensification	300–550	400–600	700	300	1/3

[a] Table headings: *a:* diameter of silver halide crystal (see Figs. 6–9); *b:* size of developed grain (see Figs. 10–14); X_{max}: maximum error due to photographic process; $\overline{X}$: root mean square error. All dimensions in A units. The sensitivity for 10 keV electrons is given as the ratio of the number of developed grains to the number of electrons with which the emulsion was irradiated.

[b] Note added in proof: Recent tests indicate that the currently supplied commercial batches of Kodak NTE have a sensitivity lower, by approximately a factor of two, than those quoted here.

d from a plane. If there is no scattering in the intervening material, the number of electrons crossing the plane per unit area will decrease with horizontal distance from the source as $\cos^3 \theta$ (increment in solid angle divided by increment in area of plane). If we consider the plane at the lower surface of an emulsion layer which overlays a thin biological section, then $\cos^3 \theta$ describes the density distribution of electrons hitting the emulsion, and at least roughly approximates the density distribution of developed grains[2] (Fig. 2b). The horizontal distance from source (r)

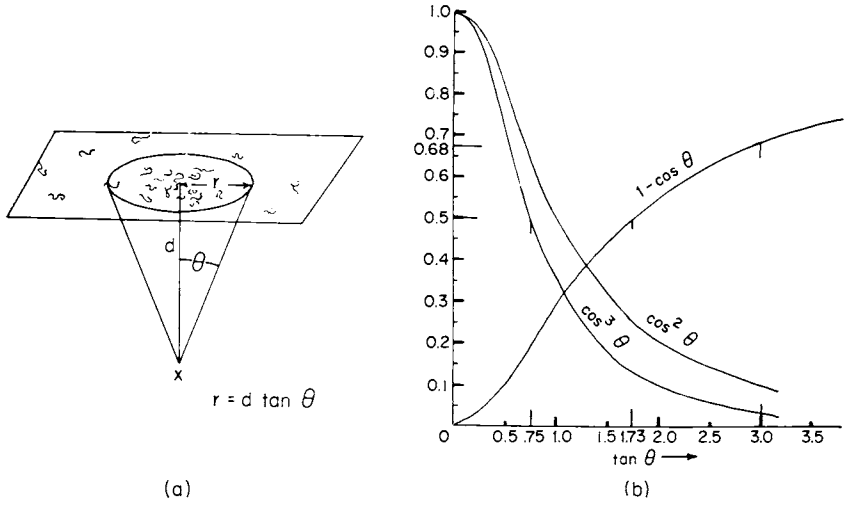

FIG. 2. Error due to distance from source to detector. (a) Schematic of radioactive source x at a distance d from a plane. (b) Graph ($\cos^3\theta$)—density distribution of electrons crossing the plane per unit area around the point source; graph ($\cos^3\theta$ and $\cos^2\theta$)—density distribution of developed grains around the point source; graph ($1-\cos\theta$)—relative numbers of electrons crossing the plane within circles of increasing area.

at which an electron hits the plane (that distance on which the geometric error depends), is directly proportional to d (Fig. 2a). In fact $r = d \tan \theta$ (θ being the angle between the vertical and the direction in which the electron leaves the source). Therefore, given d, one can determine from

[2] $\cos^3\theta$ approximates the density distribution of developed grains only if there is considerable scattering in the emulsion, since in such cases the path of the electron inside the emulsion is independent of its angle of incidence. This would be the case in emulsion layers above 400 Å with radiation energies of tritium (average 6 keV). In certain cases where there is very little scattering in the emulsion, such as with very thin emulsion layers $<$ 400 Å, or with higher energy radiation, the density distribution of developed grains would be closer to $\cos^2\theta$ (Fig. 2).

a graph of $\cos^3 \theta$ plotted against $\tan \theta$ or $\frac{r}{d}$ (Fig. 2b) at what horizontal distance from the source the grain density falls to any desired fraction of its value over the source.

The tendency to discuss resolution in terms of density distribution is a carry-over from optical autoradiography. Since sampling is usually small in electron microscope autoradiography, a more useful way of discussing the geometric error may be to consider the radius (r) of a horizontal circle above a point source within which a certain percentage of the total electrons fall. If we consider only the electrons emitted into the upper hemisphere, the fraction of these electrons leaving the source within a cone of half angle θ is $(1 - \cos \theta)$. [This is the ratio of the solid angle $2\pi(1 - \cos \theta)$ for the cone, to the solid angle 2π for the hemisphere.] They cross the emulsion plane within the circle of radius $r = d \tan \theta$. Therefore, from a plot of $(1 - \cos \theta)$ against $\tan \theta$ (Fig. 2b), we see that half the electrons emanating from the source hit the emulsion within a circle whose radius is 1.7 d, and two-thirds of the electrons within a circle of radius 3 d.

Whatever our preferred way of considering the geometric error, we see that it is directly linearly proportional to d, the source-detector distance.

To calculate the geometric error for an actual autoradiogram, one therefore has first to determine d. Figure 2a is an oversimplification since d in autoradiography is not just the distance from the source to the underside of the emulsion but really the distance from the source to the place of formation of the latent image—a distance which is impossible to obtain accurately. Approximately, however, d includes: (a) one-half the section thickness (since the radioactive source is on the average in the middle of the section), (b) the whole thickness of any intervening material between section and emulsion, and (c) in a much more complicated way some fraction of the emulsion thickness depending on the amount of scattering within the emulsion.[3] With emulsion layers currently used—i.e., 600–1300 Å—and with radiation from tritium, a compromise value for d of the emulsion can be $t_e/3$ (t_e being emulsion thickness). The total autoradiographic d would then be $t_s/2 + t_i/1 + t_e/3$ (t_s being section thickness, and t_i thickness of any intervening material between the section and the emulsion). Primarily, then, to decrease the geometric error one must decrease the specimen thickness (source-detector distance), the

[3] In cases of little scattering the value approaches 1/2 emulsion thickness, but beyond a certain thickness (i.e., approximately 400 Å for tritium radiation) the emulsion contributes a progressively smaller percentage to the total d [2].

section thickness being more important than emulsion thickness in this respect.

It is important to emphasize that since both errors which limit resolution—that due to the photographic process (E_p) and that due to geometry (E_g)—vary independently of each other, the total error (root mean square error E_t) is not a simple sum of the two, but rather the square root of the sum of their squares:

$$E_t = \sqrt{E_g^2 + E_p^2}$$

Therefore, if either error is much larger it will become dominant and little can be gained by improving the other.

Sensitivity

Technically the opposite side of the coin to resolution is sensitivity. Ideally one wants to detect every electron emitted. As sections become thinner this becomes increasingly more important. As emulsions with progressively smaller grains become available one may reach theoretically limiting sizes for the formation of the latent image. As long as one is above that limit, the primary problem in technique is that of obtaining maximum developability.

Contrast

Another problem to be solved when striving for increased resolution via thinner sections is that of enhancing the notoriously low contrast of autoradiographic specimens.

Quantitation

Finally, one would like to have a way of quantitatively evaluating electron microscope autoradiographic results. For that purpose emulsion thickness and silver halide crystal distribution as well as section thickness must be known.

PROCEDURES

Emulsion Layers

Since uniform and controlled emulsion layers are important for quantitative work, for optimum sensitivity, and for resolution, a good deal of attention has been focused on their formation. Several methods have been proposed for producing emulsion layers for autoradiography. These include dipping specimens in diluted liquid emulsion or dropping this emulsion onto the specimens [6, 7, 11, 17], centrifuging the emulsion directly onto specimen grids [5], and preforming thin layers of emulsion in metal loops [4, 12, 15] or on agar [4] before applying them to the section. One cannot prejudge these techniques. The test lies with the

resultant emulsion layer. An optimum emulsion layer for maximum resolution consists of closely packed silver halide crystals without much overlap. A gain in sensitivity can be obtained at the expense of resolution by multilayering the emulsion. Yet one loses both sensitivity and resolution by using layers in which the silver halide is not tightly packed [2, 3]. To obtain optimum layers, much depends on the coating tech-

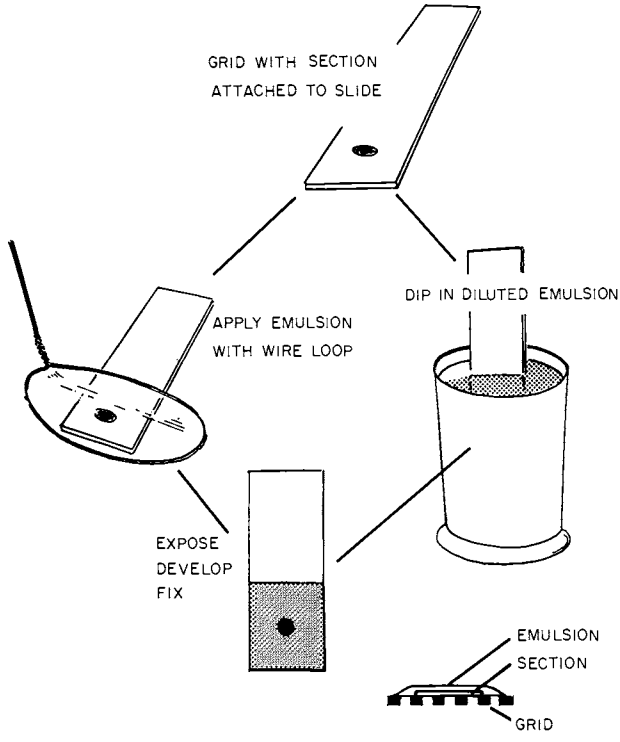

FIG. 3. Two possible procedures for applying emulsion over sections mounted on grids. Caro and VanTubergen [4] and Hay and Revel [7].

nique, on the substrate on which the emulsion is coated, and on the emulsion itself. For instance many investigators first place the section on a specimen grid and then put the emulsion over it (two typical examples are shown in Fig. 3); others have recommended placing the specimen on flat surfaces for coating [14, 17]. In our experience, coating the section while it is on a metal grid may cause trouble, especially when liquid emulsions are used, since the silver halide crystals tend to to collect at grid bars. Therefore, in cases in which sections for coating are placed on metal grids, better results are obtained when preformed

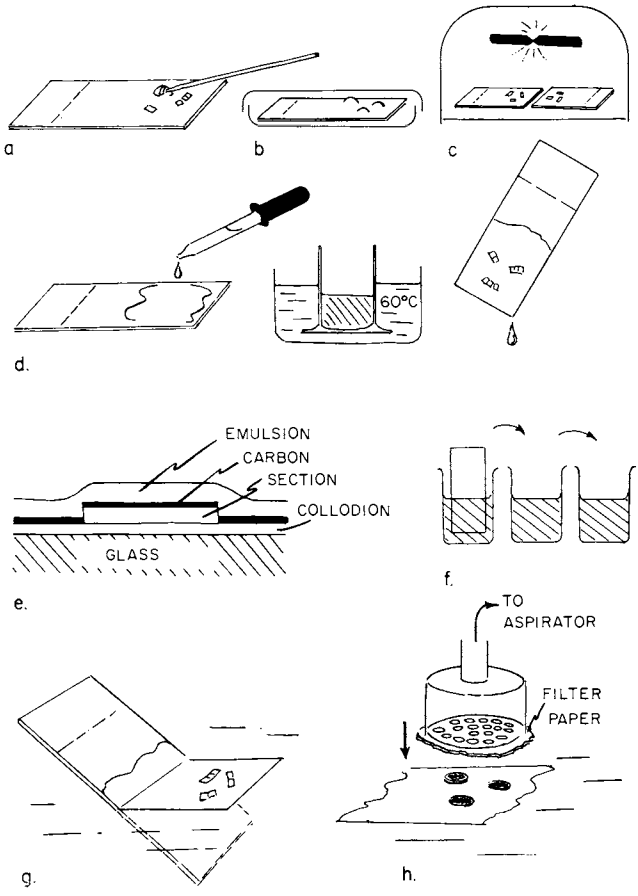

FIG. 4. Specimen preparation procedure on flat substrate [17]. (a) Ribbons of sections are placed on collodion coated slides and allowed to dry; (b) sections are stained in a tightly closed petri dish by drops of stain placed over the individual ribbons. After the staining period the stain is flushed off with distilled water; (c) the stained sections are vacuum coated with a thin layer of carbon, Union Carbide Spectroscope SPK (50 Å); (d) liquid emulsion, which is kept at 60°C, is dropped over the section and then drained and dried in a vertical position. Dipping the specimen into liquid emulsion is equally satisfactory; (e) the final specimen sandwich; (f) slides are developed in a series of beakers, with distilled water rinse between successive chemicals, the sequence being: developer, 3% acetic acid stop bath for 10 seconds, non-hardening fixer (20% sodium thiosulfate + 2.5% potassium metabisulfite) for 1 minute, three rinses in distilled water; (g) specimen sandwich is stripped onto a water surface, and grids are then placed over the tissue sections; (h) a procedure for picking up the specimen from the water surface by suction onto a moist filter paper applied over a filter plate.

emulsion layers are used. If, however, specimens are first placed on a flat surface, very uniform close-packed layers can be obtained by using either liquid or pregelled emulsion. Figure 4 shows the specimen preparation procedure recommended by us [17]. The section lies flat on a collodion-coated slide, and the thin carbon layer between it and the emulsion provides a substrate of very uniform physical properties. This procedure results in clean uniform emulsions but requires stripping the specimens off the slide after photographic processing (Fig. 4g) before they can be placed on viewing grids—an additional step in specimen preparation.

Different emulsions provide unique problems of their own. The Ilford L4 emulsion coats very nicely when gelled in metal loops. However, the finer grained emulsions such as the centrifuged Kodak NTE [17] or the Gevaert Nuc 307 [6] do not form in loops easily, and are best coated in liquid form. A flat substrate is here even more important. One way to form good monolayers using these emulsions is to keep them warm, $\sim$ 60°C, drop them onto a flat surface, and then drain and dry them at room temperature (Fig. 4d).

Another advantage of coating the emulsion while the section is mounted on a flat substrate is that it provides a criterion for evaluating the quality of a formed layer independent of the coating procedure employed.

Thin emulsion layers on glass slides show, in reflected white light, interference colors dependent on their thickness. We measured the thickness of layers having different interference colors with a Normarski interferometer [17]. Figure 5 shows these interference colors correlated with

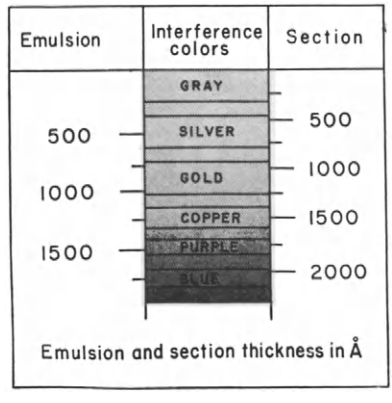

FIG. 5. Interference color—thickness scale for sections and emulsion. Interference colors of section on water and of emulsion on glass slide ([17], Table I).

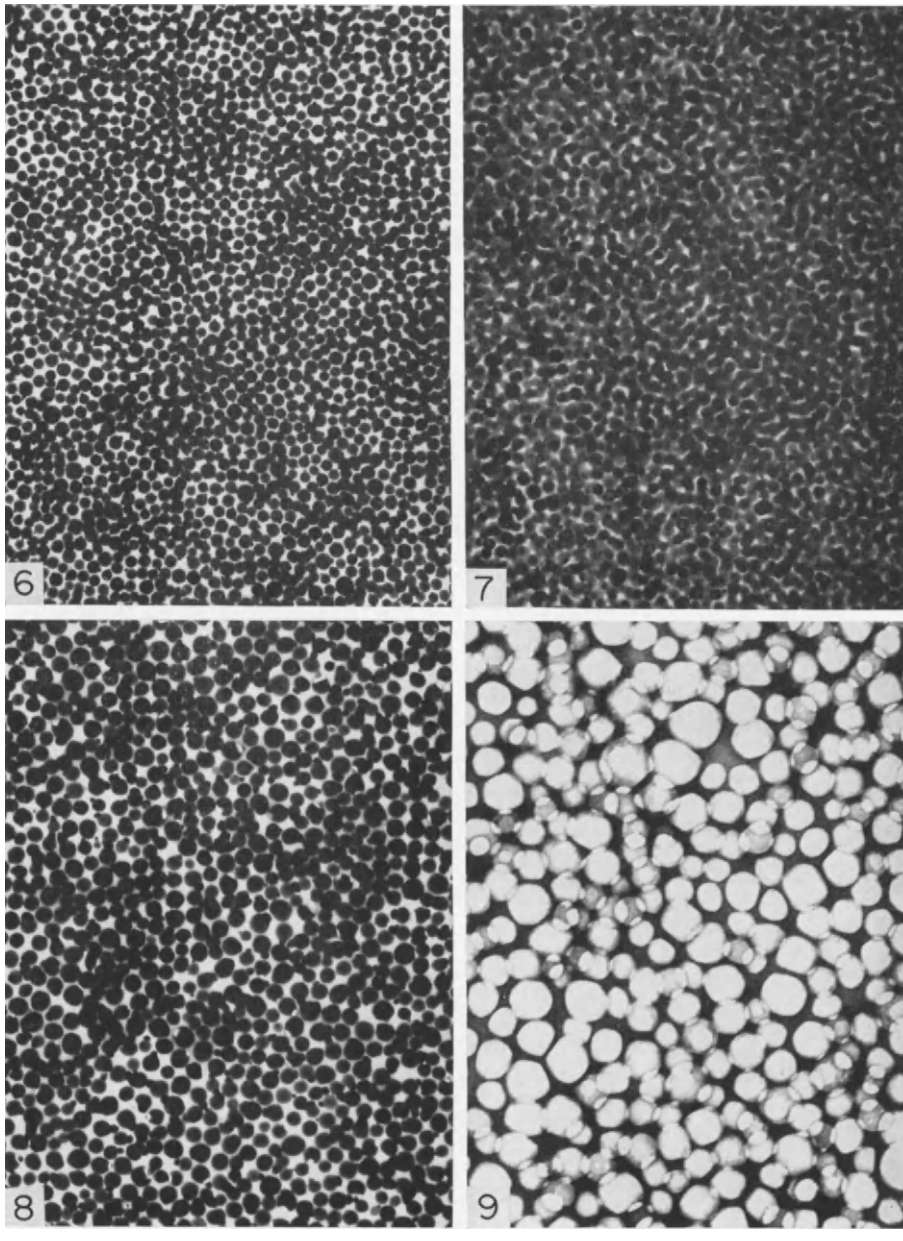

FIGS. 6–9. Emulsion layers. Magnification: 30,000 ×.

FIG. 6. Monolayer of centrifuged Kodak NTE emulsion. Interference color, silver to light gold measured thickness, 600 Å.

FIG. 7. Slightly overlapped layer of centrifuged Kodak NTE emulsion. Interference color, gold; measured thickness, 1000 Å.

measured thickness. These data have been validated for both the Ilford L4 and centrifuged Kodak NTE emulsions. We further determined by interferometry that the thickness remained constant on a microscopic level as long as the interference color remained uniform to the naked eye. When emulsion layers of different thickness were examined with the electron microscope, we found that a silver to pale gold layer of Kodak NTE (600 Å) was a monolayer (Fig. 6), and that a deep gold layer (1000 Å) already showed considerable overlap (Fig. 7). A silver to gold layer of the Gevaert Nuc 307 is a monolayer (Fig. 8) for that emulsion, and a purple layer (1300–1500 Å) is a monolayer for the Ilford L4 emulsion (Fig. 9).

The uniformity of interference color can thus be a criterion for an adequate coating procedure, and the interference color itself a criterion for emulsion thickness.

For quantitative work one has to know the exact thickness of an emulsion layer over a particular section. Interference colors can be viewed over the sections in the darkroom (yellow safe light Wratten filter OA) where they appear as density differences. A more accurate way to make this determination is available if developers are used that do not attack the silver halide crystals, such as Dektol or Elon-ascorbic acid [8]. In such cases the developing procedure can be interrupted after the specimen has been developed and stopped, but before it is finally fixed. If at that stage the slide is washed and dried, the interference colors can then be viewed in white light without introducing background. (The interference colors are not affected by the section underneath.) Fixation then follows in the usual manner.

Sensitivity

Although of considerable importance, the problem of obtaining maximum sensitivity has not received as much attention from investigators as has emulsion coating. A few years ago, at a meeting of the Royal Microscopical Society, Pelc suggested that grains as small as 100 Å may still be sensitive to radiation from tritium [13]. The Kodak NTE with a silver halide crystal size averaging 470 Å is at present the smallest

---

FIG. 8. Monolayer of Gevaert Nuc. 307 emulsion. Interference color, silver to gold. Such uniform layers of this emulsion were not obtained consistently.

FIG. 9. Monolayer of Ilford L4 emulsion. Interference color, purple; measured thickness, 1500 Å. (The emulsion gelatin was stained with phosphotungstic acid and the emulsion layer was then fixed. The images of the silver halide crystals are thus negatively stained ghosts. A close-packed monolayer of Ilford L4 is otherwise difficult to photograph without grossly disturbing the silver halide crystals due to the high beam intensity necessary for adequate illumination.)

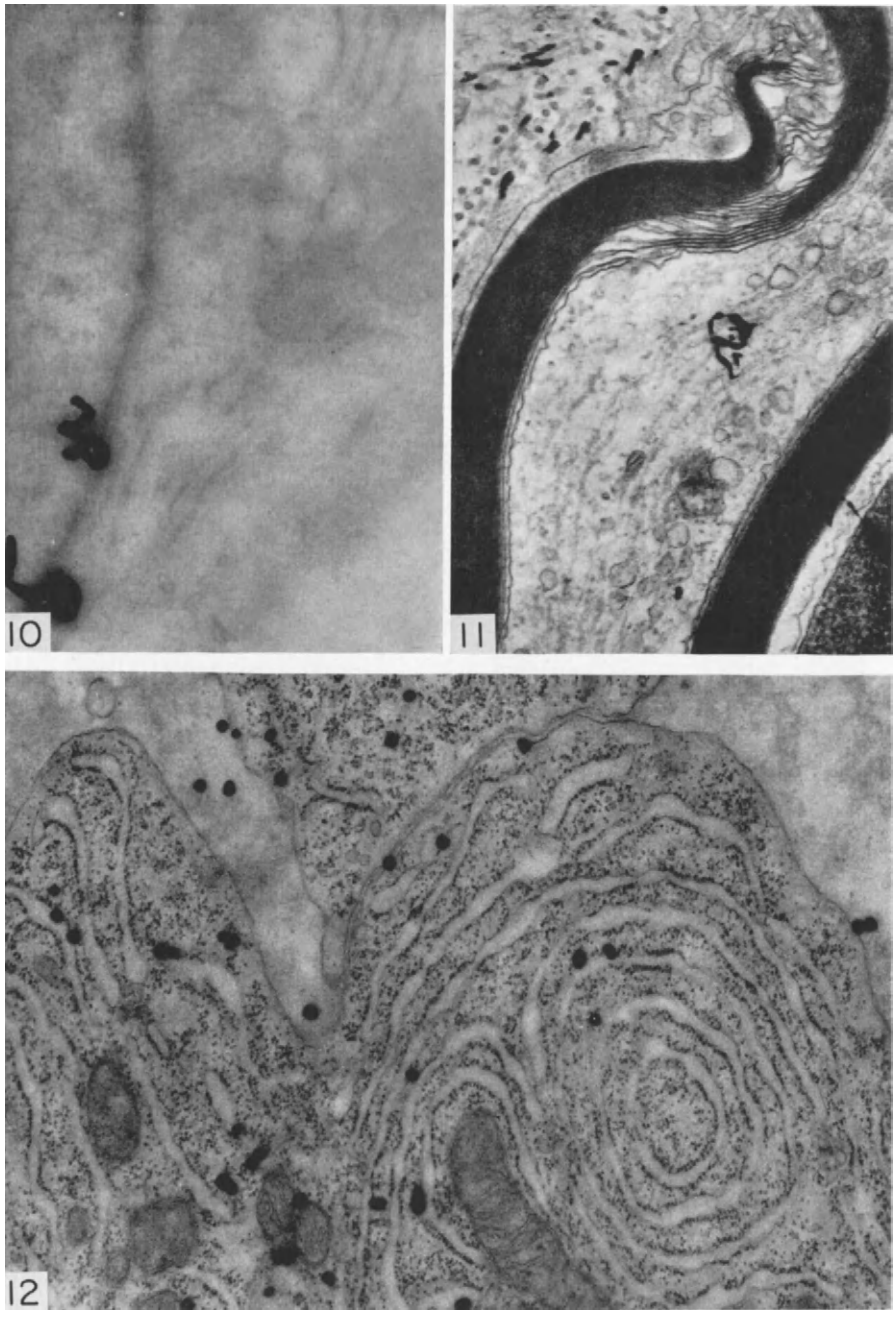

FIGS. 10–12. Autoradiograms using Ilford L4 emulsion with different embedding, staining, and developing procedures. Sections (interference color, light gold) were coated with a monolayer of Ilford L4 emulsion (emulsion interference color, purple). Approximate magnification: 30,000 ×.

grained emulsion commercially available. The very high sensitivity of this emulsion to tritium if special developing procedures are employed (Table I) indicates that Pelc's analysis was correct. We are still a long way from silver halide grains which are smaller than the theoretical limit for sensitivity to radiation of this energy.

The technical question is how to get the maximum sensitivity, i.e., the largest ratio of developed grains to electrons hitting the emulsion. (For electron microscope autoradiography this ratio is expected to stay below 1.)

There are several factors which affect sensitivity. These are evident to different extents in different emulsions and for different developing procedures. As a general rule the smaller the silver halide crystal or the smaller the developed grain desired, the more carefully one has to protect the latent image from oxidation or maybe even enhance it before development. We compared the sensitivity of the Kodak NTE and Ilford L4 emulsions using various developing and storing procedures [2, 17]. Monolayers of these two emulsions were first irradiated with low doses of 5 and 10 keV electrons. The intensity of radiation was measured with a Faraday cage. The irradiation was kept low enough to minimize the probability that any silver halide crystal was hit more than once. After development, we obtained a ratio of developed grains to electron hits (Table I). The relative sensitivities obtained were compared with data from actual autoradiograms. Data obtained from such a study are only comparative and do not represent the absolute sensitivity values to be obtained in autoradiography.

In summary our findings were: (1) Whereas no obvious latent image fading was observed in irradiated Ilford L4 layers developed by Microdol X after storage in air for as long as 2 months, the fine grained Kodak emulsion needed storage in helium to keep the latent image from fading even when coarse grained development by Dektol was used. (2) A

FIG. 10. Tissue: mesenchymatous cell of adult newt *Triturus*, labeled with ^{3}H-thymidine. Stain: section is unstained and has no carbon layer. Embedding medium: methacrylate. Development: Microdol X for 3 minutes at 24°C.

FIG. 11. Tissue: axon of peripheral nerve in the newt, *Triturus*, labeled with ^{3}H-leucine. Stain: Aqueous uranyl acetate for 5 minutes followed by lead citrate [16] for 15 minutes. Stained section was coated with a carbon layer ($\sim$ 50 Å). Embedding medium: Epon 812. Development: Microdol X for 3 minutes at 24°C. (Note dense stain deposits over collagen at upper left.)

FIG. 12. Tissue: mesenchymatous cell of the newt, *Triturus*, labeled with ^{3}H-leucine. Stain: lead cacodylate [10]. Stained section is coated with a carbon layer ($\sim$ 50 Å). Development: *p*-phenylenediamine (1.1% in 12.6% Na_2SO_3, see [1] and [4]).

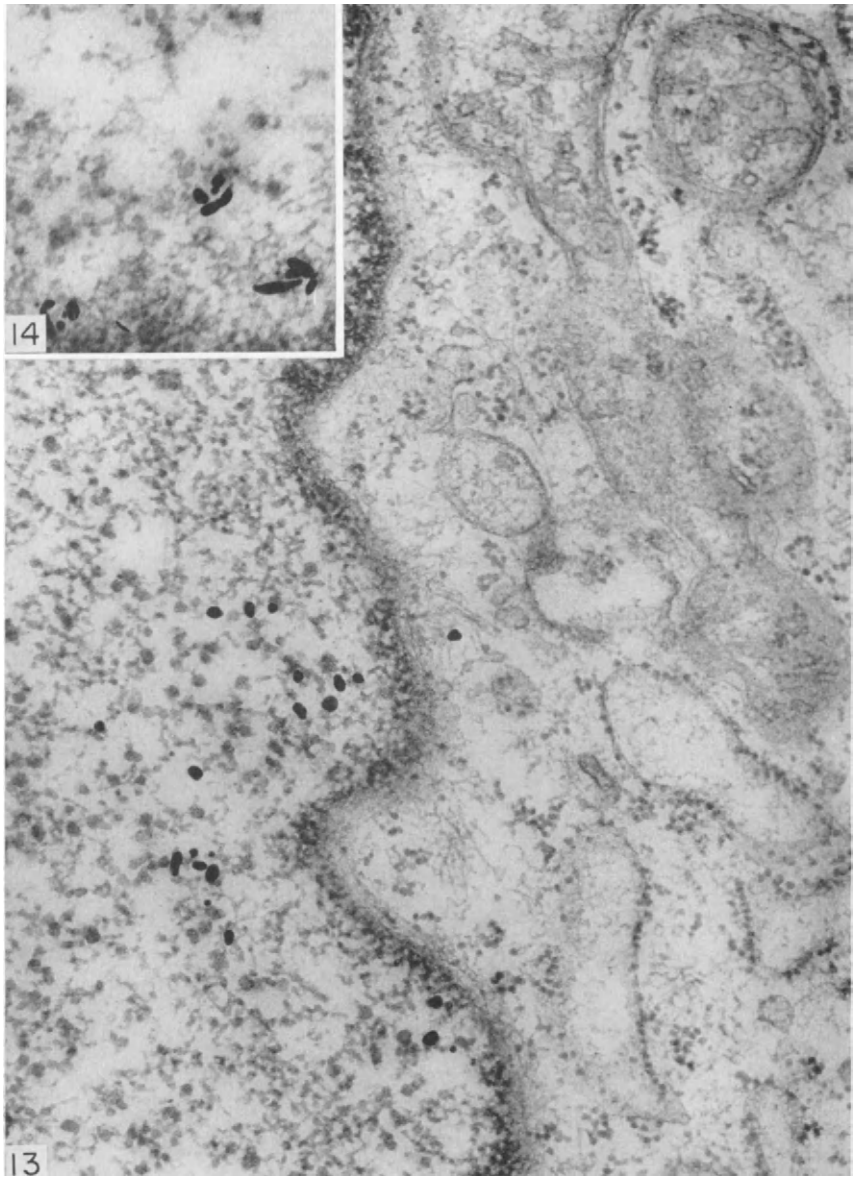

FIGS. 13 and 14. Autoradiograms using Kodak NTE emulsion. Sections (interference color-silver) were coated with a monolayer of Kodak NTE (emulsion interference color-silver). Approximate magnification 60,000 ×.

FIG. 13. Tissue: mesenchymatous cell of the newt, *Triturus*, labeled with ^{3}H-thymidine. Stain: 2% uranyl acetate for 5 minutes followed by lead citrate [16] for 10 minutes. Stained section covered with a carbon layer (~ 50 Å). Embedding medium: methacrylate. Development: gold latensification—Elon ascorbic acid [17].

FIG. 14. Tissue: same as in Fig. 13 except developed by Dektol for 1 minute at 24°C.

distinct loss of sensitivity was observed when the emulsion was in direct contact with the biological sections (tissue fixed in OsO_4). With the Ilford L4 emulsion it was most noticeable when fine grained development by *p*-phenylenediamine [4] was attempted [1]; with the Kodak emulsion it was marked even with coarse grained development by Dektol. Sensitivity can be maintained in both cases if approximately 50 Å of carbon is evaporated over the section before coating with emulsion. (3) No fine grained development of the Kodak NTE emulsion was possible without first enhancing the latent image. This can be done by "gold latensification," a process which deposits gold onto latent images before development [9, 17]. After such a procedure one can obtain small developed grains with very high sensitivity. We used an Elon-ascorbic acid developer [8]. Developed grains with this developer can range from 100 Å to over 1000 Å, depending on the developing time. Because of the difficulty of differentiating very small developed grains and also since no significant gain in over-all resolution can be expected from developed grains much smaller than the silver halide crystals (see foregoing arguments), we chose to develop for 400–500 Å grains (Fig. 13).

The actual sensitivity ratios obtained are given in Table I. Note that gold latensification enhanced sensitivity in the Kodak NTE emulsion also for Dektol development, without affecting the grain size. We expect that it should similarly affect sensitivity in other emulsions and may prove valuable in high sensitivity development of the finer grained emulsions of the future.

Contrast

Specimens prepared for electron microscope autoradiography have very low contrast unless some special manipulation is introduced to enhance it. Figure 10 shows such a typical autoradiogram in which the contrast has not been enhanced. Most procedures for enhancing contrast involve specimen manipulation—staining or gelatin removal, or both—after the photographic process is complete (for review see Caro and VanTubergen [4]). These procedures involve a risk of removing or disturbing developed grains. We have recently suggested a procedure for enhancing tissue contrast while leaving the emulsion gelatin intact [17]. This involves staining the tissue sections and then coating the stained section with a 50 Å carbon layer. The carbon protects the stain from a destaining action of the developing fluids. The resultant high contrast is independent of the emulsion or of the embedding medium used (see Figs. 11 through 14). Very thin sections can thus be used, decreasing the geometric error considerably.

A word of caution on prestaining. Prestaining may extract radioactive

compounds and for any quantitative study the sensitivity should be checked against an unstained section. Furthermore, the tissue can easily be overstained, resulting in an unpleasantly dense preparation in which the developed grains are hard to distinguish from the tissue components. In addition, the use of lead stains [10, 16] results frequently in dense deposits found over specific areas (chromatin, mitochondrial membranes, extracellular collagen, etc.) (Fig. 11). Shortening the staining period tends to minimize this effect. No explanation can be offered at the moment for this phenomenon. It may in itself prove interesting in the study of electron microscope stains. Aqueous uranyl acetate gives a clean preparation, yet of much lower contrast than that obtained with lead. The exact staining time depends on the tissue and embedding medium, of course.

It is clear that the final technique for electron microscope autoradiography has not yet been proposed. The outlook for further advances is more optimistic than a few years ago. Quantitative autoradiography with the electron microscope is not just a possibility but is in many ways easier than with the light microscope. Furthermore we know that even the smallest grained commercially available emulsion is well above the limit of sensitivity for tritium labeled compounds. Smaller grained emulsions therefore can be expected in the near future. With these emulsions will come new techniques for coating and developing. We hope that what we have so far learned about high sensitivity fine grained development and criteria for judging uniformity of emulsion thickness will prove applicable to these new procedures. Since it is obvious that errors due to the photographic process can be decreased, it is well to re-emphasize that we can fast approach a point of diminishing returns unless we can simultaneously decrease the geometric error. For instance, using the formula for total error presented earlier in this paper and assuming a constant geometric error of 900 Å, the total error would decrease as a result of decreasing the photographic error (see Table I) as depicted in the tabulation:

E_g	E_p		E_t
900	1800		2020
900	900	(Ilford L4, Microdol X developed)	1270
900	300	(Kodak NTE, Elon-ascorbic acid developed)	950
900	0		900

Progress in decreasing the photographic error enables us to invert a statement made by Pelc a few years ago [13] and state that the primary limitation in autoradiographic resolution is no longer the photographic process but comes from the geometric error primarily due to section thickness.

SUMMARY

Considerable improvements have been achieved in recent years in the technique of specimen preparation for autoradiography with the electron microscope. In this paper we outline the primary aims of such specimen preparation, describe several procedures suggested for achieving these aims, and discuss some possible advances along these lines in the future.

REFERENCES

1. Bachmann, L., and Salpeter, M. M., *Naturwissenschaften* **51**, 237 (1964).
2. Bachmann, L., and Salpeter, M. M., *in* "Symposium on Quantitative Electron Microscopy" (G. Bahr, ed.). *Lab. Invest.* Suppl. Vol. 14, p. 1041 (1965).
3. Caro, L. G., *J. Cell Biol.* **15**, 189 (1962).
4. Caro, L. G., and VanTubergen, R. P., *J. Cell Biol.* **15**, 173 (1962).
5. Dohlman, G. F., Maunsbach, A. B., Hammerstrom, L., and Applegren, L. E., *J. Ultrastruct. Res.* **10**, 293 (1964).
6. Granboulan, P., *J. Roy. Microscop. Soc.* **81**, 165 (1963).
7. Hay, E. D., and Revel, J. P., *Devel. Biol.* 7, 152 (1963).
8. Hamilton, J. F., and Brady, L. E., *J. Appl. Phys.* **30**, 1893 (1959).
9. James, T. H., *J. Colloid Sci.* 3, 447 (1948).
10. Karnovsky, M. J., *J. Biophys. Biochem. Cytol.* **11**, 729 (1961).
11. Koehler, J. K., Muhlethaler, K., and Frey-Wyssling, A., *J. Cell Biol.* **16**, 73 (1963).
12. Moses, M. J., *J. Histochem. Cytochem.* **12**, 115 (1964).
13. Pelc, S. R., *J. Roy. Microscop. Soc.* **81**, 131 (1963).
14. Pelc, S. R., Coombes, J. D., and Budd, G. C., *Exptl. Cell Res.* **24**, 192 (1961).
15. Revel, J. P., and Hay, E., *Exptl. Cell Res.* **25**, 474 (1961).
16. Reynolds, E. S., *J. Cell Biol.* 17, 208 (1963).
17. Salpeter, M. M., and Bachmann, L., *J. Cell Biol.* **22**, 469 (1964).

DISCUSSION

DR. DROZ: When silver grains are underdeveloped, the coiled grains are often broken into three or four segments, and it is an illusion to believe that the resolving power is increased in this way. Do you agree?

DR. SALPETER: I agree that a silver grain which is fragmented due to underdevelopment does not improve resolving power.

DR. GRANBOULAN: It is not clear that the discrete dots produced by underdevelopment or physical development improve resolution. *A priori*, I would think that the average distance from the point source to these dots is about the same as the distance from the point source to the center of a coiled filament.

DR. SALPETER: Whether physical development does or does not improve resolution depends primarily on the growth process of the silver grain during develop-

ment. Unfortunately, this is a process we know very little about. We have therefore had to postulate the worst possible condition, i.e., that the silver grain grows randomly as we diagrammed in Fig. 1. In such a case, the center of a fully developed grain may be as much as half the diameter of the developed grain from the site of the latent image. The center of a small physically developed grain would then be closer to the latent image and the resolution would be improved by their use. If, on the other hand, one could show that the large silver grain grows symmetrically around the latent image or around the silver halide crystal, then the grain size would not significantly alter the resolution.

We are hoping to answer this question by following the growth of developed grains in exposed dilute emulsion layers stained with phosphotungstic acid after development but before fixation. In this way, one can visualize simultaneously both the developed grain and the silver halide crystal from which it grows. Our preliminary observations indicate that a chemically developed grain may in fact cling more closely to the silver halide crystal than we postulated in Fig. 1. It is, however, too early to say for sure.

DR. ROSS: The point of location of the latent image does not necessarily provide information regarding the resolution, because the latent image is not clearly related to the course of radiation. Hence, crystal size, and the distance between the source of radiation and the emulsion, remain paramount in determining resolution.

DR. LEBLOND: What precautions must be used in prestaining for electron microscope radioautography?

DR. SALPETER: The stain should be clean, and it should be prevented from evaporating during the staining period. Lead staining can be troublesome, especially for certain tissues. In such cases, aqueous uranyl acetate or nitrate for 1–3 hours provides a somewhat lower contrast, but a much cleaner specimen.

DR. LEBLOND: How do you explain that, even though you do not extract gelatin, you obtain good visibility?

DR. SALPETER: Removing the gelatin is unnecessary for obtaining high contrast in prestained specimens since the gelatin layer is only a few hundred Å thick and is a low-density material.

DR. GRANBOULAN: In general, the finer the grains, the less drastic the necessity to remove gelatin from the sections. With Gevaert NUC 307 (grain diameter 700 Å), we can easily count the grains over the sections without removal of the gelatin. We think photographs are better after gelatin removal, although the procedure is delicate and must be adapted to each preparation by trial and error. Until now, all our published pictures have been made of sections from which the gelatin was removed, such as those in *J. Microscopie* (1962, **1**, 75).

We use our new emulsion from Kodak-France in multilayers with a large amount of gelatin on top of the grains; thus, its removal is always necessary.

DR. LEBLOND: Dr. Kopriwa, by comparing coated sections of tritium-labeled methacrylate, has observed that the Kodak NTE emulsion is much less sensitive and more difficult to use than Ilford L4 and Gevaert 307. Thus, we are not using NTE at all for routine work.

DR. GREULICH: Have you tried preparing emulsion layers on plastic rather than glass, to obtain more uniform layers?

DR. SALPETER: We have not tried plastic substrates. We use a glass slide coated with celloidin and then with carbon. This procedure provides a very uniform substrate for emulsion coating.

DR. REVEL: The technique used by our group is the one described previously

(Revel, J. P., and Hay, E. D., *Z. Zellforsch.* 1963, **61**, 110; Hay, E. D., and Revel, J. P., *Develop. Biol.* 1963, **7**, 159).

We have found that, in general, we could obtain clearer radioautograms when the emulsion was prevented from reaching the reverse of the specimen grids. The celloidin film, apart from its intrinsic value for electron microscopy, seals the holes in the grid which are not covered by sections. Each grid is checked for imperfections (holes or tears in the celloidin substrate) before use. To mount the specimen grids prior to dipping we proceed as follows: A strip of double-sided Scotch brand tape is applied to a clear glass slide, and a piece of Band Aid tape with perforations of slightly smaller diameter than the grids to be used is applied to the Scotch tape. The grids are then deposited over the perforations in the Band Aid and sealed by gentle pressure along the edge. The Band Aid adhesive is waterproof and allows the grids to be detached easily even after several months.

We do not routinely use celloidin-coated slides because we have encountered some problems in detaching the films after prolonged storage.

DR. SALPETER: We found that much more uniform emulsion layers are obtained over sections that are mounted on a celloidin-coated glass slide and then coated with a thin layer of carbon, than over sections mounted on specimen grids. Another advantage of forming emulsion layers on a glass slide-mounted specimen is that the thickness and uniformity of the emulsion can be evaluated by its interference colors. This provides a basis for quantitative electron microscope radioautography.

DR. PELC: The membrane method of electron microscope radioautography which we have designed proves to be useful and reliable (Pelc, S. R., Coombes, J. D., and Budd, G. C., *Exptl. Cell Res.* 1961, **24**, 192; Budd, G. C., and Pelc, S. R., *Stain Technol.* 1964, **39**, 295). Perspex (lucite) slides (3 inches by 1 inch) with 7 mm holes are covered with a thin layer of Formvar; a methacrylate or araldite section is placed on the Formvar film above the center of a hole and covered with liquid photographic emulsion. After exposure, the preparation is processed and stained if desired. Then the slide is inverted, a small drop of water is put through the hole onto the section, and a grid is fixed by drying. The grid is then cut out with a needle, and is ready for use. With careful handling, approximately 75% of the preparations started can finally be used.

DR. DROZ: In my laboratory, we have used the dipping technique either on grids or on celloidin-coated slides. Definitely, the quality of the radioautograph is improved by the latter technique, which allows a uniform distribution of the silver grains, and also prevents the passage of emulsion between the grid and the supporting glass.

COMPARISON OF EMULSIONS AND TECHNIQUES IN ELECTRON MICROSCOPE RADIOAUTOGRAPHY

PHILIPPE GRANBOULAN

Institut de Recherches sur le Cancer, Villejuif (Seine), France

During the past 3 years radioautography at the electron microscope level has made great progress. Already it has become an important method in cytology and has led to several very valuable investigations. However, we feel that improvements of this technique are still possible and that it has not yet fulfilled all of its promise.

The problems we deal with here can be divided into three parts: the first is theoretical; the second is practical and concerns the routine cytological technique; the third concerns the new fine grain emulsions.

THEORETICAL DATA

Three types of factors govern the effectiveness of radioautography. These are: photographic, isotopic, geometric.

With regard to the *photographic* factors, we depend entirely on the physicists and photochemists to prepare emulsions of the desired grain diameter and sensitivity.

Concerning *isotopes,* tritium electrons are the softest of all electrons emitted by any isotope and, therefore, are most frequently used in electron microscope radioautography. However, ^{14}C has also been used [5], and ^{125}I seems to be promising because of its short half-life and low-energy electrons [14, 17, 23, 30, 32].

We shall deal here only with the *geometric* factors which we can more easily control.

Let us first consider a few characteristics of emulsions:

A photographic emulsion is actually a suspension of silver halide pseudocrystals in a colloid, gelatin.

Each crystal obeys "the all-or-none law."

The smaller the diameter of the crystal, the lower the percentage of silver.

Two kinds of gelatin are present in the photographic emulsion:

a. The first, *adsorbed* onto the grain, is required for the sensitivity and the stability of the emulsion [21]. Physicists think that

this layer is a shell around the crystal about 50 Å thick [25]. If we accept this value it will play an important role in the very fine grain emulsion. For instance, if we consider an undeveloped crystal of 1500 Å in diameter, the gelatin is 7 per cent of its thickness and it is equal to 15 per cent of the cross section ($2\pi R\ dR/\pi R^2$). But if we consider a crystal of 100 Å in diameter, the thickness of the adsorbed gelatin is equal to that of the crystal, and its solid angle will be twice that of the crystal. Thus this shell can no longer be neglected with respect to the sensitivity or to the resolution.

b. The second kind of gelatin is in solution. It raises some practical problems which are discussed in the section on new fine grain emulsions. It is important to know that some emulsions contain relatively little gelatin, and are easy to handle (classic nuclear emulsions such as G5, K5, L4, and NUC 307 fall into this category); others, however, are rich in gelatin and are much more difficult to handle.

Resolving Power

We propose a model with the following characteristics: The emulsion is spread as a compact monolayer of crystals with equal diameter [4, 10]. The adsorbed gelatin is neglected in our evaluation. We are dealing with a point source. It is supposed that the nature of radiation is analogous to light in a transparent medium; there is no variation of the linear transfer energy, all electrons have the same energy, only the first crystal hit is reduced, and there is no scattering. With these assumptions in mind, the probability for a grain to be hit is proportional to its solid angle corrected with respect to its shielding effect, as defined by Caro [4].

Nomenclature for Figures 1, 2, and 3

r: radius of the grain

e: one half the thickness of the section

x: distance between the projection of the point source and the center of the grain we are considering

k: ratio $\frac{r}{e}$

Our geometric model has a sixfold rotational symmetry.

Therefore, we can find all possible situations of the projection of the point source within a triangular field of the monolayer of crystals, representing one-sixth of the entire field.

The projection of the point source may be: in the center of a crystal (case I); in between two crystals (case II); at equal distance from the centers of three crystals (case III). See Fig. 2.

We obtain the series of solid angle curves (without correction for the shielding effect) shown in Fig. 1.

We propose to define contrast as the slope of the curves (derivative of the function). This notion is similar to the gamma as known in photography. The slope of the curves diminishes with the value of k. The

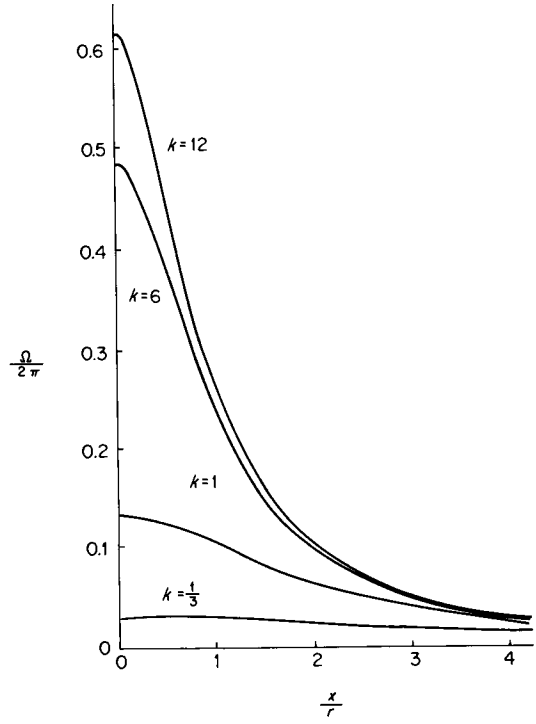

FIG. 1. Variation of the solid angle as a function of the distance and the diameter of the crystals. The solid angle is plotted against the distance, which is expressed in a relative unit $(\frac{x}{r})$. Parameter k is inversely proportional to the radius of the crystal. The shielding effect is neglected in our equation.

contrast must be considered because good resolution without contrast could not give an accurate radioautograph.

The diagram in Fig. 2, using approximations of the same kind as Caro proposed [4], shows the variation of the spreading of the image as the diameter of the grain decreases. It takes into account the shielding effect, and has been drawn with the assumption that the point source is located below the center of one grain (case I).

The dark sectors are proportional to the ratio of the corrected solid angle for the considered crystal and the maximum solid angle (of the crystal nearest the source). This ratio indicates the probability for a grain to be hit. Thus the image spread is increased as the grain diameter diminishes (Fig. 2).

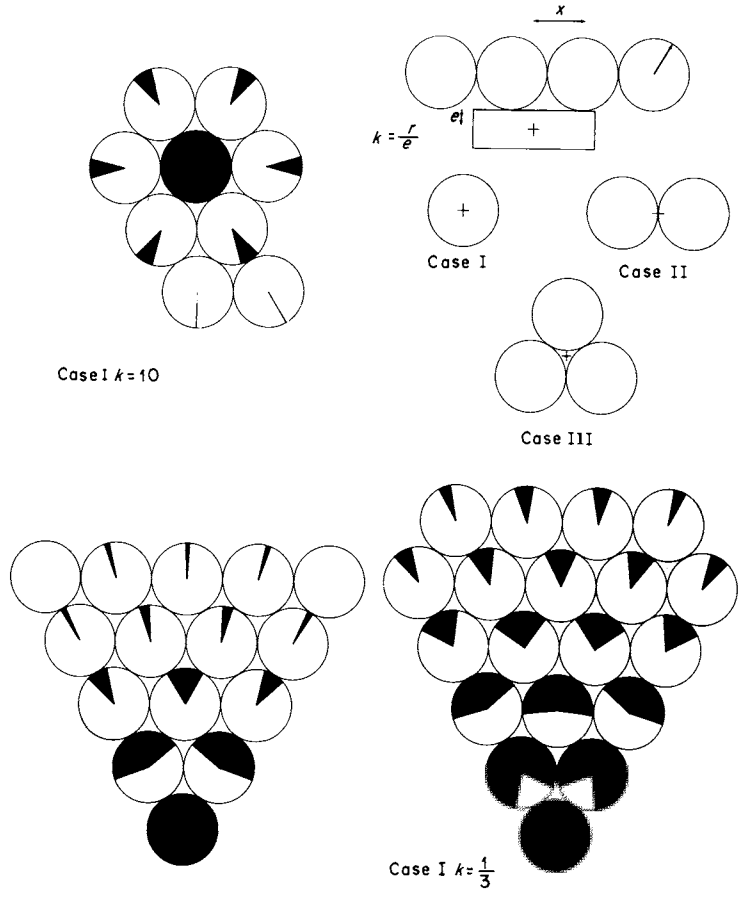

FIG. 2. Probability of a crystal being reduced at a given distance of a point source. The shielding effect is evaluated here. According to the position of the point source in relation to the center of the nearest crystals, three limited cases can be considered: cases I, II, III of this chart. We calculated case 1 only (projection of the point source in the center of the nearest crystal). This is the most favorable hypothesis. If we took into account the other cases, the results would be still less favorable. The dark sectors are proportional to the probability for a crystal to be reduced. The diagram shows the image spread (loss of contrast) when the parameter k, which is proportional to the radius of the crystal, diminishes (see text).

If we consider many point sources, each one of them reducing only one crystal, a particular fact becomes apparent. For instance, in case I, $k = \frac{1}{3}$, considering the first ring of six crystals around the central crystal, the probability of reducing a grain at this distance is 6×80 per cent $=$ 480 per cent, which is almost fivefold more than the most exposed grains (100 per cent). We have to sum up the probability for all the grains at a given distance from the source as shown in Fig. 3. The distribution of the values is similar to that obtained by Caro [4]. This figure allows us

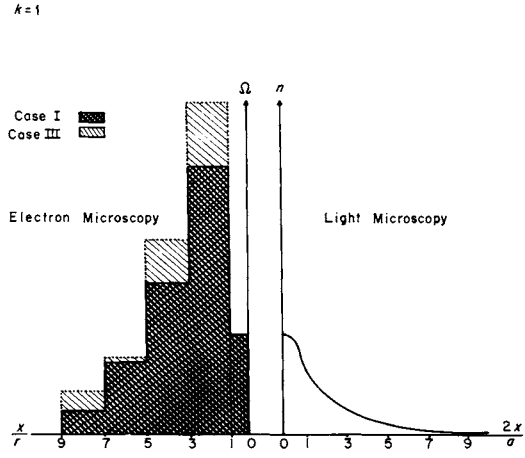

FIG. 3. Comparison of the patterns for light and electron microscopy concerning resolution. The hatched histogram represents the most unfavorable conditions in electron radioautography (case 3) and the darker cross hatching represents the most favorable conditions (case 1). They are drawn for $k = 1$. The continuous curve corresponds to the blackening in light microscope radioautography according to the equation given in the text. The level of maximum blackening is arbitrarily chosen.

to compare the discontinuous pattern of resolution with that described by Doniach and Pelc [7]; that is to compare

$$n = A \int_{y=b}^{y=a} \frac{dy}{(\delta + y)^2 + x^2} \quad \text{with } \delta = e, k = \frac{r}{e} = 1$$

Obviously r is taken for half the thickness of the emulsion, that is, $a = 2r$.

Thus the diagram for electron microscopy is much more severe than the continuous curve of light radioautography.

All these considerations emphasize the idea that, in our case, the important factor is the distance of the crystal from the point source.

In conclusion, we have analysed the resolving power only as it is affected by the geometric factor of crystal diameter. This model has two peculiar characteristics: *discontinuity* and *conic projection*.

It is interesting to consider that this geometric model alone—beyond any photographic or isotopic factor—poses the problems of contrast and resolution. We can therefore speak of "geometric resolution" and it would also be possible to define a "geometric sensitivity." But even if our model can explain certain aspects of contrast, it also has its limitations: (1) The "geometric resolution" is limited by the thickness of the ultrathin sections. The loss of resolution is evident in Fig. 2 for $k = \frac{1}{3}$, which corresponds to crystals of 150 Å in diameter and to sections which are 450 Å thick. (2) If there are two classes of crystal diameters mixed in one emulsion, the "geometric sensitivity" of the smaller crystals will be much inferior to that of the larger ones, and if the smaller crystals are a minority in the population, they will probably play no role in improving the resolution. For this reason it is important to obtain an emulsion which is as homogeneous as possible.

We have neglected the *emulsion properties* other than crystal size: Bachmann and Salpeter (1) have studied some of these aspects, but the minimal dimension of the gelatin layer adsorbed onto the crystals has still to be determined. We have also neglected an *isotopic factor;* it is difficult to evaluate the energy loss along the track within one or several silver halide crystals. Indeed, in small crystal emulsions, several crystals can be reduced by a single electron (5).

These two factors (emulsion and isotopic) would tend to decrease the resolution calculated by the geometric model. The experimentally measured resolving power will be less. The smaller the crystal, the greater the discrepancy between geometric and experimental data.

The geometric model presented here has primarily theoretical value, and data which may be calculated should be considered as approximations only.

ROUTINE CYTOLOGICAL TECHNIQUE

We shall consider first the ideal conditions, and afterwards the practical method we employ.

What Are the Requirements for the Routine Technique in a Nonspecialized Laboratory?

The technique should provide simple procedure, easy handling; sufficient resolution and sensitivity, and perfectly reproducible results.

An ideal emulsion must be: rich in silver bromide, i.e., contain more than 90 per cent; it must have grains which are small enough to give an adequate resolution relative to the dimensions of the chief intracellular organelles. On the other hand it is not necessary to use an emulsion with extremely small crystals for thin sections since the factor limiting the

resolution is chiefly the thickness of the section rather than the diameter of the crystals.

We feel that the most important practical factor is the silver-to-gelatin ratio. Emulsions with undeveloped crystals below 700 Å in diameter are very rich in gelatin. Therefore, they cannot be used without concentration, which is a source of many difficulties.

We had hoped to find the ideal emulsion in NUC 307 from Gevaert, although it should be possible to obtain a still smaller crystal diameter with the same silver-to-gelatin ratio. NUC 307 is advantageous because of its high silver content and its small crystal diameter, which is one half of that of L4 (0.7 μ instead of 1.4 μ). Unfortunately, some batches of this product have not been reliable in the past.

In summing up, we think that, for cytological purposes, it is much more advantageous to obtain an emulsion which is regularly of very high quality than to improve resolution without perfect reliability.

What Is the Ideal Substratum?

That is to say, what is the ideal surface for coating? *We think that the layering must be made on a relatively large and flat surface.*

An even surface is an important factor for permitting homogeneous layering. It is important to remember that a membrane on a grid is not an even surface; this is evident if we look at a grid with shadow-casting or one covered with a very diluted emulsion. A large surface is required for good reproducibility and easy control. The ideal method is the elegant coating technique of Kopriwa and Leblond [16], as used in light radioautography. Large surfaces are desirable in order to reduce the edge effects to a minimum. The beaker used for dipping must be deep enough to allow a large part of the slide (about 4 cm) to be covered at once, and large enough to allow good mechanical agitation.

Routine Method in Use

The routine method we use is very reliable. It resulted from further development of previous investigations.

Some authors have been dipping the whole grids covered with sections into the emulsion [13, 26, 32]. Other investigators have used membranes without grids for coating, but the emulsion was not applied by dipping [24, 27]. Another method has recently been described by Salpeter and Bachmann [29] where the dipping is replaced by dropping a small quantity of concentrated NTE emulsion on a glass slide. We still feel that the dipping procedure is an extremely important aspect of the membrane technique, and is its main advantage. The experience we have had with this technique in association with Dr. B. Droz during the

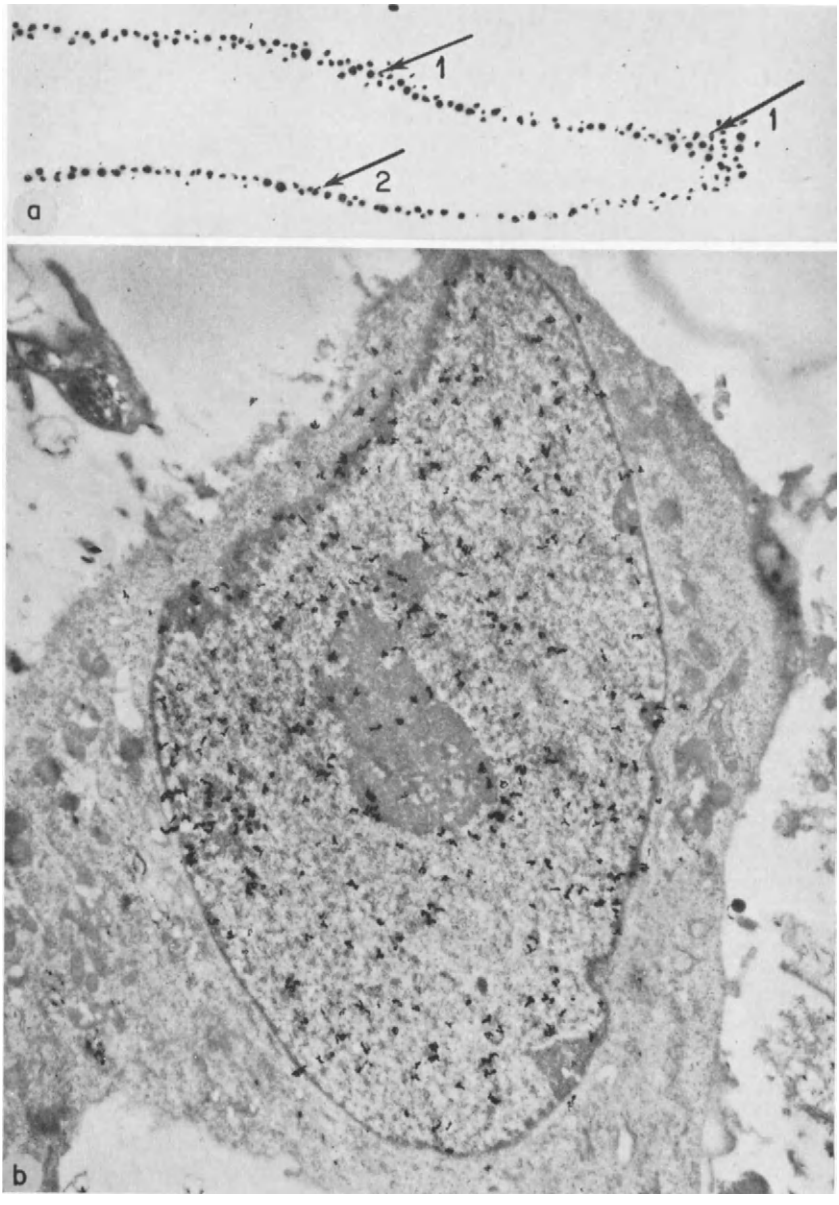

FIG. 4. (a) Control of the coating of NUC 307 carried out on glass slide by dipping. Formalin fixation. GMA embedding. 1: tangential section; 2: perpendicular section showing the monogranular layering. There exist some "holes" without crystals, pulled off during the sectioning process. Magnification: 20,000 ×. (b) Monkey kidney cell 24 hours after infection by SV40 virus and labeled with ^{3}H-thymidine. Coating of NUC 307 with the dipping technique. Exposure time: 9 days. Gelatin not removed. Magnification: 12,000 ×.

past 20 months has confirmed this view. Furthermore, regular testing of the background on the grids outside the sections has given us much lower and more constant values than with other methods.

In order to have a large coating surface, we use glass slides covered with a thick layer of collodion (Parlodion, 1.0 g in 100 ml amyl acetate). The previously cleaned slides are dipped into this solution and allowed to dry at room temperature. Then the sections are laid down onto the membranes with a plastic ring [20].

In the darkroom—under safe-light illumination (Kodak Wratten series 2 filter)—a quantity of NUC 307 is melted at 37°C and then diluted to about one-fourth with distilled water. It is necessary to have moderate agitation and sufficient time in order to get a homogeneous suspension. The slides are coated by dipping according to Kopriwa and Leblond [16]. After dipping, the emulsion is allowed to gel, and is then dried and stored at 4°C in storage boxes for the exposure time.

The development must be strong enough for the grains' characteristic coiled shape to be seen easily at the usual magnification. For cytological purposes it may be necessary to have the entire nucleus or even the whole cell on the screen of the electron microscope, and the grains should therefore be readily visible. We are not sure that underdevelopment is desirable, in spite of possibly better resolution. Normal development is probably more reproducible as far as the number of grains per electron is concerned. Usually we develop for 5 minutes in D 19 at 18°C. Figure 4 illustrates the result of this technique and shows that it can be used for studies on nucleolar metabolism (as presented elsewhere [8]).

After fixing in buffered hyposulfite without hardener [12], the glass slides are rinsed and then dried at room temperature. Afterward, the membrane is floated on distilled water and either a single grid is slipped under the floating membrane at the site of the sections or several grids are laid down with caution over the membrane which is then picked up in the usual way (Fig. 5).

A Few Points for Further Emphasis

(1) To prevent the membrane from floating off during dipping and the subsequent processes, it is recommended that the bottom of the slides be bordered by dipping the lower few millimeters in concentrated collodion. In the subsequent handling we never dip our slides deeper than to the upper limit of the more dilute collodion which forms the actual membrane. The removal of the membrane from the slide is always easy, provided the collodion membrane is thick enough.

(2) The ideal layer is monogranular. However, we feel that a small number of excess grains affects the resolution less than an incomplete

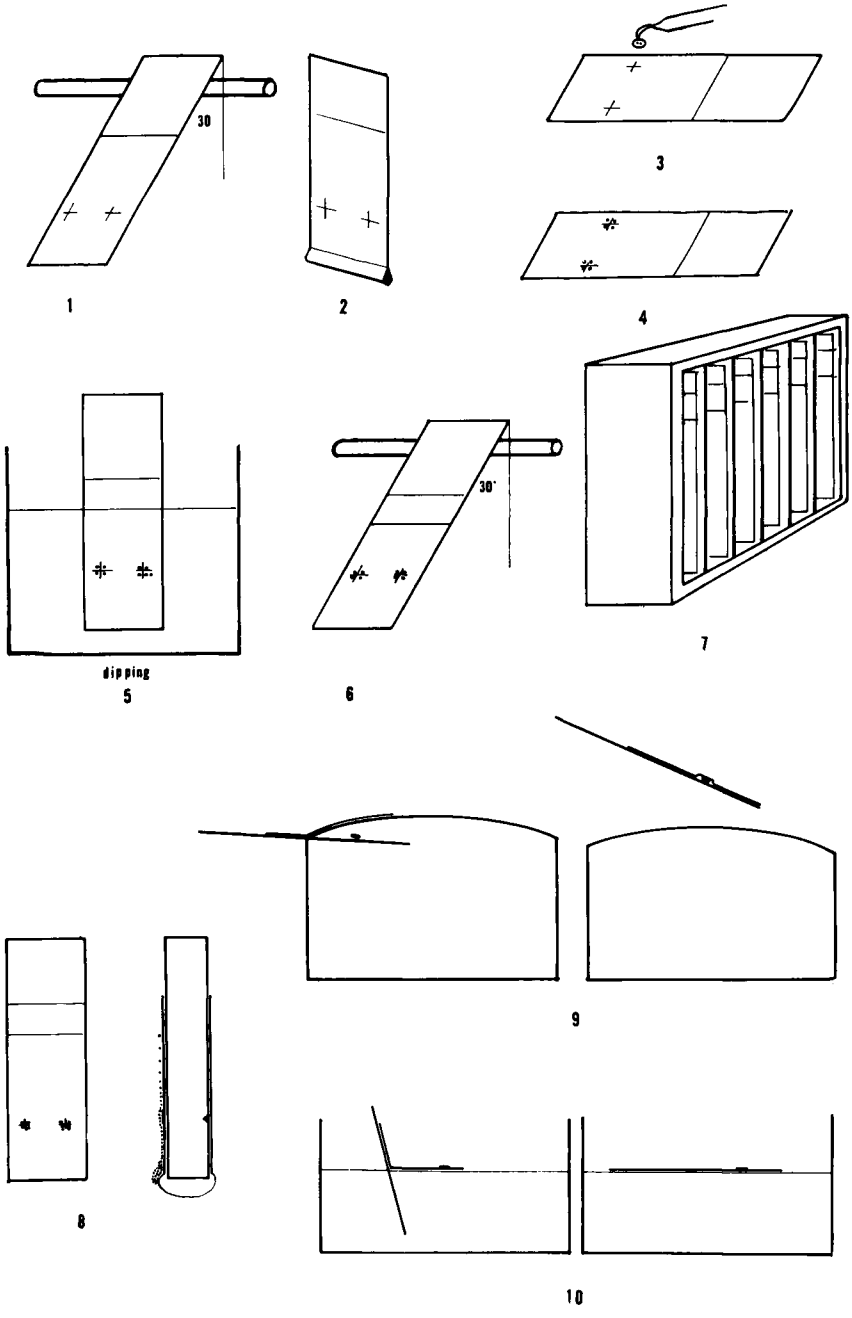

FIG. 5. Technique for electron radioautography on glass slides as described in this paper: (1) Drying of the collodion membranes. (2) Rim of concentrated solu-

layer. Direct electron microscope examination of the layer is not reliable enough. A good control technique is to fix the membrane covered with emulsion in formalin, and then to embed it in water-soluble plastics, like glycol methacrylate (GMA) [18] or 2-hydroxypropylmethacrylate (HPMA) [19]. Ultrathin transverse sections of the layer are cut with an ultramicrotome and examined with the electron microscope (Fig. 4). This method shows much better the exact position of each grain within the gelatin layer than does direct examination.

(3) Our technique does not necessarily require the removal of the gelatin. With GMA specimens the examination and grain count may be carried out without removal of the gelatin layer and without staining. But in order to get good pictures with excellent contrast, it is better to take off the gelatin. This allows adequate staining. As acetic acid [12] attacks the collodion, it is desirable to place a layer of carbon onto the collodion before putting the specimens onto the slides.

The carbon layer has been proposed by Bachmann and Salpeter [1] for preventing the emulsion from being desensitized by the section. Unlike our procedure, this layer is put between the section and the emulsion. The usefulness of this carbon film has been tested by systematically checking the sensitivity of emulsions with an electron microscope [1].

(4) Bacterial contamination is an important problem during manufacture of the gelatin and the emulsion. In order to avoid contamination during our procedure, we rinse our containers with alcohol and discard the batch after having utilized it once.

The Problems of Quantitative Radioautography

Should quantitative studies be carried out, the technical problems to be solved are more complex.

(a) Constant sensitivity is required, that is to say, strictly equal layering regardless of the presence of sections. With the method here described, the coating of the emulsion seems to be very homogeneous and reproducible from one slide to another during the same experiment,

---

tion of collodion on the bottom of the glass slides. (3) Deposit of ultrathin sections on the marks by means of a plastic ring. (4) The glass slide is ready for the coating of the emulsion. (5) Dipping. (6) Gel formation on all the glass slides at the same angle: 30°. (7) Open box containing the glass slides for development, fixing, and rinsing. (8) Three successive layers on the glass slide: developed emulsion, section, collodion. (9) and (10) Floating the membrane with sections on distilled water. (9) A grid is slipped under each group of sections. Then the glass slide is lifted and the grid carries the three layers. (10) Alternative method: the membrane is entirely floated off. Grids are deposited on sections and the membrane is picked up with a filter paper. In this case the sections are between the grids and the collodion.

provided that the following factors are constant for all the slides which are handled together: the dilution of the emulsion, the depth of dipping; the position of the sections on the slide, as there exists a gradient in the emulsion along the slide (for us, 2 cm from the lower edge), the temperature and moisture of gelling, the conditions of drying, and the conditions of the photographic process. This allows reproducible blackening from one slide to another. But all these considerations still neglect the presence of sections.

(b) Additional difficulties arise from the presence of sections of biological material. It does not seem to be possible to get perfectly identical thicknesses of sections from one block to another.

Within the same section, there are differences in thickness of cytological structures according to their hardness and density.

It seems to us that quantitative measurement is handicapped by the unevenness of the surface of the section. Ideal quantitative radioautography would require a modification of the present cutting technique. The only way to escape this difficulty is to refer the activity to a standard source located in the section and preferably in the cell itself, as has been proposed previously [2, 3, 22, 23, 28, 31].

In conclusion, the tissue section is the main limiting factor for resolution and quantitative work. With this in mind, we shall treat the third problem.

THE NEW EMULSIONS WITH VERY SMALL CRYSTALS

The new emulsions discussed here will be, in our opinion, generally useful for the study of small particles not embedded in a plastic (macromolecules, viruses). These emulsions are very different from those we have already mentioned (Ilford G5, K5, L4, Gevaert NUC 307), which have a grain diameter equal to or more than 700 Å. As a matter of fact, by "new emulsions" we mean Kodak NTE introduced by Bachmann and Salpeter [1] and an emulsion prepared for us by Kodak-Pathé, Vincennes, France [11]. These emulsions share two particular features: the percentage of silver to gelatin is low (about 50 per cent in our case) and the sizes of the undeveloped crystals are very variable.

For these reasons it is necessary to purify and concentrate these products before use.

The technique for use of these emulsions is not yet entirely worked out. However, the method we have described is the only way, in our opinion, to use very fine grain emulsions [11]. It has already given interesting results (Figs. 6-8).

The principle of this method is as follows: a Lippman-type emulsion is centrifuged producing a different type of emulsion (the supernatant)

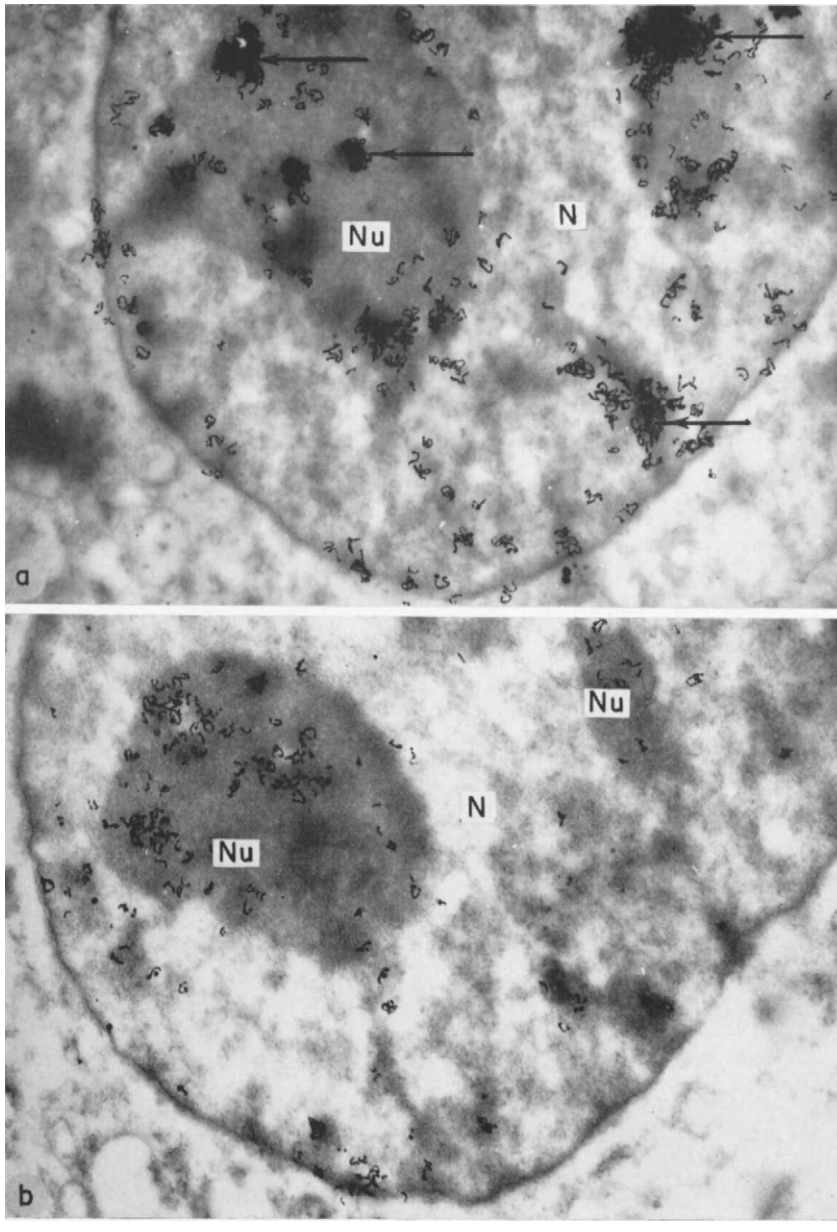

FIG. 6. (a) Mouse fibroblast labeled with ^{3}H-thymidine. Experimental emulsion from Kodak-Pathé (France) unpurified. Presence of many clumps of silver (at arrows) on the nucleus (N) and nucleolus (Nu). Magnification: 27,000 ×. (b) Same specimen, same emulsion, no clumps (see text). N = nucleus; Nu = nucleolus. Magnification: 27,000 ×.

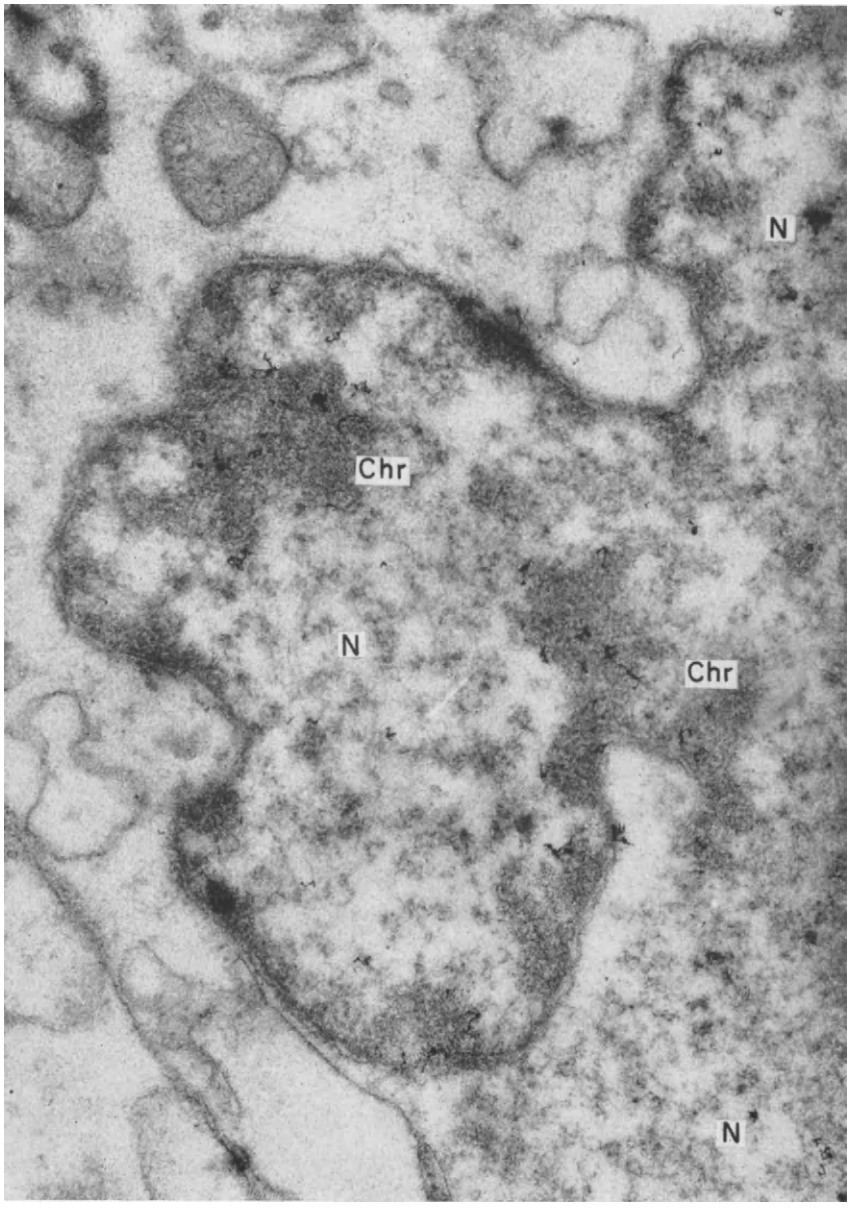

FIG. 7. Portion of a monkey kidney cell in cell culture labeled with ^{3}H-thymidine. Experimental emulsion from Kodak-Pathé. Reduced silver grains are located on chromatin zones (Chr) of the nucleus (N). Exposure time: 3 weeks. Development: D 19. Magnification: 36,000 ×.

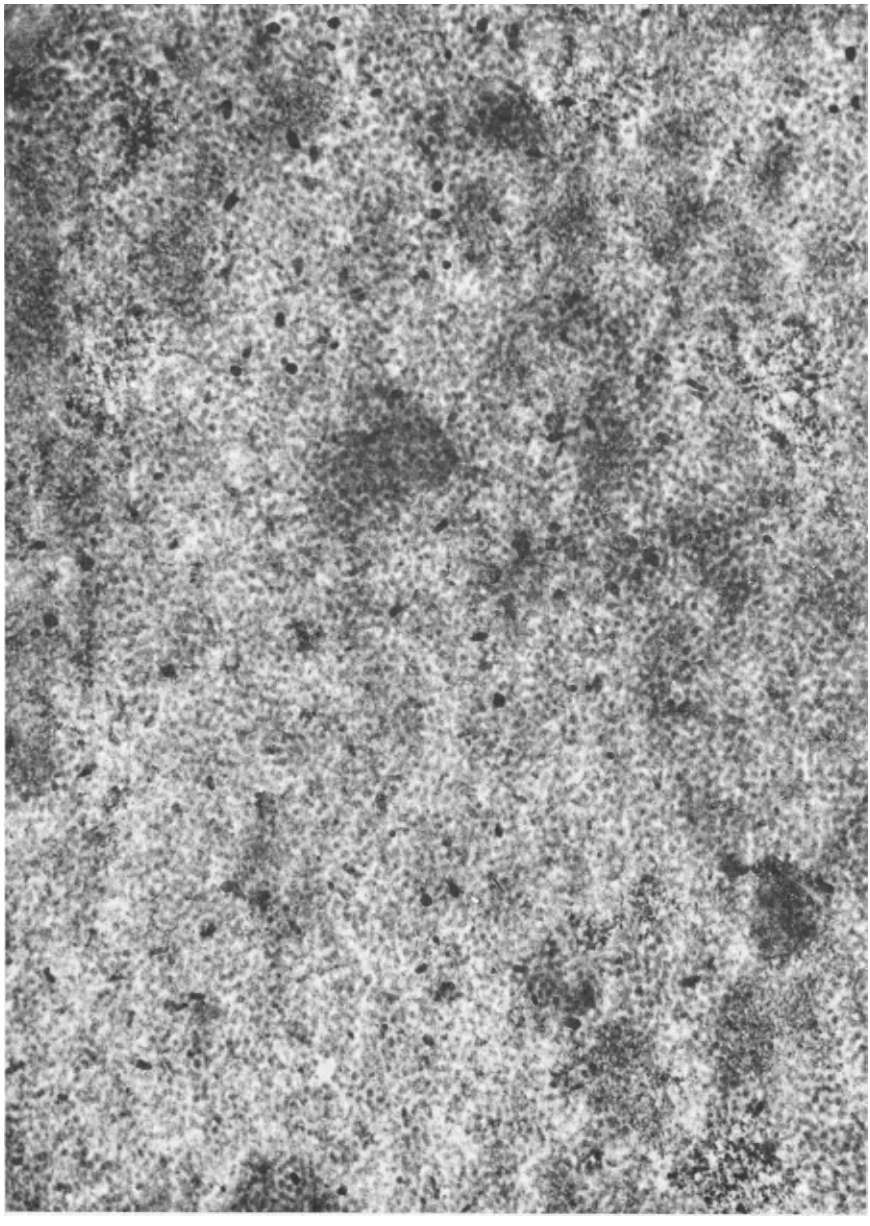

FIG. 8. Portion of a nuclear inclusion of SV40 virus in a monkey kidney cell, 4 days after infection and labeling with ^{3}H-thymidine. Experimental emulsion, Kodak-Pathé. Exposure time: 3 weeks. Development: D 19. Very small developed grains. Magnification: 45,000 ×.

which is very much diluted and has undeveloped crystals of a diameter of 300 to 350 Å (including the shell of gelatin). The concentration and coating of this emulsion are both carried out by centrifugation.

Procedure

(a) *Granulometric Separation.* The goal is to eliminate the coarsest crystals as well as the clumps of particles or other contaminants in order to keep only the finest grains. The separation can be made only by centrifugation. The viscosity of the emulsion must be lowered prior to sedimentation by dilution to one-tenth of the original concentration and heating at 37°C during centrifugation, which is carried out for 2 hours at 3000 rpm. The pellet is discarded and the supernatant which contains the finest crystals is used. The measurement of the diameter of the crystals, to measure the degree of purification, must be done by surface replica or shadow casting. In order to determine the diameter of the crystal following the usual practice, it would be necessary to measure particles stripped of their shell of gelatin. However, for our purpose it has been sufficient to compare the shadow-cast crystals before and after the first centrifugation (Fig. 9).

(b) *The Coating.* The supernatant has to be concentrated first since the emulsion is very much diluted during purification. This concentration is also performed by centrifugation, which seems to be the only method of modifying the silver-to-gelatin ratio. Centrifugation has been used before, but has been applied directly onto grids and only for emulsions with a high silver-to-gelatin ratio [6, 15]. With such emulsions the benefit of this difficult handling is greatly diminished. In the present work, the layering is carried out on large concave cylindrical lenses (surface about 20 cm^2) with a radius of curvature which corresponds to the radius of centrifugation. These lenses are covered with a membrane as used in electron microscopy. The use of large surfaces has the same advantages for control and reproducibility as it does in the dipping technique.

After precipitation, the layer is gelled, then poured off with care and allowed to dry. The next steps are performed according to the technique already described in the section on routine cytological techniques.

FIG. 9. (a) NTE emulsion diluted. Shadow casting; heterogeneity of crystal diameter. Magnification: 25,000 ×. (b) New experimental emulsion from Kodak-Pathé (France) very much diluted. Shadow casting; heterogeneity. Magnification: 25,000 ×. (c) Same emulsion as for (b), after centrifugation according to our technique. Shadow casting. The clumps and the biggest crystals have disappeared. Only the smallest crystals are present, and they are relatively homogeneous. Magnification: 25,000 ×.

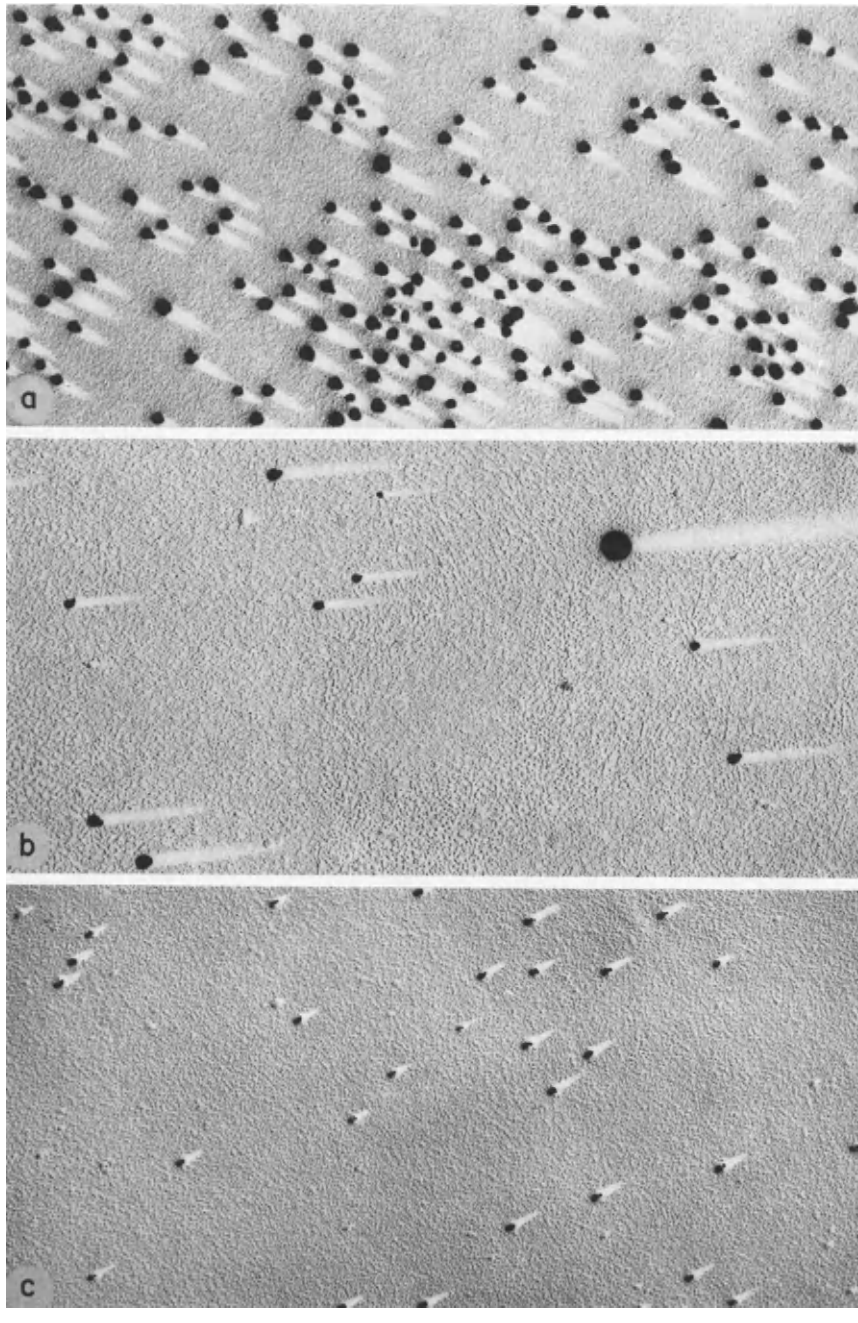

FIG. 9

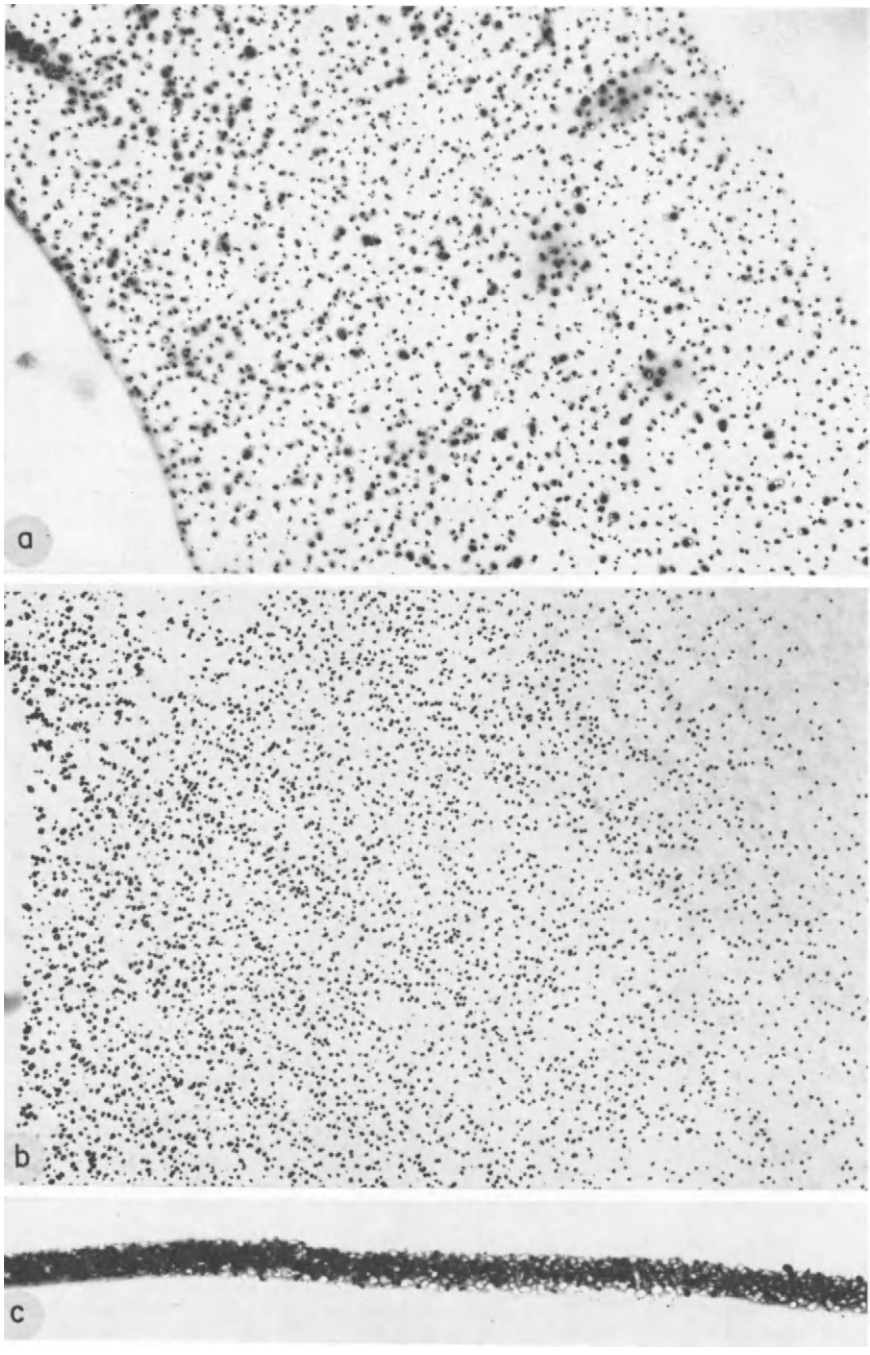

FIG. 10

For control, some membranes coated with emulsion are embedded in a plastic for sectioning. The embedding produces some artifacts due to the fineness of the grains but it has the advantage of showing the organization of the sensitive crystal layer (Fig. 10).

Concerning this procedure, two points must be emphasized:

(1) We have been using this emulsion in multilayers. The emulsion NUC 307 was initially used in multilayers as well, before we were regularly able to produce monolayers. We are not sure whether monolayers are also desirable for the Lippmann emulsion because of the adsorbed gelatin.

(2) Our procedure does not lead to a complete precipitation of all the crystals in the suspension. It is conceivable that finer grain emulsions can be manufactured, and thus the technique may still be improved. The question is to know how far the sensitivity is maintained.

A procedure for modifying the silver-to-gelatin ratio, also based on centrifugation, has been proposed by Bachmann and Salpeter [1]. But these authors do not use the supernatant; on the contrary, they resuspend a part of the pellet and the coating is not carried out by centrifugation.

CONCLUSIONS AND SUMMARY

There exist two different techniques of radioautography at the electron microscope level.

The first one is to apply emulsion on thin sections for cytological investigations. This technique is standardized; the limiting factor is the thickness of the section. The best emulsion for this purpose is thought to be similar to NUC 307 Gevaert, but should be regularly produced in perfectly reliable samples. The technique of layering by dipping glass slides without grids is very useful. It gives good reproducibility and uniformity of thickness of the emulsion. Since the principal difficulties of layering are solved, it is possible to study some problems of resolution and sensitivity on a practical basis. In spite of the present lack of perfect reproducibility of the thickness of ultrathin sections, this technique al-

FIG. 10. (a) New experimental emulsion from Kodak-Pathé (France) undiluted and without separation. Coating by dipping. Formalin fixation. GMA embedding. The layering is uneven, poor in crystals, and very thick. Magnification: 12,000 ×. (b) Same emulsion undiluted. Layering by centrifugation. The evident gradient may be due to insufficient acceleration. Magnification: 12,000 ×. (c) Same emulsion diluted, purified, and layered by the technique presented here. This layer is very rich in silver halide crystals. Alcohol fixation. HPMA embedding. Magnification: 20,000 ×.

ready offers possibilities for quantitative studies and allows comparison of the metabolism in different cells at high resolution [9].[1]

A second technique of high resolution radioautography is proposed for the study of small isolated particles. An emulsion of extremely small grain is used (from Kodak-Pathé, Vincennes, France). We propose a technique for purification by means of centrifugation. The advantage of this technique is the ability to separate a fraction of the finest grains which are alone used for coating. It is suggested that this method may be useful in the field of molecular biology.

ACKNOWLEDGMENTS

The author is very much indebted to Dr. W. Bernhard for his continuous interest and useful advice. We have had many stimulating discussions with Prof. Agr. Bernard Droz and Dr. L. G. Caro.

We gratefully acknowledge Dr. G. Sorenson for his help in the English translation and Mme. J. Burglen for her excellent technical assistance.

The new experimental emulsion from Kodak-Pathé (France) and the NTE emulsion from Kodak-Rochester have been provided by the courtesy of Dr. R. Audran (Kodak-Pathé, Vincennes, France), whose collaboration has been extremely helpful in our study. Dr. Nicole Granboulan has carried out the biological applications.

REFERENCES

1. Bachmann, L., and Salpeter, M. M., *Naturwissenschaften* **10**, 237 (1964).
2. Budd, G. C., and Pelc, S. R., *Stain Technol.* **39**, 294 (1964).
3. Caro, L. G., *J. Biophys. Biochem. Cytol.* **10**, 37 (1961).
4. Caro, L. G., *J. Cell Biol.* **15**, 189 (1962).
5. Caro, L. G., *J. Roy. Microscop. Soc.* **83**, 127 (1964).
6. Dohlman, G. F., Maunsbach, A. B., Hammarstrom, L., and Appelgren, L. E., *J. Ultrastruct. Res.* **10**, 293 (1964).
7. Doniach, I., and Pelc, S. R., *Brit. J. Radiol.* **23**, 184 (1950).
8. Granboulan, N., and Granboulan, P., *Exptl. Cell Res.* 34, 71 (1964).
9. Granboulan, N., and Tournier, P., *Ann. Inst. Pasteur* (1965) in press.
10. Granboulan, P., Symp. "Cytochemical Progress in Electron Microscopy," *J. Roy. Microscop. Soc.* **81**, 165 (1963).
11. Granboulan, P., and Audran, R., *Compt. Rend.* **259**, 3201 (1964).
12. Granboulan, P., Granboulan, N., and Bernhard, W., *J. Microscop.* **I**, 75 (1962).
13. Hay, E. D., and Revel, J. P., *Develop. Biol.* 7, 152 (1963).
14. Kayes, J. K., Maunsbach, A. B., and Ullberg, S., *J. Ultrastruct. Res.* **7**, 339 (1962).
15. Koehler, J. K., Muhlethaler, A. B., and Frey-Wyssling, A., *J. Cell Biol.* **16**, 73 (1963).
16. Kopriwa, B. M., and Leblond, C. P., *J. Histochem. Cytochem.* **10**, 269 (1962).
17. Kuhn, N. O., and Harford, C. G., *Science* **141**, 355 (1963).

[1] Since the preparation of this manuscript, better quantitative results have been obtained due chiefly to sections of more uniform thickness (R. M. Franklin and N. Granboulan, submitted to *J. Mol. Biol.*).

18. Leduc, E. H., and Bernhard, W., *Symp. Intern. Soc. Cell Biol.* "The Interpretation of Ultrastructure" (R. J. C. Harris, ed.), p. 21. Academic Press, New York, 1962.
19. Leduc, E. H., and Holt, S. J., *J. Cell Biol.* **26**, 137 (1965).
20. Marinozzi, V., *J. Ultrastruct. Res.* **10**, 433 (1964).
21. Mees, C. E. K., "The Theory of the Photographic Process." Macmillan, New York, 1954.
22. Moses, M. J., *J. Histochem. Cytochem.* **12**, 115 (1964).
23. Nadler, N. J., Young, B. A., Leblond, C. P., and Mitmaker, B., *Endocrinology* 74, 333 (1964).
24. Pelc, S. R., Coombes, J. D., and Budd, G. C., *Exptl. Cell Res.* **24**, 192 (1961).
25. Pouradier, J., and Roman, J., *Sci. Ind. Phot.* **23**, 4 (1952).
26. Revel, J. P., and Hay, E. D., *Exptl. Cell Res.* **25**, 474 (1961).
27. Roberts, J. M., and Chow, P. C., Fourth Intern. Conf. Nuclear Phot. 4th, Munich, Sept. 1962.
28. Ross, R., This volume, p. 273.
29. Salpeter, M. M., and Bachmann, L., *J. Cell Biol.* **22**, 469 (1964).
30. Stein, O., and Gross, J., *Exptl. Cell Res.* **31**, 208 (1963).
31. Van Heyningen, H. E., *Anat. Record* **148**, 485 (1964).
32. Young, B. A., and Kopriwa, B. M., *J. Histochem. Cytochem.* **12**, 438 (1964).

APPLICATION OF FREEZE-DRYING AND FORMALDEHYDE-VAPOR FIXATION TO RADIOAUTOGRAPHIC LOCALIZATION OF SOLUBLE AMINO ACIDS[1]

EARL P. BENDITT, GEORGE M. MARTIN, AND HOWARD PLATTER[2]

Department of Pathology, University of Washington, Seattle, Washington

INTRODUCTION

Localization of large molecules susceptible to fixation *in situ* by ordinary fixatives and demonstration by radioautography has been eminently successful. Although while attempts to localize soluble compounds and to demonstrate them by radioautography have been made, all suffer from the drawback: lack of a fixing step in the procedure [1, 4, 7, 9, 15]. This provides the possibility of movement of the compound during tissue preparation, application of the emulsion, and subsequent exposure.

In this laboratory we have been exploring the combination of freezing-dehydration and fixation with vapor reactants for application to the histochemical problem of soluble molecules such as histamine and acetylsalicylic acid and for use with various demonstrating reactions including radioautography [3, 11, 12, 17]. Others have applied similar techniques to the demonstration of the catecholamines [5, 8]. The basic principle of the technique is as follows: (1) Quick freezing of appropriately sized pieces of tissue under conditions designed to minimize ice crystal artifacts and to hold various intracellular and tissue items *in situ*. (2) Dehydration (after Altmann and Gersh, see Benditt *et al.* [2]) from the frozen state under conditions which will maintain localization and tissue architecture. (3) Application of reagents in the vapor state suitable for a given compound. The requirements of this last step are that the reagent, or combination of reagents, form covalent bonds with the small molecular substance and maintain them *in situ* by cross-linking them with immediately adjacent tissue elements or with formed polymers. This communication presents a preliminary résumé of some experiments utilizing the combination of freeze-drying and vapor fixation of the dried tissue for localization of the intracellular soluble forms of an amino acid.

[1] This work was supported in part by U.S. Public Health Service grants H-03174, AM-04826, and 2T-1-GM-100. Work was assisted by Mrs. Grace Warren and Mrs. Mary Derr.

[2] Summer Premedical Student Research Trainee.

MATERIALS AND METHODS

The material chosen for the initial exploration of the technique was a strain of human fibroblasts grown as monolayer cultures on cover slips. The advantages of such a system are: (1) large numbers of a uniform population of cells could be obtained [13]; (2) a high level of radioactivity could be introduced under conditions of known amino acid composition in the extracellular medium; time sequences could then be studied by incubating the cover slips briefly for known time intervals in the medium containing the isotope-labeled amino acid; (3) on one cover slip a series of observations could be made, including (a) counts of initial total radioactivity, (b) counts after application of the fixative as vapor, (c) determination of the percentage retention of isotope after exposure to solvents and (d) radioautography.

Preparation of Monolayers

Diploid human skin fibroblast cultures were established by explant techniques from foreskins of newborn babies and maintained in Waymouth's medium supplemented with 10 per cent newborn calf serum (heated to 56°C for 30 minutes) and penicillin (50 units/ml). The studies reported here were performed with strain Andrew Martin (AM) at the 5th to 14th passages (6 weeks to 6 months of continuous cultivation). Trypsinized cells (approximately 50,000 cells/ml) were allowed to attach to 22 mm square cover slips (#1 thickness, Gold Label) in 35 mm plastic petri dishes, as previously described [13, 14]. A total of 100,000–125,000 cells were plated per dish. After 20–72 hours incubation at 37°C in 5% CO_2–air, the monolayers were used for the experiments. At this stage, the monolayers were not confluent except for a few patches in para-central areas.

Pulsing Technique

Immediately before incubation in radioactive media, the monolayers were rinsed in a modified Hank's balanced salt solution buffered with 0.02 *M* tris(hydroxymethyl)aminomethane–HCl (pH 7.4 at 37°C) instead of bicarbonate. 3,4-^{3}H-L-proline hydrochloride having a specific activity of 5 curies per mmole (lots No. 46-283-101 and 46-287-12, New England Nuclear) was added to Waymouth's medium without proline supplemented with 10 per cent newborn calf serum and penicillin (50 units/ml) and buffered with 0.02 *M* Tris–HCl (pH 7.4 at 37°C) instead of bicarbonate to give final concentrations of tritiated proline ranging from 5 μc/ml to 400 μc/ml. Pulsing was always performed by immersing the cover slips in a Columbia staining jar containing 10 ml of the radioactive media. Incubation times varied from 15 seconds to 108 minutes

(at 37°C). In early experiments, cover slips were then rinsed in 5 changes of Tris buffered Hank's balanced salt solution in Columbia staining jars (10 ml per jar). In most of the experiments, however, cover slips were successively agitated in 3 staining dishes, each containing 500 ml Tris buffered Hank's solution and maintained at 37°C. With short incubation times (< 9 minutes), the cover slips were handled one at a time with a watchmaker's forceps, pulsed, and rinsed. For longer incubation times, groups of 4 to 8 cover slips were processed simultaneously, rinsing being carried out with a stainless steel cover slip carrier (Lipshaw, Detroit). Excess fluid was drained from each cover slip immediately after incubation (except in the case of 15-second and 1-minute incubations) and after the final rinse by touching to absorbent tissue paper. After a total of 8 cover slips had been processed, the first rinse was discarded, the container rinsed with distilled water, and 500 ml of fresh Tris buffered Hank's solution was added; this was now employed as the final rinse. The previous final rinse was now used as the second rinse while the previous second rinse became the first rinse. This operation was repeated until a batch of 24–40 cover slips had been processed.

Fixation

Immediately after the final rinse cover slips to be freeze-dried were instantly frozen by quenching in isopropane chilled just to freezing by liquid nitrogen. These were then dehydrated in an apparatus previously described [2]. In certain experiments, groups of cover slips were also fixed in 95 per cent alcohol or in 4 per cent formaldehyde formalin in 50 per cent alcohol at room temperature for periods of 11–20 hours. After fixation they were washed in 5 changes of fresh fixative in Columbia jars (10 ml per jar) and air dried.

Exposure to the vapor fixative, paraformaldehyde, was performed in a desiccator (160 mm inside diameter) maintained at the desired temperature in an air oven. Fifteen to twenty grams of the solid paraformaldehyde (Matheson, Coleman and Bell, 35140) was placed in a dish on the perforated porcelain platform of the desiccator and beside it, when used, a saturated solution of NaI in water. The cover slip monolayers were placed at the bottom of the jar, either vertically in stainless steel cover slip holders or cell side up in small petri dishes. The temperature of the vapor was measured and preadjusted to the desired level prior to exposure of the tissues. The whole apparatus was kept in a hood.

Measurement of Radioactivity

A windowless gas flow counter (Model D47, Nuclear, Chicago) with automatic sample changer and T3 time delay valve was employed to

measure the radioactivity of the cover slip monolayers. Although the efficiency of counting of tritium in such a system is very low, the levels of radioactivity which were achieved in this system were easily sufficient for analytical purposes (100 to 500 times the background).

Radioautography

In order to minimize direct handling of the monolayers, the cover slips were attached to standard microscope slides with small strips of tape (with adhesive on both sides). Using a loop constructed of 1 mm diameter stainless steel, the slides were covered with a "bubble" obtained by mixing 2 parts of Eastman Kodak N.T.B. #2 emulsion with 1 part 1 per cent aqueous solution of Ivory flakes at 40°C. The excess emulsion was drained off, and the slides dried and exposed for periods of 3 days to 3 weeks before developing and counterstaining with hematoxylin and eosin.

Cell and Grain Counts

The total number of cells per cover slip was estimated after radioautography and counterstaining by means of a modified Chalkley method [6]. A total of 16 fields were counted at a magnification of 400 $\times$ with a calibrated 10 mm square net micrometer disc (divided into 100 component squares). In a typical experiment, the mean total cells per cover slip of a group of 22 replicate monolayers was 148,772 with a standard deviation of $\pm$ 20,200. Radioautographic grain counts were performed with the same disc at a magnification of 1000 $\times$; in each of 25 fields, grains in 4 component squares were counted over cell cytoplasm and background.

EXPERIMENTAL OBSERVATIONS

The Time Curve of Uptake of Free Amino Acids

It was first necessary to determine the free amino acid uptake curve by the fibroblasts. For this purpose a series of cover slips, grown simultaneously, were pulsed with 5 μc of proline per ml of medium for times varying from 20 seconds to 108 minutes. After pulsing with the incubation medium containing the labeled amino acid, each cover slip was washed as indicated above to remove the excess amino acid. At each time period (20 seconds, 1, 3, 9, 18, 54, 108 minutes) duplicate cover slips were treated in each of the following ways: (a) fixed for 16 hours in 50% ethanol containing 4% formaldehyde; (b) frozen, dried from the frozen state for 4 days, fixed for 16 hours at 60°C in paraformaldehyde vapor. In addition, two sets of cover slips were treated before incubation in the medium containing labeled proline by immersion in unlabeled Hank's

balanced salt solution (without Tris or bicarbonate buffers) heated to 80°C for 5 minutes. Duplicate sets of these were then treated as described above. The radioactivity in the cover slips was counted and the counts per minute per cover slip calculated. Counts for each pair of cover slips were averaged and the data are shown in Fig. 1.

The alcoholic formalin was used to fix proteins and other large molecular complexes and was intended to dissolve out the free amino acids and any small metabolic products of these. The frozen-dried cells not exposed to any solvent action were used to provide a measure of the

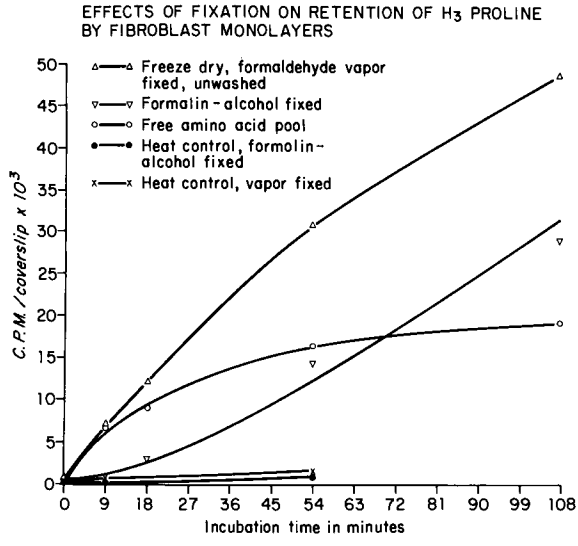

FIG. 1. Time curves of uptake of soluble and incorporated amino acid (^{3}H-proline) by fibroblast monolayers.

total amino acids present both free in cells and those incorporated into protein. The difference between these two curves, therefore, represents the free amino acid pool. As can be seen in the charts, the formalin-alcohol fixed cells exhibited a characteristic uptake into protein with a lag phase in the first 10–20 minutes and a rapid and steady rise thereafter continuing through the 108 minutes. The curve of total radioactivity, on the other hand, rises rapidly with only a slight lag in the first minutes. The difference, representing the soluble amino acid pool, rises rapidly at the outset and then plateaus at about 1 hour.

Evidence that the uptake of soluble as well as "fixed" amino acid is a metabolically conditioned phenomenon is given in the bottom two lines of Fig. 1. Here we see that heat-killed cells showed no significant uptake

of radioactivity in the 54-minute time period studies irrespective of the kind of fixation.

With this information, experiments could then be designed to find out the optimal conditions for fixing the soluble amino acids.

Conditions for Fixation of Soluble Amino Acids

From the curves described in the preceding section it became clear that the maximum differential between total amino acids and bound amino acids, in other words the soluble amino acid pool, occurred at about 10 minutes. Therefore for the remainder of the experiments, designed to test the effects of fixation on solubilization of amino acids, 10 minutes exposure to the labeled amino acid was used. All cover slips were then quenched in the freezing mixture and dried in the frozen state as described.

A variety of temperatures and times up to 21 hours of fixation with paraformaldehyde with and without deliberate control of the water vapor pressure were tried. Up to the present the best conditions regularly achieved for fixation of proline are a vapor temperature of 80°C in the presence of a water vapor saturation of 23% (provided by the saturated NaI solution). As shown in Table I, 21 hours exposure to the formalde-

TABLE I. *The Effect of Time in the Presence of a Controlled Water Vapor Pressure[a] on Fixation in Formaldehyde Vapor at 80°C*

Time (hours)	Countable radioactivity[b]	
	After exposure to fixative	After rinsing in water
2	48	71
4	56	72
21	19	79

[a] About 23% saturation, in equilibrium with saturated NaI solution [see "Handbook of Chemistry" (N. A. Lange, ed.), p. 1422. Handbook Publ., Inc., Sandusky, Ohio, 1956].

[b] Per cent retained following treatment when compared with immediately preceding state.

hyde vapor minimizes the leaching by water of the radioactivity which could be detected after the fixation step (Column 3). However the gain in percentage (71–79%) of retained label is small when compared with the loss in measurable activity suffered during fixation. This *apparent* loss in radioactivity (seen in Table I, column 2) occurs regularly with increasing exposure to the vapor fixative. It does not seem to be due to loss of label ^{3}H- from the compounds or loss of compounds from the

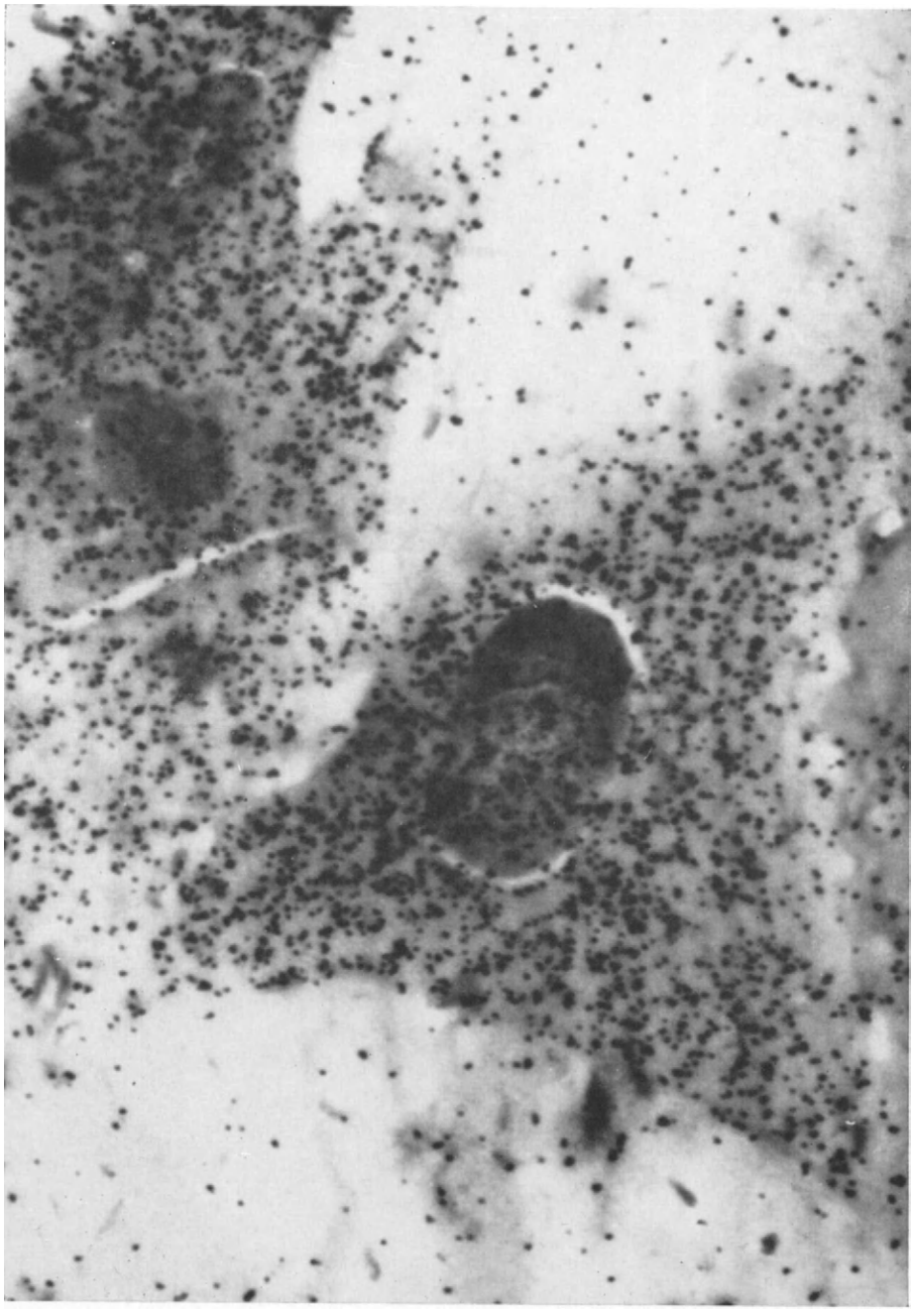

FIG. 2. Radioautograph of fibroblast monolayer cells incubated 10 minutes in medium containing 400 μc ^{3}H-proline per ml. Fixed in formaldehyde vapor at 80°C for 4 hours with 23 per cent humidity. Exposed 7 days. Hematoxylin-eosin counterstain. Magnification in microscope: × 160; in photomicrograph, × 1280.

tissue, but to absorption of the low energy β-particles by the polymerized material added during fixation.

Radioautography

Figure 2 shows a representative radioautograph of monolayer fibroblast cells. It is clear from this and many other preparations that the radioactivity is confined within cell boundaries. No differential disposition of the label within the cell can be made out. The presence of label over the nucleus is due in part to the fact that these are whole cells (not a section) and cytoplasm overlies the nucleus. The distribution after a shorter time or with a short "chase" may well show differential localization.

By count the ratio of grains over the cell to background in this case is greater than 10:1. The background regularly is variable due to factors not yet clear. One thought was that this was due to reduction of silver by residual aldehyde. However, when semicarbazide was used in an effort to remove possible free aldehyde and hence lower the background, no significant improvement occurred.

DISCUSSION

Previous attempts to localize by histochemical means, and we include here radioautography as a form of histochemistry, compounds soluble in aqueous or nonaqueous media have usually not attempted fixation. The most recent attempts were by Appleton [1], who used frozen sections cut at —10°C and dry stripping film attached at —20 to —30°C and maintained at the low temperature. The drawback of this and the similar technique used by Fitzgerald [9] and others comes immediately in the sectioning. It is a well known fact that during cutting of a frozen block with a knife the ice block melts at the knife edge. In fact this is the mechanism of the cutting process. Furthermore, the temperatures used permit substantial movements of water because the eutectic points of the salts in the tissues are quite low [2]. Thus there are many opportunities for diffusion or movement of unfixed substances.

Introduction of covalent bonding and polymer formation in cells and tissues under conditions designed to prevent movement of the substances provides a way around these difficulties. It was with the aim of inducing such bond and polymer formation that we originally used formaldehyde vapor on frozen-dried tissues for the purpose of fixing the highly soluble histamine [12].

The property of forming resinous products on reaction with other chemicals is one of the most useful characteristics of formaldehyde and

is the basis of its immense industrial importance in the synthetic resin industry. Under suitable conditions, the molecules of many compounds are linked together by methylene groups when subjected to the action of formaldehyde [16]. It has long been known that formaldehyde reacts with amines, imines, phenols, imidazoles, indoles, and sulfhydryl groups. In aqueous solution most of these reactions proceed smoothly at moderate temperatures. In the case of the imine group of proline this has been shown to occur [10]. Two distinct mechanisms are probably involved in resin-forming reactions: (1) the polycondensation of simple methylol derivatives, and (2) the polymerization of double-bonded methylene compounds [16]. Although in some cases the mechanism is definitely one or the other of the above, it is often not clear which is followed and both may play a part in some instances.

It is not clear from the experiments described to what the radioactive amino acid—proline in this instance—is tied in the cells by the fixation. However there are many compounds present in tissues, including proteins, sugars, unsaturated lipids, perhaps some of the nucleic acids, and small molecules, which may be linked to each other and to the proline by the formaldehyde. In addition to this type of linking, formaldehyde forms polymers with itself and these may help to build the fixing medium [16]. Evidence suggesting that soluble substances originally present in the cells are mainly responsible for the polymer formation with formaldehyde in the vapor comes from the following information: As noted in the experiment in Table I, extending the exposure of the cells to formaldehyde vapor from 4 hours to 21 hours causes a more than 70 per cent decrease in countable radioactivity. However, if one first treats the tissue with aqueous alcohol and then exposes overnight to formaldehyde vapor no such reduction in measurable activity occurs. Presumably this is due to loss of those substances contained in the cells which can be linked by formaldehyde. Otherwise the formation of the formaldehyde polycondensation products should reduce the radioactivity measured.

The use of reagents in the vapor phase which have the property of forming polymers with tissue constituents and with themselves provides a powerful technique applicable to a variety of freely soluble compounds of varying molecular weight. In this instance we have concentrated our attention upon formaldehyde. This has been done because formaldehyde is such a highly reactive substance and because it is particularly reactive with amine or imine groups. Other substances having similar properties are available and may be necessary since lipids, some sterols, and some aromatic compounds may not be fixed by formaldehyde even under the present conditions. In these instances other types of reactions, such as

oxidation by osmic acid vapor, may be suitable. Elsewhere we will report some experiments with other compounds.

The experiments described here were carried out on monolayers of cells cultured *in vitro*. In the present instance this was done as a matter of convenience. However, we know from previous experience that the same effects can be achieved by exposing the requisite small frozen-dried pieces of tissue to the formaldehyde vapor under the conditions presented here [3, 12, 17]. This has been followed by the usual embedding either in paraffin or plastic. The plastic has the advantage that thin sections (1 μ or less) can be made. These give superior resolution both in radioautography and with the highest powers of the light microscope. We still hope, though it may not be possible, eventually to attain morphological preservation with freeze-drying so that this technique can be applied at the electron microscope level.

SUMMARY

The aim of the work described here was to find a set of conditions capable of fixing soluble forms of amino acids in cells for radioautographic localization. The combination of freezing dehydration and exposure to formaldehyde vapor at 80°C in the presence of 20 per cent saturation of the gas phase with water vapor provided a high retention of soluble amino acids. Radioautographic localization showed the amino acids to be confined within the cell boundaries of cultured fibroblasts in monolayers on cover slips. A consideration of the mechanism of fixation suggests that it probably involves the formation of methylene bridges between adjacent molecules, particularly those containing free primary or secondary amines. In addition to this there may very well be formation of larger polymers with formaldehyde itself.

The general procedure of combining freezing dehydration and fixation in the dry state by gaseous reagents capable of forming covalently linked polymers with soluble substances is a powerful technique. It is potentially applicable to the fixation of a wide variety of small molecules containing radioactive labels which can be demonstrated by radioautography as well as by other histochemical reactions.

REFERENCES

1. Appleton, T. C., *2nd. Intern. Congr. Histochem. Cytochem. (Program & Abstracts)*, p. 97. Springer-Verlag, Berlin, 1964.
2. Benditt, E. P., Lagunoff, D., and Johnson, F. B., *Arch. Pathol.* **72**, 546 (1961).
3. Benditt, E. P., Lagunoff, D., and Holcenberg, J., *Ann. Histochim.* **8**, 221 (1963).
4. Branton, D., and Jacobson, L., *Stain Technol.* **37**, 239 (1962).
5. Carlsson, A., Falck, B., and Hillarp, H., *Acta Physiol. Scand.* **56**, Suppl. 195 (1962).

6. Chalkley, H. W., *J. Natl. Cancer Inst.* **4**, 47 (1944).
7. Edwards, L. C., and Udupa, K. N., *J. Biophys. Biochem. Cytol.* **3**, 757 (1957).
8. Eränko, O., *J. Histochem. Cytochem.* **12**, 487 (1964).
9. Fitzgerald, P. J., *Lab. Invest.* **10**, 846 (1961).
10. French, D., and Edsall, J. T., *in* "Advances of Protein Chemistry" (M. L. Anson and J. T. Edsall, eds.), Vol. 2, p. 278. Academic Press, New York, 1945.
11. Holcenberg, J., and Benditt, E. P., *Lab. Invest.* **10**, 144 (1961).
12. Lagunoff, D., Phillips, M., and Benditt, E. P., *J. Histochem. Cytochem.* **9**, 534 (1961).
13. Martin, G. M., *Nature*, **201**, 1338 (1964).
14. Martin, G. M., *Proc. Soc. Exptl. Biol. Med.* **116**, 167 (1964).
15. Miller, O. L., Jr., Stone, G. E., and Prescott, D. M., *in* "Methods in Cell Physiology" (D. M. Prescott, ed.), p. 237. Academic Press, New York, 1964.
16. Walker, J. F., *in* "Formaldehyde" (American Chemical Society Monograph Series), 2nd Ed. Reinhold, New York, 1953.
17. Wilske, K. R., and Ross, R., *J. Histochem. Cytochem.*, in press.

INTERCHANGE OF PROTEIN BETWEEN NUCLEUS AND CYTOPLASM[1]

LESTER GOLDSTEIN

Department of Biology, University of Pennsylvania, Philadelphia, Pennsylvania

INTRODUCTION

Two years ago at a similar symposium of this Society, I reported [5] on the progress that had been made up to that time on the study of two previously unknown classes of proteins in amebae that seem to be primarily localized within the cell nucleus.

Two conditions moved us to study these proteins. Our knowledge of the behavior and physiological role of nuclear proteins—even of the widely studied histones—is relatively minuscule and it is our belief that nuclear proteins may be "behaviorally" different from the proteins of the cytoplasm. Secondly, the behavior of one of these protein classes is so unexpected that the seeming uniqueness of its actions is itself sufficient to arouse an investigator's interest. More important, however, is the suggestion from these actions that the proteins may play a large role in the interaction between cytoplasm and chromosomes.

BACKGROUND

The essential characteristics of these two classes of protein were established by a variety of experiments [1, 2, 4]. It has been determined, by experiments with radioactively labeled cells, that the two classes together make up over 90 per cent of the total nuclear proteins of *Amoeba proteus*—the species upon which most of the experiments herein described have been performed. The class of proteins that is of primary interest is the one that has been shown to be in much higher concentration in nucleus than in cytoplasm but is in a constant state of back and forth migration between nucleus and cytoplasm. (This means, of course, that the migration, in one direction at least, must occur by mechanisms other than diffusion.) We have chosen for the present to call this class *cytonucleoproteins* (CNP). The other class of proteins does not appear to leave the nucleus during the normal cell interphase

[1] The work reported here was supported by grant GM-06774 from the U.S. Public Health Service.

(but Prescott [7] has evidence that they may be leaving at a slow rate when the interphase is greatly prolonged). This latter group we refer to as *nonmigrating proteins*. Our evidence suggests that histones are not a substantial fraction of either class of proteins.

The discovery of CNP was based on the initial observation that radioactivity that left a transplanted nucleus laden with ^{14}C-protein was found localized almost completely in the two nuclei, if the host was unlabeled at the outset and retained its own nucleus (Fig. 1). All subsequent experiments confirm the view that CNP must be shuttling back and forth between cytoplasm and nuclei, and spending most of the time in the nuclei. (We assume that in a normal cell the shuttling occurs between the cytoplasm and a single nucleus, but this is essentially impossible to demonstrate directly. Prescott [7] has indirect evidence that this is so.) In an experimental cell such as that shown in Fig. 1, the radioactivity was observed to be on the average 2.6 times more concentrated in the grafted nucleus than in the host cell nucleus. This consistent inequality led to the conclusion, substantiated by many experiments, that the nucleus contained another class of proteins (comprising, as calculations from the data in Table II show, about 37% of all the nuclear proteins) that was nonmigrating during the interphase between cell divisions.

A variety of experiments leave little doubt that the label we see, and which we take as a marker for the two classes of proteins, is indeed in protein [1, 2]. It also has been established that CNP shows varying degrees of "specificity" in interspecies grafts [1], that the rate by which the distribution of label between host and donor nuclei reaches equilibrium has a Q_{10} of approximately 1.3 [2], that CNP and nonmigrating proteins show very little metabolic breakdown over at least 4 cell generations [2], that both classes are uniformly distributed *throughout the cell* during mitosis [2, 7], and that both classes of protein are probably synthesized—at least in part—in the cytoplasm [2].

Having established the above, we continued to refine some of our experimental procedures and projects in our sustained effort to understand what part these proteins play in the physiology of the cell. In this paper we report on our endeavors: (a) to determine the localization of the proteins in the nucleus and in the cytoplasm; (b) to determine the proportion and relative concentration of CNP in nucleus and cytoplasm; (c) to comprehend the mechanism by which the CNP concentration difference in the two compartments is maintained; and (d) to extract, purify, and characterize the proteins specifically. With respect to these objectives, this can be considered only a progress report.

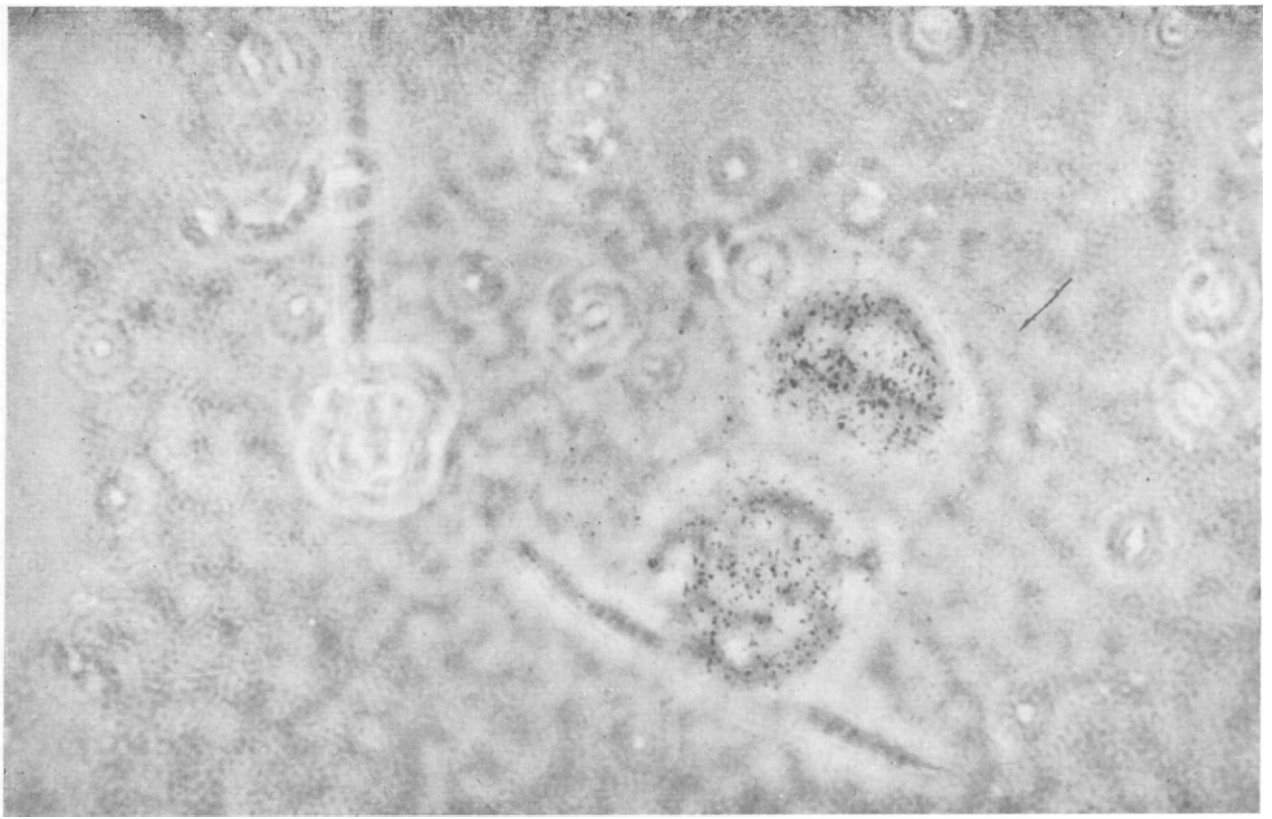

FIG. 1. Autoradiograph of part of a squashed ameba (out of focus) into which was grafted a ^{14}C-L-lysine labeled nucleus 20 hours before fixation. Radioactivity is almost completely localized in the two nuclei. Magnification: *ca.* 500 ×.

EXPERIMENTAL

Localization of CNP and Nonmigrating Proteins in the Nucleus

We had reported earlier that examination of sectioned cells into which ^{3}H-protein-labeled nuclei were grafted showed the radioactivity to be more or less uniformly distributed through the nucleus. In fact, in both host cell nucleus and grafted nucleus, it was not possible to detect particular associations of label with any structure visible in the light microscope; we took this to mean that neither class of proteins was a significant component of such features as nucleoli or nuclear envelope or any invisible structure, since no localized high concentration of radioactivity was discernible.

This view of intranuclear protein localization has been altered by the results of more recent investigations. We now have a better view as a result of experiments in which centrifugation of cells helped reveal structural associations that had been missed earlier.

Nuclei were transplanted from amebae[2] whose proteins were heavily labeled with a variety of ^{3}H-amino acids (arginine, histidine, leucine, lysine, proline, phenylalanine, tryptophan, and tyrosine) into unlabeled amebae and, after a post-operative incubation of at least 6 hours, were centrifuged. For centrifugation the experimental cells were placed in ameba medium layered over 30 per cent Ficoll in a 0.2 ml centrifuge tube and spun in a microcentrifuge (Micro-Chemical Specialties Co.) at 10,000 *g* for 20 minutes in a refrigerator at approximately 4°C. Within 2 minutes after the current to the centrifuge was reduced to zero, the cells were fixed by squashing on slides in the usual fashion [1]. The centrifugation procedure derives from a method developed by Rabinovitch and Plaut [8]. Autoradiography and other processing was carried out as previously described. (For details of methods not described here, see Byers *et al.* [1].) With experience it became possible to determine with considerable certainty which end of the cell was centrifugal and which centripetal [3].

Examination of the centrifuged cells at once revealed a striking feature: the label in the more radioactive nucleus of a cell had been caused to stratify, but the label in the less radioactive (or host cell) nucleus was apparently unmoved by the centrifugal forces (see Fig. 2). It is evident, however, that not all of the label in the grafted nucleus was stratified; rather the concentration of autoradiographic grains over the centripetal

[2] All donor labeled cells in the original experiments discussed in this paper were removed from media containing radioactive material at least 12 hours prior to nuclear transplantation experiments. This reduced the pool of intracellular acid-soluble radioactivity to a relatively insignificant size by the time of the operation.

end of that nucleus was seen to be approximately the same as the concentration over the host nucleus. From this we conclude that it is only the nonmigrating proteins that are sedimentable and associated with some intranuclear structure, whereas CNP seem not to be associated with any (at least stratifiable) structure. Our preparations do not permit a clear discrimination of internal nuclear structure and, thus, at present we cannot even be certain that the sedimentable nuclear radioactivity is asso-

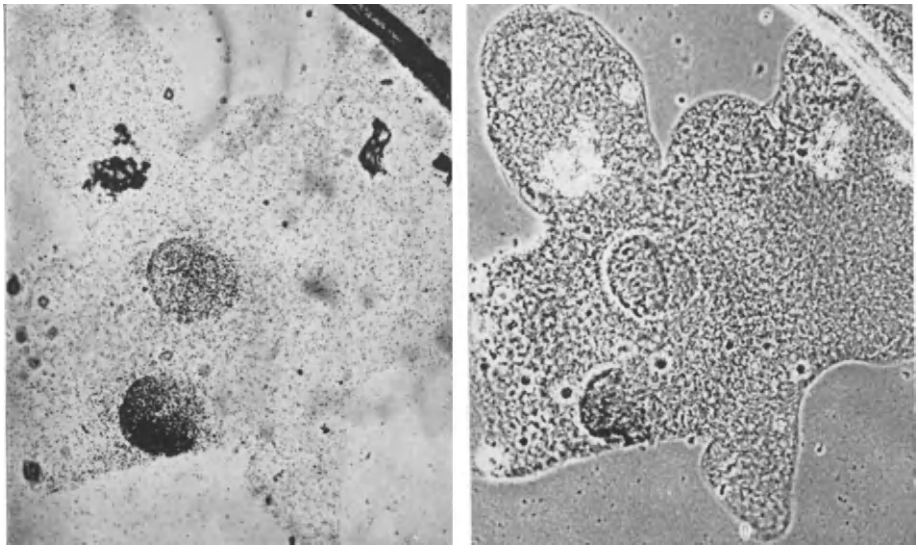

FIG. 2. Autoradiograph (left) and phase-contrast view (right) of part of a squashed ameba into which was grafted a ^{3}H-protein nucleus approximately 24 hours before centrifugation followed by immediate fixation. Centrifugal end of cell is toward left; lower nucleus is the grafted one. Magnification: *ca.* 200 ×.

ciated with nucleoli, which seem to be the only microscopically detectable nuclear structures that are stratified. Our present (not very clear) view of cytological detail, in fact, leads us to suspect that the sedimentable label is *not* associated with nucleoli. It is evident that we will have to employ more refined methods (probably at the electron microscope level) to determine precisely with what structures the intranuclear protein label is associated.

Localization of CNP in the Cytoplasm

Our earlier studies, which included centrifugal analysis, revealed little of *cytoplasmic* CNP localization. But, again, our recent use of centrifugation has shown more than we had been able to discover previously.

When cells treated like those described in the above section (or, in some cases, the same cells) were examined for distribution of autoradiographic grains over the cytoplasm, the label appeared to be distributed more or less uniformly through almost all of the cytoplasm. This distribution of radioactivity contrasts markedly with the distribution of cytoplasmic organelles and other materials, which are stratified into rather distinct layers by centrifugation [3]. There are two exceptions to the uniformity of autoradiographic grain distribution over the cytoplasm.

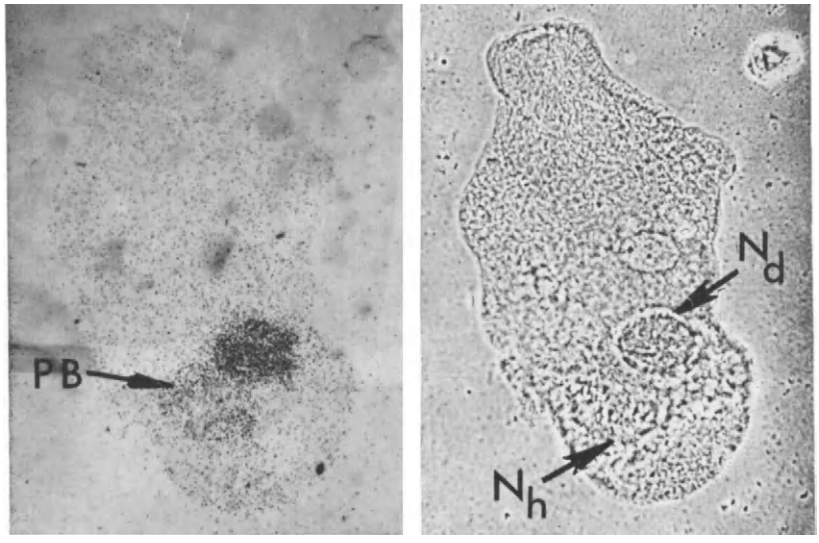

FIG. 3. Autoradiograph (left) and phase-contrast view (right) of a squashed ameba into which was grafted a ^{3}H-protein nucleus approximately 24 hours before centrifugation, followed by immediate fixation. Centrifugal end is toward bottom. PB, Perinuclear band; N_d, grafted nucleus; N_h, host cell nucleus. Magnification: *ca.* 200 ×.

In well-fed cells, the concentration of autoradiographic grains is low over the centrifugal end, obviously because the unlabeled food vacuoles make up the bulk of the cytoplasm in that region. The other, and more interesting, exception is that in many cases there is seen a "band" of higher radioactivity extending from one side of the nucleus in what may be any direction in any particular cell (Fig. 3). In whatever direction this band of radioactivity extends, it almost always appears to be only on one side of the nucleus and usually extends for one or two nuclear diameters from the nucleus.

These phenomena seem to relate to the observations—in uncentri-

fuged cells—of a decreasing gradient of radioactivity extending away from the nucleus in *all* directions for about 1 to 2 nuclear diameters into the cytoplasm. This latter observation was heretofore unexplained but now seems to be due to the presence of some kind of perinuclear structure that, as a first guess, may be concerned with the transport of CNP into and out of the nucleus. Here, too, electron microscopic studies should be carried out to discover the structural basis of these radioactivity patterns.

Quantitative Aspects of the Distribution of CNP in Nucleus and Cytoplasm

A variety of matters, such as an interest in the machinery responsible for the maintenance of unequal concentrations of CNP on either side of the nuclear envelope, has prompted us to investigate in a careful quantitative way a number of features of CNP distribution in the cell. We earlier knew, for example, that the nuclear concentration of CNP was between 40 and 240 times greater than the cytoplasmic concentration [1] and that this concentration difference is maintained in the face of what seemed like an almost equal concentration of *total* protein in both compartments. Data like these, however, were from either indirect or crude experiments and a more rigorous analysis seemed in order.

(1) *Relative Concentration of Total Protein in Nucleus and Cytoplasm*

To obtain a standard by which to compare our experimental results, we determined the relative amount of protein label in nucleus and cytoplasm. Amebae were grown on ^{3}H-amino acid-labeled *Tetrahymena* for at least 2 generations, by which time the concentration of label in nucleus and cytoplasm relative to one another would have reached (we assumed) an equilibrium state. Cells from such a population were freeze-substituted and then "fixed" with acetic acid, embedded in paraffin, sectioned at 2 μ, and processed for autoradiography with Kodak NTB-2 liquid emulsion (see Fig. 4). Autoradiographic grain counts were made over *ca.* $1.5 \times 10^4\ \mu^2$ of cytoplasm and *ca.* $5.5 \times 10^2\ \mu^2$ of nucleus on the average. The concentration of grains per unit area is shown for 14 cells in Table I. Note that the nucleus is approximately 2¼ times as radioactive as the cytoplasm. According to interference microscope measurements performed on this material by Professor A. W. Pollister, the nucleus and cytoplasm have the same dry mass per unit area and, thus, there is no need to make the corrections for self-absorption that Maurer and Primbsch [6] find necessary for other kinds of material. We feel confident, therefore, in concluding that the grain count distribution shown in

Table I is a measure of the relative concentration of protein in nucleus and cytoplasm.

(2) *Relative Concentration of CNP in Nucleus and Cytoplasm*

Our previous attempts to estimate the relative concentration of CNP in nucleus and cytoplasm were hampered by the fact that the difference

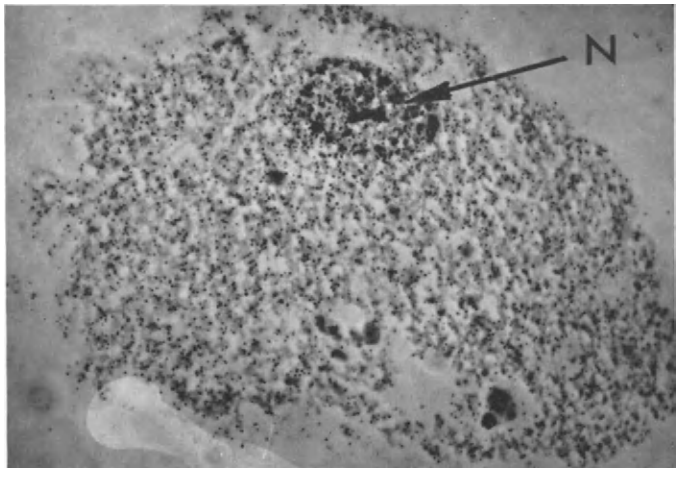

FIG. 4. Autoradiograph of a 2 μ section through a cell that had been grown in the presence of ^{3}H-amino acids for more than 2 cell generations. The section is Giemsa stained. Magnification: *ca.* 500 ×.

TABLE I. *Comparison of ^{3}H-Protein Activity in Nucleus and Cytoplasm of "Uniformly" Labeled Amoeba proteus (Number of Grains/25μ^2)*

Cell	Nucleus	Cytoplasm
A1A (IV)	18.98	8.68
A1C (I)	14.60	6.53
A1A (II)	10.96	5.29
A1A (III)	17.58	6.57
A3A (IV)	17.32	6.92
B3A —	11.47	6.31
A3A (III)	13.45	6.98
A3A (II)	14.70	5.54
A3A (I)	11.51	5.18
B1A (I)	12.29	5.72
B1B (I)	16.38	6.44
B1A (II)	12.61	6.14
B1B (II)	16.60	6.74
B1A (III)	14.53	6.08
	$\overline{X} = 14.45 \pm 1.37$	$\overline{X} = 6.37 \pm 0.47$

in concentration was so great that no autoradiographs could be obtained that would permit reasonable grain count determinations to be made in both nucleus and cytoplasm of the same cell. If the grain concentration over nucleus was sufficient for assay, little or no activity would be detectable over cytoplasm; if the grain concentration over the cytoplasm was high enough for reasonable estimation, the autoradiographs over nucleus would be almost a solid mass of black grains.

To circumvent this difficulty, *enucleate* cells that had received ^{3}H-protein nuclei at least 6 hours before were freeze-substituted and processed as those described in the above section. In this instance, however, alternate sections were placed on different slides and some were kept under autoradiographic emulsion long enough for nuclear grain counts (generally 2–4 hours) and slides with adjacent sections were kept under emulsion long enough for cytoplasmic grain counts (approximately 5–10 days). The grain counts were adjusted for the difference in emulsion exposure times and we calculated that the nucleus contained an average of 61 per cent of the CNP of the cell (see column marked "Mononucleate" in Table II). Since the nucleus makes up only about 2 per cent of the volume of the cell, the nuclear concentration of CNP is approximately 75–80 times as great as the cytoplasmic concentration. This, you will recall, compares with the approximately 2¼-fold difference in concentration of

TABLE II. *Comparison of CNP Content of Nuclei and Cytoplasm in Mononucleate and Binucleate Cells*

	Per cent of total cell CNP label in nuclei	
Cells	Mononucleate	Binucleate (both nuclei combined)
3a + 3b	53	79
6a + 6b	41	57
13a + 13b	41	79
1a + 1b	63	76
14a + 14b	84	89
4a + 4b	77	85
12a + 12b	66	85
10a + 10b	79	84
23a + 23b	63	69
20a + 20b	65	71
25a + 25b	37	88
	$\overline{X} = 61\%$	$\overline{X} = 78.5\%$
Therefore the cytoplasmic share is:	39%	21.5%
Ratio of nuclear CNP/cytoplasmic CNP is:	*1.56*	*3.65* (or *1.82* for each nucleus)

total protein and thus dramatically calls attention to a remarkable concentration gradient for CNP.

[To arrive at the proper concentration relationships in a mononucleate cell it is necessary to account for the contribution by labeled nonmigrating nuclear proteins to the total nuclear autographic grain count. This contribution was estimated from analyses of the binucleate members of a pair of cells (see next section) by the following formulation:

$$\text{Per cent of total cell radioactivity in non-migrating protein in binucleate cell} = \frac{N_1 - N_2}{N_1 + N_2 + \text{Cyto}_B} = X$$

$$\text{Per cent nuclear activity in CNP in mononucleate cell} = N_3 - X = Y$$

$$\text{Per cent of cell's total CNP in nucleus of mononucleate cell} = \frac{Y}{Y + \text{Cyto}_M}$$

N_1 = "Total" radioactivity in grafted nucleus in binucleate cell.
N_2 = "Total" radioactivity in host cell nucleus in binucleate cell.
N_3 = Per cent of "total" cell radioactivity in nucleus of mononucleate cell.
Cyto_B = "Total" radioactivity in cytoplasm of binucleate cell.
Cyto_M = Per cent of "total" cell radioactivity in cytoplasm of mononucleate cell.

These calculations are based on a number of assumptions and some of the estimates are not very accurate. Certainly the differences between members of a pair (Table II) is sufficiently variable to suggest restraint in the formulation of definitive conclusions. There is, however, sufficient internal consistency of the averaged values in this and other sections to suggest that we are not far from the mark in some of our more general conclusions.]

(3) *Comparison of Relative Concentration of CNP in Nucleus and Cytoplasm of Mononucleate and Binucleate Cells*

We had noted in earlier experiments that there seemed to be a difference in relative concentration of cytoplasmic CNP label between mononucleate and binucleate cells. This led us to investigate whether this was true, alert to the possibility that detection of a difference of this sort might lead to an insight into the nature—or at least the site—of the mechanism responsible for the maintenance of the CNP concentration difference between nucleus and cytoplasm.

The following experiment was designed to compare the relative activities of mononucleate and binucleate cells. The sister cells of a recent division of an unlabeled cell were used as paired cells: one was enucleated and the other not. Into each of these host cells was grafted a nucleus from one sister cell or the other of a relatively recent division of a ^{3}H-protein labeled cell. The recipient cells were then kept paired through all further processing—which was identical to the processing described in the previous section. (In fact, the cells described in the

preceding section *were* the mononucleate cells discussed in this section.) Carrying out the experiment in the fashion described, e.g., paraffin blocks with but 2 paired cells, led to a considerable loss by the end of the complete processing. We thus were left with a total yield of only 11 pairs usable for the final analysis, although our initial group consisted of over 50 pairs. Particularly distressing, moreover, is the fact (revealed by examination of Table II) that keeping the cells paired through the entire experimental processing apparently did not yield data better than would have resulted from lumping all mononucleate cells in one group and all binucleate cells in another.

The data in Table II seem to show that the cytoplasm of the binucleate cell has a smaller share of CNP than does the mononucleate cell cytoplasm, whereas the ratio of nuclear activity to cytoplasmic activity for mononucleates versus binucleates (1.56 versus 1.82) is fairly close and cannot be shown to be significantly different. Taken together, these figures suggest that some enzyme-like mechanism—perhaps in the nuclear envelope—is responsible for the maintenance of a constant proportionality between the two compartments, irrespective of the absolute quantities and/or volumes involved. Even this conclusion, however, is a deceptive simplification because the data refer only to the distribution of *labeled* CNP, while there exists an easily overlooked difference in the *amount* of CNP in mononucleate and binucleate cells.

If we set the amount of CNP in a normal mononucleate cell at 100 (61 parts in nucleus, 39 parts in cytoplasm), then the amount in a binucleate is 161 (2×61 parts in nuclei, 39 parts in cytoplasm at the time of the operation). From this we see that 21.5 per cent (the proportion of radioactivity) of 161 equals 35 parts for the cytoplasmic share of CNP and this is close to the 39 parts in the cytoplasm of the mononucleate cell. This means that the distribution between the two compartments is probably identical in amount and in concentration for both mononucleate and binucleate cells.

Regrettably, then, we find that we really have learned nothing of the mechanism by which the CNP concentration difference is maintained. All we seem to have achieved is some confidence that our analytical methods are reasonable ones. Perhaps some clues will be forthcoming if and when we can change the relative amount of CNP in the cell independently of any change in the number of nuclei or by some other procedure of that sort.

Attempts at Isolation and Purification of the Nuclear Proteins

In the face of frustration following several attempts to characterize physicochemical properties of CNP and nonmigrating proteins by *in situ*

methodology, we have turned to extraction procedures followed by traditional biochemical methods. The biochemical methods require, of course, relatively large amounts of material; in fact, the more conventional methods would probably—in this instance—require millions of isolated nuclei. We believe that isolated nuclei may be far from normal (indeed, Prescott [7] has shown rapid leakage of protein from isolated *A. proteus* nuclei), so that we feel compelled to seek other methods for "isolating" nuclei.

Nuclei from amebae that contained high specific activity ^{3}H-proteins were grafted into unlabeled cells in large numbers and each cell was placed in an ice bath immediately after each operation. In such cells *all* the radioactivity, even that which may pass to the cytoplasm, will be of nuclear origin and we can then assume that we have, in effect, isolated radioactive nuclei in sacs of unlabeled cytoplasm—thereby avoiding artifacts induced by routine nuclear isolation procedures. (It should be noted that the donor cells were removed from labeled media at least 12 hours before the operations; this precaution, along with the cold temperature storage, we believe effectively prevents the incorporation of low molecular weight precursors into macromolecules after the operation.) In this manner, approximately 100 nuclei were "isolated" for each attempt to extract and purify nuclear proteins. The 100 or so cells containing the radioactive nuclei were mixed with 10^6 to 2×10^6 unlabeled cells packed by centrifugation and an equal volume of ameba medium. The entire mixture was homogenized with a Potter-Elvejhem glass homogenizer in an ice bath for about 5 minutes and the homogenate was centrifuged at 25,000 *g* for 1 hour. The supernatant fluid, which contained on the order of 80 per cent of the radioactivity of the operated cells, was used in all subsequent procedures. Following fractionation, the radioactivity of each protein fraction was assayed in a liquid scintillation system.

We have tried 3 fractionation procedures: (a) differential solubility in varying concentrations of acetone; (b) electrophoresis in polyacrylamide gels; (c) differential solubility in varying concentrations of ammonium sulfate. The first two methods have given ambiguous results thus far and will require modifications if they are ever to prove useful. The ammonium sulfate fractionation procedure yielded clear results, an example of which is shown in Table III. Although the results are clear, they are disappointing in view of the fact that the label is present in significant amounts in all fractions (in fact, the specific activity of radioactive protein is roughly the same for each fraction). This suggests that the proteins we are dealing with are a heterogeneous mixture—at least with respect to ammonium sulfate solubility—and that attempts at *in vitro* characterization may be very difficult indeed.

TABLE III. *Fractionation of Nuclear Protein Radioactivity by Means of Ammonium Sulfate Solubilities*

Fraction[a]	Per cent total extract radioactivity
0–0.50	9
0.50–0.71	25
0.71–0.90	16.5
0.90–1.20	16
1.20–1.60	10
1.60–2.10	3
Final supernatant solution	20.5

[a] Represents the material that is insoluble in the indicated grams of ammonium sulfate added to 3.5 ml of ameba extract solution continuously maintained in an ice water bath, except for the intervals when the solution was centrifuged to sediment a precipitate. The centrifuge rotor temperature was maintained at 2° ± 1°C.

The Effect of Actinomycin D on the Nuclear Proteins

The use of one sort of inhibitor or another is often helpful in illuminating aspects of cellular physiology, but rarely with free-living amebae. One exceptional inhibitor is actinomycin D, which very effectively inhibits ribonucleic acid (RNA) synthesis in *A. proteus*. Because of this effectiveness and because of its presumed action on cellular genetic systems (see, e.g., Reich *et al.* [9]) we investigated the effect of actinomycin D on the two classes of proteins in which we are interested.

Nuclei from cells that had incorporated ^{3}H-leucine for about 24 hours and then had been incubated in unlabeled medium for another 24 hours were transplanted into unlabeled amebae that had been incubated in 70 μg actinomycin D/ml (a concentration that reduces the incorporation of ^{3}H-nucleosides into RNA by over 90 per cent) for from 2 to 78 hours. The operated cells were further incubated in the inhibitor solution for 19 to 25 hours before being fixed and processed for autoradiography. After development, grain counts of the autoradiographs were performed; in some cells the nuclear activity was assayed, in others the cytoplasmic activity was assayed.

We expected that, if actinomycin D had affected the association of CNP or nonmigrating proteins with an intranuclear structure, the effect would be indicated by a significant alteration in the 2.6:1 ratio of donor-to-host nuclear radioactivity. If, e.g., the association of CNP with intranuclear materials was inhibited, we could expect that the ratio might rise; if the nonmigrating protein association were affected, the ratio might diminish. In 25 experimental cells the mean ratio of donor-to-host nuclear

radioactivity was found to be 3.25:1 but the "*t* test" reveals this not to be significantly different from 2.6:1. (The preincubation time of the host cell in actinomycin D—2 to 78 hours—was of no significance.) If the rise in the ratio were meaningful, it would suggest that less CNP was being "bound" in the nucleus and that, therefore, the amount in the cytoplasm would be greater. Analysis of the cytoplasmic activity reveals, however, also no significant increase in actinomycin-treated cells.

DISCUSSION AND CONCLUSION

Our goal—to understand the physiological roles played by CNP and the nonmigrating proteins—remains elusive. The accumulation of data does, however, continue to illuminate certain aspects of the nature and behavior of these proteins and we are optimistic enough to feel that a deeper understanding may come after the acquisition of not too many more clues.

We now see the beginnings of an insight into the structural associations within the nucleus of CNP and of the nonmigrating proteins. That the two classes can be separated *in situ* by centrifugation urges us to seek refined microscopic techniques to pinpoint the specific structures involved. When we determine with precision the localization of chromatin and nucleoli and the particular radioactive fractions in the nucleus, we shall be—we believe—well on the way to removing several uncertainties about the roles played by these proteins.

This capacity to separate the two protein classes by centrifugation may prove to have an additional value for *in vitro* studies. If the *in vivo* structural associations are maintained after cell homogenization, it may be possible to achieve separations of the proteins from each other and from other components of a cell homogenate by traditional centrifugation methods, and this possibility is being investigated.

The latter possibility has particular importance in view of the results of our attempts to isolate and purify the proteins by other methods. Our best efforts have shown that as far as ammonium sulfate solubilities are concerned the nuclear proteins are a heterogeneous lot. Thus, if useful separations and purifications are to be achieved, we must look to fractionation methods that are dependent on other properties of the proteins and hope that CNP and nonmigrating proteins have properties *in vitro* that distinguish them from other cellular proteins.

The results of extensive labors to describe the quantitative aspects of nuclear and cytoplasmic proteins must be considered a disappointment at this time. We have determined that, whereas for total protein the nuclear concentration is about 2¼ times that of the cytoplasm, for CNP

the nuclear concentration is some 80 times that of the cytoplasm and this means that 60–65 per cent of the cell's total CNP is in the nucleus at any one time. Moreover, the distribution of CNP between nucleus and cytoplasm of mononucleate and binucleate cells seems to be identical and provides, therefore, none of the anticipated clues to the mechanism by which the concentration difference is maintained. Perhaps some day the knowledge of the quantitative relations may be put to some worthwhile use, but for now it is simply additional background material.

Finally, experiments with actinomycin D have shown us that neither CNP nor nonmigrating proteins seem to be associated with DNA in a way that could be blocked by the action of that antibiotic. At this moment, that seems like a minor clue, indeed.

SUMMARY

This is a report of recent progress in the study of the migrating proteins (CNP) and nonmigrating proteins of the *Amoeba proteus* nucleus. It has been shown that the nonmigrating proteins are sedimentable by centrifugation *in situ* in the nucleus, whereas CNP are not. CNP are largely nonsedimentable in the cytoplasm but those CNP molecules in the cytoplasm immediately surrounding the nucleus do seem to be associated with some sedimentable cytoplasmic structure.

Quantitative studies have shown that the nuclear concentration is about 2¼ times the cytoplasmic concentration of total protein. For CNP, however, the nucleus has 75–80 times the concentration of the cytoplasm and, thus, has 60–65 per cent of the cell total. Comparisons of CNP distribution between nucleus and cytoplasm of mononucleate versus binucleate cells show no significant differences, thereby effectively masking any clue to the mechanism by which the CNP concentration is kept different on either side of the nuclear envelope.

Attempts at isolation of the nuclear proteins have thus far shown the material to be a fairly heterogeneous group of proteins, foreboding thereby a difficult course for fruitful *in vitro* studies.

Actinomycin D appears to have little or no effect on the association of either CNP or nonmigrating proteins with the nucleus.

REFERENCES

1. Byers, T. J., Platt, D. B., and Goldstein, L., *J. Cell Biol.* **19**, 453 (1963).
2. Byers, T. J., Platt, D. B., and Goldstein, L., *J. Cell Biol.* **19**, 467 (1963).
3. Daniels, E. W., *J. Protozool.* **11**, 281 (1964).
4. Goldstein, L., *Exptl. Cell Res.* **15**, 635 (1958).
5. Goldstein, L., *Symp. Intern. Soc. Cell Biol.* **2**, 129 (1963).
6. Maurer, W., and Primbsch, E., *Exptl. Cell Res.* **33**, 8 (1964).
7. Prescott, D. M., *Symp. Intern. Soc. Cell Biol.* **2**, 111 (1963).

8. Rabinovitch, M., and Plaut, W., *J. Cell Biol.* **15**, 525 (1962).
9. Reich, E., Goldberg, I. H., and Rabinowitz, M., *Nature* **196**, 743 (1962).

Discussion

Dr. Prescott: The discovery of migratory proteins is most certainly important, even though their function is unknown. Perhaps they function as a reverse messenger, communicating cytoplasmic demands to the nucleus.

We have timed the release and return of the protein to the nucleus during division. All the labeled protein is released to the cytoplasm abruptly at late prophase, and about 90% of it has returned to the nucleus by 20 minutes after cytokinesis.

Does the figure of 80 for the nuclear/cytoplasmic ratio of protein concentration include both cytonucleoproteins and nonmigratory protein?

Dr. Goldstein: The concentration of cytonucleoproteins alone is 80 times greater in nucleus than cytoplasm.

Dr. Prescott: Does the maintenance of label in the nuclear-specific proteins over a period of four cell cycles imply little or no turnover of these proteins?

Dr. Goldstein: A detectable increase in the cytoplasm of cells after four divisions suggests that there is a significant but small turnover of these proteins.

Dr. Schultze: With regard to mammalian tissues, I did not find evidence of migration of protein between nucleus and cytoplasm of liver cells, presumably because ordinary methods would not detect a quick exchange back and forth. In muscle cells, where the nuclear activity is concentrated in the nucleolus, such a movement from cytoplasm to nucleus would be very unlikely.

Dr. Allfrey: If protein synthesis were to be inhibited by administration of Puromycin to cells containing *hot* cytoplasm, but receiving a *cold* nucleus, would the hot protein move into the nucleus under these conditions?

Dr. Goldstein: The highest nontoxic concentrations of Puromycin used are without significant effect on amino acid incorporation in amebae.

AMINO ACID DEPRIVATION AND DEOXYRIBONUCLEIC ACID SYNTHESIS IN *TETRAHYMENA*[1]

G. E. STONE AND D. M. PRESCOTT

Department of Anatomy, University of Colorado Medical Center, Denver, Colorado

Aside from the event of cell division itself, deoxyribonucleic acid (DNA) synthesis is currently the only point of reference on which the search for additional specific synthetic events forming the progress of the cell cycle can be based. By definition, some of these unknown events can be expected to occur at single specific time segments within the cycle. Histones, for example, have been demonstrated to double in amount in the nucleus simultaneously with DNA synthesis [1, 4, 6]. The study by Gall [6] showed that histone increase is linked very closely to that particular DNA replicating at any given moment of time. None of these studies have distinguished, however, between actual synthesis of histone in the nucleus and, alternatively, its simple accumulation from the cytoplasm in step with DNA replication [3].

Some of the studies presented in this paper were intended to show the effects of amino acid deprivation, imposed at various times in the cell cycle, on progress through the cycle, and specifically on the initiation and maintenance of DNA synthesis. This experimental approach was considered one means of testing the proposition that the timing and continuity of the cell cycle is composed, in part, of the sequential appearance of new proteins. The work subsequently led into a study of the maintenance and turnover of soluble pools of thymidine derivatives in relation to the cell life cycle, and these results are also reported here. Methodological details not given here can be found in a study by Stone and Prescott [13].

All of the work was carried out on *Tetrahymena* grown at 29°C primarily in synthetic medium [5] supplemented with 0.04% (w/v) of proteose peptone. Under these conditions the generation time is 225 minutes. The positions and relative lengths of the subsections of the cell cycle (determined by incorporation of ^{3}H-thymidine into DNA) are

[1] Supported in part by Biology Division, Oak Ridge National Laboratory, operated for the Atomic Energy Commission by Union Carbide, and in part by National Science Foundation grant GB-1635.

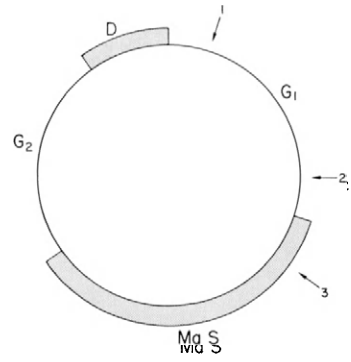

FIG. 1. The cell life cycle of *Tetrahymena pyriformis* strain HSM grown at 29°C in supplemented medium. G_1 (30% of the cycle) and G_2 (25% of the cycle) are in reference to macronuclear DNA synthesis (S, 35% of the cycle), and *D* (10%) represents the period of cytokinesis. The numbers 1, 2, and 3 refer to times at which cells were deprived of essential amino acids.

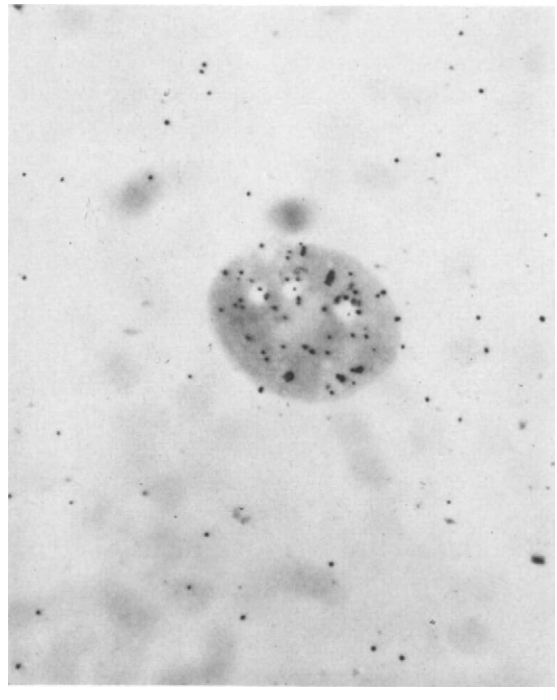

FIG. 2. Cells incubated with ^{3}H-thymidine after deprival of histidine and tryptophan during G_1. Note the radioactivity over the cytoplasm and lack of concentration over the nucleus. Magnification: approx. × 1000.

shown in Fig. 1 and are as follows: the period from the end of cytokinesis to the beginning of DNA synthesis (G_1) occupies the first 30% of interphase; DNA synthesis (S phase) occupies the next 35% of interphase; the period between the end of DNA synthesis and the beginning of cytokinesis (G_2) takes up the last 25% of interphase, and cytokinesis requires about 10% of the total generation time. The experiments were carried out on small groups of *Tetrahymena* moving through the cycle in synchrony. Synchrony was achieved by initial selection of dividing cells from a logarithmic phase culture with a braking pipette [7, 11].

When cells in any part of the G_1 period were transferred to a medium lacking histidine and tryptophan (both are absolute requirements for *Tetrahymena*), the cycle could not be completed and division did not occur. If the deprivation of histidine and tryptophan was imposed any time after the S period had begun, cells finished the cycle, completed division, and came to rest in the next G_1 (unless the deprivation of amino acids was relieved). These observations indicated that the transition from G_1 to S is a key point with respect to the supply of amino acids

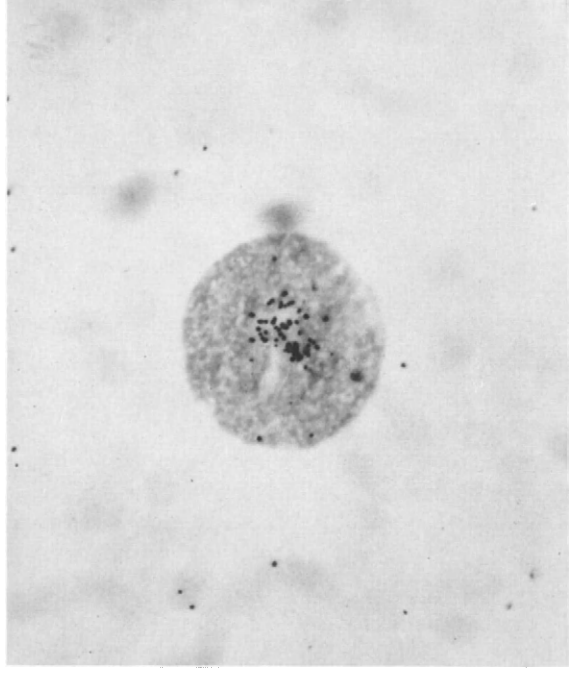

FIG. 3. An autoradiograph of a cell deprived of histidine and tryptophan in early S and incubated in ^{3}H-thymidine medium for 30 minutes. DNA synthesis is not interrupted by the deprivation.

and suggested a study of ^{3}H-thymidine incorporation into DNA in relation to amino acid deprivation. Cells transferred during G_1 to a medium lacking the two amino acids failed to incorporate ^{3}H-thymidine into macronuclear DNA when the normal time for the beginning of the *S* period was reached (Fig. 2). If the cells were deprived of the amino acids *after* the G_1 to S transition had already occurred, ^{3}H-thymidine in the medium was readily taken up and incorporated into macronuclear DNA (Fig. 3). (Although no macronuclear incorporation of ^{3}H-thymidine occurred subsequently in cells deprived of amino acids during G_1, some radioactivity was taken up into the cytoplasm. This radioactivity was not acid soluble but could be removed by deoxyribonuclease digestion. Further studies have shown that this apparent cytoplasmic synthesis of DNA takes place in the mitochondria and is discussed in detail elsewhere [12].) This first set of experiments led to the tentative conclusion that amino acid deprivation prevented the new synthesis of one or more proteins that were required for the initiation of DNA synthesis. Rather than rely only on ^{3}H-thymidine incorporation as an indicator of DNA synthesis, however, Feulgen microspectrophotometric measurements of DNA were made on cells deprived of the two essential amino acids in G_1. Surprisingly, these measurements indicated that cells deprived any time prior to the beginning of DNA synthesis and allowed to incubate for a time that would normally carry them well beyond the *S* period, contained on the average, 20 per cent more DNA than the G_1 macronucleus (Fig. 4). Consequently, it had to be concluded that DNA synthesis is initiated in the absence of the two amino acids but that ^{3}H-thymidine from the medium cannot be used for this partial synthesis.

At this point the experiments were interpreted by us as evidence that cells in the G_1 condition lack certain enzymes required to produce thymidine triphosphate (TTP) from exogenous thymidine or other pyrimidine sources. *Tetrahymena* is able to satisfy all of its pyrimidine requirements with uracil (uracil and cytidine are normally the only two pyrimidine sources in the synthetic medium), and it is probable that TTP is synthesized from uracil through deoxyuridine monophosphate as shown in Fig. 5. It had to be concluded that at least one enzyme [either thymidine monophosphate (TMP) or thymidine diphosphate (TDP) kinase] common to both pathways of TTP synthesis was absent in G_1 cells. Hotta and Stern [8] have shown that thymidine kinase (for the conversion of thymidine to thymidine monophosphate) is absent from G_1 cells in *Lilium* anthers and appears at the beginning of S. The G_1 absence of this same enzyme in *Tetrahymena* could explain the failure of cells deprived of amino acids to utilize ^{3}H-thymidine for DNA synthesis, but the absence of an additional enzyme or enzymes would have to

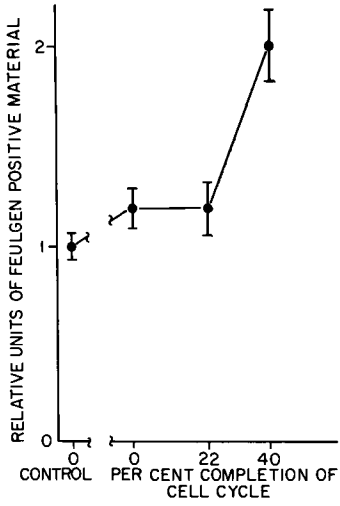

FIG. 4. Relative units of Feulgen-positive material of: cells measured immediately after division (control); cells deprived at 0 time, incubated for 24 hours, and then measured; cells deprived at 22 per cent completion of the cell cycle (just prior to DNA synthesis), incubated for 24 hours, and then measured; and cells deprived at 40 per cent completion of cell cycle (after DNA synthesis has been initiated) and allowed to continue through division. The values for the daughter cells were doubled, as were the 95 per cent confidence limits, in order to illustrate directly that cells deprived at 40 per cent completion did double their DNA in spite of amino acid deprivation.

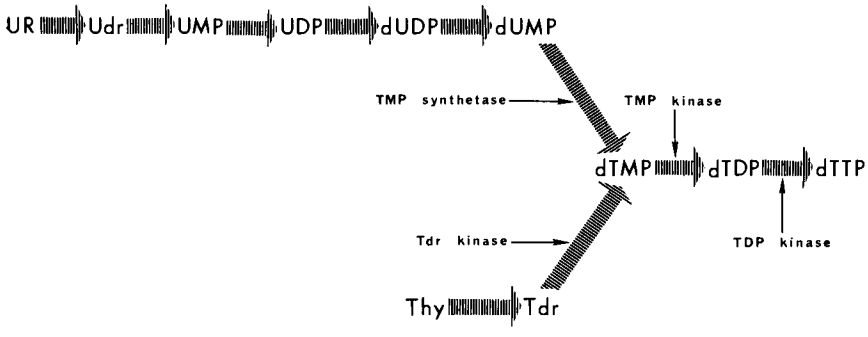

FIG. 5. Two pathways by which thymidine triphosphate (TTP) is probably formed in *Tetrahymena* for DNA synthesis. UR = uracil, Udr = uridine, UMP = uridine monophosphate, UDP = uridine diphosphate, dUDP = deoxyuridine diphosphate, dUMP = deoxyuridine monophosphate, Thy = thymine, Tdr = thymidine, dTMP = thymidine monophosphate, dTDP = thymidine diphosphate, dTTP = thymidine triphosphate. See Bessman [2] for details.

be postulated to explain the failure of uracil conversion to TTP, since thymidine is not on this latter pathway. We are inclined to believe, in part because of experiments described below, that this latter deficiency in the pathway of TTP synthesis is in TMP kinase, TDP kinase, TMP synthetase, or some combination of these. The points of action of these enzymes are shown in Fig. 5. Perhaps the most important part of this interpretation is the presumed, sudden appearance of the missing enzyme(s) in the TTP synthesis system at a precisely timed point in the cycle, i.e., at the G_1 to S transition. Imposition of amino acid deprivation is ineffective in stopping DNA synthesis once the transition point has been passed. Therefore, the missing enzyme(s) is synthesized only at the beginning of S, or at least the enzyme(s) formed at this point is adequate to carry the cell through a full S period.

In the foregoing scheme of events, the 20 per cent increase in DNA following G_1 deprivation of amino acids remains to be explained. It seemed most likely to us that this limited increase in DNA takes place at the expense of a pool of TTP carried over into G_1 from the round of DNA synthesis of the preceding cycle. On the basis of this possibility and because the experiments suggest that the first primary effect of amino acid deprivation is an interference with TTP production, we turned to more direct studies of the maintenance and turnover of the soluble pools of thymidine derivatives in relation to the cell cycle in *Tetrahymena*.

In order to follow changes in pools of thymidine derivatives in single cells or in small synchronous groups, a method of dry autoradiography was developed [10]. In this procedure the soluble materials usually extracted in preparation for autoradiography are retained within the cell by rapid air drying of the cell directly on a slide and covering with a dry autoradiographic emulsion. Any radioactive, soluble materials then contribute to the autoradiographic image of the cell. The technique can also be varied in such a way that soluble materials are extracted from the air-dried cell and deposited on the slide in a small, limited area around the cell. Since radioactivity in this deposited material can be detected by dry autoradiography, the presence of radioactive, soluble pools in a single cell can be visualized directly and a semiquantitative estimate of the amount of such extractable radioactivity also obtained.

In the first experiment, *Tetrahymena* in G_1 or in G_2 were incubated in full nutrient medium containing ^{3}H-thymidine. Using the dry autoradiographic technique, no uptake of ^{3}H-thymidine into a soluble pool could be detected in either period (see Fig. 6). This suggests a lack of turnover of the thymidine derivative pool(s), and is consistent with the interpretation that thymidine kinase is not present in the G_1 or G_2 cell.

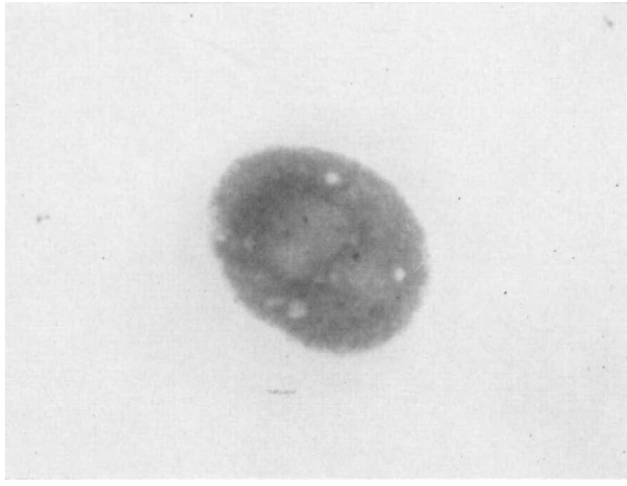

FIG. 6. A "dry" autoradiograph of a cell incubated in ^{3}H-thymidine medium during G_1. No detectable radioactivity has been taken up into the soluble pool of the cell.

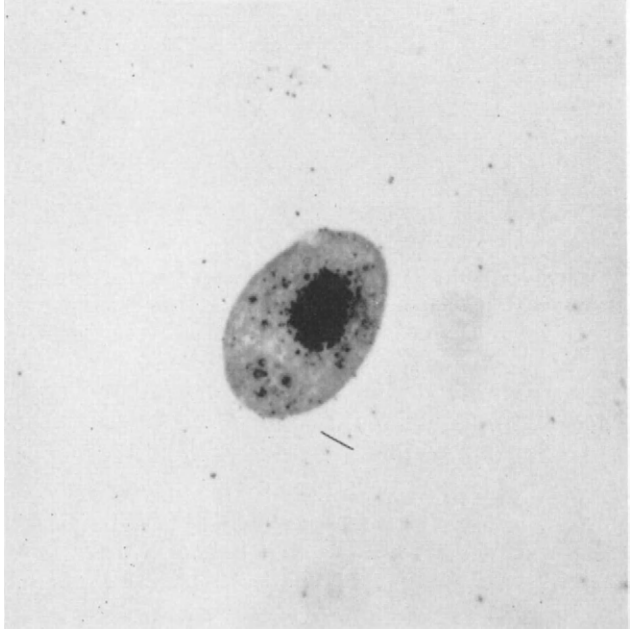

FIG. 7. A "dry" autoradiograph of a cell incubated in ^{3}H-thymidine medium during S. The autoradiographic image over the macronucleus is due to both soluble and DNA incorporated material.

If cells in S were incubated with ^{3}H-thymidine, air dried, and autoradiographed by the dry method, all radioactivity was found to be localized in the macronucleus (Fig. 7). This procedure would detect any radioactivity in soluble pools as well as that incorporated into DNA, but would not distinguish between them. When the soluble materials in such a cell were extracted and deposited around the cell before autoradiography, the autoradiographic image shown in Fig. 8 was the result.

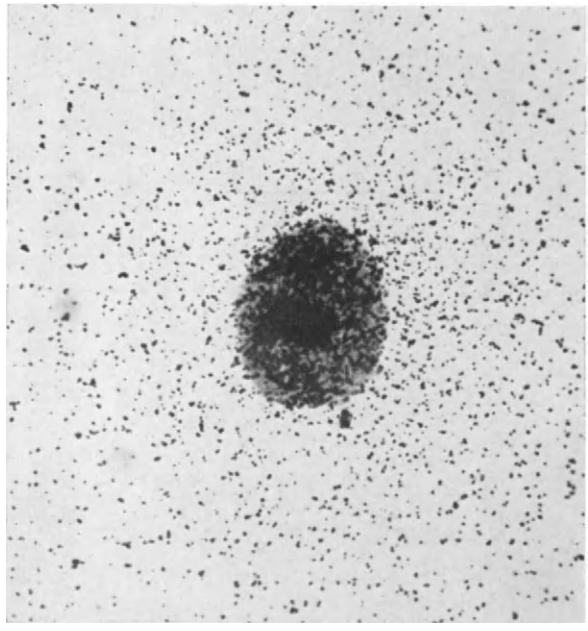

FIG. 8. A "dry" autoradiograph of a cell incubated with ^{3}H-thymidine medium during S and extracted in such a manner that soluble materials were deposited on the slide in a restricted area around the cell. This cell should be compared with Fig. 7.

In this case a large amount of soluble ^{3}H-thymidine and its soluble derivatives has been extracted from the macronucleus. The extraction from the cell is evidently incomplete since a heavy autoradiographic image is also present over the cytoplasm. The radioactivity remaining in the macronucleus is most likely that which has been incorporated into DNA. The experiment demonstrates that during S there is a large pool of thymidine and undoubtedly of its phosphorylated derivatives engaged in active turnover in the macronucleus. (A separate set of studies have shown that the soluble pool of thymidine derivatives in *Tetrahymena* consists of TMP, TDP, and TTP [9].)

Since a large pool of soluble derivatives of thymidine could be

demonstrated in the macronucleus during S, it was then possible to determine whether such pool materials are retained in G_2 and carried over through cell division into G_1 to be utilized in the next S period. In a preliminary experiment, cells in late S were incubated with ^{3}H-thymidine. When the cells were well into G_2, they were washed free of exogenous radioactivity, allowed to divide and enter G_1, air dried on slides, and extracted by the procedure which allowed deposition of the extracted materials around the cell. The subsequent dry auto-

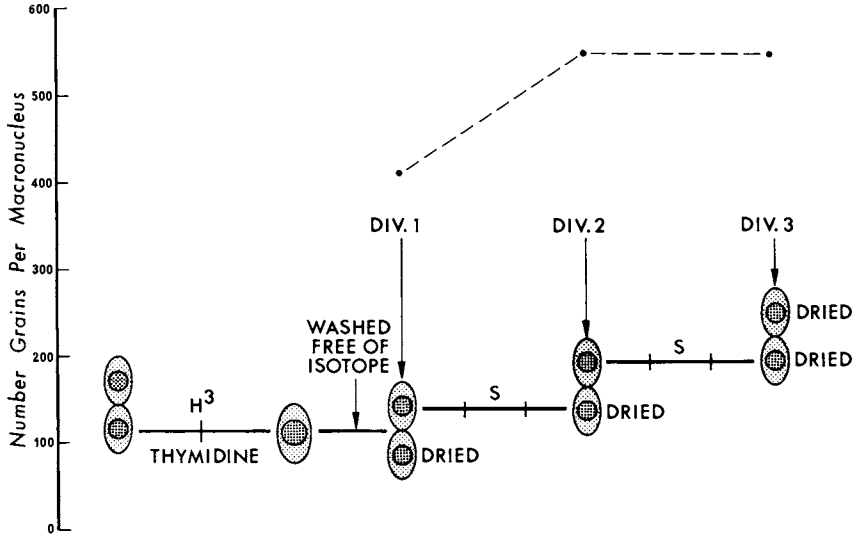

FIG. 9. Diagram of carryover and utilization of thymidine derivative, acid-soluble pools in *Tetrahymena*. The DNA and the thymidine derivative, acid-soluble pools of the macronucleus were labeled in cycle 1 with a short pulse of ^{3}H-thymidine. ^{3}H-thymidine was removed from the medium before the end of cycle 1. In cycle 2 radioactive precursors remaining in the acid-soluble pool are incorporated into DNA. The increase in radioactivity in DNA is shown in the graph above. No increase occurs in cycle 3 since turnover of the pool has exhausted all radioactive, soluble precursors. See text for further explanation.

radiograph of the preparation showed that these G_1 cells contained a radioactive, soluble pool of ^{3}H-thymidine derivatives. Since this soluble radioactivity was not lost from the living cells during the G_2 washings carried out to remove the exogenous ^{3}H-thymidine, it is probable that the retained soluble derivatives of ^{3}H-thymidine are phosphorylated, i.e., TMP, TDP, and/or TTP. (The cytoplasmic membrane of *Tetrahymena* is impermeable to at least TMP and TTP.)

In a more extended version of this type of experiment, cells were incubated in ^{3}H-thymidine during S and washed free of exogenous radio-

activity in G_2. These cells contain both DNA-incorporated and soluble radioactivity after the washing. As each cell reached division one of the daughter cells in each case was dried on a slide and the other was allowed to proceed through the cycle to the next division. One of the daughters of this second division was air dried on the same slide with the daughter from the first division. The remaining cell was cultured to the third division and both daughters were air dried on the same slide that held their ancestors. All of these cells were subjected to acid extraction to remove all soluble materials and then autoradiographed. The experimental design and the results of grain counts of macronuclei of daughters fixed after division 1, 2, and 3 are shown in Fig. 9. If the amount of radioactivity in a daughter macronucleus from division 2 is multiplied by 2 (to correct for the halving at division), it is clear that the amount of radioactivity is significantly more than the radioactivity in its ancestor macronucleus from division 1. This is good evidence that the radioactive, soluble pool material carried through division 1 was incorporated into DNA during the subsequent S period, thereby adding to the radioactivity already incorporated during the previous S period. No significant amount of radioactive material could have remained in soluble pools for utilization in the final S period (between the second and third divisions) because the level of incorporated radioactivity in the individual daughters of division 3 added together is just equal to that found at division 2. For further details on these experiments see Stone *et al.* [14].

SUMMARY

We arrive at the following summary. *Tetrahymena* contains a pool of thymidine derivatives (TMP, TDP, and TTP) which is carried over from one round of DNA synthesis to the next in the subsequent cell cycle. When a cell arrives at the beginning of DNA synthesis these pool materials are used for synthesis of DNA, and, in close correlation with this event, enzymes necessary for replenishment of TTP are rapidly synthesized. When the synthesis of these enzymes ceases is not known, but this probably occurs during S itself. During the period between consecutive S phases these enzymes required for TTP production disappear and must be resynthesized with each cycle.

Finally, we are disinclined to believe that maintenance or development of pools of DNA precursors are normally involved directly in the control of DNA synthesis. However, the appearance of those certain enzymes required for production of DNA precursors only at the beginning of DNA synthesis can serve as an example of the type of timed

derepression within the genome which must be operating in continuous sequence to maintain the orderly progress of biosynthetic events which make up the cell life cycle.

References

1. Alfert, M., *Exptl. Cell Res. Suppl.* **6**, 227 (1959).
2. Bessman, M. J., *in* "Molecular Genetics" (J. H. Taylor, ed.), p. 1. Academic Press, New York, 1963.
3. Bloch, D. P., and Brack, S. D., *J. Cell Biol.* **22**, 327 (1964).
4. Bloch, D. P., and Godman, G. C., *J. Biophys. Biochem. Cytol.* **1**, 17 (1955).
5. Elliot, A. M., Brownell, L. E., and Gross, J. A., *J. Protozool.* **1**, 193 (1954).
6. Gall, J. G., *J. Biophys. Biochem. Cytol.* **5**, 295 (1959).
7. Holter, H., *Compt. Rend. Trav. Lab. Carlsberg* (*Ser. Chim.*) **24**, 399 (1943).
8. Hotta, Y., and Stern, H., *Proc. Natl. Acad. Sci., U.S.* **49**, 648 (1963).
9. Jacobson, K. B., and Prescott, D. M., unpublished observations, 1963.
10. Miller, O. L., Jr., Stone, G. E., and Prescott, D. M., *in* "Methods in Cell Physiology" (D. M. Prescott, ed.), Vol. I, p. 371. Academic Press, New York, 1964.
11. Stone, G. E., and Cameron, I. L., *in* "Methods in Cell Physiology" (D. M. Prescott, ed.), Vol. I, p. 127. Academic Press, New York, 1964.
12. Stone, G. E., and Miller, O. L., Jr., *J. Cell Biol.* **23**, 89A (1964).
13. Stone, G. E., and Prescott, D. M., *J. Cell Biol.* **21**, 275 (1964).
14. Stone, G. E., Miller, O. L., Jr., and Prescott, D. M., *J. Cell Biol.* (accepted for publication).

Discussion

Dr. Leblond: Since you stated that, under certain conditions, mitochondria may synthesize deoxyribonucleic acid (DNA), perhaps Dr. Chèvremont and you might tell us what your views are on the subject.

Dr. Chèvremont: We have demonstrated that under the influence of some "preprophasic inhibitors" of mitosis, DNA is detectable inside the cytoplasm, more precisely, in modified mitochondria. The latter are then Feulgen-positive and are labeled by tritiated thymidine. This DNA does not come from the nucleus. These results are obtained by treatment of cells with either acid deoxyribonuclease (not with the neutral DNAase), or with an isomer of adrenochrome as well as with a few other factors, but not with every substance or factor which modifies mitochondria. By these methods, we observed mitochondrial DNA in the cells of chick, mouse, and human embryo. In addition, the same results were seen in normal tissue cultures without adding any substance, but by merely cooling the cells under certain conditions.

As a hypothesis, we have suggested that a synthesis of DNA—or of large precursors—normally takes place in the mitochondria during "preparation" for mitosis. These substances would be brought into the nucleus during the frequent contacts that normally occur between mitochondria and nucleus, as clearly seen in cinematographic records of living cells. The observations of mitochondrial DNA are interesting from the point of view of cytoplasmic inheritance.

DR. PRESCOTT: We have not been able to detect DNA in mitochondria in ciliates by Feulgen staining. For the present, we assume, as others do, that the mitochondrial DNA is the basis for a nucleus-independent genetic system with no transfer of DNA between nucleus and mitochondria.

DR. LEBLOND: Could the DNA observed in mitochondria be synthesized by a virus?

DR. CHÈVREMONT: The well-known DNA cytoplasmic inclusions due to viruses are quite different from the mitochondrial DNA I have observed.

DR. PRESCOTT: No virus-like bodies have been seen in *Tetrahymena* mitochondria labeled with ^{3}H-thymidine, but that does not rigorously exclude the possibility of virus activity as an explanation for mitochondrial DNA synthesis.

CYTOPLASMIC PROTEIN SYNTHESIS IN CELLS OF VARIOUS TYPES AND ITS RELATION TO NUCLEAR PROTEIN SYNTHESIS

BRIGITTE SCHULTZE, P. CITOLER, K. HEMPEL, KARIN CITOLER, AND W. MAURER

Institut für Medizinische Isotopenforschung der Universität Köln, Deutschland

INTRODUCTION

It has previously been shown that the application of various labeled amino acids results in very similar autoradiographic blackening patterns for the different tissues in the organism of various animals [32]. These results were confirmed and completed by using 11 tritiated amino acids for the investigation of protein metabolism in mice, rats, rabbits, guinea pigs, and pigeons. Quantitative evaluation by grain counting showed that, apart from a few exceptions, application of all the different amino acids results in a very similar relative distribution of grain densities in the organism. For all the animals examined the various cell types could be grouped according to their different protein metabolism. In all animals there are certain cells with a high protein turnover, such as protein-secreting cells, and others with a low protein turnover, such as connective tissue and muscle.

The protein metabolism per unit volume varies by a factor of 1 to 50 in the different cell types. Considering these big differences in protein metabolism and the completely different function and morphology of the different cell types, one would not expect the cellular protein metabolism to be regulated according to a simple generally valid scheme. This paper gives good evidence that the protein metabolism of a cell follows a generally applicable pattern in which the controlling factor is represented by the volume of the cell nucleus.

MATERIALS AND METHODS

Animals

Thirty-six male and female mice (Copenhagen strain, average body weight 20 gm), 25 male and female Wistar rats (average body weight 180 gm), 4 female rabbits (Blaue Wiener, average body weight 2000 gm), 5 male and female guinea pigs (340 gm), and 2 female pigeons (330 gm) received radioactive labeled amino acids. The animals were fed

a standard diet (Altromin-R) with normal protein content. Twelve hours prior to the application of amino acids the food was removed from the cages; water was given *ad libitum*.

The labeled amino acids were mostly injected intraperitoneally or intravenously or, in some cases, fed by a stomach tube.

Most of the animals were sacrificed 1 hour after application of the labeled amino acids; the rabbits, however, were killed after 3 hours. In a series of 11 mice and 11 rats, the times of sacrifice varied between 5 minutes and 3.5 hours. The animals were decapitated in slight ether narcosis.

Labeled Amino Acids

^{14}C-L-amino acids (as algae protein; 0.23 mc/mg protein; 13 μc/gm body weight), ^{14}C-L-lysine (7.7 mc/mmole; 13 μc/gm body weight), ^{35}S-L-methionine (9000 mc/mmole; 50 μc/gm body weight), and 11 different tritiated amino acids (50 μc/gm body weight) of high specific activity as listed in Table I were used for these experiments.

TABLE I. *List of Tritiated Amino Acids of High Specific Activity Used in These Experiments*

^{3}H-Amino acids	Specific activity (mc/mmole)	Mouse	Rat
Glycine-[α-*T*]	5,075	3	
DL-Alanine-[α-β-T_2]	4,500	3	2
DL-Leucine-[γ-δ-T_2]	2,820	1	12
DL-Serine-[α-*T*]	3,500	2	
DL-Lysine-[γ-δ-T_2]	30,000	2	1
DL-Arginine-[α-β-T_2]	3,000	2	1
D-Phenylalanine-[2,4-T_2]	13,000	1	
L-Phenylalanine-[2,4-T_2]	15,000	2	1
L-Tyrosine-[3-*T*]	5,100	13	1
DL-Proline-[1,2-T_2]	2,500	3	2
DL-Tryptophan-[5-*T*]	2,000	2	

Autoradiographic Technique

Small tissue samples were fixed in formalin (6 per cent)–trichloroacetic acid (TCA) (0.5 per cent) to which the corresponding "cold" amino acid was added (0.1 mg/ml) for 24 hours at 4°C and embedded in paraffin. Three-μ thick sections were deparaffinized, covered with stripping film AR 10 (Kodak, London) or liquid emulsion G5 (Ilford, London), and exposed between 1 and 30 days. The autoradiographs were

then developed and fixed under constant conditions, and some of them were mounted immediately without staining. Most of them were stained with hematoxylin-eosin through the emulsion.

Quantitative Evaluation of the Autoradiographs by Grain Counting

For quantitative estimation of the incorporated activity, grain counts and micrometric measurements were performed in the following way:

1. The number of grains was counted over the entire counting grid (6400 μ^2). From the average for a great number of counting grids, the mean grain number per square micron was calculated. This value is a measure for the *mean activity per milliliter tissue.*
2. The number of grains situated over the nuclei was counted for several hundred nuclei of each cell type. Simultaneously, the corresponding nuclear area was measured with an ocular micrometer. The grain number per single nucleus was plotted as a function of its nuclear area (Fig. 6). Or the mean grain number per nucleus for a certain cell type was plotted as a function of the corresponding mean nuclear area (Figs. 7 and 8). This calculated mean value for the grain number per unit area represents *incorporated activity per unit nuclear volume.*
3. The number of grains situated over all nuclei and the grain number localized over the whole cytoplasmic area in the counting grid were counted separately for a great number of counting grids. The ratio of the grain number over the cytoplasm to the grain number over all nuclei is equal to the *ratio of incorporated activity in the whole cytoplasm of a cell to the incorporated activity in the whole cell nucleus.* The countings were performed for experimental times between 5 minutes and 3.5 hours.
4. Simultaneously with the grain countings mentioned in point 3 above, the area of all nuclei in all counting grids was measured with an ocular micrometer. The quotient of the sum of all nuclear areas measured to the area of all counting grids is equal to the *ratio of nuclear volume to whole cellular volume* (nuclear volume in per cent of cell volume in Fig. 11).

This method of estimation of activity ratios and ratios of volumes is only applicable if the nuclei of the tissue are distributed randomly. In general, constant values became evident after evaluating the first few counting grids. In these experiments 10 to 20 counting grids (6400 μ^2 each) were evaluated for each measurement.

RESULTS

Autoradiographs after Application of ^{14}C-, ^{35}S-, and 11 Different ^{3}H-Amino Acids

Figure 1 shows unstained autoradiographs of the stomach of the rat after application of ^{14}C-amino acids, ^{3}H-DL-leucine, and ^{35}S-L-methionine. Highest grain density was always found over the chief cells, much less over the epithelia, and the lowest grain density over the submucous layer. However, it is evident that the *relative* distribution of the different grain densities is equal for all three amino acids.

This is demonstrated much more distinctly in Fig. 2, which depicts unstained autoradiographs of the stomach of the mouse after application of 10 different tritiated amino acids. Again the relative distribution of the grain densities is the same for all the different amino acids. Only the application of DL-alanine results in a slightly different picture, i.e., less intensive grain density over the epithelia.

Figure 3 shows unstained autoradiographs of the adrenal gland of the mouse after injection of 6 different tritiated amino acids. With all tritiated amino acids and also with ^{14}C- and ^{35}S-labeled amino acids, there is the same relative distribution of grain densities: high grain density over the cortex, especially over the outer fasciculata, somewhat lower density over the glomerulosa, and very low grain density over the medulla. The medulla has a higher grain density only after injection of DL-alanine.

The same autoradiographic pictures of the pancreas were obtained after injection of ^{14}C-, ^{35}S-, and ^{3}H-labeled amino acids, as is shown in Fig. 4 for the pancreas of the mouse after injection of 10 different tritiated amino acids. High grain density was found over the exocrine pancreas but a much lower one over the Langerhans islands.

Comparably high relative grain density was always found over the cells of the choroid plexus (as is demonstrated in Fig. 5 for the choroid plexus of the mouse after injection of 6 different tritiated amino acids). This means that the relative incorporation of labeled amino acids into the choroid plexus is always high. However, Fig. 5 also shows that, in contrast to all other ^{3}H-amino acids used, ^{3}H-alanine, ^{3}H-glycine, and ^{3}H-serine are only slightly incorporated into ganglionic cells.

As these few examples show, a very similar relative incorporation pattern of amino acids into the various organs of mice, rats, rabbits, guinea pigs, and pigeons was found. Quantitative evaluation by grain counting resulted in the same relative distribution of grain densities for many organs. There are only a few major exceptions. Especially the

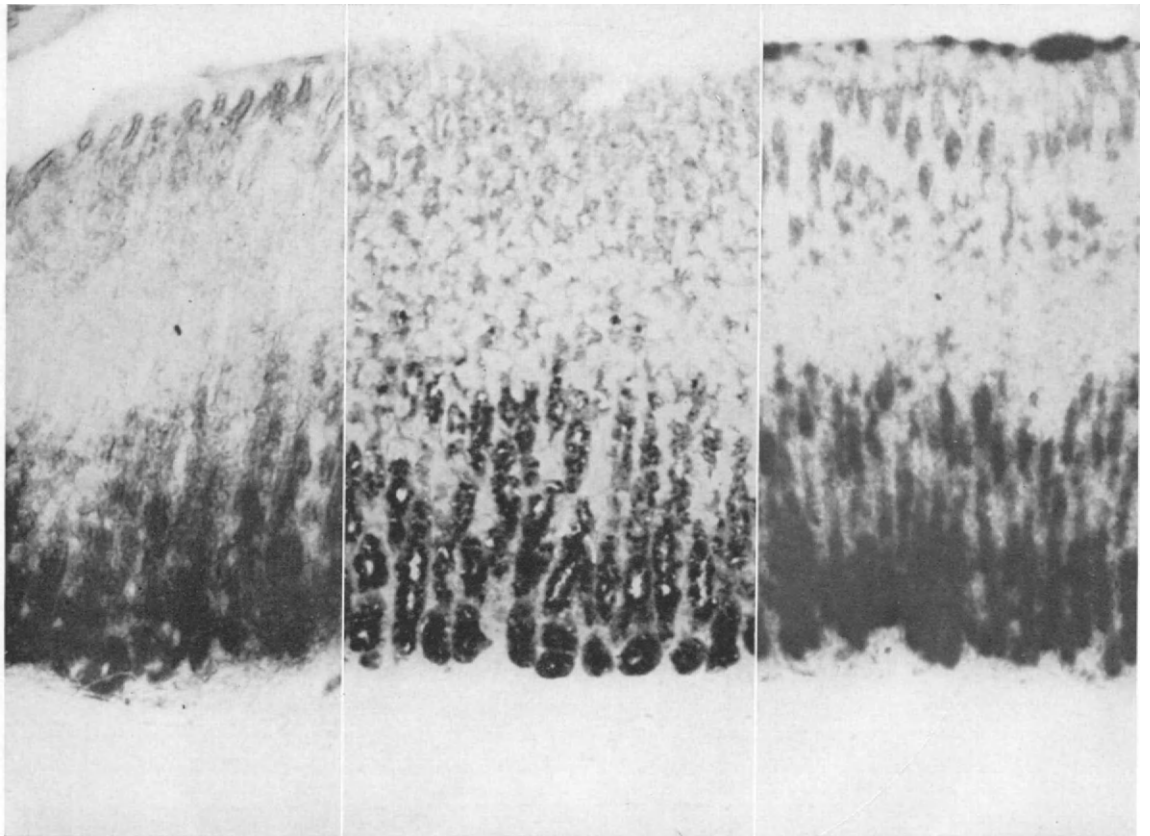

FIG. 1. Unstained autoradiographs of the stomach of the rat after application of ^{14}C-amino acids, 180 minutes (left); ^{3}H-DL-leucine, 90 minutes (center); and ^{35}S-amino acids, 90 minutes (right).

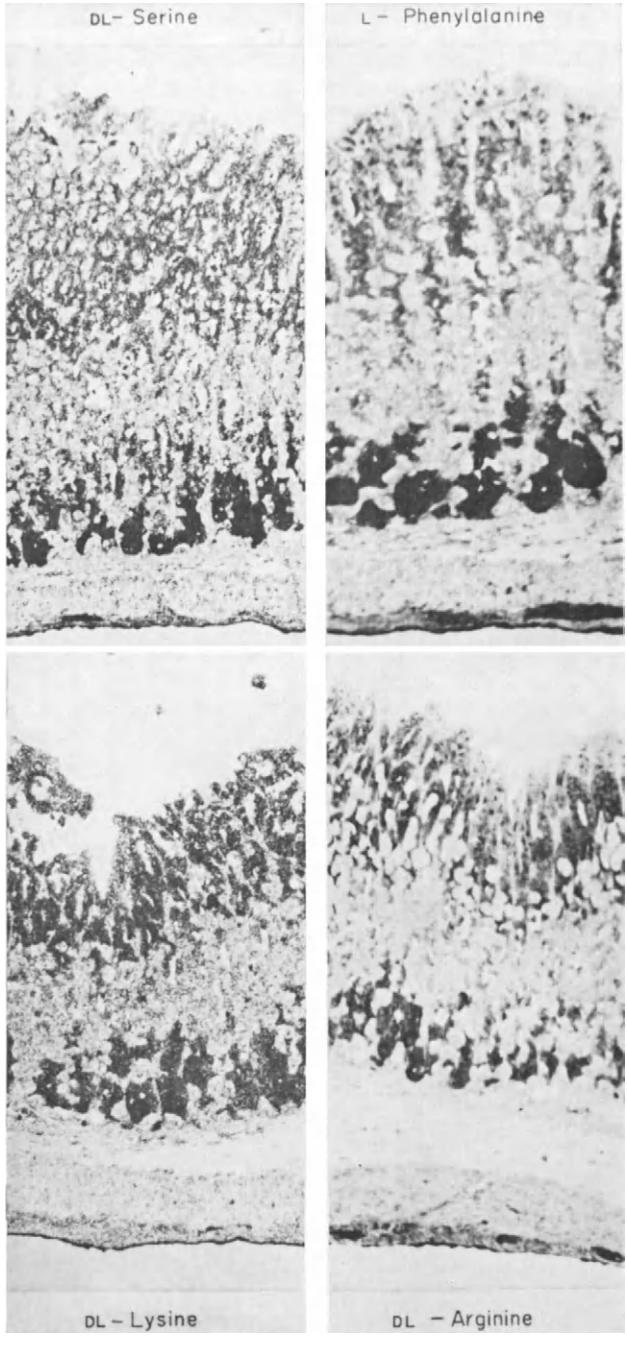

FIG. 2. Unstained autoradiographs of the stomach of the mouse 60 minutes

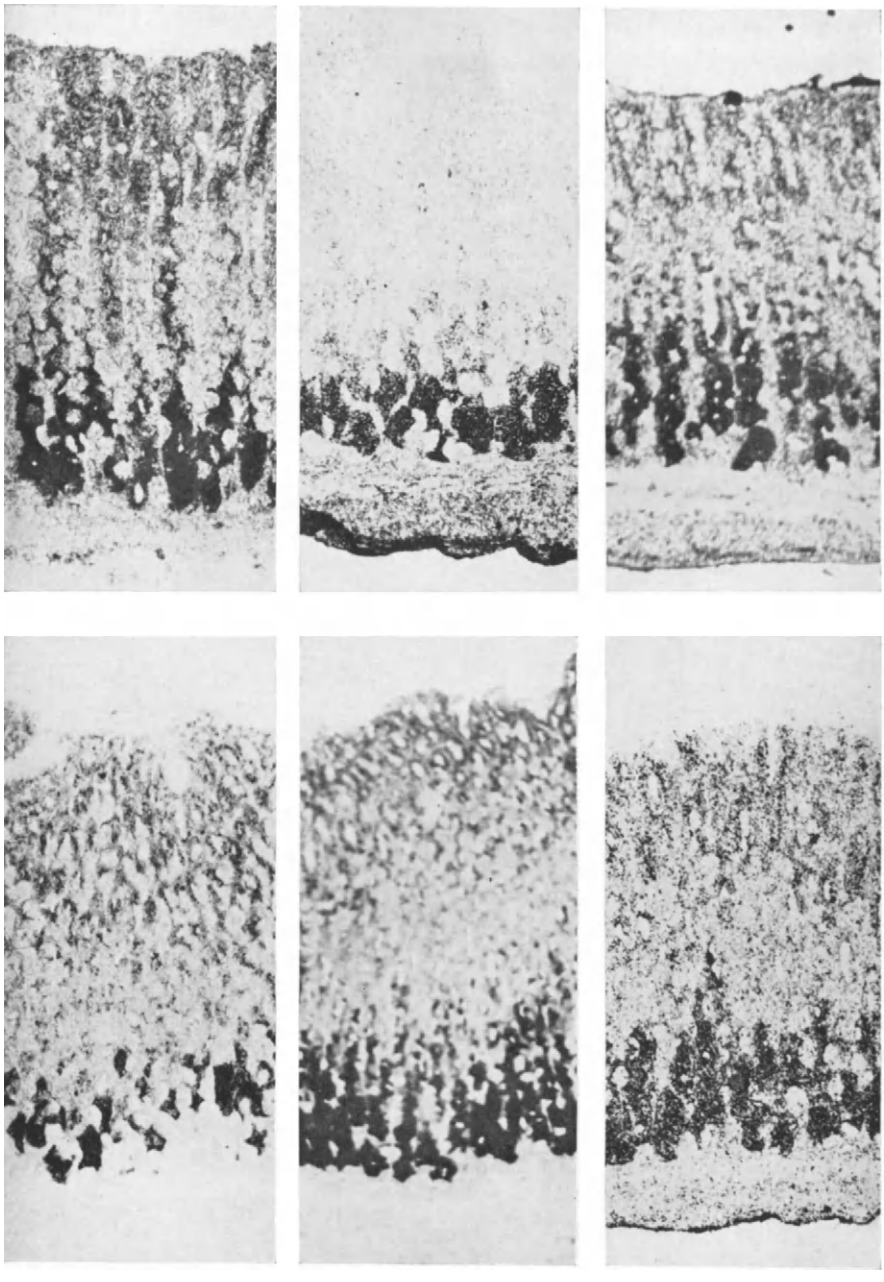

after application of 10 different tritiated amino acids.

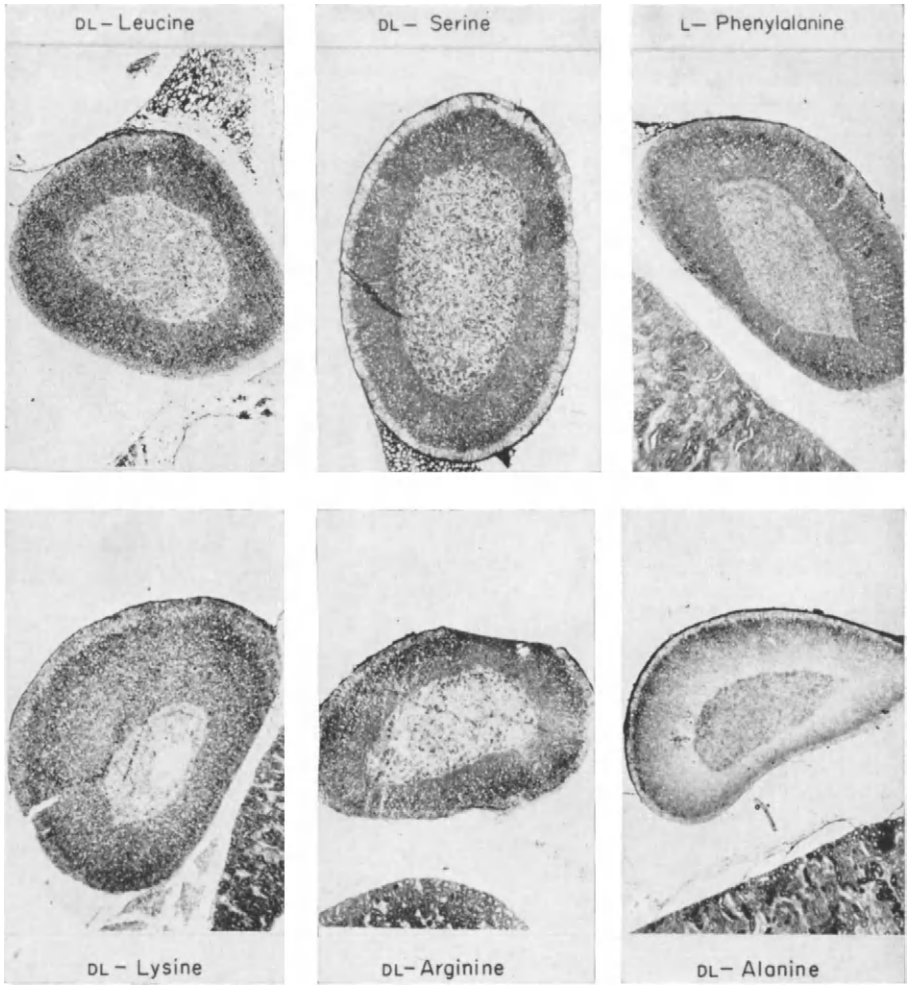

FIG. 3. Unstained autoradiographs of the adrenal gland of the mouse 60 minutes after application of 6 different tritiated amino acids.

application of DL-alanine resulted in incorporation patterns more or less different from most other labeled amino acids. Furthermore, the incorporation pattern of tritiated serine and glycine into the kidney differed from that of other amino acids. And finally, as mentioned previously, there is less incorporation of tritiated alanine, serine, and glycine into the ganglionic cells of the brain than of all other amino acids, while the relative grain density over the choroid plexus and the peripheral ganglionic cells did not differ from other amino acids.

The autoradiographic results obtained with all the different amino acids show that the amino acid incorporation of the various cell types in the organism is typical for these cell types. For instance, the ganglionic cells always have a very high incorporation rate regardless of their location in the organism. On the other hand, muscle cells in the whole organism incorporate only small amounts of amino acids.

Due to their different amino acid incorporation—measured as grain density, representing incorporation rate per ml—certain groupings of cells can be made. There are cells with very high incorporation rates, for instance, protein-secreting cells such as pancreas epithelia, epithelia of the serous salivary gland, and the chief cells of the stomach, as well as ganglionic cells, choroid plexus, adrenal cortex, cells of the reticuloendothelial system, and others. Another group with an amino acid incorporation about 2 to 4 times lower consists, among others, of the crypt cells, liver epithelia, and tubulous epithelia of the kidney. Finally, there is a group of cells with a very low—about 30 to 60 times lower—incorporation rate, consisting of muscle cells, cartilage, connective tissue, and the white substance in the nervous system. The same grouping of cells was found in all animal species investigated.

A detailed description of the incorporation of ^{14}C- and ^{35}S-labeled amino acids as well as of ^{3}H-leucine into the tissues of rats and mice, studied by means of autoradiography, has already been given by Schultze *et al.* [32]. Reproductions of autoradiographs of other organs can be found in that paper. The results described there and in this paper are in good agreement with previously published studies by Niklas and Oehlert [22], Bélanger [3], and Leblond *et al.* [17], using ^{35}S-methionine to investigate protein metabolism in different organs of the rat, and with Ficq and Brachet's results [11] for mice using ^{14}C-phenylalanine. Special investigations of protein metabolism were performed for the central nervous system [1, 2, 7, 9, 12, 26], for the tissues of the eye [24] and ear [16, 28], as well as for bone [15] and spleen [34]. Autoradiographic studies of protein synthesis within the individual cell showed that the incorporation pattern for the different cell structures is also independent of the different amino acids [27, 31].

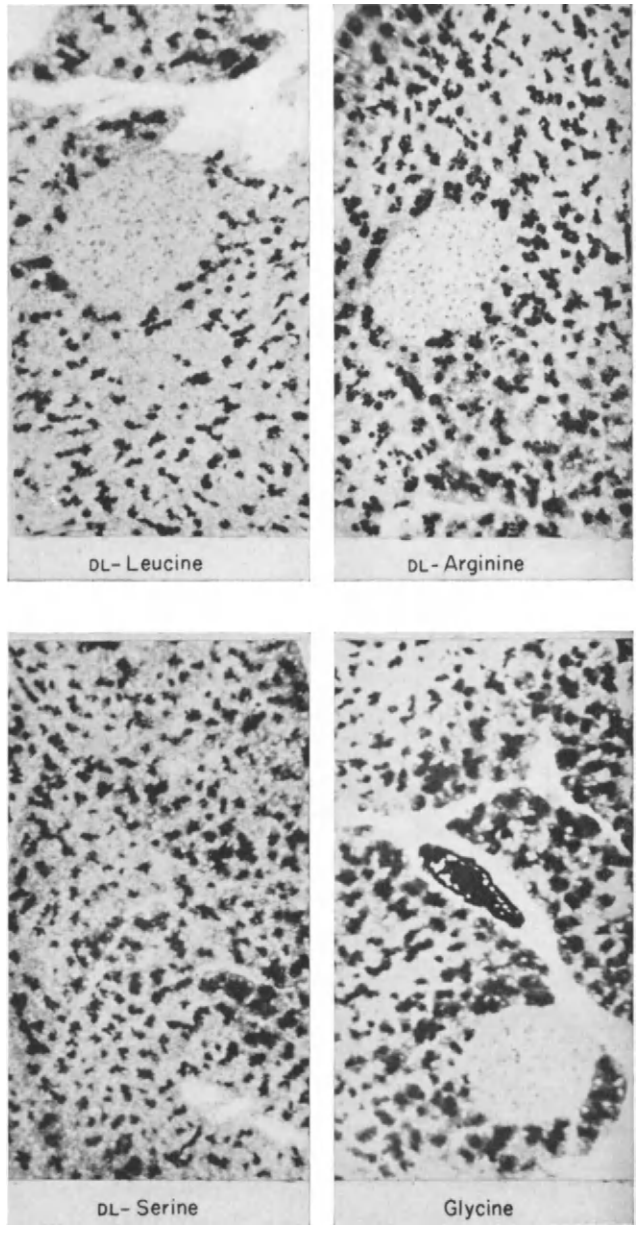

FIG. 4. Unstained autoradiographs of the pancreas of the mouse 60 minutes

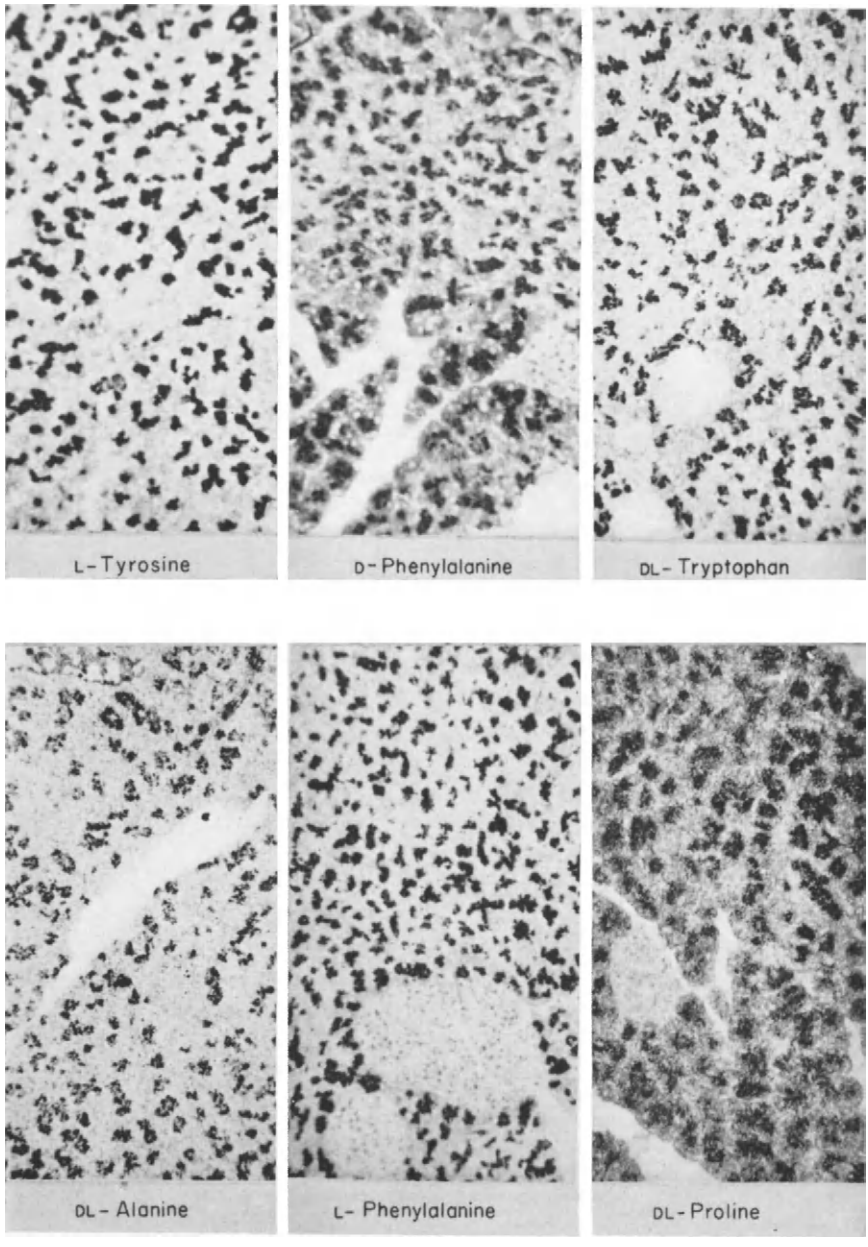

after application of 10 different tritiated amino acids.

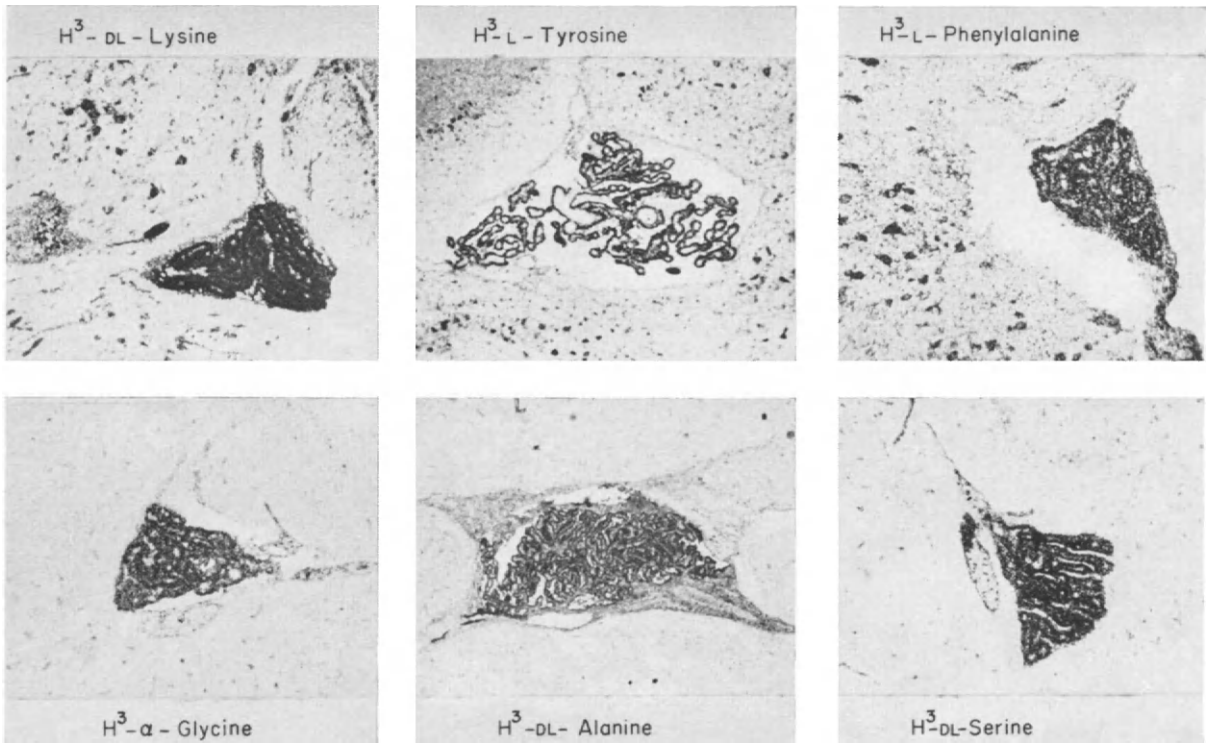

FIG. 5. Unstained autoradiographs of the choroid plexus of the mouse 60 minutes after application of 6 different tritiated amino acids.

DISCUSSION

Grain Density in the Autoradiographs as a Relative Measure of the Protein Synthesis Rate

As to the question of whether the radioactivity in the histological section after application of labeled amino acids is entirely due to newly synthesized protein, one must consider that during the histological procedure commonly used the protein is precipitated while all water- and alcohol-soluble substances are dissolved, especially those labeled free amino acids still present. In our laboratory, histological sections of animals injected with ^{14}C-labeled amino acids were prepared as usual for autoradiography but were then treated according to common chemical methods used for isolating protein. ^{14}C-activity losses of only 0–5 per cent were found by counting in a flow counter [32]. Droz and Warshawsky [10] also reported that at least 91–97 per cent of the radioactivity retained in histological sections (Bouin fixation) after labeled amino acid injection is firmly bound to protein, presumably by peptide bonds.

The most striking result of this paper is the far-reaching similarity of the autoradiographs with so many different labeled amino acids. Apart from a few exceptions, the incorporation of labeled amino acids always results in a very similar incorporation pattern in the organism. It must be emphasized that this is only valid for the *relative* distribution of the label within the organism. The *absolute* amount of incorporated activity depends on the percentage of injected amino acid which is incorporated into the protein of the whole organism and is quite different for the different amino acids. It was found that almost 50 per cent of the injected tritiated leucine is incorporated into protein while only 5 per cent of the glutamic acid is utilized and 95 per cent is catabolized [7]. To obtain equal absolute grain densities for a certain tissue autoradiographically, the individual autoradiographs have to be exposed for different lengths of time.

The correspondence of the autoradiographs with the different amino acids provides good evidence that the incorporation rates measured autoradiographically actually represent protein synthesis.

Equation (1) shows the correlation between the incorporated activity and the turnover rate R:

$$\begin{aligned}\text{Incorporated amino acid activity}\\ \text{between injection } (0) \text{ and sacrifice } (T) &= R \cdot \int_0^T s_t \cdot dt \\ &= R \cdot s_{\text{mean}} \cdot T\end{aligned} \qquad (1)$$

The left side of the equation represents the activity which is incorporated per unit volume of tissue during the time interval between the beginning ($= 0$) and the end of the experiment ($= T$). A relative measure for the

incorporated activity per unit volume is the grain density. R is the amino acid incorporation rate (mass per unit time) related to 1 ml. In a steady state the incorporation rate is equal to the catabolic rate; therefore R represents the turnover rate; s_t is the specific activity of the free amino acid at the site of synthesis as a function of time t. After injection, this specific activity of the precursor rises quickly from zero to a maximum and decreases slowly toward zero again. The incorporated activity varies with time T as $\int_0^T s_t \cdot dt$. This integral can be replaced by the product: mean specific activity in 0–T times T.

It is easy to see that the incorporated activity in the different tissues—measured as grain density—is a relative measure of the turnover rate *only* if the mean specific activity of the free amino acid is the same during the experiment for all the different cell types. For more details see Maurer [18].

For ^{35}S-methionine, the same specific activity for liver, brain, muscle, and serum was actually measured in our laboratory [8]. It should be emphasized that an equal specific activity of the free amino acid has nothing to do with variable concentrations of the free amino acids in tissues or organs like the brain. The amount of incorporated activity only depends on the mean specific activity of the precursor. If the mean specific activity of the free amino acid is *too* low, as, e.g., for alanine, glycine, and serine in the brain, possibly because of retarded entrance into the brain, the incorporated *activity* will be low too, although the protein synthesis (incorporated mass per unit time) may be quite high. It is worthwhile noting that the relative grain density over the choroid plexus and the ganglionic cells of the myenteric plexus after application of these amino acids does not differ from that of the other amino acids.

Equation (2) shows that, in the case of *de novo* synthesis of protein molecules, the incorporation rate (R) of the different amino acids should be proportional to the amino acid composition of the fast-turnover protein:

$$R_{aa_1}:R_{aa_2}:R_{aa_3}:\ldots = M_{aa_1}:M_{aa_2}:M_{aa_3}:\ldots \qquad (2)$$

where R_{aa_x} is the turnover rate of aa_x and M_{aa_x} is per cent of aa_x in the protein.

If the amino acid composition (M_{aa_x}) of the fast-turnover fraction of the protein is the same for all cells, the correlation of the incorporation rates (R_{aa_x}) will also be the same for all cells. The turnover rates of the different amino acids correspond to the proportion of an amino acid in the protein. If the amino acid composition for the different protein frac-

tions of a cell differs, the amino acid composition of the fraction with the fastest turnover predominates.

If the proportion of one amino acid is extremely high, such as cystine in the hair follicle, the incorporation rate of this amino acid into the hair follicle will also be high. This was actually shown in previous experiments with ^{35}S-amino acids [32].

The extensive correspondence throughout the autoradiographs obtained by using so many different amino acids suggests that not only the mean specific activity of the free amino acids but also the amino acid composition of the fast-turnover protein should actually be similar in the whole organism. Thus, the incorporation rates measured autoradiographically should represent protein synthesis. The correspondence of the autoradiographs is as complete as the degree of fulfillment that the two prerequisites reach.

There are special conditions to be considered for the incorporation of D-amino acids. These tritiated D-amino acids are not diluted by the inactive amino acids of the pool; thus, they have the same high specific activity in the organism as in the preparation for injection. A very small incorporation of derivatives of ^{3}H-D-amino acids could, therefore, result in high grain densities without representing a correspondingly high protein turnover. Since most of the tritiated amino acids used were in the DL-form, a possible influence of the D-amino acid on the autoradiographic pattern should be taken into consideration.

The ^{3}H-DL-alanine incorporation pattern for a number of cell types differs more or less from that of other amino acids. Since the values for the ratio of total cytoplasmic to total nuclear incorporation for alanine do not differ from those for other amino acids, the different incorporation pattern could possibly be due to variations of the specific activity of the free alanine for the different cell types or to the close relationship of alanine to other metabolic processes.

The different autoradiographic picture of the kidney which is produced by some amino acids such as ^{3}H-serine and ^{3}H-glycine may be related to the complicated renal function of secretion, reabsorption, and excretion of amino acids.

Quantitative Evaluation of Nuclear Protein Synthesis

The number of grains per nucleus was counted for different cell types in mice, rats, rabbits, and pigeons after application of various labeled amino acids. Simultaneously, the nuclear area was measured micrometrically. The results are shown in Fig. 6, where the grain number per nucleus is plotted on the ordinate while the nuclear area is expressed in square microns on the abscissa. Each point in the curves represents one

single nucleus of the corresponding cell type. The curves show very clearly that the grain number per nucleus increases quite linearly with the nuclear area. The variations in the vertical direction are mainly statistical variations, due to the statistical character of the radioactive decay. The rather linear correlation shows that the grain density is equal for all nuclei within one cell type. This means that all nuclei have the same amino acid incorporation per unit volume and that the amino acid incorporation into the whole nucleus is proportional to the volume of the nucleus.

This is not only true for the nuclei within one single cell type, but was also found to be true for the nuclei when comparing different cell types. Figure 7 shows the relationship between the mean grain number per nucleus and the mean nuclear area for 39 different cell types of the mouse after application of tritiated L-tyrosine. Here, too, is a linear relationship, although not as pronounced as that in the single cell types shown in Fig. 6. Some types of nuclei (as those of Lieberkühn's crypts, pyloric glands, plexus myentericus, spermatogonia, and skeletal and heart muscle) vary from the linear relationship by a factor of 2. With other amino acids it could be shown that these types of nuclei vary from the mean value in the same direction and to a similar extent. Thus, the grain density of the crypt cell nuclei is high for all amino acids.

Once again the general linear relationship between amino acid incorporation and nuclear area means that the grain density (grains per square micron) is very similar for all kinds of nuclei. Consequently, incorporation into the whole nucleus is, within certain limits, proportional to the volume of the nucleus for very many different cell types.

Similar results to Fig. 6 were described for mouse cells after X-ray irradiation [13] and for cancer cells [6, 14, 20].

If the very different cytoplasmic grain densities on the autoradiographs were left out, the autoradiographic picture would be very monotonous because of the nearly equal grain density over the different types of nuclei. The typical differences in the grain density of the individual cell types depend overwhelmingly on differences of the cytoplasmic incorporation rates.

Figure 8 shows the same relationship between nuclear volume and amino acid incorporation (as was demonstrated in Fig. 7 for cells of the mouse) for 26 different types of nuclei of rat after injection of tritiated

---

FIG. 6. Grain number per nucleus as a function of nuclear area for individual nuclei within one cell type. Each point equals one nucleus; 60 minute experiments for 4 different tissues with 8 different ^{3}H-amino acids. Similar results were obtained for pancreas epithelia and smooth muscle.

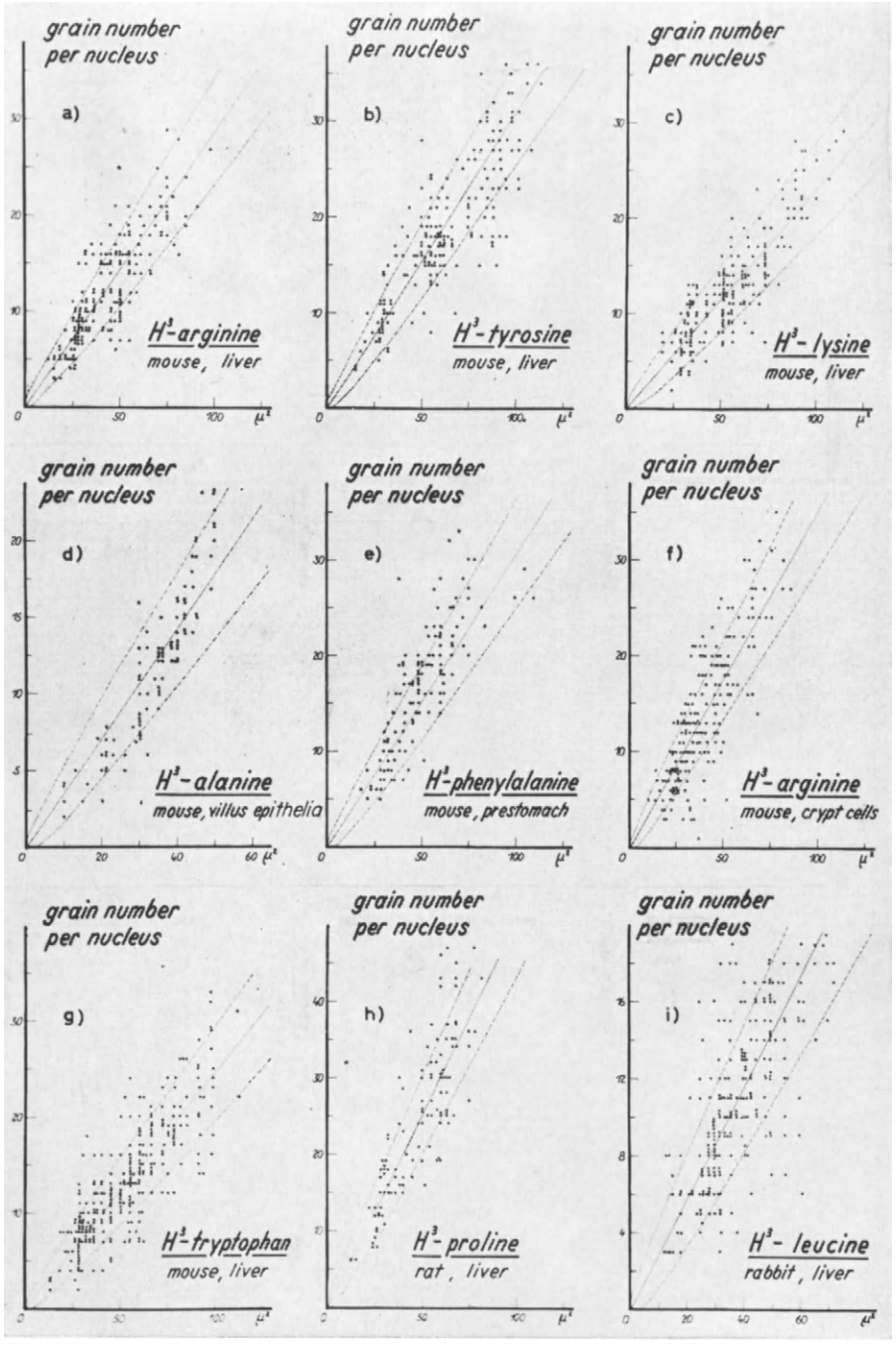
grain number per nucleus
a)
H³-arginine
mouse, liver
grain number per nucleus
b)
H³-tyrosine
mouse, liver
grain number per nucleus
c)
H³-lysine
mouse, liver
grain number per nucleus
d)
H³-alanine
mouse, villus epithelia
grain number per nucleus
e)
H³-phenylalanine
mouse, prestomach
grain number per nucleus
f)
H³-arginine
mouse, crypt cells
grain number per nucleus
g)
H³-tryptophan
mouse, liver
grain number per nucleus
h)
H³-proline
rat, liver
grain number per nucleus
i)
H³-leucine
rabbit, liver

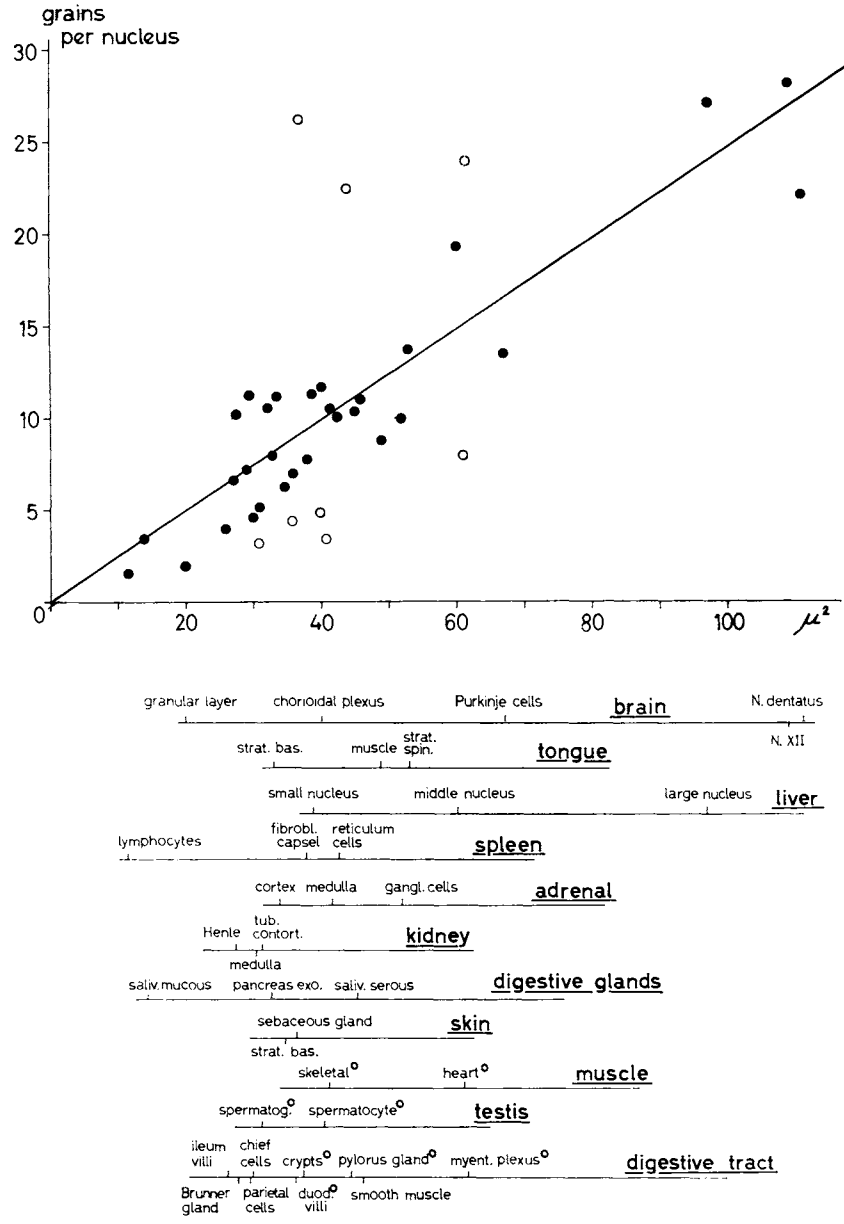

FIG. 7. Mean grain number per nucleus as a function of mean nuclear area for 39 different cell types (mouse). Each point equals one cell type; 60 minute experiment with ^{3}H-tyrosine.

leucine [25]. A similar result was obtained for ^{3}H-L-phenylalanine in the mouse [7]. No linear relationship was found for ^{3}H-DL-alanine. In describing the autoradiographs, the different behavior of DL-alanine has already been mentioned.

The nuclei of a single cell type can differ in volume because of the increase in volume between two mitoses, because of polyploidy, and because of individual variations. The linear curves in Fig. 6 for liver show that there is the same protein synthesis per unit volume, also in nuclei with different polyploidy and correspondingly differing nuclear volume. This could lead to the conclusion that the DNA content of a nucleus is the determining factor in protein synthesis. However, as shown in Figs. 7 and 8, the protein synthesis of the big nuclei of ganglionic cells

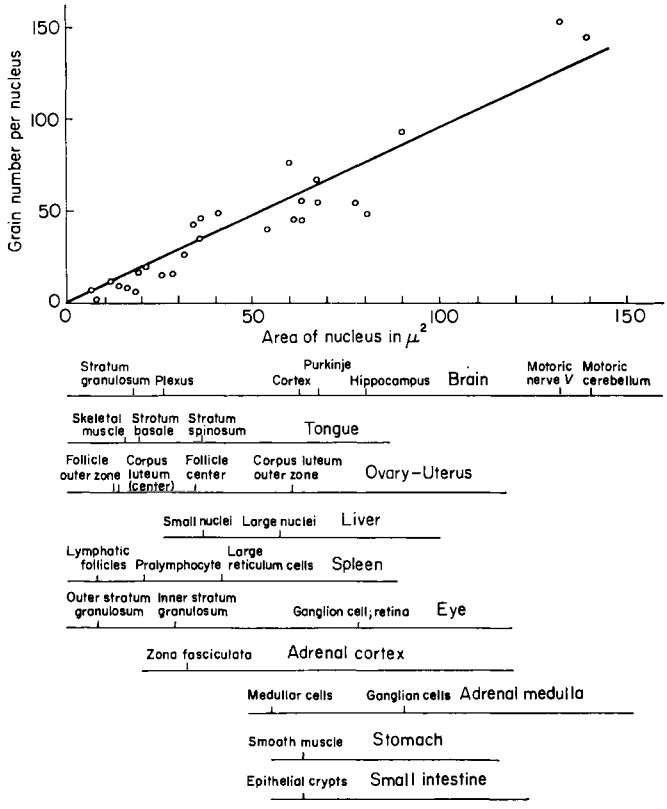

FIG. 8. Mean grain number per nucleus as a function of mean nuclear area for 26 different cell types (rat). Each point equals one cell type; 90 minute experiment with ^{3}H-DL-leucine.

is much higher than the protein synthesis of the small muscle nuclei in spite of the same DNA content.

Assuming that the concentration of protein is also approximately the same in the different nuclei, the constant turnover rate per unit nuclear volume found would lead to the interesting conclusion that the mean life-span of nuclear protein should have a similar value for different cell types. According to biochemical experiments of Niklas *et al.* [23], there is some experimental evidence that the mean life-span of the nuclear protein in rat is in fact about 1 day for different types of nuclei, while the mean life-span of the cytoplasmic protein of different cell types varies between about 1 and 50 days.

Quantitative Evaluation of the Cytoplasmic Protein Synthesis

According to the counting method described under Materials and Methods, Quantitative Evaluation, point 3, the ratio of incorporation of different amino acids into the whole cytoplasm of a cell to that into the total nucleus was determined for many cell types. The results are summarized in Table II. The values were not corrected for the differences in β-self-absorption [19] in the cytoplasm and nucleus. Thus, they should actually be somewhat higher. But the influence of β-self-absorption affects all values in the same direction and to a similar extent, as was experimentally confirmed for different cell types.

Table II (horizontal lines) shows that the ratio of amino acid incorporation into the whole cytoplasm of a cell to the incorporation into the total nucleus is strikingly constant for different ^{3}H-amino acids. Again this provides good evidence that the amino acid incorporation measured represents protein synthesis and, further, that metabolically active protein has a very similar composition in cytoplasm and nucleus.

Only the value for ^{3}H-arginine is as a rule considerably lower—by a factor of about 1.4—for all the different cell types. The lower value for ^{3}H-arginine might be due to the higher arginine content of the fast-turnover fraction of the nuclear protein, perhaps the histones. On the other hand, it should be emphasized that the values for ^{3}H-lysine do not differ from those of the other amino acids investigated.

Comparing the different cell types in Table II, it is evident that for the majority of cell types the ratio of total cytoplasmic to total nuclear incorporation is rather constant and has a value of about 7. Lower values for this ratio were found for some cell types listed at the top of Table II. On the other hand, for the exocrine pancreas epithelia the ratio is higher and has a value of about 14 (mean value of I-VIII, 60 minutes) or of 9.6 for ^{3}H-arginine. It should be emphasized that in this respect ^{3}H-alanine does not differ from the other amino acids. This contrasts to its

TABLE II. *Ratio of Total Cytoplasmic to Total Nuclear Amino Acid Incorporation for Different Cell Types of Mouse and Rat after Application of Different Tritiated Amino Acids*

Nuclear volume (% of cell volume)	Cells	Mouse									Rat	
		I	II	III	IV	V	VI	VII	VIII		IX	X
		Alanine	Leucine	Serine	Phenyl-alanine	Tyro-sine	Trypto-phan	Pro-line	Ly-sine	Mean I-VIII	Ar-ginine	Tyro-sine
30	Lieberkühn's crypts		2–3	2.2						2.4		
20	Choroid plexus	5.3	4.8	4.2	4.2	4.5			4.3	4.6		4.2
20	Ganglionic cells (CNS)		5.1[a]		7.4[b]	6.9[c]			6.2[a]	6.4		8.4[a]
15	Villi epithelia (small intestine)	5.0	5.4		5.1	5.4	5.1		4.5	5.1	3.1	4.6
14	Pylorus glands	3.1	4.0	4.2	3.8	3.3			3.5	3.7	2.2	4.2
14	Adrenal medulla		7.3	5.7	3.1	3.5	4.3			4.9	2.9	4.5
14	Pancreas endocrine	6.1	5.0	4.9	6.5		4.5			5.4		5.0
14	Salivary gland (serous)	6.9	7.2	7.5		7.2			6.8	7.1	6.9	6.0
12	Brunner's glands	5.8	5.6	7.3	7.2	5.2			5.4	6.1	5.5	5.1
12	Adrenal cortex	5.3	5.8	6.4	7.2	7.4	6.0		6.1	6.3	4.9	5.6
9	Kidney medulla	5.6		4.5	6.1	4.4	4.2		5.5	5.1	3.0	5.4
9	Liver	7.6	7.9	6.8	8.0	7.7	7.5	7.5	7.1	7.5	5.8	7.1
8	Kidney cortex	6.6		6.4	6.4	6.3	5.7		6.0	6.2	4.1	5.2
8	Kidney (Henle)	6.0	8.5		6.8	6.5	6.8		6.1	6.9	3.6	6.8
8	Pancreas exocrine	13.5	13.4	12.5	17.5	15.8	16.5	13.4		14.7	9.6	15.0
5	Salivary gland (mucous)	6.9	7.1			8.3			6.8	7.3	6.9	7.3
4	Smooth muscle	7.0	7.2	7.1	7.6	6.0	6.4		6.1	6.8	3.6	6.0
3	Heart muscle	6.1	10.5	7.7	6.5	6.7	9.5		6.1	7.6	6.6	6.9
1.3	Skeletal muscle	6.3	7.1	7.1	8.4	9.2	7.1		7.8	7.6		6.7

[a] Nucleus dentatus. [b] Nucleus olfactorius. [c] Nucleus XII.

more or less different behavior concerning the mean grain density over the different cell types.

In Table III these activity ratios for the liver cells of different animals, using different amino acids, are compared. The ratio is always approximately 7 and does not depend on the animal species.

TABLE III. *Ratio of Total Cytoplasmic to Total Nuclear Amino Acid Incorporation for the Liver of Mouse, Rat, Rabbit, and Pigeon after Application of Different Amino Acids*

Animal	Amino acid	Liver
Mouse	^{3}H-Amino acids (mean value of 8 different)	7.5
Rat	^{3}H-L-Tyrosine	7.1
Pigeon	^{3}H-DL-Leucine	6.8
	^{3}H-DL-Lysine	6.8
Rabbit	^{3}H-DL-Leucine	7.4

Of course, this constant ratio of cytoplasmic to nuclear incorporation (shown in Tables II and III) represents mean values for the cells of a certain cell type. However, this seems to hold true for the individual cell too. In certain favorable cases where the cell borders were easily recognized, the number of grains over the cytoplasm and over the nucleus were counted and the corresponding cytoplasmic and nuclear areas were measured simultaneously. The volumes of nucleus and cytoplasm and the corresponding activity per total volume were then calculated. The ratio between cytoplasmic and nuclear activity was found to be rather constant for the different cells examined, and had similar values as listed in Table II. Of course, this latter method of evaluation is of limited accuracy.

In Fig. 9 the values of the ratio of cytoplasmic to nuclear ^{3}H-L-tyrosine incorporation of the whole cell of the adrenal cortex (mouse) are plotted

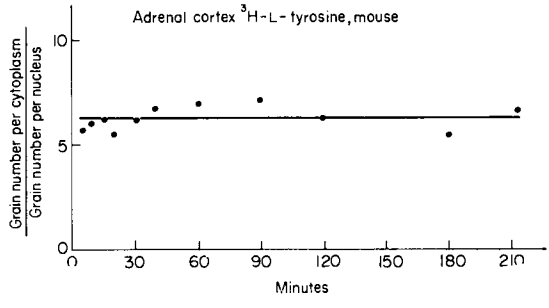

FIG. 9. Ratio of total cytoplasmic to total nuclear incorporation as a function of time. Adrenal cortex of the mouse labeled with ^{3}H-tyrosine.

as a function of time. There is a constant ratio between 5 and 315 minutes. For other cell types too, and with different amino acids, the ratio became constant after about 30 minutes. This means that after an initial period of equilibration of the free amino acid in the cytoplasm and nucleus, the increase in activity with time is the same for the cytoplasm and nucleus, and that the incorporated activity represents protein synthesis in the two cell compartments. It is very improbable that the curve in Fig. 9 could be the final result of migration of labeled protein from nucleus to cytoplasm and vice versa, because the same ratio of 7 for liver *and* muscle cells would then be quite incomprehensible, considering the big differences in the relative volumes of cytoplasm and nucleus.

The exocrine pancreas epithelia, which show an exceptionally high ratio of about 14 (Table II), seem to be no real exception. It is known that after short experimental times the grains appear over the ergastoplasm. As time increases, more and more grains are found over the zymogen granules [35]. Grain counts such as those performed for cells of the adrenal cortex (Fig. 9) were carried out for the exocrine pancreas epithelia and showed that the ratio of cytoplasmic to nuclear incorporation has a value of about 7 for short-time experiments and that this value increases with time. However, a value of about 7 was found for long experimental times too, when only those grains over the ergastoplasm were counted as "cytoplasmic activity" and those grains over the zymogen granules were excluded. Here, special conditions seem to exist which need further clarification.

The considerably lower value for the Lieberkühn's crypts (in Table II) is in line with the observation that the value for the ratio of cytoplasmic to nuclear incorporation obviously tends to decrease in all cells with an increased metabolic function (as shown in Table IV). Thus, lower values for the ratio of cytoplasmic to nuclear amino acid incorporation was found in regenerating liver cells [4], in trained heart muscle compared to normal [21], in fetal heart muscle compared to that of the mother [21], and especially in carcinoma cells [6]. Under the effect of butter yellow, the value of the ratio for liver cells decreases with increasing changes to adenoma and finally to carcinoma cells until it reaches a very low value of about 0.9 in the carcinoma cells [14, 20]. On the other hand, 2 hours after application of CCl_4 [5] to mice, the relatively high ratio of cytoplasmic to nuclear incorporation of 13.2 was found for the parenchymal cells of the centroacinar region in the liver lobules. On autoradiographs the grain density of these cells is 10 times less compared with normal liver cells; this means that these cells have a considerably reduced protein metabolism. In general, all experimental results obtained and listed in Table IV suggest that cells with a high

TABLE IV. *Ratio of Total Cytoplasmic to Total Nuclear Amino Acid Incorporation in Different Cell Types of Mouse and Rat under Normal and Pathological Conditions as well as in Tumor Cells*

Tissue	Normal			Tumors		Reference
				Adenoma	Carcinoma	
	1	2	3	4	5	
Mouse						
Liver, after application of CCl_4 (1, central; 2, normal; 3, peripheral)	13.2	7.5	6.6			[5]
Hepatitis (1, central; 2, normal; 3, peripheral)	9.1	7.5	7.7			[5]
Spontaneous mammary carcinoma (3, hypertrophic glands; 4, adenoma; 5, carcinoma)			3.0	2.1	1.2	[6]
Rat						
Hepatectomy (2, control; 3, hepatectomy)		7.5	5.9			[4]
Heart muscle (2, control; 3, training)		7.5	6.1			[21]
Heart muscle (2, mother; 3, fetus)		7.5	5.6			[21]
Butter yellow carcinoma (3, DAB–liver; 4, adenoma; 5, carcinoma)			6.5	2.4	0.94	[14, 20]

metabolic activity have more or less small values for the ratio of cytoplasmic to nuclear incorporation and vice versa.

Derivation of a Generally Valid Incorporation Scheme by which the Very Different Protein Metabolism in the Different Cell Types is Controlled

Considering the results described above, a generally valid incorporation scheme can be derived from the autoradiographic results. As shown in Figs. 6, 7, and 8, the protein synthesis of the whole nucleus depends on the volume of the nucleus. A big nucleus has a high protein turnover, a small nucleus a low one. On the other hand, Tables II and III demonstrate that the protein synthesis in the whole cytoplasm is always a very similar multiple of that in the whole nucleus. That means that the cytoplasmic protein synthesis is also proportional to the nuclear volume.

The very different grain densities of the different tissues on the autoradiographs can be easily explained by this simple incorporation scheme as shown in Fig. 10 for the autoradiographs of liver and muscle after application of ^{3}H-leucine. In the liver, the grain density over nucleus and cytoplasm is almost the same. This is due to the fact that in the liver the ratio of cytoplasmic to nuclear protein synthesis is approximately equal to the ratio of the volume of the two cell structures. The amino acid incorporation per unit volume is then similar in the nucleus and cytoplasm. In the muscle cell, as compared with the liver cell, the ratio of nuclear to cytoplasmic volume is quite different. In the autoradiograph of the muscle cell there is a single nucleus with a high grain density. Over the cytoplasm the grain density is approximately 10 times lower. This autoradiograph was purposely exposed much longer than the liver autoradiograph. Had the exposure time been the same for both, muscle and liver nuclei would have had a similar grain density. But then, only a few grains would be situated over the cytoplasm of the muscle cell. In summary, the small nucleus of the muscle cell also has a small protein synthesis rate. But it also applies for the muscle cell that the cytoplasmic protein synthesis is about 7 times that of the nucleus (Table II). However, this proportionally small cytoplasmic protein synthesis is distributed throughout a cytoplasmic volume 100 times bigger. This leads to a very small grain density over the cytoplasm. This is the quantitative explanation of the small grain density for tissues like muscle, connective tissue, and others.

The curve in Fig. 11 is a consequence of the incorporation scheme described. There is a linear relationship between the grain density over a certain cell type and the percentage of nuclear volume related to the total cellular volume. The amino acid incorporation per milliliter tissue

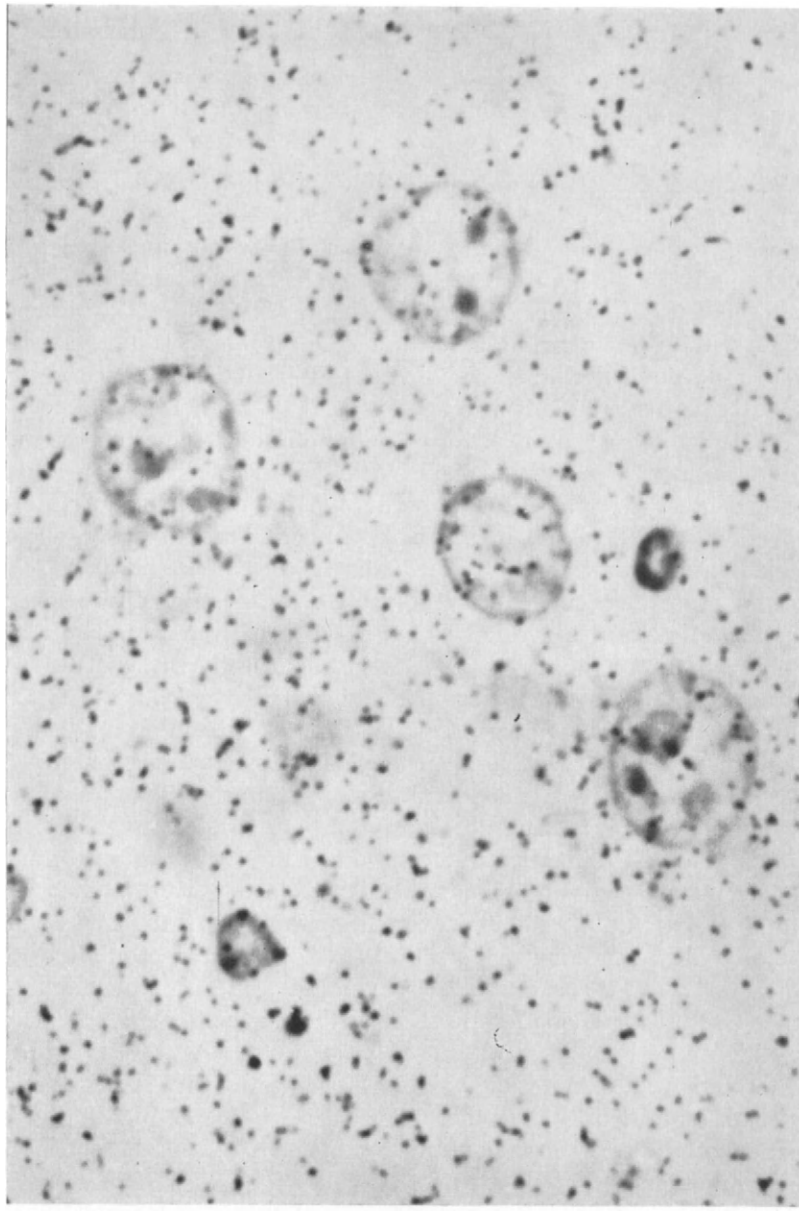

FIG. 10. Autoradiographs of the liver (this page) and the skeletal muscle (opposite page) of the mouse. Labeled with ^{3}H-leucine, 60 minutes.

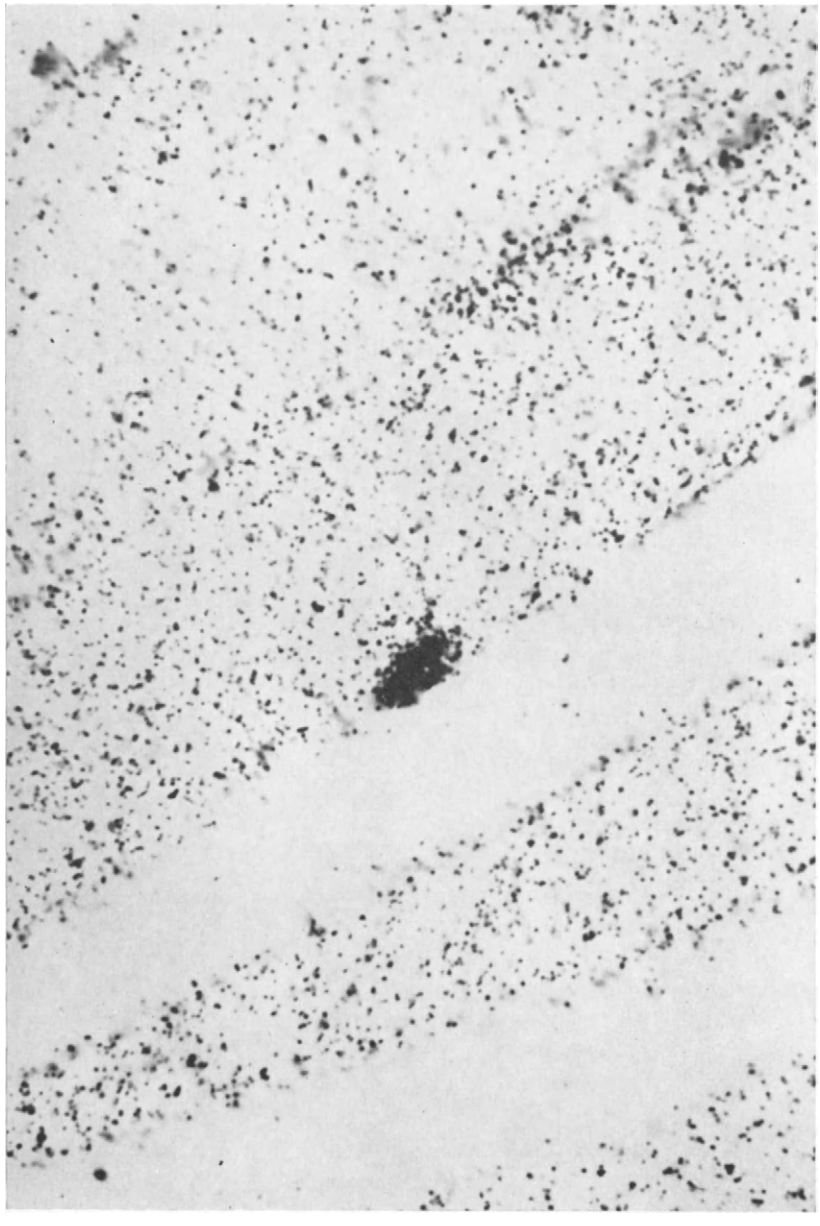

(measured as grain density) only depends on the proportion of the volume of all nuclei within this milliliter tissue. This proportion, however, is nothing more than the percentage of nuclear volume related to the total cellular volume. According to the incorporation scheme described, an approx-

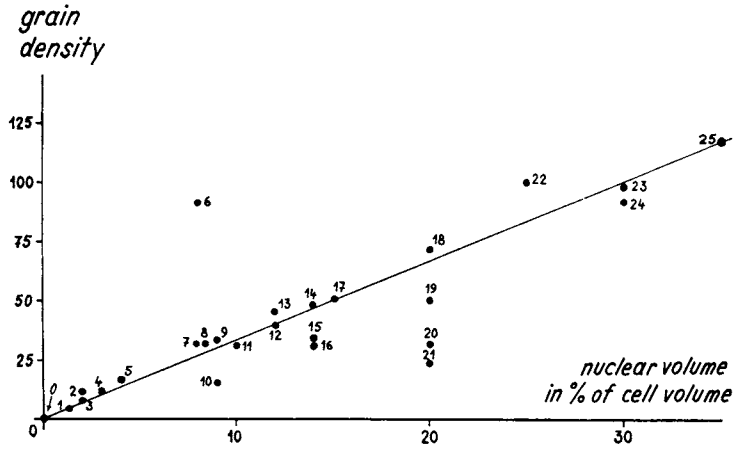

FIG. 11. Relationship between mean grain density and the nuclear–cellular–volume ratio of the corresponding cell type for 26 different cell types. Grain density equals the average of the relative grain density for tyrosine, phenylalanine, arginine, lysine, and tryptophan. Each numbered point corresponds to one cell type as follows:

0. Erythrocytes
1. Skeletal muscle
2. Fibroblasts
3. Muscle (tongue)
4. Heart muscle
5. Smooth muscle
6. Pancreas exocrine
7. Kidney cortex
8. Kidney (Henle)
9. Liver
10. Kidney medulla
11. Salivary gland (mucous)
12. Adrenal cortex
13. Brunner's glands
14. Salivary gland (serous)
15. Pancreas endocrine
16. Adrenal medulla
17. Villus epithelia
18. Prestomach epithelia
19. Tongue epithelia
20. Ganglionic cells (CNS)
21. Choroid plexus
22. Chief cells (stomach)
23. Crypt cells (small intestine)
24. Plasmocytes
25. Myenteric plexus

imately linear relationship is to be expected between protein synthesis and the percentage of the nuclear volume related to the cellular volume.

The possibility of establishing one common incorporation scheme for so many cell types leads to the conclusion that the protein metabolism of a cell is much more fundamentally controlled than would be expected for cells differing so greatly in function and morphology.

Proportionality Between Protein and RNA Turnover in the Different Tissues

As already described [30, 33], similar autoradiographs were obtained after application of labeled amino acids and labeled RNA precursors, such as tritiated cytidine and uridine. Apart from the different intracellular distribution of the grains, both kinds of autoradiographs have a very similar blackening pattern throughout the different organs and tissues of the organism. Figure 12 gives an example for the adrenal gland of the mouse after application of tritiated cytidine and leucine.

Quantitative evaluation by counting grains [30, 33] per unit area resulted in very similar relative grain densities for both RNA precursors and amino acids for the different cell types. There are only a few exceptions.

This agreement of the autoradiographic results for labeled amino acids and RNA precursors suggests that for those cell types the protein synthesis rate is, within certain limits, proportional to the RNA synthesis rate. Consequently, the nuclear volume is a measure for the nuclear RNA synthesis rate too. This was directly confirmed by Schneider and Maurer [29] in experiments with ^{3}H-cytidine. The results correspond to those in Fig. 6. This proportionality of the turnover rates for protein and RNA should not be confused with the proportionality between the protein *turnover rate* and the RNA *content* in a cell, as pointed out by Caspersson and Brachet.

The proportionality of protein and RNA synthesis rates may be responsible for the strikingly constant ratio of cytoplasmic to nuclear protein synthesis. Proportional amounts of protein and RNA are synthesized in the cell nucleus. The messenger RNA then migrating to the cytoplasm may induce a corresponding synthesis of cytoplasmic protein there.

SUMMARY

Application of 14 different ^{3}H-, ^{35}S-, and ^{14}C-labeled amino acids to mouse, rat, rabbit, guinea pig, and pigeon results in autoradiographs of a very similar blackening distribution over the various cell types. Obviously the relative grain density represents relative protein turnover rates of the various cell types. Some exceptions are discussed.

For the different cell nuclei of the organism an approximately equal protein synthesis rate per unit nuclear volume was found. This means that the protein synthesis rate in the whole nucleus depends on the volume of the nucleus.

Since the protein synthesis rate in the total cytoplasm of a cell is, in the majority of the cell types, a fixed multiple of the nuclear synthesis

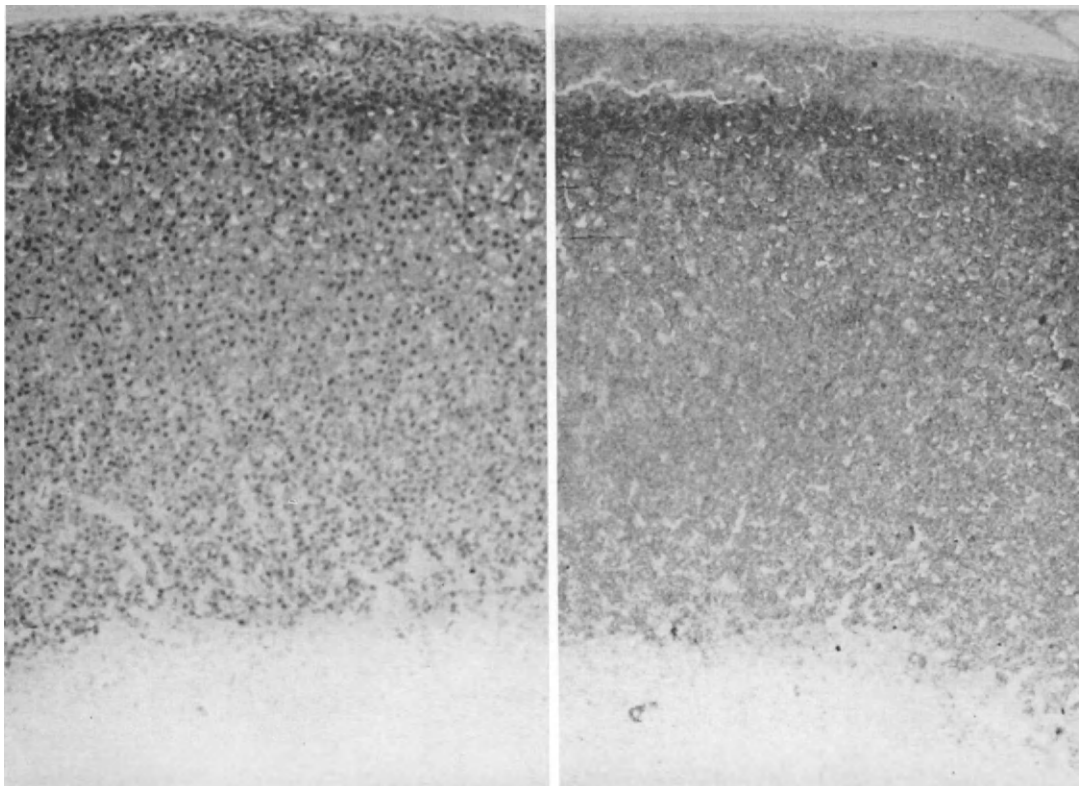

FIG. 12. Autoradiographs of the adrenal cortex of the mouse after application of tritiated cytidine, 180 minutes (left); and tritiated leucine, 60 minutes (right).

rate, the cytoplasmic protein synthesis rate depends on the nuclear volume as well.

These results lead to a generally valid scheme for cellular protein synthesis by which the great differences in the protein metabolism of the different cell types can be understood.

The protein synthesis per unit volume of the various cell types shows a linear relationship to the ratio of nuclear volume to whole cellular volume for the corresponding cell type, which can be understood as a consequence of the incorporation scheme described.

References

1. Altman, J., *Nature* **199**, 777 (1963).
2. Altman, J., *J. Histochem. Cytochem.* **11**, 741 (1963).
3. Bélanger, L. F., *Anat. Record* **124**, 555 (1956).
4. Busanny-Caspari, W., and Maurer, W., in preparation.
5. Citoler, P., and Maurer, W., *Beitr. Pathol. Anat. Allgem. Pathol.* **128**, 359 (1963).
6. Citoler, P., and Maurer, W., *Beitr. Pathol. Anat. Allgem. Pathol.* **129**, 73 (1963).
7. Citoler, P., Citoler, K., Hempel, K., Schultze, B., and Maurer, W., *Zschr. Zellforsch.* (in press).
8. Deimel, M., and Maurer, W., *Biochem. Z.* **334**, 462 (1961).
9. Droz, B., and Verne, J., *Acta Neuroveget. (Vienna)* **20**, 372 (1959).
10. Droz, B., and Warshawsky, H., *J. Histochem. Cytochem.* **11**, 426 (1963).
11. Ficq, A., and Brachet, J., *Exptl. Cell Res.* **11**, 135 (1956).
12. Fischer, J., Kolousek, J., and Lodin, Z., *Nature* **178**, 1122 (1956).
13. Gerbaulet, K., Maurer, W., and Brückner J., *Biochim. Biophys. Acta* **68**, 462 (1963).
14. Hempel, K., Lennartz, K.-J., and Maurer, W., *Beitr. Pathol. Anat. Allgem. Pathol.* **126**, 381 (1962).
15. Koburg, E., *Beitr. Pathol. Anat. Allgem. Pathol.* **124**, 108 (1961).
16. Koburg, E., and Plester, D., *Acta Oto-Laryngol.* **54**, 319 (1962).
17. Leblond, C. P., Everett, N. B., and Simmons, B., *Am. J. Anat.* **101**, 225 (1957).
18. Maurer, W., *Colloq. Ges. Physiol. Chem. 10th, Mosbach, 1959.* Springer, Berlin, p. 1.
19. Maurer, W., and Primbsch, E., *Exptl. Cell Res.* **33**, 8 (1964).
20. Maurer, W., Lennartz, K.-J., and Hempel. K., *Radioact. Isotop. Klin. Forsch.* **5**, 512 (1963).
21. Müller, D., and Maurer, W., in preparation.
22. Niklas, A., and Oehlert, W., *Beitr. Pathol. Anat. Allgem. Pathol.* **116**, 92 (1956).
23. Niklas, A., Quincke, E., Maurer, W., and Neyen, H., *Biochem. Z.* **330**, 1 (1958).
24. Nover, A., and Schultze, B., *Arch. Ophthalmol.* 131, 554 (1960).
25. Oehlert, W., and Schultze, B., *Beitr. Pathol. Anat. Allgem. Pathol.* **123**, 101 (1960).
26. Oehlert, W., Schultze, B., and Maurer, W., *Beitr. Pathol. Anat. Allgem. Pathol.* **119**, 343 (1958).
27. Oehlert, W., Schultze, B., and Maurer, W., *Beitr. Pathol. Anat. Allgem. Pathol.* **122**, 289 (1960).

28. Plester, D., Koburg, E., and Hempel, K., *Ann. Histochim.* **7**, Suppl. 2, 91 (1962).
29. Schneider, G., and Maurer, W., *Acta Histochem.* **15**, 171 (1963).
30. Schultze, B., and Maurer, W., *International Atomic Energy Agency Symp.*, TTS/63, Vienna (1961).
31. Schultze, B., Oehlert, W., and Maurer, W., *Beitr. Pathol. Anat. Allgem. Pathol.* **120**, 58 (1959).
32. Schultze, B., Oehlert, W., and Maurer, W., *Beitr. Pathol. Anat. Allgem. Pathol.* **122**, 406 (1960).
33. Schultze, B., Oehlert, W., and Maurer, W., *Biochim. Biophys. Acta* **49**, 35 (1961).
34. Tischendorf, F., and Linnartz-Niklas, A., *Acta Anat.* **48**, 7 (1962).
35. Warshawsky, H., Leblond, C. P., and Droz, B., *J. Cell Biol.* **16**, 1 (1963).

Discussion

Dr. Fitzgerald: I noticed that the incorporation of ^{3}H-leucine into the cytoplasm, relative to that in the nucleus, was greater in the pancreas than in the other organs. Is the difference related to the presence of zymogen granules?

Dr. Schultze: The ratio of cytoplasmic/nuclear incorporation (whole cell structure) is fairly constant in most cells, but pancreas is an exception. For all amino acids examined, the value is higher in the pancreas of rats and mice; at 60 minutes it is approximately double the value found in other cells. But the ratio of counts over ergastoplasm only/nucleus has the same value as in other tissues, that is, about 7. This does not offer any explanation, however, since radioactive material found in the region of zymogen granules should originate from synthesis in the ergastoplasm. This problem needs more experimental work.

Dr. Tonna: Did you obtain similar results for bone and cartilage cells as for other cells?

Dr. Schultze: Cartilage and bone cells have the same relative incorporation rate with different amino acids, but the ratio of cytoplasmic over nuclear incorporation in these cells has not been estimated.

Dr. Goldstein: Your data suggest that the rate of protein synthesis per unit volume is constant no matter what the nuclear volume is. On the other hand, Chèvremont reported that interference microscope measurements revealed that rather marked changes in protein concentration in the nucleus occur during the cell cycle. How do you reconcile these seemingly contradictory results?

Dr. Schultze: Concerning the changes in protein concentration in the nucleus during the cell cycle I must emphasize that our results represent the rate of protein synthesis. This synthesis rate is independent of the concentration and must not be correlated to the amount of protein, which may change.

Dr. Goldstein: Would you comment further on the migration of protein between nucleus and cytoplasm?

Dr. Schultze: Concerning the movement of proteins between nucleus and cytoplasm, the ratio of amino acid incorporation into the entire cytoplasm to that into the whole nucleus is constant between 3 minutes and 250 minutes after injection. A shift of protein in one direction would be detectable. In muscle cells, for instance, in which the concentration of the radioactive material is 10 times higher in the nucleus than in the cytoplasm, it is very unlikely that a diffusion equilibrium of labeled proteins exists. This is true for other cell types too (see Table II). On the other hand, in liver cells the conditions are different. In these cells the concentration

of the radioactive material is approximately equal in nucleus and cytoplasm. A quick exchange of labeled proteins back and forth would probably not be detectable.

DR. LEBLOND: The existence of a relation between nuclear size and rate of protein synthesis is important. It is difficult, however, to understand the phenomenon, because of the presence in the nucleus of several labeled proteins and ribonucleic acids (RNA) with different rates of metabolism.

Thus the grain counts over nuclei at 1 hour after *RNA* precursor injection correspond to the simultaneous presence of three labeled substances with different turnover times (Amano *et al.*, *Exptl. Cell Res.* 1965, 38, 314). Similarly, at 1 hour after *protein* precursor injection there are several labeled proteins in nuclei, some of cytoplasmic origin as suggested by the article of Goldstein at this symposium, and some of nuclear origin since they arise in isolated nuclei (Allfrey, V., *6th Canadian Cancer Conference* 1965, Academic Press, New York). Hence, the interpretation of your observations requires the identification of one substance at a time by kinetic or histochemical analysis in nuclei of various sizes.

DR. PELC: I do not agree that the graphs used by Amano *et al.* to analyze RNA synthesis in nuclei can unambiguously be interpreted as triphasic curves. They might well be biphasic and indicate exponential breakdown, eventually slowed down by reutilization of precursors.

DR. LEBLOND: The presence of the same pattern in four locations is taken as evidence in favor of the presence of three rather than two labeled RNA's in the nucleus. This conclusion is in line with recent biochemical analyses by Mirsky and Allfrey indicating the existence of three types of RNA in nuclei. Whatever the case may be, it is essential to realize that, after injection of either RNA or protein precursors, there are several labeled products in the nucleus.

DR. SCHULTZE: There are, of course, deviations from the constant relationship of cytoplasmic to nuclear incorporation, and also from the linear increase of nuclear incorporation with the nuclear volume. But in general, these relations exist and variations are minor, considering the differences in protein metabolism among the different cell types, numbering about 50. I am quite aware that I only measure the sum of all the rapidly turning-over fractions of proteins.

PROTEIN SYNTHESIS IN LYMPHOCYTES[1]

N. B. EVERETT, RUTH W. CAFFREY,
W. O. RIEKE, AND M. ROY SCHWARZ

Department of Biological Structure, University of Washington, Seattle, Washington

INTRODUCTION

The study of the lymphocyte is probably beset with more problems than that of any other cell type despite intensive research, particularly within recent years. The problems concern its origin, life-span, fate, extent of recirculation, and function. Functional considerations include its potential for elaborating substances important to the body in health and disease as well as its possible role in hemocytopoiesis, e.g., to serve as a stem cell for other types of blood cells. The problems are complicated by the fact that lymphocytes are not of a uniform cell type and investigators have not always agreed on the morphological characteristics of these cells. This complication with morphology has been appropriately expressed by Yoffey's statement [41] that "one thinks of the lymphocyte in negative terms, defining it rather by the absence of characteristics which other white cells possess, than by positive attributes of its own."

Thoracic duct lymph (TDL) has served as the source of lymphocytes for most investigators in studies of lymphocyte production as well as for a great variety of related studies. This seems appropriate since from the thoracic duct large numbers of lymphocytes can be easily obtained which are relatively uncontaminated by other cell types. Additionally, these are believed to be representative of the lymphocyte population, particularly those from lymph nodes. Appropriately stained smears of thoracic duct lymph show that lymphocytes cover a wide spectrum with respect to size, and are generally classified as large, medium, and small (Fig. 1). In studies from this laboratory [33] with rats, lymphocytes classified as large have a nuclear index of 110 or more μ^2. (The nuclear index is defined as the product of two nuclear diameters measured at right angles.) Approximately 1 per cent of the cells in TDL are large. Lymphocytes having nuclear indexes of less than 110 μ^2 and more than 56 μ^2 are considered medium and those with nuclear indexes of 56 μ^2 or less are classified as small. Approximately 4 per cent of the cells in TDL are medium and the great majority, about 95 per cent, are small. Studies

[1] Supported by U.S. Atomic Energy Commission contract AT(45-1)-1377.

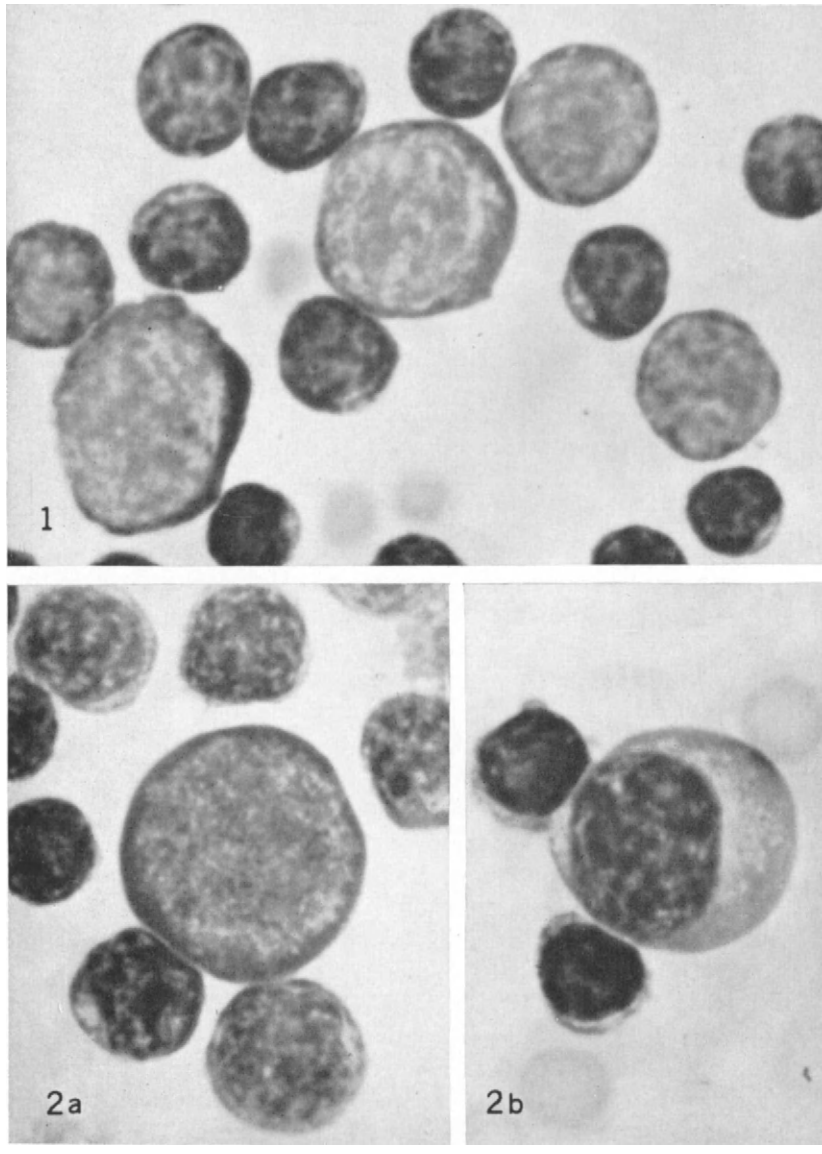

FIG. 1. Photomicrograph showing typical large, medium, and small lymphocytes of TDL. Magnification: 1500 × .

FIG. 2. Large lymphocytes of TDL. a, Cell with intensely basophilic cytoplasmic rim which is believed to be a plasma cell precursor. b, Large cell with abundant pale staining cytoplasm which is believed to be a precursor of medium and small lymphocytes. Magnification: 1550 × .

have shown that large lymphocytes are derived from stem cells of the node and that the developmental sequence, through a series of divisions, is large lymphocyte → medium lymphocyte → small lymphocyte [12, 13, 34]. The small lymphocytes comprise a nondividing population since they do not incorporate tritiated thymidine. They apparently retain the mitotic potential, however, since they have been shown to enlarge, entering the medium size category, and then undergo deoxyribonucleic acid (DNA) synthesis when appropriately stimulated [16, 17, 19, 28]. Thus, the class of medium-sized lymphocytes can include some cells derived from small lymphocytes as well as those derived from the large cell precursors. That the large lymphocytes of the TDL are not of a homogeneous type is evidenced by differences in staining [31], as well as by differences in submicroscopic structure [6, 42]. With conventional stains some of the large cells are round with a small amount of highly basophilic cytoplasm; others have more abundant cytoplasm which is pale staining (Fig. 2). The cells with intense basophilia are undoubtedly the same as those which have been shown by electron microscopy to have an abundant rough endoplasmic reticulum and are plasma cell precursors [6, 42]. These have been reported to synthesize γ-globulin [38] as well as to develop into mature plasma cells [18, 36]. The cells with the more abundant pale-staining cytoplasm are believed to be precursors of small lymphocytes.

Recent studies from this laboratory have shown that there are two populations of small lymphocytes in the rat with respect to site of origin, circulating life-span, and likely with respect to function [7, 15]. One population is short-lived and has a circulating life-span of 3–6 days. The other population, long-lived, appears to have a potential life-span comparable to that of the animal. These long-lived cells have been labeled and recovered from TDL at periods up to 1 year post-thymidine [11]. Approximately 90 per cent of the small lymphocytes in thoracic duct lymph of rats are long-lived and recirculate from blood to lymph. These long-lived cells are found in lymph nodes, spleen, and Peyer's patches, but are not ordinarily found in thymus or bone marrow [14, 15].

With respect to function of lymphocytes, an increasing body of information indicates their involvement both directly and indirectly in immune mechanisms (see review by Yoffey [41]). It is, in fact, now generally agreed that lymphocytes are the cells primarily involved in the homograft reaction, and it is probable that small cells mediate the response [3, 4, 21]. Experiments suggest that contact of lymphocytes with the homograft is necessary for graft destruction [1, 39, 40]. Attardi *et al.* [2], using a single cell technique, have shown that small lymphocytes as well as plasma cells are capable of inactivating bacteriophage and thus show antibody activity. Furthermore, the studies of Gowans and his

associates [17, 19, 20] as well as those of Porter and Cooper [28], provide convincing evidence that small lymphocytes may undergo hypertrophy and divide in response to antigenic stimulation. Studies in our laboratory have also shown hypertrophy of small lymphocytes which has followed irradiation or pertussis treatment [15, 16]. This hypertrophy, primarily cytoplasmic, suggests an immunologically active phase for these cells.

If the various lymphocytes have a direct role in immune mechanisms, it is likely that it would involve the elaboration of some protein substance in response to the immunological stimulus. Accordingly, studies were undertaken to assess protein synthesis of lymphocytes obtained from the thoracic duct lymph of control and stimulated rats with the view that the data might provide clues relative to lymphocyte function. Tritiated methionine and leucine have been used as precursor substances, and assessments of protein synthesis were made from radioautographs prepared with Eastman Kodak liquid NTB3 emulsion.

As pointed out previously [23], all cells elaborate protein even in the absence of bodily growth and this synthesis has been classified into 3 main types: (1) that associated with the formation of new cells; (2) that due to the elaboration of the various types of secretory, structural, and circulating materials; and (3) that attributable to turnover of intracellular material. Since large and medium lymphocytes are known to divide, attempts have been made to assess the extent of protein synthesis in these cells which is for cell renewal as well as that which is for export or intracellular turnover. This assessment has been made by comparing the time curve of labeling intensity for cells labeled with amino acids to similar curves obtained from a parallel set of experiments using ^{3}H-thymidine as a specific DNA precursor.

PROTEIN SYNTHESIS IN RELATION TO CELL RENEWAL

For the amino acid experiments, each of seven male rats weighing 135–170 gm was given a single intravenous injection of ^{3}H-methionine (specific activity 148 mc/mmole) in the amount of 4 μc/gm body weight. At intervals of 15 minutes, 4, 8, 24, 36, and 96 hours post-injection, TDL was collected by means of a Reinhardt fistula [30]. Radioautographs of smear preparations were made as previously described [13] and these were exposed for 8 weeks. In the parallel thymidine experiments each rat was given a single intravenous injection of ^{3}H-thymidine (1.9 c/mmole) in the amount of 1 μc/gm body weight.

In the ^{3}H-methionine experiments 100 per cent of the TDL large lymphocytes were labeled at 15 minutes and at all successive intervals sampled through 24 hours post-injection (Fig. 3). After 24 hours the

percentage of labeled cells was less than 100 per cent because the intensity of label for many cells after this time was below the level detected by the radioautographic procedure. The average grain count of the large lymphocyte was 32 at 15 minutes and increased to 53 at 4 hours. By 8 hours it had decreased slightly to 49. Between 8 and 18 hours the average grain count for the large cell decreased from 49 to 15, which reflects a 70 per cent loss in radioactivity. The increase in labeling intensity between 15 minutes and 4 hours after ^{3}H-methionine injection was not apparent in the thymidine experiments since the availability time

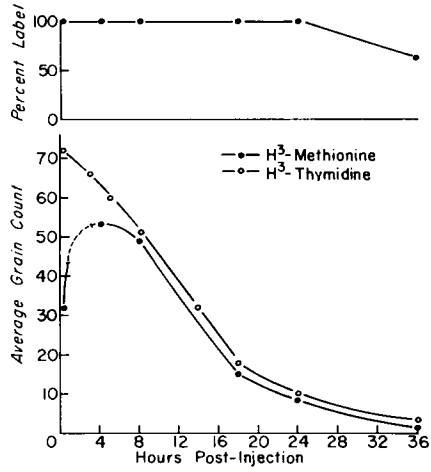

FIG. 3. Labeling patterns of large TDL cells. In the lower part of the figure the rates at which radioactivity disappears from large lymphocytes labeled *in vivo* with ^{3}H-methionine and with ^{3}H-thymidine are compared. The graph in the upper part of the figure shows that 100 per cent of the large cells were labeled with ^{3}H-methionine during the critical period of the comparison, 8 to 24 hours post-injection.

of ^{3}H-thymidine is less than 20 minutes [29]. The availability time of labeled amino acids is approximately 1 hour [32]. After the initial rise, the rate of decline in average grain count of the large lymphocyte population labeled with ^{3}H-methionine was essentially the same as that for cells labeled with ^{3}H-thymidine (Fig. 3). Thus it appears that in considering the total population of large cells, practically all protein synthesis is related to division.

Like the large lymphocytes, 100 per cent of the medium cells were labeled at short intervals after ^{3}H-methionine (Fig. 4). Although the average grain count of the medium cell was less than that of the large lymphocyte, the density of silver grains per unit area was comparable. The range of labeling intensity was greater for the medium than for

the large cell, and a few medium lymphocytes (usually intensely basophilic) had 4–5 times as many grains as the average medium cell. Although the generation time of the medium lymphocyte is not known and cannot be readily calculated, since, as indicated above, some may arise from hypertrophied small cells as well as through division of larger precursors, the rate of disappearance of radioactivity makes it highly probable that label is lost at a faster rate than can be accounted for by mitosis alone. For instance, between 18 and 24 hours, a time when the percentage of labeled medium lymphocytes remained constant in both the ^{3}H-methionine and ^{3}H-thymidine experiments, the medium lym-

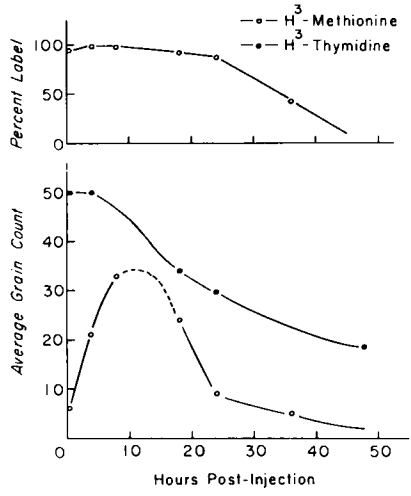

FIG. 4. Protein synthesis in control versus "activated" lymphocytes. In the lower part of the figure the rates at which radioactivity disappears from medium lymphocytes labeled *in vivo* with ^{3}H-methionine and with ^{3}H-thymidine are compared. The graph in the upper part of the figure shows that essentially 100% of the medium lymphocytes were labeled with ^{3}H-methionine during the critical period of the comparison, 18 to 24 hours post-injection.

phocyte population lost 63 per cent of its labeled protein, whereas the loss of labeled DNA was only 12 per cent. Thus it appears that for the medium lymphocyte approximately 20 per cent of the loss in labeled protein was due to cell division and the remainder, approximately 80 per cent, may be attributable to export and/or intracellular turnover.

The small lymphocytes, like the large and medium cells, labeled immediately after injection of ^{3}H-methionine. Although not all small lymphocytes were labeled under the conditions described, it was found that 100 per cent evidenced labeling after increasing the exposure time or the dosage level of labeled amino acid (Fig. 5). Labeling intensities

of small cells were fairly uniform at early intervals after isotope administration, with grain counts ranging from 3 to 10 per cell. The extent of labeling of these cells in relation to time is shown in Fig. 6. It may be noted that once the small lymphocytes reached maximal labeling their loss of radioactivity was at the rate of approximately 50 per cent in 12

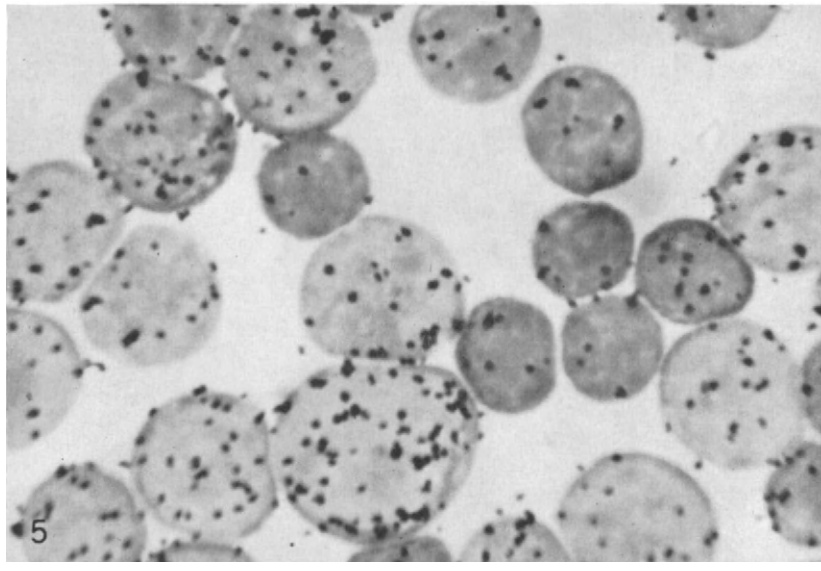

FIG. 5. Radioautograph of TDL lymphocytes from a rat after a subcutaneous injection of ^{3}H-leucine (30 μc/gram body weight); 14 day exposure. Magnification: 1500 × .

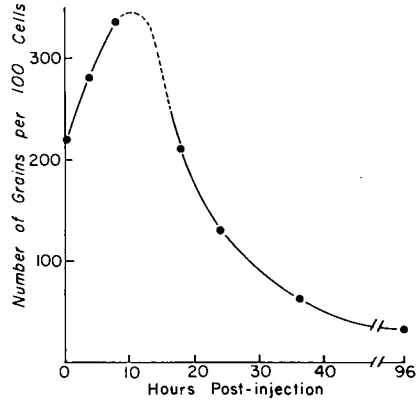

FIG. 6. Graph showing disappearance of label from TDL small lymphocytes after *in vivo* labeling with ^{3}H-methionine.

hours. This disappearance of labeled protein is almost entirely attributable to intracellular turnover and/or export rather than to cell renewal, since it is known that 90 per cent of the small cells in lymph have a very long life-span and recirculate from blood to lymph [15].

The distribution of silver grains over the lymphocytes indicated that protein synthesis was proceeding in both the nucleus and cytoplasm of all the cells.

MORPHOLOGICAL CHANGES IN THE SMALL TDL LYMPHOCYTE DUE TO STRESS

Studies on the morphology and size distribution of lymphocytes have shown that the average small cell in healthy animals has a nuclear index of 36 μ^2 with only a small amount of cytoplasm. A small percentage

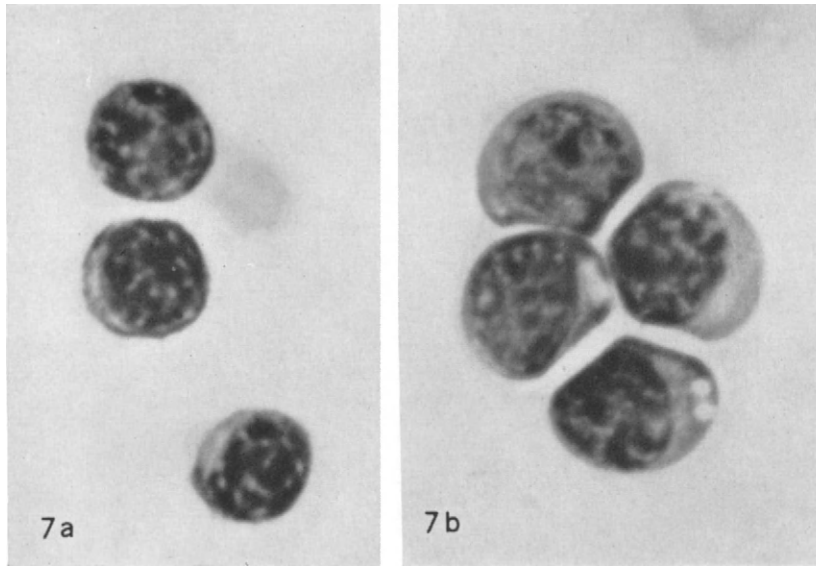

FIG. 7. Photomicrographs showing control (7a) and activated (7b) small lymphocytes. Magnification: 1500 × .

(*ca.* 10 per cent) have a slightly larger nucleus and more abundant cytoplasm. In animals receiving an antigenic stimulus such as pertussis vaccine, the size distribution of small lymphocytes in TDL shifted so that the average cell had a nuclear index of 49 μ^2 and more abundant pale-staining cytoplasm [15]. A greater enlargement of small lymphocytes has been observed in thoracic duct lymph of animals recovering from sublethal irradiation. These enlarged or activated small lymphocytes are shown in relation to control cells in Fig. 7.

Following 300 r of total body irradiation, approximately 90 per cent of the long-lived small lymphocytes became pycnotic and were removed from circulation during the first 48 hours following exposure [16]. Approximately 10 per cent of the small cells survived this dose and the average cell size increased, reaching a maximum at about 10 days post-irradiation. Transfusion of ^{3}H-thymidine labeled long-lived cells to irradiated animals showed that the post-irradiation enlargement was mediated through the irradiated animal and was not due to the direct action of irradiation on the cell. In spite of the increase in size, most of the activated lymphocytes were small, that is, incapable of division as shown by their failure to incorporate ^{3}H-thymidine. Although a small percentage of the activated cells may enter the medium-sized category and divide, it is believed that the morphological changes represent, in most cases, an immunologically active phase in the life cycle of the long-lived small lymphocyte.

PROTEIN SYNTHESIS IN THE ACTIVATED SMALL LYMPHOCYTE

In view of the morphological changes which occur in long-lived small lymphocytes subjected to various stimuli, it was decided to compare labeled amino acid incorporation in the activated cells with that of nonactivated small lymphocytes to determine if the morphological changes were associated with changes in protein synthesis.

The problem was first approached by using smears of the TDL from both controls and from animals given an intraperitoneal injection of pertussis vaccine (5×10^{9} cells). Labeled amino acid was administered 1 hour prior to thoracic duct cannulation and 4 to 7 days post-pertussis. In the pertussis-treated animals from 30–50 per cent of the small cells were activated. It is to be noted that in the controls 5–10 per cent of the cells were also judged from their morphological appearance to be activated. The cells in each slide were classified as either activated or nonactivated and the total number of grains over 100 cells of each type were counted. These preliminary studies indicated that the average grain count of activated small lymphocytes was approximately twice that of non-activated cells.

In a second approach to the problem, *in vitro* experiments were employed using ^{3}H-leucine as the protein precursor and sublethally irradiated rats as the source of activated cells. These experiments offered certain advantages over the *in vivo* experiments, namely: they provided a higher percentage of activated cells; allowed for better control of ^{3}H-amino acid concentration in the incubation medium; and eliminated the complication of labeled noncellular proteins in the radioautographic

preparations. These *in vitro* experiments also allowed for assessing the reliability of grain count determinations in estimating the rate of protein synthesis. Two types of experiments were used in this evaluation. In one, the amount of ^{3}H-leucine was varied with a constant incubation time of 20 minutes, and in the second, the amount of ^{3}H-leucine was constant (50 μc/ml media) and the incubation time was varied. The specific activity of the leucine was 5100 μc/mmole. It may be observed (Fig. 8) that the average grain count per cell was directly proportional to the amount of ^{3}H-leucine added. Likewise, the average grain count was directly proportional to the period of incubation (0–120 minutes).

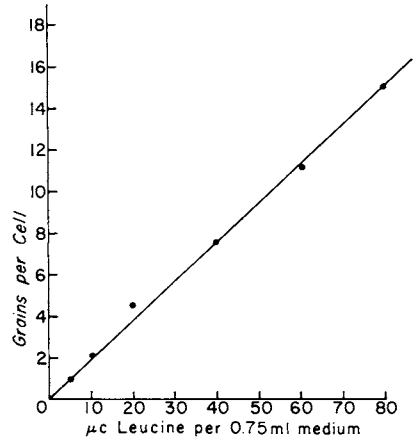

FIG. 8. Graph showing that average grain count over the small lymphocytes was proportional to the amount of ^{3}H-leucine added to the incubation medium.

Thirteen male Sprague-Dawley rats between 100 and 200 gm body weight were given 300 r of total body irradiation using a cobalt-60 source. During the second week post-irradiation lymph was collected from each rat by means of a Reinhardt fistula. Thoracic duct lymph from a non-irradiated control was processed with each experimental animal. The cells were counted, centrifuged, and resuspended in homologous serum. Approximately 20×10^{6} cells from each experimental and control rat were incubated at room temperature in identical media consisting of homologous serum and ^{3}H-leucine in a concentration of 50 μc/ml. After 20 minutes to 1 hour of incubation the cells were washed once by centrifuging and resuspending in Hank's balanced salt solution. Following a second centrifugation the cells were resuspended in a few drops of homologous serum and smears were made for radioautography. The slides were exposed for 1 to 3 weeks, depending upon the period of incubation, and grain counts were made on 100 small lymphocytes

encountered at random in each slide. Labeled activated cells are shown in Fig. 9. The results of the grain count determinations for the irradiated and control animals are summarized in Fig. 10. In all cases the average grain count was significantly higher in small lymphocytes of the ex-

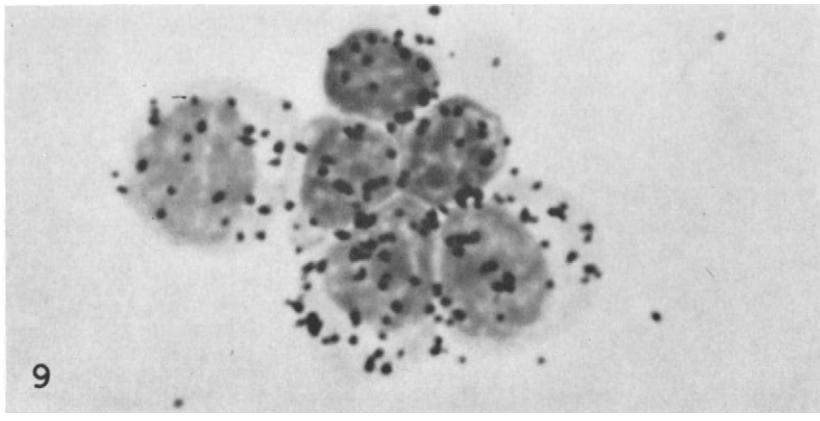

FIG. 9. Radioautograph of TDL small lymphocytes from an irradiated animal cultured *in vitro* with ^{3}H-leucine. Note the three activated (enlarged) cells which show a higher grain count than the smaller nonactivated cells. Magnification: 1500 × .

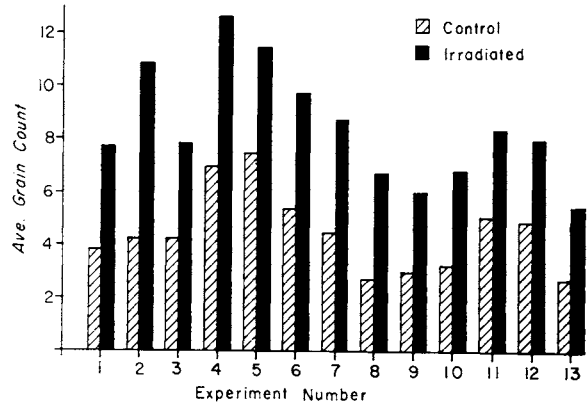

FIG. 10. Comparison of the *in vitro* uptake of ^{3}H-leucine in small lymphocytes of TDL from control and irradiated rats.

perimental animals. The small lymphocytes of experimental animals were predominantly of the activated variety, whereas those of controls were essentially all nonactivated. An average of all the experiments indicated that the small lymphocytes of irradiated rats synthesized protein at a rate 90 per cent higher than in nonirradiated controls.

DISCUSSION

The experiments reported here are in accord with the earlier autoradiographic studies of Pinheiro *et al.* [27] and Rieke and Schwarz [32] showing that 100 per cent of the lymphocytes are labeled by a single injection of tritiated amino acid and that the larger cells are more heavily labeled than the smaller ones.

The present studies indicate that practically all of the protein synthesized by the large cell population in TDL is associated with mitosis and cell renewal, while the major portion of that synthesized by the medium cells (80 per cent) and practically all of that produced by small cells is for purposes other than cell renewal. It should be emphasized, however, that these results are not in conflict with the view that some large lymphocytes may synthesize protein for purposes other than mitosis since the considerations apply to the total population of large lymphocytes in TDL. There is, in fact, good evidence that some of the large cells in TDL are plasma cell precursors [6, 18, 36, 42] and that they synthesize γ-globulin [38]. It is still a subject of considerable controversy as to whether the mature plasma cells or the immature blast forms have the major role in γ-globulin synthesis and export [26, 35]. Radioautographic studies using tritiated amino acids offer a direct approach to this problem, and the recent studies of Mitchell [24, 25] lend strong support to the view that it is the mature cell which is more actively engaged in protein synthesis for export.

The studies of Mitchell [24, 25] and those of Rieke and Schwarz [32] showed that, in comparison to plasma cells, there is little turnover of protein in small lymphocytes. Mitchell concluded that small lymphocytes synthesize only a small amount of fairly stable protein. The present studies as well as those of Rieke and Schwarz are not in accord with this conclusion, but show that protein turnover is occurring in the small lymphocyte with a half-time renewal rate of 12 hours for the labeled fraction.

The current study also shows that the rate of protein synthesis in small lymphocytes may be increased by conditions of antigenic stress and that this increase is associated with a change in the morphology of the cells, suggesting a more active phase. The activated small lymphocyte has a slightly larger nucleus with looser chromatin and more abundant cytoplasm with numerous small "nonstained bodies" and vacuoles. The "nonstained bodies" are probably the same as the multivesicular bodies observed by electron microscopy [42]. Janus green staining shows they are not mitochondria. The cytoplasm is not highly basophilic as compared with that of the mature plasma cell.

These activated cells are believed to be comparable to those previously described by a number of investigators. Their morphology is similar to that described by Downey and McKinlay [9] for the type III lymphocyte prevalent in certain diseases, by Dougherty and Frank [8] as stress lymphocytes observed in adrenalectomized rats, by Holub [22] as the "reactive small lymphocyte" present in TDL cultures exposed to antigenic stimuli, and by Binet and Mathé [5] as the "active cell" during the host versus graft reaction. The active cell in homograft rejection has been characterized by electron microscopy as having the morphological features of the small lymphocyte except for a peripheral distribution of chromatin and a relatively large amount of vesicular cytoplasm containing numerous non-membrane associated ribosomes [39]. These cells are easily distinguished from plasma cells which have an abundant rough-surfaced endoplasmic reticulum.

Very little information has thus far been obtained as to the types of protein synthesized by the lymphocytes. Recent advances in such techniques as immunophoresis combined with radioautography offer a promising method for approaching the problem. Initial success has been achieved in this laboratory with this combination method employing liquid NTB emulsion. The method entails culturing lymphocytes in a medium containing ^{14}C-amino acids. The lymphocyte proteins as well as the incubation medium are then exposed to immunophoresis and the immunoplates are coated with NTB liquid emulsion. These preliminary studies [10], as well as related studies by Slonecker [37], indicate that small lymphocytes synthesize proteins of the α-globulin variety as detected by electrophoretic studies. Since the α-globulins are not recognized as immunoglobulins and do not participate in the agglutination or precipitation reactions which are characteristic of classic antibodies, the problem as to the role of the α-globulins and thus the small lymphocyte in immunology remains obscure. The use of radioactive amino acids and radioautography combined with immunoelectrophoresis offers promise in approaching these problems.

SUMMARY

An assessment was made of the extent of protein synthesis for cell renewal in thoracic duct lymphocytes as well as that which is for export or intracellular turnover. This was done by comparing the time curves of labeling intensity for cells labeled *in vivo* with ^{3}H-methionine to similar curves obtained from a parallel set of experiments using ^{3}H-thymidine as a specific DNA precursor. The results indicated that essentially all protein synthesis of large lymphocytes and approximately 20 per cent

of that of medium lymphocytes is related to division. All small lymphocytes evidenced protein synthesis which was attributable to intracellular turnover and/or export.

In vitro experiments, using ^{3}H-leucine as a protein precursor, showed that activated small lymphocytes from rats receiving 300 r of γ-irradiation, synthesized protein at a rate 90 per cent higher than small lymphocytes of nonirradiated controls. The increased protein synthesis is believed to reflect an immune-like response, since the resultant activation of small cells has been shown to be mediated through the irradiated animal and is not a direct effect of irradiation upon the cells.

References

1. Algire, G. H., Weaver, J. M., and Prehn, R. T., *Ann. N.Y. Acad. Sci.* **64**, 1009 (1957).
2. Attardi, G., Cohn, M., Horibata, K., and Lennox, E. S., *J. Immunol.* **92**, 346 (1964).
3. Billingham, R. E., Brent, L., and Medawar, P. B., *Nature* **172**, 603 (1953).
4. Billingham, R. E., Silvers, W. K., and Wilson, D. B., *Lancet* **I**, 512 (1962).
5. Binet, J. L., and Mathé, G., *Ann. N.Y. Acad. Sci.* **99**, 426 (1962).
6. Braunsteiner, H., and Pakesch, F., *Wien. Z. Inn. Med. Grenzg.* **41**, 58 (1960).
7. Caffrey, R. W., Rieke, W. O., and Everett, N. B., *Acta Haematol.* **28**, 145 (1962).
8. Dougherty, T. F., and Frank, J. A., *J. Lab. Clin. Med.* **42**, 530 (1953).
9. Downey, H., and McKinlay, C. A., *Arch. Internal Med.* **32**, 82 (1923).
10. Epstein, L., personal communication (1964).
11. Everett, N. B., and Caffrey, R. W., *Anat. Record* **148**, 279 (1964).
12. Everett, N. B., Reinhardt, W. O., and Yoffey, J. M., *Blood* **15**, 82 (1960).
13. Everett, N. B., Rieke, W. O., Reinhardt, W. O., and Yoffey, J. M., *Ciba Found. Symp.* "Haemopoiesis, Cell Production and Regulation" (G. E. W. Wolstenholme and Maeve O'Connor, eds.). Published by J. & A. Churchill Ltd., London, p. 43 (1960).
14. Everett, N. B., Caffrey, R. W., and Rieke, W. O. *Proc. IX Congr. Intern. Soc. Hematol.* **3**, 345 (1964).
15. Everett, N. B., Caffrey, R. W., and Rieke, W. O., *Ann. N.Y. Acad. Sci.* **113**, 887 (1964).
16. Everett, N. B., Caffrey, R. W., and Rieke, W. O., *Radiation Res.* **21**, 383 (1964).
17. Gowans, J. L., *Ann. N.Y. Acad. Sci.* **99**, 335 (1962).
18. Gowans, J. L., and Knight, E. J., *Proc. Roy. Soc. (London) Ser.* B **159**, 257 (1964).
19. Gowans, J. L., Gesner, B. M., and McGregor, D. D., *Ciba Found. Study Group* **10**, 32 (1961).
20. Gowans, J. L., McGregor, D. D., Cowen, D. M., and Ford, C. E., *Nature* **196**, 651 (1962).
21. Hildemann, W. H., *Transplantation* **2**, 38 (1964).
22. Holub, M., *Ann. N.Y. Acad. Sci.* **99**, 477 (1962).
23. Leblond, C. P., Everett, N. B., and Simmons, B., *Am. J. Anat.* **101**, 225 (1957).
24. Mitchell, J., *Australian J. Exptl. Biol. Med. Sci.* **42**, 347 (1964).

25. Mitchell, J., *Australian J. Exptl. Biol. Med. Sci.* **42**, 363 (1964).
26. Nossal, G. J. V., and Mäkelä, O., *J. Exptl. Med.* **115**, 209 (1962).
27. Pinheiro, P., Leblond, C. P., and Droz, B., *Exptl. Cell Res.* **31**, 517 (1963).
28. Porter, K. R., and Cooper, E. H., *J. Exptl. Med.* **115**, 997 (1962).
29. Quastler, H., Sherman, F. G., Brecher, G., and Cronkite, E. P., *Proc. Second Conf. Peaceful Use Atomic Energy, Geneva,* Vol. 22, p. 202 (1958).
30. Reinhardt, W. O., and Li, C. H., *Proc. Soc. Exptl. Biol. Med.* **58**, 321 (1945).
31. Reinhardt, W. O., and Yoffey, J. M., *J. Physiol.* **136**, 227 (1957).
32. Rieke, W. O., and Schwarz, M. R., *Blood* **23**, 502 (1964).
33. Rieke, W. O., Everett, N. B., and Caffrey, R. W., *Acta Haematol.* **30**, 103 (1963).
34. Rieke, W. O., Caffrey, R. W., and Everett, N. B., *Blood* **22**, 674 (1963).
35. Schooley, J. C., *J. Immunol.* **86**, 331 (1961).
36. Schooley, J. C., and Berman, I., *Blood* **16**, 1133 (1960).
37. Slonecker, C. E., *Anat. Record* **145**, 287 (1963).
38. Wesslen, T., *Acta Dermato-Venereol.* **32**, 265 (1952).
39. Wiener, J., Spiro, D., and Russell, P. S., *Am. J. Pathol.* **44**, 319 (1964).
40. Woodruff, M. F. A., *Ann. N.Y. Acad. Sci.* **64**, 1014 (1957).
41. Yoffey, J. M., *Ann. Rev. Med.* **15**, 125 (1964).
42. Zucker-Franklin, D., *J. Ultrastruct. Res.* **9**, 325 (1963).

Discussion

Dr. Everett: A percentage of lymphocytes in cultures from blood is not stimulated by antigens. This observation could be related to the fact that there are two varieties of small lymphocytes in blood. Blood has a much higher percentage of short-lived lymphocytes than does thoracic duct lymph, and it is likely that these are the ones which do not respond to antigenic stimulation. In rats, at least, it seems to be the long-lived small lymphocyte which responds to antigenic stimulation.

Dr. Schwarz: While small lymphocytes are transformed into immature-appearing cells by phytohemagglutinin, an extract of the kidney bean, such a response is not considered by all authors to be antigenic in nature. In any event, the number of cells responding to this mitogenic agent *in vitro* is unclear, because too little is known about (a) the number and kinds of cells which die during culture; (b) the number, proliferative rates, and progeny of the cells which do divide; and (c) the number that persist without being transformed.

Dr. Leblond: It appears that, under antigenic stimulation or stress, some small lymphocytes can transform into fairly large, basophilic, divisible cells known as pyroninophilic cells, blast cells, graft rejection cells, etc. However, there does not seem to be evidence that this transformation can take place in the absence of antigenic stimulation or stress. For several years, Whitelaw, at the Ontario Cancer Institute in Toronto, cultured individual small lymphocytes from human and rat blood under continuous microscopic observation for up to 12 days and did not see enlargement and mitosis of these cells. However, when phytohemagglutinin was added to the medium used for blood cell culture, there was enlargement and mitosis of the small lymphocytes.

It would thus appear that, under steady state conditions and without antigenic stimulation, large and medium-sized lymphocytes do not come from small lymphocytes.

Dr. Everett: Dr. Leblond, you have summarized very well our views relative to the kinetics of lymphocytes. We have no evidence that medium-sized lymphocytes

are derived from small lymphocytes in the normal course of development. We recognize, however, that under appropriate stimulation some small lymphocytes enlarge sufficiently to enter the medium-sized class. It appears that these enlarged cells may divide to form other small lymphocytes.

DR. KOBURG: It is difficult to explain those conditions in the human where there are large numbers of lymphocytes with a hyperplastic lymphatic tissue, but the immune response is very weak. There may then be a high proportion of lymphocytes which cannot be activated.

DR. ALLFREY: Since low doses of X-rays inactivate the nuclear adenosine triphosphate (ATP) synthetic system (Stocken and Ord), the use of 300 r may lead to reduced levels of nuclear ATP and to reduced synthetic capacities in surviving lymphocytes.

DR. EVERETT: We recognize that 90% of the small lymphocytes are destroyed by 300 r. The 10% which persist enlarge and show increased protein synthesis. We have shown that this stimulation or activation is mediated through the animal and not from the direct effect of irradiation upon the small cells. I would add that we have shown the same relative increase in protein synthesis in small lymphocytes after antigenic stimuli. It seems likely that the activation of small lymphocytes by irradiation, which is indirect, is comparable to an immune response and may in fact be homologized with phenomena of autoimmune disease.

FATE OF NEWLY SYNTHESIZED PROTEINS IN NEURONS

B. DROZ[1]

Département de Biologie, Commissariat à l'Energie Atomique, Saclay, France

INTRODUCTION

The synthesis of proteins in nerve cells has been investigated by means of radioautography in the course of the past 10 years. On the basis of experiments in which radioactive sulfur-labeled amino acids were administered to intact animals, it was concluded that nerve cell bodies are the sites of a synthesis of protein [3, 8, 11, 12, 13, 19, 21, 24, 26–29]. Most authors have emphasized that protein synthesis is surprisingly large in nerve cells, as compared with most other cells of the body.

The purpose of this paper is to survey the kinetic behavior of proteins in neurons, as derived by radioautography after administration of tritium-labeled amino acids. The preparations were first examined in the light microscope [6]. More recently, the results were confirmed and extended with the electron microscope.

TURNOVER OF PROTEINS IN NEURONS

Biochemical Results

Ever since it was first suggested that proteins turn over in the brain [14], attempts have been made to estimate the life-span of protein in the nervous system. Thus, after intracisternal injection of ^{35}S-methionine, the half-life of brain proteins in rats was stated to be 13.7 days [16]. When ^{14}C-labeled amino acids were injected and the flux of amino acid into the brain proteins of mice was calculated, a series of turnover values was found, ranging from 3 to 15 days with ^{14}C-lysine and from 4 to 27 days with ^{14}C-leucine [23]. This "spectrum of turnover rates" reflected the heterogeneity of brain proteins [23, 33]. It must be emphasized that, when working on the whole brain by biochemical techniques, the data obtained are by no means specific for nerve cell bodies, since the material examined includes many nerve cell processes, glial cells of various categories, ependymal cells, and also blood vessels.

[1] Dr. B. Droz was a Fellow of the Rockefeller Foundation (1960–1962) in the Department of Anatomy at McGill University.

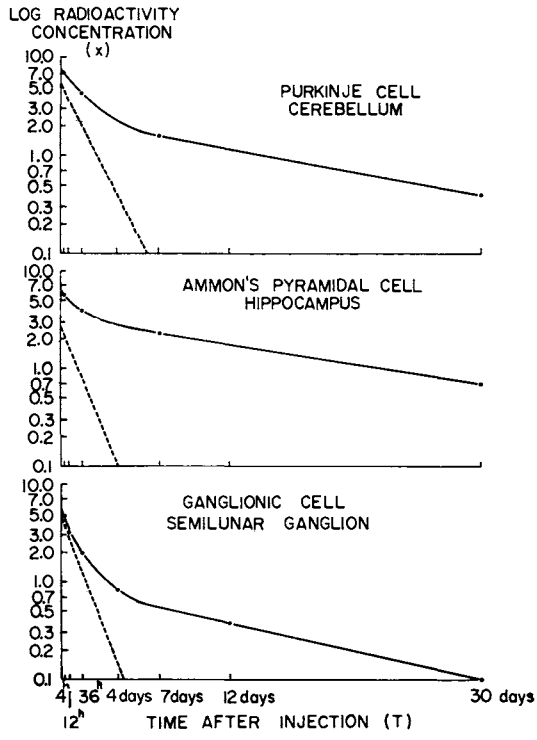

FIGS. 1–3. Decay curves of radioactive proteins in three types of nerve cell body.

FIG. 1 (top). Labeled proteins in Purkinje cells (cerebellum in rat) after ^{3}H-leucine injection.

FIG. 2 (middle). Labeled proteins in pyramidal cell (cornu Ammonis of hippocampus in rat) after ^{3}H-leucine injection.

FIG. 3 (bottom). Labeled proteins in ganglionic cells (semilunar ganglion of the trigeminal nerve in mouse) after ^{3}H-arginine injection.

The log of the radioactivity concentration (x) is plotted against time after injection. The right part of the curve has a straight line portion, the slope of which corresponds to the rate ($-k_2$) at which one class of protein turns over, that is, 5.8 to 7.2 per cent per day. By extrapolating to time 0, this line in turn may be subtracted from the corresponding portion of the original curve. The difference yields a straight line of steep slope ($-k_1$) indicating that 71 to 111 per cent of the second class of protein turnover in 1 day within the perikaryon. Thus two classes of protein may be distinguished: a rapidly turning over one of rate $-k_1$ and a slowly turning over one of rate $-k_2$, such that:

$$x = x_1 e^{-k_1 t} + x_2 e^{-k_2 t}$$

in which x_1 and x_2 may be graphically determined by extrapolating back to zero time. Taken from B. Droz and C. P. Leblond, *J. Comp. Neurol.* **121**, 331 (1963).

Radioautographic Results

In contrast, radioautography allows one to detect the radioactivity in individual neurons as distinct from their surrounding structures. Since the reliability of radioautography for the detection of newly synthesized proteins has been decisively established [9], this method is suitable for investigating the turnover of proteins within the neuron itself.

The kinetics of the disappearance of newly synthesized proteins were examined in the Purkinje cells of the cerebellum, the pyramidal cells of the cornu Ammonis in the hippocampus, and in the ganglionic cells of the semilunar ganglion of the trigeminal nerve.

After injection of a labeled amino acid such as ^{3}H-leucine or ^{3}H-arginine, the radioautographic reaction over the nerve cell bodies reaches a maximum around 90 minutes. Then, the radioactivity of cell bodies decreases progressively as shown by grain counts (Figs. 1, 2, and 3). All the decay curves obtained in plotting the log of the radioactivity concentration of the perikaryon versus time show the same pattern: they consist of an initial portion which decays rapidly and of a terminal portion which decays slowly. The analysis of such time curves [36] indicates the existence of two classes of proteins (Table I): a rapidly turning

TABLE I. *Turnover Time of Proteins in Three Types of Nerve Cell Body as Calculated from the Decay Curves of Labeled Proteins after Labeled Amino Acid Injection*

Neuron	Injected amino acid	Life-span (days)	
		Migratory	Sedentary
Purkinje cell (cerebellum)	^{3}H-Leucine	1.4	13.7
Pyramidal cell (hippocampus)	^{3}H-Leucine	0.9	17.3
Ganglionic cell (semilunar ganglion)	^{3}H-Arginine	1.1	13.7

over protein, which leaves the cell body in about 1 day, and a slowly turning over protein, which spends about 2 weeks in the perikaryon [6].

STEPS IN THE ELABORATION OF PROTEINS IN NEURONS

At short time intervals after injection of a labeled amino acid, the newly labeled proteins at their sites of synthesis are visualized by the radioautographic reaction. Later, proteins elaborated in one cell structure may be transported into another structure and their pathways of migration can be traced by radioautography.

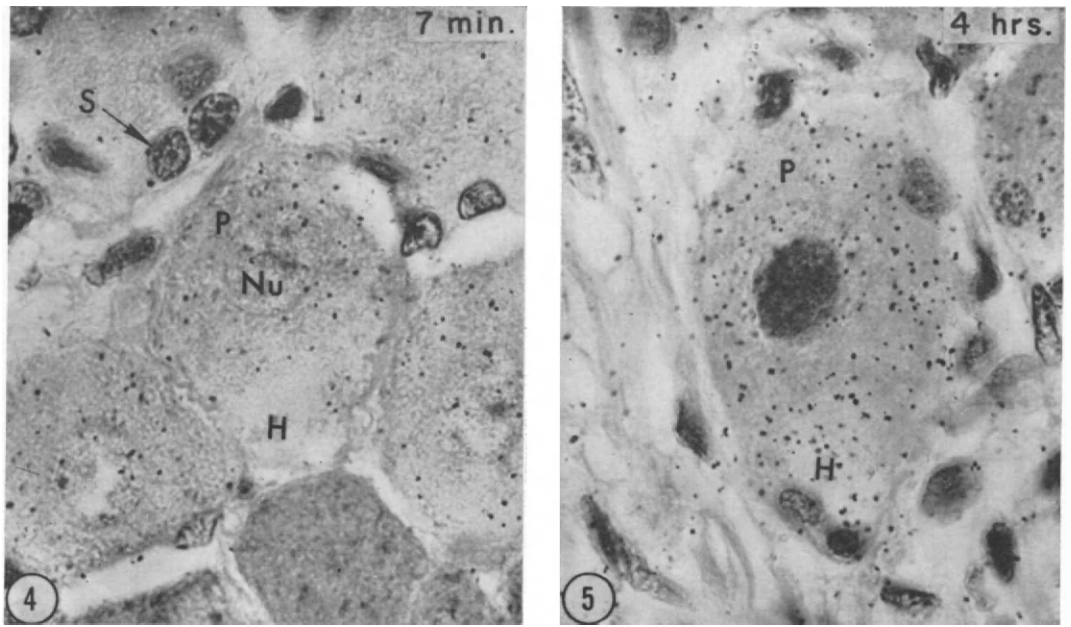

FIGS. 4 and 5. Hematoxylin and eosin stained radioautographs of semilunar ganglion of 80-gm rats given a single injection of ^{3}H-leucine and sacrificed after 7 minutes (Fig. 4) and 4 hours (Fig. 5).

FIG. 4. After 7 minutes, the silver grains are scattered over the nucleus (Nu) and perikaryon (P) with the exception of the axon hillock (H). A few grains may be seen over satellite cells (S).

FIG. 5. After 4 hours, the radioautographic reaction has increased over the perikaryon, but now silver grains accumulate over the axon hillock.

Both figures taken from B. Droz and C. P. Leblond, *J. Comp. Neurol.* **121**, 327 (1963).

Sites of Protein Synthesis in Neurons

As early as 7 minutes (Fig. 4) and 15 minutes (Fig. 6) after injection of ^{3}H-leucine, the radioautographic reaction seen over the perikaryon, and also over the nucleus, indicates that these structures are the sites of protein synthesis. On the contrary, the axon hillock (Fig. 4, H) and the axon proper (Fig. 6, A), both of which lack ribosomes, give no evidence of protein synthesis. Furthermore, by 15 minutes, electron microscopy (Figs. 6 and 7) shows that the label contained in the perikaryon is confined to the ergastoplasm of the Nissl substance, the ribosomes of which are presumably the sites of protein synthesis.

Intraneuronal Pathways of Migration

With the passage of time, radioactivity is detected in regions which were previously unlabeled. Thirty minutes after injection (Figs. 8, 9, and 11), silver grains may still be seen over the ergastoplasm of the Nissl substance, but at that time numerous silver grains overlie the vesicles and flattened sacs of the Golgi zone. The appearance of radioactivity in the Golgi zone indicates that proteins synthesized in the Nissl substance have migrated into the Golgi zone and have accumulated there.

By 4 hours, the axon hillock, which was previously unlabeled, becomes radioactive (Fig. 5). Thus, labeled proteins have moved into the axon hillock.

After 24 hours, the label is present in the proximal regions of the axons (Fig. 10). Since local synthesis cannot account for the presence of labeled proteins within the axon (Figs. 5, 12, and 13), it is concluded that proteins synthesized in the nerve cell body have moved into its axon within 1 day. This finding suggests that the rapidly turning over protein, which spends about 1 day in the perikaryon, is a migratory protein.

The distribution of silver grains over the axons at that time shows that only a few grains (6 per cent) seem to be related to mitochondria; about 18 per cent are located over the axolemmal membrane, whereas most of them (76 per cent) are spread over the axoplasm. From time to time, instead of being randomly distributed, the neurotubules and neurofilaments are packed in one region of the axon, presumably in the course of fixation. The radioautographic reaction shows a clump of silver grains superimposed on the packed neurotubules and neurofilaments (Fig. 10). This circumstantial evidence would indicate that the labeled proteins transported along the axons are mainly related to the neurofilaments and/or neurotubules.

As far as the identity of newly synthesized proteins is concerned, we

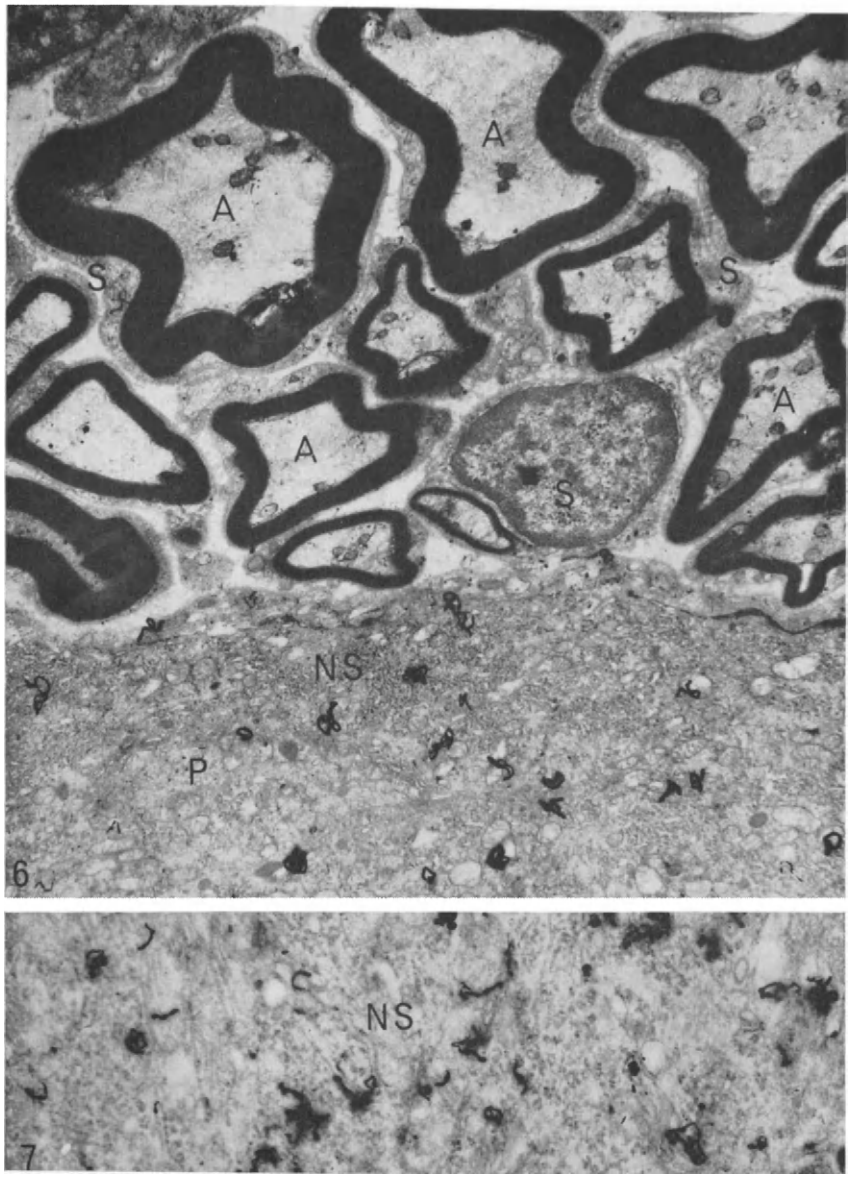

FIGS. 6 and 7. Electron microscope radioautograph of semilunar ganglion of 40-gm rat 15 minutes after an intraperitoneal injection of ^{3}H-leucine.

FIG. 6. Glutaraldehyde fixation and OsO_4 postfixation. Methacrylate–Ilford L4 emulsion diluted 1/6, developed in Microdol X for 5 minutes. Exposure time: 8 months. Karnowsky staining. Magnification: 7200 ×. The silver grains seen over the perikaryon (P) are mainly distributed over the Nissl substance (NS). A few grains

can only speculate. The presence of enzymatic activities such as choline-acetylase specifically found in the axon [18] and, to a lesser degree, acetyl cholinesterase, indicates that the enzymes have migrated from the nerve cell body, since the axon cannot account for the synthesis of such proteins. These enzymes, therefore, would share, at least in part, in the axonal migration of protein.

KINETICS OF THE AXONAL PROTEINS

Massive migration of proteins was shown to take place in the central nervous system, e.g., the hippocampus, cerebellum, medulla oblongata, and spinal cord [6] as well as in peripheral nerves and ganglia [5–7, 27, 31]. In contrast to the structural complexity of the central nervous system, the relatively simpler anatomy of peripheral nerves makes it possible to trace the movement of the labeled proteins in *individual axons*, with the exclusion of the other nerve components. The reason for success may be that after a single injection of ^{3}H-leucine, only a *short* segment of axon is labeled; but after multiple injections (every 3 hours over a 24-hour period), the proteins continuously elaborated by the nerve cell body label a *longer* segment of axon. Hence, the probability of detecting a labeled axon in nerve cross section is increased and the tracing of the label along the nerve is facilitated (Fig. 13).

Polarity of the Axonal Flow of Proteins

In the semilunar ganglion, as well as in the spinal ganglia, the axons originating from the ganglionic cells show a bifurcation into a "T." One branch of the "T" enters the peripheral nerve and terminates peripherally as sensory nerve endings; the second one enters the nerve roots and reaches the central nervous system, to which it carries sensory impulses. This special relation of the nerve cell body to its bipolar axon led us to examine whether the polarity of the impulse is related to that of the axoplasmic migration.

Labeled proteins elaborated by ganglionic cells were found to migrate both ways, that is, peripherally along the axons of the peripheral nerve toward the sensory nerve endings and centrally along the axons of

---

may be seen over satellite and Schwann cells. (S). No reaction occurs in the axon (A).

FIG. 7. Glutaraldehyde fixation and OsO_4 postfixation. Methacrylate–Gevaert NUC 307 emulsion diluted 1/2, developed in D 19 for 2 minutes. Exposure time: 12 months. Gelatin was digested in 2 per cent acetic acid. Magnification: 21,600 ×. Silver grains overlie the ergastoplasm of the Nissl substance (NS) which corresponds to the actual sites of protein synthesis.

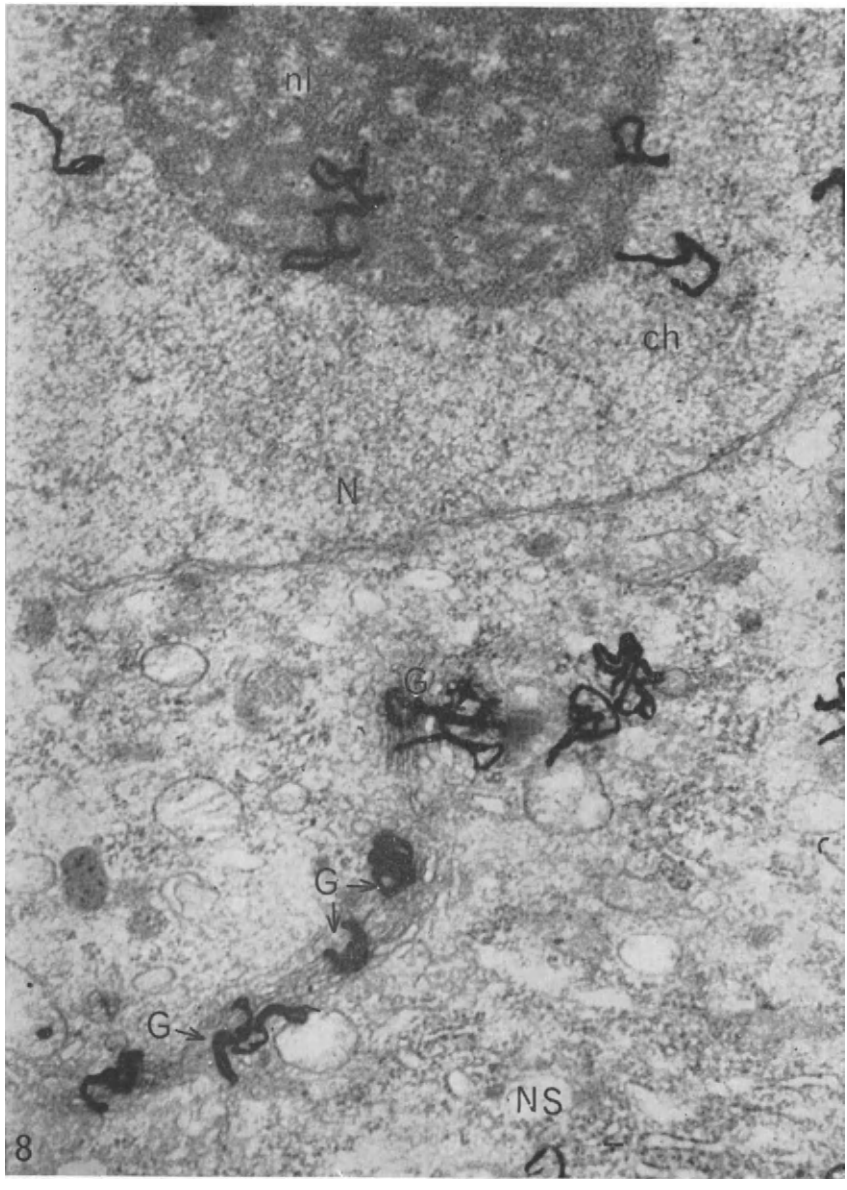

FIG. 8. Electron microscope radioautograph of a semilunar ganglionic cell 30 minutes after ^{3}H-leucine injection (same technique as Fig. 6). Magnification: 21,600 ×. Note incidentally the reaction over the nucleolus (nl) and chromatin (ch) of the nucleus (N). In the perikaryon, silver grains accumulate mainly over the vesicles and flattened sacs of the Golgi zone (G) as compared with the Nissl substance (NS).

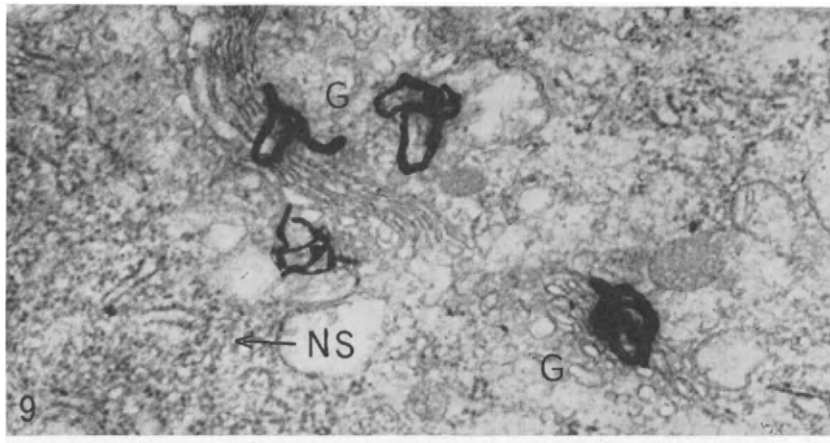

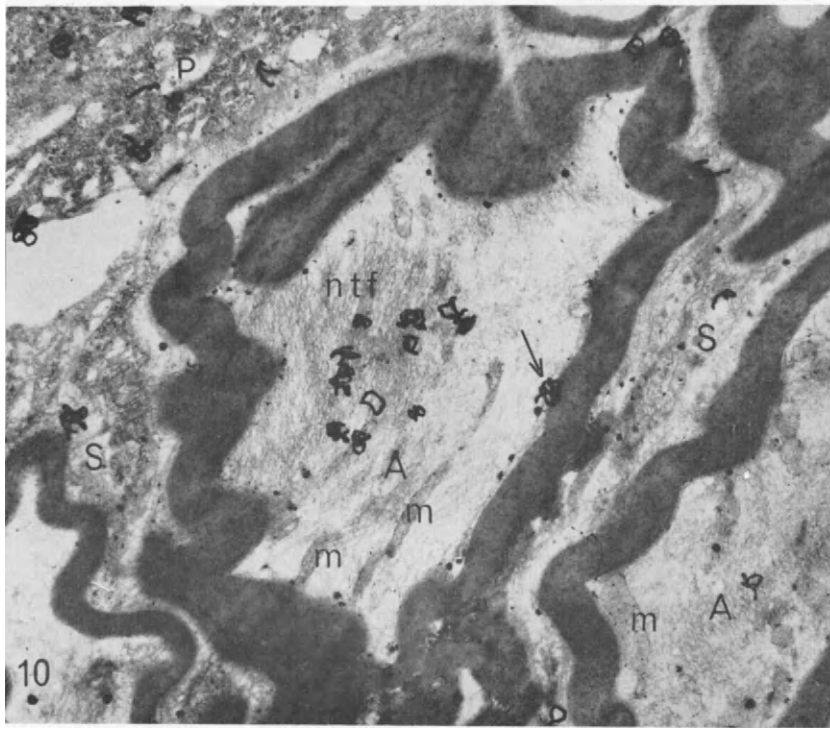

FIG. 9. Electron microscope radioautograph of a semilunar ganglionic cell 30 minutes after ^{3}H-leucine injection (same technique as Fig. 6). Magnification: 28,800 ×. Silver grains overlie the Golgi zone (G).

FIG. 10. Electron microscope radioautograph of an axon in the semilunar ganglion 24 hours after ^{3}H-leucine injection (same technique as Fig. 6). Magnification: 10,800 ×. In the axon (A), the packed fibrillar material (ntf), which corresponds to the neurofilaments and neurotubules of the axoplasm, is the site of an intense radioautographic reaction. The arrow points to a grain which overlies the axolemmal membrane. No reaction occurs over the mitochondria (m). Note also that the reaction persists over the perikaryon (P) of a ganglionic cell and over the Schwann cells (S).

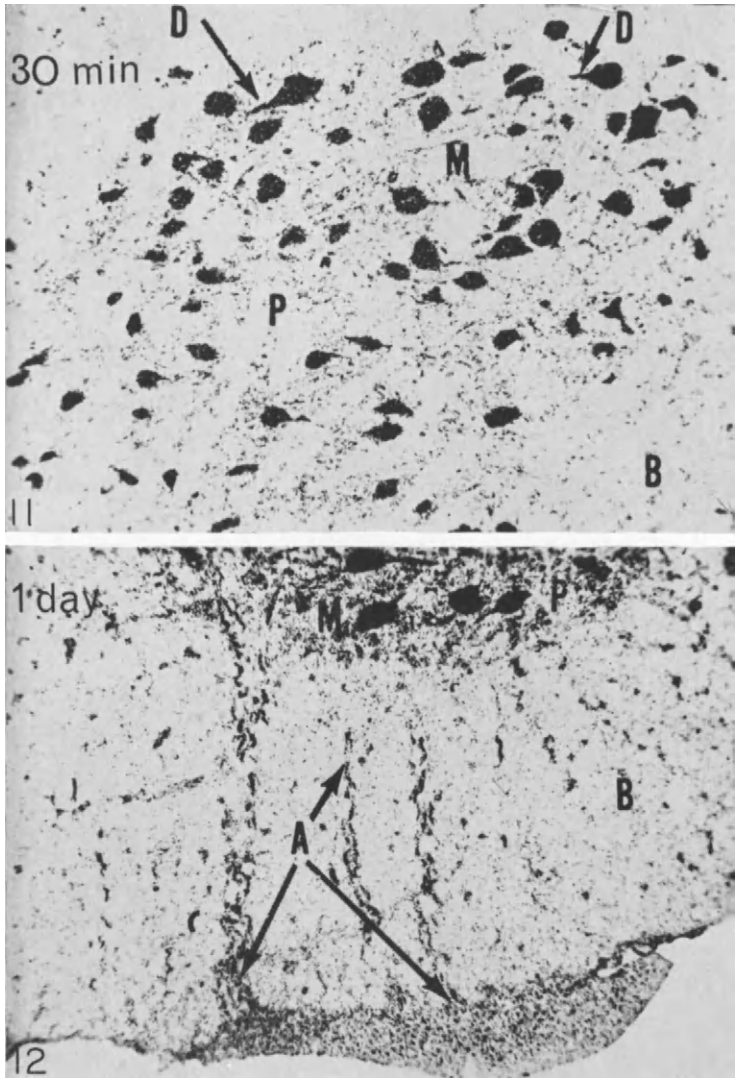

FIGS. 11 and 12. Unstained radioautographs of the spinal cord of 250-gm rats after injection of ^{3}H-leucine.

FIG. 11. The radioautographic reaction, 30 minutes after injection, is intense over the nerve cell bodies of motor neurons (M) and spreads over the base of the dendrites (D). The neuropile (P) and the white matter (B) show a rather weak reaction. No reaction occurs over the axons in the white matter.

FIG. 12. Twenty four hours after the first of a series of multiple injections (every 3 hours over a 24 hour period), the neuropile (P) shows a strong reaction. The motor neurons (M) are still extremely radioactive and the reaction extends now over their axons (A) which cross the white matter (B) to reach the ventral roots (at the bottom). Thus, proteins synthesized in the nerve cell bodies have moved into the axons. From B. Droz and C. P. Leblond, *J. Comp. Neurol.* **121**, 345 (1963).

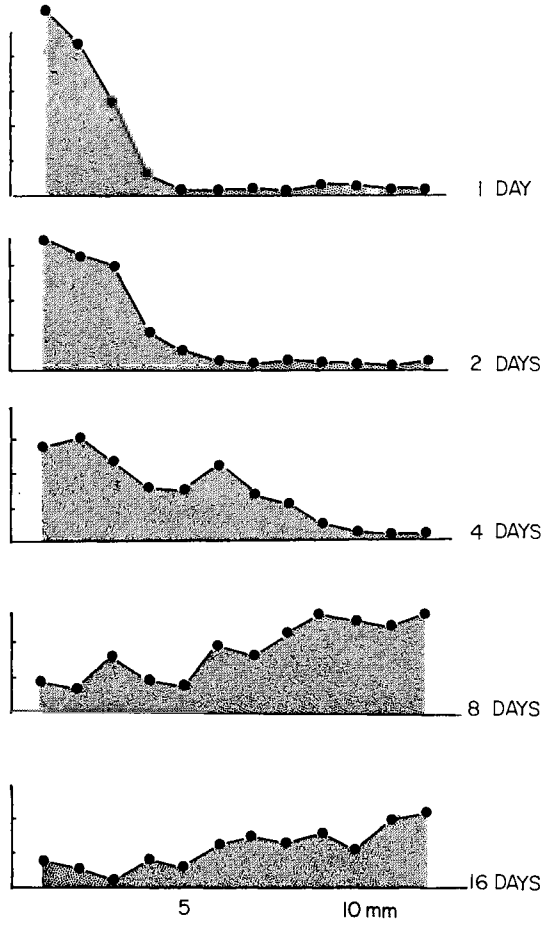

FIG. 13. Profile of the radioactivity along the maxillary axons of 45 gm rats given multiple injections of ^{3}H-leucine (every 3 hours over a 24 hour period) and sacrificed 1, 2, 4, 8, and 16 days after the first injection of the series. Radioautographs of nerve cross sections were prepared every millimeter along a certain length. Grain counts were made over 100 axons contained in the field of an ocular grid placed over the center of each nerve section. The average number of grains per axon is plotted against the distance in millimeters from the semilunar ganglion. By 1 and 2 days, the radioactivity is located in the proximal region of the axons, that is close to the cell bodies of the ganglionic cells. In the distal region of the axons, the very low number of grains corresponds to the axonal background. At 4 days, the radioactivity extends farther. Finally, by 8 and 16 days, the axonal radioactivity returns back to a low level in the proximal regions and reaches a high level in the distal ones.

the roots toward the central nervous system. Thus, the polarity of the axonal flow is independent of that of the nerve influx. In conclusion, the axonal migration of protein may be described as cellulifugal. The cell body would then act as a dispatching center of axoplasmic protein.

Velocity of Migration of Axonal Proteins

The velocity at which the axonal proteins move may be defined as the longest distance covered by the radioactive axonal proteins per unit of time (Fig. 13). Velocity is expressed in millimeters per day (Table II).

TABLE II. *Velocity of Protein Migration along the Axons*[a]

Subjects	Maxillary nerve [4]	Hypoglossal nerve [7]	Sciatic nerve [4]
Young (45-gm rats)	2.0	2.2	2.5[b]
Adult (250-gm rats)	0.9	0.6	0.8

[a] Results expressed as millimeters per day.
[b] From Rambourg and Droz [27a].

Contrary to Weiss and Hiscoe's opinion [35], the velocity of axonal protein migration seems to be independent of the length of the nerve (compare sciatic with hypoglossal or maxillary nerve). The most important feature to which we would like to draw attention is the difference of velocity observed in young and adult animals. The velocity of migration is higher in young growing rats, in which nerves are still increasing in length and diameter, than in adult animals. It is suggested that a supplement of axoplasmic proteins is required for the growth of the axons in young rats.

Turnover Rates of the Axonal Proteins

According to a theory proposed by Nadler (quoted by Droz [4]), the turnover rate of proteins per axonal cross section was calculated and found to be 7.5 and 6 per cent per hour in maxillary axons of 45-gm and 250-gm rats, respectively.

RADIOAUTOGRAPHY AS A TOOL FOR INVESTIGATING THE AXONAL MIGRATION OF PROTEINS

The concept of axonal migration of proteins has been derived from experiments in which axoplasmic material dammed up in front of a nerve section or constriction [15, 18, 35]. However, in such experiments, it is difficult to decide what part is taken by migration or by local synthesis in response to the injury. Hence, the conclusions obtained from experiments on *interrupted* neurons cannot be safely extended to *intact*

neurons. The results of previous experiments carried out with labeled amino acids suggested a movement of radioactivity along whole nerves, that is, including not only axons but also glial or Schwann cells, connective tissue cells, and blood vessels [22, 27, 29–34]; however, such conclusions could not be confirmed by several authors [2, 17, 20, 25, 28].

To provide a decisive demonstration of the axonal flow theory proposed by Weiss [34, 35], it is necessary to analyze the movement of protein in the axon proper and not in the nerve as a whole. In other words, it is important to *trace labeled proteins in the axons* themselves. This goal may be attained by high resolution radioautography not only in peripheral nerves but also in the central nervous system [4–7].

An axonal migration of proteins will be proved convincingly only if the following conditions are demonstrated to be fulfilled:

(1) *The axoplasmic proteins should not be produced* in situ. Although the Mauthner axons of the goldfish, which contain ribonucleic acid (RNA) [10a], seem to be capable of synthesizing proteins [10b], the evidence presented here is that such protein synthesis does not take place in the axoplasm of the rat.

(2) *The axoplasmic proteins must be elaborated in the nerve cell body, then pass to the axon and travel along its length.* Since the labeled proteins found in axons (Figs. 11–13) are not produced *in situ,* they may come from two possible sources: first, the Schwann or glial cells, which encompass each axon; second, the nerve cell body, from which the axon originates.

Let us consider the first possibility. It has been found that proteins synthesized in Schwann cells decay at the same rate all along the length of peripheral nerves. This means that, if Schwann cells transfer their labeled proteins to the axon, they would do it at the same rate all along the nerve and, therefore, radioactivity would appear simultaneously in proximal as well as in distal regions of the axon. Such is not the case: the labeled proteins appear first in the proximal regions of the axons, then they reach progressively more distal regions.

On the other hand, the second possibility, which deals with the passage of labeled proteins from the nerve cell body into its axon, fits the experimental data. In neurons, proteins are synthesized in the ergastoplasm of the Nissl substance (Figs. 6 and 7). Contrary to a recent misconception [1], the new proteins migrate to and accumulate in the Golgi zone (Figs. 8 and 9). Then, labeled proteins invade the axon hillock (Fig. 5), enter the axon (Figs. 10 and 12), move along its length (Fig. 13), and finally reach the nerve endings such as motor end plates [4] and synaptic knobs [4, 7].

The kinetic behavior of the newly synthesized proteins draws atten-

tion to the existence of two classes of protein: first, "migratory" ones, which rapidly leave their sites of synthesis in the perikaryon to enter the axonal process; second, "sedentary" ones which turn over slowly within the cell body (presumably ensuring the renewal of cell organelles).

(3) *The axonal migration of proteins insures the renewal of the axoplasmic proteins.* The axoplasmic proteins are continuously catabolized, presumably broken down by the proteolytic enzymes present in the central and peripheral nervous system [23, 33]. Since the axon is unable to synthesize its own proteins, the axon must receive new proteins manufactured by the nerve cell body to compensate for the loss of protein. This fact establishes that the axon is dependent on the nerve cell body, at least as regards protein metabolism. The integrity of the axonal cytoplasm, that is, the continuity, axon–cell body, is required to maintain the axon in a normal state; if not, the axon degenerates.

This feature is the so-called "trophic function" of the nerve cell body. The most important role of the nerve cell body is to purvey the axon with axoplasmic proteins and thus maintain integrity. In other words, at the cellular level, the existence of "migratory" proteins which move along the axon may be considered as both the morphological and the functional expression of the renewal of the axoplasmic proteins.

SUMMARY

After labeled amino acid injection, radioautography shows that the proteins newly synthesized in the nerve cell body disappear gradually with time. Analysis of the decay curves points to the existence of two classes of protein: "sedentary" ones, which turn over in 2 weeks; and "migratory" ones, which leave the perikaryon in 1 day. In the neuron, protein synthesis is shown to take place in the nerve cell body and not in the axon. Proteins newly synthesized in the ergastoplasm of the Nissl substance migrate to and pile up in the Golgi zone. Then, labeled proteins enter the axon hillock and, later, the axon proper, along which they move distally. Most of the labeled proteins found in the axons are related to the neurotubules and neurofilaments and, to a lesser degree, to the axolemmal membrane. The polarity of the migration may be rated as cellulifugal as observed in the "T" branch of the ganglionic axons. The velocity of the axonal migration is 0.6–0.9 mm per day in adult and 2–2.5 mm per day in young growing rats. Since the axon is not capable of elaborating its own proteins, the axoplasmic proteins are continuously manufactured by the cell body and transported within its axon all along its length to compensate for the loss of axonal proteins. This cellulifugal migration characterizes the turnover of the axonal proteins.

ACKNOWLEDGMENTS

I would like to express my gratitude to Dr. C. P. Leblond for his generous help during many experiments and for his constant advice. I wish to thank Dr. P. Granboulan, who kindly initiated me into the field of electron microscope radioautography. I am grateful to Dr. M. Vaughan for her help in the writing of the manuscript and to Mrs. J. Boyenval and Mr. J. Costa for their technical assistance.

REFERENCES

1. Bunge, R. P., and Bunge, M. B., *Anat. Record* **145**, 213 (1963).
2. Clouet, D. H., and Waelsch, H., *in* "Regional Neurochemistry" (S. S. Kety and S. Elkes, eds.), p. 243. Pergamon Press, London, 1961.
3. Cohn, P., Gaitonde, M. K., and Richter, D., *J. Physiol.* **126**, 7P (1954).
4. Droz, B., Thesis Ph.D., McGill University, 1964.
5. Droz, B., and Leblond, C. P., *Science* **137**, 1047 (1962).
6. Droz, B., and Leblond, C. P., *J. Comp. Neurol.* **121**, 325 (1963).
7. Droz, B., and Leblond, C. P., *Compt. Rend. Assoc. Anat.* **122**, 103 (1964).
8. Droz, B., and Verne, J. *Acta Neuroveget. (Vienna)* **20**, 372 (1959).
9. Droz, B., and Warshawsky, H., *J. Histochem. Cytochem.* **11**, 426 (1963).
10. (a) Edstrom, A., *J. Neurochem.* **11**, 309 (1964). (b) Personal communication, 1964.
11. Fischer, J., Kolousek, J., and Lodin, Z., *Nature* **178**, 1122 (1956).
12. Flanigan, S. J., Gabrielli, E., and McLean, P., *Arch. Neurol. Psychol.* **77**, 588 (1957).
13. Ford, D. H., Hirschman, A., Rhines, T., and Ziniberg, S., *Exptl. Neurol.* **4**, 444 (1961).
14. Friedberg, F., Tarver, H., and Greenberg, D. M., *J. Biol. Chem.* **173**, 355 (1948).
15. Friede, R., *Exptl. Neurol.* **1**, 441 (1959).
16. Gaitonde, M. K., and Richter, D., *Proc. Roy. Soc. (London) Ser.* **B 145**, 83 (1956).
17. Goslar, H. G., and Schultze, B., *Z. Mikroscop. Anat. Forsch.* **64**, 556 (1958).
18. Hebb, C. O., and Waites, G., *J. Physiol.* **132**, 667 (1956).
19. Klika, E., and Lodin, Z., *Acta Histochem.* **10**, 198 (1960).
20. Koenig, E., and Koelle, G. B., *Science* **132**, 1249 (1960).
21. Koenig, H., *J. Biophys. Biochem. Cytol.* **4**, 785 (1958).
22. Koenig, H., *Trans. Am. Neurol. Assoc.* **83**, 162 (1958).
23. Lajtha, A., *Intern. Rev. Neurobiol.* **6**, 1 (1964).
24. Leblond, C. P., Everett, N. B., and Simmons, B., *Am. J. Anat.* **101**, 225 (1957).
25. Miani, N., *Nature* **185**, 541 (1960).
26. Oehlert, W., and Schultze, B., *Intern. Conf. Radioisotopes Sci. Res. UNESCO, RIC.* 17. Pergamon Press, New York, 1957.
27. Rambourg, A., Thèse de Doctorat en Médecine, Nancy, France, 1961.
27a. Rambourg, A., and Droz, B., unpublished data, 1964.
28. Schultze, B., and Oehlert, W., *Strahlentherapie* **38**, 68 (1958).
29. Sloper, J. C., Arnott, D. J., and King, B. C., *J. Endocrinol.* **20**, 9 (1960).
30. Taylor, A. C., *Intern. Congr. Cell Biol. XIth, Excerpta Med. (abstr.)* **77**, 44 (1964).
31. Verne, J., and Droz, B., *Experientia* **16**, 77 (1960).
32. Waelsch, H., *in* "Biochemistry of the Central Nervous System" (O. Hoffman Ostenhof, ed.), p. 36. Pergamon Press, London, 1958.

33. Waelsch, H., and Lajtha, A., *Physiol. Rev.* **41**, 709 (1961).
34. Weiss, P., *in* "Regional Neurochemistry" (S. S. Kety and S. Elkes, eds.), p. 220. Pergamon Press, London, 1961.
35. Weiss, P., and Hiscoe, H., *J. Exptl. Zool.* **107**, 315 (1948).
36. Zilversmit, D. B., Entenman, C., Fishler, N. C., and Chaikoff, I. C., *J. Gen. Physiol.* **26**, 333 (1943).

Discussion

Dr. Everett: I would like to know if Dr. Droz has noted an accumulation of labeled protein at the nerve terminals in relation to synaptic vesicles.

Dr. Droz: Yes, I have observed an accumulation of labeled protein in motor end-plates of the hypoglossal nerve in young growing rats. Since this observation was made with the light microscope, I do not know if this accumulation of label is related to the synaptic vesicles.

Dr. Revel: Is there any label in the smooth endoplasmic reticulum of the axon? If the label is over the filaments of the axoplasm, as I understand, where and how is it released from the membrane-bounded elements of the Golgi?

Dr. Droz: Most of the silver grains appear to be related to the neurotubules and neurofilaments of the axoplasm. The presumed release of labeled protein from the Golgi zone to these structures was not seen in our radioautographs.

Dr. Salpeter: Are you sure that there is no protein synthesis in the axoplasm?

Dr. Droz: We believe that there is none. The available evidence is based on experiments such as the following: Sections of sciatic nerve were radioautographed 24 hours after the first of a series of injections of ^{3}H-leucine (total dose: 58 μc/gm body weight). The radioautographs were exposed for 6 months. The number of grains per unit area of axon was found to be twice as high as that of the background. It is difficult to decide whether this extremely weak reaction over the axons is an artifact due to crossfire radiation from the Schwann cells or is the result of a slight protein synthesis, possibly in mitochondria.

Dr. Leblond: Dr. S. Ochs has some evidence that the migratory protein of axons is present in the axonal fluid rather than in organelles. Do enzymes go from the perikaryon along the whole length of the nerves? Is not migration too slow to account for the passage of enzymes to terminal synapses?

Dr. Droz: In the case of the axons of young growing rats, our observations suggest that migratory proteins are not diluted in the axoplasmic matrix, but are mainly related to neurotubules and neurofilaments. Since no significant protein synthesis can be detected in axons, the axonal enzymes are probably manufactured in the nerve cell body, then pass into the axon. This interpretation is consistent with the damming up of choline acetylase in the proximal stump of a sectioned nerve and its disappearance in the distal segments (Hebb, D. O., and Waites, G., *J. Physiol.* 1956, **132**, 667). I stated above that, in the hypoglossal nerve, the accumulation of labeled proteins was observed in motor end-plates 16 days after injection of ^{3}H-leucine. This finding would indicate that, if migratory proteins are progressively broken down in the course of their travel along the axon, a substantial amount of new protein reaches the nerve endings.

Dr. Coimbra: Friede demonstrated an accumulation of oxidative enzymes in the central stump of ligated nerve (Friede, R., *Exptl. Neurol.* 1959, **1**, 441). Have you done this type of experiment with labeled amino acids, in order to have more direct evidence of protein migration along the axon?

DR. DROZ: I carried out such experiments combining a constriction of the postganglionic fibers of the superior cervical ganglion and radioautography after administration of labeled amino acids. Unfortunately, under these conditions, it is not possible to decide what is due to the local injury and what is due to axonal migration. On the basis of these results, I felt it necessary to seek decisive evidence of axonal migration only in intact neurons.

DR. CARNEIRO: You said that the proteins which migrate to the axons are produced in the ergastoplasm, move to the Golgi zone, and from there pass to the axon. I wonder whether it is really possible to make such a categorical statement. It is possible that some protein by-passed the Golgi apparatus and migrated directly into the axon.

DR. DROZ: Grain counts have been made at several time intervals from 10 minutes to 6 hours over the Nissl substance, the Golgi zone, and the neurofilament–neurotubules of the perikaryon in spinal ganglionic cells. On the basis of this kinetic study, it is not possible to decide with certainty whether the Golgi complex is a required step in the elaboration of neurofilament–neurotubules.

PROTEIN SYNTHESIS IN THE EAR UNDER NORMAL AND PATHOLOGICAL CONDITIONS[1]

E. KOBURG AND K. HEMPEL[2]

Klinik für Hals-, Nasen-, und Ohrenheilkunde der Medizinischen Akademie Düsseldorf, Düsseldorf, Germany, and Institut für Medizinische Isotopenforschung der Universität Köln, Köln, Germany

INTRODUCTION

Adequate approaches to the study of metabolic processes of the organ of hearing and the organ of equilibration situated in the bone-protected inner ear have been lacking for a long time. However, the development of the autoradiographic technique and the introduction of low energy β-emitters such as sulfur ^{35}S, carbon ^{14}C, and tritium ^{3}H have changed things a great deal. This is especially true in the study of protein metabolism.

In 1953 Bélanger [1, 2, 3] started with his investigations of the inner ear by means of ^{35}S-labeled compounds. His experiments encouraged us to continue his work by studying protein metabolism of the inner ear of guinea pigs, rats, mice, and pigeons [6, 8–13, 16–18, 21, 26]. The results of these experiments are summarized in this report.

METHODS

Pigeons (5 birds weighing between 165 and 380 gm), male albino mice (9 animals between 15 and 20 gm), rats (3 animals between 200 and 217 gm) and guinea pigs (29 animals between 180 and 580 gm) received tritiated amino acids[3] by intraperitoneal or intravenous injection. Another experiment with 5 guinea pigs was done by feeding yeast (*Torula torulopsis*) which was grown in a medium containing ^{35}S-sodium sulfate. After sacrifice the animals were dissected with isolation of the temporal bones and opening of the bulla tympanica. For decalcification the bones were suspended for 1–3 days in a solution of hydrochloric acid (17 ml of a 25 per cent solution), $AlCl_3$ (14 gm),

[1] Supported by grants of the Deutsche Forschungsgemeinschaft.

[2] The authors are greatly indebted to Prof. Dr. W. Maurer for valuable help and advice. The experiments were in part performed in the Institut für Med. Isotopenforschung der Univ. Köln.

[3] The tritiated amino acids were synthesized by Dr. K. Hempel.

and formic acid (14 ml of an 85 per cent solution) in 200 ml water. Only in the case of mice was the whole skull decalcified, so that, after sectioning, the brain and the different sensory organs appeared in the same, or in subsequent, levels.

Serial paraffin sections (5–7 μ) were prepared for autoradiography using Kodak AR 10 stripping film and Ilford G5 or K2 liquid emulsions. For staining hematoxylin and eosin were used. Quantitative examination was done by means of grain counting. In order to compare the results of different experiments with one another, relative values were calculated by taking the incorporation rate of the ganglionic cells of the hearing organ to be 100 and expressing the remaining tissue grain counts in percentages of the incorporation rate of the ganglionic cells.

RESULTS

In the first section the pattern of protein synthetic activity within the different structures of the hearing organ of birds and mammals will be described. Another section will deal with the organ of equilibration. The third section will try to give a synopsis of protein metabolism in different ganglionic cells and in the tissues of sensory organs.

Although various amino acids (^{3}H-leucine, ^{3}H-lysine, ^{3}H-phenylalanine, ^{3}H-tyrosine) were used as precursors, the relative incorporation pattern remained nearly unchanged from one animal to another and—with certain restrictions—even from one species to another. Similar observations with other organs have been made by Maurer and his colleagues [14, 15]. Only when thio-amino acids were used, were results with tissues rich or lacking in sulfur found to diverge from those obtained with sulfur-free amino acids. In the case of the inner ear this is true preferably with the epithelium of the limbus spiralis cochleae, which is supposed to secrete the matrix of the tectorial membrane. As has already been pointed out by Bélanger [1–3], after administration of ^{35}S-thio-amino acids there is a relative accumulation of ^{35}S activity in that area. This is easy to understand, since the tectorial membrane consists in part of sulfomucopolysaccharides.

Protein Synthesis in the Hearing Organ

Birds. In the outstanding structures of the hearing organ, i.e., in the sensory cells, the ganglionic cells, and the secretory epithelium, the rates of protein metabolism reveal characteristic differences.

Figure 1 shows an unstained autoradiograph of a cross section of the cochlea of a pigeon, 2 hours after injecting ^{3}H-leucine. The strongest incorporation can be seen in the ganglionic cells. The sensory cells have

about 50% less incorporation. Nearly in the same range is the turnover rate of the secretory epithelium of the tegmentum vasculosum. The tectorial membrane shows only a very slight incorporation of labeled material. The relative turnover rates are listed in Table I.

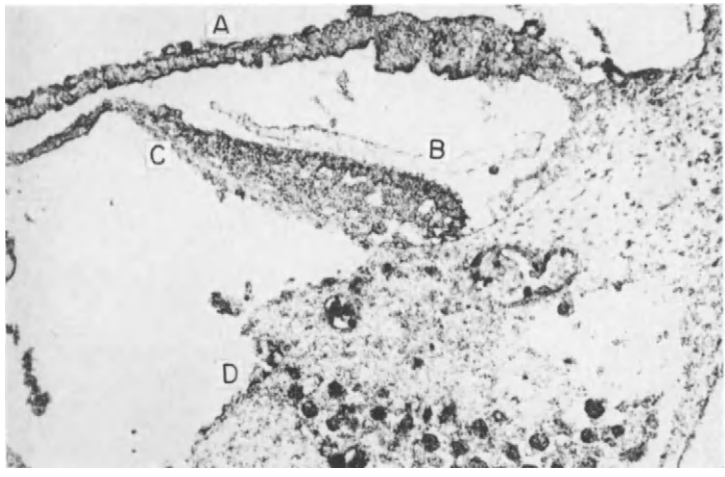

FIG. 1. Unstained autoradiograph of the hearing organ of a pigeon, 2 hours after administration of ^{3}H-leucine. A, tegmentum vasculosum; B, membrana tectoria; C, sensory cells and sustaining cells; D, ganglionic cells. Magnification: × 100.

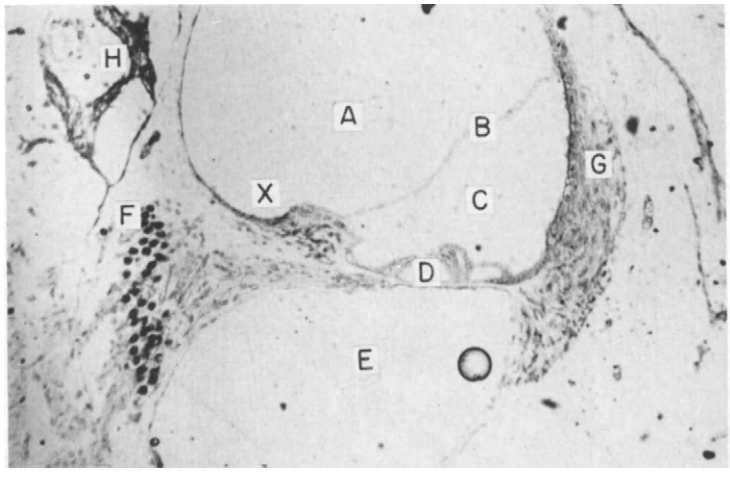

FIG. 2. Unstained autoradiograph of the second turn of the cochlea of a guinea pig, 2 hours after injecting ^{3}H-leucine. A, scala vestibuli; B, Reissner's membrane; C, ductus cochlearis; D, Corti's organ; E, scala vestibuli; F, ganglion spirale cochleae; G, ligamentum spirale with stria vascularis; H, plexus cochlearis with blood vessels, X, mediobasal linings of scala vestibuli. Magnification: × 60.

TABLE I. *Mean Relative Amino Acid Incorporation Rates of Different Tissues of the Hearing Organ of Various Species*[a]

Tissues	Guinea pig			Rat			Mouse	Pigeon	
	^{3}H-Leucine	^{3}H-Lysine	^{3}H-Phenylalanine	^{3}H-Leucine	^{3}H-Lysine	^{3}H-Phenylalanine	^{3}H-Leucine	^{3}H-Leucine	^{3}H-Lysine
Ganglionic cells	100	100	100	100	100	100	100	100	100
Plexus cochlearis	91	92	97						
Stria vascularis	72	71	67	62	59	63	73	—	—
Tegmentum vasculosum	—	—	—	—	—	—	—	41	38
Connective tissue cell of spiral ligament	72	63	61	48	52	50	59	—	—
Spiral ligament facing scala vestibuli and scala tympani	63	61	62	44	41	43		—	—
Mediobasal lining of scala vestibuli	58	59	61	45	42	43		—	—
Boettcher's cells	83	80						—	—
Reissner's membrane	54	52	39	30	32	31	58	—	—
Epithelium of the limbus spiralis	34	36	38	30	30	31	36		
Membrana tectoria	0	0	0	11	13	12	7	13	6
Sensory cells (hair cells)	53	54	45	36	33	39	44	50	54
Sustaining cells	51	49	45	36	33	37	42		

[a] The grain density of the ganglionic cells was arbitrarily taken to be 100, this being the standard for comparison.

Mammals. The hearing organ of mammals, e.g., of a guinea pig, reveals a pattern of protein synthetic activity similar to that of the pigeon. Figure 2 shows an unstained autoradiograph of the second turn of the cochlea from a guinea pig, 2 hours after injecting ^{3}H-leucine. Again the ganglionic cells have the highest rate of protein turnover, whereas the vascular stria has about 70 per cent, and the sensory cells have only about 40–50 per cent of the activity of the ganglionic cells. The relative turnover rates of the different tissues of the inner ear of guinea pigs, rats, and mice are listed in Table I.

The ganglionic cells of the spiral ganglion are rather uniform with respect to their size and—at least at first sight—to their autoradiographic grain density. Grain counting reveals that there are, indeed, only small variations between neighboring cells of one turn; however, there are considerable differences between cells of different turns.

TABLE II. *Protein Turnover of Ganglionic Cells of the Ganglion Spirale Cochleae, in Normal and Noise-Exposed Guinea Pigs Labeled with ^{3}H-Phenylalanine*

Guinea pig	Mean grain no. per total cell area	Mean cell area (μ^2)	Mean grain density	Mean approximate protein turnover per total cell volume
Expt. no. 19, normal				
Turn I	32.33	103.30	0.34	284
Turn II	23.90	90.25	0.28	188
Turn III	25.86	96.83	0.29	220
Turn IV	26.30	105.41	0.26	220
Expt. no. 24, noise				
Turn I	38.69	90.0	0.45	302
Turn II	41.20	82.84	0.53	316
Turn III	40.43	77.83	0.55	309
Turn IV	42.43	92.64	0.51	367

Table II contains the results of grain counting over comparable areas of the ganglionic cells of the four turns. The animal for which values are given in the upper part of Table II is representative of a series of 6 animals. It may be seen that the incorporation of ^{3}H-phenylalanine is highest in the ganglionic cells of the basal turn and decreases gradually toward the apical turn.

When animals are exposed to moderate noise the incorporation behavior changes slightly. The lower part of Table II contains the rates of protein synthesis of the ganglionic cells of the different turns from one animal of a series being exposed to a broad spectrum noise of 90 decibels for 48 hours. All animals, normal as well as noise-exposed, were sacri-

ficed 1 hour after administration of ^{3}H-phenylalanine. Contrary to normal animals, after exposure to noise the incorporation rate of the ganglionic cells does not decrease toward the apical turn. Moreover, when liver is taken as a standard for comparison, the ganglionic cells seem to reveal a slight general increase in their protein synthetic activity shortly after prolonged exposure to noise, thus suggesting that noise of moderate intensity might give rise to an enhanced consumption of cellular protein.

The receptors of acoustic stimulation are localized in the organ of Corti. Figure 3 shows a stained autoradiograph of the organ of Corti

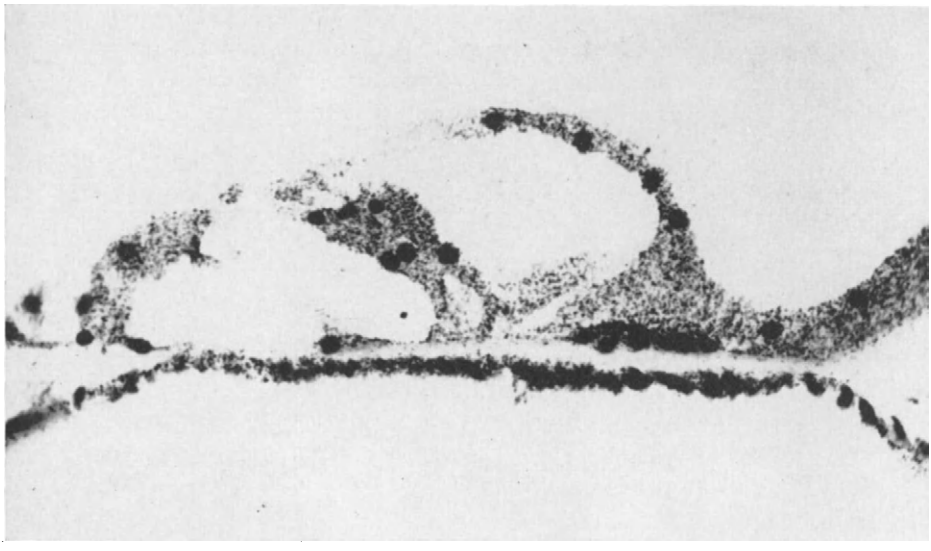

FIG. 3. Autoradiograph of the organ of Corti of a guinea pig, basal turn, 2 hours after injecting ^{3}H-leucine. Hematoxylin and eosin stain. Magnification: × 500.

of the basal turn of a guinea pig, 2 hours after injecting ^{3}H-leucine. There is no difference in the grain density between the sustaining cells and the hair cells. Even after exposure to noise there is no change. However, after prolonged administration of streptomycin the turnover rate of the organ of Corti is reduced, whereas for the ganglionic cells it remains unchanged [22].

The very dark stained basophilic cell layer underneath the cells of Deiters, i.e., the cells of Boettcher, were always found to incorporate protein precursors at a high rate. The strong basophilia indicating a large content of ribonucleic acid (RNA) and the pronounced protein synthetic activity of these cells are all the more interesting since nothing is known concerning their function.

In the upper right part of Fig. 2 there is another strongly labeled tissue with unknown function. It always accompanies the vessels of the tractus spiralis arteriosus et venosus within the modiolus. Examined with higher magnification, this tissue looks exactly like the plexus chorioideus of the brain or like the ciliary body of the eye. In addition to the morphological resemblance the rates of protein synthesis of the tissues in

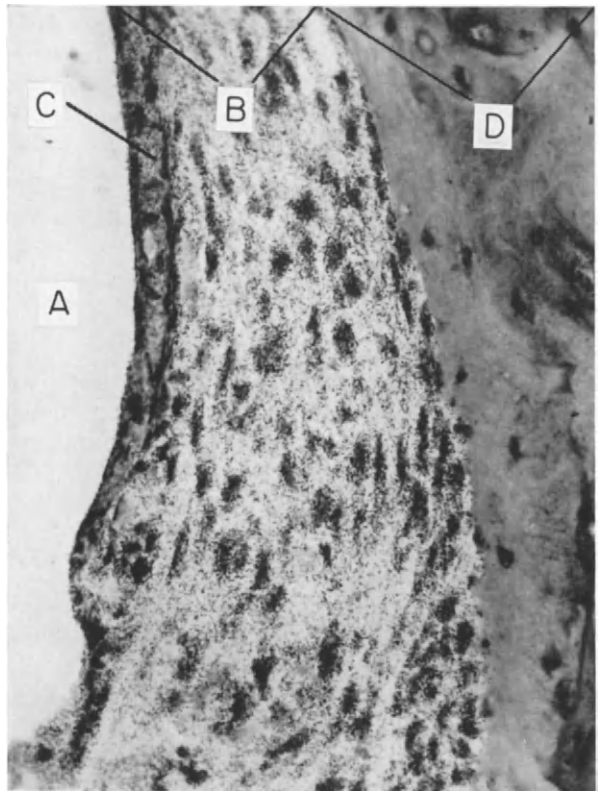

FIG. 4. Autoradiograph of the spiral ligament of a guinea pig, 2 hours after injecting ^{3}H-leucine. A, endolymphatic space; B, ligamentum spirale; C, stria vascularis; D, labyrinthine bone. Hematoxylin and eosin stain. Magnification: × 300.

question are very similar. We therefore decided to call this tissue plexus cochlearis.

Another important structure of the cochlea is the spiral ligament with the stria vascularis. Figure 4 shows a stained autoradiograph of the spiral ligament of a normal guinea pig, 2 hours after injecting ^{3}H-leucine. The epithelium of the stria vascularis, which is lining the endolymphatic space, has a very high rate of protein turnover. The connective

tissue cells in the spiral ligament have only a slightly lower rate. The epithelium of the stria vascularis is supposed by the majority of investigators, to be involved in the production of endolymph. Nothing particular is known regarding the function of the large connective tissue cells in the spiral ligament.

In our autoradiographs the area of tissue lining the scala vestibuli between the lateral wall of the modiolus and the spiral limbus (marked by X in Fig. 2) was always strongly blackened. The amino acid incorporation was of the same order as that of the connective tissue cells of the spiral ligament and only slightly below that of the stria vascularis.

In one series of experiments the perilymph of the scala vestibuli and in another series the perilymph and the endolymph were continuously removed by puncturing the spaces, making tiny drill holes into the lateral wall of the cochlea, and sucking off the liquid with small glass capillaries. After about 20 minutes the flow came to a standstill, obviously due to exhaustion. At this moment ^{3}H-tyrosine was injected. The animals were sacrificed after 1 hour. For control the untouched contralateral cochlea was also prepared. Both the control and the drained cochlea were sectioned, mounted, and autoradiographed together. In both groups, that with only the perilymph and that with the perilymph plus the endolymph being drained, the incorporation of tyrosine was increased in the stria vascularis, the spiral ligament lining the scala vestibuli, the mediobasal lining of the scala vestibuli (see X in Fig. 2), and—surprisingly—in the plexus-like formation within the modiolus, the plexus cochlearis. Although this change in the rate of incorporation might above all be merely a response to injury, it is interesting that only those tissues which are supposed to be concerned with the production of inner ear liquids show an increased incorporation. However, more information will be necessary to cast more light on the still obscure problem of inner ear liquid production.

Protein Synthesis in the Equilibration Organ

Pigeon. The equilibration organ of the pigeon presents some peculiarities. Although the maculae staticae (Fig. 5A) can be found in the same position and the same configuration as in mammals, there are two different types of cristae in birds. The one (Fig. 5B) in the ampulla of the external or horizontal semicircular canal is the same in appearance as it

FIG. 5. Unstained autoradiographs of the equilibration organ of the pigeon, 2 hours after injecting ^{3}H-leucine. A, macula sacculi; B, crista in the external ampulla; C, crista in the posterior ampulla with septum cruciatum (s) on either side. The planum semilunatum (p) has nonsensory epithelium. Magnification: × 90.

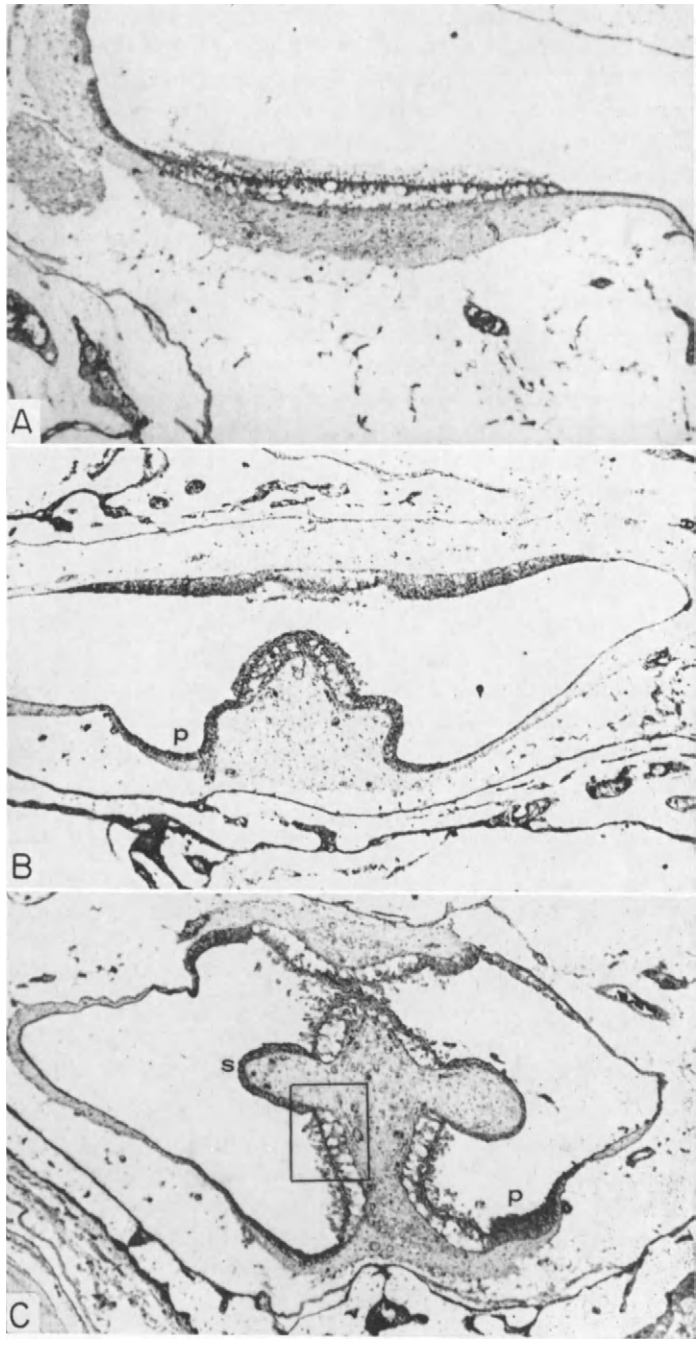
A
P
B
S
P
C

is in mammals. The crista in the ampulla of the posterior semicircular canal has a large area covered with sensory cells, which, as Fig. 5C shows, is divided into three parts by a septum cruciatum on either side. This septum cruciatum bears nonsensory epithelium. The second peculiarity is that opposite to the cristae there is another area covered with sensory epithelium.

Two hours after injecting ^{3}H-leucine or ^{3}H-lysine, the incorporation of labeled material is highest within the nonsensory epithelium of the planum semilunatum, and within those nonsensory epithelia adjacent to the sensory epithelium opposite to the cristae. Even the epithelium of the septa cruciata reveals a slightly higher protein turnover rate than does the sensory epithelium. Within the sensory epithelium itself (Fig. 6), there are more grains above the sustaining cells than above the hair cells. Toward the endolymphatic space there are many dot-like structures covered with grains. Some of these may be protruding processes of sustaining cells [4], but the most remote ones, especially in the left part of Fig. 6A (macula), correspond to the organic matrix of the statoliths.

Mammals. With the exception of those anatomical peculiarities of the organ of equilibration in birds, mammals have generally the same incorporation pattern of protein precursors within the vestibular organ.

The epithelium of the planum semilunatum has a slightly higher protein turnover than have the sensory cells. This has been pointed out by Schreiner [24], who studied the guinea pig's equilibration organ. Table III gives a comparison of relative protein turnover rates of hearing and equilibration organs in pigeons, guinea pigs, and mice. The relative turnover rate in the epithelium of the planum semilunatum is approximately the same as that in the epithelium of the stria vascularis, thus suggesting that those structures might have a similar function. Such an observation is in good accord with the results of electron microscope studies which show that both epithelia have an ultrastructure very closely related to each other and indicate that both might have a secretory function.

In contrast with the pigeon, there is no significant difference in grain density between the sensory cells and the sustaining cells, but again labeled material was found in the organic matrices lying above the sensory epithelia. Figure 7A demonstrates that even 1 hour after giving ^{3}H-phenylalanine many grains, the number of which is distinctly above the background, can be found over the matrix of the cupula. It is interesting to see that in the same animals *no* grains could be detected above the tectorial membrane of the cochlea.

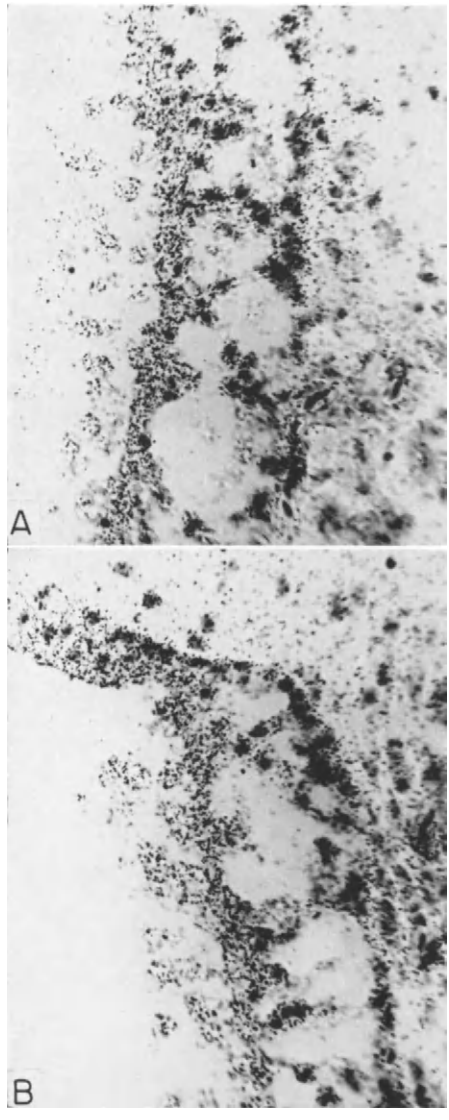

FIG. 6. Sensory epithelium with sustaining cells of a pigeon's equilibration organ, 2 hours after injecting ^{3}H-leucine. A, macula statica; B, area of crista ampullaris corresponding to that of Fig. 5C marked by a rectangle. The upper left of Fig. 6B shows nonsensory epithelium of the septum cruciatum. Hematoxylin and eosin stain. Magnification: × 400.

Comparison of Protein Metabolism in the Inner Ear with That in Different Sensory Organs and Ganglionic Cells

The relative protein turnover rates presented in Table III reveal that in mammals there is no significant difference in the protein synthetic activity between the hearing and the equilibration organs. Only the

TABLE III. *Protein Turnover of the Inner Ear (Equilibration and Hearing) of Pigeon, Guinea Pig, and Mouse*

	Pigeon		Guinea pig		Mouse	
Organ, tissue	Grains per 1440 μ^2	Relative turnover rate	Grains per 1440 μ^2	Relative turnover rate	Grains per 1440 μ^2	Relative turnover rate
Equilibration organ						
Ganglion vestibulare	726	139	1623	125	1032	132
Epithelium, planum semilunatum	607	116	627	48	406	52
Crista ampullaris						
Hair cells	448	86	594	46	391	50
Sustaining cells	536	103	607	47	—	—
Epithelium, septum cruciatum	568	109	—	—	—	—
Cupula	363	69	529	41	—	—
Maculae staticae						
Hair cells	453	87	590	46	389	50
Sustaining cells	504	96	595	46	—	—
Statolith membrane	285	54	542	42	—	—
Hearing organ						
Ganglionic cells	522	*100*	1299	*100*	782	*100*
Stria vascularis	—	—	873	67	571	73
Tegmentum vasculosum	222	42	—	—	—	—
Reissner's membrane	—	—	511	39	446	57
Hair cells	269	51	582	45	405	52
Sustaining cells	246	47	582	45	408	52
Membrana tectoria	78	15	0	0	0	0

ganglionic cells of the ganglion vestibulare are relatively more active. In pigeons, however, the ganglionic cells not only have different metabolic rates, but there is a striking difference between the two organs, with the equilibration organ by far surpassing the hearing organ. Perhaps this difference reflects the situation of a flying bird, which obviously must rely much more upon its equilibration organ than quadruped mammals.

The differences in protein metabolism between neighboring, but

functionally unequal, ganglionic cells such as presented in Fig. 8 and between the two parts of the inner ear (Table III) gave rise to a more detailed study in order to compare the protein synthetic activity of various types of ganglionic cells and of sensory organs. In a qualitative

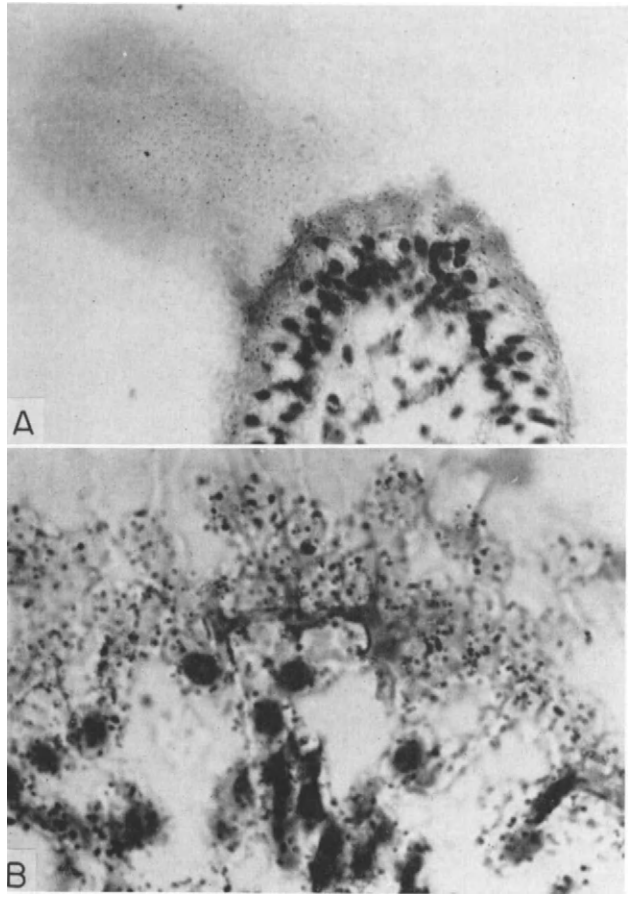

FIG. 7. Autoradiographs of the crista ampullaris of a guinea pig, 1 hour after injecting ^{3}H-phenylalanine. A, crista ampullaris with labeled material in the cupula; magnification: × 400. B, sensory epithelium of the crista ampullaris. Hematoxylin and eosin stain. Magnification: × 1000.

way such studies have been done already [5, 7, 19, 20, 25]. The present report gives a more quantitative evaluation.

A synopsis of 8 types of ganglionic cells of both brain and sensory organs from a mouse, 20 minutes after injecting ^{3}H-leucine is given in Fig. 9. The photographs are made of the same autoradiograph with the

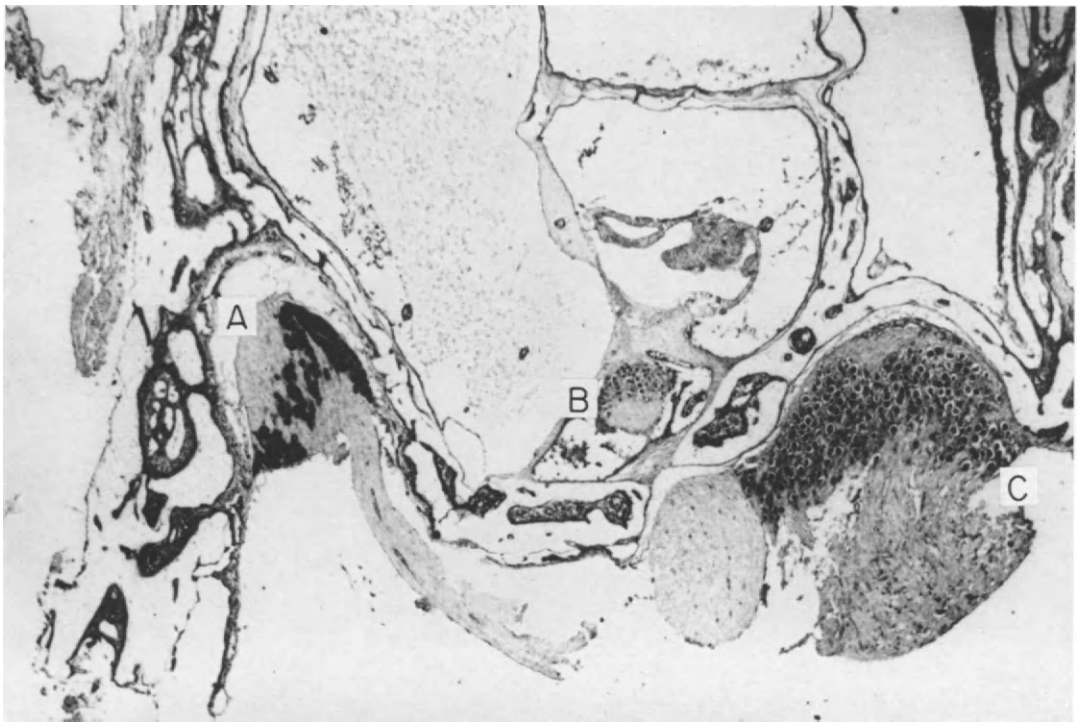

FIG. 8. Unstained autoradiograph of the labyrinth of a pigeon, 2 hours after injecting ^{3}H-leucine. A, ganglion geniculi N. VII; B, ganglion cochleare N. VIII; C, ganglion vestibulare N. VIII. Magnification: × 50.

same magnification, so that the grain density and the size of the cells are directly comparable. It is easy to see that there are big variations in the grain density, i.e., in protein turnover per unit volume, and in cellular size.

In ganglionic cells—whose function is in some respects more individual than that of, e.g., a liver cell—it should be of interest to have an estimate of the metabolic rate not only per *unit volume,* but per *total cell volume.* The total volume of ganglionic cells can be estimated roughly from the diameters, and by multiplying that volume by the rate of protein metabolism per unit volume as revealed by grain counting, one gets an impression of the wide range of variation in cellular function among different ganglionic cells. The results of such an estimation are listed in Table IV.

TABLE IV. *Protein Turnover of Various Ganglionic Cells of the Mouse, with ^3H-Leucine Labeling*

Cell	Mean cell area sectioned (μ^2)	Relative amino acid incorporation per unit volume	Mean protein turnover per total cell volume
Cerebellum, granular cells	12.8	= 1	= 1
Cerebellum, Purkinje cells	96.2	1.8	38
Ganglion retinae	38.6	1.3	7
Olfactory lobe, mitral cells	128.5	1.2	46
Ganglion spirale cochleae	59.9	1.2	13
Ganglion vestibulare	97.5	1.6	31
Ganglion gasseri N. V Ganglion geniculi N. VII	288.0	2.0	243

There is another point of view of interest. As was already mentioned, the ganglionic cells of the spiral ganglion are rather uniform in cellular size and rate of cellular protein synthesis, with only a relatively small range of variation according to changes in functional activity (see Table II). Other ganglia, however, reveal considerable differences in cellular size as well as in the degree of basophilia and the grain density, i.e., the protein turnover rates. This is shown in Fig. 10A, which shows an autoradiograph of the ganglion semilunare N. V from a mouse, 20 minutes after injecting ^3H-leucine. Figure 10B is an autoradiograph of the ganglion vestibulare N. VIII from a guinea pig, 1 hour after injecting

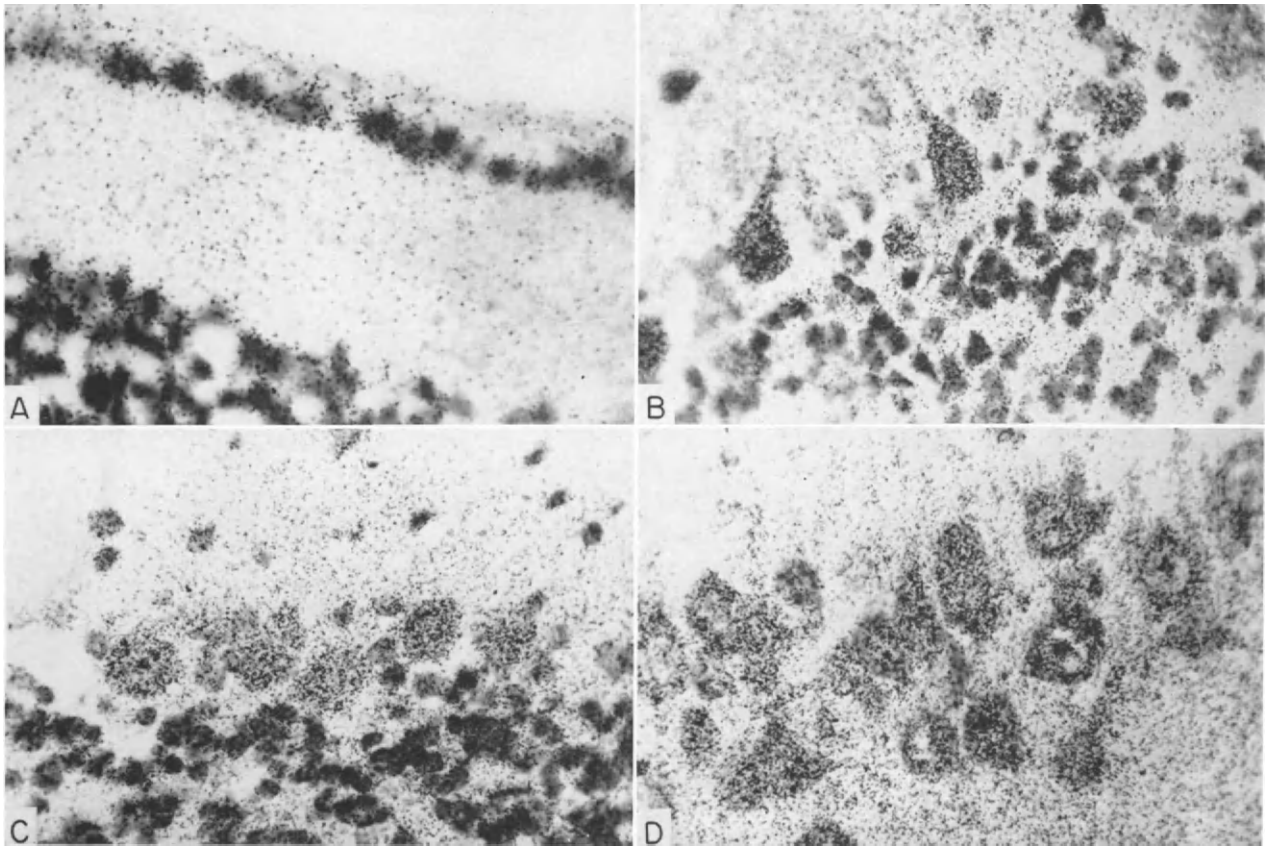

FIG. 9. Various ganglionic cells of a mouse, 20 minutes after injecting ^{3}H-leucine. A, retina; B, mitral cells of the olfactory lobe; C, Purkinje cells of cerebellum; D, hippocampus; E, ganglion geniculi N. VII; F, nucleus terminalis dors.

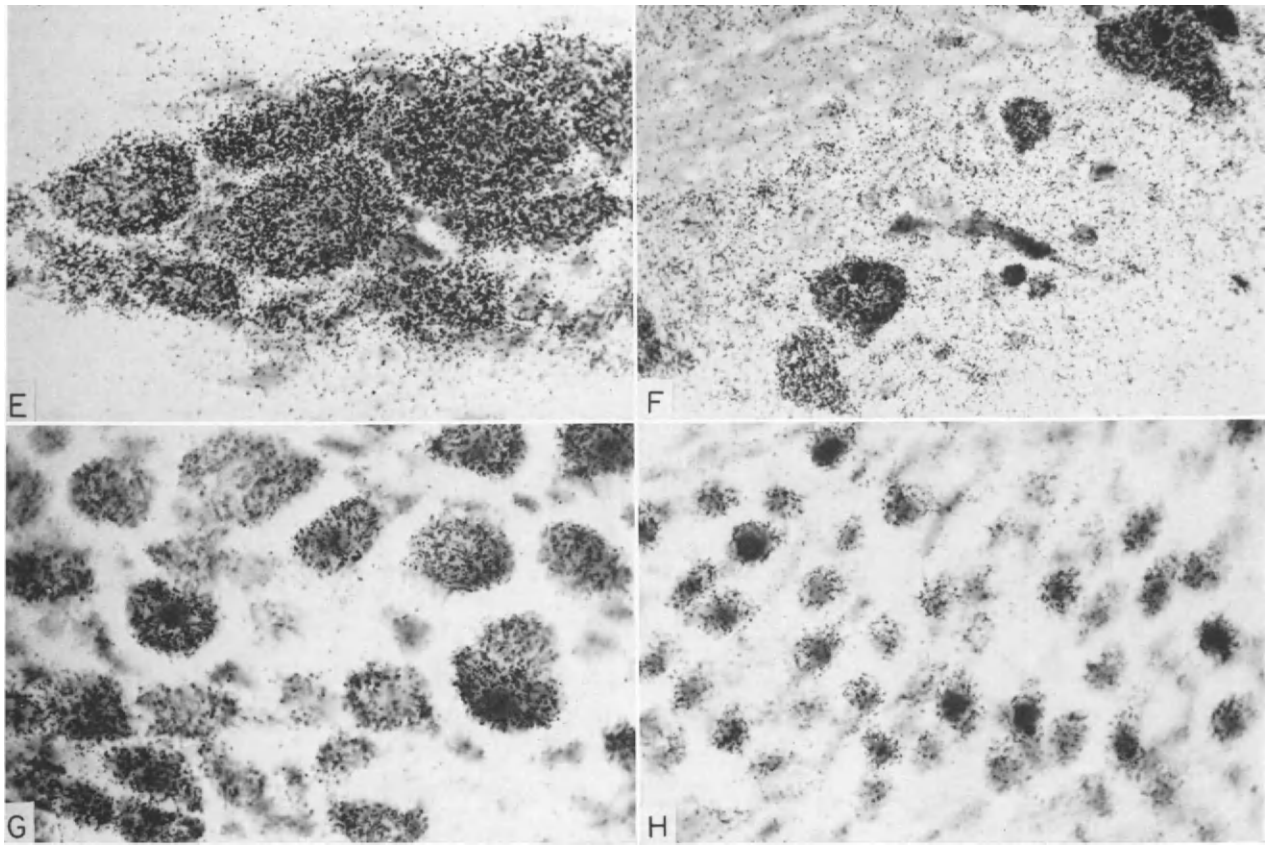

N. VIII; G, ganglion vestibulare; H, ganglion spirale cochleae. Hematoxylin and eosin stain. All photographs were taken from the same autoradiograph with the same magnification (× 750).

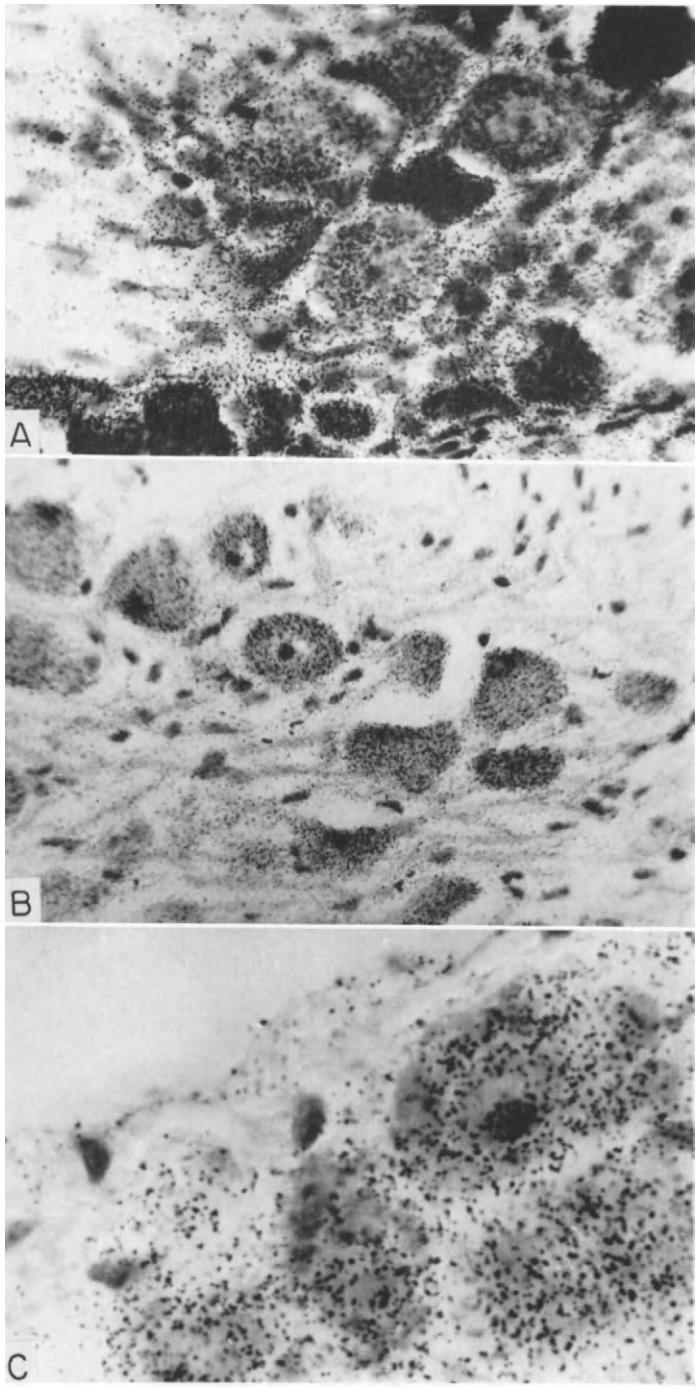
A
B
C

^{3}H-phenylalanine. In Fig. 10A especially there are big variations in cellular activity as revealed by cytoplasmic basophilia and nucleolar protein synthesis. Nucleolar protein synthesis only occurs in cells which are very active in protein synthesis [5, 10, 27]. Distinct protein synthesis within the nucleolus of a ganglionic cell of the ganglion geniculi N. VII is visualized in Fig. 10C.

TABLE V. *Protein Turnover of Sensory Organs of the Mouse, Labeled with ^{3}H-Leucine*

Organ, tissue	Total grain number	Total tissue area (μ^2)	Mean grain density	Mean/Relative protein turnover (ganglion spirale cochleae = 100)
Eye				
Retina, ganglionic cells	2306	5040	0.45	102
Retina, granule cells	1855	5040	0.36	82
Corpus ciliare	1745	5040	0.34	77
Olfactory organ				
Olfactory lobe:				
Mitral cells	2457	5040	0.48	109
Granule cells	1975	5040	0.39	88
Glomerula olfactoria	1783	5040	0.35	79
Nose, olfactory epithelium	1950	5040	0.38	86
Hearing organ				
Ganglion spirale cochleae	2216	5040	0.44	100
Sensory cells, Corti	390	1680	0.23	52
Stria vascularis	537	1680	0.32	73
Reissner's membrane	432	1680	0.25	57
Equilibration organ				
Ganglion vestibulare	2962	5040	0.58	132
Sensory epithelium				
Crista ampullaris	178	800	0.22	50
Maculae	403	1920	0.22	50

Table V contains a synopsis of relative amino acid incorporation rates per unit volume, which yield a comparison of protein turnover within the structures of sensory organs, *i.e.*, of the eye, ear, and nose. Concerning the metabolic rates of the organ of Corti, it must be borne in mind that

FIG. 10. Autoradiographs of ganglionic cells. A, ganglion semilunare N. V, mouse, ^{3}H-leucine, with different stages of functional activity; × 750. B, ganglion vestibulare, guinea pig, ^{3}H-phenylalanine; × 750. C, ganglion geniculi N. VII, rat, ^{3}H-phenylalanine; × 1250.

this tissue is only nourished by diffusion. As a result the availability of injected labeled material in the organ of Corti is delayed and reduced [17]. So the values given for the organ of Corti should be corrected for this delay in availability by a certain percentage. Nevertheless, there will remain differences in the rate of protein turnover from one sensory organ to another.

The question whether a classification depending on the intensity of protein metabolism, such as intended for the inner ear and some nervous tissues in this report, yields information concerning the function and the limits of functional capacity under normal and pathological conditions is tempting, but cannot yet be decided. In order to answer this question, further investigation in this promising field will be necessary.

SUMMARY

The pattern of protein synthetic activity within the structures of the inner ear—hearing and equilibration organ—is demonstrated by means of autoradiography with labeled protein precursors. The ganglionic cells appeared to have the highest rate of protein metabolism, while sensory epithelia have only a moderate turnover. Similar results could be obtained with other sensory organs, i.e., with the eye and the olfactory organ. In a synopsis the turnover rates of sensory organs and of different ganglionic cells were compared.

ACKNOWLEDGMENT

The technical assistance of Miss Erika Hinterleitner is gratefully acknowledged.

REFERENCES

1. Bélanger, L. F., *Science* **118**, 520 (1953).
2. Bélanger, L. F., *Science* **123**, 1074 (1956).
3. Bélanger, L. F., *J. Histochem. Cytochem.* **8**, 447 (1960).
4. Engström, H., personal communication (1964).
5. Erb, W., and Maurer, W., *Z. Naturforsch.* **17b**, 268 (1962).
6. Freese, M., Dissertation, Düsseldorf (1964).
7. Goslar, H. G., and Schultze, B., *Z. Mikroskop. Anat. Forsch.* **64**, 556 (1958).
8. Hussein, A., Dissertation, Düsseldorf (1964).
9. Koburg, E., *Arch. Ohr.-, Nas.- u. Kehlk. Heilk.* **178**, 150 (1961).
10. Koburg, E., *Verhandl. Deut. Ges. Pathol.* **46**, 238 (1962).
11. Koburg, E., and Meyer zum Gottesberge, A., *Arch. Ohr.-, Nas.- u. Kehlk. Heilk.* **183**, 280 (1964).
12. Koburg, E., and Plester, D., *Acta Oto-Laryngol.* **54**, 319 (1962).
13. Koburg, E., and Plester, D., *Arch. Ohr.-, Nas.- u. Kehlk. Heilk.* **179**, 332 (1962).
14. Maurer, W., "Über die Grösse des Umsatzes von Organ and Plasmaeiweiss, 10." Colloquium d. Ges. f. physiol. Chemie, Springer, Berlin-Göttingen-Heidelberg, 1959.

15. Maurer, W., and Koburg, E., *in* "Biochemie des Hörorgans" hrsg. v. S. Rauch, Thieme, Stuttgart, 1964.
16. Meyer zum Gottesberge, A., *Acta Oto-Laryngol. Suppl.* **163**, 46 (1960).
17. Meyer zum Gottesberge, A., and Plester, D., *Arch. Ohr.-, Nas.- u. Kehlk. Heilk.* **178**, 145 (1961).
18. Neveling, R., Koburg, E., and Stupp, H., *Arch. Ohr.-, Nas.- u. Kehlk. Heilk.* **183**, 247 (1964).
19. Nover, A., and Schultze, B., *Arch. Ophthalmol.* **161**, 554 (1960).
20. Oehlert, W., Schultze, B., and Maurer, W., *Beitr. pathol. Anat. allgem. Pathol.* **119**, 343 (1958).
21. Plester, D., *Arch. Ohr.-, Nas.- u. Kehlk. Heilk.* **176**, 667 (1960).
22. Plester, D., and Koburg, E., unpublished data (1964).
23. Plester, D., Koburg, E., and Hempel, K., *Ann. Histochim. Suppl.* **2**, 91 (1962).
24. Schreiner, L., *Klin. Wochschr.* **40**, 1016 (1962).
25. Schultze, B., Oehlert, W., and Maurer, W., *Beitr. pathol. Anat. allgem. Pathol.* **120**, 58 (1959).
26. Schwartzkopf, J., *Arch. Ohr.-, Nas.- u. Kehlk. Heilk.* **182**, 435 (1933).
27. Stöcker, E., *Verhandl. Deut. Ges. Pathol.* **46**, 242 (1962).

Discussion

Dr. Droz: By radioautography it has been shown that the visual cells of rats and mice are the site of a continuous synthesis of protein (Nover, A., and Schultze, B., *J. Graefes. Archiv. Ophthalmol.* 1960, **161**, 554). We have further observed that the synthesis of protein takes place in the inner segment of the rod and that, with the passage of time, the newly formed proteins migrate toward and into the outer segment (Droz, B., *Anat. Record* 1963, **145**, 157; Droz, B., Rambourg, A., and Olivier, L., *Compt. Rend. Soc. Biol.* 1963, **157**, 2136).

The incorporation of labeled amino acids into the proteins of the retina may be modified by stimulation. Comparison of radioautographs of the retinae of mice maintained in darkness with others stimulated by light flashes reveals that the incorporation of ^{35}S-methionine decreases by about 42 per cent in the inner segment after light stimulation. A slight decrease is also observed in the bipolar and ganglionic cells of the retina. Since the permeability of the cell membrane changes in the course of stimulation, it is difficult to decide whether this phenomenon is related to a decrease in protein synthesis, or to a decrease in the uptake of free labeled precursor.

Dr. Koburg: I am not quite sure whether your flashes of light did not act upon the ribonucleic acid (RNA) in a direct way. Can repeated flashes be considered as a physiological stimulus? In our case, the intensity of noise to which the animals were exposed was still in the range that can be tolerated. If you expose animals to shock waves or other kinds of acoustic trauma, there seems to be a complete breakdown of RNA synthesis and protein synthesis (Humberger and Hydèn, *Acta Oto-laryngol.* 1945, **61**, and others).

Dr. Bélanger: Since the cells in the limbus spiralis reach peak labeling at 1–2 hours after injection of a radioactive amino acid, whereas the cells of the tectorial membrane reach peak labeling at 1–4 days, it may be that labeled material synthesized in the cells of the limbus spiralis migrates slowly into the tectorial membrane.

Dr. Koburg: In some recent experiments with ^{35}-S thioamino acids, we saw the distribution which Dr. Bélanger just described, i.e., labeling of the epithelial cells of the limbus spiralis after 1 hour and migration of label after longer periods

into the tectorial membrane. However, the differences found when comparing the incorporation of tritiated amino acids into the tectorial membrane and into the cupules may be influenced by differences in the composition of these structures and in the availability of precursor.

DR. TONNA: Might not some of the differences you obtained when comparing the protein-synthetic activity of similar organs in different animal species reflect differences in age?

DR. KOBURG: I do not believe that the variations between the different animals and species are caused by differences in age. We always used rather young animals, which had reached puberty but were still growing. The weight ranged between 250 and 300 gm for guinea pigs, between 150 and 200 gm for rats, and between 15 and 20 gm for mice.

DR. PELC: There was a paper by Dohlman and Ormerod* on this subject. What is your opinion?

DR. KOBURG: I remember this paper of Dohlman and Ormerod. After administration of ^{35}S-sulfate they saw the radioactivity appear first in the secretory epithelium and later in the cupula, the otolith membranes, and the tectorial membrane. At that time, radioactivity was no longer to be seen in the secretory epithelium. No radioactivity appeared in the sensory epithelium. The authors took these results as indicating the pathways of secretion of endolymph.

* Dohlman, G., and Ormerod, F. C., *Acta Oto-Laryngol.* **51**, 435 (1960).

AMINO ACID UTILIZATION IN THE SYNTHESIS OF ENAMEL AND DENTIN MATRICES AS VISUALIZED BY AUTORADIOGRAPHY[1]

R. C. GREULICH AND H. C. SLAVKIN

Department of Anatomy, School of Medicine, and Division of Oral Biology, School of Dentistry, University of California, Center for the Health Sciences, Los Angeles, California

INTRODUCTION

Although taking its embryonic origin in ectoderm, the organic matrix of dental enamel acquires and maintains a mineral phase which is qualitatively similar to that occurring in the mesodermally derived organic matrix of dentin. It has been demonstrated repeatedly that, as in bone, the bulk of dentin matrix is composed of the fibrous protein, collagen. Analyses of enamel matrix, on the other hand, indicate that while it too is fundamentally proteinaceous, it contains little if any collagen. On ontogenetic and chemical grounds, therefore, the ability of enamel matrix to mineralize presents a biological paradox, the resolution of which has become the subject of increasing experimental interest.

Attempts to elucidate a mineralizing mechanism common to both matrices have thus far been unsuccessful, partly because of technical difficulties associated with isolation and chemical analysis of the highly mineralized organic substrate of enamel. Another inhibiting factor has been the relative paucity of information regarding metabolic activity in enamel matrix, both during and following its mineralization.

Of the techniques available for investigation of matrix chemistry and metabolism, perhaps none possesses so much potential as autoradiography. The report which follows will serve to review and interpret certain aspects of protein synthesis in dentin and enamel matrices which have been demonstrated by autoradiography. New findings based on the application of tritiated amino acid precursors are reported, including quantitative observations involving grain counting techniques. The latter provide data regarding the respective amino acid compositions of rapidly growing enamel and dentin matrices, as well as some preliminary information regarding the rates at which individual amino acids are utilized in their formation.

[1] This investigation was supported by research grant GM-09748 and by training grant T1-DE 89-01, National Institutes of Health, U.S. Public Health Service.

THE TOOTH AS AN EXPERIMENTAL OBJECT

Histology of the Rodent Tooth

As in man, tooth formation in the rodent is largely a postnatal event. Consequently, events relating to the formation of the matrices of dentin and enamel can be observed for several weeks following birth. During odontogenesis, the enamel matrix arises as a secretion from a single layer of epithelial cells, the *ameloblasts*, while dentin matrix is secreted by a layer of differentiated mesenchymal cells, the *odontoblasts*. Initially, the odontoblastic layer lies in close approximation to the ameloblastic layer, but as dentin and enamel matrices are elaborated between them, the cell

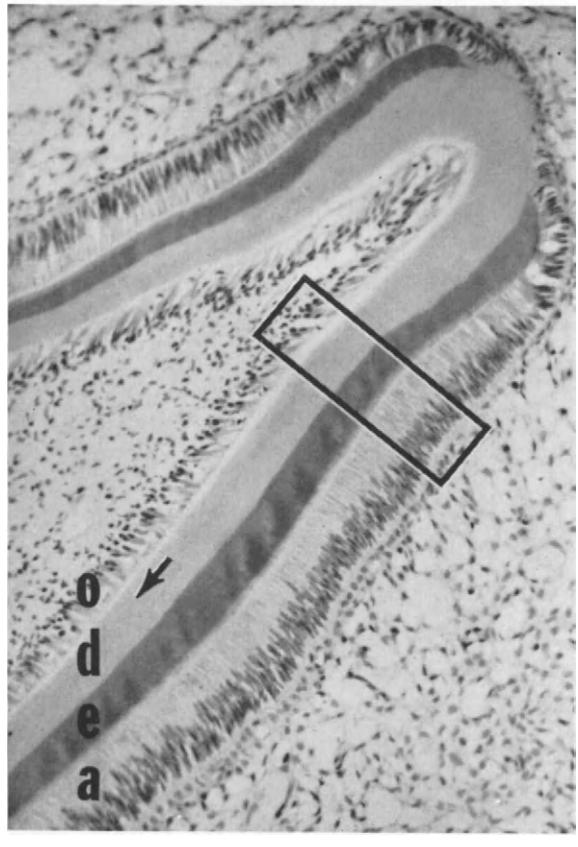

FIG. 1. Longitudinal (mesiodistal) section through the coronal portion of a molar cusp of a 6-day-old rat. The rectangular region illustrates the region examined autoradiographically in this study. Abbreviations: (a) ameloblast, (e) enamel, (d) dentin, (o) odontoblast; the arrow indicates the line of demarcation between predentin and dentin. Magnification: × 150.

elements become progressively separated. Such is the situation illustrated in Fig. 1, which demonstrates a cusp from a rapidly growing rat molar 6 days after birth, by which time discrete layers of enamel and dentin matrix are present. An area typical of that used in the course of the observations reported below is outlined in the illustration. The section is from a decalcified jaw, and so portrays the organic matrices of dentin and enamel (d, e, Fig. 1), as well as the morphology of the cells responsible for their formation (o, a). In the living state, the dentin and enamel matrices are heavily impregnated with mineral. Characteristically, however, a layer of nonmineralizing predentin (Fig. 1, arrow) is interposed between the odontoblasts and the dentin matrix proper.

Until very recently, it was thought that the mineral component of enamel was deposited intracellularly, concomitant to transformation of the apical cytoplasm of the ameloblast which rendered it calcifiable. Electron microscope demonstration [21] of a tortuous but intact plasma membrane interposed between the active ameloblast and the mineralizing enamel has served to discredit this long-held histological view. More significantly, it has served to place the process of enamel formation within a physiological framework analogous to that of dentin formation, i.e., specific accumulation of mineral salts within a preformed extracellular organic matrix, comprised principally of fibrous protein.

The uniqueness of the association between dentin and enamel matrices is also worthy of note. As far as we are aware, there is no other site in the body where one can encounter, in such quantity and intimate association, two embryologically and chemically disparate extracellular protein substrates. The extent to which autoradiographic observations have served in the past to provide information regarding their similarities and differences will now be reviewed briefly.

Early Studies of Matrix Formation by Autoradiography

Labeled organic constituents were first identified autoradiographically in the dentin and enamel of demineralized tooth sections following introduction of carbon-14 in the form of bicarbonate ion [9]. Figure 2 illustrates a typical autoradiograph obtained in the course of this early study. Inadequate histological preservation precluded any detailed study of the fate of ^{14}C-labeling in enamel matrix. However, it was suggested that the ^{14}C in dentin matrix had been incorporated into collagen [10]. Essentially similar organic labeling was also described in the growing tooth following administration of ^{35}S-sulfate, the uptake of which was ascribed to sulfated mucopolysaccharide synthesis [1].

With the development of labeled precursors possessing greater chemical specificity, these initial observations concerning the formation of

organic matrices were expanded and refined. Thus, precursors such as ^{35}S-methionine [2, 16], ^{35}S-cystine [2], ^{14}C-labeled hexoses [14], and ^{3}H-glycine [3] were utilized for studies of organic synthesis in the growing tooth. Comparison of the results from these and more recent studies reveals that the distribution of autoradiographic reactions in growing dentin and enamel matrices follows a generally similar pattern, irrespective of the isotopic precursor applied. This pattern will be described in detail below.

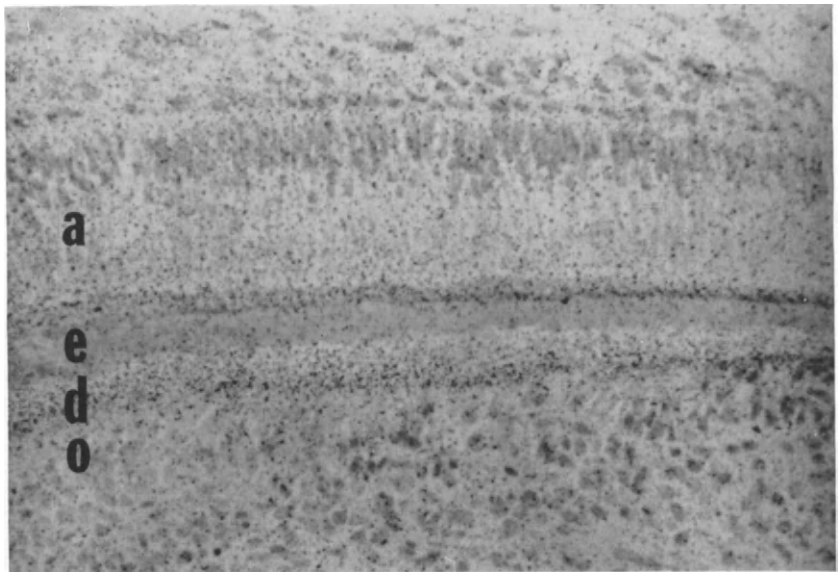

FIG. 2. Autoradiograph of tooth from newborn rat sacrificed 4 hours after administration of ^{14}C in the form of bicarbonate ion [9]. Autoradiographic reactions are localized over the predentin layer (d) and the tips of the odontoblasts (o). The thin layer of enamel matrix (e) present at this time is also seen with reaction, as is the ameloblastic cytoplasm (a). Magnification: × 360.

Since the present report is concerned with the behavior of amino acid precursors, final mention should be made of the reliability of the autoradiographic technique for demonstrating protein synthesis in the tooth. This was previously tested [13] in the rodent tooth, using methionine labeled in different positions with ^{14}C, ^{35}S, or ^{3}H. The results clearly demonstrated that, irrespective of label, the sites of initial incorporation and subsequent distribution were essentially identical. Consequently, it is assumed that sites of incorporation of tritiated amino acids observed autoradiographically in the present study accurately portray protein synthesis in the odontogenic apparatus.

UTILIZATION OF TRITIATED AMINO ACIDS IN MATRIX FORMATION

Materials and Methods

Qualitative and quantitative observations have been made on the distribution of twelve tritiated amino acids. Each was administered as a single intraperitoneal injection to Long-Evans rats at 6 days of age. The doses ranged from 25 to 100 μc (Table I) and the animals were

TABLE I. *Tritiated Amino Acids: Type, Specific Activity, Dosage, and Autoradiographic Exposures Used in Studies of Amino Acid Utilization during Odontogenesis*

Amino acid	Specific activity (mc/m*M*)	Dose (μc)	Exposure time (days)
2,3-^{3}H-L-Alanine	100	100	15
^{3}H-L-Arginine	200	50	43
^{3}H-Glycine	194	50	7
^{3}H-DL-Histidine	34	50	15
^{3}H-DL-Isoleucine	100	100	15
^{3}H-L-Leucine	65	100	7
Methyl-^{3}H-L-Methionine	10	50	7
2,3-^{3}H-L-Phenylalanine	200	50	15
3,4-^{3}H-L-Proline	50	25	15
3-^{3}H-DL-Serine	10	100	15
^{3}H-DL-Tyrosine	55	50	15
2,3-^{3}H-DL-Valine	460	100	15

sacrificed at intervals ranging from 15 minutes to 24 hours following injection. Mandibles and maxillae were removed immediately after sacrifice, stripped of most adherent soft tissue, and were fixed in Hollande's solution. Fixation was followed by demineralization in 18.5% aqueous Versene (sodium ethylenediaminetetraacetate), buffered to pH 7.0 with 1 *N* HCl. The decalcified tissues were then embedded in nitrocellulose-paraffin and mesiodistal sections were cut at 5 μ. Replicate samples were left unstained or were stained by the periodic acid-Schiff (PAS) technique prior to autoradiography.

Autoradiographs were prepared by the dipping technique [17] using Eastman Kodak NTB2 emulsion, and were developed after exposures ranging from 7 to 43 days. After photographic fixation and washing, the PAS-stained specimens were counterstained with Harris' hematoxylin, while the unstained preparations were stained with Harris' hematoxylin and eosin B.

The developmental status of a rat tooth (or one of its individual cusps) is closely correlated with the postnatal age of the animal [11]. Hence, in undertaking both qualitative and quantitative observations,

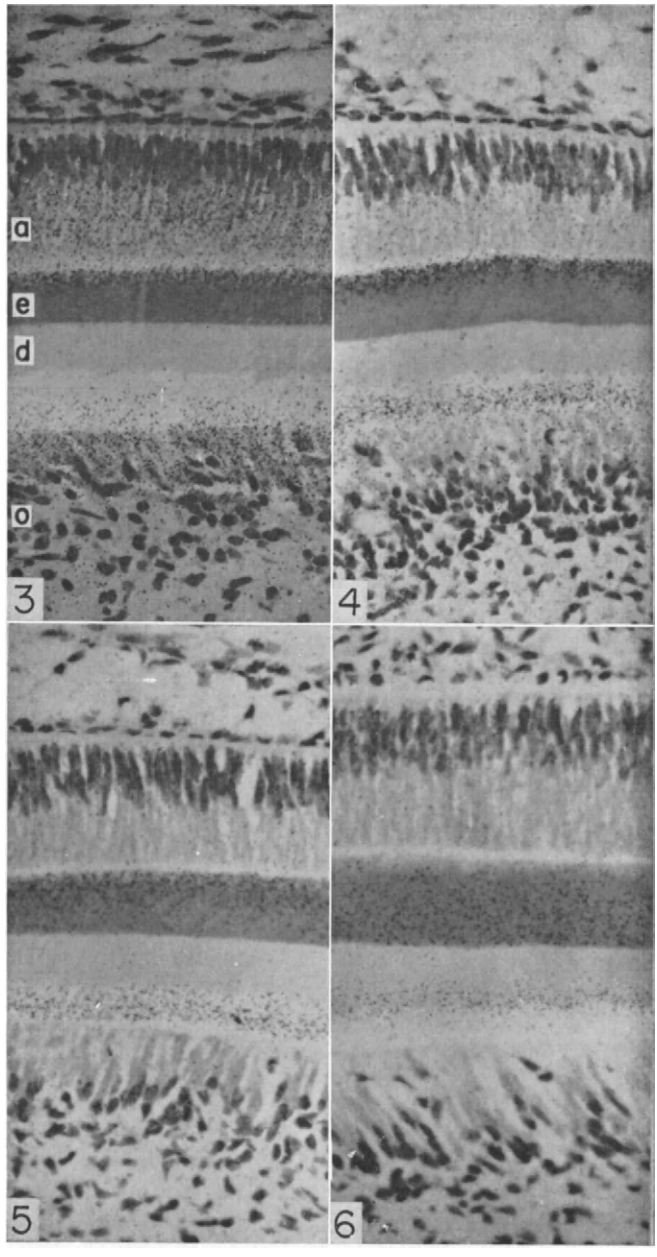

FIGS. 3–6. Autoradiographs demonstrating ^{3}H-proline uptake in enamel and dentin matrices of rat molar cusps (labeled as in Fig. 1). Magnification: × 340.

Thirty minutes after administration of the label (Fig. 3), the reaction is seen over the cytoplasm of the ameloblasts and odontoblasts, extending slightly into the adjacent matrices.

attention was restricted to the mesial cusp of the second molar, particularly to the region outlined in Fig. 1.

Qualitative Observations

The processes of incorporation and translocation of labeled matrical proteins are best exemplified by autoradiographs of teeth from animals given tritiated amino acids, since the low energy of the tritium β-particle lends itself to high resolution. The qualitative aspects of ^{3}H-proline distribution in the rat molar during the first 24 hours after administration are illustrated in Figs. 3–6.

Thirty minutes after injection (Fig. 3), the radioautographic reaction in the *dentinogenic* system is restricted to the cytoplasm of the odontoblasts, as well as to the extracellular predentin matrix immediately adjacent to it. With increasing time intervals following isotope administration, the bulk of the reaction is seen to be displaced from the cytoplasm into the predentin matrix. At 1 and 5 hours (Figs. 4 and 5), a distinct band of radioactive material may be visualized in the predentin layer. During the interval from 5 to 24 hours, displacement of this band continues, such that by 24 hours the band lies in the dentin matrix immediately distal to the predentin layer (Fig. 6).

The pattern of ^{3}H-proline uptake in dentin matrix confirms, in every respect, those observations made with the wide variety of isotopic precursors mentioned previously. Chemically, the labeled matrix component is presumed to be collagen, which was being formed in the odontoblastic cytoplasm at the time of ^{3}H-proline administration. During the succeeding 24 hours, as the level of circulating radioactive precursor decreased, collagen synthesis continued, but its labeling proportionately diminished. Since dentin formation occurs in an appositional manner, a discrete layer of labeled collagen was deposited in the predentin, and subsequently was displaced away from the odontoblasts as new unlabeled matrix collagen was formed behind it. Dentin matrix already present at the time of injection did not become labeled.

Initial ^{3}H-proline localization in the *amelogenic* system was also cellular, and by 30 minutes (Fig. 3) labeled material was particularly

---

One hour after administration (Fig. 4), the reaction over the intracellular regions is considerably reduced whereas that in the predentin and enamel matrix regions is more intense.

At 5 (Fig. 5) and 25 hours (Fig. 6) after administration of labeled material, little or no reactivity is discernible intracellularly. The label appears to diffuse throughout the enamel matrix, whereas in dentin it appears as a discrete band adjacent to the predentin-dentin junction.

prominent over the apical cytoplasm of the ameloblasts and the adjacent enamel matrix. Examination of the autoradiographs at serial time intervals thereafter revealed that, unlike dentin, the newly synthesized material was not transferred to the matrix as a reaction band. Instead, all the enamel matrix, including that already present at the time of injection, gradually accumulated labeled components (Figs. 4–6). This pattern has previously been described for ^{3}H-glycine [22] and ^{3}H-histidine [12], and has been termed "diffusive" to distinguish it from the discrete "bandlike" reaction in dentin [22]. A comparable translocation of ^{14}C-bicarbonate and of ^{35}S-sulfate in enamel matrix had also been suggested previously [15], although on the basis of inadequately preserved material.

The patterns of incorporation and translocation of the remaining ^{3}H-amino acid precursors used in the present study were examined in optimally exposed autoradiographs (Table I), and were generally similar to ^{3}H-proline. Thus, initial cellular accumulation was soon followed by transfer of labeled material into the respective matrices. The ultimate pattern of matrix reaction was bandlike in the dentin and diffuse in the enamel, irrespective of the precursor applied. Since the bulk of radioactive material appeared to be localized in the matrices at 24 hours, it was concluded that the secretion of labeled matrix components from cells to matrices was essentially completed during the first 24 hours after a single injection of a labeled amino acid.

Comparative observation of reaction intensities in the same sample at 24 hours also revealed that a given amino acid precursor was utilized with varying efficiency in the formation of enamel and dentin matrices. Following ^{3}H-histidine, for example, the enamel matrix was intensely labeled relative to the minimal reaction of the adjacent dentin matrix. By contrast, ^{3}H-glycine labeling at 24 hours was much greater in dentin than in enamel matrix. These findings were in general accord with the variations in matrix amino acid concentration previously established by chemical analysis of dentin and enamel (Table II). The tendency toward agreement between chemical and autoradiographic observations suggested the need for more precise data upon which to compare the utilization of the various amino acid precursors, and led to the application of autoradiographic grain counting.

Quantitative Observations

Technique. Grain counting was performed on the same optimally exposed preparations that had previously been examined qualitatively (Table I). A strip of the odontogenic apparatus approximately 11 μ wide under oil immersion optics (1500 diameters) was outlined by means of an ocular grid (Fig. 7). Counts were made of all silver grains lying

directly above each component tissue element in the strip (e.g., ameloblasts, enamel matrix, dentin matrix, predentin, and odontoblasts). Two strips were counted for each amino acid at each time interval. The length of each tissue element was measured and recorded and, following correaction for background fog (< 7 grains/1000 μ^2), the grain count over each was expressed in terms of grains per unit length.

TABLE II. *Range of Amino Acid Concentrations in Fetal Enamel and Dentin Obtained by Chemical Analysis (Expressed as Residues per 1000)*

Amino acid	Enamel matrix[a]	Enamel matrix[b]	Collagen[c]
Alanine	14–21	56	108–112
Arginine	25–31	31	51–52
Glycine	68–84	97	308–329
Histidine	58–62	30	4.7–6.5
Hydroxyproline	0–3.5	0	98–101
Isoleucine	27–33	30	5.3–6.8
Leucine	83–97	96	24–27
Methionine	38–49	21	5.3–6.8
Phenylalanine	23–41	51	15–16
Proline	152–261	146	115–116
Serine	58–78	76	33–41
Tyrosine	49–64	—	4.9–6.4
Valine	33–43	45	25–27

[a] Human [5], ox [7], pig [18].
[b] Unerupted human, stored in formalin [18].
[c] Human Dentin [5].

Variations in the plane of histological section introduced significant differences in the length of the constituent tissue elements. Hence, "standard" lengths were calculated for each tissue element, i.e., the arithmetic means derived from measurement of 41 individual odontogenic strips. These standards are tabulated in Fig. 7, and the grain counts from each experimental section were ultimately adjusted by proportionality to fit them.

Comparison of Matrical Amino Acid Incorporation. Since the degree of utilization of the different amino acid precursor substances varied greatly, and since minor variations in dosage were unavoidable, the utility of absolute grain counts was limited. As a consequence, quantitative comparisons both between amino acids and between animals sacrificed serially after administration of the same amino acid were expressed in relative terms.

Comparison was undertaken of the distribution of amino acids between the enamel and dentin matrices at 24 hours following injection. The data were expressed in terms of the percentage occurrence of silver grains, and confirmed the qualitative impression of differential utilization.

Nearly 90 per cent of matrix-localized silver grains was related to enamel following administration of ^{3}H-histidine, while after ^{3}H-glycine administration about 80 per cent of silver grains was localized over dentin. These and other selected examples of the distribution of matrical reac-

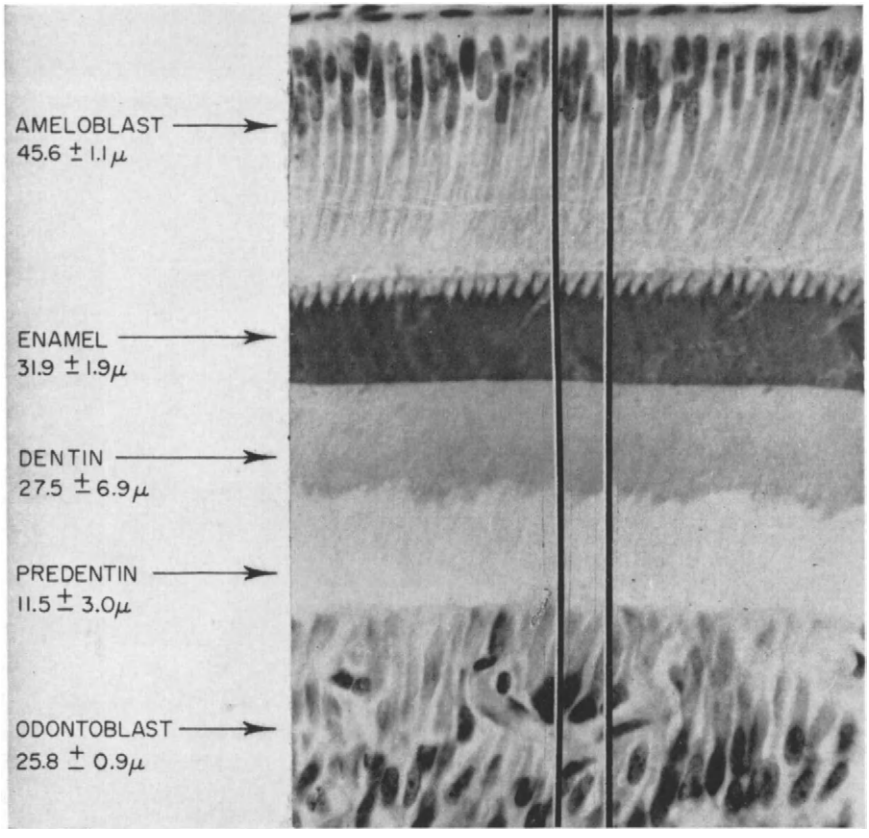

FIG. 7. Photomicrograph of the rat odontogenic apparatus. The heavy black lines indicate a typical sector through which grain counts were made. The arithmetic mean values for the length of the constituents of the odontogenic apparatus are also given (see text for fuller explanation). Magnification: × 800.

tions are illustrated in Fig. 8, which emphasizes the range of affinities of amino acids for the two matrices.

Examination of these data suggested the possibility that a relationship might be established between the observed grain count distribution in the two matrix components and their respective content of amino acid residues. To this end, reference was made to results of chemical analyses of dentin and enamel matrices available in the literature (Table II).

Some variation exists in the values derived by different investigators for the amino acid composition of enamel matrix, but for the most part the data are in reasonable agreement. Moreover, the values for collagen in dentin matrix appear to be quite consistent irrespective of the investigator or the source of the sample. Therefore, for the same concentration

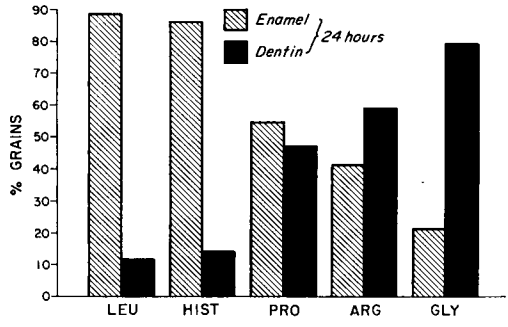

FIG. 8. Graph demonstrating the partitioning of grains between the enamel and dentin matrices at 24 hours following the administration of tritiated amino acids (see text).

of enamel and dentin matrix, Table II suggests that a relatively constant relationship can be derived for the comparative incidence of a given amino acid in the respective matrices. Histidine, for example, occurs in enamel matrix protein with nine times greater concentration than in an equal mass of dentin collagen, a relationship which is also reflected in the comparison of autoradiographic grain counts. Glycine, on the other hand, is some four to five times more frequent in its occurrence in dentin collagen than in enamel matrix, again as suggested by our autoradiographic observations.

This coincidence between the results of chemical analysis and quantitative autoradiography was pursued further in an effort to establish whether a full similarity could be established. An assumption vital to this comparative treatment was that the concentration of proteins must be equal in enamel and dentin matrices. This assumption is manifestly invalid in the adult tooth wherein the protein concentration in enamel is less than 1 per cent [20]. However, there is good evidence that in the fetal state enamel protein concentration approaches 20 per cent [4], a value virtually comparable to the concentration of collagen in fetal dentin.

The results of autoradiographic quantitation are presented graphically in Fig. 9 for nine representative amino acids.[2] The cross-hatched bars

[2] Since hydroxyproline of collagen is known to arise by conversion of proline

represent the ratios obtained by relating the silver grain concentration in enamel matrix to that in dentin matrix at 24 hours after amino acid administration. Accompanying each bar is the corresponding range of ratios derived from several chemical analyses of amino acid concentrations taken from the literature (Table II), including one series of values

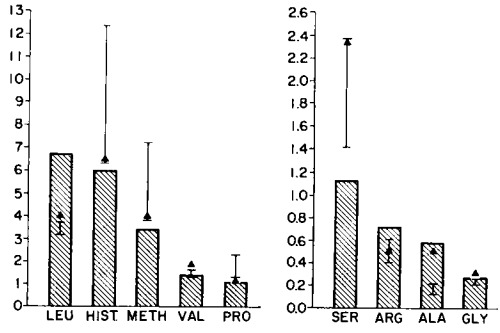

FIG. 9. Graphic representation of the ratio of grain counts in enamel matrix to that in the dentin matrix for nine tritiated amino acids, 24 hours following administration (cross-hatched bars). The range of ratios obtained by chemical analyses of amino acid concentration in the respective matrices is represented by the straight lines. Separate values (solid triangles) are also indicated for the ratio obtained by chemical analysis of formalin-preserved molars (see text).

obtained by chemical analysis of human impacted third molars stored in formalin [18]. These are expressed separately (solid triangles in Fig. 9). Comparison of the ratios obtained from quantitative autoradiography with those from chemical analysis demonstrates reasonable agreement, particularly with those derived on the basis of analysis of formalin-treated teeth. Only two amino acids, namely leucine and serine, yielded grain count ratios distinctly at variance with those anticipated on the basis of amino acid composition. The trend toward agreement otherwise suggests that factors other than experimental errors may be responsible for the variations in leucine and serine content. These will be discussed further in the following section.

DISCUSSION

Qualitative observation of the cellular site of initial incorporation and subsequent extracellular migration of labeled matrical components

(see Ross and Benditt [19]), it is assumed that autoradiographic images stemming from ^{3}H-proline administration reflect the presence of both labeled proline and hydroxyproline. Consequently, in comparing the chemical analyses of dentin collagen to the grain count ratios, combined content of proline and hydroxyproline were taken into account.

following administration of a variety of amino acid precursors confirms in every respect the results of previous autoradiographic investigations of odontogenesis. Thus, it is clear that the labeled precursors applied here are utilized in dentinogenesis for the synthesis of the collagenous component of dentin matrix. Coupled with investigations by others, our present results strongly support the concept that collagenesis is initially an intracellular event, followed rapidly by extrusion and fibrillar aggregation in the extracellular milieu [3, 19]. Once formed, the collagen of dentin matrix remains in a stable form, undergoing neither metabolic exchange nor physical intermixing with adjacent unlabeled matrix collagen. The fact that at least 90 per cent of the organic component of dentin matrix is collagen [20] would further suggest that the amino acid incorporation observed here reflects the synthesis of only that protein.

Amino acid incorporation in the amelogenic system is also initially cellular. Unlike dentin, migration of labeled enamel matrix components does not occur in the form of a discrete layer. Instead, there is a progressive tendency for mixing of the labeled component with the older, unlabeled matrix. This pattern of matrix labeling would tend to support the suggestion [6] that the state of aggregation of fetal enamel matrix may be that of a thixotropic gel.

The question of the chemical nature of the labeled material in enamel matrix cannot be answered satisfactorily on the basis of these data. It seems likely that, unlike dentin collagen, enamel matrix consists of a mixture of protein entities, the synthesis of some or all of which is demonstrated by the autoradiographic technique. There is inferential evidence from the present results to suggest that the labeled components are structural rather than actively metabolic in their function, since no appreciable loss of enamel matrix reaction occurs during the first 24 hours after amino acid administration. Indeed, previous investigations of ^{3}H-glycine [22] and ^{3}H-proline [8] have revealed no significant loss in enamel matrix reaction intensity over periods up to 168 hours after administration.

With the exceptions of leucine and serine, among the 12 amino acids that have been examined thus far, reasonable agreement exists between the amino acid ratios in dentin and enamel derived chemically or by autoradiographic grain counts. Consequently, the autoradiographic method of analysis would appear to provide a fair reflection of the physiological and biochemical processes which operate in the formation of matrix proteins.

In undertaking our comparisons we have chosen to overlook the possible influence of a number of metabolic factors, such as availability time, pool size, reutilization, etc. Initial attempts to evaluate their role

in the apparently anomalous behavior of leucine and serine have involved examination of the movement of labeled components from the cells to the matrices. The ratio of the grain count in the matrix to the total number of grains in both cells and matrix at any time interval after injection provides a convenient, though approximate, means for expressing the efficiency of amino acid utilization in matrix synthesis. Data of this type are expressed graphically in Fig. 10 for ^{3}H-leucine and ^{3}H-

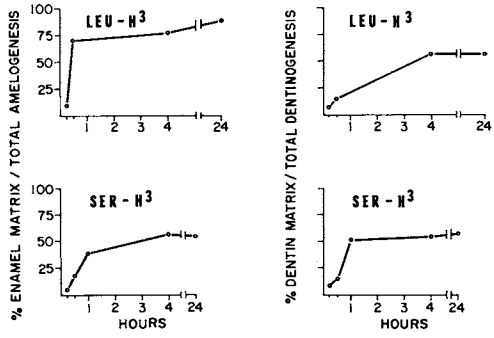

FIG. 10. Graphic representation of the relative rates of increase in reactivity of enamel (left) and dentin (right matrices during the first 24 hours following administration of ^{3}H-leucine (above) and ^{3}H-serine (below). (See text for further explanation.)

serine. The efficiency of utilization of these amino acids appears to be essentially comparable in dentinogenesis, as might be anticipated if but a single protein is elaborated. In enamel matrix, on the other hand, ^{3}H-leucine is utilized more rapidly and more completely than is ^{3}H-serine.

This contrast may account in part for the discrepant values obtained by quantitative autoradiography for the content of these amino acids in enamel matrix. Serine is not efficiently utilized for enamel matrix synthesis during the first 24 hours. Mechanisms such as pool dilution and/or differential membrane transport may be active in impeding enamel matrix labeling after serine administration. Additional investigation, particularly over time periods beyond 24 hours, should provide more precise information regarding the extent to which these factors are involved.

In the case of leucine, more appears in the enamel matrix at 24 hours than would be anticipated on the basis of chemical analysis. The data regarding transfer rate (Fig. 10) suggest that leucine is utilized for matrix synthesis with an extraordinarily high degree of efficiency. While further experimental investigation is needed to settle the question, it seems possible that leucine may contribute through its own local

catabolism to the formation of other labeled precursor compounds, which in turn are then utilized for matrix synthesis. Unpublished results from this laboratory have demonstrated, for example, that the ameloblast is extremely active in anabolic synthesis involving acetate, one of the products which may be anticipated from leucine breakdown.

SUMMARY

Qualitative and quantitative autoradiographic techniques have been applied in the study of protein synthesis associated with the formation of the matrices of dentin and enamel. Examination of autoradiographs of rat molars taken from animals sacrificed up to 24 hours following administration of a series of twelve amino acids reveals a qualitatively similar pattern of incorporation. Initially, amino acid utilization occurs in those cells responsible for matrix synthesis, i.e., ameloblasts and odontoblasts. Within 1 hour after injection, labeled matrix components are transferred from cell to extracellular milieu.

In the dentin matrix, labeling occurs in the form of a discrete band of radioactive matrix, and presumably reflects the presence of labeled collagen. In the enamel matrix, labeled material diffuses through pre-existing enamel matrix, so that ultimately the entire matrix layer is homogeneously labeled. The identity of the matrix protein or proteins in enamel is unknown.

Grain counting techniques have been applied in an attempt to compare the utilization of the various amino acid precursors in matrix synthesis. Quantitation of the autoradiographic images not only emphasizes the dynamic metabolic state of these tissues during odontogenesis, but provides as well a reasonably accurate reflection of their quantitative amino acid composition.

Acknowledgments

The authors wish to thank Dr. R. W. Young for providing the specimens of teeth and to gratefully acknowledge the technical and secretarial assistance of Mrs. Zoja Trirogoff and Mrs. Shirley Gold.

References

1. Bélanger, L. F., *J. Dental Res.* **34**, 20 (1955).
2. Bélanger, L. F., *Anat. Record* **124**, 555 (1956).
3. Carneiro, J., and Leblond, C. P., *Exptl. Cell Res.* **18**, 291 (1959).
4. Eastoe, J. E., *Nature* **187**, 411 (1960).
5. Eastoe, J. E., *Arch. Oral Biol.* **8**, 633 (1963).
6. Eastoe, J. E., *in* "Bone and Tooth" (H. J. J. Blackwood, ed.) p. 269. Pergamon Press, New York, 1964.
7. Glimcher, M. J., Mechanic, G., Bonar, L. C., and Daniel, E. J., *J. Biol. Chem.* **236**, 3210 (1961).

8. Greulich, R. C., *Intern. Assoc. Dental Res. Proc.* p. 110 (1963).
9. Greulich, R. C., and Leblond, C. P., *Anat. Record* **115**, 559 (1953).
10. Greulich, R. C., and Leblond, C. P., *J. Dental Res.* **33**, 859 (1954).
11. Hoffman, M. M., and Schour, I., *Anat. Record* **78**, 233 (1940).
12. Hwang, W. S. S., Tonna, E. A., and Cronkite, E. P., *Nature* **193**, 896 (1962).
13. Karpishka, I., Leblond, C. P., and Carneiro, J., *Arch. Oral Biol.* **1**, 23 (1959).
14. Kumamoto, Y., and Leblond, C. P., *J. Dental Res.* **35**, 147 (1956).
15. Leblond, C. P., Belanger, L. F., and Greulich, R. C., *Ann. N. Y. Acad. Sci.* **60**, 629 (1955).
16. Leblond, C. P., Everett, N. B., and Simmons, B., *Am. J. Anat.* **101**, 225 (1957).
17. Messier, B., and Leblond, C. P., *Proc. Soc. Exptl. Biol. Med.* **96**, 7 (1957).
18. Piez, K. A., *in* "Fundamentals of Keratinization" (E. Butcher and R. Sognnaes, eds.), p. 173. American Association for the Advancement of Science, Washington, D.C., 1962.
19. Ross, R., and Benditt, E., *J. Cell Biol.* **15**, 19 (1962).
20. Stack, M. V., *Ann. N.Y. Acad. Sci.* **60**, 585 (1955).
21. Watson, M. L., *in* "Fundamentals of Keratinization" (E. Butcher and R. Sognnaes, eds.), p. 161. American Association for the Advancement of Science, Washington, D.C., 1962.
22. Young, R. W., and Greulich, R. C., *Arch. Oral Biol.* **8**, 509 (1963).

Discussion

Dr. Tonna: I agree with Dr. Greulich, that the general distribution of label which appears after administration of a large variety of amino acids is similar. I don't know, however, why enamel shows the peculiar phenomenon of protein diffusion through the matrix.

Dr. Ross: Dr. Greulich compared the uptake of label in enamel to that in dentin, for each of 12 different amino acids. He felt that the enamel-to-dentin ratios remain relatively unchanged at the later times, when mineralization had already begun to occur. The extent of loss of protein matrix and retention of labeled amino acids in this matrix remains to be resolved.

Dr. Leblond: Mr. H. Warshawsky has used ^{3}H-proline and -tyrosine in investigating enamel formation in the rat. At early intervals (5–15 minutes after injection) the radioautographic reaction predominated in the ribosome-rich supranuclear region of secretory ameloblasts. By 30 minutes, the silver grains were arranged in long axial rows corresponding to the Golgi apparatus (which in these cells is tubular; *J. Cell Biol.* 1963, **16**, 629). The appearance of radioactivity in the matrix began at this time (30 minutes) and progressed to a maximum reached toward 4 hours. These results seem to be in full agreement with those of Dr. Greulich.

PROTEIN SYNTHESIS AND CELLS OF THE SKELETAL SYSTEM[1]

EDGAR A. TONNA

Medical Research Center, Brookhaven National Laboratory, Upton, Long Island, New York

SKELETAL PROTEINS

Unlike other tissues (excluding teeth) the skeletal system consists of three major nonliving compartments, namely: the mineral, water, and organic phases. Except for a certain amount of water, these substances are found in the external environment of skeletal cells called the matrix. Analyses of compact bone reveal that by weight 72.17 per cent is mineral, 3.68 per cent water, and 24.15 per cent organic matter [7, 8]. Because of the differences in density of the various phases, approximately 54 per cent is mineral, 8 per cent water, and 38 per cent organic matter [19, 20]. Since the skeletal system also contains much cartilage in addition to compact bone, these values will vary considerably. Differences can also be found in samples taken from different animal species or from different tissue areas of the same animal, and in samples taken from animals of different ages [7].

The organic matter making up the skeletal system consists of approximately 90 to 96 per cent collagen, 1.24 per cent mucopolysaccharide–protein complex, and 3 to 9 per cent protein material, largely coming from vascular material which for our purpose can be considered adventitious to true bone. Analyses of cartilage mucopolysaccharide–protein samples (free from hydroxyproline) reveal that the complex consists of only 18 per cent protein and 83 per cent chondroitin sulfate [5]. Keratosulfate is also found in bone and cartilage; this complex, however, constitutes less than 1 per cent of the total mucopolysaccharides [14]. The major protein composition of the skeletal system, therefore, consists of the matrical proteins collagen and mucopolysaccharide–protein and a variety of cellular proteins. Although the bulk of the skeletal protein is extracellular, the cells play a pertinent role in the manufacture of protein precursors. These precursors undergo orientation, polymerization, and maturation after they are liberated from cells into the skeletal matrix.

[1] Research supported by the U. S. Atomic Energy Commission.

CELLULAR COMPOSITION OF THE SKELETON AND CELLULAR FUNCTION

The living phase of the skeletal system consists of a variety of pleomorphic cells and cellular populations whose initial origin stems from undifferentiated pleuripotential mesenchymal cells. In addition to the necessary manufacture of protoplasmic proteins, many of the skeletal cells actively participate in matrical protein-precursor synthesis. Fibrogenic, osteogenic, and chondrogenic cells are all capable of collagen and mucopolysaccharide–protein complex precursor formation. Sufficient evidence is available for acceptance of the fact that protein precursors (protofibrils) are synthesized intracellularly and are then elaborated extracellularly for eventual polymerization [10, 12, 17, 22]. These cells obviously contain the necessary power requirements (energy supply), biochemical mechanisms, quantity and rate control systems (enzymatic catalysis), the quality control mechanism (deoxyribonucleic acid), and the ribonucleic acid assembly lines for protein precursor production. In addition, they can secrete into the surrounding matrix a variety of substances which would insure the continued extracellular process of precursor orientation, polymerization, and maturation into the definitive protein structure (Fig. 1).

For a more comprehensive understanding of skeletal biology, it is therefore necessary to study the synthesis of matrical proteins including

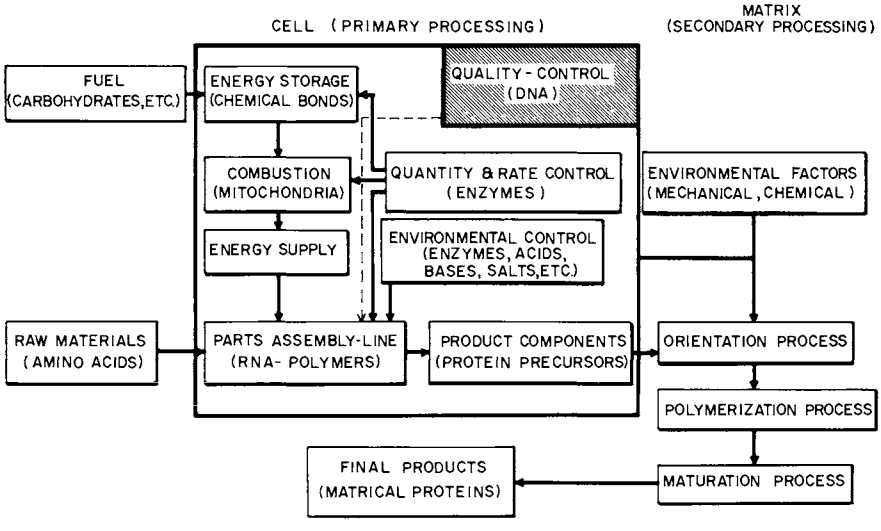

FIG. 1. A schematic representation of the biphasic protein processing system showing the cell's role in the primary internal phase and the secondary extracellular phase.

the important primary role of cells in protein precursor formation. These investigations must encompass studies of the cellular uptake and turnover of amino acids, evaluation of the differences in the activity of different cell types, and of similar cells at various sites within the skeletal system. Comparable data must be obtained from birth to old age. More important, the cellular potential for protein precursor production must be evaluated, since it is of biological and medical interest to know the emergency response and reparative capacity of the system at different ages.

AUTORADIOGRAPHIC ASSESSMENT OF PROTEIN SYNTHESIS

Autoradiography offers a simple, highly informative, and precise means by which many of the facets of protein synthesis can be effectively studied. In addition, the skeletal system lends itself very favorably to autoradiographic analysis because of the stability of skeletal protein. The matrices of bone and cartilage reveal a histological map from which the amount of labeled protein deposited and the apparent movement of labeled protein during growth, repair, etc., can be followed and evaluated from one time period to the next.

^{3}H-labeled amino acids offer the advantage of high resolution autoradiography, since with tritium, radioactivity can be detected within a range of about 1 μ. To date a number of ^{3}H-amino acids have been used to study protein synthesis in the skeletal system, including glycine [6, 25, 32, 33], leucine [6], methionine [6], histidine [29, 31], and proline [18, 26]. A study of fibroblastic collagen production in healing wounds using ^{3}H-proline was also reported by Ross and Benditt [21].

The Use of ^{3}H-Amino Acids in Matrical Protein Synthesis

When a given ^{3}H-labeled amino acid is injected into an organism for the study of skeletal protein synthesis, the appearance of labeled protein does not necessarily indicate that the ^{3}H-label is present exclusively within the same amino acid, since some injected amino acids undergo hydroxylation or metabolic transformations by which other amino acids are synthesized from atoms constituting the injected amino acid. This is probably also true for the administration of essential amino acids, since evidence is available [11] showing that during catabolism products are formed which can be reutilized in the synthesis of nonessential amino acids (Fig. 2). On the other hand, it has been shown that when glycine is administered to animals, the amino acid is preferentially incorporated into collagen [15, 23]. In any event, the question of concern in autoradiography is not whether the original form of the administered amino acid appears in newly deposited matrical protein, but how much of the cellu-

lar turnover of injected ^{3}H-amino acids is representative of matrical protein synthesis and how much is needed for protoplasmic turnover. Labeled matrical protein represents, for the most part, collagen and mucopolysaccharide–protein, with only insignificant amounts of other proteins found within the matrix.

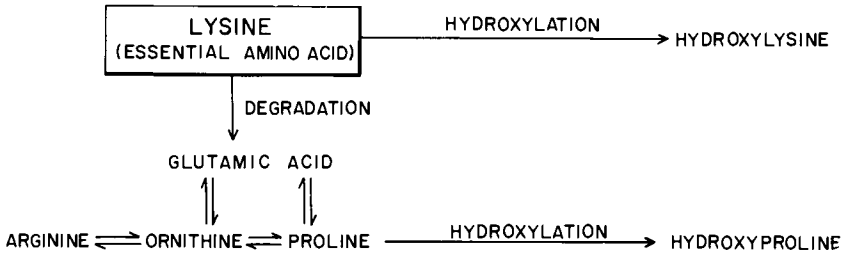

FIG. 2. A diagram showing a number of chemical interrelationships which can take place following administration of lysine and illustrating the synthesis of a variety of amino acids.

Table I compares grain counts deposited over bone and cartilage matrices in femora of young mice, not treated with enzyme or treated with collagenase or hyaluronidase; the mice were sacrificed 8 hours following administration of ^{3}H-glycine, histidine, and proline. The autoradiographic results with enzymes, although crude, were sufficient to show that the grains appearing over bone and cartilage matrix were essentially due to matrical proteins, largely collagen. Therefore, autoradiography using ^{3}H-amino acids largely represents a study of matrical protein synthesis.

Skeletal cells appear to use large quantities of amino acids for matrical protein formation, but comparatively little for turnover of protoplasmic proteins. Evidence is available from autoradiographic studies using ^{3}H-histidine [31], ^{3}H-glycine [32, 33], and ^{3}H-proline [26] in which osteoclasts were consistently shown with very low grain counts. These cells are highly active metabolically but not involved in matrical protein synthesis. Bone and cartilage cells which terminate their matrical protein synthetic activity following growth of the organism and during aging also showed the presence of very few autoradiographic grains [25, 29].

Concerning the distribution of reduced silver grains in autoradiograms of bone and cartilage following the administration of ^{3}H-amino acids, the investigator must bear in mind that variations in the ratios of collagen (C) to mucopolysaccharide–protein complex (MPC) in bone versus cartilage exist and that some differences can be significant [5, 7, 8]. One must also be cognizant of the possible significant variations in re-

TABLE I. *The Removal of Reduced Silver Grains from ^{3}H-Amino Acid Autoradiographs of Mouse Femora by Treatment with Hyaluronidase and Collagenase*[a,b,c]

	Epiphyseal plate (matrix)			Metaphyseal trabeculae (osteoblastic collagen)		
Treatment	^{3}H-Histidine	^{3}H-Glycine	^{3}H-Proline	^{3}H-Histidine	^{3}H-Glycine	^{3}H-Proline
Hyaluronidase:						
No treatment	2.39	5.52	2.60	3.39	25.80	9.62
4 hours	1.65	4.01	2.08	1.74	21.33	5.80
8 hours	1.69	3.68	1.87	1.56	20.08	4.93
Collagenase:						
No treatment	2.39	5.52	—	3.39	25.80	—
3 hours	0.61	1.48	—	0.88	2.75	—
8 hours	0.63	0.76	—	0.96	1.25	—
16 hours	0.83	0.74	—	1.04	0.82	—

[a] Mice: 2 weeks old; sacrificed 8 hours after administration of ^{3}H-amino acid.

[b] Each value represents an average 200–300 areas (6.25 μ each).

[c] Average background ~ 0.13 grains/area.

sults due to the removal of samples from different sites within the same animal [7], differences due to the age of the animals used, and differences between similar tissues taken from different animal species [8, 16]. In a recent theoretical study it was shown that with a bone C/MPC ratio of 79:1 and cartilage C/MPC ratio of 1:1 the number of grains attributed to MPC overlying bone was ~ 1 per cent for ^{3}H-glycine, histidine, proline, and lysine. Over cartilage, on the other hand, 5, 33, 8, and 17 per cent of the overlying grains were attributed to MPC, respectively [27].

There are three additional situations involved in the assessment of ^{3}H-amino acid autoradiographs which significantly affect the interpretation of the data, namely: (1) availability of injected ^{3}H-amino acids to cells situated in different regions of the skeleton, (2) the reutilization by skeletal cells of labeled materials which become available to them sometime after the initial uptake of injected ^{3}H-amino acid, and (3) the size of the body pool for a given amino acid which may be different in animals of different ages resulting in a change in the "specific activity" of the label. These parameters will be discussed more fully later.

In terms of a dynamic understanding of skeletal protein synthesis, it is not sufficient to have data which reflect events taking place at one age. Neither is it sufficient to possess data for normal protein uptake and turnover without having data reflecting the capacity of cells to accelerate or reactivate protein synthesis following trauma. This is because cells of the skeletal system, including cells of other tissues as well, undergo several phases of activity throughout the life-span of the organism during which the potential for protein synthesis may be altered. These phases include growth, post-growth activity, aging, and the response to trauma. It is imperative, therefore, that for a more comprehensive understanding of protein synthesis by a given tissue system, each of these phases should be considered in the experimental design.

Materials and Methods Used for Autoradiographic Assessment

The methods which were used in the present studies of protein synthesis by the skeletal system involve: (1) autoradiographic grain counting of cells from early time periods (e.g., 5 minutes) to 14 days after ^{3}H-amino acid administration, (2) analysis of the grain count data and curve analysis after semilogarithmic plotting, and (3) microscopic and micrometric analysis of the apparent movement of label following the continued deposition of new matrix. All the studies included cells of the osteogenic layer of the periosteum, metaphyseal–trabecular–endosteal osteoblasts, epiphyseal plate cartilage cells (proliferative and hypertrophic zones), and cells of articular cartilage. These cell populations were studied in the femora of mice (5 to 52 weeks of age) of the Brookhaven

National Laboratory strain of Swiss albino. The left femora were generally fractured at mid-shaft prior to the subcutaneous administration of ^{3}H-amino acids. ^{3}H-histidine was given in quantities of 1 μc/gm body weight (specific activity 1.7 curies/mmole), ^{3}H-glycine in quantities of 5 μc/gm body weight (specific activity 50 mc/mmole), and ^{3}H-proline in 2 μc/gm body weight (specific activity 1.0 curie/mmole). The femora and upper half of the tibia were removed intact, fixed in 10% formalin, processed histologically, and finally paraffin embedded and blocked. Five micron sections were cut and autoradiographs were prepared using NTB3 Kodak liquid emulsion. ^{3}H-histidine sections were exposed in a cold, dry atmosphere for 30 days. ^{3}H-glycine and ^{3}H-proline sections were exposed for 16 days prior to photographic development. One set of slides was stained with hematoxylin and another set with hematoxylin and eosin.

AUTORADIOGRAPHIC STUDIES (^{3}H-HISTIDINE, -GLYCINE, AND -PROLINE)

Skeletal Cell ^{3}H-Amino Acid Turnover

After administration of either ^{3}H-histidine, -glycine, or -proline to 5-week-old mice, the label first appeared largely over the cytoplasm of cells. All skeletal cell types became labeled, but not all the cells comprising a given type were seen labeled as early as 5 minutes after administration of ^{3}H-amino acids. Osteoclasts and osteocytes were poorly labeled throughout the entire study period, but new osteocytes and osteocytes formed shortly after ^{3}H-amino acid administration were well labeled. The latter cells were labeled substantially by reutilization. Periosteal and endosteal osteoblasts as well as cartilage cells of both the epiphyseal plate and articular cartilage were highly labeled. This is especially true for metaphyseal osteoblasts and epiphyseal cartilage cells. Fewer grains were seen over preosteoblasts than over osteoblasts. The perichondrial regions of the periosteum were more abundantly labeled than the rest of the periosteum. This is also true of the cells at the periphery of the epiphyseal plate. Metaphyseal endosteal cells incorporated larger amounts of labeled material than did other skeletal cells, and at an earlier time period. Maximum grain counts were reached after 15 minutes by metaphyseal osteoblasts and after 30 minutes by the other skeletal cells (Fig. 3). The increased activity of metaphyseal cells at earlier time periods is believed to reflect, at least in part, an increased availability of ^{3}H-amino acids via the well-developed circulatory system of this region. At 30 minutes silver grains increased in number over cells and appeared as well over the matrix contiguous with the cells. The silver grains formed a continuous band over newly formed matrices of cortical bone,

metaphyseal trabecular bone, and bone at the secondary centers of ossification. The apparent movement of silver bands was traceable in autoradiographs from one time period to the next as additional unlabeled matrix was deposited (see Figs. 4 and 10). Silver band formation was not prominent in ^{3}H-histidine autoradiographs, but very pronounced with

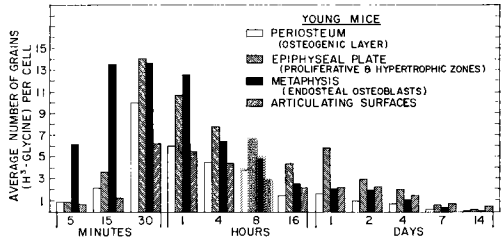

FIG. 3. A histogram illustrating the uptake and turnover of ^{3}H-glycine by various femoral cell populations in 5-week-old mice. Assessment is made by autoradiographic grain counting. Note particularly the differences between osteoblasts of periosteal and metaphyseal origin (taken from [32]).

^{3}H-glycine and -proline. Cartilage matrices were labeled diffusely throughout the study but never in sharp bands. A continuous loss of label from cells to matrix was observed in all cells except osteoclasts and mature osteocytes.

At the metaphysis, the newly deposited osteoblastic trabecular matrix was labeled, but the cartilage core of the trabeculae was unlabeled. With increasing time the label appeared deeper within the trabeculae as more matrix was deposited and further along the metaphysis as longitudinal trabecular growth proceeded. Simultaneously with these events, silver grains which were deposited earlier over the cartilage matrix of the epiphyseal plate at the proliferative and hypertrophic zones, appeared over the degenerative zone of the plate by 16 hours and eventually over the trabecular cartilage core. By this time, however, the trabecular label deposited by osteoblasts had progressed further along the metaphysis.

With increasing time more and more grains were deposited over bone and cartilage matrices while cellular labeling became weaker, so that by the fourth day very few grains were seen above cells and by the seventh day cellular labeling was essentially negative (Figs. 4 and 5).

Autoradiographs of older animals revealed the same distribution of silver grains over all cell types as was observed in younger mice, but the protein synthetic activity was much lower (Fig. 6). The rates of uptake, turnover time, and total amount of labeled amino acid used differed significantly from those of young cells, except in metaphyseal osteoblasts. These cells revealed an uptake and turnover very much

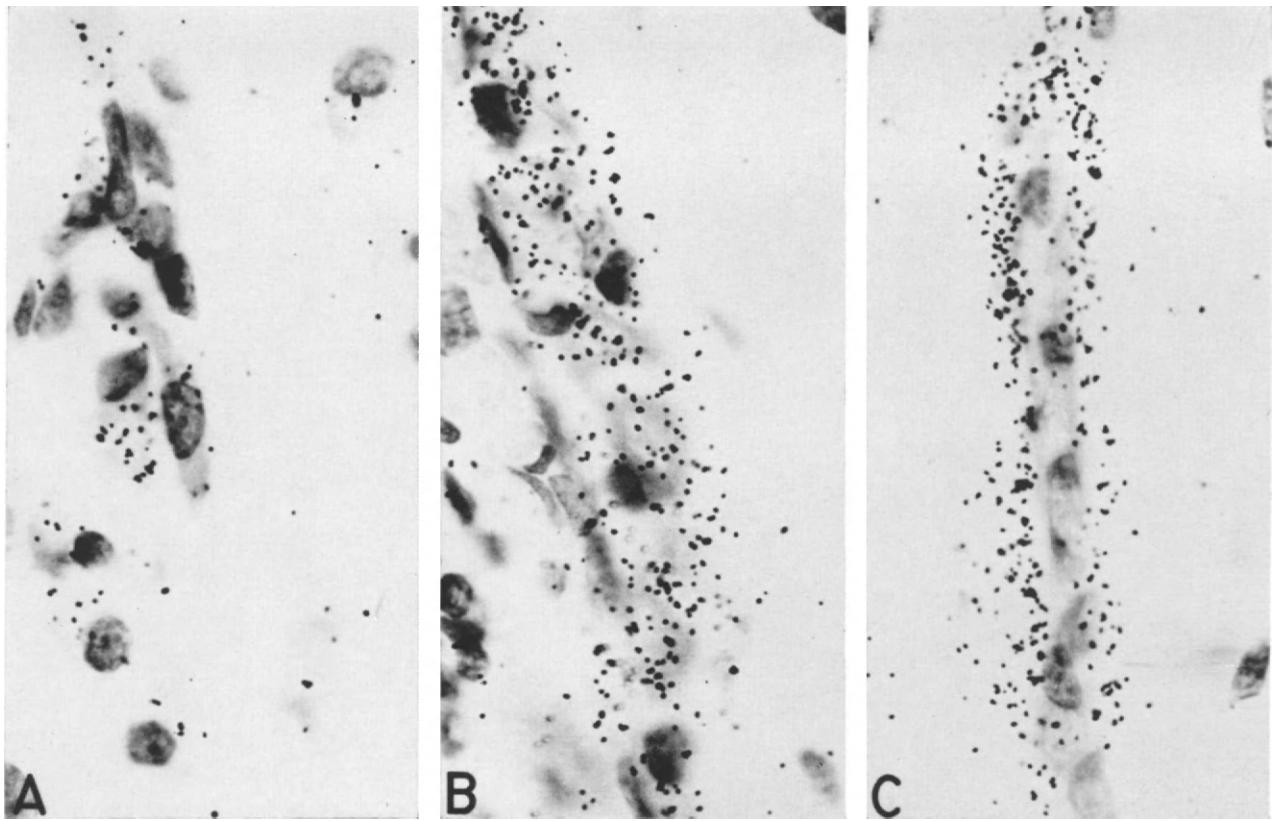

FIG. 4. An autoradiographic series showing turnover of ^{3}H-proline (A) 15 minutes, (B) 30 minutes, and (C) 4 hours after its administration by metaphyseal osteoblasts of 5-week-old mouse femora. New trabecular bone matrix is evidenced by the appearance of bands of silver grains. Hematoxylin stained. Magnification: × 1000.

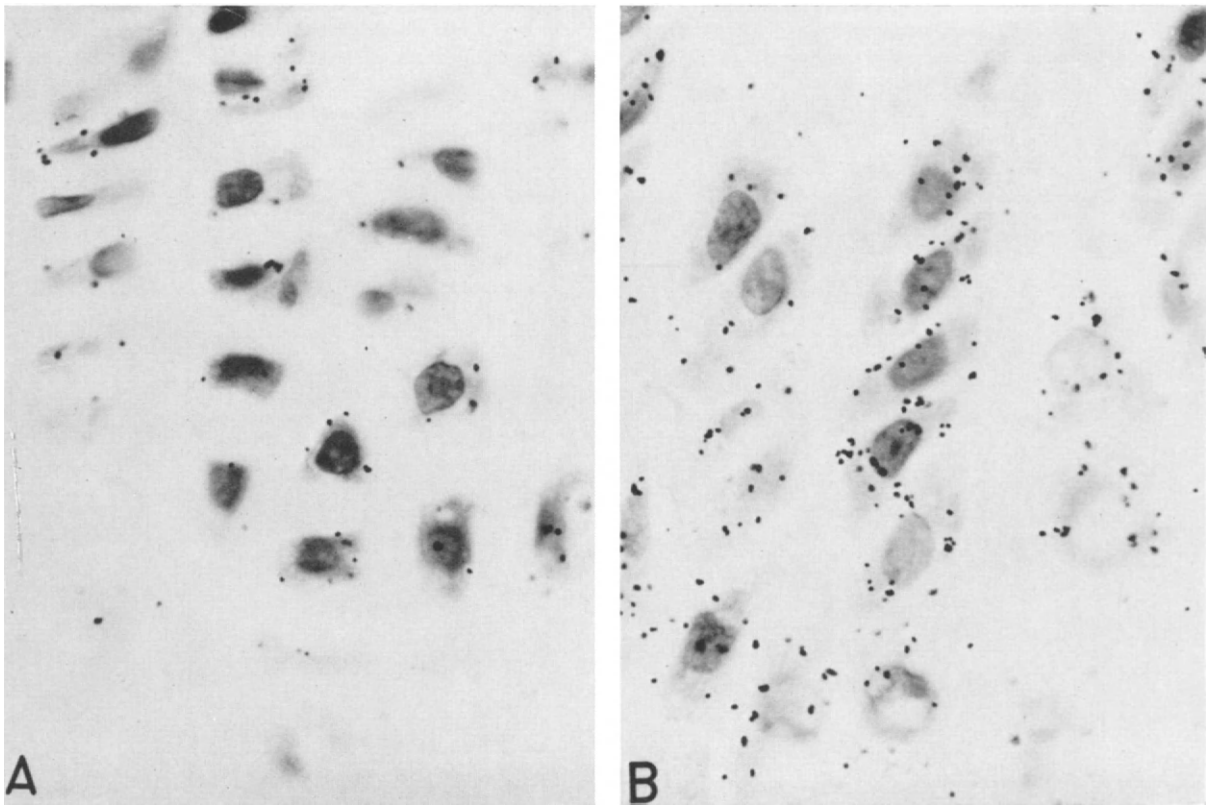

FIG. 5. An autoradiographic series showing turnover of ^{3}H-proline by cartilage cells of the distal epiphyseal plate of 5-week-old mouse femora. The photomicrographs represent (A) 15 minutes, (B) 30 minutes, (C) 1 hour, and (D)

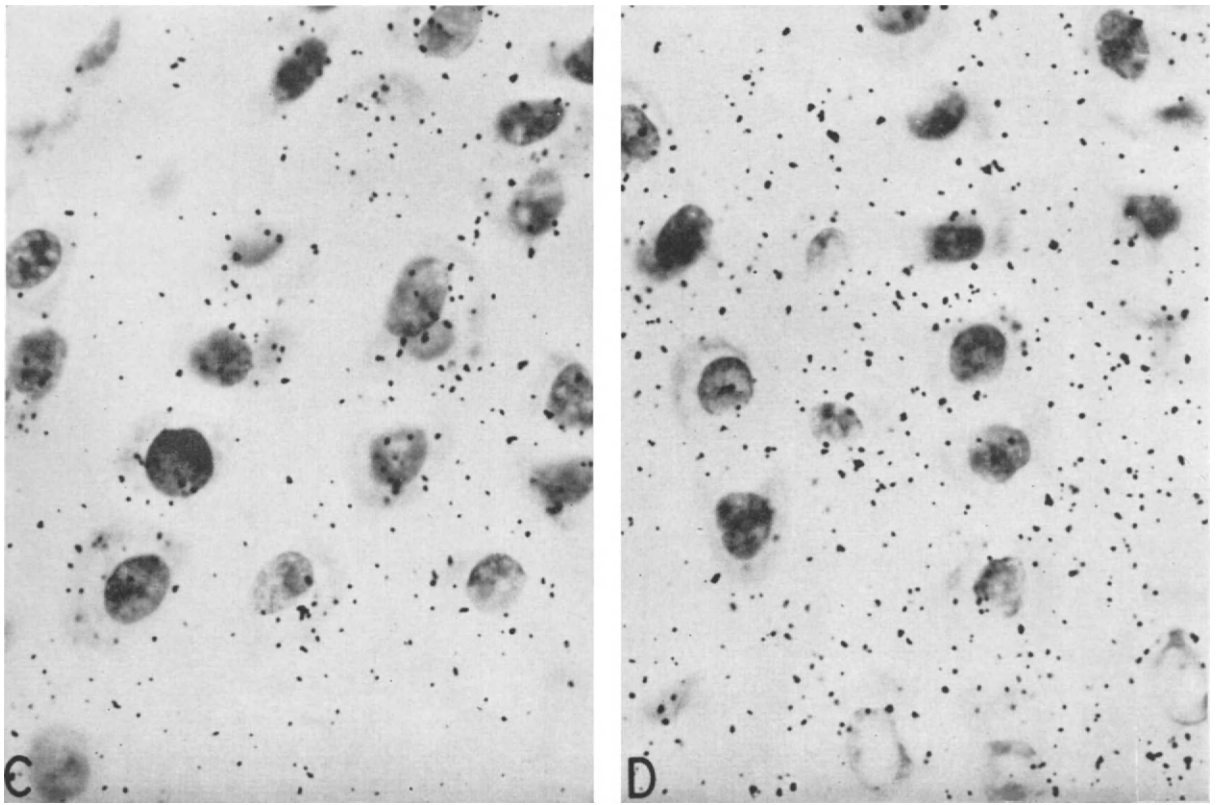

4 hours after administration of ^{3}H-proline. Note the progressive cellular uptake and turnover of label marking newly deposited cartilage matrix. The distribution of the extracellular label is diffuse. Hematoxylin stained. Magnification: × 1000.

similar to that seen in young mice. Their grain counts were lower and the peak labeling time was maintained at 30 minutes, whereas peak labeling of other skeletal cells of older mice occurred at about 4 hours (Fig. 7).

Reduced protein synthetic activity was observed in adult mice at the perichondrial zones of the periosteum and subepiphyseal foci. These foci

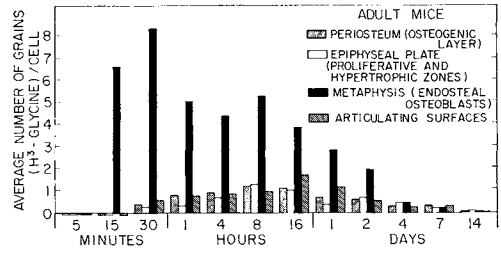

FIG. 6. A histogram illustrating the uptake and turnover of ^{3}H-glycine by various femoral cell populations in 52-week-old mice. Assessment is made by autoradiographic grain counting. Note particularly the remarkable difference between metaphyseal osteoblasts and other cell populations at this age. Compare with the histogram of 5-week-old rats (Fig. 3).

represent the remaining vestiges of metaphyseal activity during closure of the epiphyseal plate. Labeling of skeletal cells was generally weak in older animals, largely due to plate closure. No significant labeling of the epiphyseal plate was observed with ^{3}H-histidine. Matrical bands of silver grains which are always seen over bone matrices of young mice after ^{3}H-glycine and ^{3}H-proline administration were not seen in older mice except for an occasional short line at the subepiphyseal region of the metaphysis.

Variations in Turnover During the Life-Span of the Mouse

Although injected amino acids may be converted to other amino acids or used for the synthesis of a large variety of molecules, for our purpose their utilization by skeletal cells can be considered twofold: amino acids are utilized (1) in protoplasmic synthesis and (2) in the manufacture of the matrical proteins collagen and mucopolysaccharide–protein. In order to gain insight into the collagen turnover of amino acids, the number of autoradiographic silver grains which appeared over skeletal cells following ^{3}H-amino acid administration was counted over a number of time periods. The data were used in a manner analogous to the use of radioactivity data in an analysis of a mixture of two independently decaying radioisotopes. Protoplasmic synthetic activity and matrical protein precursor synthetic activity were considered the two components of

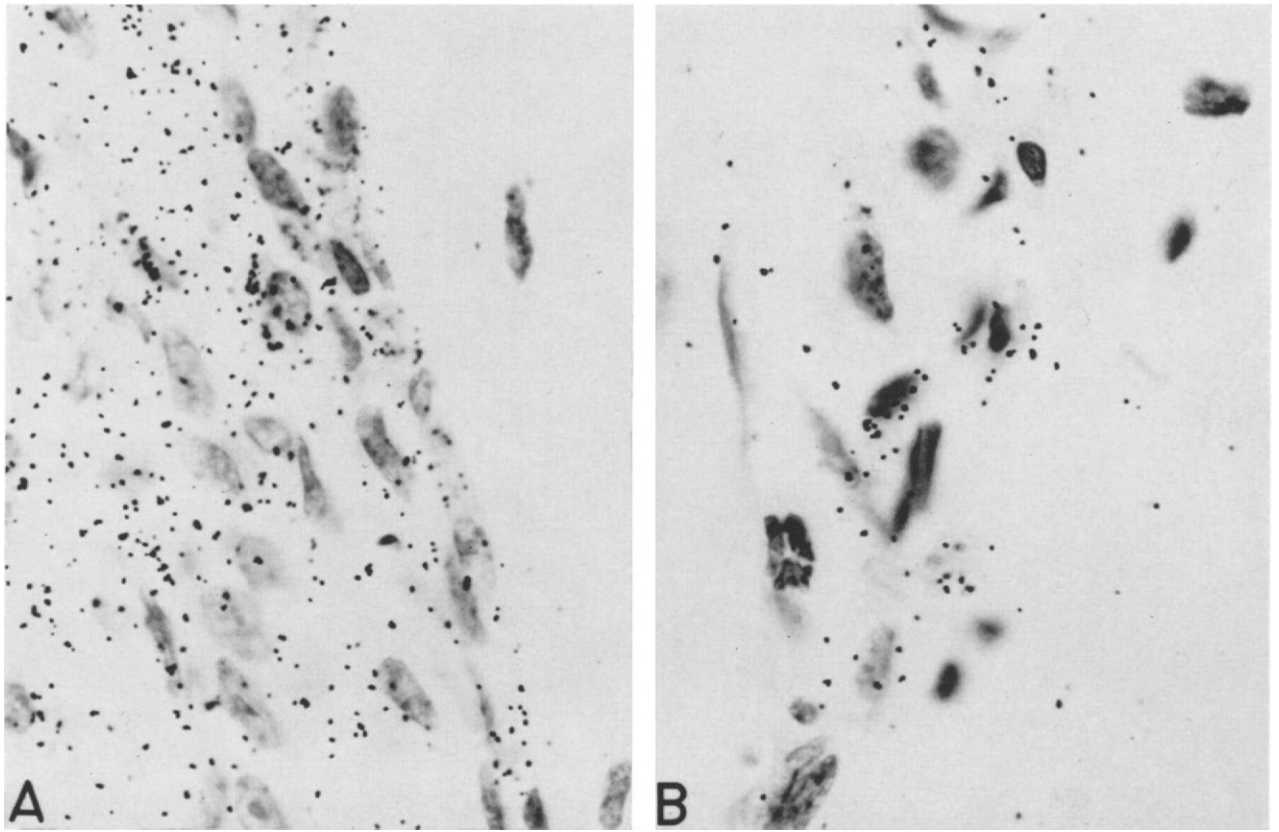

FIG. 7. Autoradiographs of femoral periosteum (perichondrial zones) showing peak labeling at (A) 30 minutes and (B) 1 hour after ^{3}H-proline administration in mice (A) 5 weeks and (B) 52 weeks of age. Hematoxylin stained. Magnification: × 1000.

the mixture. The total activity A of the mixture consists of the sum of the activities of the individual components A_1 and A_2. Similarly, the protein synthetic activity A is the sum of the protoplasmic synthetic activity of the cell A_1 and the manufacture of matrical protein precursors A_2. Since, autoradiographically, the activity is assesed by counting the numbers of grains over cells,

$$A = A_1 + A_2$$

Assuming that turnover results in exponential decay for A_1 and A_2,

$$A_1 = A_1{}^0\ e^{-\lambda t} \text{ and } A_2 = A_2{}^0\ e^{-\lambda t}$$

where A^0 is taken as the peak grain count at a given time $t = 0$, and λ is the turnover constant. Therefore, the cellular activity at $t > 0$ is given as

$$A_t = A_1{}^0\ e^{-\lambda_1 t} + A_2{}^0\ e^{-\lambda_2 t}$$

Contributions by the individual components of the mixture are revealed by semilogarithmic plotting of the average grain counts observed over a given cell population against time.

Following semilogarithmic plotting and curve analysis of the ^{3}H-glycine grain count data of young mice, reasonably good two exponential curve component systems were obtained (Table II). In each cell population the fast component in hours represents turnover of matrical proteins, whereas the slow component in days represents turnover of protoplasmic proteins. The turnover time of the latter is no doubt extended by some degree of reutilization. It is interesting to note that the turnover rate of matrical proteins appears to be quite similar for all skeletal cell types except for metaphyseal osteoblasts. However, this may also be true for these cells, if it were not for the increased availability time which they enjoy. In any event, similar turnover times do not imply that the same total amount of protein material was actually turned over during the growth period, since the availability of the label and duration of cell activity vary.

In a similar curve analysis of the grain count data of older mice (Table II), a straightening out of the curves was revealed with a suppression of the two-component feature observed in young mice. This is probably not true for metaphyseal endosteal osteoblasts of older mice, since they maintain an elevated amino acid uptake and turnover activity in comparison to other cell types.

It is interesting to state that these crude data show that protein turnover times vary substantially between young and old mice, and that the turnover rate of structural protoplasmic proteins is less sensitive to changes in metabolic function and age than is the turnover rate of amino acids utilized in matrical protein precursor formation.

TABLE II. *Approximate Half-times of First and Second Curve Components Obtained from Semilogarithmic Plots of the Average Grain Counts of Young and Adult Mouse Skeletal Tissues versus Time*

Curve components	Age	Metaphysis	Epiphysis	Periosteum	Articular cartilage
1st (hours)	Young	2.5	4.0	4.0	3.5
	Adult	2.5	7.0	6.0	7.0
2nd (days)	Young	2.5	2.9	3.2	5.2
	Adult	1.6	3.8	3.3	3.2

Assessment of the Proteosynthetic Potential

The levels of protein synthetic activity observed in normal bones reflect only the growth, development, and remodeling demands placed upon cells during a given time period. The addition of the parameter of aging revealed a diminution in the protein synthetic activity with increasing time. In order to understand the protein synthetic activity of skeletal cell populations more fully, data must be obtained which reveal not only their degree of participation in protein synthesis at any given time, but their ability to respond to emergency situations. In keeping with this concept a number of important questions need serious consideration, namely: When skeletal cells synthesize matrical proteins, is the synthetic process operating at maximum capacity? Does the reduction in the protein synthetic activity of skeletal cells with increasing age imply that the cells are any less capable of participating in protein synthesis if the need should arise? Is the post-trauma reactivation of the process of proliferation in the periosteum of old mice accompanied by reactivation of protein synthesis in regions far removed from the site of trauma?

In an attempt to answer these questions the left femora of 12 mice, 5 and 52 weeks of age, were fractured at midshaft. Five days later the mice were given a subcutaneous injection of ^{3}H-glycine or ^{3}H-histidine. On the sixth day, the mice were sacrificed and the hind limbs were removed and processed for autoradiography. Details of the process have been stated in the materials and methods section of this article.

^{3}H-glycine autoradiographs of young mice showed active protein synthesis occurring throughout the fracture site and elsewhere. Although most of the grains were observed over extracellular regions of the tissue 6 days after fracture, some sparsely labeled cells were still seen. The matrices of the cartilaginous and prechondrogenic portions of the fracture callus were heavily but diffusely labeled. At the periphery of the callus, silver bands appeared over active sites of trabecular bone formation. On studying the periosteal and endosteal surfaces of the shaft from the fractured ends to the limits of the perichondrial regions the following was observed: silver grains were not present over cortical bone below the active cartilaginous callus. Grains were noted at the region of trabecular bone formation. Beyond the periphery of the callus, the activity of both the periosteum and endosteum was similar to that observed in the unfractured femora described earlier in this article. The fracture did not appear to disturb significantly the protein synthetic process normally taking place in regions away from the fracture site.

^{3}H-glycine autoradiographs of 52-week-old mice also revealed very active protein synthesis throughout the fracture site. The distribution of grains was similar to that described over the fractures of 5-week-old mice, but with the important exception of the periosteal and endosteal activity. As described earlier, normal femora of 52-week-old mice exhibited at best a weak periosteal and endosteal protein synthetic activity. The activity was moderate only at the perichondrial zones of the periosteum and in some scattered endosteal foci where some trabecular or subcortical remodeling activity remained. In the fractured femora, however, active protein synthesis was observed along the entire length of the periosteum except for the perichondrial regions. Definitive silver bands were seen over a layer of new bone recently deposited on both the anterior and posterior cortical surfaces of the shaft (Fig. 8). The rapidity with which this new layer of bone is deposited is remarkable, since it would take 4 to 5 days for the nontraumatized femoral periosteum of 5-week-old mice to form the amount deposited within 1 day in 52-week-old mice at sites distant from the fracture callus (compare Fig. 8B with Fig. 10C). Endosteal activity was also stimulated in certain regions, but to a much lower degree. The epiphyseal plate and articular cartilage were not disturbed by midshaft fractures. Examination of the intact tibias within the same slides showed no stimulation of periosteal protein synthetic activity. Stimulation of protein synthesis was limited to the traumatized bone.

These results are in agreement with and complement studies reported earlier on the behavior of periosteal cells following trauma [24, 28, 30]. It was shown that 32 hours after fracture periosteal cell proliferation was stimulated from 3 to 25 per cent in 5-week-old mice [28]. Respiratory enzyme activity of the periosteum, however, could not be elevated appreciably following femoral trauma at 5 weeks of age [24]. Apparently the cells were respiring at a near maximum level. The ^{3}H-glycine results showed that the protein synthetic activity was not appreciably enhanced in the periosteum following stimulation of cell proliferation. The level of protein synthetic activity of the cells at the fracture does not appear to differ from the level seen elsewhere in the periosteum. Thus, it would appear that protein synthetic activity of osteogenic cells of the periosteum at 5 weeks of age is at or near maximum capacity and proceeds largely undisturbed following trauma.

In 52-week-old mice cell proliferation was stimulated in fractured femora from a level of 0.3 to 10.5 per cent in the periosteum away from the fracture site [30]. Respiratory enzyme levels were also shown to increase [24]. ^{3}H-glycine results showed stimulation of active protein

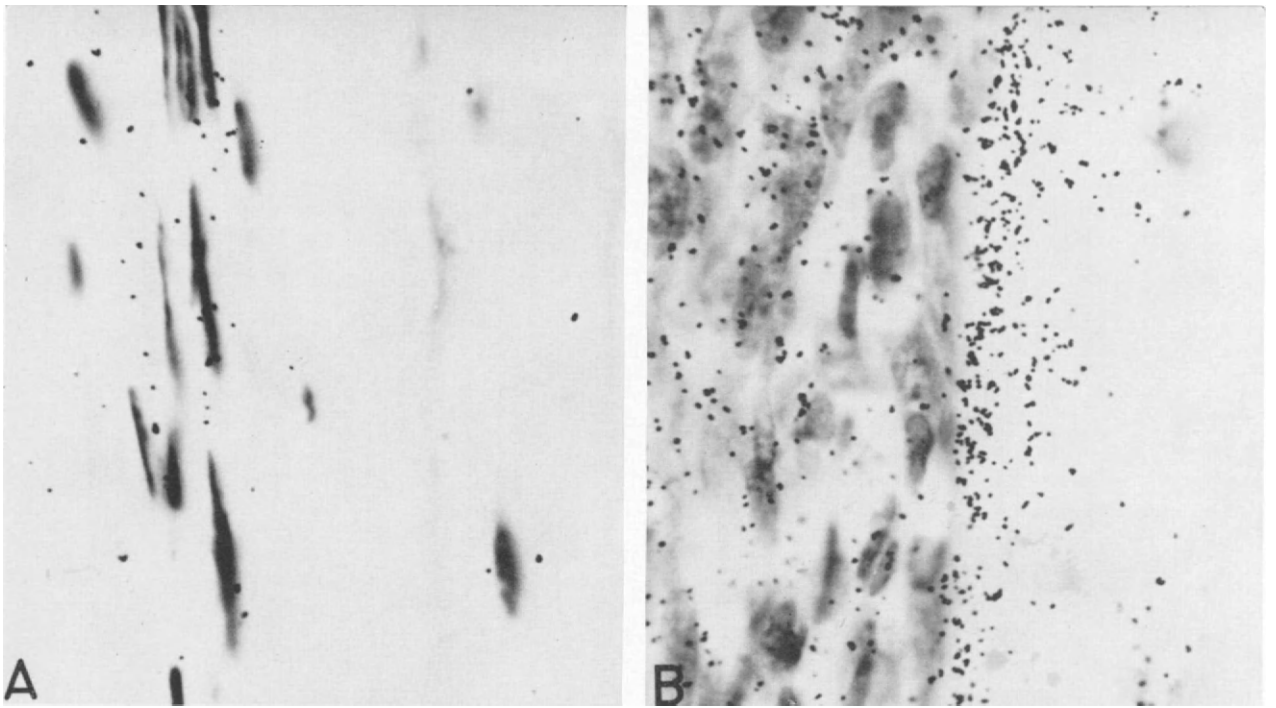

FIG. 8. Autoradiographs were made from the periosteum of a 1-year-old mouse whose left femur was fractured 6 days earlier and on the fifth day ^{3}H-glycine was administered. A shows the uptake seen at the unfractured right femur. B (a comparable site with A) shows the thickened osteogenic layer of the periosteum following stimulation of cell proliferation and the deposition of a layer of new bone matrix. Note that the initial deposition of label is scanty (farthest point away from periosteum) and within a short time an intense band is formed. This is probably due to the rapidity with which new bone was laid down. Under normal conditions of growth in 5-week-old mice it would have taken about 4 to 5 days to produce what appears in 1-year-old mice within 1 day following fracture. The periosteal site selected in B is a considerable distance away from the future callus. Hematoxylin stained. Magnification: × 1000.

synthesis at the fracture site and periosteum at 52 weeks of age. Reduced demands for growth at 52 weeks of age and the degree of cellular aging accumulated during life did not eliminate nor diminish the capacity of cells for protein synthetic activity. However, autoradiographs showed that the uptake of label by periosteal cells of fractured femora did not differ from the uptake of the unfractured controls. Protein synthesis was not activated in old-looking, spindle-shaped periosteal cells of 52-week-old mice. Active protein synthesis was associated with the newly generated cell population following stimulation of cell proliferation. Apparently, the protein synthetic processes cannot be directly stimulated in the old periosteal cells as a result of trauma. At this time the morphological and biochemical effects of cellular aging are evident, but these cells have not lost their capacity to divide and are capable of regenerating new revitalized populations of bone and cartilage cells following trauma, which in all respects appear similar to these newly generated skeletal cells and will continue at the fracture site until the demands for repair are fulfilled. It was shown in a previous study that away from the fracture site stimulation of cell proliferation in the periosteum of both young and older mice diminished, so that by the fourth or fifth day the normal nontraumatized levels were again reached [30]. Protein synthesis stimulated in this region also continues for a limited time only.

^{3}H-histidine autoradiographs revealed a picture similar to that found with ^{3}H-glycine and ^{3}H-proline, but the events were not as dramatic.

Micrometric Analysis

In a study of bones and teeth using ^{3}H-glycine, Carneiro and Leblond [6] observed that the presence of labeled material in newly deposited bone matrix appeared as discrete bands of silver grains in autoradiographs. Tonna *et al.* [32] charted the course of these autoradiographic silver bands in the femora of growing mice. It was shown that the activity of the periosteum and endosteum varied considerably depending on the region of the femur with which they were associated. By and large, active protein synthesis by cells of the periosteum was observed at the proximal half of the femur while the cells of the endosteum were actively synthesizing protein in the distal half of the femur. Several silver bands which appeared at one surface of the femoral shaft at about 30 minutes after ^{3}H-glycine administration were observed to cross the entire thickness of the shaft by the seventh and fourteenth day. This is clearly illustrated by the endosteal bands in Fig. 9. It is also of interest to note that, although initially silver bands appeared almost simultaneously along a given bone surface, their rate of progression toward the opposite surface of the shaft differed. Significant differences were

noted in the rate of progression along the length of any given band. The proximal periosteal bands showed greater protein synthetic activity at their center and a gradual diminution as one moved away from the center. The distal endosteal bands showed increasing activity along their length as one moved more distally (Fig. 9).

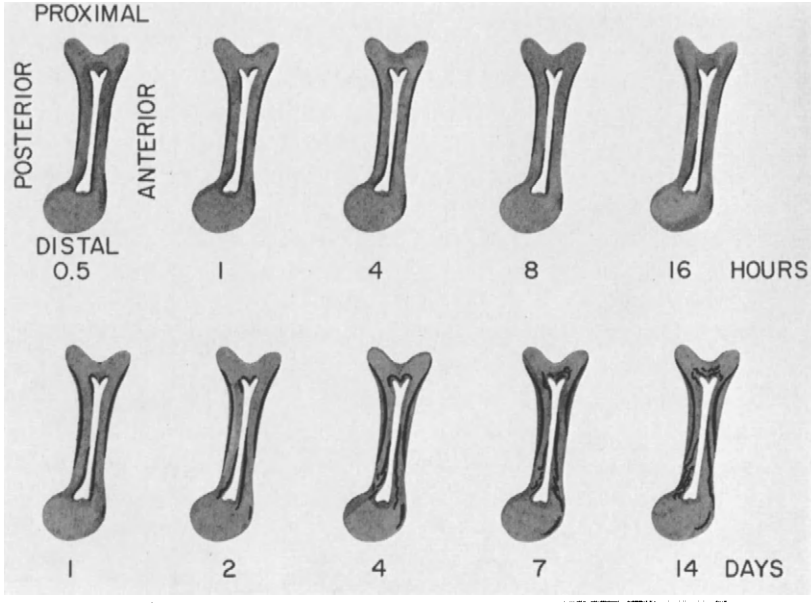

FIG. 9. The incorporation of label as seen in autoradiograms of 5-week-old mouse femora is illustrated diagrammatically as new bone is deposited from 30 minutes to 14 days after ^{3}H-glycine administration. Note the largely periosteal activity at the proximal end and the endosteal activity at the distal end at this age (taken from [32]).

In order to evaluate the differences in protein synthetic activity of the femoral bone surfaces, a filar micrometer was used to measure the progressively larger distance existing between the leading edge of the silver band and the original surface of deposition with time following ^{3}H-glycine administration (Fig. 10). It must be remembered that, since the protein synthetic activity reflected by any given silver band varies widely along its length, the values shown in Table III represent only average activity values. In addition, the band shapes differ in the same animal from one bone to the next and in animals of different ages and species.

With respect to the daily rate of protein synthesis over a 14-day observation period, the values appeared to vary with the growth pressures

TABLE III. *Micrometric Analysis of the Autoradiographic Movement of Silver Grains Deposited Over the Femora of Young Mice Following ^{3}H-Glycine Administration*[a]

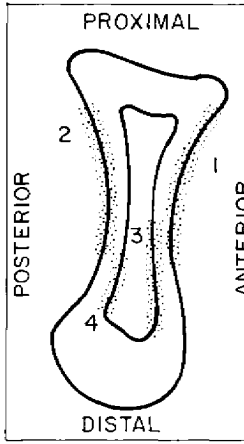

Region Analyzed	HOURS					DAYS					Average Daily Rate Over 14 d Period (μ/d)
	0.5	1	4	8	16	1	2	4	7	14	
1	1.8	3.9	2.7	2.4	4.7	6.9	12.9	19.8	35.6	46.3	3.3
2	1.4	2.9	3.2	4.3	5.2	11.9	20.2	35.5	45.3	88.8	6.3
3	1.9	3.0	3.8	4.7	6.8	6.5	12.8	15.7	32.2	96.1	6.9
4	1.7	2.4	3.7	5.1	5.6	6.1	10.5	15.2	29.9	48.0	3.4
Average	1.7	3.1	3.3	4.1	5.6	7.9	14.1	21.6	36.4	69.8	5.0

[a] Each value (μ) represents an average of 25 measurements made along each specific region with a filar micrometer.

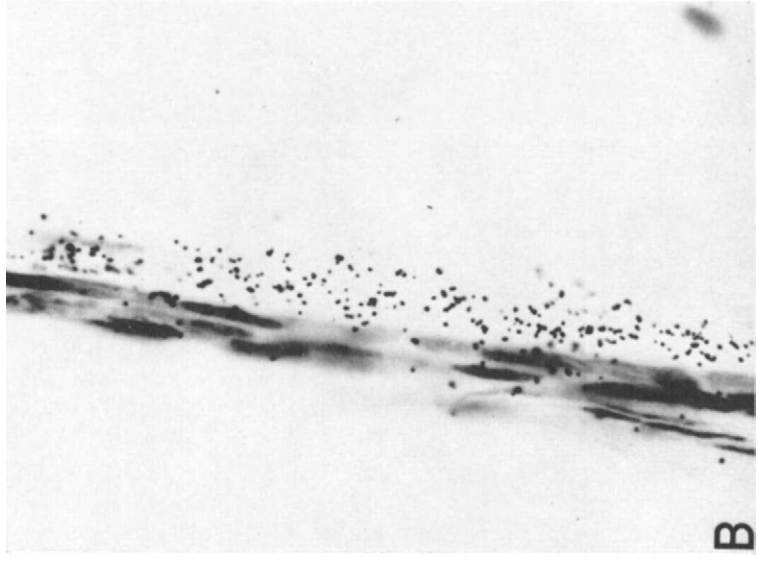
B

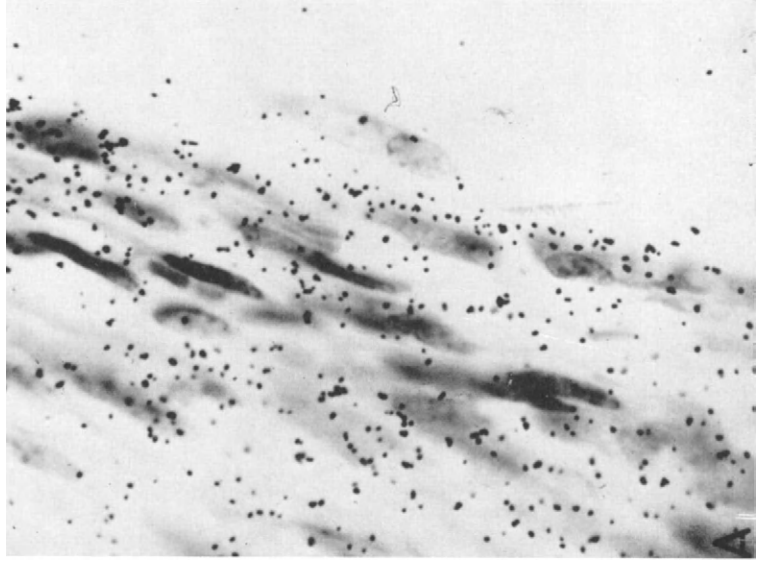
A

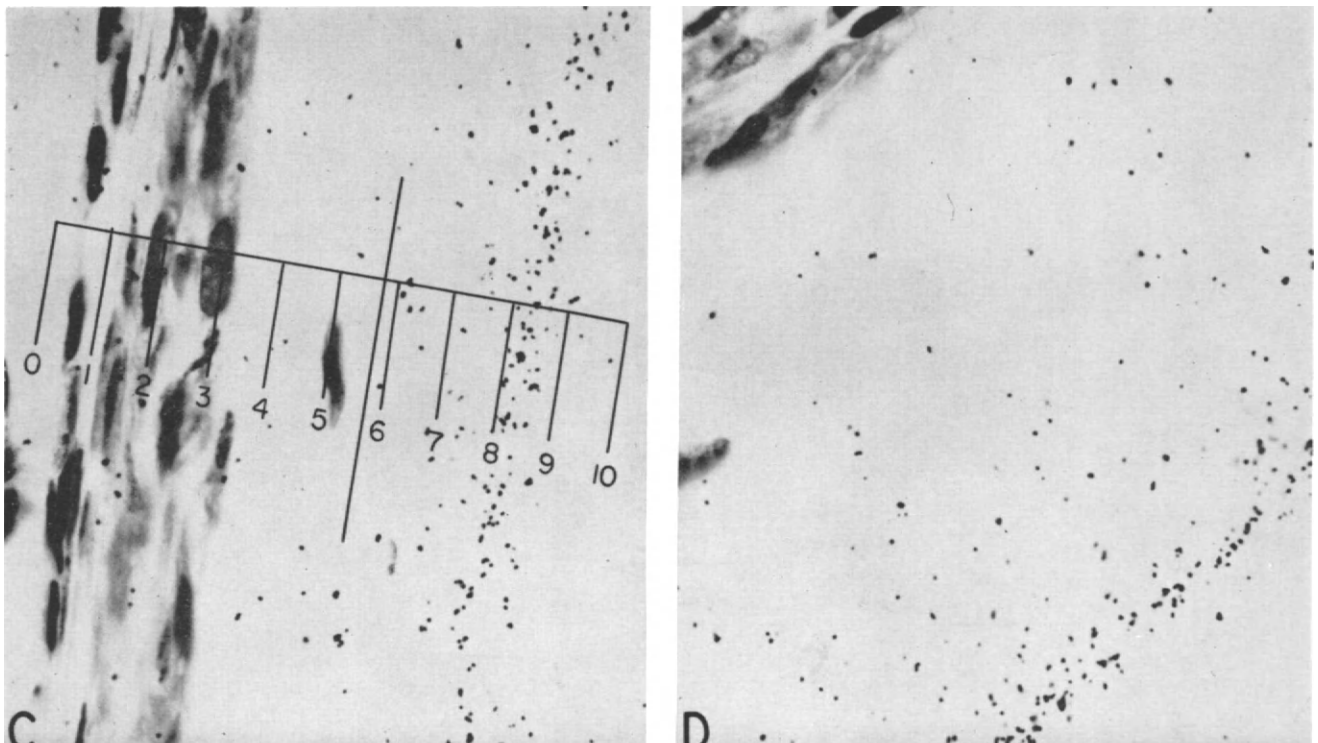

FIG. 10. An autoradiographic series showing, in the femora of 5-week-old mice, the continued periosteal deposition of new cortical bone as evidenced by the band of silver grains formed after (A) 1 hour, (B) 1 day, (C) 7 days, and (D) 14 days after ^{3}H-glycine administration. A filar micrometer (used in the analyses) is pictured in C. The vertical line is movable along the horizontal scale. Hematoxylin stained. Magnification: × 1000.

existing along the skeletal surfaces from one period of growth to the next. The proximal anterior periosteal band and distal posterior endosteal band exhibited similar average daily rates of protein synthesis (3.3 and 3.4 μ/day). The proximal posterior periosteal and distal anterior endosteal bands were double these values, but similar to each other (6.3 and 6.9 μ/day).

^{3}H-proline autoradiographs revealed comparable events. Histidine, which constitutes only 2 in 419 amino acid residues in the collagen polymer, did not produce discrete silver bands, but the distribution of the matrical label was not unlike the other amino acids.

Availability and Reutilization of ^{3}H-Amino Acids

Injected amino acids reach cells and are incorporated intracellularly with unbelievable speed. Borsook *et al.* [1] showed that 2-^{14}C-imidzole-L-histidine injected intravenously in mice had nearly all disappeared from circulation within less than 10 minutes. Within 40 minutes 18 to 47 per cent of the injected histidine was incorporated into visceral proteins. Autoradiographs of adult frog tissues previously injected intraperitoneally with ^{14}C-glycine revealed labeled cells within 5 minutes [13]. Labeled bone and cartilage cells were also seen as early as 5 minutes in autoradiographs of mouse tissues previously injected subcutaneously with ^{3}H-glycine [32] and ^{3}H-proline [26]. Labeled cells can probably be detected earlier than 5 minutes after ^{3}H-amino acid administration.

The rapidity with which injected ^{3}H-amino acids become available to cells, by whatever route, introduces a parameter of significant import into the interpretation of autoradiographs. This point is well illustrated in Figs. 3 to 6. Certain cell types, e.g., endosteal osteoblasts, revealed the accumulation of larger grain counts than other cell types prior to peak labeling. This was observed in both young and adult mice. It is entirely possible that these variations were due in a significant part to differences in vascularization of the tissues, which vary the availability time. In addition, evidence exists to indicate that endosteal osteoblasts turn over larger total amounts of material, exhibiting a shorter half-time (Table II). The degree to which each parameter contributed to the observations is unknown. On this basis, the grain count data are representative of a complex set of circumstances rather than a simple uptake phenomenon. Therefore, comparisons between the data of different cell types or between cells from animals of different ages, must be made only with the greatest caution.

Another difficulty exists when comparing grain count data obtained from animals of widely different ages. This difficulty has its basis in the likely possibility that the pool size for the particular ^{3}H-amino acid

injected differs in young and old animals. Since ^{3}H-amino acids are generally administered to animals in μc/gm body weight, changes in the "specific activity" alter the base line for comparison. Unfortunately, the body pool size for any given amino acid in animals of different ages is not as yet available. Therefore, this parameter must be kept in mind when comparing data of animals of different ages.

Reutilization of previously injected ^{3}H-amino acids is still another factor which adds to the complexity of the interpretation of the results. Significant amounts of ^{3}H-thymidine available through the breakdown of lymphocytes and necrotized liver cells is known to be reutilized by different cell types [2, 3, 4, 9]. No doubt reutilization also occurs following ^{3}H-amino acid administration, and to a significant degree. Cortical bone serves as an excellent medium for the autoradiographic assessment of the degree of reutilization by cells of the skeletal system. It was noted that, during the continuous deposition of matrical proteins, the autoradiographs initially revealed an intense band of silver grains which appeared to progress away from the cells as new matrix was deposited. These silver bands consisted of a dense population of grains with a sharply delineated leading edge and an after "trail" of grains showing a decreasing population density (Fig. 11). Micrometric analysis showed that the initial dense bands have a width of $\sim$ 9.5 μ, and grain trails of $\sim$ 28.5 μ. Approximately 2 days are required to produce the dense band and 6 to 8 additional days for the trail. Since the uptake of injected labeled amino acids occurs in minutes while the bulk of matrical proteins is turned over in hours, the continued turnover of labeled matrix reflects reutilization.

It can be seen from Table IV that the number of grains appearing

TABLE IV. *Average Micrometric and Grain Count Analyses of the Matrical Silver Bands Appearing in Autoradiographs over Mouse Femoral Cortex 14 Days After ^{3}H-Amino Acid Administration*[a,b]

Areas studied	Width of region (μ)	^{3}H-Glycine	^{3}H-Proline
Region A[c]	$\sim$ 9.5	19.3	34.4
Region B[d]	$\sim$ 28.5	9.0	11.5
Regions A + B	$\sim$ 38.0	28.3	45.9
A + B/B	—	31%	40%

[a] Mice 5 weeks old.

[b] Each value represents 25 measurements. The width was obtained with a filar micrometer. The grain counts were made with a reticle having two parallel lines equal in distance to the length of the cell responsible for the portion of the band being analyzed.

[c] The densely populated band initially deposited.

[d] The sparsely populated "trail" of silver grains following the initial band.

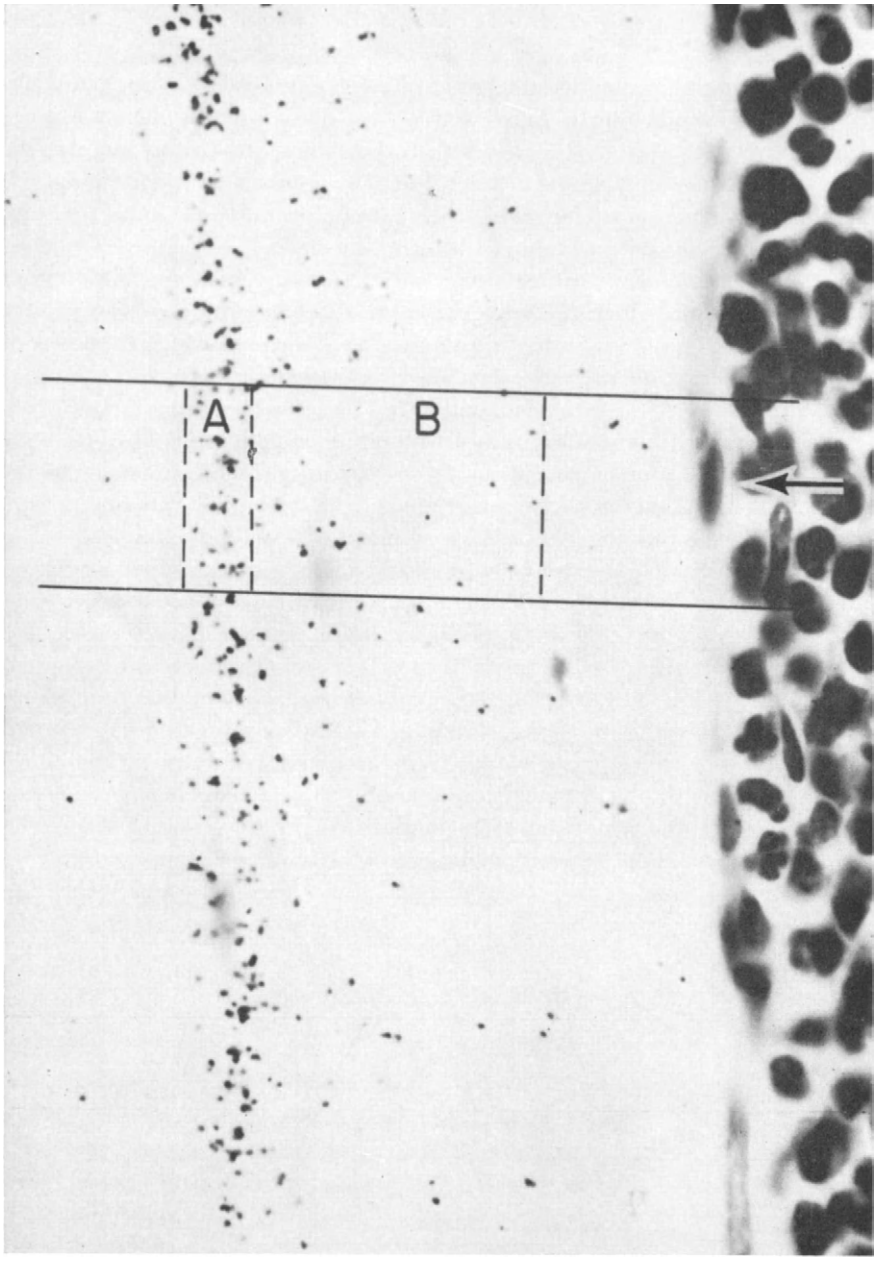

FIG. 11. The autoradiograph of a 5-week-old mouse femur 14 days after ^{3}H-proline administration illustrating endosteal bone formation evidenced by the overlying silver grains. A and B represent rectangles of matrix laid down by a single endosteal osteoblast (arrow). A shows the initial band and B the "trail" resulting from reutilization of ^{3}H-proline. Hematoxylin stained. Magnification: × 1000.

over the matrix is several times larger than the peak grain counts obtained over cells ($\sim$ 10 grains/cell for ^{3}H-glycine and $\sim$ 4 grains/cell for ^{3}H-proline 30 minutes after administration of ^{3}H-amino acid). Furthermore, the grain numbers found in the trail of the dense bands constitute a significant portion of the total number of grains turned over. It seems obvious, therefore, that an investigator must exercise prudence in drawing conclusions based on autoradiographic grain count data.

GENERAL CONCLUSIONS

Earlier reports of autoradiographic studies of the skeletal system using ^{3}H-amino acids [6, 18, 25, 26, 29, 31, 32, 33] and the present results showed that injected amino acids were first utilized by cells for protoplasmic needs and the manufacture of matrical protein precursors. Uptake of amino acids was extremely rapid at all ages studied and already evident within 5 minutes of amino acid administration. Initial turnover and peak labeling of cells was noted at about 30 minutes in young mice. In older mice, except for metaphyseal endosteal osteoblasts, peak labeling was not observed until about 4 hours after administration of ^{3}H-amino acids. Cellular labeling diminished with time, so that by 4 hours in young and somewhat longer in older mice, few grains were seen over cells. Turnover of label, however, did not terminate abruptly after the release of the initial pulse of injected amino acid, because of the reutilization of the continued supply of labeled products from the breakdown of cells and cellular components of other tissues. Reutilization was detected in autoradiographs for about 6 to 8 days after administration of labeled amino acids. The evidence was recorded in autoradiographs by the presence of a "trail" of silver grains over cortical bone.

Significant variations in uptake and turnover were seen in different skeletal cells at all ages; the absolute differences, however, are believed to be masked by the availability, reutilization, and dilution of injected labeled amino acids. Distribution patterns of silver grains in animals of different age were similar for ^{3}H-histidine, -glycine, and -proline. The intensity of the markers differed, however, because of the differences in specific activity, in autoradiographic exposure time, the number of histidine, glycine, and proline molecules used in the synthesis of a given matrical protein, and varied metabolic patterns.

Endosteal osteogenic cells revealed the highest protein synthetic activity followed by cartilage cells of the epiphyseal plate, osteogenic cells of the periosteum, and cartilage cells of the articular surfaces. The distribution of label in cartilage matrix was diffuse, while in trabecular and cortical bone it appeared in discrete bands. As additional matrix was

formed, the cartilage label appeared lower down the epiphyseal disc and finally within the cartilage cores of developing metaphyseal trabeculae. Similarly, trabecular and cortical bands of label appeared farther away from the cell source. Because of longitudinal growth, the trabecular bands were also seen lower down the metaphysis with increasing time. A distinctive pattern of protein synthesis was seen along the periosteal and endosteal surfaces of bone, which accounted for the familiar growth and remodeling dynamics of the skeleton. The periosteal surfaces were active at the proximal half of the mouse femur and the endosteal surfaces were active at the distal portion in young mice. The proximal anterior periosteal band and distal posterior endosteal band exhibited similar average daily rates of protein synthesis, whereas the proximal posterior periosteal and distal anterior endosteal bands revealed double the activity. If the different rates of daily synthesis are pooled, approximately 5 μ of cortical bone is deposited per day over a 14-day period in the femora of 5-week-old mice.

With respect to variations in protein synthesis with age, a significant reduction in activity was seen following cessation of bone formation and growth. With increasing time, however, the activity diminished further as the effects of aging accumulated. It is of significant interest to note that active protein synthesis is apparently not a capacity of old periosteal cells, even when traumatized. However, the capacity for cell proliferation remains [30] and, following trauma, activation of periosteal cell proliferation results in the formation of a rejuvenated population of both bone and cartilage cells capable of intense protein synthetic activity at the site of trauma and along the entire shaft.

Application of isotope methodology and autoradiography has proved to be of great utility in expanding our knowledge of understanding of the dynamic behavior and potentialities of the skeletal system within the last decade. The use of tritiated amino acids has focused our attention on protein synthesis and furnished us with several bonuses, namely: (1) a better understanding of skeletal growth and remodeling phenomena, (2) an appreciation and assessment of varying cellular potentialities in different kinds of skeletal cell populations, (3) insight into the gerontological aspects of skeletal physiology, and (4) an assessment of the magnitude of the reutilization phenomenon.

Although autoradiographic methods and their application are simple enough, they are not without limitations and pitfalls. Those difficulties which are inherent in the autoradiographic technique itself are well known and need not be reiterated. However, difficulties which arise from the complex nature of the biological system and which place a serious limitation on the interpretation and full assessment of our data are not

well known. Needless to say, our understanding of protein synthesis and its ramifications through the application of autoradiographic methods will be limited so long as our knowledge of availability, reutilization, and variations with age in amino acid pool size are limited.

Since variation is a natural attribute of living things, comparative autoradiographic analysis will remain at best semiquantitative, for want of an absolute baseline.

SUMMARY

A series of autoradiographic studies of the femora of mice 5 to 52 weeks of age using ^{3}H-glycine, ^{3}H-proline, ^{3}H-histidine were described. These studies included the assessment of cellular uptake, utilization, and turnover of ^{3}H-amino acids in matrical protein precursor formation. Four skeletal cell populations were compared, namely: those of the osteogenic layer of the periosteum, metaphyseal–endosteal–osteoblasts, and cartilage cells of the epiphyseal plate and articular surfaces. Fracture studies were described in an attempt to assess the protein synthetic potential of cells at different ages. Micrometric measurements were also made to determine the protein synthetic activity present at various bone surfaces. In addition, the degree of ^{3}H-amino acid reutilization was estimated from the autoradiographs.

Acknowlegments

The author wishes to thank Miss M. Pavelec for her fine technical assistance and Mr. R. F. Smith, for the photomicrography.

References

1. Borsook, H., Deasy, C. L., Haagen-Smith, A. J., Keighley, G., and Lowy, P. H., *J. Biol. Chem.* 187, 839 (1950).
2. Bryant, B. J., *Exptl. Cell Res.* **27**, 70 (1961).
3. Bryant, B. J., *Exptl. Cell Res.* **32**, 209 (1963).
4. Bryant, B. J., *J. Cell Biol.* 18, 515 (1963).
5. Campo, R. D., and Dziewiatkowski, D. D., *J. Biol. Chem.* **273**, 2729 (1962).
6. Carniero, J., and Leblond, C. P., *Exptl. Cell Res.* 18, 291 (1959).
7. Eastoe, J. E., *in* "The Biochemistry and Physiology of Bone" (G. H. Bourne, ed.), Chapter IV, p. 81. Academic Press, New York, 1956.
8. Eastoe, J. E., and Leach, A. A., *in* "Recent Advances in Gelatin and Glue Research" (G. Stainsby, ed.), p. 173. Pergamon Press, New York, 1958.
9. Fichtelius, K.-E., and Diderholm, H., *Acta Pathol. Microbiol. Scand.* **52**, 11 (1962).
10. Fitton Jackson, S., *in* "The Cell" (J. Brachet and A. Mirsky, eds.), Vol. VI, p. 387. Academic Press, New York, 1964.
11. Fruton, J. S., and Simmonds, S., "General Biochemistry," 2nd ed., Chapters 31 and 32, p. 723. Wiley, New York, 1958.
12. Godman, G. C., and Porter, K. R., *J. Biophys. Biochem. Cytol.* 8, 719 (1960).
13. Kemp, N. E., and Hibbard, E., *J. Exptl. Zool.* **145**, 73 (1960).

14. Meyer, K., Hoffman, P., and Linker, A., *Science* **128**, 896 (1958).
15. Neuberger, A., and Slack, H. G. B., *Biochem. J.* **53**, 47 (1953).
16. Piez, K. A., and Likins, R. C., *in* "Calcification in Biological Systems" (R. F. Sognnaes, ed.), p. 411. Amer. Assoc. Advan. Sci., Washington, D.C., Publ. No. 64, 1960.
17. Porter, K., *in* "Symposium on Connective Tissue: Intercellular Macromolecules," p. 167. Little, Brown, Boston, Massachusetts, 1964.
18. Revel, J. P., and Hay, E. D., *Z. Zellforsch.* **61**, 110 (1963).
19. Robinson, R. A., and Cameron, D. A., *Clin. Orthop.* **9**, 16 (1957).
20. Robinson, R. A., and Elliott, S. R., *J. Bone Joint Surg.* **39A**, 167 (1957).
21. Ross, R., and Benditt, E. P., *J. Cell Biol.* **15**, 99 (1962).
22. Rouiller, C., *in* "The Biochemistry and Physiology of Bone" (G. H. Bourne, ed.), p. 107. Academic Press, New York, 1956.
23. Slack, H. G. B., *in* "Nature and Structure of Collagen" (J. T. Randall, ed.), p. 51. Butterworths, London, 1953.
24. Tonna, E. A., *J. Gerontol.* **14**, 159 (1959).
25. Tonna, E. A., *J. Gerontol.* **19**, 198 (1964).
26. Tonna, E. A., Study in progress (1964).
27. Tonna, E. A., *Lab. Invest.* **13**, 1238 (1964).
28. Tonna, E. A., and Cronkite, E. P., *J. Bone Joint Surg.* **43A**, 352 (1961).
29. Tonna, E. A., and Cronkite, E. P., *J. Gerontol.* **17**, 353 (1962).
30. Tonna, E. A., and Cronkite, E. P., *J. Bone Joint Surg.* **44A**, 1557 (1962).
31. Tonna, E. A., Cronkite, E. P., and Pavelec, M., *J. Histochem. Cytochem.* **10**, 601 (1962).
32. Tonna, E. A., Cronkite, E. P., and Pavelec, M., *J. Histochem. Cytochem.* **11**, 720 (1963).
33. Young, R. W., *Anat. Record* **143**, 1 (1962).

Discussion

Dr. Greulich: I would question the significance of measurements of migration rates of labeled bone matrix over long experimental periods. In view of the relatively great increase in bone length of the 5-week-old mouse during the 14-day-period of experimental observation, how significant are data which suggest twofold differences in migration rates of labeled matrix in discrete areas of bone? The data indicate a comparable rate over a 16-hour period.

Dr. Tonna: The units refer to analysis of specific, comparable regions only. In an attempt to produce some constancy in the analytical method, only the regions of maximum activity were examined. Obviously, if one were to move away from these regions, different values would be obtained.

Dr. Leblond: The bands observed in the matrix of bones after injection of labeled amino acids are identical to those occurring after injection of organic matrix precursors other than amino acids, as described with Greulich after injection of ^{14}C-bicarbonate (see Bourne, G., "The Biochemistry and Physiology of Bone," p. 325, Academic Press, New York, 1956). In fact, these bands behave in the same manner as the bands due to labeled bone salts, as observed in undecalcified sections after injection of ^{32}P-phosphate (with G. W. Wilkinson, L. F. Bélanger, and J. Robichon, *Am. J. Anat.* 1950, **86**, 289).

Dr. Bélanger: The curved radioautographic band observed in rat diaphysis by Dr. Tonna differs from the straight band depicted in other investigations (*Am. J. Anat.* 1950, **86**, 289). Is this due to age differences? In young rats (10 gm), it ap-

pears that the mid-diaphyseal osteoblasts are more differentiated and perhaps better equipped for manufacturing protein.

DR. TONNA: I am not sure that osteoblasts at mid-shaft differ in activity from those elsewhere, although such differences might provide an explanation for the curved pattern. It is indeed true that there are differences in the shape and extension of the bands at different ages. Variations in band shapes can also be demonstrated from one bone to the next in the same animal, or by differences in the plane of sectioning.

DR. LEBLOND: Like Dr. Tonna, we have observed that the bone matrix deposited immediately after injection is intensely labeled, while that deposited during the next few days is also labeled, though only to a moderate extent, thus constituting in radioautographs what Dr. Tonna has aptly called "trail." This trail is probably due to the fact that some of the labeled precursors taken up in other tissues may be gradually released and then utilized in the region under study.

The trail may be conveniently reduced by shortening the exposure time. We have also tried to do so by administering a chaser, that is, fairly large doses of unlabeled amino acid within a short time after injection of the labeled one; but this procedure has not been as successful as we had hoped in getting rid of the trail.

DR. PELC: A chaser frequently does not work in living animals because of the pools in the organism and because the chaser is rapidly converted to a different substance, e.g., by phosphorylation. If the concentration of a chaser is high enough to be effective, it is likely to be physiologically dangerous.

DR. FITZGERALD: Is your reactivation of protein synthesis at a distance from the site of fracture the result of an increase of vascularity, a locally diffusing "wound hormone," or some other triggering mechanism?

DR. TONNA: The effects do not seem to be due to increased vascularity since the changes occur within 12 hours. I do not know the cause of this reactivation, but it could be due to a number of interrelated complex parameters such as change in O_2/CO_2 ratios, changes in pH, etc.

SYNTHESIS AND TURNOVER OF COLLAGEN IN PERIODONTAL TISSUES

J. CARNEIRO[1]

Laboratory for Cell Physiology, Faculdade de Medicina, São Paulo University, São Paulo, Brazil

INTRODUCTION

Even if it is not possible here to review the extensive literature on collagen formation, a few remarks seem appropriate. In the past, several theories have been proposed to explain the origin of collagen fibers. Some histologists believed that the fibers were a product of the intercellular milieu arising under the influence of enzymes released by fibroblasts, while others felt that the fibers were formed within the cells and then released to the outside [21]. A third hypothesis was that the fibers arise in the extracellular spaces, but as a condensation of material secreted by the cells [8].

This last hypothesis received considerable support when radioautographic evidence indicated that the protein collagen arises within the cell cytoplasm, but is promptly released to the outside [4]. Since Porter and his collaborators [24, 25] had shown that collagen fibers are not seen within the cell but are in contact with its outside surface, it was concluded that collagen was secreted in the form of a soluble molecule which would then be arranged into fibers on the outside [4, 9, 27, 29]. Indeed, the soluble form of collagen, the so-called tropocollagen molecule, has been shown to be the building stone of collagen fibers [15].

Recently we became interested in the formation and metabolism of the collagen fibers present in the periodontal membrane. The collagen present in this structure showed a high turnover. It was then decided to study the time sequence of collagen formation and breakdown in the several groups of fibers which constitute the periodontal membrane. Other periodontal tissues (bone, cementum) were also examined. Considering that no strictly specific label is available for collagen, we used collagenase digestion to test how much of the label injected as ^{3}H-glycine

[1] This work was supported by grants from the Fundação de Amparo à Pesquisa do Est. de S. Paulo, Conselho Nacional de Pesquisas, the Rockefeller Foundation, and the Canadian Medical Research Council.

or ^{3}H-proline was really within collagen. Bacterial collagenase appears to offer some advantages as a histochemical tool, especially if combined with radioautography.

MATERIALS AND RESULTS

As collagen is an abundant protein in the body, its formation can be studied in many tissues. The organic matrices of bone and dentin contain about 95 per cent collagen [28, 34]. These two tissues, by the amount of collagen and by the fact that the respective collagen secreting cells are oriented, constitute excellent models to study collagen synthesis by radioautography [4]. The periodontal membrane, also called ligament, which forms the attachment of the teeth to the alveolus, is also rich in collagen fibers. These fibers are adherent to the root cement by one side and to the alveolar bone or to the cementum of another tooth by the other side. They are arranged in bundles which constitute the several ligaments classified by Black: (1) *trans-septal fibers*, going from one tooth to the next one, passing over the alveolar crest; and (2) *alveolar fibers*. The latter can be subdivided into four parts, which are (starting from the cervical end of the root) crest fibers, horizontal fibers, oblique fibers, and apical fibers [11].

Two experiments were performed on mice injected with 5 μc per gm body weight of ^{3}H-proline (generally labeled; specific activity 43 mc/mmole) or 2-^{3}H-glycine (specific activity 13 mc/mmole). The mice injected with ^{3}H-proline were sacrificed at ½, 4, 8, and 24 hours after a single intraperitoneal injection of the labeled amino acid. In the experiment with ^{3}H-glycine, the animals were similarly injected and sacrificed ½, 4, and 35 hours, 7 and 45 days after the injection. For comparison, other mice received either 4,5-^{3}H-DL-leucine (150 mc/mmole) or ^{3}H-methyl-DL-methionine (7.2 mc/mmole) and were sacrificed at the same time intervals as the ones injected with ^{3}H-glycine.

In all collagen-secreting cells (fibro-, osteo-, cemento-, and odontoblasts), the incorporation of ^{3}H-glycine was much higher than the incorporation of ^{3}H-methionine or ^{3}H-leucine. The amount of radioactivity present in those cells after ^{3}H-proline was comparable with the amount found after ^{3}H-glycine, as far as it could be detected by the darkening of the photographic emulsion. Indeed all observations made with ^{3}H-glycine were confirmed in the mice injected with ^{3}H-proline.

Collagen formation and turnover were studied in osteoblasts of alveolar bone, in odontoblasts of incisor teeth, in fibroblasts of periodontal membrane, and in cementoblasts of molar teeth. In each case the radioactivity was found first in the cells (½ hour after labeling) and then in the extracellular spaces (Figs. 1 and 2). In dentin, cementum,

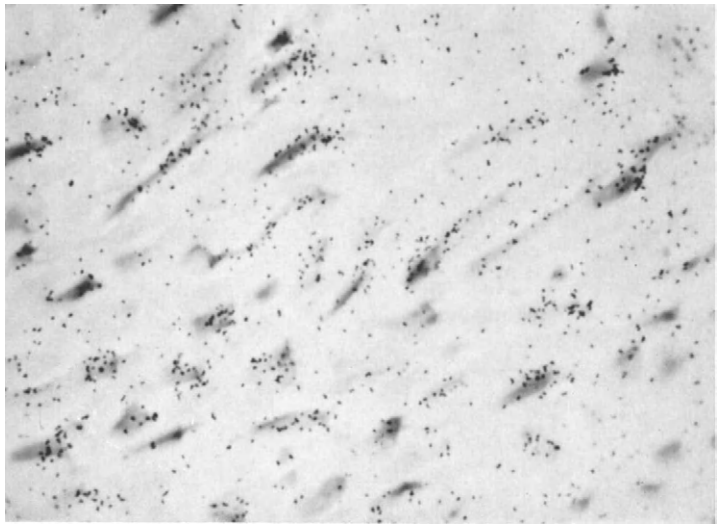

FIG. 1. Radioautograph of periodontal membrane 30 minutes after injection of ^{3}H-glycine. The label is mainly intracellular. Only a few grains are seen over the intercellular spaces. Radioautograph exposed 83 days, stained by hematoxylin and eosin. Magnification: 700 ×.

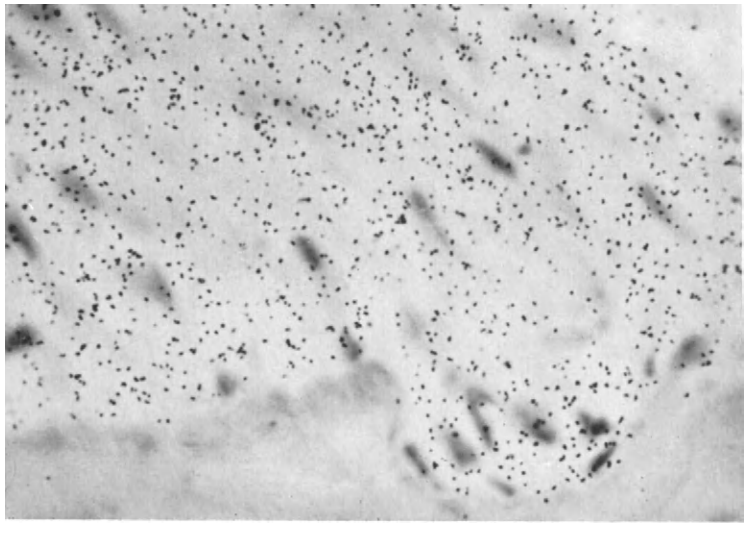

FIG. 2. Radioautograph of periodontal membrane 35 hours after injection of ^{3}H-glycine. The label now is mainly extracellular. Radioautograph exposed 83 days, stained by hematoxylin and eosin. Magnification: 700 ×.

and bone, the radioactivity soon decreased in the cells while increasing in predentin, precementum, and prebone, respectively (4 hours), appearing later in the calcified part of each tissue (8 hours or more).

Grain counts made at several time intervals after injection showed that once the label is incorporated into the collagen of a calcified tissue, it remains unchanged, unless the tissue is resorbed (Fig. 3). In periodontal membrane, however, the high incorporation of the label was followed by a rather fast decrease (Fig. 3). This result indicates that

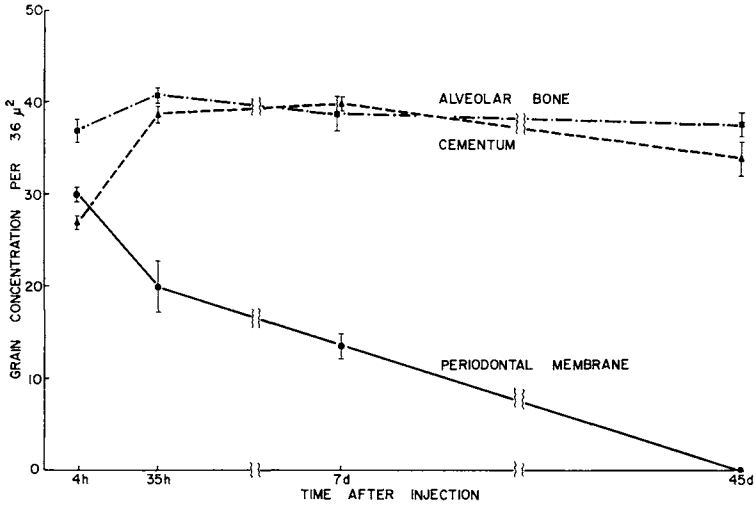

FIG. 3. Time sequence of ^{3}H-glycine incorporation into periodontal membrane, alveolar bone, and cementum of adult mice. Grain counts made at the level of the root apex. Each figure is the average of 20 grain counts in teeth from 2 mice. Vertical bars represent standard errors. In bone and cementum, the label stays without appreciable change for 45 days, except in areas of resorption. In contrast, there is a rapid decrease in the grain counts in the periodontal membrane. Radioautographs exposed 83 days.

collagen turns over in periodontal membrane, whereas it is stable in other investigated sites.

For a more detailed study of periodontal membrane, grains were counted over the crest fibers, the horizontal and oblique fibers, and the apical fibers (according to Black's classification). It was observed that the turnover of collagen is higher in the apical and crest fibers than in the horizontal and oblique fibers.

Effect of Collagenase

Even if all the evidences show that in collagen-secreting cells most of the label injected as proline or glycine is incorporated in newly formed

collagen, neither amino acid is specific for collagen. In order to determine how much of the label was taken by collagen itself and how much by other macromolecules, we used collagenase to remove the labeled collagen. Purified *Clostridium* collagenase is a very specific enzyme which does not attack any other protein except collagen [2, 32]. It is inactive also against mucopolysaccharides [20]. Young rats (average body weight 112 gm) were injected with either 3,4-^{3}H-proline (specific activity 5000 mc/mmole) or 2-^{3}H-glycine (specific activity 107 mc/mmole) and sacrificed 20 minutes, 4 (Figs. 4 and 5), and 48 hours after injection. Tissues were fixed in Carnoy, embedded in paraffin, and sectioned at 5 μ. Some slides were treated by collagenase in distilled water for 5 hours at 37°C (Fig. 5). Control slides were incubated with distilled water under similar conditions. All slides were then radioautographed.

At the first time interval (20 minutes) all the label was intracellular. About 50 per cent of the radioactivity present in odontoblasts, fibroblasts and osteoblasts could be removed by collagenase (Tables I and II). At

TABLE I. *Effect of Collagenase on Grain Counts over Odontoblasts (Incisor Tooth) and Osteoblasts (Alveolar Bone)*

	Grains per 136 μ^{2a}			
	20 minutes		4 hours	
	Odontoblasts	Osteoblasts	Odontoblasts	Osteoblasts
Control	26.6	25.3	13.8	12.2
Collagenase	12.8	13.5	11.9	10.5

[a] Each number is the average of 20 grain counts made in radioautographs from 2 rats injected with ^{3}H-proline.

TABLE II. *Effect of Collagenase on Grain Counts over Periodontal Membrane*

	Grains per 136 μ^{2a}	
	20 minutes	4 hours
Control	10.9	12.7
Collagenase	6.3	8.3

[a] Each number is the average of 20 grain counts made in radioautographs from 2 rats injected with ^{3}H-proline.

4 and 48 hours there was a pronounced decrease in the amount of radioactivity present in these cells. This residual radioactivity was not removed by collagenase (Table I) and probably represents labeled structural proteins [and perhaps some ribonucleic acid (RNA) in the animals injected with glycine]. However, the label which appeared in prebone and predentin at 4 hours and in bone and dentin at 48 hours was completely removed by collagenase (Figs. 6 and 7).

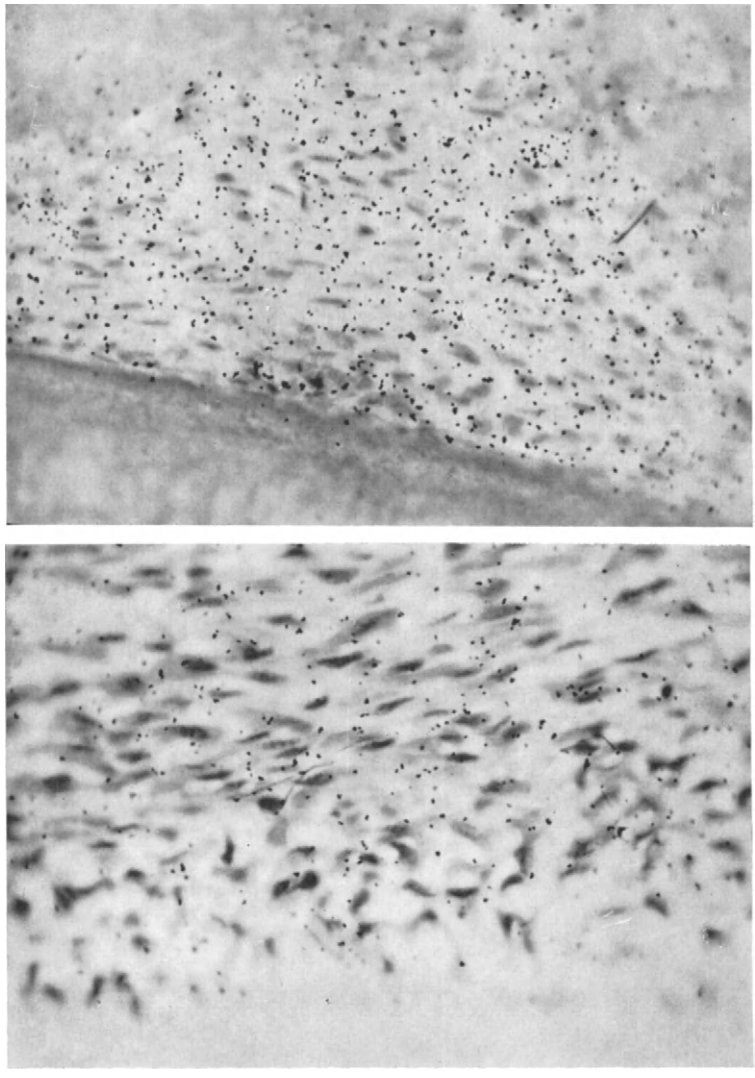

FIGS. 4 AND 5. Radioautographs of periodontal membrane from young rats injected with ^{3}H-glycine 4 hours before sacrifice. Figure 4 is a control preparation. The section shown in Fig. 5 was treated by collagenase. The enzyme removes a large amount of the label. Radioautographs exposed 15 days, stained by hematoxylin and eosin. Magnification: 700 ×.

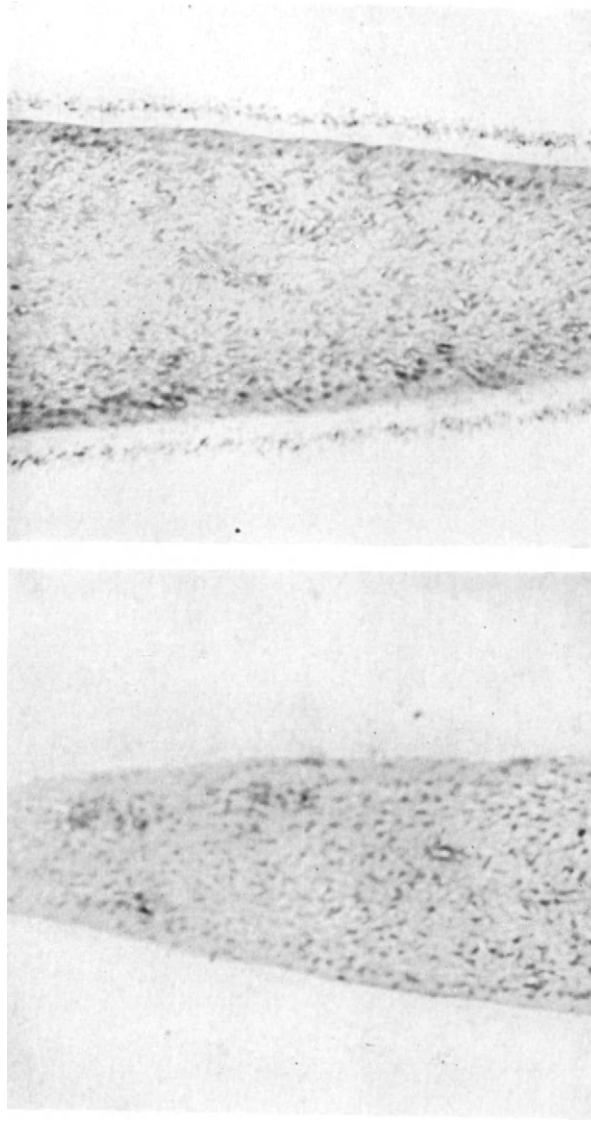

FIGS. 6 AND 7. Radioautographs of incisor teeth from young rats injected with ^{3}H-glycine 48 hours before sacrifice. Figure 6 is a control preparation, showing a layer of radioactive dentin separated from odontoblasts by nonradioactive dentin produced after the injected labeled glycine was utilized. The section shown in Fig. 7 was treated by collagenase, which removes all the label. Radioautographs exposed 15 days, stained by hematoxylin and eosin. Magnification: 700 ×.

The radioactivity present in cells known not to secrete collagen (liver cells, epithelial cells) was not removed at all by collagenase. This result confirms the specificity of the enzyme.

DISCUSSION

Problem of Collagen Labeling

Stetten and Schoenheimer [36] showed that collagen could be labeled by feeding animals with labeled proline, and that the label appears in the proline and hydroxyproline of collagen. Later Stetten [35] made the observation that labeled hydroxyproline is not incorporated into collagen. He concluded that the hydroxyproline of collagen is derived from proline and that the conversion takes place after a peptide or larger molecule is formed. This is an unfortunate situation, since hydroxyproline on account of its specificity would be the best collagen label for radioautography.

In the absence of a specific precursor, several labeled substances have been used in radioautographic studies of collagen formation. At least for dentin (odontoblasts) it was shown that after injection of ^{14}C-labeled bicarbonate or glucose, the label appears mainly in collagen. A much better precursor, however, is ^{3}H-glycine as we showed before [4]. This amino acid accounts for 32.5 per cent of all amino acid residues in collagen [3]. ^{3}H-Proline is also a convenient precursor [27, 30] since it is incorporated into collagen as proline or hydroxyproline and, taken together, these two amino acids constitute 23 per cent of the residues in collagen [3]. We found that ^{3}H-glycine and ^{3}H-proline gave comparable results.

Collagen Synthesis and Turnover

In most organs the turnover of collagen is very slow [23, 37]. Kao *et al.* [18] observed that among aorta, skin, tendon, and uterus only the last organ showed appreciable synthesis and turnover of collagen.

In contrast, the present results show a high rate of synthesis, as well as rapid turnover of collagen, in the periodontal membrane. Synthesis and turnover are particularly active in the crest and apical fibers. This may be a consequence of the lateral pressures and tensions to which teeth are subjected during mastication, with the main effect on the proximal and distal ends of the root. It was indeed shown that increased stress produces a widening of the periodontal membrane [26, 39], while disuse produces its atrophy [6, 7].

There are in the literature a number of observations which support our conclusion that the periodontal membrane is the site of a high col-

lagen turnover. For example, the periodontal membrane is sensitive to conditions which impair collagen synthesis, such as deficiencies in ascorbic acid [38] or protein [5, 12, 19, 31]. Both deficiencies are known to produce an atrophy of the periodontal membrane, the tooth becoming loose in the alveolus.

It must also be pointed out that collagen is not only the main constituent of periodontal membrane [1, 10, 33], but it may be different from that found elsewhere, since there is more neutral-soluble than acid-soluble collagen, contrary to other tissues [22]. As neutral-soluble collagen is synthesized before the acid-soluble fraction, a high content of the first is characteristic of tissues in which new collagen is being produced. Acid-soluble collagen is formed by aggregation of the smaller particles present in the neutral-soluble fraction [13, 14, 16, 17].

SUMMARY

The results presented in this article show that the periodontal membrane is the site of a high rate of synthesis and rapid turnover of collagen. This result was reached after injection of either ^{3}H-proline or ^{3}H-glycine, the most abundant amino acids in collagen. Collagen formation in bone, cementum, and dentin was also briefly described.

Bacterial collagenase was utilized to confirm the nature of the labeled material present in collagen-secreting cells after injection of ^{3}H-proline or ^{3}H-glycine. Under the conditions of the experiment, the purified enzyme used did not remove any label from noncollagen-secreting cells (liver, kidney), but removed about 50 per cent of the label present in the cytoplasm of collagen-secreting cells. The label found in extracellular collagen at 4 hours or later time intervals was completely removed by the enzyme.

ACKNOWLEDGMENTS

I wish to thank Dr. C. P. Leblond, Department of Anatomy, McGill University, for his suggestions during the preparation of this article. The collaboration of Dr. F. Fava de Moraes (Department of Histology, Faculty of Odontology, University of São Paulo, Brazil) is also acknowledged. Part of the experimental work was done with him.

REFERENCES

1. Araya, S., Ishiwara, T., and Saito, S., *J. Dental Res.* **40**, 225 (1961).
2. Bidwell, E., and van Heyningen, W. E., *Biochem. J.* **42**, 140 (1948).
3. Bowes, J. H., and Denten, R., *Biochem. J.* **42**, 358 (1948).
4. Carneiro, J., and Leblond, C. P., *Exptl. Cell Res.* **18**, 291 (1959).
5. Chawla, T. N., and Glickman, I., *Oral Surg. Oral Med. Oral Path.* **4**, 578 (1951).
6. Cohn, S., *J. Dental Res.* **40**, 707 (1961).
7. Coolidge, E. D., *J. Am. Dental Assoc.* **24**, 1260 (1937).

8. Doljanski, L., and Roulet, F., *Arch. Pathol. Anat. Physiol.* **291**, 260 (1933).
9. Fernando, N. V. P., and Movat, H. Z., *Lab. Invest.* **12**, 214 (1963).
10. Fullmer, H. M., *J. Dental Res.* **41**, 223 (1962).
11. Glickman, I., *in* "Clinical Periodontology," 2nd ed., p. 33. McGraw-Hill, New York, 1962.
12. Goldman, H. M., *J. Periodontol.* **25**, 87 (1954).
13. Green, N. M., and Lowther, D. A., *Biochem. J.* **71**, 55 (1959).
14. Harkness, R. D., Marko, A. M., and Muir, H. M., *Biochem. J.* **56**, 558 (1954).
15. Hodge, A. J., and Schmitt, F. O., *in* "Macromolecular Complexes" (M. V. Edds, Jr., ed.), p. 19. Ronald Press, New York, 1961.
16. Jackson, D. S., *Biochem. J.* **65**, 277 (1957).
17. Jackson, D. S., and Bentley, J. P., *J. Biophys. Biochem. Cytol.* 7, 37 (1960).
18. Kao, K.-Y. T., Hilker, D. M., and McCavack, T. H., *Proc. Soc. Exptl. Biol. Med.* **106**, 335 (1961).
19. Kerr, D. A., *J. Dental Res.* **41**, 302 (1962).
20. MacLennan, J. D., *Bull. N.Y. Acad. Med.* **30**, 997 (1954).
21. Mallory, F. B., *J. Med. Res.* **10**, 334 (1903).
22. Michi, T., Imagawa, Y., and Araya, S., *J. Dental Res.* **42**, 756 (1963).
23. Neuberger, A., and Slack, H. G. B., *Biochem. J.* **53**, 47 (1953).
24. Porter, K. R., *Biophys. J.* **4**, 167 (1964).
25. Porter, K. R., and Papas, G. D., *J. Biophys. Biochem. Cytol.* **5**, 153 (1959).
26. Ramfjord, S. P., and Kohler, C. A., *J. Pediodontol.* **30**, 95 (1959).
27. Revel, J.-P., and Hay, E. D., *Z. Zellforsch.* **61**, 110 (1963).
28. Rogers, H. J., Weidemann, S. O., and Parkinson, A., *Biochem. J.* **50**, 537 (1952).
29. Ross, R., and Benditt, E. P., *J. Biophys. Biochem. Cytol.* **11**, 677 (1961).
30. Ross, R., and Benditt, E. P., *J. Cell Biol.* **15**, 99 (1962).
31. Ruben, R. P., McCoy, J., Person, P., and Cohen, D. W., *Oral Surg.* **15**, 1061 (1962).
32. Seifter, S., Gallop, P. M., Klein, L., and Meilman, E., *J. Biol. Chem.* **234**, 285 (1959).
33. Smith, D., *J. Dental Res.* **41**, 250 (1962).
34. Stack, M. V., *Ann. N.Y. Acad. Sci.* **60**, 585 (1955).
35. Stetten, M. R., *J. Biol. Chem.* **181**, 31 (1949).
36. Stetten, M. R., and Schoenheimer, R., *J. Biol. Chem.* **153**, 113 (1944).
37. Thompson, R. C., and Ballou, J. E., *J. Biol. Chem.* **208**, 883 (1954).
38. Waerhaug, J., *J. Periodontol.* **29**, 87 (1958).
39. Wentz, F. M., Jarabak, J., and Orban, B., *J. Periodontol.* **29**, 117 (1958).

Discussion

Dr. Tonna: I agree that the grains over bone represent labeled collagen. After all, 95–99% of bone matrix is collagen, while roughly 1% is *mucopolysaccharide*–protein. We have been doing similar enzyme treatments of bone and cartilage, and have found that, if we extend the period of collagenase treatment, we start removing large chunks of partially digested collagen. Presumably, the ±1% mucopolysaccharide–protein intimately associated with collagen also comes off physically with the collagen. But on the other hand, if one treats bone with hyaluronidase to remove only mucopolysaccharide–protein, the decrease in the grain count is so small as to be within the error range. Therefore, the removal cannot be detected.

Dr. Ross: The labeled material present in cells and not removable by col-

lagenase is of interest. Is it possible that this may represent collagen that is protected from reaction with the enzyme, or is it due to proteins that are not susceptible to collagenase?

DR. CARNEIRO: We believe that the radioactivity left in the cells after collagenase treatment is in other proteins than collagen. As nascent collagen has the same amino acid sequence as mature collagen with only a difference in the proline–hydroxyproline ratio (which does not affect its susceptibility to the enzyme), it is easily digested by collagenase, as was indeed shown by biochemists.

DR. BÉLANGER: Is your collagenase bacterial in origin?

DR. CARNEIRO: There are differences between the collagenase produced by bacteria and that found in tadpoles. We use that from the bacterium *Clostridium histolyticum*. This collagenase is purified by ion exchange chromatography (Worthington Biochem. Corp.); only purified collagenase should be used. In our hands, this collagenase has given good and consistent results.

We introduced several modifications to the technique described by Green (1960).* The sections are covered with a thin celloidin film, and the temperature of the enzyme solution is kept constant (37°C) throughout the 5-hour digestion period. On each slide of hard tissues, sections of liver are added as controls. Under our conditions, collagenase decreased the grain count over liver cells by less than 5%. After collagenase treatment of bone or dentin, the noncollagenous elements remain in the section. Indeed, cells and their processes are more clearly seen after collagenase treatment; the limits of the cytoplasm are clearly defined.

DR. TONNA: Incidentally, any fixative employing formalin diminishes the ability of collagenase to remove collagen. Carnoy fixation is adequate.

DR. LEBLOND: Some years ago, Hancox observed that osteoclasts placed on a gelatin layer dug out a hole in the gelatin. The interpretation may be that osteoclasts secrete a collagenase, and perhaps they may resorb bone by digesting the collagen matrix.

Recently, Dr. Bélanger presented evidence indicating that osteocytes can cause resorption of the bone tissue by which they are immediately surrounded. Does Dr. Bélanger know whether osteocytes (and perhaps also osteoblasts and osteoclasts) have the ability to secrete a collagenase?

DR. BÉLANGER: When fresh sections of bone are incubated on the surface of a photofilm, the gelatin is digested under the large osteocytes. Around these cells, alpha-radiographs show decreased organic matrix density, and X-ray microradiographs show concomitant loss of salt. This type of resorption we call "osteolysis," to distinguish it from "osteoclasia," which may be a form of phagocytic activity.

DR. GREULICH: With regard to your interesting finding that the collagen of periodontal ligament turns over at a fairly rapid rate, I would like to know if the rates of loss of ^{3}H-proline or -glycine from the three regions of periodontal ligament differ.

DR. CARNEIRO: We did not find clear-cut differences in the loss of label from the three regions of the periodontal membrane, whatever precursor was used.

* Green, J. A., *Stain Technol.* **35**, 273-276 (1960).

SECRETION OF PROTEIN ENZYMES BY THE ACINAR CELLS OF THE RAT PANCREAS[1]

HUBERTA E. VAN HEYNINGEN

Department of Anatomy, McGill University, Montreal, Canada

INTRODUCTION

The acinar cells of the pancreas produce the proteins which constitute the digestive enzymes of the pancreatic juice. In the rat, the acinar cells produce the pancreatic enzymes continuously and at a rather rapid rate [14]; these two aspects render the rat pancreas a suitable organ for the study of protein secretion.

The polarized organization of the pancreatic acinar cells has allowed an assessment of the sequence and rate of protein secretion with the light microscope. In the three concentric zones into which they divided the pancreatic acini, Warshawsky *et al.* [14] measured the relative protein concentration as well as the radioactivity at various intervals after ^{3}H-leucine injection. From the relative specific activities provided by these data, they deduced how each cellular zone participates in the secretion of protein. First, the protein is synthesized in the basal, i.e., basophilic zone of the cell and then it migrates via the middle zone, containing Golgi elements and zymogen granules, to the distal zone, consisting primarily of zymogen granules; finally it is released in the duct system as pancreatic secretion. The synthesis and intracellular migration of the protein proceeds amazingly rapidly; the entire process from amino acid incorporation to extrusion of the protein has been estimated to last approximately 1 hour [6].

As is often the case, subdivisions useful in the light microscope do not have their counterpart in the equivalent study with the electron microscope. Division of the acini into zones, while useful for light microscopy, was not suitable for radioautography with the electron microscope; instead the clear definition of cell organelles made it possible to assign radioactivity to them. Therefore, in the present study protein synthesis and migration are considered in terms of the various cell organelles involved, independently of the zone in which they are located.

[1] This investigation was supported by grant 5 T1-GM-721-04 from the U.S. Public Health Service.

EXPERIMENTAL

Details of the technique used for radioautography with the electron microscope have been previously published [13]. In studies of this nature, some quantitative evaluation of the number of grains over cell organelles is indispensable. The least bias is introduced in the grain counts if the layer of emulsion over the sections is of reproducible and even thickness. Pilot experiments revealed that the most even distribution of emulsion over the grid was obtained if the grid was placed directly on

TABLE I. *Percentage Distribution of Grains Over the Components of the Pancreatic Acinar Cells at Various Intervals after Injection of ^{3}H-Leucine*[a]

Site	1 minute	10 minutes	30 minutes	1 hour	3½ hours	12 hours
Basal ergastoplasm[b]	76	60	27	9	19	18
Golgi complex[c]	—	14	13	5	3	4
Zymogen granules	9	10	38	57	53	41
Acinar lumen[d]	—	—	1	9	5	7
Intergranular ergastoplasm[e]	—	5	18	17	14	24
Nucleus	3	6	2	1	4	2
Mitochondria	12	5	1	2	2	4
S.D.[f]	17	5	5	3	6	9

[a] From H. E. van Heyningen [13].

[b] Denotes the ergastoplasm in the basal half of the cell, free from zymogen granules.

[c] Including prezymogen granules.

[d] Includes the grains over microvilli.

[e] Denotes the ergastoplasm in the upper half of the cell, among the zymogen granules.

[f] Standard deviation, calculated as $\frac{\sqrt{n}}{n}$.

the supporting glass slide and a Formvar film covered them both. As to the distribution over each square of the grid, a Formvar film reinforced with collodion was found to give a more even emulsion layer than a Formvar film alone. Therefore preparations were made with collodion-reinforced Formvar films, which thus served a dual purpose: attachment of the grids to the glass slides and support for the sections. These preparations were dipped in Ilford nuclear track emulsion L-4, diluted 1:5 with distilled water, then exposed, and finally developed with Kodak Microdol-X. The material consisted of pancreas of young rats that had received an injection of ^{3}H-leucine at various time intervals prior to fixation with osmium tetroxide. In the electron micrographs, the distribution of grains over the various cell organelles was determined as a function of time after injection (see Table I).

OBSERVATIONS

The *ergastoplasm* (granular endoplasmic reticulum) is distributed unequally throughout the pancreatic acinar cell. In the basal half of the cell, numerous long flat parallel cisternae, studded with regularly spaced ribosomes, occupy the entire space between nucleus and plasma membrane except for a few mitochondria. This region (termed basal ergastoplasm) corresponds to the strong basophilia seen with the light microscope. In the apical half of the cell the many zymogen granules leave only little space for the ergastoplasm (termed intergranular ergastoplasm), in which, compared to its basal counterpart, the cisternae tend to be wider and much shorter, with more free ribosomes between them.

As early as 1 or 2 minutes after injection of ^{3}H-leucine, a few silver grains were present over the pancreatic acinar cells and nearly all of these were over the basal ergastoplasm (Fig. 1). Since these intervals are presumably too short for any appreciable protein migration, and since free amino acids do not register [2], these grains should signify only newly synthesized protein. It may be concluded that the synthesis of protein occurs in the basal ergastoplasm. The lack of grains over the intergranular ergastoplasm may indicate absence of protein synthesis in this location, or else may be due to the low total radioactivity at these early intervals.

The resolution of the present technique allows the localization of the protein synthesis in the ergastoplasm irrefutably, but does not reveal whether the ribosomes, the membranes, or the contents of the ergastoplasmic cisternae are involved. However, in the thyroid gland where the cisternae are naturally dilated, the silver grains at early intervals after ^{3}H-leucine injection straddle the ribosome-studded membranous walls of the ergastoplasmic cisternae, whereas at later intervals they overlie the cisternal contents [7]; apparently, the protein is synthesized in the membrane-bound ribosomes, from where it migrates into the cisternal lumen. In analogy with the findings in the thyroid, it is likely that the pancreatic protein follows the same course, i.e., synthesis in the ribosomes and subsequent migration into the narrow cisternal lumen. That the ribosomes are responsible for the synthesis of enzymic proteins has also been demonstrated in biochemical studies on the pancreas of the guinea pig [12]. Ribosomes being the site of protein synthesis is in concordance with current views on the involvement of the three classes of ribonucleic acid (RNA) in protein synthesis [15]. In fact, arrays of ribosomes (termed polysomes or ergosomes) can be considered the assembly lines for the mass production of protein [10].

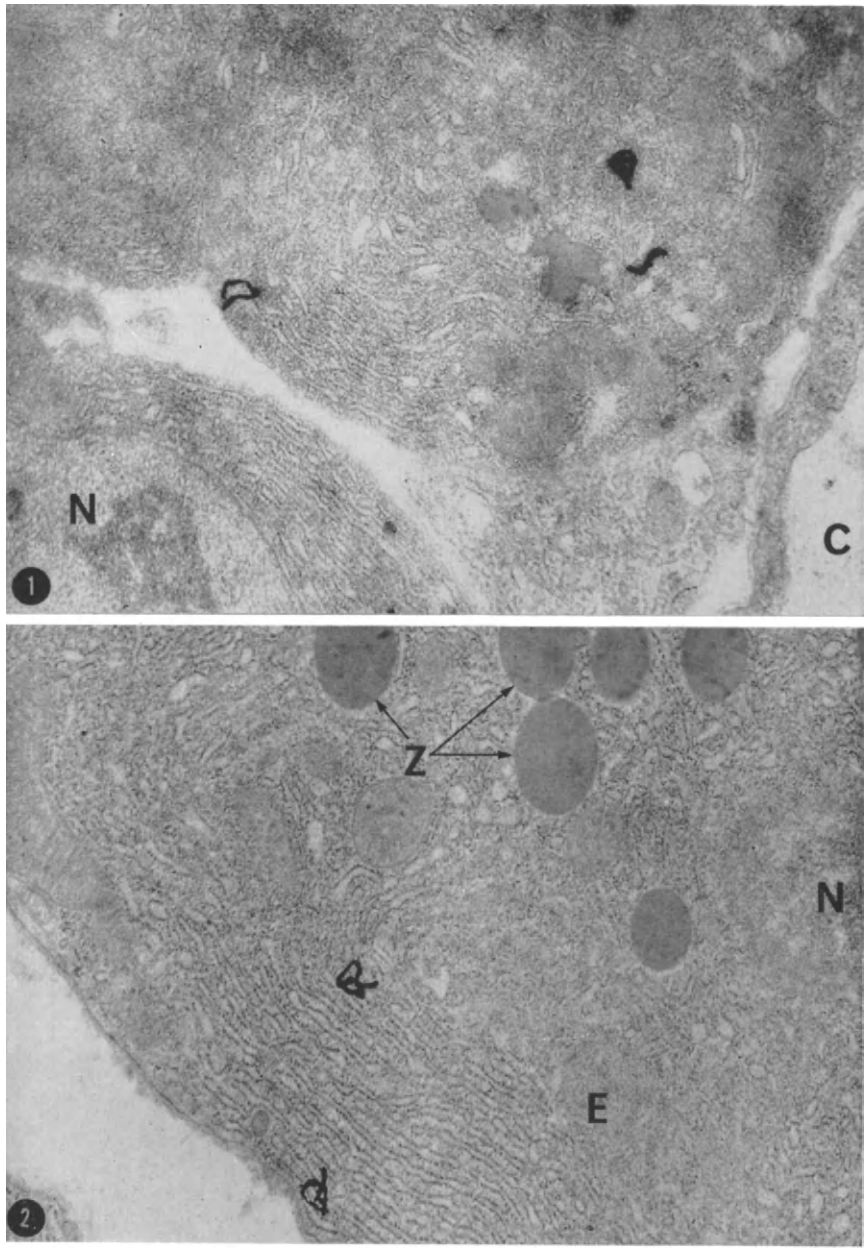

FIG. 1. Portion of several pancreatic cells at the periphery of an acinus; nucleus (N) of one of acinar cells at left, endothelium of a capillary (C) at right. This preparation was obtained from pancreas fixed 1 minute after the injection of ^{3}H-

The *Golgi complex* is located approximately in the center of the acinar cell, with fractions among the zymogen granules. The elements of the Golgi complex (Fig. 3) comprise: numerous small vesicles (also called microvesicles); stacked smooth-surfaced flattened cisternae (also called saccules), some of which are in part distended to vacuoles; and separate Golgi vacuoles. Frequently, granules less dense than zymogen granules, but in the same size range, are present in the Golgi complex. They are called prezymogen granules and, because of their spatial relationship to the Golgi region, they will be considered here with the other Golgi elements.

Whereas at early intervals after ^{3}H-leucine injection, the Golgi complex is not labeled, there is a definite reaction at later intervals (10, 20, and 30 minutes; see Figs. 3 and 4). Since 10 minutes may be sufficient time to allow intracellular protein migration, and since the Golgi complex was not labeled at earlier intervals, the labeled protein in the Golgi must have come from the basal ergastoplasm. Thus, the newly synthesized protein migrates from the basal ergastoplasm to the Golgi complex. To know the exact way by which the protein passes through the Golgi complex is of fundamental importance. At the intervals studied, silver grains were present over Golgi vesicles, saccules, and vacuoles, as well as over prezymogen granules, but the percentages were not sufficiently diverse to suggest a time sequence within the Golgi complex. The first of the Golgi elements to contain the newly synthesized proteins may be the vesicles. In the pancreas of the guinea pig, electron microscopic radioautographs showed the radioactivity in the Golgi vesicles to precede that in the other Golgi components [1]. Morphological evidence has suggested that the Golgi vesicles originally arise as smooth-walled "blebs" budding off from the ergastoplasmic cisternae [16]. These observations would assign to the Golgi vesicles the role of taking the protein from the ergastoplasmic cisternae to the Golgi complex.

On the other hand, the form in which the protein departs from the Golgi complex may be the prezymogen granules. The frequent demonstration of continuous series linking empty Golgi vacuoles to dense, mature zymogen granules [3, 9] provides morphological evidence that

---

leucine. The silver grains are located over the granular endoplasmic reticulum (ergastoplasm), indicating the presence of labeled protein which, in view of the short time interval involved, must have been synthesized there. The synthesis of protein is thus believed to occur in the basal ergastoplasm.

FIG. 2. Corner of a pancreatic acinar cell, occupied by tip of nucleus (N), a few stray zymogen granules (Z), and abundant ergastoplasm (E). This preparation was obtained from pancreas fixed 10 minutes after the injection of ^{3}H-leucine. Many grains are still found over the basal ergastoplasm at this time.

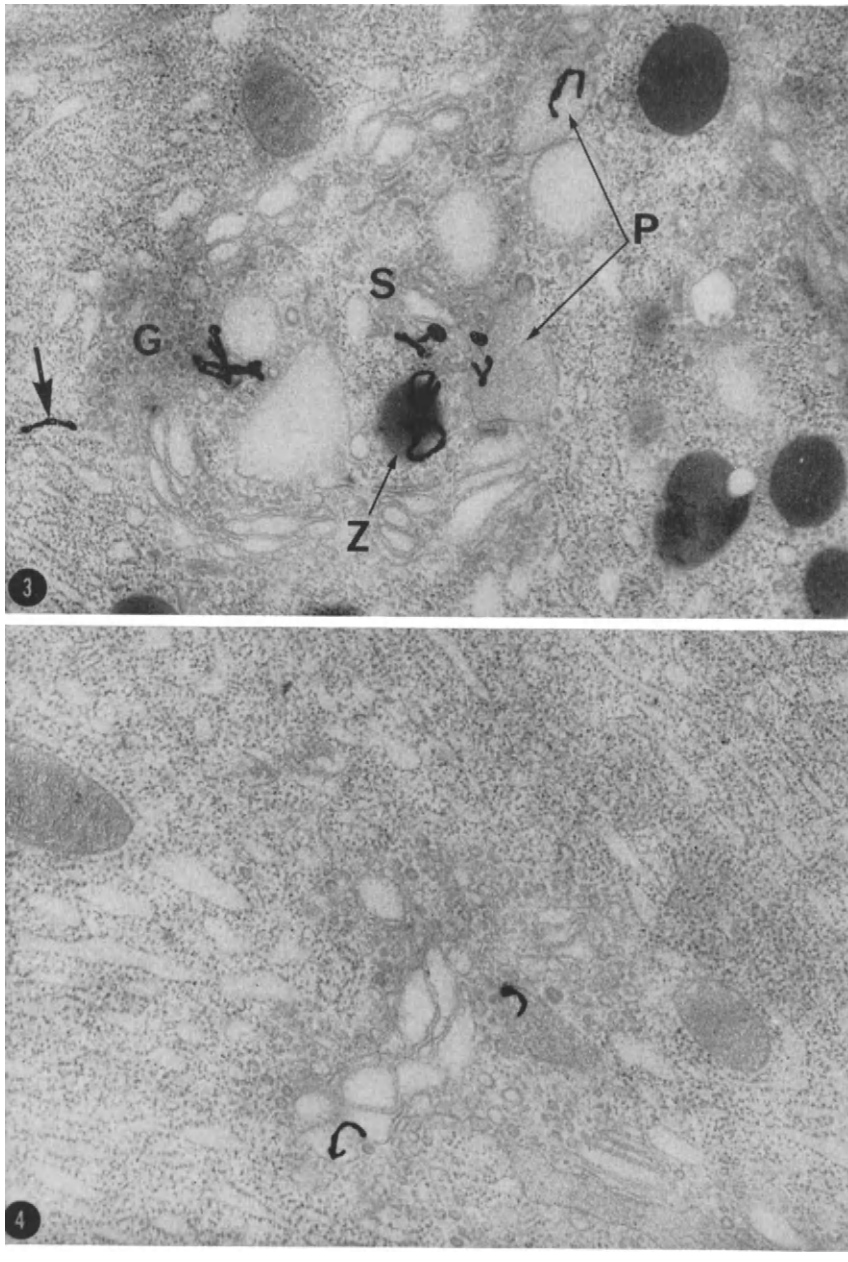

FIG. 3. Golgi region of a pancreatic acinar cell 10 minutes after injection of ^{3}H-leucine. Various elements of the Golgi complex are labeled, e.g., small vesicles (G), saccules (S), prezymogen granules (P), as well as a zymogen granule (Z).

the prezymogen granules be considered immature zymogen granules, which would contain the protein leaving the Golgi complex. Although radioactivity appears in the prezymogen granules at about the same time as the other Golgi elements are labeled (Fig. 3), this does not necessarily deny its later rank in the Golgi sequence, but may simply allude to the speed with which the protein traverses the Golgi complex.

The *zymogen granules* occupy predominantly the apical half of the acinar cell. Generally they are spherical, have a homogeneous, electron-opaque content, and are enclosed in a smooth membrane. Already at 30 minutes after injection of ^{3}H-leucine, numerous zymogen granules are labeled, but the peak of radioactivity in the zymogen granules was found at 60 minutes (Fig. 5). Since at that interval the Golgi complex is no longer labeled significantly, the labeled protein in the zymogen granules must have come from the Golgi complex. Thus, the labeled protein migrates in the form of zymogen granules from the Golgi complex to the apex of the cell.

At still later intervals (3½ and 12 hours), most of the labeled protein has left the acinar cells, but some of the remaining radioactivity can be found in the zymogen granules. This may imply that the zymogen granules which were formed first do not necessarily also leave the acinar cell first.

The *acinar lumen* is located between the apices of the acinar and occasional centroacinar cells and may have canalicular extensions between adjacent acinar cells. After ^{3}H-leucine injection, the lumen was found to be labeled significantly at the 60-minute interval only (Fig. 5). The lack of radioactivity in the lumen at later times suggests that the protein released by the zymogen granules does not remain in the lumen, but immediately proceeds further.

The manner of release involves the fusion of the membranes of granule and cell apex, so that the content of the zymogen granule becomes continuous with the lumen. In this location the appearance of the zymogen is often different from that in intact zymogen granules; a possible explanation may be provided by the finding that a greater

---

Grain at left (heavy arrow) is still over the ergastoplasm. It is believed that the labeled protein migrates from the ergastoplasm to the Golgi complex where, with prezymogen granules as an intermediate step, it is packaged into zymogen granules. The simultaneous labeling of the various components alludes to the rapidity of the process.

FIG. 4. Golgi complex of a pancreatic acinar cell, 30 minutes after injection of ^{3}H-leucine. The grains over the Golgi complex are regarded as being due to protein, which has migrated here from the basal ergastoplasm.

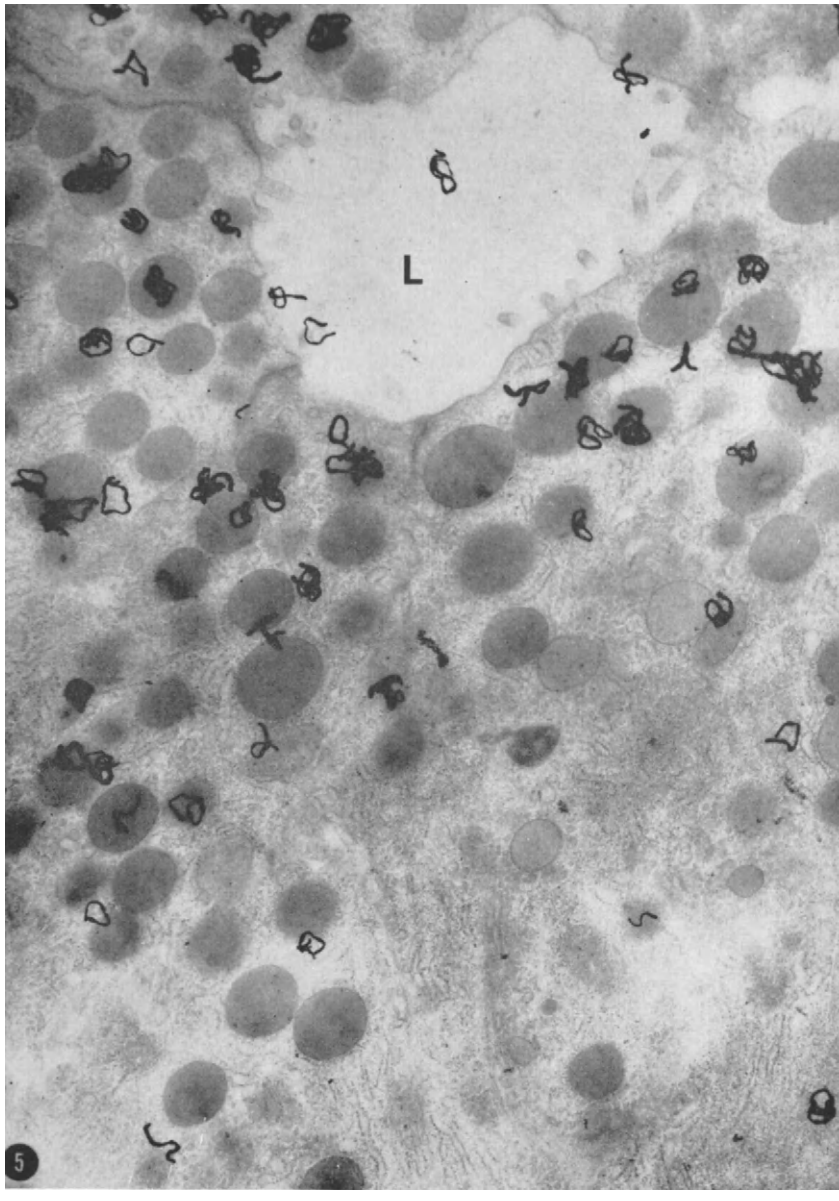

FIG. 5. Apices of pancreatic acinar cells, encircling an acinar lumen (L). This preparation was obtained from pancreas fixed 60 minutes after injection of ^{3}H-leucine. Many zymogen granules are labeled and apparently contain the protein, which was packaged in the Golgi complex. The grains over the acinar lumen are presumably due to protein released by zymogen granules into the lumen.

dilution or a change in pH brings about alterations in the solubility properties of the zymogenic proteins [3].

Besides the zymogenic proteins, which are released into the lumen (the so-called exportable proteins), the acinar cell also contains *sedentary proteins*, i.e., proteins which are part of the framework of the cell itself. These proteins are synthesized simultaneously with the zymogenic proteins, but at a much slower rate. Nadler [6] has estimated that the turnover time of the sedentary proteins is in the order of 62.5 hours, versus 3–6 minutes for the exportable proteins in the ergastoplasm. At the later intervals (3½ and 12 hours) after ^{3}H-leucine injection, when most of the exportable proteins have left the acinar cell, some of the remaining radioactivity is found in the basal and intergranular ergastoplasm. This persistent label presumably represents sedentary proteins in the acinar cells.

The *nucleus* is located centrally in the basal half of the cell, and the *mitochondria* are located anywhere throughout the cytoplasm, but frequently line up along the plasma membrane of the basal half of the cell. At all intervals studied these cell organelles account for only a small percentage of the silver grains observed. Even though at no interval was their labeling significant, the few grains present may possibly also represent sedentary proteins in these organelles.

DISCUSSION

The pattern of protein secretion described in the pancreas of the rat [13,14] agrees closely with that observed in the fasted and refed guinea pig [1]. One point of difference, however, may be the condensing vacuoles of the guinea pig which, originating as Golgi vacuoles, gradually accumulate heterogeneous flakes of a material of the same density as that of the zymogen granules, until they become identical to mature zymogen granules. The heavy labeling of these condensing vacuoles at an interval preceding the labeling of the zymogen granules sustains the theory that these vacuoles are indeed the precursors of the mature zymogen granules. In the normal rat pancreas these condensing vacuoles are not encountered, but it is believed that they correspond to the prezymogen granules discussed above.

The described sequential involvement of cell organelles in protein secretion is not unique for the pancreas. Other cell types to which electron microscopic radioautography has been applied, e.g., the fibrocytes of healing wounds [11], the chondrocytes of differentiating cartilage [8], the fibroblasts and epidermal cells of salamander skin [4], and the follicular cells of the thyroid gland [7], all exhibit the same successive

labeling of cell organelles as in the pancreas. In all these cell types the same basic pattern is followed for the production of extracellular protein. First the protein is synthesized in the granular endoplasmic reticulum. From there the newly synthesized protein migrates to the Golgi complex, whose role may involve the packaging of the protein into membrane-bound granules (pancreas), vacuoles (chondrocytes), or small vesicles (thyroid). In addition, indirect evidence has suggested that in the Golgi complex carbohydrate components may be added to the secretory product [7]. From the Golgi complex the protein migrates in the form of granules, vacuoles, or vesicles to the surface of the cell and is finally released into the extracellular compartment.

SUMMARY

The secretion of protein enzymes by the acinar cells of the pancreas can be divided into three steps: protein synthesis, migration, and release. The synthesis of the protein occurs in the basal ergastoplasm, presumably in relation to the ribosomes. From there, the newly synthesized protein migrates, possibly via the lumen of the ergastoplasmic cisternae, to the Golgi complex. In the Golgi complex the protein eventually accumulates in prezymogen granules, which later become zymogen granules. In this form the protein then migrates to the apex of the cell, where it is released from the zymogen granules into the acinar lumen.

REFERENCES

1. Caro, L. G., and Palade, G. E., *J. Cell Biol.* **20**, 473 (1964).
2. Droz, B., and Warshawsky, H. J., *Histochem. Cytochem.* **11**, 426 (1963).
3. Ekholm, R., Zelander, T., and Edlund, Y., *J. Ultrastruct. Res.* **7**, 61 (1962).
4. Hay, E. D., and Revel, J. P., *Develop. Biol.* **7**, 152 (1963).
5. Hokin, L. E., *Biochim. Biophys. Acta* **18**, 379 (1955).
6. Nadler, N. J., *J. Cell Biol.* **16**, 24 (1963).
7. Nadler, N. J., Young, B. A., Leblond, C. P., and Mitmaker, B., *Endocrinology*, **74**, 333 (1964).
8. Revel, J. P., and Hay, E. D., *Z. Zellforsch.* **61**, 110 (1963).
9. Rhodin, J. A. G., "An Atlas of Ultrastructure." Saunders, Philadelphia, 1963.
10. Rich, A., *Sci. Am.* **209**, 44 (1963).
11. Ross, R., and Benditt, E. P., *2nd Ann. Meeting Am. Soc. Cell Biol.* p. 157 (1962).
12. Siekevitz, P., and Palade, G. E., *J. Biophys. Biochem. Cytol.* 7, 619 (1960).
13. van Heyningen, H. E., *Anat. Record* **148**, 485 (1964).
14. Warshawsky, H., Leblond, C. P., and Droz, B., *J. Cell Biol.* **16**, 1 (1963).
15. Watson, J. D., *Science* **140**, 17 (1963).
16. Zeigel, R. F., and Dalton, A. J., *J. Cell Biol.* **15**, 45 (1962).

Discussion

Dr. Ross: How do you explain the increase in per cent label over basal ergastoplasm after it had already increased, realizing this is a relative percentage?

Dr. van Heyningen: Since after 60 minutes most of the radioactivity has left the acinar cells, the percentages at 3½ and 12 hours are taken from a smaller total, and thus represent only a small amount of radioactivity.

Dr. Goldstein: Why do you believe that 1 minute is too short an interval after administration of labeled amino acid for it to be incorporated into protein somewhere in the organism and then migrate to the endoplasmic reticulum of the pancreas?

Dr. van Heyningen: If the protein would migrate from the periphery of the cell inward, the grain concentration would be expected to be initially higher over the periphery of the cell than over the more interior ergastoplasm; with time, the situation would be reversed. However, when I counted the grains over the peripheral and the interior ergastoplasm as two separate categories, this was not the case; the ratio of the two percentages did not change with time, so supposedly protein synthesis occurs in the ergastoplasm and, in fact, in both regions simultaneously.

Dr. Pelc: Diffusion rates in water are of the order of 10–20 μ per second for substances with a molecular weight of 200–300. We found by water-soluble autoradiography a speed of the order of 1–2 μ per second for ^{3}H-thymidine moving from the peritoneum into the intestinal epithelium across the smooth muscle, etc.

Dr. Leblond: Specific activity measurements (that is, ratio of grain counts over protein content) were carried out with Warshawsky and Droz in rats given ^{3}H-leucine using three zones of pancreatic acini: ergastoplasm, proximal zymogen region (containing the Golgi complex and zymogen granules), and distal zymogen region (containing only zymogen granules) (*J. Cell Biol.* 1963, **16**, 1). Calculations were made by Nadler using the classic method, which assumes that, under steady state conditions, any entering molecule mixes instantly with those already present, and that any molecule in the pool has equal probability of departing. With these assumptions, mean turnover time of the label was about 5 minutes in the ergastoplasm and 12 minutes in the Golgi complex. These results indicate that the synthesis of protein, their migration to the Golgi, and their packaging as zymogen granules in this zone are extremely rapid phenomena.

Dr. Nadler: The concept of turnover time which classically refers to the time taken to replace an amount equal to the contents of a pool may not strictly apply when we begin to peer into minute structures such as the ergastoplasm or the Golgi complex. For instance, consider what might be going on in the cisternae of the endoplasmic reticulum. There, instead of each molecule having equal probability of departing, the newly synthesized molecules could be moving along in a more or less orderly procession from the sites of entry to those of exit. In such a case, it may be more appropriate to speak of the rate of migration of molecules, rather than of turnover time. The turnover time might then become the "mean transit time."

The experimental evaluation of turnover time (mean transit time) of the protein label has practical applicability. In a preliminary theoretical approach to this problem (unpublished), the average speed of migration of labeled protein molecules in the cisternae of acinar pancreatic cells has been calculated. Using the 5 minute figure

quoted by Dr. Leblond as mean transit time, and estimating the longest dimension of the membranes of the endoplasmic reticulum to be of the order of 5 μ, it works out that the average speed of migration of protein molecules in the cisternae may be of the order of 0.5 μ per minute. Therefore, in answer to Dr. Goldstein's question, even if we disregard the time taken for the synthesis of new protein, I suspect that if, 1 minute after injection of a labeled amino acid, the label is found throughout the ergastoplasm, then this would represent its site of synthesis. Indeed, 1 minute is too short a time for a protein molecule migrating at that rate to spread throughout the ergastoplasm from another site. The ergastoplasm would thus be the site of synthesis.

SYNTHESIS AND SECRETION OF COLLAGEN BY FIBROBLASTS IN HEALING WOUNDS[1]

RUSSELL ROSS[2]

Departments of Pathology and Oral Biology, Schools of Medicine and Dentistry, University of Washington, Seattle, Washington

INTRODUCTION

Collagen, the principal structural protein of the connective tissue, constitutes approximately one-third of all body protein, and serves not only in the function of support, as in cartilage, bone, and tendon, but also as part of a milieu for the transmission of, and interaction between, many important substances. The healing skin wound presents an opportunity for the study of the role played by the fibroblasts in the synthesis of this protein. A clearer understanding of how the fibroblast functions in wound healing would provide a basis for further examination of the pathological alterations of this important biological process, as well as the more fundamental problems associated with protein synthesis.

The fibroblast, like the osteoblast and the chondroblast, has been shown to contain a configuration of organelles and subcellular systems consistent with that demonstrated in cells actively engaged in the synthesis of protein for export [9, 14, 16]. The principal morphological feature of this cell is the very extensive development of the rough endoplasmic reticulum, apparently randomly dispersed throughout its cytoplasm. In addition, the fibroblast contains an abundant Golgi complex, numerous mitochondria, vesicles, vacuoles, dense bodies, and peripheral cytoplasmic aggregates of filaments, measuring approximately 50 Å in diameter [11, 14, 16]. This cell type usually contains a large nucleus with a prominent nucleolus as well. From cell to cell within a wound there is no apparent, orderly arrangement of the organelles of the fibroblast such as that seen in the pancreatic acinar cell (Fig. 1) [20].

The characteristic polarity of the organelles of the acinar cells of the pancreas facilitates autoradiographic studies of this particular organ, whereas the apparently random distribution of the organelles of the

[1] Supported by grants DE-01703-03 and HE-03174 from the U.S. Public Health Service.

[2] Dr. Ross is the holder of a Career Development Research Award (DE-K3-9053) from the U.S. Public Health Service.

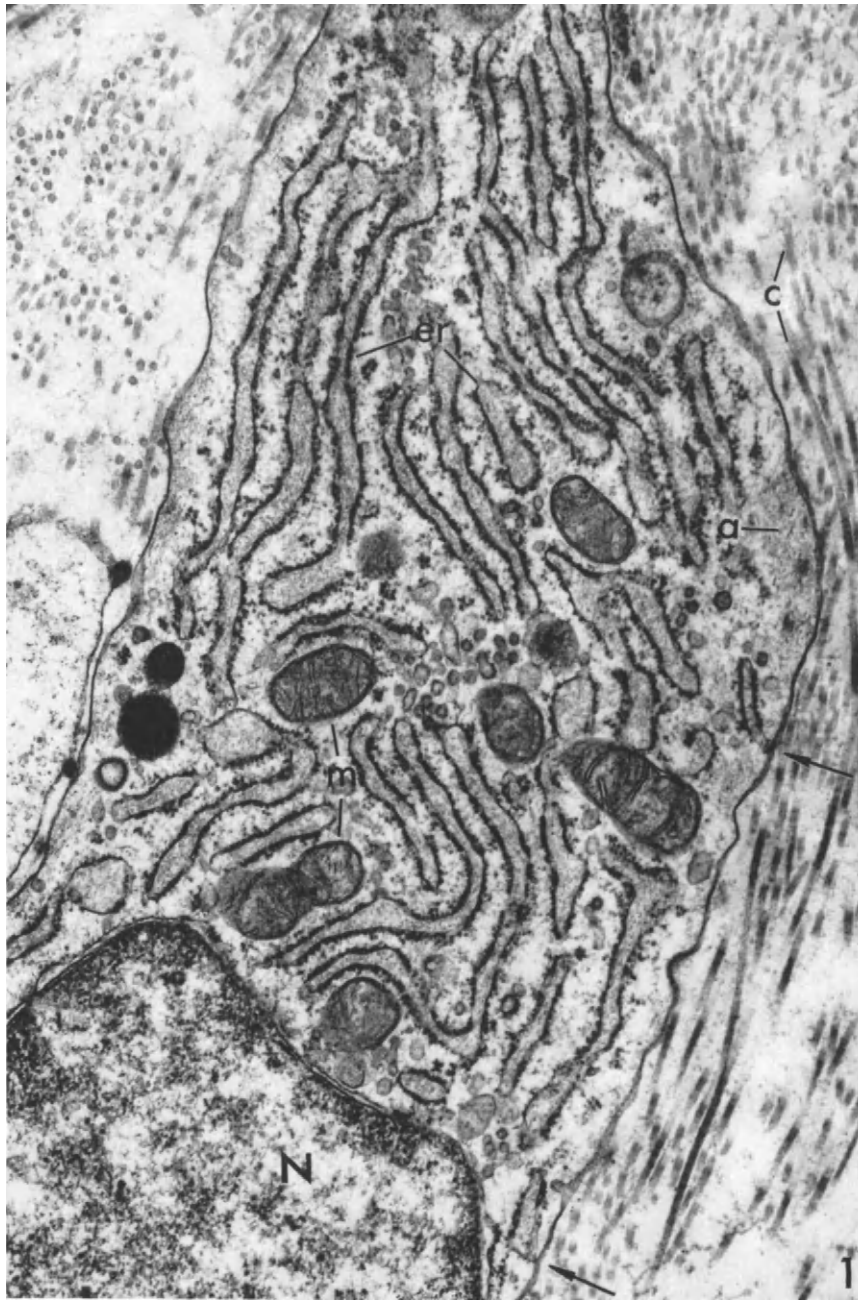

FIG. 1. This electron micrograph is from a representative area of a 7-day-old skin wound in a guinea pig. The fibroblast in this picture is surrounded by numerous

fibroblast adds a degree of complexity to any interpretation of autoradiographic studies of protein synthesis by the cells of the connective tissues.

Electron microscope autoradiography has been used to examine the sequence of participation of the various cellular organelles during the processes of synthesis and secretion of the collagen molecule into the extracellular environment [7, 13]. This same approach in studies of the regenerating limb bud, pancreatic acinar cells, and the thyroid is demonstrated in several of the chapters in this symposium. The purpose of this chapter is to present the results of investigations of the utilization of tritiated proline by wound fibroblasts as seen by high resolution autoradiography. This will be discussed further in relation to the problems of quantitative electron microscope autoradiography. In addition, previous studies of healing wounds using techniques of light microscope autoradiography will be reviewed.

LIGHT MICROSCOPE AUTORADIOGRAPHY

Earlier studies utilizing ^{3}H-glycine and ^{3}H-proline were performed in guinea pigs weighing approximately 300 gm containing a series of 7-day-old wounds. Wounds were removed at 30 minutes, 1 and 4 hours, 1, 3, and 7 days after the intraperitoneal administration of the labeled amino acid. This time period was chosen because the cells of the wounds are actively engaged in collagen synthesis during this interval. The wounds were fixed in 1.5 per cent glutaraldehyde for 2 hours, then postfixed in 2 per cent osmium tetroxide for 1 hour and subsequently embedded in epoxy resin. The light microscope autoradiographs were prepared with 1 μ sections cut from the epoxy-embedded wounds. Representative autoradiographs at 1 hour and 24 hours after the administration of ^{3}H-proline are shown in Figs. 2 and 3. The observations of these autoradiographic studies were quantitated by determining the number of grains per unit area of cells and extracellular collagen at each time period, using a modified Chalkley procedure [2, 15]. The results of the quantitative evaluation of these investigations are presented in Fig. 4. These investigations, and those of others [3, 7], have demonstrated a passage of amino acid through the cells and into the collagen.

The combination of ½–1 μ sections of epoxy-embedded tissues covered

---

collagen fibrils (c) and ground substance. The extensive ergastoplasm (er) so characteristic of these cells is evident, as well as numerous mitochondria (m) and a portion of the nucleus (N) of this cell. Peripheral cytoplasmic aggregates of filaments (a) and two sites where the ergastoplasmic cisternae appear to lose their ribosomes and merge with the plasma membrane (arrows) are noted. Magnification: 29,600 ×.

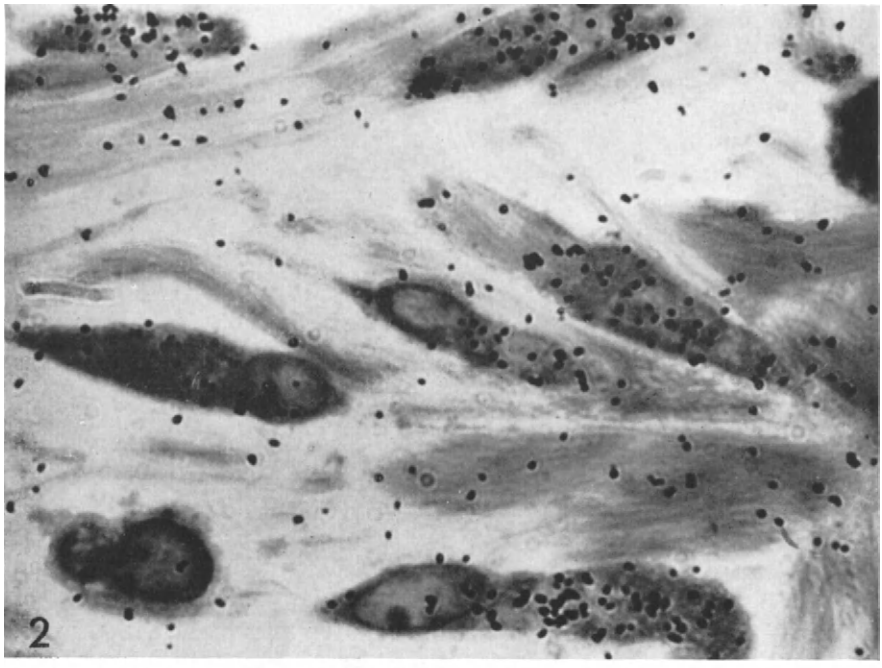
2

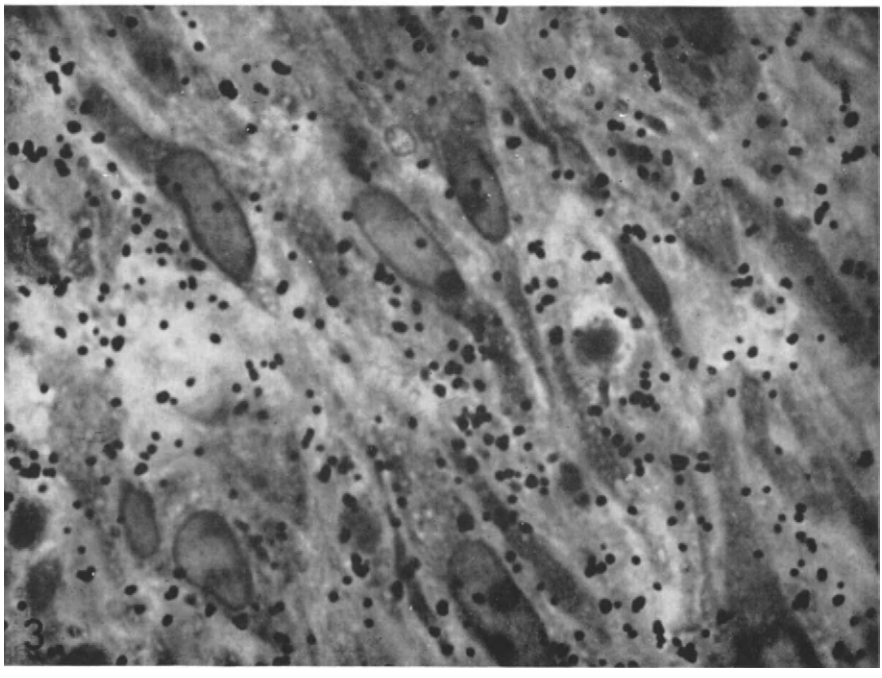
3

by thin layers of uniform nuclear track emulsion provide optimal resolution for autoradiographs at the light microscope level. A number of different stains can be used after developing the autoradiographs to provide good contrast. Beyond the advantage of optimum resolution,

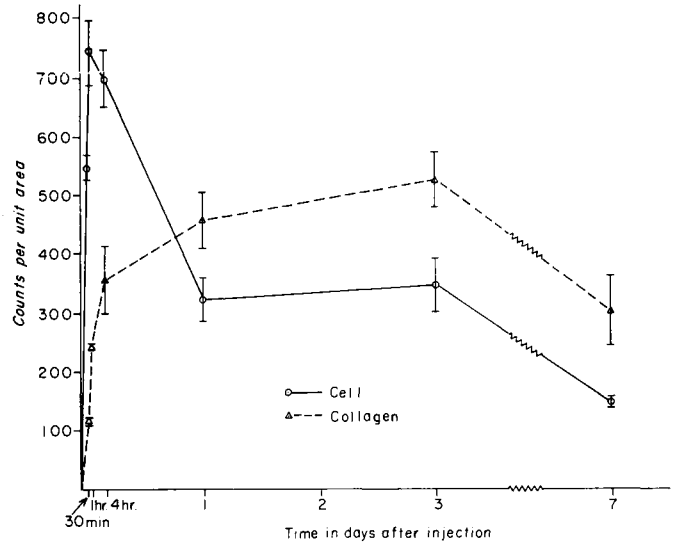

FIG. 4. This graph is a composite of the numbers of counts obtained from a series of normal guinea pigs administered ^{3}H-proline, after 5 weeks exposure of the slides. The points represent means, and the bars, the standard errors for each mean. The abscissa represents the time periods after intraperitoneal injection. It can be seen that the fibroblasts rapidly take up the label, and are maximally labeled within 1 hour and remain heavily labeled until 4 hours, after which they lose their content of isotope. Concomitantly, the collagen is rapidly labeled from 30 minutes to somewhere between 4 and 24 hours.

however, this approach also enables the observer both to visualize and to photograph the specimens with the tissue and the developed silver grains in the same focal plane, thus facilitating observations in these studies. Further information regarding the participation of the various subcellular constituents in the passage of amino acid through the

---

FIG. 2. A light microscope autoradiograph from a 7-day wound 1 hour after the administration of ^{3}H-proline. The cells are seen to contain most of the label at this time. Magnification: 2000 ×.

FIG. 3. An autoradiograph from another wound from the same animal as that seen in Fig. 2. In this case the wound was removed 24 hours after giving ^{3}H-proline. Here the isotope is located primarily over the extracellular collagen fibrils. Magnification: 2000 ×.

fibroblasts is provided by examining electron microscope autoradiographs of a similar sequence. Since the fibroblast does not display an orderly arrangement of its organelles, a quantitative study of this phenomenon would be helpful in obtaining a clearer understanding of this process in this particular cell type.

MATERIALS AND METHODS

Male guinea pigs weighing 250–300 gm were wounded with 6 linear incisions in the dorsal skin. The wounds were allowed to heal for 7 days, at which time each animal was given 3,4-^{3}H-L-proline (20 μc/gm body weight). A wound from each animal was removed 15 and 30 minutes, and 1, 2, 4, 8, and 24 hours after the administration of ^{3}H-proline. These wounds were routinely prepared for electron microscopy after being fixed with 1.5 per cent glutaraldehyde and post-fixed with 2 per cent osmium tetroxide. Sections (ca. 1000 Å thick) were subsequently coated with Ilford L-4, nuclear track emulsion and were exposed for 10 weeks prior to developing them. Further details may be found in a previous article of Ross and Benditt [17].

Randomly taken electron microscope autoradiographs were counted by a modified Chalkley procedure [2] to determine the number of grains per unit area of endoplasmic reticulum. Golgi complex, peripheral cytoplasm, and extracellular collagen for each time period. A clear plastic grid containing 450 intersections was used to determine the per cent area in each micrograph occupied by each of the organelles. The number of silver grains overlaying each compartment was also tabulated. From these observations, a determination of the number of silver grains per unit area of each compartment was derived for each micrograph. In marginal cases, if two thirds or more of a grain lay over an organelle, the grain was counted as related to that organelle. If the grain appeared to be equally distributed over two structures, a coin was flipped. The errors inherent in this approach will be discussed elsewhere in this chapter, as well as in the other presentations in this symposium.

The intracellular compartment labeled "peripheral cytoplasm" consisted of peripheral vesicles, vacuoles, or peripheral cytoplasmic aggregates of fine filaments. It was not always possible to determine which of these underlay a grain; therefore, they were lumped into this single category.

ISOTOPE LOCALIZATION IN SUBCELLULAR COMPARTMENTS

Fifteen minutes after the administration of ^{3}H-proline, large numbers of silver grains can be seen to be located primarily in relation to cisternae of rough endoplasmic reticulum. This is easier to visualize in those cells

where the cisternae are sufficiently dilated so that the problem of determining whether the silver grains are located close to ergastoplasmic ribosomes or cisternal contents is easier to resolve. There are some grains located over Golgi vesicles and cisternae as well at this time; the largest proportion, however, lay over the rough endoplasmic reticulum. There is very little extracellular label present at this time (Fig. 5).

Within 30 minutes of giving ^{3}H-proline, the localization is similar to that seen at 15 minutes, although there are more silver grains present over the Golgi complex. At this time a relatively small number of grains lay over peripheral cytoplasm and extracellular collagen fibrils. Many of the profiles of the rough endoplasmic reticulum display developed silver grains over them as well (Fig. 6).

At 1 and 2 hours the amount of label over the ergastoplasm and Golgi complex remains high, and the number of silver grains over peripheral cytoplasmic constituents and collagen continues to increase (Figs. 7 and 8).

Beyond 2 hours a decrease in the amount of isotope related to both the ergastoplasm and the Golgi complex can be seen. The amount of label over peripheral cytoplasmic components is high after 4 hours, and collagen appears to continue to increase in its content of labeled proline.

Eight hours after ^{3}H-proline administration, the number of silver grains over the cellular constituents has decreased, with the exception of the peripheral cytoplasmic elements, whereas the amount of label over the collagen fibrils remains high (Fig. 9). This pattern continues throughout the remainder of the 24 hours of observation in this experiment (Fig. 10).

These observations are consistent with those previously demonstrated for the pancreatic acinar cell [5, 19], the chondroblast [12], and the thyroid [8]. In those studies the sequence of passage of amino acid through the cells was from ergastoplasm to Golgi, to secretion vesicles, or zymogen granules, with eventual secretion from the cells after varying periods of storage.

QUANTITATION

Two types of quantitative data were obtained from the results of these studies. They consisted of: (a) determinations of the relative distribution of isotope in each of the compartments (in per cent) with time and (b) the distribution of the concentration of isotope (in numbers of grains per unit area of organelle) in each organelle with time.

The results of the relative distribution of developed silver grains are presented in Table I. These results are compatible with the qualitative observations already described.

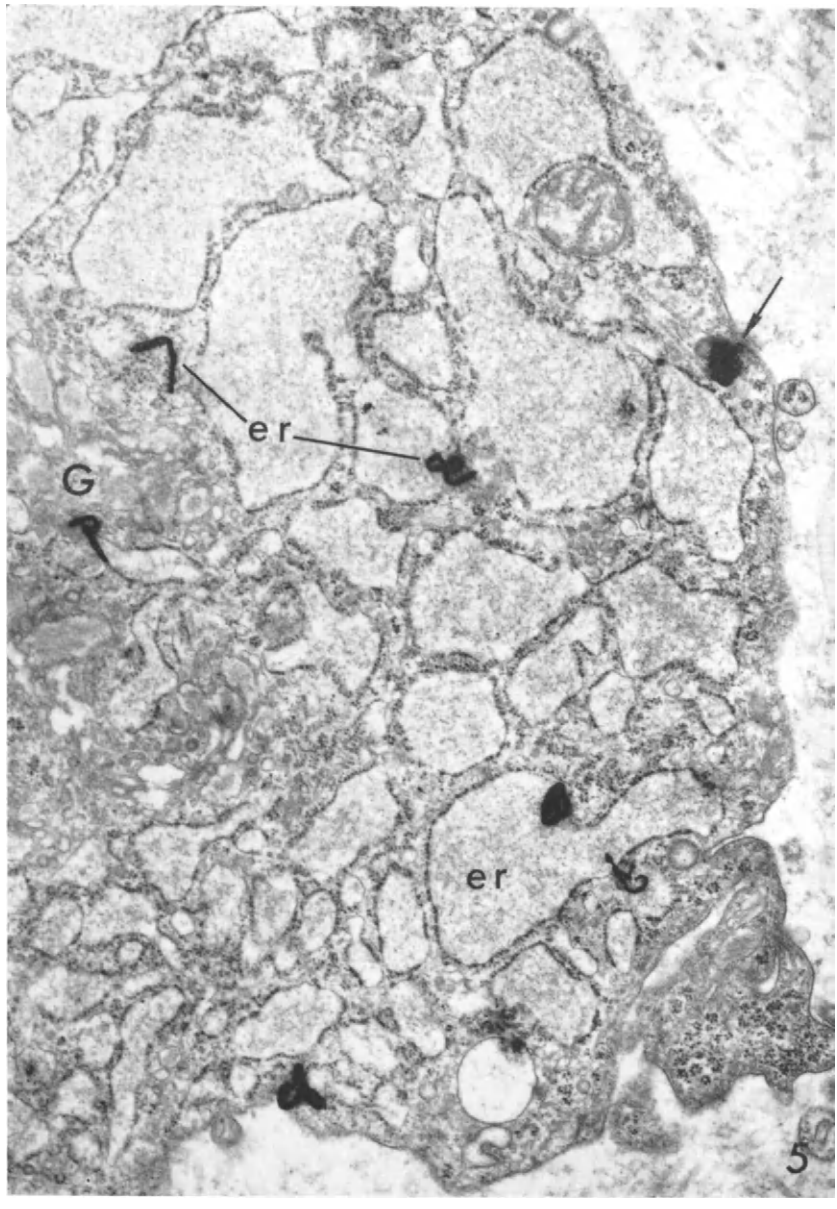

FIG. 5. An electron microscope autoradiograph 15 minutes after ^{3}H-proline administration. The developed silver grains are located primarily over rough endoplasmic reticulum (er). Two grains are present over peripheral cytoplasmic structures (arrows) as well. In the vicinity of the Golgi complex (G) the ergastoplasmic membranes are devoid of ribosomes and one silver grain is located between these two components. Magnification: 25,200 ×.

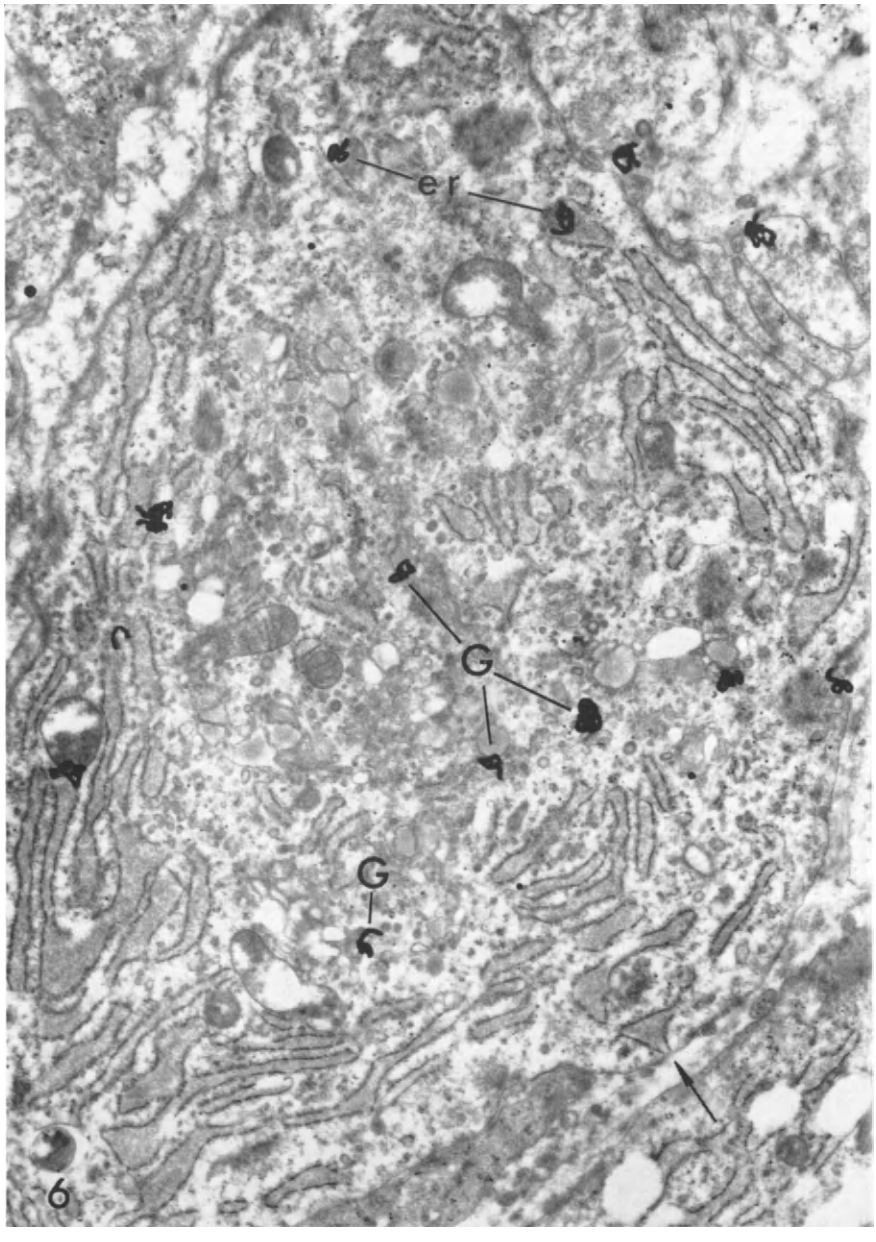

FIG. 6. A fibroblast from a wound 30 minutes after giving ^{3}H-proline is seen in this autoradiograph. In this particular cell, both Golgi (G) components and ergastoplasm (er) are labeled. An area of proximity between ergastoplasm and the plasma membrane is denoted by an arrow. Magnification: 19,800 ×.

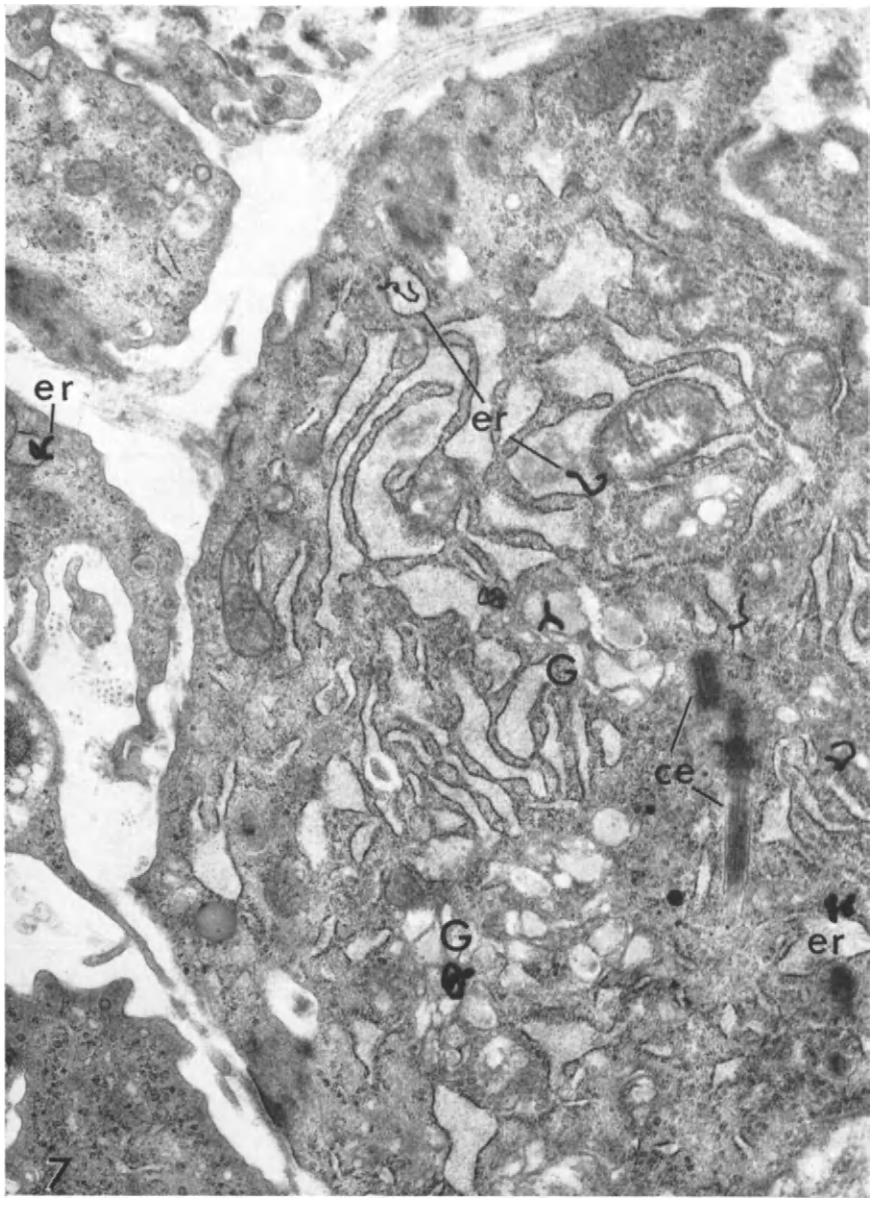

FIG. 7. An autoradiograph from a 7-day-old wound 1 hour after administering ^{3}H-proline. The organelles labeled in the fibroblasts in this micrograph are the ergastoplasm (er) and Golgi complex (G). Two centrioles (ce) are also visible in this cell. Magnification: 17,600 ×.

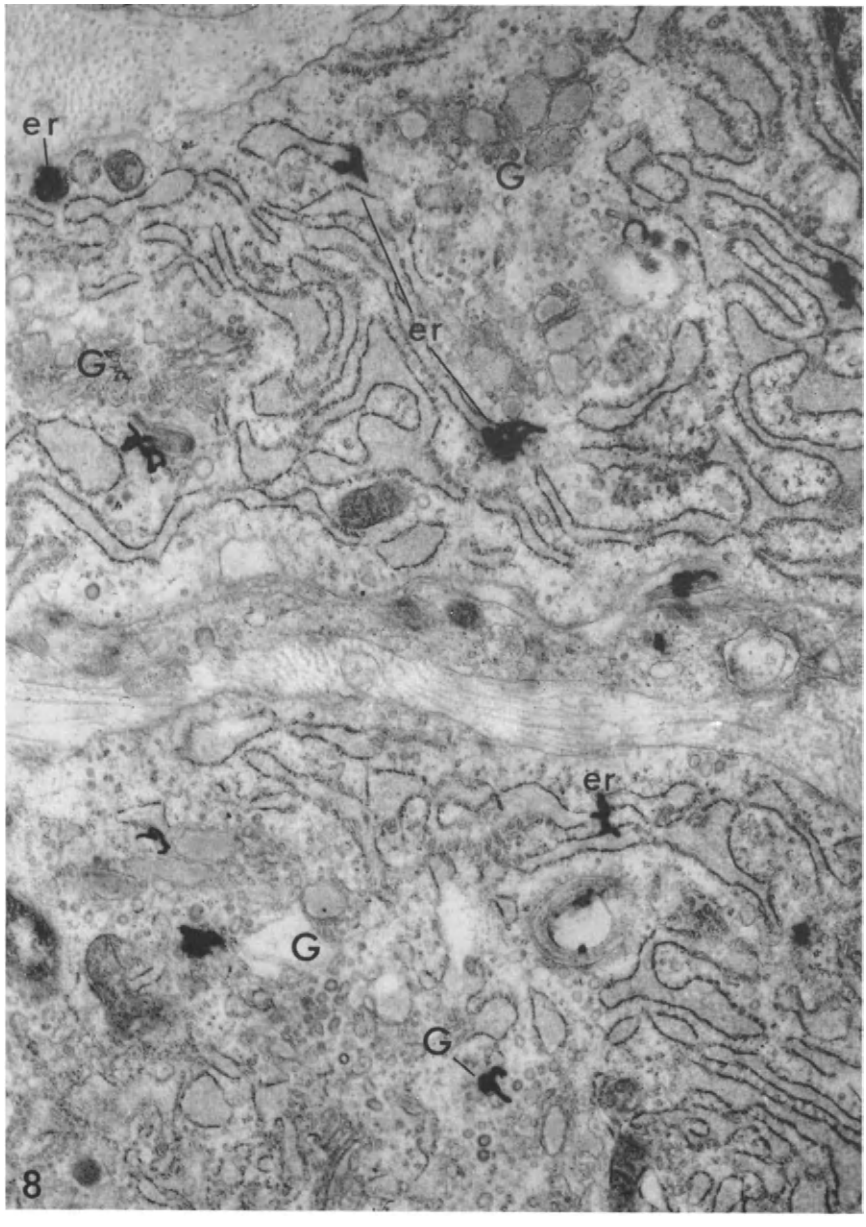

FIG. 8. An autoradiograph 2 hours after ^{3}H-proline administration. Parts of two fibroblasts are present in which the rough endoplasmic reticulum (er) and Golgi zones (G) appear to contain the amino acid. Magnification: 16,200 ×.

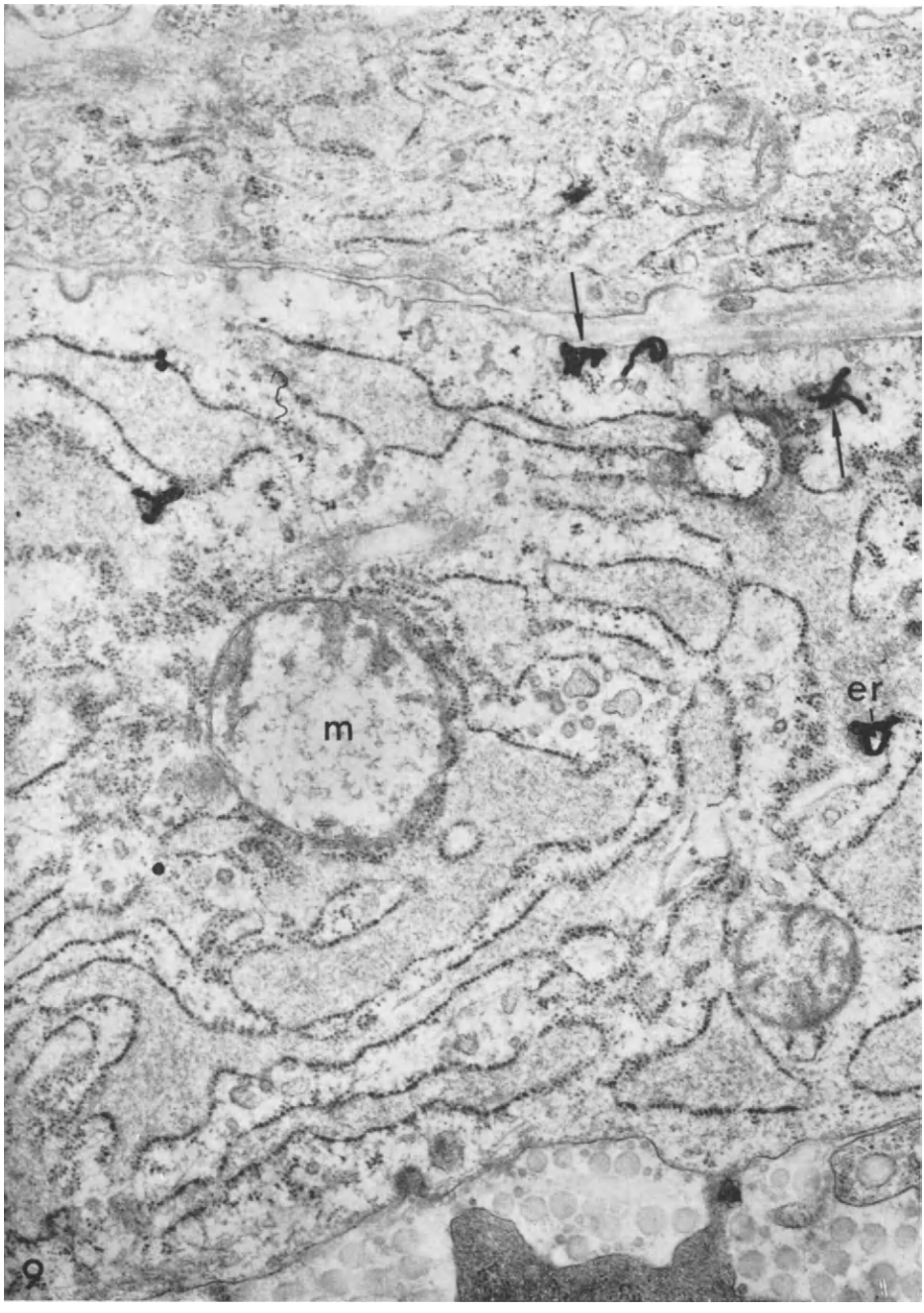

FIG. 9. This micrograph is from a 7-day wound 8 hours after the intraperitoneal administration of ^{3}H-proline. Ergastoplasm (er) and peripheral cytoplasmic vesicles (arrows) are labeled. One silver grain lay equally over collagen and cell periphery and it is not possible to determine the site of its origin. A large mitochondrion (m), possibly an artifact of fixation, is seen in this cell as well. Magnification: 19,000 ×.

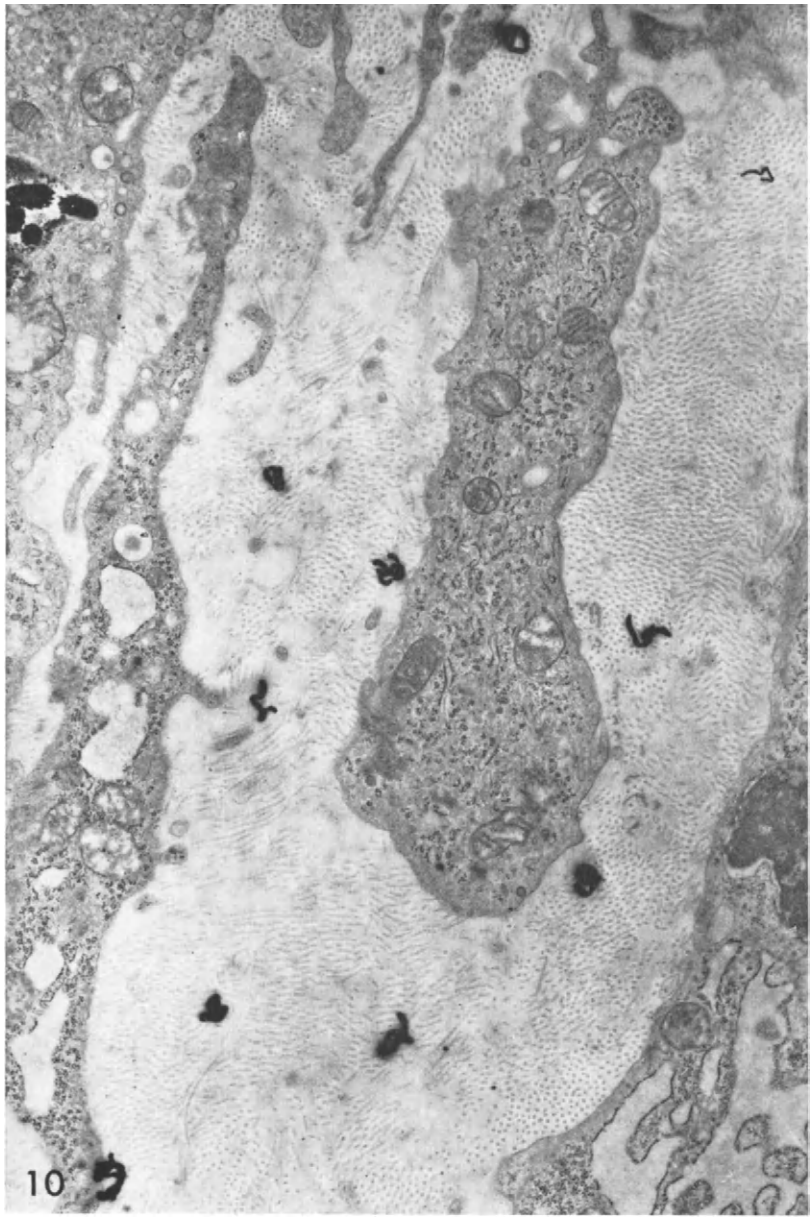

FIG. 10. An autoradiograph 24 hours after giving ^{3}H-proline. In this case the extracellular collagen fibrils are the only elements containing isotope in this picture. Magnification: 15.300 ×. Reproduced with the permission of Pergamon Press [13].

TABLE I. *Relative Distribution of Activity with Time*

Location	Percentage activity						
	15 Min	30 Min	1 Hr	2 Hr	4 Hr	8 Hr	24 Hr
Ergastoplasm	74	59	48	35	28	13	6
Golgi	8	14	15	11	4	3	2
Peripheral cytoplasm	4	10	12	13	15	20	7
Collagen	8	10	17	35	46	51	78

The observations of the change in concentration of developed silver grains with time are presented in Table II and Fig. 11. Several important similarities and differences are discernible on comparing the observations of the relative distribution of isotope (as per cent) with the concentration of isotope (as grains per unit area). These are described below.

Ergastoplasm

Both the relative numbers of grains and the concentration of label are at a maximum in the ergastoplasm 15 minutes after the intraperitoneal administration of ^{3}H-proline. However, beyond this initial maximum, the relative amount of label appears to decrease in the ergastoplasm, but the concentration remains at this maximal level for 2 hours before it begins to drop off. This is probably related to the length of time required

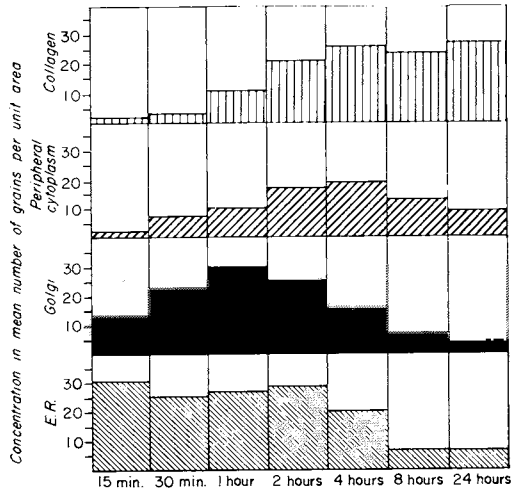

FIG. 11. Concentration of activity of ^{3}H-proline in organelles or collagen with time. This histogram represents the change in concentration of silver grains with time over the four compartments measured in this study. Each bar represents the mean, and the standard errors for each of these means can be found in Table II.

TABLE II. *Change in Concentration (in number of grains/unit area) of Compartment with Time*

	15 Minutes		30 Minutes		1 Hour		2 Hours		4 Hours		8 Hours		24 Hours	
Location	Mean	SE	Mean	SE	Mean	SE	Mean	SE	Mean	SE	Mean	SE	Mean	SE
Ergastoplasm	30.3	±3.0	25.0	±1.7	26.5	±2.7	28.0	±1.9	20.2	±1.8	6.6	±1.0	6.0	±2.0
Golgi	13.3	±3.9	22.5	±3.9	29.9	±3.0	24.9	±5.5	15.1	±3.2	6.5	±1.2	3.4	±2.5
Peripheral cytoplasm	2.6	±1.1	7.3	±1.6	9.9	±1.8	16.8	±3.1	18.8	±2.8	13.1	±0.9	8.9	±2.7
Collagen	1.9	±0.8	3.1	±0.7	10.6	±1.8	20.7	±1.8	25.5	±2.4	22.8	±2.5	26.2	±2.4

for the isotope to arrive in the tissues after intraperitoneal administration, and reflects the absence of a true "pulse" of label.

Golgi

The relative amount of ^{3}H-proline in the Golgi zone never reaches that found in the ergastoplasm (Table I); both of these compartments, however, attain the same maximum concentration of isotope (Table II). In addition, the concentration of proline in the Golgi complex appears to begin to decrease before it does so in the ergastoplasm. Unfortunately the limitations in the resolution of this technique do not permit a clear differentiation between these two events. This is discussed in greater detail below.

Peripheral Cytoplasm

Even at its maximum, the relative amount of label in this compartment, like the Golgi, remains low. The relative amount of label (per cent) does not reach a maximum until 8 hours after giving ^{3}H-proline; however, the concentration of label in this zone (Table II and Fig. 11) reaches a maximum 2 hours after administration of the isotope, and begins to decrease later than that in both the ergastoplasm and the Golgi complex.

Collagen

The relative grain count (per cent) continues to increase until 24 hours, whereas the concentration of isotope reaches a maximum within 4 hours, and then becomes stable (Fig. 11).

There is a continual shift in the position of labeled amino acid as it passes from one compartment of the cell to another during the processes related to synthesis and secretion of collagen. Such motion precludes the possibility of detecting a clear picture, by determination of relative activity alone (per cent), of the passage of label through each compartment except at the very beginning and end of the process. To do this, it is advantageous to determine the concentration of proline in each compartment with time. This would serve as an approximation of the specific activity in each organelle with time. If any subtleties exist in the pathway taken by the label, or if there is more than one pathway, then each individual route would not be evident if only a determination of relative amounts of label were available, as in previous studies [5, 19].

Unfortunately, there are limitations to the accuracy of concentration determinations when emulsions with silver grains the size of those in the Ilford L-4 emulsion (0.14 μ) are used. Elsewhere in this symposium Salpeter has presented the mathematical basis for calculating the combined error due to photographic and geometric errors in electron micro-

scope autoradiographs. Caro [4] has also discussed the problem of resolution. With the Ilford L-4 emulsion it is not possible accurately to relate the filamentous silver grains to objects much smaller than 0.35 μ [1].

It is less difficult to relate developed silver grains to the ergastoplasm and the Golgi complex than other structures in the fibroblasts, as the former are usually sufficiently large to establish such a relation. However, in the case of peripheral cytoplasmic elements or smaller structures, it is not possible to determine which organelle is related to a developed grain. Although the calculated maximum error imposes restrictions on an analysis of grain distribution, a pattern of distribution with time is quite apparent, and a quantitative approach affords further possible insight into this data.

The major limitations in the interpretations of these autoradiographic studies are the lack of information concerning specific activities in the tissue of the substances being studied and the absence of a steady state. Such information would permit a kinetic analysis of the data that is not presently possible. The quantitation of grain concentration in cell organelles with time can only serve as a crude approximation to the specific activities in tissue, but unfortunately this is the best form of data presently available in this kind of investigation. Hopefully, further advances in methodology will permit more accurate analysis of the events as they occur within the cells.

PASSAGE OF ISOTOPE THROUGH THE ORGANELLES OF THE FIBROBLAST

There are at least two logical, possible pathways that amino acids can traverse in the fibroblast during their incorporation into protein and eventual secretion from the cell: (a) the first of these is the one already presented, namely, from the ergastoplasm to the Golgi, to peripheral vesicles, to the extracellular regions; (b) the second possible pathway is from the ergastoplasm directly to the extracellular environs.

Morphologically, the fibroblast displays many areas where the ergastoplasm approximates the plasma membrane and in some instances both membranes appear to fuse (Figs. 1 and 6) [16]. In other areas strings of vesicles can be seen interspersed between the cisternae of the endoplasmic reticulum and the plasma membrane. Both of these present possible sites where material from the ergastoplasmic cisternae could move directly out of the cell, thus by-passing the remaining subcellular compartments.

There is no question that at least part of the administered ^{3}H-proline passed through the Golgi complex. This area has been demonstrated to be active in the synthesis of mucopolysaccharide [6, 10] and it may pos-

sibly serve as a site of formation of protein-polysaccharide complexes which would comprise part of the "ground substance" of the connective tissue, thereby explaining the label seen in this compartment.

In analyzing the results of grain concentrations it is helpful to imagine an analogous system with four compartments of relatively constant size in which the label passes in the sequence demonstrated by the relative grain counts. If such a situation existed, one would also expect each of these compartments to rise to maximal concentration and decrease from this maximum in the same sequence: ergastoplasm, Golgi, peripheral cytoplasm, collagen. All of the observations of change in concentrations are in agreement with this sequence except for the earlier decrease from maximum in the Golgi than occurs in the ergastoplasm. If the two occurrences were sufficiently distinct in time, then this observation would be consistent with the possibility of a shunt from the ergastoplasm that by-passes the Golgi. Unfortunately they are so close that it is not possible to separate these two events statistically. Perhaps with emulsions containing smaller silver grains [18] and with intravenous administration of label to obtain more of a "pulse," it may be possible to separate more clearly these two events, if they are indeed separate. However, it should be noted that these studies do not support the concept that all of the material that passes through the endoplasmic reticulum also passes through the Golgi. Such findings, coupled with observations of areas in the fibroblast interpretable as potential or actual communications of the ergastoplasm with the cell surface, provide the opportunity of suggesting that material may be secreted directly from the endoplasmic reticulum to the extracellular spaces. Although a common pathway of amino acids appeared to have been established in those systems already studied, the possibility that other modes of passage may exist should be entertained if we are to obtain a clear understanding of the numerous and varied roles played by each subcellular system in various cells during the synthesis, storage, modification, and secretion of proteins.

SUMMARY

The morphology of fibroblasts and studies of their utilization of proline in collagen synthesis in healing wounds by both light and electron microscope autoradiography are presented.

Quantitation by determination of both relative activity of organelles and concentration of isotope in organelles are presented and the problems of this approach as related to the limitations in resolution are considered. Previous studies have presented only relative activities, whereas the advantages of determining concentrations in cell organelles allows a clearer separation of events within the cell. The possibility of other pathways

through cells than that of ergastoplasm, to Golgi, to secretion vesicles, should be entertained if a clearer understanding of the function of the various subcellular systems in different cell types is to be attained.

ACKNOWLEDGMENTS

The author is deeply grateful to Professor Earl P. Benditt, in collaboration with whom much of this work was done. He should also like to acknowledge the technical help of Mrs. Dawn Bockus, Miss Leslie Caldwell, and Miss Franque Remington, and the secretarial assistance of Mrs. Jo Steepy.

REFERENCES

1. Bachmann, L., and Salpeter, M. M., *Symp. Quant. Electron Microscopy 1964, Lab. Invest.* **14**, 1041 (1965).
2. Chalkley, H. W., *J. Natl. Cancer Inst.* **4**, 47 (1944).
3. Carneiro, J., and Leblond, C. P., *Exptl. Cell Res.* **18**, 291 (1959).
4. Caro, L. G., *J. Cell Biol.* **15**, 189 (1962).
5. Caro, L. G., and Palade, G. E., *J. Cell Biol.* **20**, 473 (1964).
6. Godman, G. C., and Lane, N., *J. Cell Biol.* **21**, 353 (1964).
7. Hay, E. D., and Revel, J. P., *Develop. Biol.* 7, 152 (1963).
8. Nadler, N. J., Young, B. A., Leblond, C. P., and Mitmaker, B., *Endocrinology* **74**, 333 (1964).
9. Palade, G. E., and Siekevitz, P., *J. Biophys. Biochem. Cytol.* **2**, 671 (1956).
10. Peterson, M., and Leblond, C. P., *J. Cell Biol.* **21**, 143 (1964).
11. Porter, K. R., *Biophys. J.* **4**, 167 (1964).
12. Revel, J. P., and Hay, E. D., *Zeit. Zellforsch.* **61**, 110 (1963).
13. Ross, R., *in* "Advances in Biology of Skin-Wound Healing" (W. Montagna and R. E. Billingham, eds.), Vol. 5, p. 144. Pergamon Press, New York, 1964.
14. Ross, R., and Benditt, E. P., *J. Biophys. Biochem. Cytol.* **11**, 677 (1961).
15. Ross, R., and Benditt, E. P., *J. Cell Biol.* **15**, 99 (1962).
16. Ross, R., and Benditt, E. P., *J. Cell Biol.* **22**, 365 (1964).
17. Ross, R., and Benditt, E. P., *J. Cell Biol.* **27**, 83 (1965).
18. Salpeter, M. M., and Bachmann, L., *J. Cell Biol.* **22**, 469 (1964).
19. van Heyningen, H. E., *Anat. Record* **148**, 485 (1964).
20. Warshawsky, H., Leblond, C. P., and Droz, B., *J. Cell Biol.* **16**, 1 (1963).

DISCUSSION

DR. REVEL: Many fibroblasts have dilated ergastoplasmic cisternae. Do you think that this fact may reflect a relatively slow passage of newly synthesized material to the Golgi area, and thus have some bearing on the Golgi "by-pass" which you have postulated?

DR. ROSS: You wonder whether dilated ergastoplasmic sacs indicate "constipation" of the Golgi and might be related to the possibility of by-passing the Golgi. This may be a possibility, but the dilation is not necessarily an expression of pathological change.

DR. AXELRAD: How early after wounding have you looked for new protein synthesis? It would seem difficult to interpret early observations because of the complication of acute inflammatory response.

DR. ROSS: These studies were conducted in 7-day-old wounds, a time when inflammation has subsided and protein synthesis is active.

DR. PELC: What fraction of the labeled material would have to by-pass the Golgi region to explain the observations?

DR. ROSS: Let me answer your question by stating what should happen if the same fraction of the labeled material were to go through the two compartments. Under these conditions, the material would have to pass through the Golgi approximately 5 times faster than through ergastoplasmic cisternae, since both compartments attain the same maximal concentrations and the Golgi occupies one-fifth as much area of the fibroblast as does the ergastoplasm.

DR. NADLER: As Dr. Ross is aware, to establish, in a steady state, whether a protein in the ergastoplasm is the sole and whole precursor of protein in the Golgi complex, it is necessary and sufficient to show that the specific activity of labeled protein in the first compartment is equal to specific activity of labeled protein in the second when the specific activity of the latter is maximum. If the specific activities are not known, then, assuming that the protein concentrations in all compartments remain constant, the sequence of peaks of label concentration for each compartment would be identical to the sequence of specific activity peaks; and thus would give some indication of the pathway of migration. In this manner, Dr. Ross has shown that protein synthesized in the ergastoplasm migrates to the Golgi complex, the peripheral cytoplasm, and collagen.

Now, if it were observed that radioactivity disappeared entirely from the first compartment (ergastoplasm) before it appeared in the third (peripheral cytoplasm), then it would also be possible to conclude that labeled protein migrated from the first compartment (ergastoplasm) to the second only (Golgi complex), and there was no by-pass migration direct to the third (peripheral cytoplasm). However, failing this observation, it is not possible from data on radioactivity concentrations alone to deduce whether protein synthesized in the ergastoplasm goes wholly to the Golgi complex or by-passes it in part.

DR. ROSS: Dr. Nadler is correct in stating that it would be necessary to know protein concentrations to understand more than the peaks of the concentration. This would be particularly so if one did not know that the volume of compartments, i.e., ergastoplasm (ER), Golgi, etc., remain constant throughout the experiment. Since they do, the increase in rate of loss of label from Golgi compared to ER could be interpreted as either of the following: (1) increased rate of passage through Golgi; (2) by-passage of Golgi. Because the Golgi is a much smaller compartment than the ER, one would expect an increased concentration rather than a decrease, as was observed. Unfortunately, the experimental design did not provide a "pulse" of label; there is no steady state of isotope concentration and it is not possible to know the specific activity of proline, so that these results must remain suggestive at present.

DR. EVERETT: In relation to protein, is there any evidence that the Golgi apparatus does anything more than package the synthesized material?

DR. LEBLOND: Work done with Miss Peterson suggests that the role of the Golgi complex is to synthesize macromolecules of carbohydrate which then combine with the newly synthesized protein, thus making up the carbohydrate-protein combinations present in most secretions.

DR. EVERETT: Do you have convincing evidence that the peripheral cytoplasmic vesicles are concerned with transporting the synthesized material through the cell membrane?

DR. ROSS: With regard to the peripheral vesicles, it is impossible *a priori* to be sure of direction of motion of these structures. However, the progression of label through these toward the outside is compatible with our findings.

THE FORMATION OF THE BASEMENT LAMELLA IN REGENERATING SALAMANDER LIMBS[1]

JEAN-PAUL REVEL

Department of Anatomy, Harvard Medical School, Boston, Massachusetts

INTRODUCTION

The dermis of the salamander, like that of many other aquatic animals, consists of an orthogonal array of collagenous sheets, disposed in a plane parallel to the base of the epidermis [12, 18]. This very regularly organized structure is commonly called a basement lamella. While the collagenous nature of the basement lamella has been clearly established on the basis of morphological observations and by chemical analysis, there have for a long time been two opposed views about its mode of formation. Some investigators have taken the view that it is a product of the subjacent fibroblasts, a concept quite in keeping with its collagenous nature [7, 19]. Others, however, were led to conclude that the epidermis might be involved in the formation of the lamella [1, 11] (also [16] for review). On the basis of morphological observations, Edds and Sweeney [5] suggested that the lamella probably grew from the epidermal side inward. This hypothesis has now been confirmed by autoradiographic studies of protein secretion into the lamella [8, 9]. Our observations also suggested that both the fibroblasts and the epidermis appeared to contribute material to the salamander dermis. The available evidence for this concept of the growth of the lamella and for the possibility of an epidermal contribution will be summarized here.

GROWTH OF THE LAMELLA

Since the morphological data and the chemical analysis [4] of the basement lamella indicates that the only protein present is collagen, we used radioactive proline as a precursor in our experiments [9]. Tritiated proline, successfully employed as a collagen precursor in studies by Leblond and others [10, 15], is well suited for studies of collagen synthesis since it can be a precursor for about a third of the amino acid residues in collagen. We administered the amino acid intraperitoneally to salamanders whose limbs had been amputated 12 days previously.

[1] Supported in part by grants GM K3-13, 979-CIA, and GM11380 from the U.S. Public Health Service.

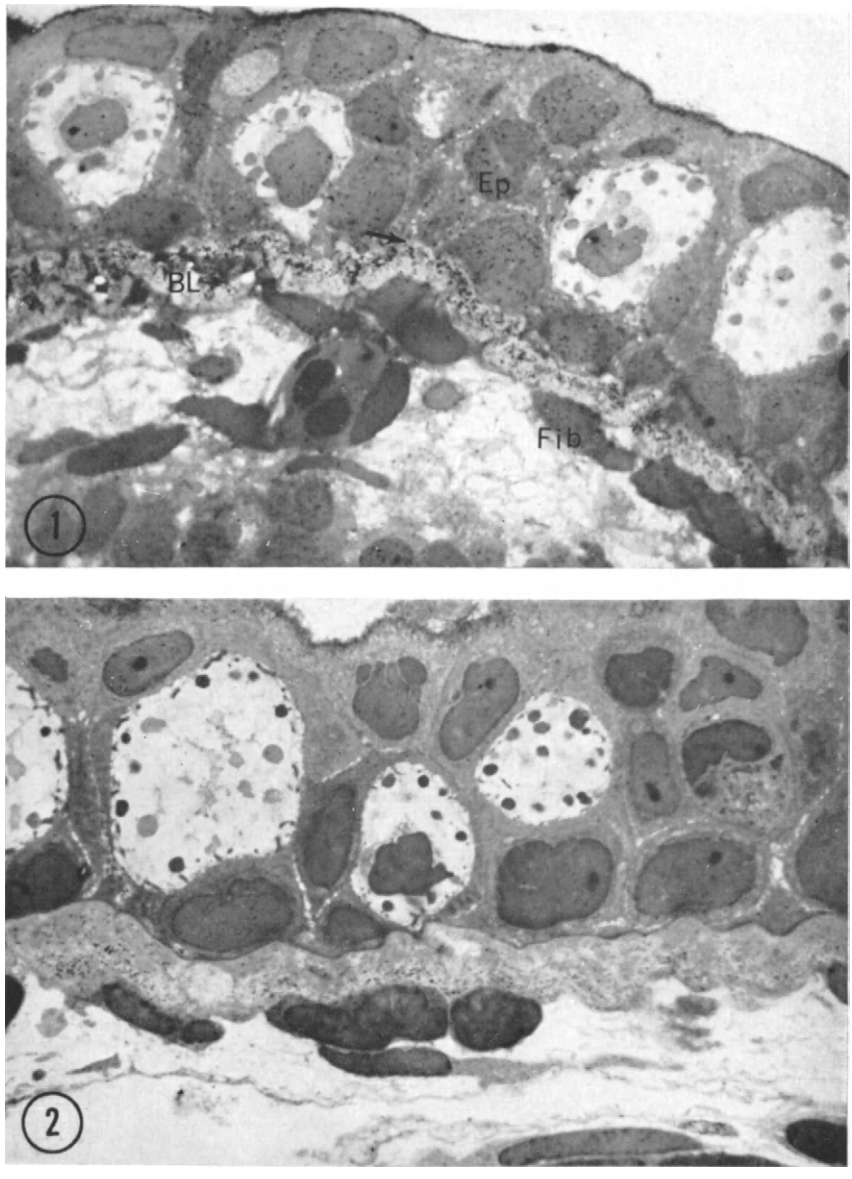

FIG. 1. A light microscope autoradiograph of a 1 μ thick section through a regenerating salamander limb treated *4 days* previously with ^{3}H-proline. The juxta-epidermal band of label secreted some 2–4 hours after injection of the isotope has been displaced inward, as unlabeled material (seen as a clear zone at the arrow) is deposited next to the epidermis. All remaining intracellular label is found in the nucleus, both in the epidermal cells (Ep) and in the fibroblast (Fib) associated

They were in the fingerbud stage of regeneration and the dermis was growing rapidly. The limbs were fixed in osmium tetroxide at different time intervals after the administration of ^{3}H-proline, and embedded in methacrylate. Sections for light and electron microscopy were coated with Ilford L4 emulsion, and processed as described in our earlier communications [9, 13, 14].

The autoradiographs obtained indicated that tritiated proline is incorporated not only into the fibroblasts at the inner surface of the lamella but also into the basal epidermal cells. The label found in fibroblast cytoplasm at an earlier time is subsequently secreted into the extracellular space and migrates upward to the base of the epidermis several microns away. Radioactivity associated with the epidermal cells is at first intense in the juxtanuclear area and then becomes concentrated in the basal cytoplasm. It appears to migrate to the junction between the epidermis and the dermis. Both the epidermal cells above and the fibroblasts underlying the dermis thus participate in the formation of a heavy extracellular juxtaepidermal band of label about 4 hours after administration of the isotope.

An examination of limbs fixed at various intervals up to a month after the incorporation of amino acid shows that the growth of the dermis does indeed take place from the epidermis inward. Four days after administration of tritiated proline one can distinguish a clear nonradioactive zone separating the labeled material from the base of the epidermis (Fig. 1). This zone presumably contains newly synthesized "cold" collagen formed after the labeled proline pool had been exhausted. With time, the original band of radioactivity is displaced further from the epidermis. It reaches the base of the dermis where it is apparently reabsorbed in 3 or 4 weeks. In the lower layers of the lamella the radioactive zone is less condensed than it was originally, presumably because the labeled collagen has been diluted by the addition of unmarked collagen to the fibrils (Fig. 2). This interpretation is in good agreement with the observation that the collagen fibrils in the lower layers of the lamella are thicker than those found in the peripheral juxtaepidermal layers [5]. It seems, therefore, that the

---

with the basement lamella (BL). This intranuclear label will persist for extended periods of time. Magnification: 700 ×.

FIG. 2. A preparation similar to that shown in Fig. 1, but from an animal sacrificed 3 weeks after injection of the radioactive precursor. At this time the lamella has reached its normal thickness. The radioactivity originally found at the junction of the dermis and epidermis is now seen in the lower half of the lamella, and appears to have been diluted, presumably by the addition of unmarked collagen. These autoradiographs indicate that the lamella grows from the epidermal side inward, and that new collagen is also added interstitially. Magnification: 700 ×.

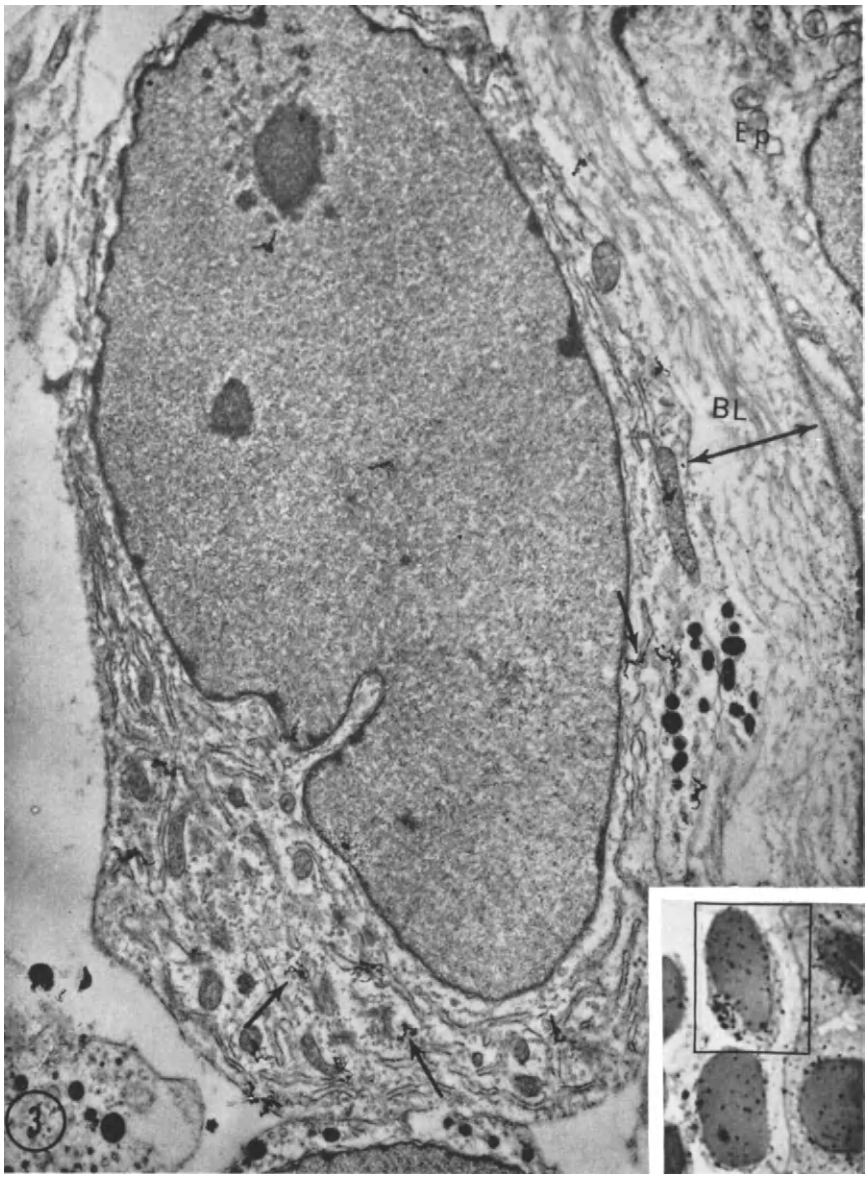

FIG. 3. An electron micrograph of an autoradiograph showing the distribution of label in a fibroblast 30 minutes after treatment with ^{3}H-proline. The radioactivity (see silver grains at the arrows) is associated with the cisternae of the endoplasmic reticulum and the Golgi area of the fibroblast. Little label can be seen at this time in the basement lamella. The inset depicts an autoradiograph of a thick section of the same cell, seen in the light microscope. There is intense radioactivity in the area of the cytoplasm which can be identified as a Golgi zone on the basis of the electron micrograph. Magnification: 10,000 ×; inset 1,000 ×.

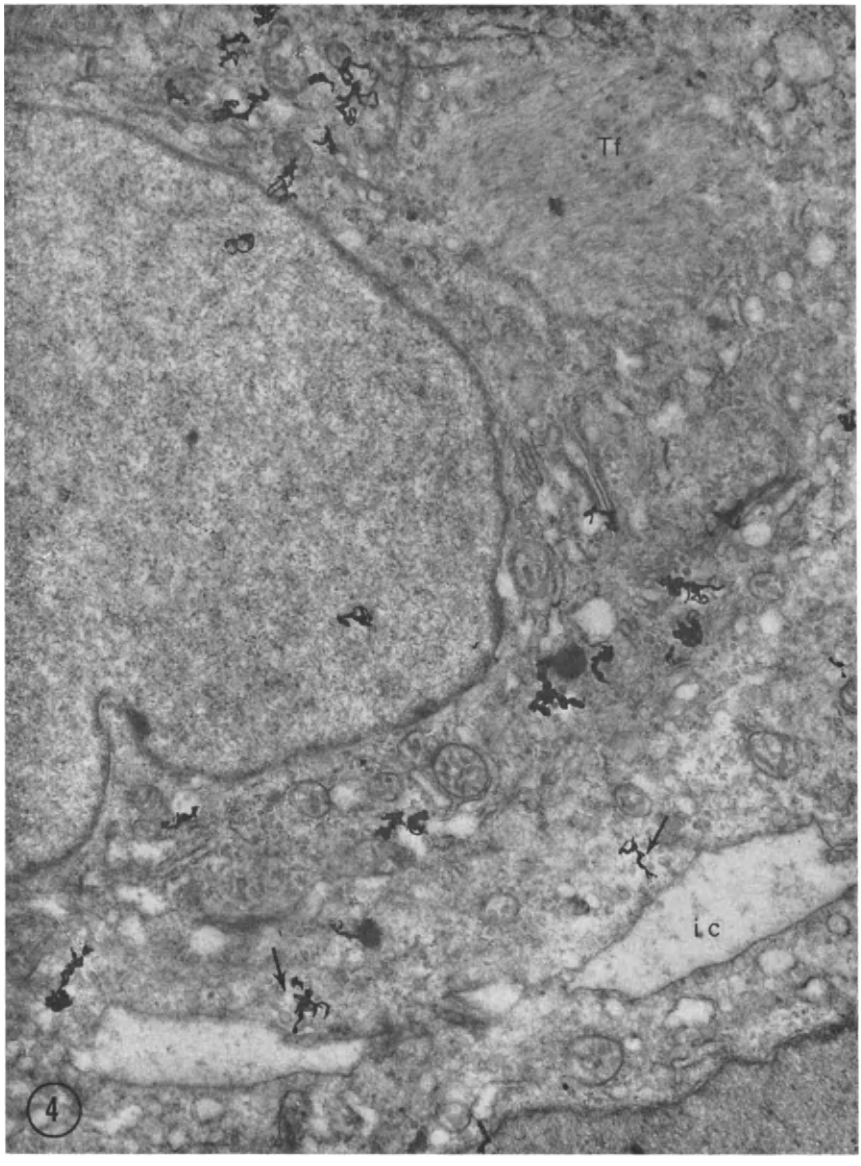

FIG. 4. A labeled epidermal cell, 30 minutes after treatment with tritiated proline. There is an accumulation of label in the perinuclear region of the cell, where most of the cell organelles are found. This section shows radioactivity concentrated in the Golgi area. Some silver grains are also found close to the plasmalemma, seemingly associated with small secretory vesicles (arrows). No incorporation of isotope can be detected in bundles of tonofilaments (Tf). The labeling pattern observed in epithelial cells suggests that they secrete a proline-rich material into the extracellular milieu (ic, interfacial canal). Magnification: 15,000 ×.

lamella grows by accretion of material at its juxtaepidermal surface, and also by some interstitial deposition of material.

CYTOLOGY OF SECRETION

Electron microscope autoradiography of thin sections through regenerating limbs fully confirms and extends the data obtained in the light microscope. Radioactivity is found over the endoplasmic reticulum of the fibroblasts and basal epidermal cells at 15 minutes, and over the Golgi area at 30 minutes (Figs. 3 and 4). The Golgi area and the endoplasmic reticulum occupy a juxtanuclear position in the epidermal cells, thus accounting for the perinuclear distribution of label observed in the light microscope. At later times the label is found over small vesicles near the base of the cells in the epidermis and near the cell membrane in the fibroblasts. The secretion of labeled material into the extracellular milieu seems to take place by the fusion of such vesicles with the plasmalemma. Clearly, then, the intracellular distribution of the label in both fibroblast and epidermal cells is in all respects similar to that observed in other protein-secreting cells, such as the pancreatic acinar cell [2, 17] or the chondrocyte [14].

Electron microscope autoradiographs show that by 4 hours the label is definitely extracellular, and the distribution of label at that time can be interpreted as showing radioactivity in both the collagen fibrils of the lamella and in the basement lamina (Fig. 5). Since, as we have already seen, the label disappears from the juxtaepidermal zone of the dermis in a few days, one could assume that the filamentous material of the lamina can be converted to striated filaments or that it has a fairly rapid turnover. It may also be that the radioactivity observed in the lamina does not represent labeling of intrinsic protein, but rather that some radioactive material is simply passing through the lamina. However tempting it may be to speculate about these or yet other possibilities, the data available at the present time only indicate that the epidermis is secreting a proteinaceous component into the same space where labeled material originating from the fibroblasts also accumulates.

NATURE OF THE EPIDERMAL CONTRIBUTION

Little discussion is needed about the product of the activity of the fibroblasts. These cells have been clearly shown to be involved in the elaboration of the collagen and protein polysaccharides of the connective tissue (for review see Fitton-Jackson [6]). The possible nature of the material contributed by the epidermis is less obvious and must be examined more closely. In our approach to this problem we have tried to

design experiments so that one could distinguish the products of the epidermis from those of the connective tissue. In a first series of attempts in collaboration with M. Edds, we removed the epidermis from the salamander larvae, at such a time after the administration of label that

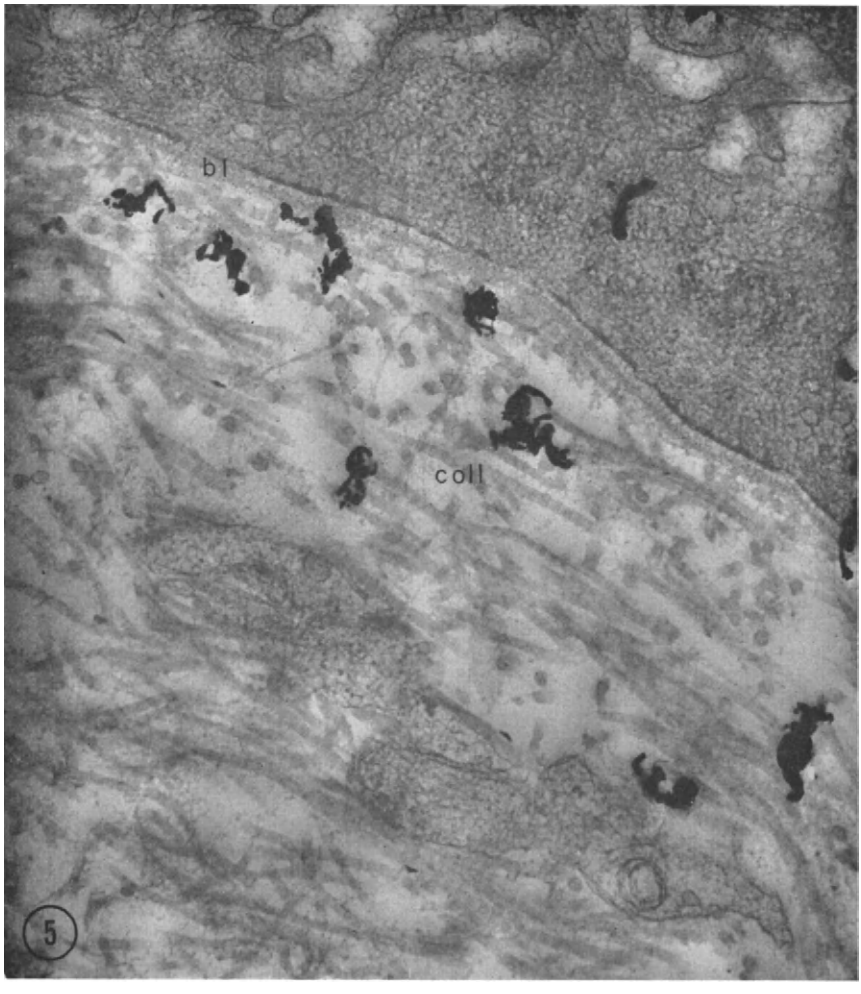

FIG. 5. The junction of the epidermis and the basement lamella in a sample fixed 4 hours after the administration of tritiated proline. The basal lamina can be seen as a finely filamentous layer, some 500 Å thick, separated from the cell membrane of the epithelial cell by a narrow clear zone. Striated collagen fibrils are found in close proximity to the lamina and elsewhere in the lamella. The radioactivity is mostly extracellular, and seems to be associated with the striated collagen fibrils, and perhaps also with the basement lamina. Magnification: 30,000 ×.

the label would still all be intracellular (1 hour). The epidermal cells were removed by sonication, washed, dialyzed, and finally hydrolyzed. The amino acids of the nondialyzable fraction were then separated by thin layer chromatography, and the radioactivity in each was counted after elution. In this fashion it was possible to show that, besides proline, epidermal pellets prepared by sonication also contained hydroxyproline, an indication of the possible presence of collagen-like protein. In this type of experiment, however, it proved difficult to eliminate completely the possibility that radioactivity found in hydroxyproline is due to a contamination by collagen extracted from the underlying connective tissue cells during the isolation.

In order to circumvent this difficulty we are now attempting to do similar experiments with epidermal cells grown in culture, under conditions where no connective tissue cells are present, in the hope that we will be able to characterize more fully the material synthesized by the epidermis. One of the systems currently under investigation is the corneal epithelium of the 12–14 day old chick embryo. The cornea is growing rapidly at this time and becomes organized into an orthogonal array of collagen fibrils strikingly reminiscent of the salamander dermis. Corneal epithelium can easily be removed with trypsin as an intact epidermal sheet, with no contamination by connective tissue cells. Since it has been shown that embryonic skin can grow and differentiate if placed in contact with killed connective tissue [3], we decided to place our stripped corneal epidermis on a substratum of killed corneal stroma, from which the connective tissue cells had been removed by osmotic lysis. Epithelium for culture is stripped from other corneas after enzymatic treatment and placed on the dead stroma. After 2 days in culture, the epithelium is exposed to tritiated proline for 2 hours. Half of each culture is fixed for autoradiography and electron microscopy 2 hours later, while the other half is used for radiochemical analysis of the amino acids of the nondialyzable fraction. Autoradiography shows an intense incorporation of labeled proline into the epidermal cells, especially the basal cells. Electron microscope observation of the cultured epidermal cells shows them to have a morphology very reminiscent of the epidermis in the salamander skin. The cells have well-developed endoplasmic reticulum and Golgi apparatus. The basement lamina, however, seems to be absent. We have as yet too little experience with this system to attempt to draw any firm conclusions as to the types of protein the epidermis may be synthesizing. It is clear, nevertheless, that radioactive proline can be identified in all the cultures, except control cultures consisting of killed stroma alone. In addition to proline, several cultures have also contained a substantial amount of labeled hydroxyproline, identified by rechromatography in a

different solvent, and by three specific color reactions. While far from being conclusive, these preliminary data raise anew the possibility that epidermal cells may indeed synthesize a protein related to those found in the connective tissue.

SUMMARY

The formation of the basement lamella in the regenerating salamander limb has been studied by autoradiographic techniques. Material for the lamella is contributed by both epidermis and fibroblasts, and the lamella grows from the epidermal dermal junction inward.

ACKNOWLEDGMENT

I wish to thank my colleague, Dr. Elizabeth D. Hay, for allowing me to use unpublished material from our previous studies in the preparation of this manuscript.

REFERENCES

1. Anderson, E., and Kollros, J. J., *J. Ultrastruct. Res.* **6**, 35 (1962).
2. Caro, L. G., and Palade, G. E., *J. Cell Biol.* **20**, 473 (1964).
3. Dodson, J. W., *Exptl. Cell Res.* **31**, 233 (1963).
4. Edds, M. V., Jr., and Sweeny, P. R., *in* "Synthesis of Molecular and Cellular Structures" (D. Rudnick, ed.), p. 111. Ronald Press, New York, 1961.
5. Edds, M. V., Jr., and Sweeny, P. R., *Proc. 5th Intern. Congr. Electron Microscopy* Vol. II, p. QQ-2. Academic Press, New York, 1962.
6. Fitton-Jackson, S., *in* "The Cell" (J. Brachet and A. E. Mirsky, eds.), Vol. VI, p. 387. Academic Press, New York, 1964.
7. Harrison, R. G., *J. Exptl. Zool.* **41**, 349 (1925).
8. Hay, E. D., *in* "The Epidermis" (W. Montagna, ed.), p. 97. Academic Press, New York, 1964.
9. Hay, E. D., and Revel, J. P., *Develop. Biol.* 7, 152 (1963).
10. Leblond, C. P., *Ann. Histochim.* **8**, 43 (1963).
11. Leeson, C. R., and Threadgold, L. T., *Acta Anat.* 44, 159 (1961).
12. Porter, K. R., *Proc. 3rd Intern. Conf. Electron Microscopy* p. 539. Royal Microscop. Soc., London, 1954.
13. Revel, J. P., and Hay, E. D., *Exptl. Cell Res.* **25**, 474 (1961).
14. Revel, J. P., and Hay, E. D., *Z. Zellforsch.* **61**, 110 (1963).
15. Ross, R., and Benditt, E. P., *J. Cell Biol.* **15**, 99 (1962).
16. Singer, M., and Andrews, J. S., *Acta Anat.* **28**, 313 (1956).
17. Warshawsky, H., Leblond, C. P., and Droz, B., *J. Cell Biol.* **16**, 1 (1963).
18. Weiss, P., and Ferris, W., *Exptl. Cell Res.* 6, 546 (1954).
19. Weiss, P., and Ferris, W., *J. Biophys. Biochem. Cytol. Suppl.* **2**, 275 (1956).

DISCUSSION

DR. BÉLANGER: Do the same epidermal cells in your material make both collagen and collagenase?

DR. REVEL: It is not known.

DR. LEBLOND: Your pictures showed that the radioactive band of newly synthesized basement material arose at the junction of epithelial cells and basement lamina and that the band appeared farther and farther from epithelial cells as new base-

ment material accumulated. On the other hand, it seemed in at least one of your pictures that the distance between the radioactive band and the fibroblast layer decreased with time. If so, there would be a turnover of the basement lamina with production on the outer surface and resorption on the inner surface. Under these conditions, there would be both growth and turnover. What do you think?

DR. REVEL: Because the band of label becomes more diffuse as the lamella grows, it is not possible to measure precisely its distance from the base of the lamella, and thus obtain direct evidence for turnover. Even so, a comparison of Fig. 1 with Fig. 2 certainly suggests that the label reaches the base of the lamella, and we believe that there probably is some turnover of the collagen, "old" collagen being removed from the inner layers while new collagen is deposited at the outer surface. It is possible that the growth and the thickness of the lamella is controlled by the relative rates of these two opposing processes.

DR. TONNA: I think your results, showing deposition of protein precursors not only across the surfaces where collagen fibrils are assembled, but also into the intercellular spaces where one never sees collagen, are fascinating. They re-emphasize the importance of the local extracellular environment and its effect in collagenogenesis.

THE ELABORATION OF THYROGLOBULIN BY THE THYROID FOLLICULAR CELLS

N. J. NADLER

Department of Anatomy, McGill University, Montreal, Canada

INTRODUCTION

The synthesis of thyroglobulin, an iodinated glycoprotein, is essential to the production of the hormones in the thyroid gland. Early experimental work [11, 19] showed that, in all thyroid follicles, thyroglobulin was located mainly in the colloid of the lumen. However, it was realized that the lumen of the follicle was unlikely to be the site where complete synthesis of thyroglobulin takes place; and there was for a long while considerable debate regarding exactly what, in the follicular cells, are the antecedents of colloid (and, therefore, of thyroglobulin). The hypothesis which was most widely held, namely, that it was the intracellular colloid droplets [8, 9, 33], has been rejected by the conclusive demonstration that these droplets are derived from the colloid in the lumen, and, therefore, cannot be its source [25]. In fact, the problem of how thyroglobulin is synthesized in the follicular cells, and how it emerges into the colloid of the lumen, could not be resolved by classical techniques alone, and had to await the advent of more modern experimental approaches.

In this regard, radioautography has proved an effective technique to determine sites of synthesis of biological substances. A tracer amount of an appropriate precursor substance tagged with radioactive label is injected into an animal. In this manner proteins being synthesized acquire the label of the precursor radioactive amino acid, and can be localized in tissues by radioautography. However, proteins may undergo migration soon after they are formed [18, 35]. Hence, the earliest location of the label should indicate the site of synthesis of proteins, whereas tracking the later locations should reveal the course of their eventual migration.

SITES OF SYNTHESIS AND MIGRATION OF THYROID PROTEINS

Thus, to investigate the synthesis and secretion of thyroid proteins [22], mice were injected with leucine labeled with tritium (^3H) and sacrificed ½ hour and 36 hours later. Radioautographs of the thyroid showed that, at the early time, silver grains in the photographic emulsion

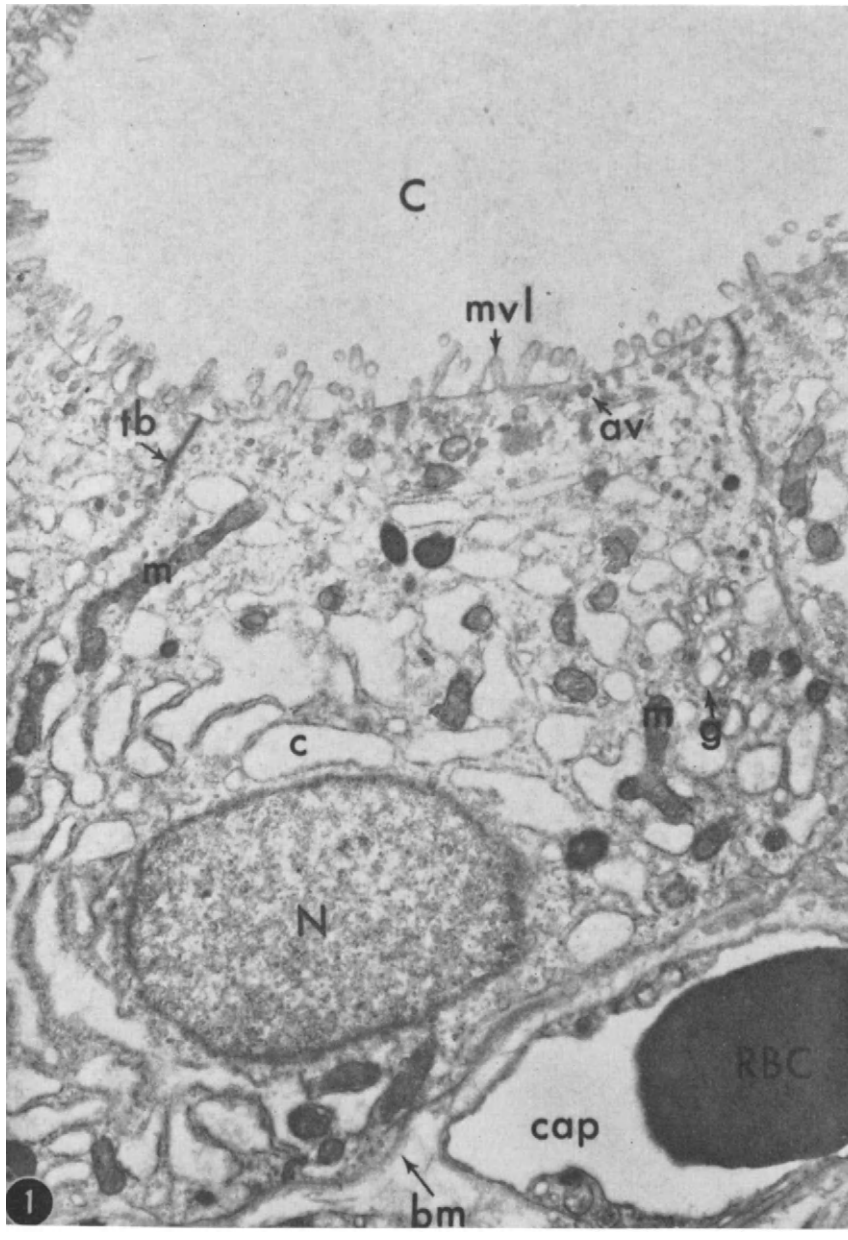

FIG. 1. Electron micrograph of a follicular cell. Magnification: about ×9000. From the top down, are shown the *colloid* (C), uniformly filling the lumen of the follicle; the *apical membrane* of the follicular cell with microvilli (mvl) and with terminal bars (tb) at the junction with the lateral membranes; the region of the

were present only over follicular cells, whereas at the later time they were also present over the colloid. Hence, protein synthesized in the cells had migrated to the colloid. Now, it has been demonstrated that the predominant protein present in the colloid is thyroglobulin [10], and that leucine is one of the most abundant amino acids in the thyroglobulin protein molecule [13]. Hence, it was inferred that the protein synthesized in the cells of the thyroid follicle, and secreted into the colloid, is the protein moiety of thyroglobulin.

This type of experiment was later repeated on a larger scale in the rat: 2.5 μc ^{3}H-leucine per gram body weight was injected, and groups were killed at 10 and 30 minutes, 4 and 36 hours, 7 and 30 days [26]. Thyroid glands were fixed in Bouin fluid, cut into sections of 5 μ and stained with periodic acid-Schiff and hematoxylin. These sections were radioautographed by the coating technique [17], using Eastman Kodak NTB2 photographic emulsion, exposing for 60 days. The radioautographs obtained at 10 minutes after injection showed a fairly uniform distribution of grains over the cytoplasm of every follicular cell and every follicle (Fig. 2). At ½ hour, the radioautographic density over the cells had increased, but was still distributed more or less evenly throughout (Fig. 5). At 4 hours, however, the grains accumulated over the region of the cells immediately proximal to the apical surface, sometimes extending to the outside to make their first appearance over the colloid of the follicular lumen (see Fig. 9). In this manner, the grains over the neighboring cells in a given follicle were arranged into well-defined rings, concentric with the cell–colloid interface. At 36 hours, these rings were no longer distinguishable; only a somewhat diffuse reaction was visible over the cytoplasm, which persisted up to 7 days, but not to 30 days. Meanwhile, a pronounced reaction was seen over the entire colloid at 36 hours and 7 days.

Since at 10 minutes after injection of ^{3}H-leucine, the radioautographic reaction, confirmed in repeated experiments, was present over every follicular cell, it means that the synthesis of protein must take place in all follicular cells and must take place continuously.

Until 30 minutes after injection of ^{3}H-leucine, labeled protein remained distributed throughout the cytoplasm of the follicular cells. However, by 4 hours analysis of grain counts revealed that more than half of this protein had migrated immediately below the apical surface

---

small *apical vesicles* (av); the *supranuclear region* with mitochondria (m), Golgi zone (g), and cisternae of the ergastoplasm (c); the *base of the cell* with nucleus (N), mitochondria, and cisternae of ergastoplasm; the *basement membrane* (bm) on the outside of the cell, and a capillary (cap) with a red blood cell (RBC).

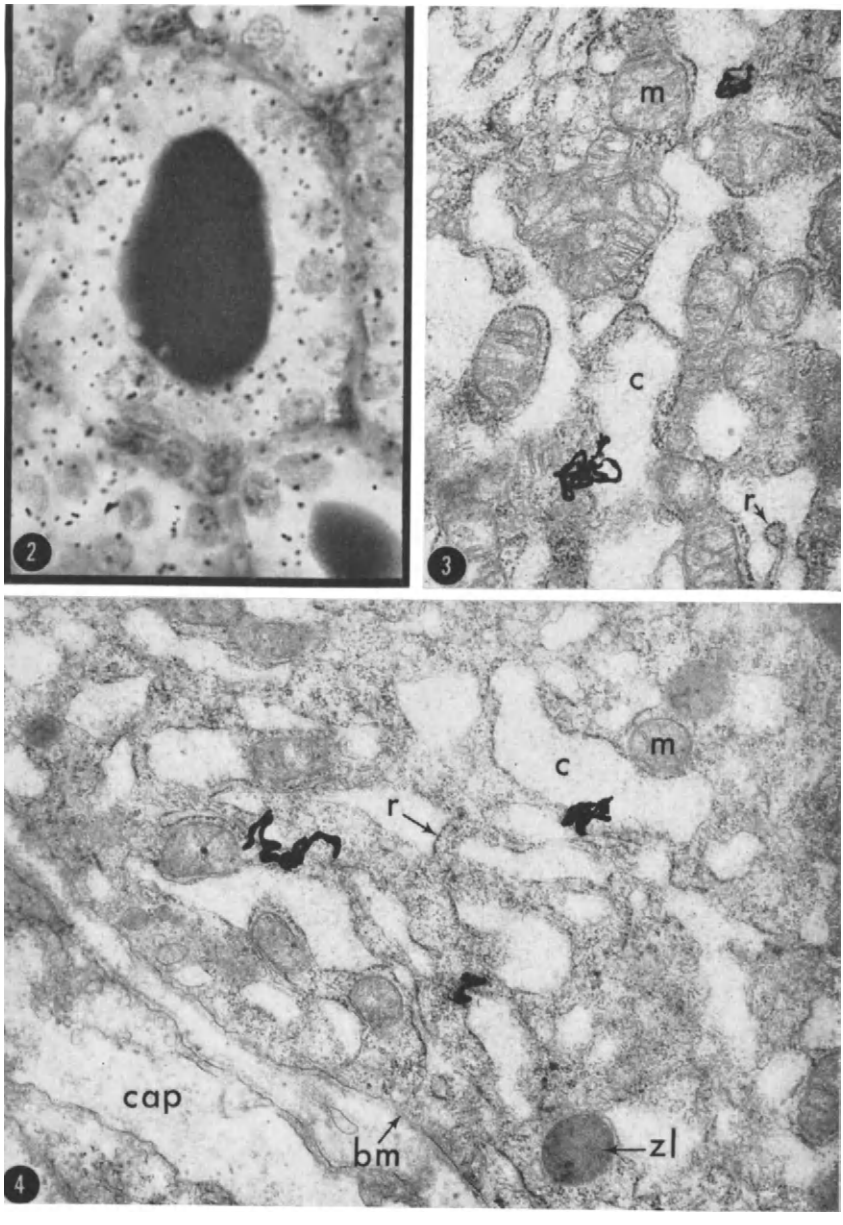

FIGS. 2–4. All preparations are coated radioautographs from rats sacrificed 10 minutes after injection of ^{3}H-leucine.

FIG. 2. Light microscope preparation stained with periodic acid-Schiff-hematoxylin. The follicle in the center shows diffuse radioactivity in the cells, but none in the colloid. Magnification: ×1200.

of most of these cells close to, and even reaching the edge of the colloid. By 36 hours, the migration of labeled proteins extended to the whole of the colloid. Since the blood level of the precursor leucine label was known to reach a very low level within minutes after injection [3], it

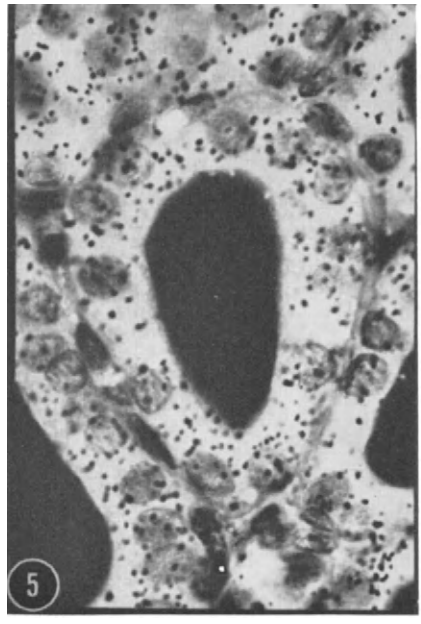

FIG. 5. Light microscope coated radioautograph of periodic acid-Schiff-hematoxylin stained preparation from rat sacrificed 30 minutes after injection of ^{3}H-leucine. Radioactivity is diffuse in cells. Magnification: ×1200.

is clear that any labeled protein appearing in the colloid 4 hours or later after injection cannot have originated direct from the blood leucine label, and must therefore have had to be derived from the follicular cells. Furthermore, it was calculated that the decrease in cellular radio-

---

FIG. 3. Electron microscope preparations (Ilford L-4 emulsion, development in Dektol). The micrograph shows mitochondria (m) and ergastoplasm with dilated cisternae (c) and attached ribosomes (r). Two black, filamentous silver grains can be localized over the ergastoplasm, straddling the walls of cisternae. Magnification: ×30,000.

FIG. 4. Electron microscope preparations (as in Fig. 3). The micrograph again shows mitochondria (m) and ergastoplasm with dilated cisternae (c) and attached ribosomes (r). A capillary can be seen (cap) separated from the base of the follicular cell by a basement membrane (bm). A zymogen-like granule (zl) can also be seen in the follicular cell. The three silver grains can be localized over the membranes enclosing the cisternae of the ergastoplasm. Magnification: ×30,000.

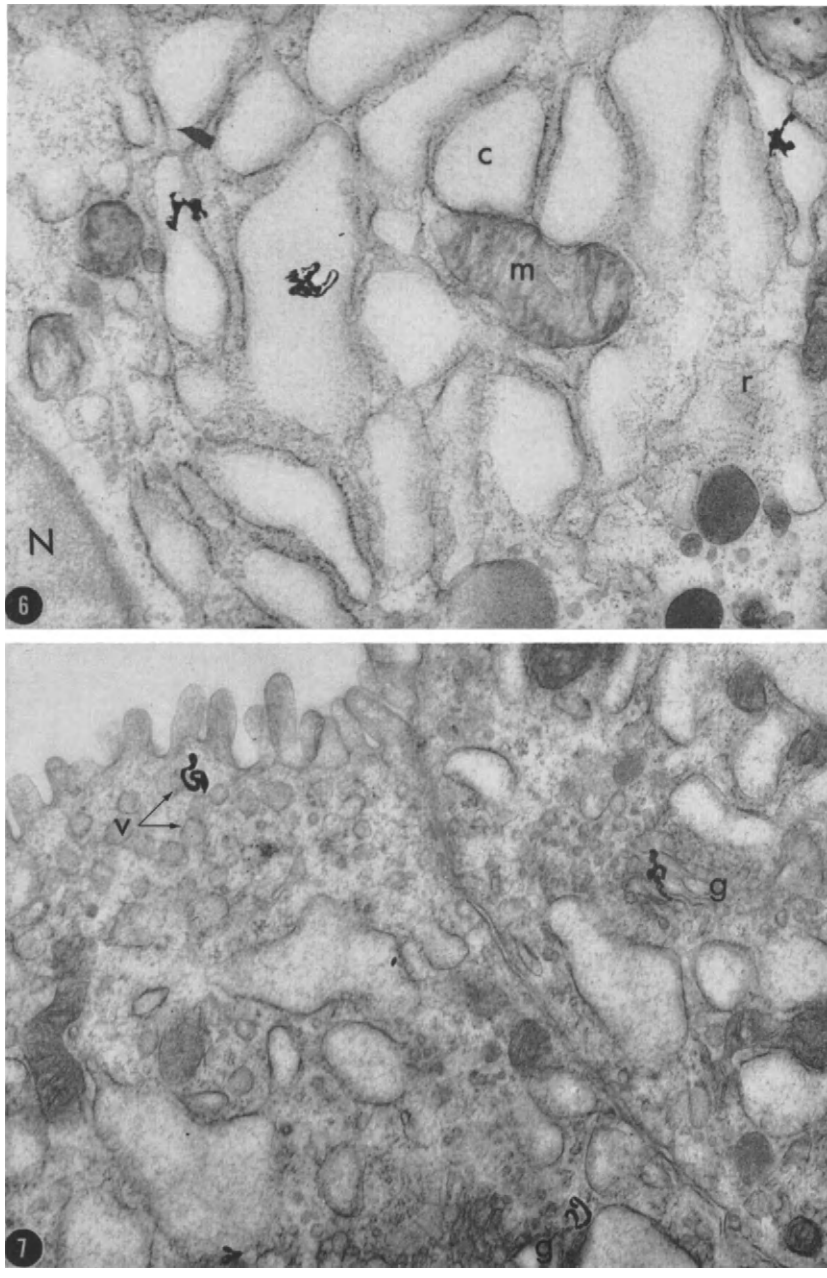

FIG. 6. Electron microscope coated radioautograph 1 hour after ^{3}H-leucine injection (Ilford L-4 emulsion; development in Dektol). Of the three silver grains over the ergastoplasm, two are over ribosomes, one is completely over the lumen of a cisterna. Magnification: ×30,000.

activity was almost equal to the increase in colloid radioactivity, confirming the conclusion that follicular cells secreted the labeled protein into the colloid [26].

More recently, a morphological analysis of the synthesis and secretion of thyroglobulin by follicular cells was carried out by applying radioautography to electron microscope sections (26). By coating ultrathin sections in such a way that the silver halide crystals in the photographic emulsion are packed closely in monolayers, it is possible to localize radioactive proteins in cytological structures visualized only with the electron microscope. In this manner, it was hoped to reveal the precise intracellular site of synthesis of the protein moiety of thyroglobulin as well as its path of migration from this site into the colloid.

The technique was carried out by Dr. B. A. Young, whose results are presented in this series. After injection of ^{3}H-leucine, thyroid glands were removed at 10 minutes, ½ hour, 1 hour, and 3½ hours, then flooded with osmic acid, chopped into small pieces, and fixed in ice-cold 1% osmium tetroxide, buffered with Veronal plus added sucrose [6]. After fixation for 1 hour, the pieces of tissue were rapidly dehydrated in a graded series of alcohol and embedded in butyl methacrylate. Using glass knives, ultrathin sections (silver to gold) were cut on a Porter-Blum microtome and mounted in carboned Formvar Athene type grids. With the electron microscope grid attached to glass slides, radioautographs were prepared by the coating technique [14]. The emulsion used was Ilford L-4 (diameter of grains 0.12 μ) diluted 1:6, which after exposure was developed in Dektol for 2 minutes or Microdol for 5 minutes [4]; or undiluted Gevaert NUC-307 emulsion (diameter of grains 0.07 μ) was developed in Kodak D-170 for 5 minutes [12, 36]. After exposure, the sections were stained with Karnovsky's stain, which also removed the gelatin of the emulsion [28]. The sections were then examined in a Siemens Elmiskop I electron microscope.

In the electron microscope (Fig. 1), thyroid follicular cells show the apical surface with irregularly arranged microvilli (mvl) protruding into the colloid-containing lumen (C), while the basal surface is separated from the extracellular spaces and capillaries by a basement membrane (bm). The ergastoplasm, composed of ribosomes and cisternae and of endoplasmic reticulum, is distributed throughout the cytoplasm of the cell. The ribosomes are present on the outer surface of the

FIG. 7. Electron microscope coated radioautographs, 1 hour after ^{3}H-leucine injection (Ilford L-4 emulsion; development in Dektol). Golgi zone (g) with dilated sacs and associated vesicles of the same size as the apical vesicles (v) can be seen. In this cell, two grains are definitely related to the Golgi zone and one to an apical vesicle. Magnification: ×30,000.

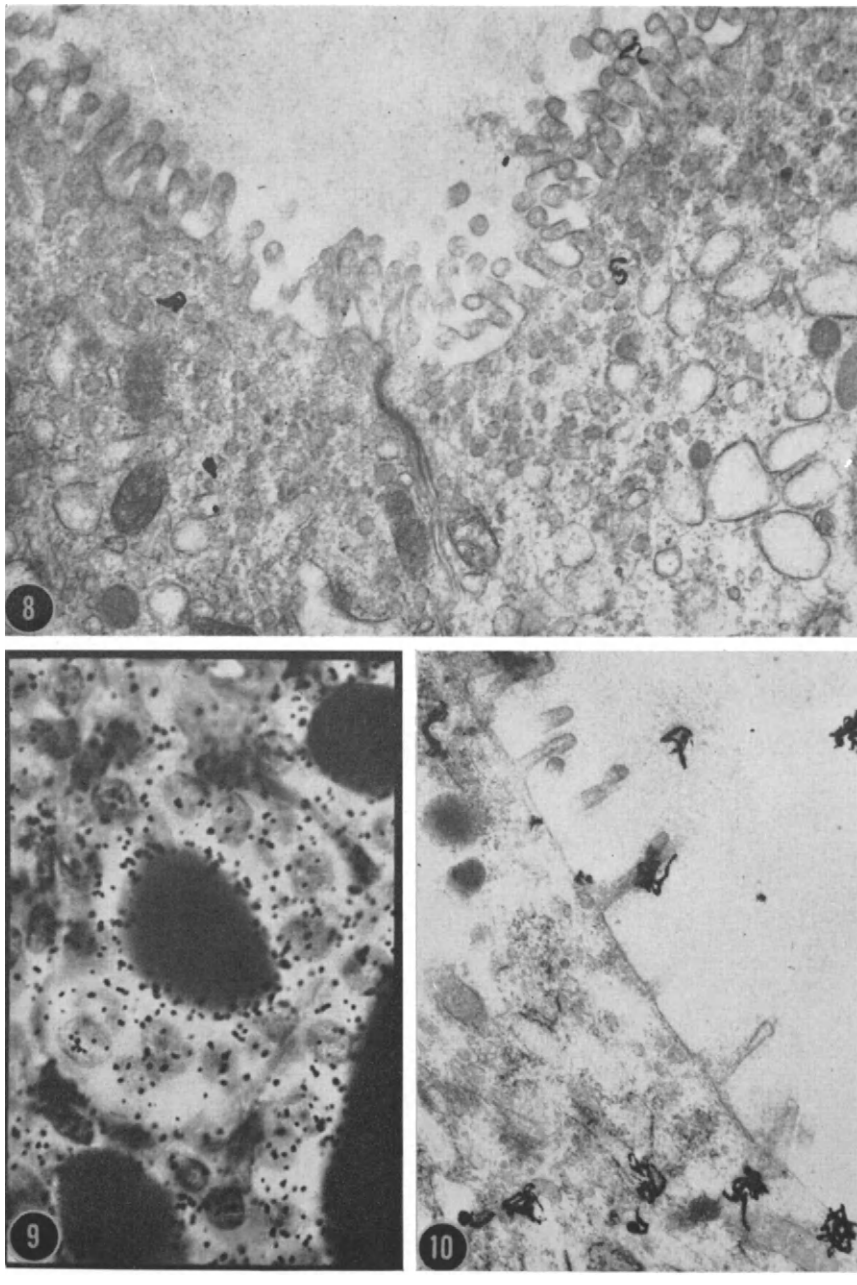

FIG. 8. Electron microscope coated radioautograph 1 hour after ^{3}H-leucine injection (Gevaert NUC-307 emulsion; development in Kodak D-170). Three silver grains are over the region of the apical vesicles, one over the colloid between microvilli. Magnification: ×30,000.

membranes enclosing the cisternae, which are often widely dilated (c). The nucleus is usually located at the base of the cell (N). In ultrathin sections, one or several groups of Golgi elements (g) are seen, which are usually in a supranuclear position. Each group consists of numerous sacs, which are often dilated and are surrounded by small vesicles of various sizes. Of these vesicles, the most numerous measure about 0.15 μ in diameter and have a homogeneous content. They are often observed to extend from the Golgi zone to the region immediately below the apical surface where they tend to gather; accordingly, they are referred to as the "apical vesicles" (av). Incidentally, two other types of cytoplasmic inclusions are commonly present, the colloid droplets which consist of irregular, pale-staining spheroids of the order of 1.5 μ in diameter, and densely staining granules of the order of 0.5 μ in diameter or less, which are referred to as "zymogen-like" granules (they probably are lysozomes).

In the investigations conducted with B. A. Young, it was reported [20] that the high resolution radioautographs (Figs. 3 and 4) prepared 10 minutes after ^{3}H-leucine injection showed nearly all the silver grains over the ergastoplasm, often straddling the ribosome-studded membranes of the cisternae. One hour after injection, when the reaction of the cytoplasm of the follicular cells was more intense, the majority of grains (about 60%) were still localized over ribosomes, but some (about 10%) were over the lumen of the cisternae (Fig. 6). A small number of grains (about 17%) were observed over the membranes and small vesicles of the Golgi zone (Fig. 7). Finally, occasional grains (about 10%) were also over the region of the apical vesicles (Figs. 7 and 8), some being ascribed to the apical vesicles close to the Golgi zone, and others to those adjacent to the cell surface. At 3½ hours after injection, although a few silver grains were still distinguished over the ergastoplasm and over the Golgi zone, the grains were more numerous over the region of the small vesicles and the apical zone of the cytoplasm and, now, also over the colloid of the follicular lumen (Fig. 10). From all the separate studies, it may be concluded that the earliest grains over the ergastoplasm appeared almost immediately after injection of the labeled precursor of thyroglobulin, the earliest grains over the Golgi at 30 minutes, over the apical vesicles at 1 hour, and over the colloid at 2½ hours.

The early electron microscope results showing nearly all the silver grains over the ergastoplasm pointed to this organelle as the site of

---

FIG. 9. Light microscope coated radioautograph of periodic acid-Schiff-hematoxylin stained preparation from rat sacrificed 4 hours after ^{3}H-leucine injection. Magnification: ×1200.

FIG. 10. Electron microscope coated radioautograph (Ilford L-4 emulsion; development in Dektol) from rat sacrificed 3½ hours after ^{3}H-leucine injection. Silver trains are seen over the apical region and the colloid. Magnification: ×30,000.

synthesis of protein in the cytoplasm. Moreover, the neat manner in which the grains appeared to straddle the membranes enclosing the cisternae of the ergastoplasm would suggest that the site of synthesis can be even further localized to these ribosome-studded membranes—a conclusion in keeping with the currently accepted view that ribosomal ribonucleic acid (RNA) plays a key role in the synthesis of protein [2, 15]. The later observations corresponding to the piling up of radioactivity in the follicular cell apex viewed with the light microscope at 4 hours were shown in the electron micrograph to be due to the appearance of labeled proteins in the apical vesicles. These results point to these apical vesicles as the vehicle by which the protein moiety of thyroglobulin emerges into the colloid of the follicular lumen. To explain by which intracellular channels the exportable protein journeys from the ergastoplasm to the apical vesicles, it was noted that, at ½ to 1 hour after injection, many grains were found over the contents of the cisternae, suggesting that the protein formed on the ribosomes outside the walls of the cisternae migrated first into the lumen of the cisternae. The next step in the journey was suggested by the observation that, when a few grains were initially observed over the apical vesicles (that is, 1 hour after ^{3}H-leucine administration), the grains were more numerous over the Golgi zone. Since it is suspected that the cisternae of the ergastoplasm may have some connection with the Golgi sacs, it is inviting to hypothesize that, through the maze of cisternae, protein molecules move to the Golgi zone and in this way reach the apical vesicles. The same sequence for protein migration from ergastoplasm to Golgi zone to the exterior has also been observed in the cells of the pancreas and in cells secreting collagen [29, 30].

MATURATION OF THE THYROGLOBULIN MOLECULE

Precisely what role the Golgi sacs may play is only conjectural. However, histochemical studies have shown frequent localization of carbohydrates to the Golgi zone, and tracer studies with ^{3}H-glucose [27] have indicated that complex carbohydrates combine with protein in this zone. Accordingly, in the Golgi zone, the carbohydrate portion may add to the protein moiety of thyroglobulin, and the newly-formed carbohydrate–protein complex would come out in the apical vesicles, seen as off-shoots of the Golgi zone, and, in this form, go to the cell apex.

By which mechanism does the labeled protein contained in the apical vesicles gain access to the colloid? The release of the content of apical vesicles to the cell surface was visualized like a bubble of soap coming to the surface of the water where it explodes, leaving a soap film. In a similar manner, the membrane of an apical vesicle reaching the cell

surface could fuse with the plasma membrane of the cell and break up to yield its contents to the colloid. A similar explanation has been accepted for the release of zymogen granules [16].

There is considerable evidence that iodination of the protein moiety of thyroglobulin takes place only on tyrosine already bound in thyroglobulin peptide linkage rather than on free tyrosine [1, 5, 31, 32, 34], it being also possible that smaller iodinated polypeptide units may subsequently polymerize into larger molecules. In fact, results of grain counts after ^{3}H-leucine revealed that the rates of synthesis and secretion of the protein moiety of thyroglobulin were unaffected by agents which normally block the iodination of the protein moiety, such as propylthiouracil [20] or acute large doses of iodide [23]; hence, the iodination phenomenon is independent of the elaboration of the protein moiety of thyroglobulin. Regarding the site of iodination in the thyroid follicle, as early as ½ minute after a single injection of radioiodine (^{125}I), the radioautographic reaction was found by light or electron microscopy to be present over the periphery of the lumen [19a], showing that the final stage in the synthesis of thyroglobulin, the iodination of the glycoprotein molecule, takes place in the follicle lumen, just at the cell–colloid interface. The few grains in the radioautographs which are consistently found over the cells are usually attributed to scatter, although it is also possible that some iodination of protein does take place in the cells. If so, the iodination in the cells must amount to less than 5% of the total iodination activity which occurs in the lumen; moreover, it may involve proteins other than thyroglobulin [7], so that its role is relatively insignificant.

RATES OF SYNTHESIS AND MIGRATION OF THE PROTEIN MOIETY OF THYROGLOBULIN

Only a portion of the proteins which are synthesized in the follicular cells is secreted into the colloid. This portion is referred to as "exportable" and represents thyroglobulin; the remainder remains behind in the cells and is referred to as "sedentary," representing protein relegated to intracellular structures.

In the light microscope radioautographs, at 10 and 30 minutes after injection of ^{3}H-leucine, the grain count over the whole of the follicular cells can be regarded as an index of the over-all rate of synthesis of proteins in the cells. At 4 hours, the grain count over the apex of the cells would be an index of the rate of accumulation of the newly formed protein moiety of thyroglobulin in the apical vesicles of these cells; and the count over the colloid in the lumen of the follicles would be an index of the rate of secretion of thyroglobulin into the colloid. From investi-

gations of this kind it was concluded [26] that, in the normal rat, all follicular cells of all follicles are continuously active at the same rate in the synthesis of proteins; and that the migration of the protein moiety of thyroglobulin from its site of synthesis to the apex of the follicular cells and into the colloid occurred at the same rate in all cells. As a result, small follicles which have relatively more cells per unit volume of lumenal colloid would concentrate newly exported protein in the lumen more rapidly.

It was also calculated [26] that, in the region of the ergastoplasm of the follicular cells, the turnover rate of newly synthesized exportable protein was about 17 percent per hour. Turnover rate may have a different significance in the case of a relatively large pool where the label is distributed homogeneously than in the case of a small compartment, such as in the cisternae of the endoplasmic reticulum, where mixing of proteins is not necessarily likely to occur. Applying a formula adapted especially for the latter example (unpublished), it was concluded that the turnover rate times the concentration of exportable protein would yield the mass of protein synthesized per unit volume of cisternae per unit time. Accordingly, to make the fullest use of this turnover rate value, it would be necessary to know the concentration of exportable protein as well as the dimensions of a unit endoplasmic reticulum; if so, it would be possible to derive the rate of synthesis of protein per unit endoplasmic reticulum in absolute figures of mass per unit time.

The grain-counting technique was also used to investigate factors which influence the rates of synthesis and secretion of the protein moiety of thyroglobulin in the follicular cells. Thus, it has been shown that these rates are diminished in the hypophysectomized rat, and are restored by injections of thyroid stimulating hormone (TSH) [24]. Also, by decreasing the concentration of iodine in the diet, thereby increasing the pituitary endogenous secretion of TSH, it was possible to stimulate the elaboration of thyroglobulin. Thus, the grain counts (Table I) were increased when rats had been placed on a low iodine diet. In such stimulated glands, there is hypertrophy of the cells in the thyroid follicle, the size of which can be measured by histological techniques. Of interest in morphology are results [20] correlating the activity of the follicular cell with the size of the cell (Table I). Thus, at 10 and 30 minutes over the base of the cells (region of ergastoplasm), when the counts were corrected per mean volume of a single follicular cell, the results were not significantly different than similarly corrected counts for rats on a high iodine diet. This means that the rate of synthesis of protein in the follicular cell is directly proportional to its size; a result which should not be too surprising since protein is synthesized in ergastoplasm and,

TABLE I. *Correlation of Thyroid Cell Volume with Rates of Protein Synthesis (Grain Counts over Ergastoplasm), Intracellular Migration (Apical Vesicles), and Release (Periphery of Follicle Lumen), in Rats on Low and High Iodine Diets*

		GRAIN COUNTS Time after ^3H Leucine							
		Over region of ergastoplasm (base of cells)				Over region of apical vesicles (apex of cells) at 4 hours		Over periphery of follicle lumen at 4 hours	
		10 minutes		30 minutes					
Diet	Mean cell height (μ)	Measured	Corrected per cell volume	Measured	Corrected per cell volume	Measured	Corrected per cell volume	Measured	Corrected per cell volume
Low iodine (stimulated thyroids)	15.2 ± 1.1	30.5 ± 2.7	0.105 ± 0.029	68.9 ± 1.5	0.204 ± 0.019	9.2 ± 1.0	1.60 ± 0.017	7.4 ± 0.71	1.61 ± 0.12[a]
High iodine	10.1 ± 0.5	19.8 ± 2.9	0.086 ± 0.018	43.4 ± 2.9	0.189 ± 0.018	7.4 ± 0.71	1.29 ± 0.12	2.9 ± 0.71	0.54 ± 0.054[a]

[a] Between low and high iodine diets, a significant difference in corrected grain counts ($p < 0.05$) exists only where figures have been underlined.

although actual figures are lacking, it is probable that the volume of ergastoplasm is proportional to the size of the follicular cell. The grain counts at 4 hours over the apex of the cells, corrected per mean volume of a single follicular cell, were also not significantly different for rats on low and high iodine diets, suggesting that the rate of concentration of newly synthesized protein in the apical vesicles is also directly proportional to the size of the cell. However, over the periphery of the lumen, the corrected counts were significantly different, indicating increased concentration of newly secreted thyroglobulin in the lumen of stimulated thyroid follicles. This follows since the total rate of protein elaborated in such follicles with large cells is increased, and, therefore, more protein will concentrate in the lumen. Moreover, time studies have shown that, after TSH stimulation, as well as the amount elaborated, the rate of migration of the protein moiety from its site of synthesis in the endoplasmic reticulum to the region of the apical vesicles to the follicle lumen is also accelerated. Finally, it has been shown previously that in every thyroid follicle the iodination of thyroglobulin occurs continuously [19] and at a rate influenced by the number and size of the follicular cells [21]. Hence, although the iodination of thyroglobulin takes place in the lumen of the follicle, the rate of iodination is governed by the cells of that follicle, probably through the elaboration of an enzyme which facilitates iodination of the glycoprotein moiety.

SUMMARY

In all follicular cells of the rat thyroid, a protein believed to be the protein moiety of thyroglobulin is synthesized continuously in the ergastoplasm, migrates from there to the apical vesicles, and thence to the colloid in the lumen. It is suggested that this protein makes its way from the ribosomes into the cisternae of the ergastoplasm, thence into the Golgi zone, next into the apical zone of the follicular cells of the apical vesicles and finally into the colloid of the follicle lumen. There in the follicle lumen, it is known that this glycoprotein moiety of thyroglobulin is iodinated with the formation of iodotyrosyl and iodothyronyl groups, thus yielding full-fledged thyroglobulin. The striking influence of the size of the follicular cell on the respective rates of each operation suggests that there may be a direct relationship between the structural content of the organelle responsible for that operation and the rate at which it proceeds.

Acknowledgments

The work reported in this article is the result of the team efforts of many members of the Department of Anatomy, some of whom have not been mentioned

in the bibliography. In particular, it is appreciated that practically no concept cited in this article regarding thyroid structure or function has evolved without the maturing guidance of C. P. Leblond.

References

1. Alexander, N. M., *Endocrinology* **74**, 273 (1964).
2. Campbell, P. N., *in* "Protein Synthesis" (R. J. C. Harris, ed.), p. 31. Academic Press, New York, 1961.
3. Caro, L. G., and Palade, G. E., *J. Cell Biol.* **20**, 473 (1964).
4. Caro, L. G., and Van Tubergen, R. P., *J. Cell Biol.* **15**, 173 (1962).
5. Cartouzou, G., Aquaron, R., and Lissitzky, S., *Biochem. Biophys. Res. Commun.* **15**, 82 (1964).
6. Caulfield, J. B., *J. Biophys. Biochem. Cytol.* **3**, 827 (1957).
7. De Groot, L. J., *New England J. Med.* **272**, 243 (1965).
8. Dempsey, E. W., and Peterson, R. R., *Endocrinology* **56**, 46 (1955).
9. De Robertis, E., *Anat. Record* **84**, 125 (1942).
10. Derrien, Y., Michel, R., and Roche, J., *Biochim. Biophys. Acta* **2**, 454 (1948).
11. Gersh, I., and Caspersson, T., *Anat. Record* **78**, 303 (1940).
12. Grandoulan, P., *J. Roy. Microscop. Soc.* **81**, 165 (1963).
13. Haurowitz, F., "Chemistry and Biology of Proteins." Academic Press, New York, 1950.
14. Hay, E. D., and Revel, J. P., *J. Cell Biol.* **16**, 29 (1963).
15. Hultin, T., and von der Decken, A., *in* "Protein Synthesis" (R. J. C. Harris, ed.), p. 83. Academic Press, New York, 1961.
16. Ito, S., and Winchester, R. J., *J. Cell Biol.* **16**, 541 (1963).
17. Kopriwa, B. M., and Leblond, C. P., *J. Histochem. Cytochem.* **10**, 269 (1962).
18. Leblond, C. P., and Amano, M., *J. Histochem. Cytochem.* **10**, 162 (1962).
19. Leblond C. P., and Gross, J., *Can. Med. Assoc. J.* **58**, 404 (1948).
19a. Leblond, C. P., Nadler, N. J., van Heyningen, H. E., Petrovik, A., Kopriwa, B., and Bénard, B., in preparation (1965).
20. Nadler, N. J., and Harrison, K., unpublished data (1964).
21. Nadler, N. J., Leblond, C. P., and Bogoroch, R., *Endocrinology* **54**, 154 (1954).
22. Nadler, N. J., Leblond, C. P., and Carneiro, J., *Proc. Soc. Exptl. Biol. Med.* **105**, 38 (1960).
23. Nadler, N. J., Leblond, C. P., and Harrison, K., *Proc. Endocrine Soc.* p. 74 (1963).
24. Nadler, N. J., and Mitmaker, B., *Proc. Endocrine Soc.* June (1961).
25. Nadler, N. J., Sarkar, S. K., and Leblond, C. P., *Endocrinology* **71**, 120 (1962).
26. Nadler, N. J., Young, B. A., Leblond, C. P., and Mitmaker, B., *Endocrinology* **74**, 333 (1964).
27. Peterson, M., and Leblond, C. P., *J. Cell Biol.* **21**, 143 (1964).
28. Revel, J. P., and Hay, E. D., *Exptl. Cell Res.* **25**, 474 (1961).
29. Revel, J. P., and Hay, E. D., *Z. Zellforsch.* **61**, 110 (1963).
30. Ross, R., and Benditt, E. P., *Abstr. 2nd Meeting Am. Soc. Cell. Biol. San Francisco, 1962* p. 157 (1962).
31. Seed, R. W., and Goldberg, I. H., *Proc. Natl. Acad. Sci.* **50**, 275 (1963).
32. Soodak, M., Maloof, F., and Sato, G., *Federation Proc.* **23**, 268 (1964).
33. Stoll, R., Maraud, R., Blanquet, P., Meunier, J., and Lachapelle, A. *Ann. Endocrinol.* **19**, 183 (1958).
34. Tishler, P. V., and Ingbar, J. H., *Endocrinology* **76**, 295 (1965).

35. Warshawsky, H., Leblond, C. P., and Droz, B., *J. Cell Biol.* **16**, 1 (1963).
36. Young, B. A., and Kopriwa, B. M., *J. Histochem. Cytochem.* **12**, 438 (1964).

Discussion

Dr. Pelc: In 1950, Doniach and Pelc incubated unfixed, frozen sections of rat thyroids with ^{131}I and obtained uniform radioautographs over the colloid, supporting the idea that binding of ^{131}I takes place throughout the colloid. Supporting evidence was obtained by incubation of whole glands in ^{131}I labeled Ringers solution. This agreed with our *in vivo* findings that iodination of the thyroid hormone is not performed by the epithelial cells.

Dr. Nadler: Radioautographs of unfixed thyroids after an injection of radioiodide, ^{125}I (by a method derived from that kindly demonstrated by Dr. Ross) suggested to Dr. Bénard that this labeled ion is soon found in the cells as well as in the lumen of the thyroid follicles. However, radioautographs of routinely fixed thyroids in which just the bound iodine is retained showed that the label is found only over the lumen of the follicles; that is, at its periphery just at the cell–colloid interface, so that the binding of iodide to the protein moiety of thyroglobulin takes place in this region of the lumen.

However, it has been shown that the rate of iodination of thyroglobulin is influenced by the follicular cells, and it is suspected that this influence is exerted by the elaboration of an oxidizing enzyme responsible for iodination. Thus, since the thyroid cells pick up iodide ions which they release into the lumen of the follicles, since they elaborate the protein moiety of thyroglobulin and since they, no doubt, elaborate the enzyme which binds iodide to thyroglobulin, then, in a strict sense, the epithelial cells *do* perform the iodination of thyroglobulin, but they effect the performance in the lumen of the follicles.

Dr. Bélanger: In rapidly dehydrating fixatives such as ethanol, the colloid of medium-sized and large follicles is distributed into three zones which by Masson or Mallory staining show no stain, blue stain, or red stain, respectively. Only the blue-stained colloid contains ^{125}I or ^{131}I at short times after injection (up to 1 hour). Is the heterogeneity significant? Is only the blue-staining colloid capable of accepting iodine?

Dr. Leblond: When the colloid is examined under living conditions or after osmic acid fixation in young adult rats, the colloid appears uniform throughout in small as well as in large follicles. But irregularities are observed with many fixatives (e.g., alcohol). The irregularities are probably artifacts.

However, artifacts may be meaningful. Thus it is not impossible that alcohol fixation might separate within the colloid a more labeled from a less labeled protein.

Dr. Revel: Is it possible that the inhomogeneous labeling observed by Dr. Bélanger with ^{125}I reflects the availability of sites which can be iodinated rather than be due to a concentration gradient of iodinating enzyme?

Dr. Nadler: While in some other species, such as mouse and man, it is true that not all follicular cells function equally, in the young adult rat (which has been the subject of most of our investigations), the cells are remarkably uniform in the rate of synthesis and secretion of the protein moiety of thyroglobulin, and also of its iodination.

With regard to the factors governing the rate of iodination in the lumen, recall first that, seconds after a single injection of radioiodine, radioautographs of routinely fixed rat thyroids reveal the presence of silver grains uniformly over the periphery of the follicle lumens, giving rise to the so-called "ring reaction" of Leblond and

Gross. This consistent observation means that iodination of thyroglobulin occurs at a uniform rate around the periphery of the follicle lumen. Now, consider in turn the three agents involved in the iodination process: iodide, the protein moiety of thyroglobulin, and the enzyme which facilitates binding. With regard to iodide, we know that, minutes after injection of radiodide, radioautographs of unfixed sections (Bénard) show a diffuse reaction over the colloid of the lumens, as well as over the cells, so that the inorganic ion is available throughout the lumen. With regard to the second agent, it has been shown (unpublished data of A. Petrovic), from spectrophotometric studies on the intensity of protein stains of the colloid, that the concentration of the protein moiety of thyroglobulin is uniform throughout the lumen of all follicles. Moreover, since the average thyroglobulin molecule is never quite saturated with iodine, it is unlikely that the rate of binding of iodine reflects simply the availability of sites which can be iodinated. This leaves us with the third possibility; namely, that iodination takes place in the periphery of the lumen because of the presence of an enzyme which is released by the follicular cells into this site; and I suspect that the relative decrease in iodination observed in the center of the lumen is due to the want of this enzyme.

DR. DROZ: The isotopic equilibrium is a method which allows replacement of iodine content of the thyroid gland by isotopic iodine ^{125}I which, with time, reaches the same specific activity as that of the iodine given in the diet (Simon, C., and Droz, B., *Proc. 5th Intern. Congr. Thyroid, Rome* 1965). In other words, after the isotopic equilibrium has been reached (in about 2 months), radioautographs of the thyroid gland reveal how the bound iodine is distributed in thyroid follicles. While most of the silver grains are located randomly over the colloid, some are constantly seen over the cytoplasm of the follicular cells, where they are mainly superimposed on the colloid droplets, free or combined to lysosomes (zymogen-like granules). I would like to know how Dr. Nadler and Dr. Leblond interpret the presence of ^{125}I in these structures.

DR. LEBLOND: Since the colloid would be fully labeled with iodine, any colloid droplet taken up into the cells would also be labeled. Some of the work of Dr. Van Heyningen here and of Dr. Wollman at the National Institutes of Health suggests that colloid droplets combine in the cells with the "zymogen-like granules" (which are probably the same structures as the "dark granules" or "lysosomes"). Hence, the labeled structures shown by Dr. Droz would in fact be combinations of these granules with colloid droplets.

WHAT RADIOAUTOGRAPHY HAS ADDED TO PROTEIN LORE

C. P. LEBLOND

Department of Anatomy, McGill University, Montreal, Canada

The steam engine was used by some biologists of the 19th century as a model to which the body might be compared. The organs were commonly described as unchanging structures, like cogs and wheels, fueled by food. When Voit and Rubner in Germany and Atwater in America [34] succeeded in keeping animals and man in nitrogen equilibrium (that is, with the ingested protein nitrogen balancing the nitrogen excreted in urine and feces), they assumed that all the excreted nitrogen came from the combustion of food (except for a minute fraction coming from worn out or damaged tissues).

Therefore, in the 1930's, when Schoenheimer and Rittenberg, Borsook, and others administered amino acids or protein labeled with heavy nitrogen to animals in nitrogen equilibrium, the expectation was that all the label would soon appear in the excreta. Instead, only one-third did. Therefore, only one-third of the ingested proteins had been used as fuel; the rest had been retained in the body. Conversely, two-thirds of the excreted nitrogen must have come from sources other than food protein, that is, from the protein making up organs and tissues. The possibility was then considered that tissue proteins were turning over and that organs were not the unchanging static structures postulated by 19th century biologists.

Radioautography was an ideal tool to find out what happened to proteins within organs and tissues. However, in 1940, the technique which consisted of placing a section in apposition with a photographic plate yielded crude pictures with poor resolution: and, in any case, no adequate radioactive precursor of proteins was available.

The situation improved in 1946, when a technique was devised with Bélanger in which sections were "coated" with liquid emulsion [5, 31], thus ensuring an intimate contact between section and emulsion and vastly improving resolution. In 1947, the introduction of the stripping film technique by Pelc provided the same benefits [44].

Meanwhile, the first tracing of labeled protein by radioautography was done unwittingly by Bloom, Curtis, and McLean in 1947, when they

injected ^{14}C-bicarbonate into rats. They found that undecalcified sections of bone caused a radioautographic reaction, which they attributed to the uptake of labeled carbonate within bone salts [6]. When this experiment was repeated at McGill in 1953, the reaction was found to persist after decalcification, so that the radiocarbon must have been taken up into bone matrix, presumably as a protein [19]. Bicarbonate was not quite adequate as protein precursor, since it could also enter carbohydrates [19]. Neither was the next substance used, ^{14}C-glycine [16, 25], since it also passed into nucleic acids [1]. From 1955 on, use was made of ^{35}S-methionine [4, 32], ^{14}C-phenylalanine [17], and other amino acids which may be considered to be specific for proteins. In 1957, there appeared on the market three amino acids (leucine, glycine, and methionine) labeled with tritium, a soft beta emitter ideally suited for radioautography. During the next few years, a large number of tritium-labeled amino acids became available. Studies of protein synthesis by means of radioautography became more and more numerous with time.

What has been achieved will now be briefly summarized. The present article consists of remarks that were to be presented at the end of the symposium (but were not, because of lack of time). In a first part, comments are made on the *procedures* used in radioautographic work. A second part deals with the *sites* of protein synthesis, and a third part with the *fate* of newly synthesized proteins.

PROCEDURES

The basic procedure is a familiar one. A labeled amino acid is injected into an animal. Within minutes the labeled amino acid appears in blood and tissues. A significant amount remains there in a free form for only a short time, at most a few hours after injection.

Proteins synthesized during that time take up the radioactive amino acid and thus incorporate its label (Fig. 1). When the animal is sacrificed and the tissues processed for histology, the unused labeled amino acid that may still be present is washed out, while the labeled protein is retained and may be detected in the sections by radioautography.

Thus, the sites of radioautographic reaction immediately after injection are sites of protein synthesis. With time, the intensity of the reactions over these sites decreases gradually (Fig. 2), because of either local breakdown or emigration of the newly formed protein.

Experimental Animals

Instead of seeking nitrogen equilibrium, it is customary today to aim at an over-all balanced equilibrium so as to maintain a *steady state* of the

various metabolic systems of the animals. For this reason, the animal of choice is an adult which has completed growth or nearly so, e.g., a 30-gm mouse. A male is preferred to avoid interference from the estrus cycle. The animal is fed a balanced diet and is tamed to avoid excitement at the time of injection. Diurnal variation may have to be taken into account, since our experience (briefly quoted on p. 16 in ref. [57]) indicates that

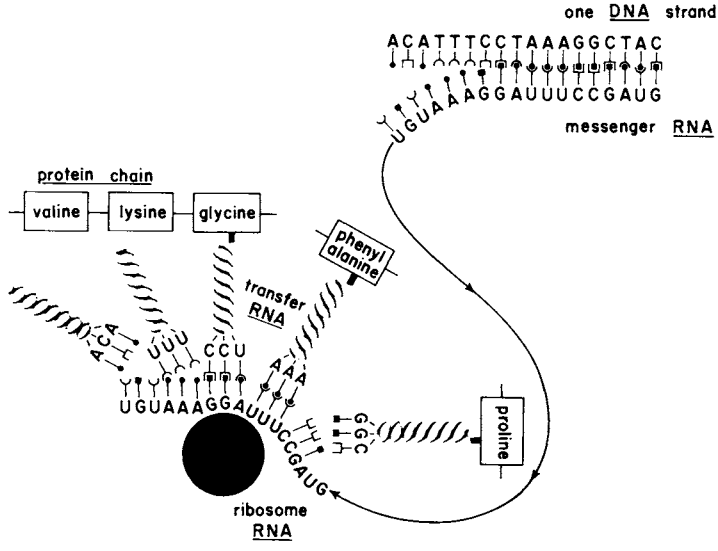

FIG. 1. Diagram of protein synthesis in cytoplasm. At upper right, a deoxyribonucleic acid (DNA) strand is represented by its bases (A, adenine; T, thymidine; C, cytidine; and G, guanine). For ribonucleic acid (RNA) synthesis, each base residue of DNA takes up the corresponding free base (adenine takes up uridine; thymidine takes up adenine; cytidine takes up guanine; and guanine takes up cytidine). Once a molecule of RNA is completed, it separates from the DNA strand and migrates out of the nucleus into the cytoplasm. In certain regions contact is established between ribosomal and messenger RNA. Then the latter successively picks up transfer RNA's, whose three bases meet with the three corresponding bases on the messenger RNA. Then, the amino acid carried by each transfer RNA is inserted onto the protein chain.

Let us for instance consider the 10th, 11th, and 12th bases of the DNA strand at upper right. All three are adenines. They give rise to a series of three uridines in the messenger RNA. When the messenger makes contact with ribosomes, one of which is depicted here as a black sphere, protein synthesis gets under way. The sequence of three uridines can only pick up a transfer RNA with three adenines, that is, the one which carries phenylalanine. When this occurs, phenylalanine is added to the growing protein chain.

In this manner, a radioactive amino acid is incorporated into a protein, which thus becomes radioactive itself and may eventually produce a radioautographic reaction.

while protein synthesis occurs continuously at all times of day, there are minor diurnal fluctuations.

With these various precautions, the sites of label uptake reveal where proteins are synthesized under steady state conditions.

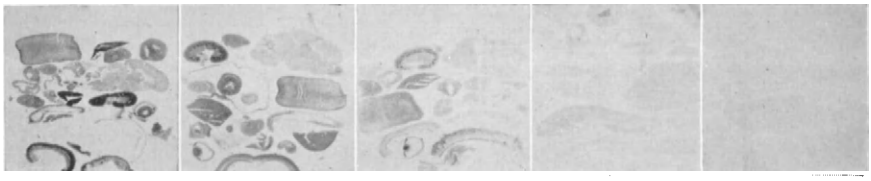

FIG. 2. Radioautographs of unstained tissues taken from rats injected with ^{35}S-methionine at the age of 3 days and sacrificed at various time intervals thereafter. At left, it is seen that ^{35}S-methionine uptake differs in different tissues. With time, the intensity of the radioautographic reactions decreases, indicating decrease in concentration of labeled proteins. In a few tissues this phenomenon may be attributed to emigration of labeled protein (e.g., the release of protein enzymes from pancreatic cells). The decrease of the reactions in other tissues is due in part to the dilution of labeled proteins in the course of growth and in part to loss of proteins by breakdown and turnover. (In adult non-growing animals, there is a similar decrease in radioactivity with time, which can only be attributed to protein turnover.) Reproduced from Karpishka and Carneiro [23].

Nature of Radioactivity in Sections after Amino Acid Injection

Does the radioactive material retained in tissue sections after labeled amino acid injection consist of protein? Since biochemists routinely use cold trichloroacetic acid to precipitate proteins, our early work on the distribution of ^{35}S-methionine with Everett and Simmons made use of organs fixed in trichloroacetic acid prior to radioautography [32]. Simultaneously, trichloroacetic acid precipitates of the same organs were examined in the Geiger counter. The Geiger counts appeared to be proportional to the radioautographic intensities. Hence, the reactions, like the Geiger counts, were attributed to newly formed protein [32]. Although cold trichloroacetic acid precipitates also contain nucleic acids, Droz and Warshawsky found only traces of radioactivity in these acids, at least after injection of labeled leucine [15]. They also showed that free leucine was not absorbed on the proteins retained in sections [15].

In theory, decisive evidence of the uptake of a labeled amino acid into a protein requires demonstration of its presence as a residue within the protein. In radioautographs, it can only be shown that amino acids are taken up in the same proportion as the corresponding residues of the protein. Thus, when ^{3}H-leucine was mixed with fresh rat blood *in*

vitro and the smears radioautographed (Fig. 3), the grain counts over reticulocytes were 5–6 times higher than when ^{3}H-tyrosine was used (Fig. 4). Since reticulocytes are known to synthesize hemoglobin—a protein with 5.3 times more leucyl than tyrosyl residues—the similarity

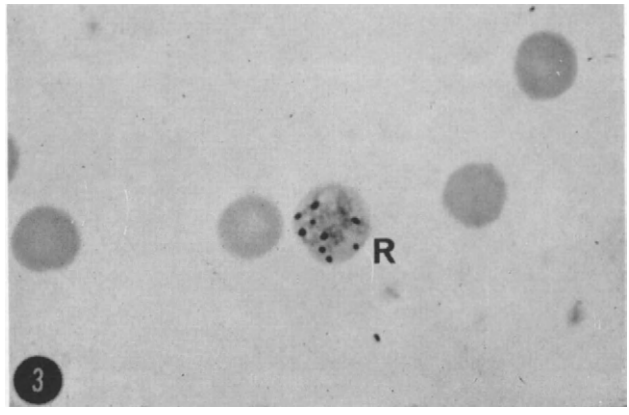

FIG. 3. Radioautograph of blood smear. Fresh rat blood was incubated for 1 minute with ^{3}H-leucine, supravitally stained with brilliant cresyl blue and smeared on glass slides. The smears were then fixed in methanol, radioautographed by the coating technique, exposed for 6 days, and post-stained with Giemsa. The cell in the center (R) contains the reticulum characteristic of reticulocytes. Furthermore, this cell is overlaid by silver grains, indicating uptake of labeled leucine. The reticulocyte is therefore a site of protein synthesis. Magnification: × 1000. Reproduced from Pinheiro *et al.* [48].

in the proportions was evidence that the radioautographs of reticulocytes were due to synthesis of this protein [48].[1]

Analysis of Results in the Light Microscope

The problem is twofold. The structure which is the source of radioactivity must be identified and then the concentration of radioisotope in this structure must be measured. Usually the identification of the source is easy, but quantitation is difficult. The theory of quantitative radioautography was formulated by Nadler in 1953 [39] and will now be summarized with emphasis on the use of tritium. Three steps may be considered. First, the *grain count* has to be measured accurately. Then, the grain count has to be related to *radiation exposure* (that is, the amount of radiation received by the emulsion during exposure time).

[1] The similarity in the radioautographic pattern of uptake of various amino acids mentioned in the articles of Schultze *et al.* and of Greulich in this volume reflects a rough similarity in the amino acid composition of many proteins.

Finally, the radiation exposure has to be related to the *radioisotope concentration* in the structure under study.

(1) The grain count is usually obtained by estimating the number of silver grains per unit area over a given structure. It is also possible to

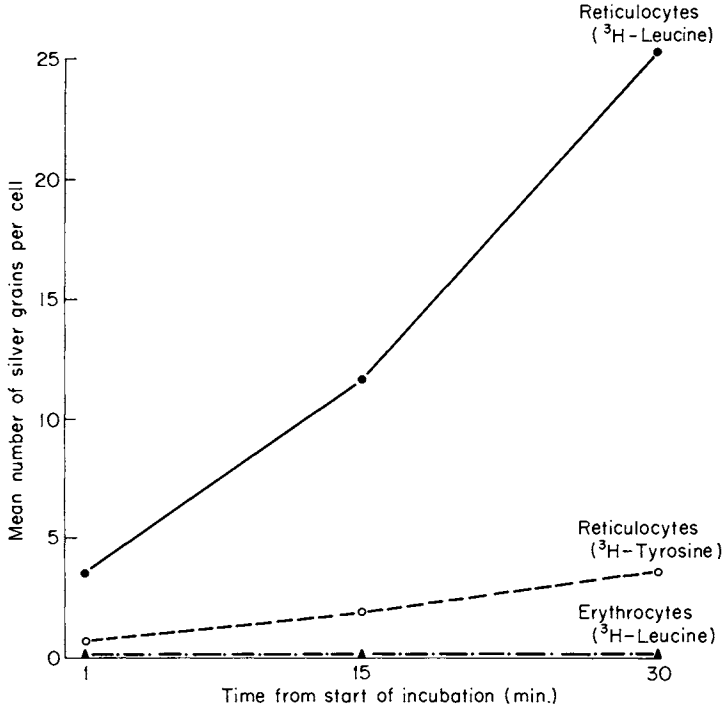

FIG. 4. Comparison between mean grain counts over reticulocytes after incubation of fresh rat blood with ^{3}H-leucine or ^{3}H-tyrosine and radioautography of the smears under identical conditions. With either precursor, reticulocytes become labeled, and the labeling increases with time. (The grain count over erythrocytes is equal to background fog.) The mean grain count is five to six times higher with ^{3}H-leucine than with ^{3}H-tyrosine at the three time intervals. Reproduced from Pinheiro *et al.* [48].

measure the intensity of radioautographic reaction by photometric or mechanical densitometry, but direct grain counting is usually preferred as it is not influenced by staining density and can be done over a discrete structure, however irregular.

The emulsion selected must be developed so as to yield grains large enough to be readily counted (in the case of AR 10 stripping film, it

is advantageous to prolong the development, e.g. 10 min in D-170). Furthermore, the grain count must be true. There must be neither addition of grains due to fogging and other artifacts, nor loss of grains due to the use of acids or other chemicals in post-staining. For instance, differentiation of hematoxylin in acid was shown by Kopriwa to be unsafe [25a].

(2) Grain count is dependent on the nature of the radiation and on the sensitivity and thickness of the emulsion as well as development procedure [39]. However, for a given radiation, e.g., from tritium, and for a nuclear emulsion of a sufficient thickness, there is, within a wide range, proportionality between *radiation exposure* and grain count, provided fading of the latent image is avoided (Figs. 15 and 16 in ref. [26]). With the widely used NTB2 emulsion, fading is prevented by exposing unstained preparations in a dry atmosphere at 4°C [26].

(3) The extent to which the *radioisotope concentration* influences radiation exposure depends largely on the extent of beta ray absorption within the structure that emits radiation (self-absorption) and within the rest of the section (tissue absorption).

In the case of tritium, Maurer and Primbsch found that the *self-absorption* within nucleolus, karyoplasm, and cytoplasm of liver was proportional to the relative densities, estimated at about 5, 1, and 1.5, respectively, in the interference microscope [37]. Grain counts (or radiation exposure) for these structures would have to be multiplied by the respective figures.

The *tissue absorption* of tritium is negligible in sections 0.1 μ thick or less. In sections up to about 3 μ thick, the absorption increases with the thickness [37]. But when sections are 3 or more μ thick, the beta rays from the deeper regions do not reach the surface, so that the thickness no longer influences radiation exposure. Because of this tissue absorption, grain counts should be related to the upper surface only of a structure. Counts over tiny structures such as a nucleolus should be done when the upper surface of the section cuts through them.

In practice, many of the difficulties due to beta ray absorption may be avoided when comparative grain counts are made on the same structure, for instance when counts over thyroid cells are compared at several times after labeled amino acid injection. The procedure is to mount the thyroids of all the animals in a single paraffin block, thus ensuring the same conditions (section and emulsion thickness, development, etc.) for all the specimens to be compared. The various grain counts are then proportional to radioisotope concentration.

Analysis of Results in the Electron Microscope

The first problem is to identify the source of the radioactivity eliciting the production of the radioautographic reaction. This is fairly easy with large sources, such as nucleus or Golgi zone (Fig. 8 in Droz's article, p. 166), but is often difficult when the source is small, as will be shown.

With a tissue source larger than a silver grain, there is usually, as in light microscopy, sufficient radioactivity emitted to produce a group of silver grains that is readily related back to the source. However, when the source is smaller than a silver grain, e.g., a ribosome, there is a limited amount of radioactive isotope present which, during the time of exposure, may emit very few radioactive particles, possibly only one and perhaps none. Thus, usually one can expect a single hit on a silver bromide crystal, which in a sensitive emulsion results in a silver grain. Therefore the radioautographic reaction will consist of scattered single grains, and the problem is to relate the collection of these grains to a particular structure in the underlying tissue. For instance, to trace newly formed glycogen [11, 12], which requires relating silver grains (about 1200 Å) to glycogen granules (about 240 Å), the distances from grain centers to suspected granules have to be measured; and the observed distribution of these distances has to be compared with the theoretical distribution expected in such cases, according to the theories of Granboulan and Salpeter given in this volume (Fig. 3, p. 47).

The second problem—quantitation—is again particularly difficult for small sources. For fairly large sources of radioactivity, the grain count is obtained by averaging the number of grains per unit area over a given structure in various localities, then, as performed by Ross in this volume, dividing the grain count by the per cent volume occupied by the structure in the tissue (measured by histometric methods) and, briefly, deriving the concentration of radioisotope in the source according to the reasoning used in light microscopy (Fig. 11, p. 286). In the electron microscope, the sections are so thin that there is neither self-absorption nor tissue absorption, and the amount of radiation emitted is directly proportional to section thickness. An exact control of section thickness would therefore be useful for quantitative work in the electron microscope. It is hoped that automatic microtomes will soon make it possible to cut sections of known thickness.

For small sources of radioactivity, a *grain count* can only be obtained by assessing the incidence of all observed grains which can be assigned to the structure under consideration. Since absorption is not a problem, this incidence is a measure of the relative *amount of radiation* emitted by

the structure. Then, this is related to the relative *concentration of radioisotope* in the structure by measuring the relative volume of the structure.

Mathematical Analysis

Mathematical analyses used in radioautography, like those in biochemistry, are usually based on the postulate that the structures considered are sufficiently simple and large to be treated as a series of pools, in each one of which the entering molecules are randomly mixed with preexisting ones, so that any molecule of the pool has the same chance to leave. Under these conditions the turnover time of protein in a structure, that is the time taken to replace an amount equal to that present, is really the mean time spent by any molecule in the pool [60].

The simplest method for measurement of the turnover time (or of its inverse, the turnover rate) is one in which absorption problems cancel out. After the precursor has left the circulation, the decrease in grain count plotted on semi-logarithmic paper versus time yields a straight line if only one labeled substance is involved, so that the negative slope gives the turnover rate, that is the inverse of turnover time, of the substance. Or the line may show two slopes, indicating the existence of two proteins with different turnovers (as in Figs. 1-3 of Droz's article, p. 160).

When the passage of a protein from one pool to another is investigated, it is necessary to make use of specific activities. A substance A is the precursor of a substance B if the specific activity curve of A plotted against time cuts the specific activity curve of B at its maximum. The measurement of specific activities usually involves two arduous tasks, the estimation of absolute concentrations of radioactivity on the one hand and the measurement of the protein content on the other hand, as discussed in ref. [57].

An unexpected benefit of the use of electron microscopy was to force reexamination of the assumptions made by biochemists and light microscopists in their mathematical analyses, that is, *random* and equal opportunities for all molecules in each pool [60]. When structures were examined in the electron microscope, it became clear that molecules often proceed in an *oriented* manner through a compartment and, therefore, classical formulations may not apply. When the molecules go along the whole length of a compartment, they may still have a normally distributed turnover time (although it would be more appropriate to speak of *transit time*), but when they follow different lengths of pathway in the compartment, their *mean transit time* then varies from low to high values without necessarily being normally distributed. New mathematical

models of migration and turnover time are being developed by Nadler to fit in with this concept.

SITES OF PROTEIN SYNTHESIS

Protein Synthesis in Nucleus and Cytoplasm of All Cells

There was a time, not too long ago, when protein synthesis in mammals was believed to be a specialized function of certain cells, such as liver cells, plasma cells, and so on [18], which would then supply the rest of the body with proteins. However, early radioautographic works revealed the widespread distribution of the reactions [19, 32] and led to the conclusion that the cytoplasm [32] as well as the nucleus [9] of all examined cells synthesized protein continuously. Thus, protein synthesis appears to be a universal phenomenon in mammalian cells, and perhaps in all animal and plant cells.

Conversely, no protein synthesis has ever been observed to take place outside cells, although a protein coming out of a cell may undergo changes or a "maturation." For instance, while thyroglobulin is synthesized in the follicular cell of the thyroid, its iodination takes place in the lumen of the follicle [40].

Cytoplasmic Protein Synthesis

The sooner a tissue is fixed after injection of a labeled amino acid, the better is the chance that the newly formed protein will still be at its site of synthesis. In work with Everett and Simmons, published in 1957, it was thought that sacrificing the animals 4 hours after injection of a labeled amino acid would be early enough to pinpoint the sites of protein synthesis in radioautographs [32]. It took a fair amount of work to realize how wrong this point of view was. Thus, in pancreatic acinar cells the time had to be reduced to 2–5 minutes after injection to be sure that most silver grains were restricted to a definite region of the cells [57]. At such early times, the reactions were located over the ribosome-rich regions of the cytoplasm, that is, over the *ergastoplasm* (Fig. 5). This is true of all cells examined so far, except for discrete reactions observed by Swift over mitochondria, indicating the possibility of a small degree of protein synthesis there [55].

The turnover time of proteins in the ergastoplasm of pancreatic acinar cells was estimated to be of the order of 5–6 minutes [57]. This time would seem to include not only the time taken for protein synthesis, that is, one or more amino acids per second according to Anfinsen [2], but also the time taken for the newly formed proteins to migrate out of the zone (that is, what was called above mean transit time).

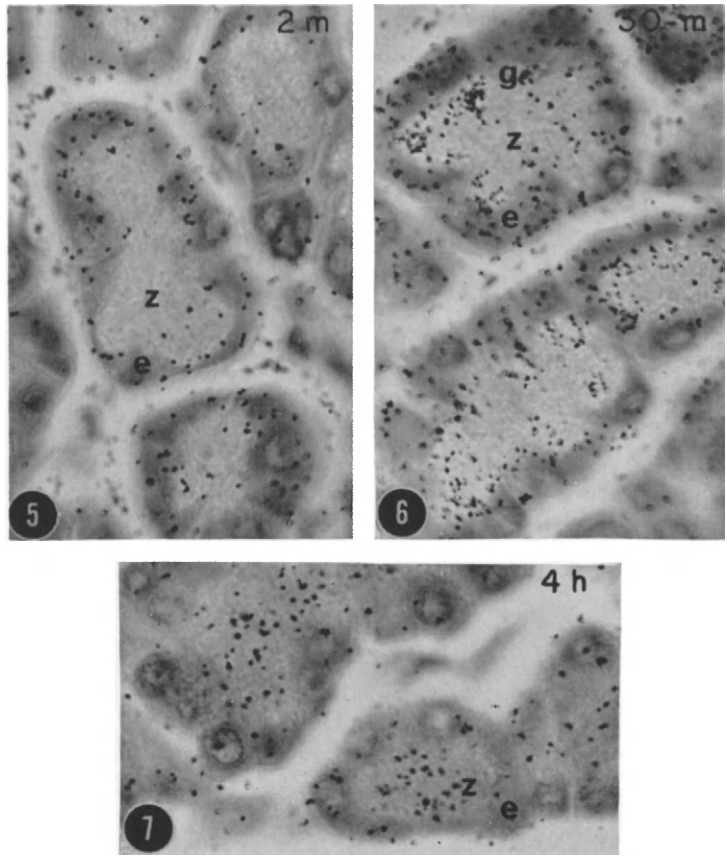

FIGS. 5, 6, and 7. Protein synthesis and migration in the acinar cells of pancreas, as seen in hematoxylin and eosin stained radioautographs of acini from rats injected with ^{3}H-leucine. Pancreatic acini are composed of several cells associated around a tiny lumen (not visible here) in such a way that their basal ergastoplasm shows as a basophilic peripheral band (e) enclosing their light-staining apical region filled with zymogen granules (z). Within the zymogen region of each cell, the proximal portion (close to the ergastoplasm) contains the Golgi complex.

At 2 minutes after injection of ^{3}H-leucine (Fig. 5), the silver grain reactions are confined to the ergastoplasm (e). At 30 minutes (Fig. 6), the reaction over the ergastoplasm (e) is slightly heavier than at the previous time intervals, but a more intense reaction is now over the proximal portion of the region of zymogen granules, where clusters of silver grains (corresponding to the Golgi region) are distinct (g), while the central portion of this region (z) shows no reaction. Later (4 hours, Fig. 7) the reactions extend to the whole zymogen region (z). Magnification: × 1000. Reproduced from Warshawsky *et al.* [57].

Nuclear Protein Synthesis

Protein is synthesized in both nucleolus and karyoplasm [30, 52]. The total amount of protein made is related to the size of the nucleus [38, 42]. Thus, a tetraploid nucleus of liver has twice the volume of, and makes twice as much protein as a diploid nucleus, so that both types of nuclei synthesize protein at exactly the same rate [7]. The rate of nuclear protein synthesis was not too different in several neurons, but was less in Sertoli cells and lymphocytes. (The rate for large, medium, and small lymphocyte nuclei was 72, 34, and 26%, respectively, of that of liver nuclei [7].) Yet, the work of Schultze *et al.*, described in this volume, makes it clear that when many types of nuclei are considered, nuclear size is roughly proportional to the amount of protein formed in the nucleus (Fig. 8, p. 125), so that the rate of this synthesis would be roughly the same in all nuclei. Probably, nuclear size is related to the rate of ribonucleic acid (RNA) synthesis, which in turn controls the rate of protein synthesis in the nucleus (and presumably in cytoplasm as well).

In conclusion, since protein synthesis occurs continuously in the nucleus and cytoplasm of all examined rat cells, and presumably in all living systems, it is likely that this continuous synthesis is a basic characteristic of life.

FATE OF PROTEINS

Three types of protein behavior may be considered: (a) The best understood is that of the proteins present in *secretions,* for instance the enzyme proteins produced by the pancreas; such proteins are elaborated in the cell and released, usually into a lumen. (b) Another readily understood case is that observed in *"renewal systems"* [28], that is, the organs in which new cells are being continuously produced (e.g., hemopoietic tissues); proteins have to be built up as new cells are formed to replace those lost. (c) A less well understood case is that of proteins undergoing intracellular turnover; they are referred to as *sedentary proteins.* The three cases will now be considered, starting with the last one.

Turnover of Sedentary Proteins

Within minutes after injection of a labeled amino acid into an adult animal, radioautographic reactions were observed over the cells of muscle, kidney, adrenal gland, and many others which, as far as we know, do not secrete protein nor undergo renewal [32]. These reactions persisted for several weeks or months, but eventually disappeared (Fig. 2). Hence, they were due to proteins that turn over.

It is likely that these proteins are used for the renewal of intracellular

components (nucleus, mitochondria, Golgi, etc.). In the *cytoplasm*, it is suspected that the lysozomes, which contain proteolytic enzymes, associate with other cell organelles and cause their lysis [59], so that the newly formed proteins would provide for the replacement of cell organelles. In the *nucleus*, it is likely that some of the proteins turn over *in situ* (Schultze *et al.*, this volume), while others migrate back and forth between nucleus and cytoplasm (Goldstein, this volume). These various types of cytoplasmic and nuclear proteins remain within the confines of the cell and are accordingly called *sedentary*.

Sedentary proteins also exist in secreting and renewing cells. For instance, when, following an injection of radioactive amino acid, the pancreatic acinar cells secrete labeled enzymes, a significant amount of radioactivity remains in the cytoplasm afterwards [57]. While some of this radioactivity may be due to reutilization of amino acids released by the breakdown of labeled proteins, the bulk of it is attributed to proteins

TABLE I. *Approximate Turnover Time of Proteins*[a]

Site	Exportable	Sedentary
Neurons	1 day (axonal proteins)	2 weeks
Thyroid cell	9 hours (thyroglobulin)	2½ weeks
Pancreas cell	1 hour (pancreatic enzymes)	2 days

[a] After Nadler, quoted in ref. [29].

turning over intracellularly, that is, to sedentary proteins. Table I, which is based on calculations neglecting reutilization, provides a comparison of the turnover time of sedentary and secretory—or exportable—proteins released by the same cell.[2]

Renewal Systems

Several organs of non-growing animals exhibit mitotic figures which yield cells replacing lost or dying cells. Thus, in the intestinal epithelium, the mitosis of the crypts provide cells which migrate onto the villus surface to replace cells lost from the villus tips. Similar cell renewal takes place in many surface epithelia [36] (e.g., epidermis), in blood-forming organs, in testis, etc. When these organs are radioautographed after injection of a labeled amino acid, active protein synthesis is found [32] in direct proportion to the number of cells being produced.

[2] Table II of Tonna's article in this volume gives the half life (turnover time $\times 0.693$) of exportable and sedentary proteins in bone and cartilage cells.

One may well wonder why body components, such as cells or individual proteins, are being renewed. A *priori*, living matter could overcome environmental hazards in two ways. First, the formation of new living matter could be triggered in case of wear or damage, and thus provide repair. Secondly, there could be continuous formation of new living matter with corresponding loss taking place whether or not there had been damage. The second procedure, although costly in terms of energy, has important advantages: simplicity since no feed-back mechanism is required to trigger synthesis, and efficiency since cells and proteins are usually cast off *before* they have a chance to become damaged by wear and tear. In modern industry, procedures of the second type have often proved more effective than those of the first, e.g., the replacement of parts of airplane engines before they have a chance to wear out. It is likely that the renewal of some cells and proteins proved beneficial and was, therefore, preserved in the course of evolution.

Secretory Proteins

One of the most exciting findings arising from electron microscope radioautography is the discovery of the complex pathway by which secretory proteins migrate from their site of synthesis—the ergastoplasm—to the outside of the cell. The pattern is that the new protein goes from ergastoplasm to Golgi complex, from where it comes out in secretion granules or vesicles, which finally take their content to the outside. The sequence has been observed in cells of cartilage by Revel and Hay [50], connective tissues by Ross and Benditt [51], thyroid by Nadler *et al.* [40], pancreas by Warshawsky *et al.* (Figs. 5–7, ref. [57]), as well as by van Heyningen [56] and Caro and Palade [10], mammary glands by Wellings and Philp [58], and probably ameloblasts.[3]

By piecing together information obtained from various cells, the detailed sequence of events appears to be as follows: (a) A messenger RNA (Fig. 1) associates with groups of ribosomes, referred to as "polysomes" and elicits protein synthesis. In secretory cells, most polysomes lie on the outer surface of the cisternae of the endoplasmic reticulum. (b) The newly formed protein leaves the polysome, crosses the cisternal membrane, and passes into the cisternal fluid, a step shown in the follicular cells of the thyroid, where silver grains appear over the lumen of cisternae (Fig. 6, p. 308). (c) The proteins are believed to be carried in microvesicles from the cisternae of endoplasmic reticulum to the Golgi saccules [10]. (d) The saccules give rise to secretion granules, e.g., the

[3] This work was the object of a demonstration by H. Warshawsky at the symposium (mentioned in the discussion of Greulich's article, p. 214).

zymogen granules of pancreatic cells (Fig. 3, p. 266), or to vesicles, e.g., the apical vesicles in thyroid cells (Fig. 7, p. 308; Fig. 8, p. 310). (e) Finally, the secretion granules or vesicles open up at the surface of the cell where they release their content (Fig. 5, p. 268; Fig. 10, p. 285; Fig. 10, p. 310).[4]

Role of the Golgi Complex

An intriguing feature of the scheme is why secretory proteins go through the Golgi complex. The classical explanation is a rather weak one, summarized in the words "packaging of secretion." Recent findings suggest two more exciting possibilities.

One is based on biochemical observations of Seed and Goldberg concerned with the formation of thyroglobulin in the thyroid gland [53]. Within minutes after administration of labeled leucine, a radioactive protein is detected which has half the size of thyroglobulin, while 30–45 minutes later labeled full-size thyroglobulin appears and increases in amount. On the other hand, radioautographs after ^{3}H-leucine injection show a reaction over the ribosomes at 10 minutes, whereas Golgi reactions appear after 30 minutes (p. 303 and following). It is, therefore, possible that the Golgi region is the site where the smaller protein molecules combine to give rise to full-sized thyroglobulin.

An equally stimulating clue was provided by the frequent finding in the Golgi region of glycoprotein, as shown by the periodic acid-Schiff technique [47] and of acidic carbohydrates, as shown by the colloidal iron technique [3]. These complex carbohydrates are also found in the secretion itself [33, 35], where their content may be high as in mucous secretions or low as in serous secretions (e.g., pancreatic acinar cells). Since glucose is used as a building stone in the course of synthesis of complex carbohydrates [13, 14], ^{3}H-glucose could be injected and radioautography used to locate the sites of synthesis of these carbohydrates.[5]

At an early time after injection, 5 minutes, strong radioautographic reactions were found over the Golgi region of goblet cells of intestine (Fig. 8), mucus-secreting cells of sublingual and submaxillary glands,

[4] Proteins which are secreted into the blood stream (like the plasma proteins released by liver cells) or into connective tissue spaces (like collagen elaborated by fibroblasts) may turn over in their new compartment. Collagen is a particularly interesting case. Radioautography indicates that the dentinal collagen is stable [8, 20, 24], in agreement with biochemical observations of very slow collagen turnover [41, 54]. However, in this volume, Carneiro reports the finding of a collagen with fairly rapid turnover in the periodontal ligament (Fig. 3, p. 250). Thus, a given type of protein may have a different turnover in different locations.

[5] This work was the object of a demonstration of Miss Marian Peterson (now Mrs. R. Neutra) at the symposium.

Brunner gland cells of duodenum, chondrocytes, etc. Moderate reactions were found over the Golgi regions of other cells, such as the chief cells of intestine (Fig. 9). At later times after injection, e.g., 1–3 hours, the reactions appeared over the secretion product. It was concluded that the

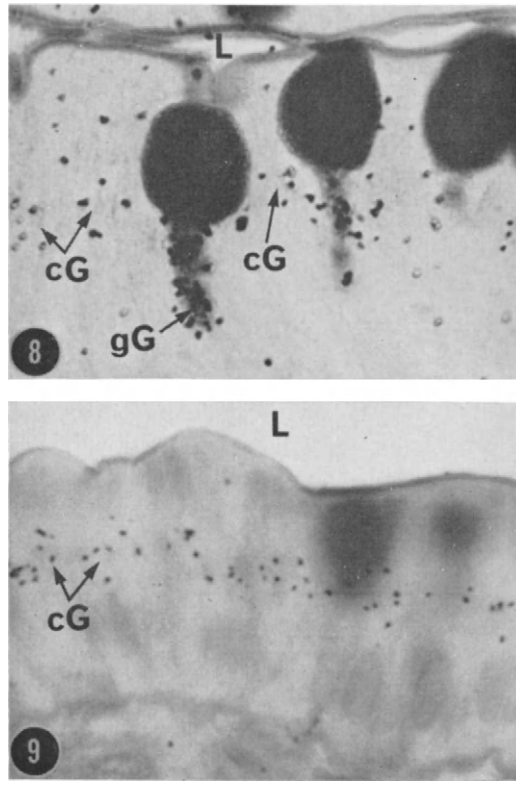

FIG. 8. Periodic acid-Schiff stained radioautograph of duodenal epithelium from 100-gm rat following ^{3}H-glucose injection. The heavily stained tadpole-shaped structures are the goblet cells; the "tails" correspond to their Golgi region (gG). Between the goblet cells lie the unstained columnar cells. At top, a narrow portion of the intestinal lumen (L) is lined on both sides by the striated border. Silver grains are accumulated over the Golgi region of goblet cells (gG). The grains scattered over the cytoplasm of chief cells predominate over their Golgi region (cG). Magnification: × 1300. Reproduced from Peterson and Leblond [47].

FIG. 9. Periodic acid-Schiff–hematoxylin stained radioautograph of colonic epithelium, 5 minutes after injection of ^{3}H-glucose into the lumen of the colon. Two goblet cells out of focus appear as two hazy spots at right. The field shows a series of columnar cells, with the intestinal lumen at top (L). Local injection allowed contact of the cells with a large dose of ^{3}H-glucose. Under these conditions, silver grains are regularly found over the Golgi region of chief cells (cG). Magnification: × 1300. Reproduced from Peterson and Leblond [46].

labeled glucose trapped in the Golgi region was incorporated into the secretion product, presumably as complex carbohydrate [46, 47].

The electron microscope showed silver grains over all the stacked Golgi saccules in the goblet cells of colon at 5 and 15 minutes after ^{3}H-glucose injection [45]. Hence, any Golgi saccule (of which the proximal ones have a narrow lumen, and the distal ones have a lumen containing a mucus-like material) would seem to provide for the synthesis of complex carbohydrates. By 1 hour, the labeled material had migrated from the Golgi region into the mucigen droplets of the mucous theca; and by 3 hours, some label was seen in the excreted mucus outside the cell. Hence, the glucose label bound as a complex carbohydrate in Golgi saccules was released as a component of mucus.[6]

In conclusion, the uptake of glucose in the Golgi region indicates that the Golgi complex provides for carbohydrate synthesis. Thus, the protein moiety coming from the ergastoplasm may not only acquire its full size in the Golgi complex, as suggested by the work of Seed and Goldberg [53], but may also combine there with carbohydrate [45–47]. The addition of a carbohydrate component to protein secretion is probably the key step in the "packaging" of secretion.

CONCLUSION

Whenever we carry out a chemical analysis or prepare a section for radioautography from an animal in steady state, we see what happens at a given time in a system in which sequential chemical reactions and intracellular migrations occur continuously. Radioautography has to be done at various times after injection of a labeled substance to visualize the sequence of events as they happen normally. Particularly, the sites of synthesis of proteins and the course of their migrations may be identified, and the rates at which these phenomena occur may be measured.

The nucleus and cytoplasm of all the cells examined synthesize protein continuously. While some proteins turn over within nucleus or cyto-

[6] It was recently observed by Miss M. Peterson that ^{3}H-galactose is also taken up in the Golgi region. Thus, at 10 minutes, a particularly intense Golgi reaction was seen over the chief cells of intestine. By 30 minutes, much radioactivity had left the Golgi and accumulated at the apical surface. Since the material present at this surface is probably part of the "cell coat" [49], it may be speculated that the cell coat contains a complex carbohydrate which is rich in galactose and, in some locations, is fairly rapidly renewed. (Ito and Revel have already reported passage of labeled protein and carbohydrate into the fuzz covering the apical surfaces of these cells in the cat [21]).

Finally, since ^{35}S-sulfate is also taken up in the Golgi complex of some cells [22, 43, 47], it is presumed that sulfated polysaccharides acquire their sulfate in the same region.

plasm, others migrate back and forth between these two parts of the cells, and others are released to the outside as secretory proteins.

A common pathway has been described in this volume for a number of secretory proteins. From the ribosomes of the ergastoplasm where they are synthesized, these proteins migrate through the cisternae of the endoplasmic reticulum into the Golgi region, where they are "packaged" as secretion granules or vesicles. Since carbohydrate macromolecules are synthesized in the Golgi region, the packaging may involve their combination with protein to make up the secretory material.

These and many other results reported in the present volume show that, in the protein field as in others, radioautography stands at the crossroads of Biochemistry and Morphology.

ACKNOWLEDGMENTS

Most of the work reported in this article was done with the support of the Medical Research Council of Canada.

Suggestions from Dr. H. van Heyningen, Mrs. R. Neutra, and especially Dr. N. J. Nadler were helpful in the writing of this article.

REFERENCES

1. Allfrey, V., Daly, M. M., and Mirsky, A. E., *J. Gen. Physiol.* **37**, 157 (1953).
2. Anfinsen, C. B., *Proc. Can. Cancer Conf.* **5**, 3 (1963).
3. Badinez, O., Gasic, G., Loebel, F., and Baydak, T. *Nature* **193**, 704 (1962).
4. Bélanger, L. F., *Anat. Record* **124**, 555 (1956).
5. Bélanger, L. F., and Leblond, C. P., *Endocrinology* **39**, 8 (1946).
6. Bloom, W., Curtis, H. J., and McLean, F. C., *Science* **105**, 45 (1947).
7. Carneiro, J., unpublished observations, 1959.
8. Carneiro, J., and Leblond, C. P., *Exptl. Cell Res.* **18**, 291 (1959).
9. Carneiro, J., and Leblond, C. P., *Science* **129**, 391 (1959).
10. Caro, L. G., and Palade, G. E., *J. Cell Biol.* **20**, 473 (1964).
11. Coimbra, A., Proc. Histochem. Soc. 1965 (in press, *J. Histochem. Cytochem.*).
12. Coimbra, A., and Leblond, C. P., *Anat. Record (Proc.)* **151**, 337 (1965).
13. Dorfman, A., *J. Histochem. Cytochem.* **11**, 2 (1963).
14. Draper, P., and Kent, P. W., *Biochem. J.* **86**, 248 (1963).
15. Droz, B., and Warshawsky, H., *J. Histochem. Cytochem.* **11**, 426 (1963).
16. Ficq, A., *Experientia* **9**, 377 (1953).
17. Ficq, A., and Errera, M., *Biochim. Biophys. Acta* **16**, 45 (1955).
18. Fisher, R. B., "Protein Metabolism." Methuen, London, 1954.
19. Greulich, R. C., and Leblond, C. P., *Anat. Record* **115**, 559 (1953).
20. Greulich, R. C., and Leblond, C. P., *J. Dental Res.* **33**, 859 (1954).
21. Ito, S., and Revel, J. P., *J. Cell Biol.* **23**, 44A (1964).
22. Jennings, M. A., and Florey, H. W., *Quart. J. Exptl. Physiol.* **41**, 131 (1956).
23. Karpishka, I., and Carneiro, J., *Anat. Record* **137**, 73 (1960).
24. Karpishka, I., Leblond, C. P., and Carneiro, J., *Arch. Oral Biol.* **1**, 23 (1959).
25. Kemp, N. E., *J. Exptl. Zool.* **133**, 227 (1956).
25a. Kopriwa, B. M., unpublished observations, 1964.
26. Kopriwa, B. M., and Leblond, C. P., *J. Histochem. Cytochem.* **10**, 269 (1962).

27. Leblond, C. P., *Ann. Histochim.* **8**, 43 (1963).
28. Leblond, C. P., *Natl. Cancer Inst.* (Monogr.) **14**, 119 (1964).
29. Leblond, C. P., *Am. J. Anat.* **116**, 1 (1965).
30. Leblond, C. P., and Amano, M., *J. Histochem. Cytochem.* **10**, 162 (1962).
31. Leblond, C. P., and Bélanger, L. F., *Anat. Record* (Proc.) **94**, 98 (1946).
32. Leblond, C. P., Everett, N. B., and Simmons, B., *Am. J. Anat.* **101**, 225 (1957).
33. Leblond, C. P., Glegg, R. E., and Eidinger, D., *J. Histochem. Cytochem.* **5**, 445 (1957).
34. Lusk, G., "The Elements of the Science of Nutrition." Saunders, Philadelphia, 1909.
35. Mandel, I. D., and Ellison, S. A., *Ann. N.Y. Acad. Sci.* **106**, 271 (1963).
36. Marques-Pereira, M. P., and Leblond, C. P., *Am. J. Anat.* **117**, 73 (1965).
37. Maurer, W., and Primbsch, E., *Exptl. Cell Res.* **33**, 8 (1964).
38. Montreuil-Langlois, M., *Xth Intern. Congr. Cell Biol.* (L'expansion, éditeur Paris) **10** (1960).
39. Nadler, N. J., *Am. J. Roentgen. Rad. Therap., Nuc. Med.* **70**, 814 (1953).
40. Nadler, N. J., Young, B. A., Leblond, C. P., and Mitmaker, B., *Endocrinology* **74**, 333 (1964).
41. Neuberger, A., and Slack, M. G. B., *Biochem. J.* **53**, 47 (1953).
42. Oehlert, W., and Schultze, B., *Proc. 1st Intern. Congr. Histochem. Cytochem.* (Paris) p. 15 (1960).
43. Otero-Vilardebo, L., Lane, N., and Godman, G. C., *J. Histochem. Cytochem.* **12**, 34 (1964); *J. Cell Biol.* **21**, 339 (1964).
44. Pelc, S. R., *Nature* **160**, 749 (1947).
45. Peterson, M., *Anat. Record* (Proc.) **151**, 399 (1965).
46. Peterson, M., and Leblond, C. P., *Exptl. Cell Res.* **34**, 420 (1964).
47. Peterson, M., and Leblond, C. P., *J. Cell Biol.* **21**, 143 (1964).
48. Pinheiro, P., Leblond, C. P., and Droz, B., *Exptl. Cell Res.* **31**, 517 (1963).
49. Rambourg, A., Neutra, M., and Leblond, C. P., *Anat. Record*, in press.
50. Revel, J. P., and Hay, E. D., *Z. Zellforsch.* **61**, 110 (1963).
51. Ross, R., and Benditt, E. P., *J. Cell Biol.* **22**, 365 (1964).
52. Sandborn, E., *Anat. Record* (Proc.) **145**, 280 (1963).
53. Seed, R. W., and Goldberg, I. H., *Proc. Natl. Acad. Sci.* **50**, 275 (1963).
54. Stack, M. V., *Ann. N.Y. Acad. Sci.* **60**, 585 (1955).
55. Swift, H. private communication (1964).
56. Van Heyningen, H. E., *Anat. Record* **148**, 485 (1964).
57. Warshawsky, H., Leblond, C. P., and Droz, B., *J. Cell. Biol.* **16**, 1 (1963).
58. Wellings, S. R., and Philp, J. R., *Z. Zellforsch.* **61**, 871 (1964).
59. Wolstenholme, G. E. W., "Lysosomes." Ciba Found. Symp., 1963.
60. Zilversmit, D. B., Entenman, C., and Fischler, M. C., *J. Gen. Physiol.* **26**, 325 (1943).

AUTHOR INDEX

Numbers in parentheses are reference numbers and indicate that an author's work is referred to although his name is not cited in the text. Numbers in italic show the page on which the complete reference is listed.

Alexander, N. M., 313 (1), *317*
Alfert, M., 95 (1), *105*
Algire, G. H., 145 (1), *156*
Allfrey, V., 322 (1), *338*
Altman, J., 115 (1, 2), *137*
Amano, M., 303 (18), *317*, 332 (30), *339*
Anderson, E., 293 (1), *301*
Andrews, J. S., 293 (16), *301*
Anfinsen, C. B., 330, *338*
Applegren, L. E., 28 (5), *39*, 58 (6), *62*
Appleton, T. C., 13 (21), 14 (1), *20*, 65 (1), 72 (1), *74*
Aquaron, R., 313 (5), *317*
Araya, S., 255 (1, 22), *255*, *256*
Arnold, J. S., 2, *5*
Arnott, D. J., 159 (29), 171 (29), *173*
Attardi, G., 145, *156*
Audran, R., 54 (11), *62*
Axelrod, D., 2, *5*

Bachmann, L., 28 (17), 29 (2, 17), 30 (17), 31 (17), 35 (1, 2, 17), 36 (17), 37 (1, 17), *39*, 49, 53, 54, 61, *63*, 289 (1), 290 (18), *291*
Badinez, O., 335 (3), *338*
Ballou, J. E., 254 (37), *256*
Baserga, R., 10, *20*
Bauer, E. C., 14 (12), *20*
Baydak, T., 335 (3), *338*
Bélanger, L. F., 1 (2), *5*, 10, *20*, 115, *137*, 177, 178, *196*, 201 (1), 202 (2, 3), 206 (15), *213*, *214*, 321 (5, 31), 322 (4), *338*, *339*
Bénard, B., 313 (19a), 314 (19a), *317*
Benditt, E. P., 65 (3, 11, 12), 67 (2), 72 (2, 12), 74 (3, 12), *74*, 75, 210, 211 (19), *214*, 217, *244*, 247 (29), 254 (30), *256*, 269 (11), *270*, 273 (14, 16), 275 (15), 278, 289 (16), *291*, 293 (15), *301*, 312 (30), *317*, 334, *339*
Bentley, J. P., 255 (17), *256*
Berman, I., 145 (36), 154 (36), *157*
Bernhard, W., 51 (12), 53 (12, 18), *62*, *63*
Bessman, M., 99 (2), *105*
Bidwell, E., 251 (2), *255*
Billingham, R. E., 145 (3, 4), *156*
Binet, J. L., 155, *156*
Blake, William, *55*
Blanquet, P., 303 (33), *317*
Bloch, D. P., 95 (3, 4), *105*
Bloom, W., 2, *5*, 322 (6), *338*
Bogoroch, R., 2, *6*, 316 (21), *317*
Bonar, L. C., 207 (7), *213*
Borsook, H., 238, *243*
Bowes, J. H., 254 (3), *255*
Boyd, G. A., 2 (5), 3 (5), 5, 10, 14 (12), *20*
Brachet, J., 115, *137*
Brack, S. D., 95 (3), *105*
Brady, L. E., 33 (8), 37 (8), *39*
Branton, D., 14 (6), *20*, 65 (4), *74*
Braunsteiner, H., 145 (6), 154 (6), *156*
Brecher, G., 147 (29), 157
Brent, L., 145 (3), *156*
Brownell, L. E., 95 (5), *105*
Brückner, J., 122 (13), *137*
Bryant, B. J., 239 (2, 3, 4), *243*
Budd, G. C., 29 (14), *39*, 49 (24), 54 (2), *63*
Bunge, M. B., 171 (1), *173*
Bunge, R. P., 171 (1), *173*
Busanny-Caspari, W., 129 (4), 130 (4), *137*
Byers, T. J., 79 (1, 2), 80 (1, 2), 82 (1), 85 (1), *93*

Caffrey, R. W., 143 (33), 145 (7, 11, 14, 15, 16, 34), 146 (15, 16), 150 (15), 151 (16), *156*, *157*
Cameron, D. A., 215 (19), *244*
Cameron, I. L., 97 (11), *105*
Campbell, P. N., 312 (2), *317*

Campo, R. D., 215 (5), 218 (5), *243*
Carlsson, A., 65 (5), *74*
Carneiro, J., 202 (13), 211 (3), *213*, 214, 217 (6), 233, 241 (6), *243*, 247 (4), 248 (4), 254 (4), *255*, *291*, 303 (22), *317*, 324, 330 (9), 332 (7), 335 (8, 24), *338*
Caro, L. G. 28 (4), 29 (3), 35 (4) 37 (4), *39*, 43 (5), 44 (4), 45, 54 (3), 47, *62*, 265 (1), 269 (1), *270*, 275 (3), 279 (5), 288 (5), 289, *291*, 298 (2), *301*, 307 (3), 309 (4), *317*, 334 (10), *338*
Cartouzou, G., 313 (5), *317*
Caspersson, T., 303 (11), *317*
Caulfield, J. B., 309 (6), *317*
Chaikoff, I. C., 161 (36), *174*
Chalkley, H. W., 68, *75*, 275 (2), 278, *291*
Chawla, T. N., 255 (5), *255*
Chichester, C. O., 14 (26), *20*
Chow, P. C., 49 (27), *63*
Citoler, K., 115 (7), 119 (7), 125 (7), *137*
Citoler, P., 115 (7), 119 (7), 122 (6), 125 (7), 129 (5, 6), 130 (5, 6), *137*
Clouet, D. H., 171 (2), *173*
Cohen, D. W., 255 (31), *256*
Cohn, M., 145 (2), *156*
Cohn, P., 159 (3), *173*
Cohn, S., 254 (6), *255*
Coimbra, A., 328 (11, 12), *338*
Collidge, E. D. 254 (7), *255*
Comar, C. L., 2, *5*
Coombes, J. D., 29 (14), *39*, 49 (24), *63*
Cooper, E. H., 145 (28), 146, *157*
Copp, D. H., 2, *5*
Cowen, D. M., 146 (20), *156*
Cowing, R. F., 14 (13), *20*
Cronkite, E. P., 147 (29), *157*, 206 (12), *214*, 217 (29, 31, 32), 218 (29, 31, 32), 222 (32), 231 (28, 30), 233 (30, 32), 234 (32), 238 (32), 241 (29, 31, 32), 242 (30), *244*
Curtis, H. J., 2, *5*, 322 (6), *338*

Dalton, A. J., 265 (16), *270*
Daly, M. M., 322 (1), *338*
Daniel, E. J., 207 (7), *213*
Daniels, E. W., 82 (3), 84 (3), *93*
Deasy, C. L., 238 (1), *243*
Debons, A. F., 14 (25), *20*
De Groot, L. J., 313 (7), *317*
Deimel, M., 120 (8), *137*
Dempsey, E. W., 303 (8), *317*
Denten, R., 254 (3), *255*
DeRobertis, E., 303 (9), *317*
Derrien, Y., *317*
Diderholm, H., 239 (9), *243*
Dittman, J. A., 14 (25), *20*
Dodson, J. W., 300 (3), *301*
Dohlman, G. F., 28 (5), *39*, 58 (6), *62*, *198*
Doljanski, L., 247 (8), *256*
Doniach, I., 9 (7), 13 (7), *20*, 47, *62*
Dorfman, A., 335 (13), *338*
Dougherty, T. F., 155, *156*
Downey, H., 155, *156*
Draper, P., 335 (14), *338*
Droz, B., 154 (27), *156*, 159 (6, 8, 27a), 160, 161 (6, 9), 162, 165 (5, 6, 7, 31), 168, 170 (4, 7), 171 (4, 5, 6, 7, 31), *173*, 261 (14), 263 (2), 269 (14), *270*, 273 (20), *291*, 298 (17), *301*, 303 (35), *318*, 323 (57), 324 (15), 325 (48), 326 (48), 329 (57), 330 (57), 331 (57), 333 (57), 334 (57), *338*, *339*
Droz, M., 115 (9), 119, 129 (35), *137*, *138*
Dziewiatkowski, D. D., 215 (5), 218 (5), *243*

Eastoe, J. E., 207 (5), 209 (4), 211 (6), *213*, 215 (7, 8), 218 (7, 8), 220 (7, 8), *243*
Edds, M. V., Jr., 293 (4), 295 (5), *301*
Edlund, Y., 265 (3), 269 (3), *270*
Edsall, J. T., 73 (10), *75*
Edstrom, A., 171 (10a), *173*
Edwards, L. C., 14 (8), *20*, 65 (7), *75*
Eidinger, D., 335 (33), *339*
Eidinoff, M. L., 3 (10), *6*
Ekholm, R., 265 (3), 269 (3), *270*
Elliot, A. M., 95 (5), *105*
Elliott, S. R., 215 (20), *244*
Ellison, S. A., 335 (35), *339*
Endicott, K. M., 10, *20*
Engström, H., 186 (4), *196*

Entenman, C., 161 (36), *174*, 329 (60), *339*
Epstein, L., 155 (10), *156*
Eränko, O., 65 (8), *75*
Erb, W., 189 (5), 195 (5), *196*
Errera, M., *338*
Evans, H. M., 2, *6*
Evans, T. C., 2, *6*
Everett, N. B., 115 (17), *137*, 143 (33), 145 (7, 11, 12, 13, 14, 15, 16, 34), 146 (13, 15, 16, 23), 150 (15), 151 (16), *156*, *157*, 159 (24), *173*, 202 (16), *214*, 322 (32), 324 (32), 330 (32), 332 (32), 333 (32), *339*

Falck, B., 65 (5), *74*
Fernando, N. V. P., 247 (9), *256*
Ferris, W., 293 (18, 19), *301*
Fichtelius, K.-E., 239 (9), *243*
Ficq, A., 10, *20*, 115, *137*, 322 (16, 17), *338*
Fischer, J., 115 (12), *137*, 159 (11), *173*
Fischler, M. C., 329 (60), *339*
Fisher, N. C., 161 (36), *174*
Fisher, R. B., 330 (18), *338*
Fitton Jackson, S., 216 (10), *243*, 298, *301*
Fitzgerald, P. J., 3, *6*, 14 (11), *20*, 65 (9), 72, *75*
Flanigan, S. J., 159 (12), *173*
Florey, H. W., 337 (22), *338*
Ford, C. E., 146 (20), *156*
Ford, D. H., 159 (13), *173*
Frank, J. A., 155, *156*
Freese, M., 177 (6), *196*
French, D., 73 (10), *75*
Frey-Wyssling, A. J., 28 (11), *39*, 58 (15), *62*
Friedberg, F., *173*
Friede, R., 170 (15), *173*
Fruton, J. S., 217 (11), *243*
Fullmer, H. M., 255 (10), 256

Gabrielli, E., 159 (12), *173*
Gaitonde, M. K., 159 (3, 16), *173*
Gall, J. G., 95, *105*
Gallimore, J. C., 14 (12), *20*
Gallop, P. M., 251 (32), *256*
Gasic, G., 335 (3), *338*
Gerbaulet, K., 122 (13), *137*
Gersh, I., 303 (11), *317*
Gesner, B. M., 145 (19), 146 (19), *156*
Clegg, R. E., 335 (33), *339*
Glickman, I., 248 (11), 255 (5), *255*, *256*
Glimcher, M. J., 207 (7), *213*
Godman, G. C., 95 (4), *105*, 216 (12), *243*, 289 (6), *291*, 337 (43), *339*
Goldberg, I. H., 91 (9), *94*, 313 (31), *317*, 335, 337, *339*
Goldman, H. M., 255 (12), *256*
Goldstein, L., 79 (1, 2, 4, 5), 80 (1, 2), 82 (1), 85 (1), *93*
Gorbman, A., 2, *6*
Goslar, H. G., 171 (17), *173*, 189 (7), *196*
Gowans, J. L., 145 (17, 18, 19), 146 (17, 19, 20), 154 (18), *156*
Granboulan, N., 51 (8, 12), 53 (12), *62*
Granboulan, P., 28 (6), 31 (6), *39*, 44 (10), 51 (8, 12), 53 (12), 54 (11), 62 (9), *62*, 309 (12), *317*
Green, J. A., *257*
Green, N. M., 255 (13), *256*
Greenberg, D. M., *173*
Greulich, R. C., 201 (9, 10), 202 (9), 206 (15, 22), 211 (8), *214*, 322 (19), 330 (19), 335 (20), *338*
Grigoleit, G., 14 (29), *21*
Gross, J., 2, *6*, 43 (30), *63*, 303 (18, 19), 316 (19), *317*
Gross, J. A., 95 (5), *105*

Haagen-Smith, A. J., 238 (1), *243*
Hamilton, J. F., 33 (8), 37 (8), *39*
Hamilton, J. G., 2, *5*
Hammerstrom, L., 28 (5), *39*, 58 (6), *62*
Hammond, J. H., 14 (31), *21*
Harford, C. G., 43 (17), *62*
Harkness, R. D., 255 (14), *256*
Harris, E. B., 9 (17), *20*
Harrison, A., 14 (31), *21*
Harrison, K., 313 (20a, 23), *317*
Harrison, R. G., 293 (7), *301*
Haurowitz, F., 305 (13), *317*
Hay, E. D., 28 (7, 15), 29, *39*, 49 (13, 26), *63*, 217 (18), 241 (18), *244*, 247 (27), 254 (27), *256*, 269 (4, 8), *270*, 275 (7), 279 (12), *291*, 293 (8, 9), 295 (9, 13, 14), 298 (14),

301, 309 (14, 28), 312 (29), *317*, 334, *339*
Hebb, C. O., 165 (18), 170 (18), *173*
Hempel, K., 115 (7, 28), 119 (7), 122 (14, 20), 125 (7), 129 (14, 20), 130 (14, 20), *137*, *138*, *197*
Hibbard, E., 238 (13), *243*
Hildemann, W. H., 145 (21), *156*
Hilker, D. M., 254 (18), *256*
Hillarp, H., 65 (5), *74*
Hirschman, A., 159 (13), *173*
Hiscoe, H., 170 (35), 171 (35), *174*
Hodge, A. J., 247 (15), *256*
Hoffman, M. M., 203 (11), *214*
Hoffman, P., 215 (14), *244*
Hokin, L. E., *270*
Holcenberg, J., 65 (3, 11), 74 (3), *74*, *75*
Hole, H., 14 (29), *21*
Holstrom, V., 14 (32), *21*
Holt, M. W., 14 (13), *20*
Holt, S. J., 53 (19), *63*
Holter, H., 97 (7), *105*
Holub, M., 155, *156*
Horibata, K., 145 (2), *156*
Hotta, Y., 98, *105*
Howard, A., 2, *6*, 13 (14, 22), *20*
Huang, T., 14 (15), *20*
Hultin, T., 312 (15), *317*
Hussein, A., 177 (8), *196*
Hwang, W. S. S., 206 (12), *214*

Imagawa, Y., 255 (22), *256*
Ingbar, J. H., 313 (34), *317*
Ishiwara, T., 255 (1), *255*
Ito, S., 313 (16), *317*, 337 (21), *338*

Jackson, D. S., 255 (16, 17), *256*
Jacobson, K. B., 102 (9), *105*
Jacobson, L., 14 (6), *20*, 65 (4), *74*
James, T. H., 37 (9), *39*
Jarabak, J., 254 (39), *256*
Jee, W. S. S., 2, *5*
Jennings, M. A., 337 (22), *338*
Joftes, D. L., 2, *6*, 10, *20*
Johnson, F. B., 65 (2), 67 (2), 72 (2), *74*

Kao, K.-Y. T., 254, *256*
Karnovsky, M. J., 35 (10), 38 (10), *39*
Karpishka, I., 202 (13), *214*, 324, 335 (24), *338*
Kayes, J. K., 43 (14), *62*
Keighley, G., 238 (1), *243*
Kemp, N. E., 238 (13), *243*, 322 (25), *338*
Kent, P. W., 335 (14), *338*
Kerr, D. A., 255 (19), *256*
King, B. C., 159 (29), 171 (29), *173*
Klein, L., 251 (32), *256*
Klika, E., 159 (19), *173*
Knight, E. J., 145 (18), 154 (18), *156*
Knoll, J. E., 3 (10), *6*
Koburg, E., 115 (15, 16, 28), *137*, *138*, 177 (9, 10, 11, 12, 13, 18), 178 (15), 182 (22), 195 (10), *196*, *197*
Koehler, J. K., 28 (11), *39*, 58 (15), *62*
Koelle, G. B., 171 (20), *173*
Koenig, E., 171 (20), *173*
Koenig, H., 159 (21), 171 (22), *173*
Kohler, C. A., 254 (26), *256*
Kollros, J. J., 293 (1), *301*
Kolousek, J., 115 (12), *137*, 159 (11), *173*
Kopriwa, B. M., 43 (32), 49 (32), 51, *62*, *63*, 305 (17), 309 (36), 314 (19a), *317*, *318*, 327 (26), *338*
Kuhn, N. O., 43 (17), *62*
Kumamoto, Y., 202 (14), *214*
Kundt, H., 14 (19), *20*

Lachapelle, A., 303 (33), *317*
Lagunoff, D., 65 (2, 3, 12), 67 (2), 72 (2, 12), 74 (3, 12), *74*, *75*
Lajtha, A., 159 (23, 33), 172 (23, 33), *173*, *174*
Lamerton, L. F., 9 (17), *20*
Lane, N., 289 (6), *291*, 337 (43), *339*
Leach, A. A., 215 (8), 218 (8), 220 (8), *243*
Leblond, C. P., 1 (2), 2, *5*, *6*, 10, *20*, 43 (23), 49, 51, 54 (23), *62*, *63*, 115, 129 (35), *137*, *138*, 146 (23), 154 (27), *156*, *157*, 159 (6, 24), 160, 161 (6), 162, 165 (5, 6, 7), 168, 170 (7), 171 (5, 6, 7), *173*, 201 (9, 10), 202 (9, 13, 14, 16), 203 (17), 206 (15), 211 (3), *213*, *214*, 217 (6), 233, 241 (6), *243*, 247 (4),

248 (4), 254 (4), 255, 261 (14), 263 (7), 269 (7, 14), 270 (7), *270*, 273 (20), 275 (3), 279 (8), 289 (10), *291*, 293, 298 (17), 301, 303 (19, 22, 25, 35), 305 (17, 26), 309 (26), 312 (27), 313 (19a, 23), 314 (26), 316 (19, 21), *317*, *318*, 321 (5, 31), 322 (19, 32), 323 (57), 324 (32), 325 (48), 326 (48), 327 (26), 328 (12), 329 (57), 330 (9, 19, 32, 40, 57), 331 (57), 332 (28, 30, 32), 333 (29, 32, 57), 334 (40, 57), 335 (8, 20, 24, 33, 40, 46, 47), 336, 337 (46, 47, 49), *338*, *339*

Leduc, E. H., 53 (18, 19), *63*
Leeson, C. R., 293 (11), *301*
Lennartz, K.-J., 122 (14, 20), 129 (14, 20), 130 (14, 20), *137*
Lennox, E. S., 145 (2), *156*
Levi, H., 10, *20*
Li, C. H., 146 (30), *157*
Likins, R. C., 220 (16), *244*
Linker, A., 215 (14), *244*
Linnartz-Niklas, A., 115 (34), *138*
Lissitzky, S., 313 (5), *317*
Lodin, Z., 115 (12), *137*, 159 (11, 19), *173*
Loebel, F., 335 (3), *338*
Lord, B. I., 11, *20*
Lotz, W. E., 2, *5*
Lowther, D. A., 255 (13), *256*
Lowy, P. H., 238 (1), *243*
Lusk, G., 321 (34), *339*

McCoy, J., 255 (31), *256*
McGavack, T. H., 254 (18), *256*
McGregor, D. D., 145 (19), 146 (19, 20), *156*
McKinlay, C. A., 155, *156*
McLean, F. C., 2, *5*, 322 (6), *338*
McLean, P., 159 (12), *173*
MacLennan, J. D., 251 (20), *256*
Mäkelä, O., 154 (26), *157*
Mallory, F. B., 247 (21), *256*
Maloof, F., 313 (32), *317*
Mandel, I. D., 335 (35), *339*
Maraud, R., 303 (33), *317*
Marinozzi, V., 51 (20), *63*
Marko, A. M., 255 (14), *256*
Marques-Pereira, M. P., *339*
Martin, G. M., 66 (13, 14), *75*
Mathé, G., 155, *156*
Maunsbach, A. B., 28 (5), *39*, 43 (14), 58 (6), *62*
Maurer, W., 85, *93*, 107 (32), 115 (7, 26, 27, 31, 32), 119 (7, 32), 120 (8), 121 (32), 122 (6, 13, 14, 20), 126 (19, 23), 129 (4, 5, 6, 14, 20, 21), 130 (4, 5, 6, 14, 20, 21), 135 (30), *137*, *138*, 177, 178, 189 (5, 20, 25), 195 (5), *196*, *197*, 327 (37), *339*
Mechanic, G., 207 (7), *213*
Medawar, P. B., 145 (3), *156*
Mees, C. E. K., 43 (21), *63*
Meilman, E., 251 (32), *256*
Messier, B., 203 (17), *214*
Meunier, J., 303 (33), *317*
Meyer, K., 215 (14), *244*
Meyer zum Gottesberge, A., 177 (11, 16, 17), *196*, *197*
Michel, R., *317*
Michi, T., 255 (22), *256*
Miller, O. L., Jr., 65 (15), *75*, 98 (12), 100 (10), 104 (14), *105*
Mirsky, A. E., 322 (1), *338*
Mitchell, J., 154, *156*, *157*
Mitmaker, B., *63*, 263 (7), 269 (7), 270 (7), *270*, 279 (8), *291*, 305 (26), 309 (26), 313 (24, 26), *317*, 330 (40), 334 (40), 335 (40), *339*
Montreuil-Langlois, M., 332 (38), *339*
Moses, M. J., 28 (11), *39*, 54 (22), *63*
Movat, H. Z., 247 (9), *256*
Müller, D., 129 (21), 130 (21), *137*
Muhlethaler, A. B., 58 (6), *62*
Muhlethaler, K., 28 (11), *39*
Muir, H. M., 255 (14), *256*

Nadler, N. J., 43 (23), 54 (23), *63*, 261 (6), 263 (7), 269 (7), 270 (7), *270*, 279 (8), *291*, 303 (22, 25), 305 (26), 309 (26), 311 (20), 313 (19a, 20a, 23), 314 (20, 24, 26), 316 (21), *317*, 325, 327 (39), 330 (40), 334 (40), 335 (40), *339*
Nemeroff, K., 10, *20*

Neuberger, A., 217 (15), *244*, 254 (23), *256*, 335 (41), *339*
Neutra, M., 337 (49), *339*
Neveling, R., 177 (18), *197*
Neyen, H., 126 (23), *137*
Niklas, A., 115, 126, *137*
Nossal, G. J. V., 154 (26), *157*
Nover, A., 115 (24), *137*, 189 (19), *197*

Oehlert, W., 107 (32), 115 (26, 27, 31, 32), 119 (32), 121 (32), 125 (25), 135 (33), *137*, *138*, 159 (26, 28), *173*, 189 (20, 25), *197*, 332 (42), *339*
Orban, B., 254 (39), *256*
Ormerod, F. C., *198*
Oster, H., 14 (19), *20*
Otero-Vilardebo, L., 337 (43), *339*

Pakesch, F., 145 (6), 154 (6), *156*
Palade, G. E., 263 (12), 265 (1), 269 (1), *270*, 273 (9), 279 (5), 288 (5), *291*, 298 (2), *301*, 307 (3), *317*, 334 (10), *338*
Papas, G. D., 247 (25), *256*
Parkinson, A., 248 (28), *256*
Pavelec, M., 217 (31, 32), 218 (31, 32), 222 (32), 233 (32), 234 (32), 238 (32), 241 (31, 32), *244*
Pelc, S. R., 2, *6*, 9 (7), 10, 13 (7, 14, 21, 22, 23), *20*, 29 (14), 33 (13), 39, *39*, 47, 49 (24), 54 (2), *62*, *63*, 321 (44), *339*
Person, P., 255 (31), *256*
Peterson, M., 289 (10), *291*, 312 (27), *317*, 335, 336, 337 (45, 46, 47), *339*
Petrovic, A., 314 (19a), *317*
Phillips, M., 65 (12), 72 (12), 74 (12), *75*
Philp, J. R., 334, *339*
Piez, K. A., 207 (18), 210 (18), *214*, 220 (16), *244*
Pinheiro, P., 154, *157*, 325, 326, *339*
Platt, D. B., 79 (1, 2), 80 (1, 2), 82 (1), 85 (1), *93*
Plaut, W., 82, *94*
Plester, D., 115 (16, 28), *137*, *138*, 177 (12, 13, 17, 21), 182 (22), *196*, *197*
Porter, K. R., 145 (28), 146, *157*, 216 (12, 17), *243*, *244*, 247 (24, 25), *256*, 273 (11), *291*, 293 (12), *301*
Pouradier, J., 44 (25), *63*
Prehn, R. T., 145 (1), *156*
Prescott, D. M., 65 (15), *75*, 80, 90, *93*, 95, 100 (10), 102 (9), 104 (14), *105*
Primbsch, E., 85, *93*, 126 (19), *137*, 327 (37), *339*

Quastler, H., 147 (29), *157*
Quincke, E., 126 (23), *137*

Rabinovitch, M., 82, *94*
Rabinowitz, M., 91 (9), *94*
Rambourg, A., 159 (27, 27a), 165 (27), 170, 171 (27), *173*, 337 (49), *339*
Ramfjord, S. P., 254 (26), *256*
Ray, R. C., 12, *20*
Reich, E., 91, *94*
Reinhardt, W. O., 145 (12, 13, 31), 146 (13), *156*, *157*
Revel, J. P., 28 (7, 15), 29, *39*, 49 (13, 26), *62*, *63*, 217 (18), 241 (18), *244*, 247 (27), 254 (27), *256*, 269 (4, 8), *270*, 275 (7), 279 (12), *291*, 293 (9), 295 (9, 13, 14), 298 (14), *301*, 309 (14, 28), 312 (29), *317*, 334, 337 (21), *338*, *339*
Reynolds, E. S., 38 (16), *39*
Rhines, T., 159 (13), *173*
Rhodin, J. A. G., 265 (9), *270*
Rich, A., 263 (10), *270*
Richter, D., 159 (3, 16), *173*
Rieke, W. O., 143 (33), 145 (7, 13, 14, 15, 16, 34), 146 (13, 15, 16), 147 (32), 150 (15), 151 (16), 154, *156*, *157*
Roberts, J. M., 49 (27), *63*
Robinson, R. A., 215 (19, 20), *244*
Roche, J., *317*
Rogers, H. J., 247 (28), *256*
Roman, J., 44 (25), *63*
Ross, R., 54 (28), *63*, 65 (17), 74 (17), *75*, 210, 211 (19), *214*, 217, *244*, 247 (29), 254 (30), *256*, 269 (11), *270*, 273 (14, 16), 275 (13, 15), 278, 285 (13), 289 (16), *291*, 293 (15), *301*, 312 (30), *317*, 334, *339*
Roth, L. J., 14 (27), *20*

Rouiller, C., 216 (22), *244*
Roulet, F., 247 (8), *256*
Ruben, R. P., 255 (31), *256*
Russell, P. S., 145 (39), 155 (39), *157*

Saito, S., 255 (1), *255*
Salpeter, M. M., 28 (17), 29 (2, 17), 30 (17), 31 (17), 35 (1, 2, 17), 36 (17), 37 (1, 17), *39*, 49, 53, 54, 61, *63*, 289 (1), 290 (18), *291*
Sandborn, E., 332 (52), *339*
Sarkar, S. K., 303 (25), *317*
Sato, C., 313 (32), *317*
Schmitt, F. O., 247 (15), *256*
Schneider, G., 135, *138*
Schoenheimer, R., 254, *256*
Schooley, J. C., 145 (36), 154 (35, 36), *157*
Schour, I., 203 (11), *214*
Schreiner, L., 182, *197*
Schultze, B., 107 (32), 115 (7, 24, 26, 27, 31, 32), 119 (7, 32), 121 (32), 125 (7, 25), 135 (30, 33), *137*, *138*, 159 (26, 28), 171 (17), *173*, 189 (7, 19, 20, 25), *196*, *197*, 332 (42), *339*
Schwartzkopf, J., 177 (26), *197*
Schwarz, M. R., 147 (32), 154, *157*
Seed, R. W., 313 (31), *317*, 335, 337, *339*
Seifter, S., 251 (32), *256*
Sherman, F. G., 147 (29), *157*
Siekevitz, P., 263 (12), *270*, 273 (9), *291*
Silvers, W. K., 145 (4), *156*
Simmel, E. B., 3 (10), *6*
Simmonds, S., 217 (11), *243*
Simmons, B., 115 (17), *137*, 146 (23), *156*, 159 (24), *173*, 202 (16), *214*, 322 (32), 324 (32), 330 (32), 332 (32), 333 (32), *339*
Singer, M., 293 (16), *301*
Slack, H. G. B., 217 (15, 23), *244*, 254 (23), *256*, 335 (41), *339*
Slonecker, C. E., 155, *157*
Sloper, J. C., 159 (29), 171 (29), *173*
Smith, D., 255 (33), *256*
Smitherman, T. C., 14 (25), *20*
Soodak, M., 313 (32), *317*
Spear, F. G., 13 (23), *20*
Spiro, D., 145 (39), 155 (39), *157*
Stack, M. V., 209 (20), 211 (20), *214*, 248 (34), *256*, 335 (54), *339*
Stein, O., 43 (30), *63*
Stern, H., 98, *105*
Stetten, M. R., 254, *256*
Stevens, C. E., 2, *6*
Stevens, G. W. W., 12, *20*
Stevens, V., 14 (25), *20*
Stirling, C., 14 (26), *20*
Stöcker, E., 195 (27), *197*
Stoll, R., 303 (33), *317*
Stone, G. E., 65 (15), *75*, 95, 97 (11), 98 (11), 100 (10), 104, *105*
Stumpf, W. E., 14 (27), *20*
Stupp, H., 177 (18), *197*
Sweeny, P. R., 293, *301*
Swift, H., 330 (55), *339*

Tarver, H., *173*
Taugner, R., 14 (19, 28, 29), *20*, *21*
Taylor, A. C., 171 (30), *173*
Thompson, R. C., 254 (37), *256*
Tischendorf, F., 115 (34), *138*
Tishler, P. V., 313 (34), *317*
Tonna, E. A., 206 (12) *214*, 217 (25, 26, 29, 31, 32), 218 (25, 26, 29, 31, 32), 220 (27), 222 (32), 231 (24, 28, 30), 233 (30), 234 (32), 238 (26, 32), 241 (25, 26, 29, 31, 32), 242 (30), *244*
Tournier, P., 62 (9), *62*

Udupa, K. N., 14 (8), *20*, 65 (7), *75*
Ullberg, S., 43 (14), *62*

Van Heyningen, H. E., 54 (31), *63*, 261 (13), 269 (13), *270*, 279 (19), 288 (19), *291*, 314 (19a), *317*, 334, *339*
van Heyningen, W. E., 251 (2), *255*
Van Tubergen, R. P., 28 (4), 29, 35 (4), 37 (4), *39*, 309 (4), *317*
Verne, J., 115 (9), *137*, 159 (8), 165 (31), 171 (31), *173*
von der Decken, A., 312 (15), *317*

Waelsch, H., 159 (33), 171 (2, 32, 33), 172 (33), *173*, *174*
Waerhaug, J., 255 (38), *256*

Wagenmann, V., 14 (28, 29), *21*
Waites, G., 165 (18), 170 (18), *173*
Walker, J. F., 73 (16), *75*
Warren, S., 2, *6*, 14 (13), *20*
Warshawsky, H. J., 119, 129 (35), *137*, *138*, 161 (9), *173*, 261 (14), 263 (2), 269 (14), *270*, 273 (20), *291*, 298 (17), *301*, 303 (35), *317*, 323 (57), 324 (15), 329 (57), 330 (57), 331, 333 (57), 334 (57), *338*, *339*
Watson, J. D., 263 (15), *270*
Watson, M. L., 201 (21), *214*
Weaver, J. M., 145 (1), *156*
Weidemann, S. O., 248 (28), *256*
Weiss, P., 170 (35), 171 (34, 35), *174*, 293 (18, 19), *301*
Wellings, S. R., 334, *339*
Wentz, F. M., 254 (39), *256*
Wesslen, T., 145 (38), 154 (38), *157*
Wiener, J., 145 (39), 155 (39), *157*
Williams, A. I., 14 (30), *21*
Wilske, K. R., 65 (17), 74 (17), *75*
Wilson, D. B., 145 (4), *156*
Winchester, R. J., 313 (16), *317*
Winteringham, F. P., 14 (31), *21*
Witten, V. H., 14 (32), *21*
Wolstenholme, G. E. W., 333 (59), *339*
Woodruff, M. F. A., 145 (40), *157*

Yagoda, H., 10, *20*
Yoffey, J. M., 143, 145 (12, 13, 31), 146 (13), *156*, *157*
Young, B. A., 43 (23, 32), 49 (32), 54 (23), *63*, 263 (7), 269 (7), 270 (7), *270*, 279 (8), *291*, 305 (26), 309 (26, 36), 313 (26), *317*, *318*, 330 (40), 334 (40), 335 (40), *339*
Young, R. W., 206 (22), 211 (22), *214*, 217 (33), 218 (33), 241 (33), *244*

Zeigel, R. F., 265 (16), *270*
Zelander, T., 265 (3), 269 (3), *270*
Zilversmit, D. B., 161 (36), *174*, 329 (60), *339*
Ziniberg, S., 159 (13), *173*
Zucker-Franklin, D., 145 (42), 154 (42), *157*